Proceedings
Le Compte rendu

The Canadian conference on building energy simulation

La Conférence canadienne sur la simulation énergétique dans les bâtiments

June 13 and 14, 2001 / le 13 et 14 juin, 2001

Published by CANMET Energy Technology Centre / Natural Resources Canada

Publié par le Centre de la technologie de l'énergie de CANMET
Ressources Naturelles Canada

Natural Resources Canada
Buildings Group

Ressources naturelles Canada
Group du bâtiment

Canada

Citation:

Various authors, eSim 2001, Canadian Conference on building energy simulation. CANMET Energy Technology Centre, Natural Resources Canada, Ottawa, Ontario, 2001.(264p)

Copies of this report may be obtained through the following:

Energy Technology Branch - CANMET
Natural Resources Canada
580 Booth Street, 13th floor
Ottawa Ontario, Canada
K1A 0E4

Disclaimer

This report is distributed for informational purposes only and does not necessarily reflect the views of the Government of Canada nor constitute adnendorsement of any commercial product or person. Neither Canada nor its ministers, officers, employees or agents makes any warranty in respect to this report or assumes any liability arising out of this report.

Références

Divers auteurs, eSim 2001, Conférence canadienne sur la simulation énergétique dans les bâtiments. Centre de la technologie de l'énergie de CANMET, Ressources naturelles Canada, Ottawa (Ontario), 2001. (264 pages)

On peut obtenir des exemplaires du compte rendu de la Conférence à l'adresse suivante :

Direction de la technologie de l'énergie de CANMET
Ressources naturelles Canada
580, rue Booth, 13e étage
Ottawa (Ontario)
Canada K1A 0E4

Renonciation

Le présent compte rendu n'est distribué qu'à titre d'information et ne reflète pas nécessairement les points de vue du gouvernement du Canada, ni ne constitue une reconnaissance d'un produit commercial quelconque ou d'une personne en particulier. Ni le Canada, ni ses ministres, ses représentants, ses agents ou ses employés n'offrent de garantie en ce qui concerne ce compte rendu ou n'assument de responsabilités s'y rapportant.

Minister of Supply & Services Canada 2001
Catalogue No. M39-79/2001
ISBN. 0-660-61650-5

Ministre des Travaux publics et des Services gouvernementaux Canada, 2001
No de catalogue : M39-79/2001
ISBN : 0-660-61650-5

102-06014/

Sim 2001

Table of Contents / Table des matières

Preface / Préface i

Organizing Committee / Comité organisateur de la conférence iii

Scientific Committee / Comité scientifique de la conférence iii

Session 1 / Séance 1

The Application of Simulation in Building Design and Guidance on Modelling Approaches 1
La simulation appliquée à la conception des bâtiments et l'orientation des formules de modélisation

La modélisation des systèmes énergétiques de bâtiment, un outil de decision 3
Laurier Nichols

The Significant Factors in Modelling Residential Buildings: Part 2 11
Julia Purdy, Ian Beausoleil-Morrison, CANMET Energy Technology Centre, Natural Resources Canada

DOE2.1E Geometric Modelling: The Basic Geometric Approach vs. The Complex XYZ Approach 19
Christopher R. Jones, Curt Hepting, EnerSys Analytics Inc.,Canada

Simulation on the Edge 26
Dr. Jon W. Hand, ESRU, University of Strathclyde, Glasgow Scotland

Session 2 / Séance 2

Energy Calculation Methods, Software Development and New Simulation Programs 33
Les méthodes de calcul de la consommation énergétique, l'élaboration de logiciels et les nouveaux programmes en matière de simulation

Revue de littérature sur les avantages et limites des méthodes de modélisation des bâtiments à des fins d'intervention commerciale: le cas d'Hydro-Québec 35
Michel Parent, Technosim; Patrice Raymond, Hydro-Québec

Simulation of Residential HVAC System Performance 43
Iain S. Walker, Jeffery Siegel, Gwladys Degenetais, Lawrence Berkeley National LAboratory, Berkeley, California, USA

Airtightness Testing and Air Flow Modelling of a Three-Unit Multifamily Building 51
Sebastiano DePani, GES Technologies, Montreal; Paul Fazio, Concordia University, Montreal

Developing Project Management and Quality Control Approaches for Improving the EE4 Building Simulation Software 58
Robert Calla, Phylroy Lopez, Paul Wyndham-Wheeler, CANMET Energy Technology Centre, Natural Resources Canada

Simulation Software to Describe the Thermal Environment of Residential Buildings Based on Detailed Physical Models 66
Akihito Ozaki, Kitakyushu University, Japan; Toshiyuki Watanabe, Shuho Takase, Kyushu University, Japan; Shigeki Iwaoka, ATOM Indoor Climate Institute, Japan

Session 3 / Séance 3

Modelling of Non-Thermal Processes: Lighting, Moisture, Material Emissions 75
La modélisation des procédés non thermiques : l'éclairage, l'humidité et les émissions produites par les matériaux

A Methodology for Detailed Calculation of Room Illuminance Levels and Light Dimming in a Room with Motorized Blinds Integrated in an Advanced Window 77
ANDREAS K. ATHIENITIS, Ph.D., P.Eng., ATHANASSIOS TZEMPELIKOS, Centre for Building Studies, Concordia University, Montreal, Quebec, Canada

Development of Analysis Software for the Optical Characteristics and Daylighting Performance of Conventional and Tubular Skylights 85
Abdelaziz Laouadi and Morad Atif, Indoor Environment Research Program, Institute for Research in Construction, National Research Council Canada

A Model for Moisture-Content Evolution in Porous Building Elements: Treatment of Irregular Regions 93
Regina Katsman, National Research Council Canada, Canada; Rachel Becker, Israel Institute of Technology, Israel

Advanced Hygrothermal Models and Design Models 101
Achilles N. Karagiozis, Oak Ridge National Laboratory Building Technology Center, Oak Ridge TN, U.S.A

Modelling of Volatile Organic Compounds Emission from Dry Building Materials 109
Hongyu Huang, Fariborz Haghighat, Department of Building, Civil and Environmental Engineering, Concordia University, Montreal, Canada

Air Conditioning Simulation 116
Hisashi YAMAZAKI, Kyushu-University, Fukuoka city Japan, Toshiyuki WATANABE, Kyushu-University, Fukuoka city Japan, Hitoshi YAMAZAKI, Kanto-Gakuin-University, Kanagawa city Japan.

Session 4 / Séance 4

The Role of Simulation in Supporting Energy Efficiency Programmes and Stock Modelling 123
Le rôle de la simulation à l'appui des programmes d'efficacité énergétique et la modélisation des ensembles de bâtiments

HOT2.XP: Energuide for Houses and the New Housing Market 125
Ted Kesik, Architecture, Landscape and Design, University of Toronto; Michael Lio, Lio Associates, Toronto, Canada

Whole Building Energy Simulation for Access to Incentive Funding: Lessons Learned from Canada's Commercial Building Incentive Program 132
Stephen Pope, François Dubrous, CANMET Energy Technology Centre, Natural Resources Canada

The Prescriptive Path - Its Construction and Place in the Commercial Building Incentive Program 138
Doug Cane Andrew Morrison, Caneta Research Inc., Mississauga, Ontario, Canada

A Residential End-Use Energy Consumption Model for Canada 144
A.S. Fung, M. Aydinalp, V. I. Ugursal, H. Farahbakhsh Canadian Residential Energy End-use Data and Analysis Centre Department of Mechanical Engineering, Dalhousie University Halifax, Nova Scotia, Canada

Real-World Integrated Design Practice and Tools: Effective Energy Performance Analysis Approaches 152
Graham Henderson, P.Eng., BC Hydro, Burnaby B.C. ; Curt Hepting, P.Eng. and Diane Ehret, EnerSys Analytics Inc. Coquitlam B.C., Canada

Session 5 / Séance 5

Modelling Conventional and Innovative HVAC Systems 161
La modélisation de systèmes classiques et originaux de CVC

Annual Simulations of Heat Pump Systems with Vertical Ground Heat Exchangers 163
Michel Bernier, Duo Randriamiarinjatoto, École Polytechnique de Montréal

Modélisation d'un chauffe-eau solaire couplé à un système à compression de vapeur 171
Stéphane Bilodeau, Simon Sansregret Groupe Énerstat Inc., Sherbrooke, Quebec.

Simulation of a Combined Space and Water Heating System Firing Pellet Fuel for Commercial/Residential Application 179
Bruce R. Clements, Bill Pearson, A.C.S. Hayden CANMET Energy Technology Centre, Natural Resources Canada

Modelling and Analysis of Building Systems that Integrate Cogeneration and District Heating and Cooling ..187
Marc A. Rosen, Wey H. Leong, Minh N. Le, Department of Mechanical, Aerospace and Industrial Engineering, Ryerson Polytechnic University, Toronto, Canada

Dynamic Simulation of Building Heating Systems Connected to a District Heating System 195
L. Yang, C. W. Snoek, CANMET Energy Technology Centre, Natural Resources Canada

Session 6 / Séance 6

Calibration, Validation and Inverse Methods 203
L'étalonnage, la validation et les méthodes inversées

Use of Soft Computing Techniques for the Evaluation of Energy Performance of Equipments in Buildings ..205
Radu Zmeureanu, Linda Farinaccio, Centre for Building Studies Department of Building, Civil and Environmental Engineering Concordia University, Montreal, Canada

Measurement and Simulation of the Thermal Environment of a Low Energy House with Air-Circulation in Brick Walls 212
Shuho Takase, Toshiyuki Watanabe, Tetsuo Hayashi, Mayuko Nagata, Masako Osato, Kyushu University, Japan; Akihito Ozaki, Kitakyushu City University, Japan; Mikiko Nakamura, Japan Science and Technology Corporation, Japan

Validation Dynamique des Modeles de Simulation des Batiments Existants 220
Marc-Antoine Roberge, Stanislaw Kajl, René Bellemare, École de technologie supérieure, Montréal, Canada

4. Validation and Calibration of a Multizone Network Airflow Model with Experimental Data 228
Amy Musser, Oliver Schwabe, University of Nebraska-Lincoln, Omaha, NE; Steven Nabinger, National Institute of Standards and Technology, Gaithersburg, MD, USA

Session 7 / Séance 7

Recent Developments in Modelling Thermal and Other Physical Processes 237
Les plus récents développements dans la modélisation des procédés thermiques et des a utres procédés physiques

Advances in Modelling Thermal Bridges in Building Envelopes 239
Stephen Carpenter, Enermodal Engineering Limited, Kitchener, ON, Canada

Demonstration of ESP-r's Adaptive Convection Algorithm 245
Ian Beausoleil-Morrison, CANMET Energy Technology Centre, Natural Resources Canada

Multi-Domain Modelling Using the ESP-r System 253
Nick Kelly and Paul Strachan, Energy Systems Research Unit University of Strathclyde, Glasgow, Scotland

Author Index / Index des auteurs 261

Preface

The CANMET Energy Technology Centre (CETC) is a leader in the development of energy simulation software for the Canadian construction industry. It develops whole-building energy analysis tools such as EE4 and HOT2000 as well as specialized programs for analyzing specific aspects of building physics (e.g. BASECALC and GS2000). The full details of CETC's energy simulation software activities can be found at http://buildingsgroup.nrcan.gc.ca.

CETC organized the *eSim 2001* conference to provide a Canadian forum for the exchange of ideas and experiences related to the development and application of building energy simulation software tools. As such, *eSim 2001* complements international events such as the biennial conferences of the International Building Performance Simulation Association.

Potential authors were invited to submit abstracts related to the following themes:

- Recent developments in methods for modelling the physical processes relevant to buildings (thermal, air flow, moisture, lighting);
- Algorithms for modelling conventional and innovative HVAC systems;
- The development of methods for modelling energy supply systems within whole-building simulation, including renewables, district heating and cooling, and combined heat and power;
- Building simulation software development and quality control approaches;
- The role of building simulation tools in code compliance and incentive programmes;
- Moving simulation into practice and removing barriers to the adoption of simulation by the building industry;
- Validation and calibration techniques;
- User interface and software interoperability issues.

Préface

Le Centre canadien de la technologie de l'énergie (CTEC) assume le rôle de chef de file en matière d'élaboration de logiciels de simulation énergétique à l'intention du secteur canadien de la construction. De fait, le CTEC œuvre à la mise au point d'outils d'analyse énergétique des bâtiments dans leur entier, tels que EE4 et HOT2000, de même que de programmes spécialisés visant à analyser certains aspects précis de la physique des bâtiments (comme BASECALC et GS2000). On retrouvera à l'adresse http://groupedubatiment.rncan.gc.ca tous les détails concernant les activités du CTEC en matière de logicels de simulation énergétique des bâtiments.

Le CTEC a mis sur pied la Conférence *eSim* afin d'établir une tribune canadienne favorisant les échanges d'idées et d'expériences reliées au développement et à l'application de logiciels de simulation énergétique des bâtiments. À ce titre, la Conférence vient compléter des événements internationaux comme les conférences biennales de l'International Building Performance Simulation Association.

Les auteurs éventuels ont été invités à présenter des résumés de travaux portant sur les thèmes suivants :

- Les plus récentes découvertes dans le domaine des méthodes relatives à la modélisation des processus physiques propres aux bâtiments (énergie ther mique, débit d'air, humidité, éclairage).
- Les algorithmes servant à la modélisation des systèmes de CVC classiques et originaux.
- L'élaboration de méthodes en vue de modéliser les systèmes d'approvisionnement énergétique à l'intérieur de la simulation globale du bâtiment, notamment en ce qui concerne les énergies renouvelables, le chauffage et la climatisation à l'aide de réseaux de quartier, la production combinée de chaleur et d'électricité.
- L'élaboration de logiciels de simulation du rendement énergétique des bâtiments et les façons de contrôler la qualité.
- Le rôle que jouent les instruments de simulation énergétique des bâtiments dans la conformité aux codes et dans les programmes d'encouragements.
- Les questions relatives à l'interface avec les utilisateurs et à l'interopérabilité des logiciels.

A scientific committee—volunteer peers from the private sector, academia, and government research communities—was assembled to review these abstracts. Each abstract was reviewed by at least two members of the scientific committee. The authors whose abstracts were accepted by this committee, then developed their works into full-length manuscripts. These manuscripts were reviewed by the scientific committee and those deemed to be of sufficiently high caliber and directly related to the eSim 2001 themes were accepted for presentation at the conference.

These proceedings act as a permanent record of the papers that were presented at *eSim 2001*. Simultaneous translation was provided at the conference. However, each paper is published here in the language (French or English) chosen by the author.

A total of 32 papers were presented at *eSim 2001*. In addition, three invited presentations were given to provide delegates with an overview of building simulation activities Europe, Japan, and the USA; however, no papers were produced for these presentations.

The 32 papers are organized in these proceedings by the seven sessions held at the conference:

- The application of simulation in building design and guidance on modelling approaches;
- Energy calculation methods, software development, and new simulation programs;
- Modelling of non-thermal processes: lighting, moisture, material emissions;
- The role of simulation in supporting energy efficiency programmes and stock modelling;
- Modelling conventional and innovative HVAC systems;
- Calibration, validation, and reverse methods;
- Recent developments in modelling thermal and other physical processes.

Pour la circonstance, on a réuni un comité scientifique, formé de pairs bénévoles provenant du secteur privé, du domaine universitaire et des organismes de recherche gouvernementaux, qui était chargé de passer en revue les résumés reçus. Ainsi, chaque document a été examiné par, au moins, deux membres du comité scientifique. Les auteurs des résumés acceptés par les membres du comité pouvaient, par la suite, développer leurs écrits en manuscrits complets. Ces derniers ont été examinés par les membres du comité scientifique. Les documents jugés d'un calibre suffisant, en plus d'être reliés directement aux thèmes de la Conférence, ont été acceptés en vue de leur présentation.

Le présent compte rendu constitue un registre permanent des documents qui ont été présentés à la Conférence eSim 2001. Un service d'interprétation simultanée a été fourni lors de l'événement. Toutefois, chaque document de présentation est publié dans la langue choisie par l'auteur (soit le français ou l'anglais).

Un total de 32 documents a été présenté à la Conférence. En outre, trois présentations spéciales ont été faites afin de fournir aux délégués un aperçu de ce qui se fait en Europe, au Japon et aux États-Unis dans le domaine de la simulation énergétique des bâtiments. Toutefois, ces présentations ne s'accompagnaient d'aucun document.

Ces 32 documents sont disposés dans le présent compte rendu en sept séances qui ont eu lieu pendant la Conférence, soit :

- la simulation appliquée à la conception des bâtiments et l'orientation des formules de modélisation;
- les méthodes de calcul de la consommation énergétique, l'élaboration de logiciels et les nouveaux programmes en matière de simulation;
- la modélisation des procédés non thermiques : l'éclairage, l'humidité et les émissions produites par les matériaux;
- le rôle de la simulation à l'appui des programmes d'efficacité énergétique et la modélisation des ensembles de bâtiments;
- la modélisation de systèmes classiques et originaux de CVC;
- l'étalonnage, la validation et les méthodes inversées;
- les plus récents développements dans la modélisation des procédés thermiques et des autres procédés physiques.

Organizing Committee
Comité organisateur de la conférence

Chair / Président : Ian Beausoleil-Morrison
Organizer / Organisatrice responsable : Julianne Bertulli
Webmaster / Webmestre : Stephanie Mombourquette

Scientific Committee
Comité scientifique de la conférence

Andreas Athienitis, Concordia University, Canada
Morad Atif, National Research Council, Canada
Ian Beausoleil-Morrison, Natural Resources Canada, Canada
Michel Bernier, Ecole Polytechnique de Montréal, Canada
Jeff Blake, Natural Resources Canada, Canada
Brian Bradley, Natural Resources Canada, Canada
Doug Cane, Caneta Research, Canada
Stephen Carpenter, Enermodal Engineering, Canada
Kamal Haddad, Natural Resources Canada, Canada
Fariborz Haghighat, Concordia University, Canada
Jon Hand, University of Strathclyde, Scotland
Jan Hensen, Technische Universiteit Eindhoven, The Netherlands
Milan Janak, Slovenska Technicka Univerzita, Slovak Republic
Christopher Jones, EnerSys Analytics Inc., Canada
Stanislaw Kajl, École de technologie supérieure, Canada
Achilles Karagiozis, Oak Ridge National Laboratory, USA
Nick Kelly, University of Strathclyde, Scotland
Ted Kesik, University of Toronto, Canada
Aziz Laouadi, National Research Council, Canada
James Love, University of Calgary, Canada
Maria Mottillo, Natural Resources Canada, Canada
Joel Neymark, Joel Neymark and Associates, USA
Michel Parent, Technosim, Canada
Julia Purdy, Natural Resources Canada, Canada
Don Stephenson, National Research Council (retired), Canada
Paul Strachan, University of Strathclyde, Scotland
Meli Stylianou, Natural Resources Canada, Canada
Ismet Ugursal, Dalhousie University, Canada
Radu Zmeureanu, Concordia University, Canada

Session 1 / Séance 1

The Application of Simulation in Building Design and Guidance on Modelling Approaches

La simulation appliquée à la conception des bâtiments et l'orientation des formules de modélisation

LA MODÉLISATION DES SYSTÈMES ÉNERGÉTIQUES DE BÂTIMENT UN OUTIL DE DÉCISION

Laurier Nichols, ing.
Dessau-Soprin
Montréal (Québec)
Laurier.nichols@dessausoprin.com

1. RÉSUMÉ

En première partie, ce document présente globalement les résultats d'une étude préliminaire qui a permis d'intéresser les administrateurs d'une commission scolaire d'opter pour un concept de mécanique offrant une meilleure performance énergétique. La modélisation du fonctionnement du bâtiment a fourni des indications crédibles en comparant les coûts globaux annuels pour diverses sources d'énergie en utilisant les différents tarifs en vigueur au moment de l'étude. Cette démarche a été à l'origine du processus décisionnel qui a conduit au choix d'un système de chauffage avec thermopompes géothermiques.

Les systèmes de chauffage, ventilation, réfrigération et de conditionnement de l'air (CVCA et R) ont une incidence majeure sur la consommation énergétique d'un bâtiment. Non seulement faut-il choisir un équipement qui permettra de rencontrer la charge maximale de conception, mais il faut s'assurer que l'équipement pourra conserver une efficacité intéressante à charge partielle. La charge usuelle d'un bâtiment, que ce soit en chauffage ou en refroidissement, se situe généralement en deçà de 50 % de la charge maximale. On comprend l'importance de choisir des équipements qui seront performants lorsqu'ils seront sollicités à un niveau de charge bien en deçà de leur puissance maximale. La présentation permettra de visualiser les résultats d'une modification de la courbe de performance pour un projet où on a eu recours à des thermopompes géothermiques combinées à des serpentins électriques de chauffage.

La modélisation des équipements CVCA nécessite de bien comprendre comment on détermine la puissance de l'appareillage en mode de climatisation ou en mode de chauffage. Les données d'entrée de certains logiciels utilisent des valeurs courantes qu'il faut connaître pour être en mesure de valider les résultats obtenus. On présentera quelles sont les conséquences d'utiliser des données inappropriées pour établir la performance d'un système utilisant un réseau de thermopompes géothermiques. Un mauvais choix des données d'entrée peut avoir un impact considérable sur les résultats d'analyse et en fausser totalement les conclusions.

Les calculs des différentes modélisations qui seront présentées ont été effectués à l'aide du logiciel DOE-2.1E.

2. INTRODUCTION

La conception des systèmes architecturaux et des systèmes énergétiques des bâtiments fait appel à une foule de connaissances de nature si diverse qu'il est très difficile d'adopter une méthodologie uniformisée sans devoir l'adapter au contexte particulier de chaque nouveau bâtiment. Par chance, au cours des années et surtout suite à l'avènement de l'ordinateur, une multitude d'outils d'aide à la conception ont été développés pour faciliter la tâche des concepteurs. Il est donc possible de compléter une étude particulière pour chaque bâtiment sans devoir y consacrer un effort extraordinaire.

Malheureusement, on constate que les outils d'analyse énergétique sont encore peu utilisés. Une évaluation d'un représentant technique d'un important fournisseur d'équipements de climatisation mentionnait qu'en dix ans de représentation, sur un nombre de plus de 1 000 projets, il a eu connaissance qu'une analyse énergétique par modélisation complète du bâtiment avait été effectuée sur moins de dix (10) bâtiments. Il mentionne aussi que pour plus 30 % de ces 1 000 bâtiments le calcul des charges de climatisation et de chauffage avait été effectué par analyse sommaire à l'aide de tableaux et formules empiriques. Selon son opinion, le calcul des charges à l'aide des outils informatiques ne se réalise que pour un pourcentage de 40 à 50 % des projets. Les logiciels de calcul des fournisseurs d'équipement ne sont utilisés que pour 35 % des concepts de nouveaux bâtiments.

Dans la province de Québec, il existe plus de 50 firmes importantes de génie conseil qui offrent des services de conception des systèmes énergétiques de bâtiment. On considère comme importante une firme qui compte plus de 40 employés à plein temps. On peut prétendre qu'il y a au total plus de 250 firmes de consultants en mécanique et électricité de bâtiment.
De ce nombre, très peu de firmes utilisent une modélisation complète pour orienter la conception d'un nouveau bâtiment. Pourtant, ce sont ces consultants qui ont le plus d'impact sur le choix de l'appareillage qui aura une incidence majeure sur sa consommation d'énergie. Il est difficile d'évaluer le pourcentage exact des firmes qui utilisent l'analyse énergétique par modélisation. Il est fort probable que cette technique n'est utilisée que pour moins de 10 % des nouveaux bâtiments.

Ce document démontre les avantages incontournables de la modélisation du fonctionnement d'un édifice pour en évaluer sa performance énergétique. Il présente, en première partie, l'analyse d'un petit bâtiment qui a fait l'objet d'une analyse de la consommation énergétique par modélisation de son comportement à l'aide du logiciel DOE-2.1.

On y présente les informations les plus pertinentes d'une première analyse qui a été l'élément déclencheur pour convaincre les responsables de la construction de ce bâtiment qu'il était opportun de concevoir des systèmes architecturaux et des systèmes mécaniques et électriques qui permettraient d'en abaisser la facture énergétique.

On présente ensuite les difficultés rencontrées lors de la modélisation requise dans le cadre du programme d'encouragement pour les bâtiment efficaces (PEBC). On discutera de la méthodologie utilisée pour la modélisation d'équipements particuliers.

3. DESCRIPTION DU BÂTIMENT

L'école primaire de Ste-Anne-de-Bellevue est propriété de la commission scolaire Marguerite-Bourgeoys située dans la banlieue ouest de Montréal. L'école comprend deux étages et un gymnase. Le premier étage est occupé par six salles de cours, une salle polyvalente, cuisinette, vestiaires, bureaux administratifs et une maternelle. Le deuxième étage est occupé par six salles de cours, une bibliothèque, une salle informatique de même qu'une salle mécanique et une salle électrique. Le bâtiment couvre une surface totale d'environ 2 900 m² (31 000 pieds carrés). L'implantation au sol est de 1 930 m² (21 000 pieds carrés). Les informations plus détaillées sont les suivantes :

4. DONNÉES GÉNÉRALES

Type de bâtiment : École primaire
Lieu : Ste-Anne-de-Bellevue, Québec
Occupation : 435 personnes ou 1 personne/0,66 m² (72 pi.²)

Horaire des occupants :
Selon l'occupation probable d'un bâtiment scolaire (école primaire)

Conditions ambiantes :
Température (calcul de charge) : 23,9 °C (75° F)
Point de consigne de chauffage : 23,3 °C (74° F)
Point de consigne de la climatisation :24,4 °C (76° F)

Données architecturales :
Superficie totale :
2 908 m² (31 309 pi.²) total qui comprend :
1 930 m² (20 778 pi.²) au rez-de-chaussée
978 m² (10 531 pi.²) pour l'étage

Construction des fenêtres : fenêtres doubles, tintées
valeur U : 3,17 SI (0,56 I-P)
valeur R : 0,31 RSI (1,79 I-P)
coefficient d'ombrage: 0,58
coefficient de gain solaire:0,50
fenestration : 33 %

Construction des murs extérieurs :
Hauteur : plancher à plancher : 3,84 m (12' 6")
Valeur U totale : 0,45 SI (0,08 I-P)
Valeur R totale : 2,2 RSI (12,5 I-P)
Le taux d'infiltration d'air frais a fait l'objet d'une analyse spécifique

Construction du toit :
Valeur U totale : 0,381SI (0,067 I-P)
Valeur R totale : 2,62 RSI (14,9 I-P)

Éclairage :
Type d'éclairage : fluorescent
Charge : 16,14 W/m² (1,5 W/pi.²)

Horaire d'usage de l'éclairage :
Selon l'usage d'un bâtiment scolaire (école primaire)

Équipement électrique :
Type d'équipement : ordinateurs, copieurs, projecteurs

Charge : 5,38 W/m² (0,5 W/pi.²) (classes, bureaux administratifs)
1,62 W/m² (0,15 W/pi.²) (gymnase)
Horaire d'usage de l'équipement :
Selon l'usage d'un bâtiment scolaire (école primaire)

Les systèmes CVCA :
Deux systèmes CVAC différents ont été étudiés. Un système de chauffage en périmètre avec convecteurs à l'eau chaude a été comparé à un système de chauffage par plinthes électriques. Le modèle de base assure une entrée d'air frais de 10 l/s (20 pcm) par personne.

L'horaire d'air frais est le suivant :
Selon l'occupation probable : 8h00 – 18h00 (5 jours par semaine)

Les systèmes de chauffage :
Le système de chauffage comprend une chaudière au gaz naturel. Le modèle de base assure une efficacité de la chaudière de 80 %. Certaines modifications ont été apportées au modèle de base pour évaluer différents taux d'air frais et différents taux d'humidité. Les résultats les plus intéressants ont été obtenus avec la comparaison entre le modèle de base au gaz et un système de chauffage de type électrique. On retrouve aussi des informations sur la différence de coût entre

un système de chauffage au gaz utilisant deux chaudières au lieu d'une seule.

5. ANALYSE PRÉLIMINAIRE

La préoccupation des administrateurs d'un parc immobilier lors de la construction d'un nouveau bâtiment sont :

- Bâtiment qui répondra aux besoins des usagers (fonctionnel et esthétique agréable)
- Coût initial qui respecte les budgets (même s'ils sont souvent trop faibles)
- Construction qui respectera les échéanciers
- Composantes qui seront durables et faciles à entretenir
- Coûts énergétiques faibles

Il demeure de la responsabilité du concepteur de faire valoir les avantages d'un concept par rapport à un autre. Pour la province de Québec, la démonstration des différences dans le coût des différentes sources d'énergie permet au concepteur d'amorcer chez les administrateurs une réflexion très captivante.

Ainsi, pour le projet d'école de la Commission scolaire Marguerite-Bourgeoys, une modélisation sommaire du bâtiment a fourni une information très crédible sur les différents concepts possibles pour permettre l'usage des différentes sources usuelles d'énergie. Les différentes options qui ont été analysées sont les suivantes (voir aussi Tableau-1) :

- Chauffage au gaz naturel avec radiation en périmètre, apport d'air neuf (10 l/s par personne), humidification à 30 % et efficacité nominale de chaudière de 80 %.

- Chauffage au gaz naturel avec radiation en périmètre, apport d'air neuf (7,5 l/s par personne), humidification à 30 % et efficacité nominale de chaudière de 80 %.
- Chauffage au gaz naturel avec radiation en périmètre, apport d'air neuf (0 l/s par personne), humidification à 30 % et efficacité nominale de chaudière de 80 %.

- Chauffage au gaz naturel avec radiation en périmètre, apport d'air neuf (10 l/s par personne), humidification à 0 % et efficacité nominale de chaudière de 80 %.

- Chauffage à l'électricité avec plinthes en périmètre, apport d'air neuf (10 l/s par personne) et humidification à 30 %.

- Chauffage au gaz naturel avec radiation en périmètre, apport d'air neuf (10 l/s par personne), humidification à 30 % et deux (2) chaudières avec efficacité nominale de 80 %.

Cette étude permet de saisir l'importance d'une analyse du fonctionnement d'un bâtiment par modélisation. Strictement pour le choix de la source énergétique pour le chauffage, tout dépendant de l'option choisie, le coût global résultant de la consommation énergétique peut faire l'objet d'une augmentation de l'ordre de 67 % (voir tableau #1). Le futur propriétaire d'un bâtiment est certainement intéressé à connaître les conséquences des diverses options possibles et bien entendu de les connaître avant la construction. Il est donc nécessaire de faire une modélisation théorique.

Même si le coût initial de construction d'une installation de chauffage à l'électricité est moins élevé, les résultats de cette étude démontrent que le coût énergétique d'une telle option est très dispendieux en comparaison du coût global d'énergie de chacune des différentes options utilisant le chauffage au gaz naturel.

Deux phénomènes sont à l'origine de cette importante différence. D'abord, les caractéristiques du tarif d'Hydro-Québec sont telles qu'un client qui consomme l'électricité pour des fins de chauffage aura à payer une surprime pour l'écart entre la puissance d'été et la puissance d'hiver. Puisqu'une école est normalement fermée pour la période estivale, il en résultera un écart important entre la puissance appelée en hiver et la puissance appelée en été. Les résultats globaux feront en sorte que le coût moyen par kWh sera relativement élevé (voir tableau #2). Une autre caractéristique du tarif d'Hydro-Québec tient compte de l'usage de la puissance raccordée. Le cas d'une école primaire est typique. Il n'y a aura presque pas d'usage de la puissance appelée en dehors des périodes d'occupation, donc le coût moyen par kWh sera plus élevé que pour une option utilisant d'autres sources d'énergie.

Cette simple démonstration illustre l'importance de faire l'analyse du fonctionnement d'un nouveau bâtiment en utilisant les techniques modernes de modélisation. Une telle analyse peut être l'élément initial d'une démarche qui fera en sorte qu'on utilisera le modèle pour non seulement valider le choix de la meilleure source d'énergie mais aussi pour optimiser le choix de l'appareillage électromécanique.

6. CHOIX FINAL DE LA SOURCE ÉNERGÉTIQUE POUR L'ÉCOLE DE SAINTE-ANNE-DE-BELLEVUE

Il est intéressant de mentionner que l'électricité a été retenue comme choix final de la source d'énergie pour le chauffage de l'école. Toutefois, l'option choisie fait appel à une technologie de chauffage qui est beaucoup plus efficace que les différentes options au gaz naturel. Les concepteurs ont opté pour une installation de chauffage de type géothermique. De plus, pour minimiser l'impact du chauffage de l'air de ventilation sur la puissance appelée en

hiver, on a prévu l'utilisation d'un récupérateur de la chaleur contenue dans le débit d'air évacué. La chaleur récupérée est utilisée pour le préchauffage de l'air de ventilation.

7. DESCRIPTION GÉNÉRALE DES SYSTÈMES ÉLECTROMÉCANIQUES DE L'ÉCOLE

L'école est munie de différents systèmes CVAC qui combinent la géothermie avec un système de thermopompes et un système conventionnel d'apport d'air frais avec récupérateur d'énergie (roue thermique). Dans le but de limiter les coûts d'immobilisation, la sélection des thermopompes a été effectuée en considérant qu'une partie de la charge de chauffage serait assurée par des serpentins de chauffage de type électrique.

8. SYSTÈME D'AIR FRAIS

Pendant les heures d'occupation, le système fourni un débit constant d'air frais de 2 618 l/s (7 670 cfm). Un récupérateur de chaleur (roue thermique) et un serpentin électrique (85 kW) assurent le chauffage de l'air frais à 18,3° C (65° F). La roue thermique récupère la chaleur avec une efficacité moyenne de 60 %. L'air frais est distribué dans l'entreplafond par l'intermédiaire d'une gaine d'alimentation qui apporte la quantité d'air neuf requis à chaque thermopompe.

9. BOUCLE D'EAU SOUTERRAINE ET BOUCLE DU RÉSEAU DES THERMOPOMPES

Le système géothermique fournit de la chaleur à l'édifice à partir d'une boucle ouverte qui puise l'eau souterraine, alimente un échangeur de chaleur et réinjecte l'eau dans le sol. À l'intérieur du bâtiment, une boucle fermée circule un mélange eau/glycol (5 % poids). Cette seconde boucle est utilisée comme circuit d'échange pour les thermopompes.

Le système de géothermie à boucle ouverte puise l'eau à l'aide d'une pompe submersible dans un puits souterrain. Pour des considérations économiques et en raison de la taille réduite du système, il a été décidé d'utiliser un débit fixe de 6,3 l/s (100 gpm). Suite à une étude de caractérisation de la disponibilité en eau souterraine, le débit de conception peut être maintenu et la température de l'eau souterraine demeure constante à 7,2 °C (45 °F).

L'eau ainsi puisée transmet sa chaleur à la boucle interne par l'intermédiaire d'un échangeur de type à plaques. La température de la boucle interne peut être réchauffée par la boucle externe pour atteindre une température maximale de conception de 6,1°C (43 °F). La température du retour d'eau à l'échangeur de chaleur a été fixée à 0 °C (32 °F) pour retirer le maximum de chaleur de la boucle souterraine tout en évitant le danger de gel de l'échangeur. La température de l'eau de retour au sol devrait être de l'ordre de 1,0 °C (33,8 °F).

La boucle interne est utilisée comme source de chaleur pour l'ensemble des thermopompes. Les thermopompes reçoivent une solution d'eau avec un léger additif de glycol à une température de 6,1 °C (43 °F). Lors d'un fonctionnement en plein régime de chauffage, chaque thermopompe peut rejeter l'eau du circuit primaire à une température de 0 °C (32 °F).

Pour les conditions d'été, le bâtiment a été conçu avec refroidissement partiel des locaux. Les locaux de la bibliothèque, la classe d'informatique et les locaux administratifs sont climatisés. Le concept de base ne prévoit pas que les thermopompes des autres locaux puissent fonctionner en mode climatisation.

En été, la boucle interne du réseau des thermopompes rejette sa chaleur dans la boucle géothermique en utilisant l'échangeur de chaleur. Le système fonctionne alors en mode inversé. La chaleur est d'abord retirée des locaux pour être ensuite rejetée dans la boucle interne. Chaque thermopompe (en mode climatisation) sera alors alimentée par la solution de la boucle interne à une température de 8,3 °C (47 °F). Le rejet de chaleur rehaussera la température de la solution eau/glycol jusqu'à un maximum de 14,4 °C (58 °F). La boucle interne sera alors refroidie par la boucle externe par l'intermédiaire de l'échangeur de chaleur. L'eau souterraine sera alimentée à une température de 7,2 °C (45 °F) pour être réchauffée à une température de 13,3 °C (56 °F).

10. RÉSEAU DES THERMOPOMPES

L'école est chauffée et refroidie partiellement avec un système de thermopompes sur une boucle fermée. Il y a un total de vingt (20) thermopompes de différentes capacités distribuées à travers l'édifice pour fournir le chauffage pour chaque zone. Le chauffage des pièces est d'abord fourni par chaque thermopompe. Lorsque la demande de chauffage dépasse la capacité de la thermopompe, un serpentin de réchauffage permet d'assurer un chauffage d'appoint pour maintenir le local à son point de consigne 22,2°C (72 °F). Chaque thermopompe a fait l'objet d'une sélection pour fournir 70 % de la puissance de chauffage calculée pour chaque zone. Un serpentin électrique permet de combler la balance du 30 % pour éviter tout abaissement de température durant les périodes de froid intense.

11. SYSTÈME DE CONTRÔLE CENTRALISÉ

Tout l'appareillage CVCA sera contrôlé par un système centralisé de régulation et de gestion de l'énergie. Le système permettra l'arrêt des composantes CVCA en dehors des périodes d'occupation. Différentes stratégies de gestion efficace de l'énergie pourront être implantées de façon à optimiser les performances des systèmes du bâtiment et en diminuer les besoins énergétiques.

12. SYSTÈME D'ÉCLAIRAGE

Les systèmes d'éclairage utilisent les appareils à rendement élevé qui sont actuellement disponible sur le marché. La majorité de l'éclairage est assuré par des appareils de type fluorescent avec tube de type T-8 et ballast électronique. Un système de contrôle permet une gestion efficace de l'éclairage pour éviter toute sur-utilisation en période non-occupée.

13. MODÉLISATION DU SYSTÈME PROPOSÉ

Le logiciel EE4 1.30 n'offre pas la possibilité de reproduire fidèlement le concept et les modes de fonctionnement qui ont été privilégiés pour ce bâtiment. Pour permettre de bien représenter le fonctionnement des systèmes CVCA, il a été nécessaire de modifier la modélisation du bâtiment proposé en utilisant le fichier d'entrée DOE-2.1E (généré par EE4).

Dans un premier temps, on a modélisé le bâtiment en utilisant le logiciel EE4, ensuite une nouvelle simulation a été effectuée en utilisant le logiciel DOE-2.1E et le fichier météorologique Montreal.bin (format CWEC – le même fichier que celui utilisé par EE4).

14. EFFET COMBINÉ DE L'ÉNERGIE REQUISE PAR LES THERMOPOMPES ET L'ÉNERGIE REQUISE POUR LES SERPENTINS ÉLECTRIQUES

Tel que mentionné précédemment, on a effectué la sélection des thermopompes pour assumer 70 % de la charge de chauffage de pointe. La balance du 30 % de chauffage de pointe doit être assurée par des serpentins électriques installés sur la conduite d'air à la sortie de chaque thermopompe.

Étant donné que ces serpentins sont inactifs pendant la majorité de l'année, il serait très pénalisant de modifier le COP de chauffage des thermopompes pour inclure l'alimentation énergétique des serpentins et ainsi diminuer la performance énergétique des thermopompes sur une base annuelle.

Il est évident qu'on doit tenir compte de l'alimentation électrique des serpentins par l'addition de leur puissance respective à l'alimentation électrique des thermopompes. Toutefois, cette addition ne doit être considérée que pour la courte période de froid intense (environ 200 heures par année dans la région de Montréal).

Une simple correction du COP en divisant la puissance de chauffage combinée du serpentin et de la thermopompe par le total combiné de leur alimentation électrique respective serait très pénalisante dans la simulation EE4. On a donc opté pour une méthode alternative plus représentative du fonctionnement simultané de ces deux appareils de chauffage.

Il a été possible de corriger le besoin énergétique de base de l'ensemble tout en modifiant le facteur de correction de l'énergie d'alimentation des appareils combiné en fonction d'une charge partielle de chauffage. Il s'agit du facteur EIR et de la courbe applicable aux thermopompes HEAT-EIR-FPLR.

15. MODIFICATION DU COP DES THERMOPOMPES

Le logiciel DOE-2.1 requiert de déterminer la valeur d'un facteur qui représente l'alimentation en énergie d'un appareil mécanique au moment où il fonctionne à pleine charge (Energy Input Ratio, EIR). Ce facteur est une fraction qui est obtenue par la division de l'énergie fournie à l'appareil par la valeur de la puissance à pleine charge. Il s'agit en fait de la valeur inverse du COP. Ce facteur est relativement simple à calculer. Dans le cas de l'usage combiné d'une thermopompe et d'un serpentin électrique, on doit établir le besoin total d'énergie des deux appareils lorsque la demande de chauffage atteint la puissance combinée des deux appareils. Le EIR est un facteur obtenu par la division de l'alimentation combiné des deux appareils par leur puissance combinée de chauffage à pleine charge. On doit mentionner que la puissance combinée de la thermopompe et du serpentin doit être donnée pour une température de la boucle interne de 21,1 °C (70 °F). Il y a une erreur dans le manuel guide du logiciel EE4 à ce sujet. On ne doit pas fournir la puissance de la thermopompe à 0 °C (32 °F) mais bien à 21,1°C (70 °F).

Dans le cas de la modélisation de ce projet, il apparaissait plus approprié de modifier la courbe de correction de puissance (HEAT-CAP-FT) en fonction de la température de la boucle interne plutôt que de donner une puissance initiale peu représentative de la puissance combinée de la thermopompe et du serpentin électrique. Puisque la température de pièce ne change pas beaucoup et que la température de la boucle interne doit être maintenue à 6.1 °C (43 °F), l'équation de correction de la puissance nominale a été modifiée pour établir une valeur constante au facteur de correction (HEAT-CAP-FT). Dans ce cas, il suffit d'utiliser le facteur (1) dans cette équation de correction.

16. MODIFICATION DU FACTEUR DE CORRECTION DE L'ÉNERGIE FOURNIE À L'APPAREIL EN FONCTION DE LA CHARGE DE CHAUFFAGE

Tel que mentionné précédemment, nous avons modifié le EIR des thermopompes pour tenir compte du fonctionnement des serpentins électriques d'appoint lors des périodes de froid intense. Il importe de préciser que le fonctionnement des serpentins n'est requis que pour de très brèves périodes. Étant donné que le système central d'air neuf alimente l'air à une température de 18,3 °C (65 °F), ce mode de fonctionnement

crée une charge de chauffage pour les thermopompes. Toutefois, l'apport d'air frais n'est requis qu'en période de jour au moment où la température extérieure s'élève en raison de l'apport de l'énergie solaire.

Il en résulte que l'occurrence d'une charge de chauffage maximale qui requiert le fonctionnement combiné de la thermopompe en mode chauffage à pleine puissance et le fonctionnement du serpentin de chauffage à pleine puissance est très faible. On réalise que le fonctionnement simultané du serpentin de chauffage et de la thermopompe sera possible que pour de très courte période occupée alors que la température extérieure s'approche du minimum annuel.

Il est donc absolument essentiel de modifier la valeur de l'énergie alimentée à l'appareil en fonction de la puissance de chauffage réellement fournie. En bref, on doit obtenir une représentation la plus exacte possible du fonctionnement à charge partielle. DOE-2.1 offre la possibilité de modifier le facteur d'alimentation en énergie en fonction de la charge. Il s'agit d'une équation linéaire ou quadratique qui réajuste l'énergie fournie à l'appareil (EIR) en fonction du facteur de charge. Ce facteur de charge est en fait le rapport de la charge de chauffage qui doit être fourni par l'appareil par rapport à la puissance maximale de chauffage. Il s'agit donc de la courbe de correction de l'énergie d'alimentation en fonction du rapport de charge de l'appareil. Le logiciel DOE-2.1 assigne un code de commande qui appelle la courbe de correction de l'énergie alimentée à charge partielle. Cette courbe est appelée par le terme HEAT-EIR-FPLR.

Dans le cas d'un fonctionnement combiné d'une thermopompe avec un serpentin électrique il s'agit d'abord d'établir une courbe de l'énergie totale requise à l'ensemble au moment où il fonctionne à charge partielle. Le chiffrier Excel permet de trouver facilement les différents points représentatifs de cette courbe et d'y obtenir les paramètres de l'équation quadratique. Le tableau #3 donne un exemple de la méthodologie suivie pour obtenir la courbe désirée. Le tableau #4 et la figure #1 donnent une comparaison des valeurs calculées par rapport à la courbe par défaut utilisée normalement par DOE-2.1.

17. CONCLUSION

La modélisation du fonctionnement simultané d'une thermopompe et d'un serpentin électrique demande une attention particulière. Les résultat de cette étude démontre q'une économie de 3 000 $/année est réalisable par une modélisation plus précise des équipements de CVCA.

EIR combiné (par défaut): 44 943 $ par année
EIR combiné corrigé : 41 899 $ par année

Tableau #1 : Comparaison du coût d'énergie des différentes options de chauffage

Gaz naturel avec 10 l/s-pers. (30 % HR)	47 645 $/année
Gaz naturel avec 7.5 l/s-pers. (30 % HR)	44 354 $/année
Gaz naturel avec 0 l/s- pers. (30 % HR)	36 919 $/année
Gaz naturel avec 10 l/s-pers. (sans humidité)	47 227 $/année
Électricité avec 10 l/s-pers. (30 % HR)	79 849 $/année
Gaz naturel avec 2 chaudières 7.5 l/s-pers et 30% HR	44 846 $/année

Tableau #2 Détail du calcul de l'option (tout électrique)
École Ste-Anne-de -Bellevue

Coût de la consommation ***Tarif M***

Tarif M Hydro-Québec (à compter du 1er mai 1998) (Même tarif au 1er mai 2002)

Calcul du coût Coût moy. 12.38115 c/kWh

31	Jan	395.5	94785	4882	0	1402	0	3526	0	0	9820	1528	11348
28	Fév	410.1	82505	4582	0	1441	0	3069	0	0	9091	1415	10506
31	Mars	385.4	79532	4767	0	1269	0	2959	0	0	8994	1400	10394
30	Avril	227.2	49885	2720	0		0	1856	0	0	4575	712	5287
31	Mai	217.3	35726	2688	0		0	1329	0	0	4017	625	4642
30	Juin	117.2	29264	1403	1195		0	1089	0	0	3686	574	4260
31	Juil	77.9	19999	964	1721		0	744	0	0	3428	533	3961
31	Aout	85	21439	1051	1633		0	798	0	0	3482	542	4023
30	Sept	171.3	32326	2050	547		0	1203	0	0	3800	591	4391
31	Oct	202.9	48397	2510	174		0	1800	0	0	4484	698	5182
30	Nov	250.4	61180	2997	0		0	2276	0	0	5273	821	6094
31	Déc	348.9	89885	4316	0	787	0	3344	0	0	8446	1314	9760

Demande : Coût de l'appel maximale de puissance pour le mois (Coût = kW x 11,97 $ x nombre de jours / 30)

Surprime : Coût pour la surprime en raison d'une puissance (hiver) qui excède 133 % de la puissance souscrite (Coût = kW (excédent) x 12,78 $)

Puiss. S : Coût additionnel résultant d'une puissance souscrite plus élevée que la puissance réelle appelée

Cons.-1 : Coût pour la 2e tranche de consommation (excédent de 210 000 kWh x nombre de jour /30)

Cons.-2 : Coût pour la 1ère tranche de consommation (inférieure à 210 000 kWh x nombre de jour /30)

Crédit alim. : Applicable seulement pour alimentation en haute tension ou mesurage en amont de la transformation par le distributeur

Redev. : Coût pour alimentation électrique par compteur (s'applique seulement pour certains tarifs)

Paramètres du tarif M : Général

tarif M	Coût de demande	11.97 $/kW	taxes	15.55 %	
	Redevance abon.	0 $/mois	Crédit alim.	0 $/kW	
	Puissance sousc.	217 kW	Coût de la surprime	12.78 $/kW	

borne inf kWh	borne sup kWh	Cout c/kWh
0	210000	3.720
210000	10000000	2.420

Équations utilisées par DOE-2.1 pour le calcul de l'énergie requise à la thermopompe

Energy = Cap x EIR (Design) x EIR(FPLR)

Energy = Énergie qui doit être fournie à l'unité pour l'heure considérée
Cap = Puissance nominale de chauffage de l'unité (heat output)
EIR (Design) = Fraction de la puissance nominale qui doit être fournie à l'unité à pleine charge (energy input)
EIR(FPLR) = Fraction de l'énergie nominale de pleine charge qui doit être fournie à charge partielle

$EIR(FPLR) = A + (B \times PLR) + (C \times PLR^2)$

A, B, et C = Coefficients de calcul de la fraction de l'énergie nominale selon la charge
PLR = Fraction de la charge pour l'heure considérée par rapport à la pleine charge

Tableau #3 – Évaluation de la courbe (HEAT-EIR-FPLR ou EIR(FPLR))

Charge de chauffage	Facteur de charge	Énergie alimentée thermopompe BTU/hre	Énergie alimentée serpentin BTU/hre	Total de l'énergie à l'ensemble BTU/hre	EIR(FPLR)
5 315	.1	2 501	0	2 501	0.107
10 630	.2	3 888	0	3 888	0.167
15 975	.3	5 250	0	5 250	0.225
21 260	.4	6 610	0	6 610	0.284
26 575	.5	7 993	0	7 993	0.343
31 889	.6	9 721	0	9 721	0.405
37 204	.7	10 919	0	10 919	0.469
42 300	.8	12 441	0	12 441	0.534
47 834	.9	12 441	5 534	17 975	0.772
53 149	1.0	12 441	10 849	23 290	1.00
Puissance de la thermopompe : 42 300 BTU/hre Puissance du serpentin électrique : 10 849 BTU/hre Rapport nominal d'énergie alimentée (EIR) : 0.438					

Tableau #4 – Comparaison pour le HEAT – EIR – FPLR ou EIR(FPLR)
(valeur calculée vs valeur par défaut)

Facteur de charge	.1	.2	.3	.4	.5	.6	.7	.8	.9	1.0
Courbe HEAT-EIR-FPLR (valeur par défaut DOE-2.1)	.178	.267	.355	.442	.529	.617	.708	.797	.898	1.0
Courbe HEAT-EIR-FPLR (valeur calculée)	.107	.167	.225	.284	.343	.405	.469	.534	.772	1.0

Figure #1

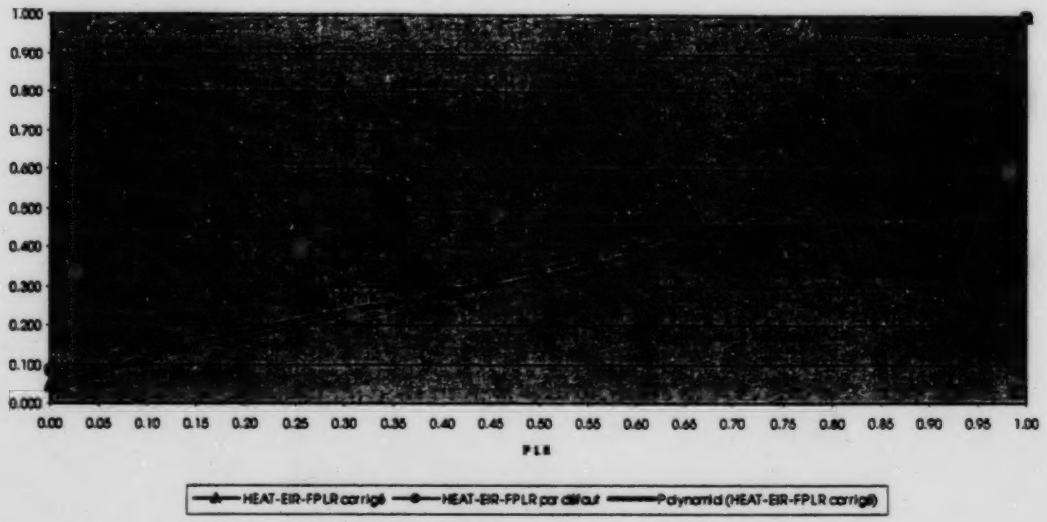

THE SIGNIFICANT FACTORS IN MODELLING RESIDENTIAL BUILDINGS: PART 2

Julia Purdy and Ian Beausoleil-Morrison

CANMET Energy Technology Centre, Natural Resources Canada, Ottawa Canada
(jpurdy@nrcan.gc.ca and ibeausol@nrcan.gc.ca)

ABSTRACT

For users and developers of energy simulation software tools, knowledge of which inputs have the greatest impact on the simulation results will dictate which areas of the building require additional development and input time.

This is the second reporting of a study examining the sensitivity of simulation results to modelling assumptions and user inputs. In this case, the sensitivity of the HVAC system's energy consumption to various furnace inputs, and the impact of the internal conditions on the annual heat load are examined.

The predicted furnace energy consumption was found to be sensitive to the simulated efficiency and the part load curve. The convective/radiant ratio of heat injection, and the set-point and set-back temperatures had the greatest impact on the predicted heating load.

INTRODUCTION

The building simulationist is forced to make numerous assumptions to abstract the complexities of reality to a model of manageable resolution — this is the art of building simulation. Deciding how to sub-divide the building into thermal zones, selecting which geometric features to include and exclude, and choosing whether to model shading by external objects are common decisions faced by the simulationist. Decisions regarding modelling resolution must be made: should an integrated air flow model be employed to calculate infiltration and inter-zone air flows or will prescribed values suffice? Should the sun be tracked to determine which internal surfaces absorb solar radiation or is it adequate to use a simpler approach?

It is obvious that excluding significant elements from the model can compromise the integrity of simulation results. However, the inclusion of unnecessary detail may also contribute to uncertainty. For example, subdividing a building into thermal zones may introduce errors if the significant heat transfer paths between the zones (inter-zone air motion, internal surface convection, and longwave radiation) are poorly characterized.

Each of these assumptions and decisions affects simulation predictions. Consequently, a solid grounding in the principles of building physics and considerable experience in the application of simulation are necessary when a tool presents the user with so many degrees of freedom. Coping with so many assumptions and decisions also requires significant time for data gathering and data input. These are two of the significant barriers impeding the further adoption of simulation by building design professions. Clearly the pragmatic design of user interfaces that focus the user's attention only on those factors that are truly significant for the problem at hand would contribute to addressing these issues. This is one of the objectives of the HOT3000 project (Haltrecht et al 1999). With this, a simplified user-friendly interface targeted at house designers and energy auditors is being integrated with a detailed building simulation program (the engine). This software relies heavily upon pragmatic assumptions and in-built defaults to streamline data entry.

The development of these pragmatic assumptions and in-built defaults is the topic of this paper. Specifically, the goal is to determine which factors have the greatest impact upon simulation results. These results will be used in the HOT3000 user interface design and in the translation of the simplified user input to the detailed simulation engine.

This paper represents the second reporting of this ongoing work and as such does not provide a comprehensive examination of the factors that impact simulation results. Part 1 of this work is to be published in the *Proceedings of the Building Simulation Conference* (Purdy and Beausoleil-Morrison, 2001). The method reported here will be extended to examine other factors in the future.

Part 1

Part 1 of this work examined factors as diverse as thermal bridging through the opaque envelope and wind shielding. The following gives a brief description of the factors examined and the conclusions determined in Part 1.

The following geometric and zoning factors were examined: sub-division of the living space into multiple thermal zones, simple versus explicit representation of windows, internal thermal mass, and shading

by overhangs and surrounding objects. The impact of heat transfer paths through the building envelope, including: thermal contact with the ground, thermal bridging through the opaque envelope, window optical and thermal properties, and air infiltration, were examined. In addition, the impact of the modelling of conditions external to the building, such as: the distribution of diffuse solar radiation, exterior temperature, the longwave radiation exchange between the building and the surrounding ground, and the ground reflected solar radiation, were examined.

It was determined, that the simulated heat load was particularly sensitive to the following parameters: the sub-zoning of the living space, the simulation of the ground contact, the thermal bridging through the opaque envelope, the modelling of infiltration into the house, the external temperature, and the ground reflected solar radiation.

It is important to note that these papers, Parts 1 and 2, treat the specific case of residential buildings in cold climates where the objectives of the analysis are to predict energy consumption and the energy impact of design alternatives.

The simulation environment used in this study is first described. The sensitivity analysis approach is then outlined and the parameters to be investigated discussed. Results are presented and finally conclusions are drawn.

SIMULATION ENVIRONMENT

A developmental version of the HOT3000 program was used in this analysis. Development of the HOT3000 simulation engine is based upon the comprehensive and extensively validated simulation program ESP-r (ESRU 2000). The interested reader is referred to Haltrecht et al (1999) for a discussion on the rationale for selecting ESP-r as the starting point for the HOT3000 development.

ESP-r applies a finite-difference formulation based on a control-volume heat-balance to represent all relevant energy flows within the building. The building is discretized by representing air volumes (such as rooms), solid-fluid interfaces (such as the internal and external surfaces of walls and windows) and plant components (such as boilers and ducts) with finite-difference nodes. Numerous nodes are placed through each fabric element (walls and windows) to represent these multi-layered constructions. A heat balance is written for each node in algebraic terms, approximating the governing partial differential equations and linking all inter-node heat flows over time and space. A simultaneous solution is then performed to determine the state of each node and the inter-nodal heat flows. The equation set is reformed and resolved for each subsequent time step of the simulation. A comprehensive review of this approach is given by Clarke (1985).

Numerous modelling capabilities have been added to ESP-r's extensible structure to support the HOT3000 development. These include the BASESIMP ground heat transfer algorithm (Beausoleil-Morrison and Mitalas 1997), the AIM-2 air infiltration model (Walker and Wilson 1990), and models to predict the performance of residential HVAC equipment. This simulation environment is referred to as ESP-r/HOT3000 throughout the paper.

ANALYSIS METHOD

Differential sensitivity analysis (DSA) is employed in this analysis. As explained by Lomas and Eppel (1992), the DSA method enables a direct examination of the sensitivity of simulation results to input parameter changes. A **base case** building model is first created and simulated using best estimates for the parameters under consideration. A series of simulations are then performed on models modified from the base case. A single input is varied in each simulation while the remaining inputs remain at their base case values. The change in the predicted parameter thus represents the direct measure of the impact of the change made to a single input, $\Delta E = E_i - E_{base\text{-}case}$. Where E_i is the simulation result attained with the modified input parameter and $E_{base\text{-}case}$ is the result for the base case.

DSA is usually applied to building simulation in the context of uncertainly analysis and validation (Macdonald and Strachan, 2000). However, it is equally applicable for identifying the parameters which most significantly affect simulation results.

A number of input parameters are examined in this sensitivity study. The descriptions of the input parameter variations and simulation results have been divided into two groups: issues relating to the HVAC equipment, and the impact of the building's internal conditions on the annual heating load.

It is important to note that the results are not presented in terms of sensitivity coefficients ($\Delta change/\Delta input$), an inappropriate metric for this type of analysis. Rather, the results reflect the sensitivity to each modelling decision, over a realistic range of possible options. For example, the manufacturer determines the capacity of a furnace, so there is relatively little uncertainty associated with these inputs; whereas, there is a larger uncertainty involved in the modelling of the convective regime generated by the HVAC equipment.

In this work, the simulation results of interest are the heating load placed upon the house's HVAC system,

integrated over the year as well as the HVAC system's energy consumption. Although the HVAC models have not yet been fully implemented in ESP-r/HOT3000, a complete furnace model is available for this analysis. The following section describes the base case for this study.

BASE CASE MODEL

The HOT3000 software is primarily targeted at modelling Canadian housing (although its approaches are equally applicable in other climates). Consequently, one of the houses at the Canadian Centre for Housing Technology (CCHT) was selected as the base case for this study. The CCHT houses (Swinton et al 2001) are built to the R-2000 energy efficiency standard (NRCan 1994) and as such represent a typical modern energy efficient Canadian house.

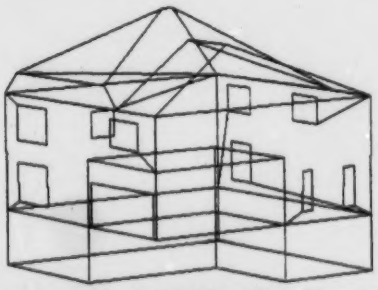

Figure 1: ESP-r/HOT3000 model of base case

The CCHT house is composed of two above-grade storeys and a fully conditioned basement. Its wood-framed construction is built upon a cast-in-place concrete foundation. With 240 m^2 of conditioned floor area (not including the basement) its size is typical of modern Canadian suburban construction. The house is well insulated: the nominal U-values of the above-grade walls and ceiling are 0.24 and 0.34 W/m^2K, respectively. The nominal U-values of the windows are 1.9 W/m^2K while RSI 2.72 covers the interior surfaces of the basement walls. As a result of careful envelope detailing, the airtightness rating of the house is 1.5*ach* at 50 Pa depressurization.

An ESP-r/HOT3000 model of the CCHT was constructed (see Figure 1). Four thermal zones were used to represent the house. The basement, the attic space, and the attached garage were each represented as thermal zones while the two storeys of living space were represented as a single zone. In the model, the living space and basement zones were conditioned by the house's HVAC system, a 19.8 kW condensing gas furnace, while the attic and garage were "free floating", varying in response to the thermal contact with the other zones and the outdoors. The contact between the basement zone and the ground was modelled with the BASESIMP model and the air infiltration was modelled with the AIM-2 model.

This ESP-r/HOT3000 simulation of the base case CCHT model predicted an annual heating load of 51.98 GJ. Since measured data were unavailable at the time, empirical validation of the ESP-r/HOT3000 model of the base case was not possible (empirical validation will be performed in the near future). The ESP-r/HOT3000 base case model, however, compared well in simulation predictions against the results of a more simplified calculation program (NRCan 2000).

HVAC SYSTEM

The following factors affecting the performance of the HVAC system were examined:

- Furnace steady-state efficiency.
- Furnace part-load curve.
- Damper control and flue opening area.
- Location of heat injection.
- Convective regime generated by HVAC equipment.

The purpose of this research is to determine which inputs are significant in simulation, to aide in the development of a user interface. As such, the factors chosen for analysis represent a reasonable data set that the user would have access to at the time of simulation. They do not, however, represent all the possible information required or available.

Furnace steady-state efficiency

The base case furnace was modelled as a condensing gas furnace with 94% steady-state efficiency. To test the significance of the furnace efficiency, the condensing gas furnace was modelled with two different efficiencies: 85% (a 9% reduction in energy efficiency), and 70% (a 24% reduction in energy efficiency).

Reducing the efficiency of the condensing gas furnace to 85% resulted in a 9.5% increase in the energy consumption of the HVAC system, see **85% efficiency** in Figure 3. This represents a one-to-one relationship between the reduction in energy efficiency and the increase in energy consumption. Further illustrating this relationship, reducing the efficiency of the condensing gas furnace to 70% resulted in a 25% increase in the energy consumption of the HVAC system. see **70% efficiency** in Figure 3.

Furnace part-load curve

The furnace will not operate at full capacity throughout the heating season, it will cycle on and off in

accordance with the heating load placed upon it. Heat is injected into each zone to maintain the set-point temperature in the spaces. To account for the impact of this cycling on the furnace performance, the HVAC model in ESP-r/HOT3000, uses part load curves (Henderson, 1998 and Barringer, 1991).

The part load curve, Figure 2, is a representation of the part load efficiency based on the part load ratio for any given hour. The part load ratio (PLR) and part load factor (PLF) are defined as: *PLR = Hourly Load / Available Capacity* and *PLF = Part Load Efficiency / Steady State Efficiency*.

To examine the impact of the reduced efficiency at different part-loads, the HVAC input file for ESP-r/HOT3000 was modified to simulate a spark ignition furnace. It can be seen in Figure 2 that the spark ignition furnace has a significantly different part-load curve from the condensing furnace. It is important to note that all other parameters relating to the furnace, including but not limited to capacity and efficiency, remained at the base case values.

Figure 2 appears to show an anomaly for the condensing furnace. It indicates that the part load efficiency of the furnace can increase slightly at part load conditions. Henderson (1998) informs the reader that this effect is due to the oversized heat exchanger at the part load.

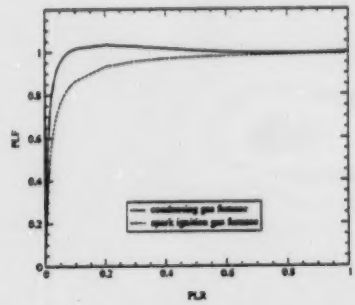

Figure 2: PLC for condensing & spark ignition furnaces.

As can be seen in Figure 3, the HVAC system's energy consumption is quite sensitive to the part-load curve selected. Changing from the condensing to the spark-ignition furnace increased the heating season energy consumption by 9.2%, see **spark ignition furnace** in Figure 3. Therefore, obtaining accurate information on the furnace type, i.e., the appropriate part-load curve, is warranted in this type analysis.

Damper control and flue opening area

For most furnaces, hot combustion air exits the house through the flue. A condensing furnace does not utilize a flue, instead using a small pipe through which the combustion air exits the house. For this reason, simulations to determine the model's sensitivity to damper control and flue diameter were performed using the spark ignition furnace.

The use of damper control has been shown to reduce the infiltration into the house, and therefore the annual heat load, see Purdy and Beausoleil-Morrison (2001). For this analysis, the impact on the furnace consumption was examined.

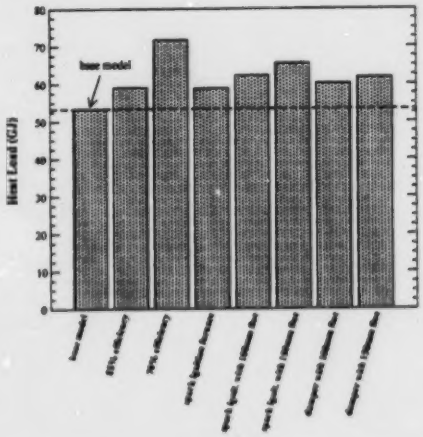

Figure 3: Sensitivity to HVAC parameters.

In the first two cases, the spark ignition furnace was modelled with a 100mm and 150mm flue, and then with damper control on the 100mm and 150mm flues. The flue diameter inputs are represented in the AIM-2 infiltration model, as they primarily impact the infiltration load on the house.

The use of damper control was shown to significantly reduce the furnace energy consumption. For the 100mm flue with damper control, see **damper with 100mm flue** in Figure 3, a 2.2% increase in furnace energy consumption throughout the heating season was calculated. This can be compared to the 5.4% increase in furnace energy consumption for the case with a 100mm flue and no damper control, see **spark ignit. with 100mm flue** in Figure 3. The difference is even more pronounced with the larger flue diameter. A 4.7% increase in furnace energy consumption as predicted for the case with damper control and a 150mm flue, see **damper with 150mm flue** in Figure 3. This is significantly lower than the 10.2% increase

for the case without damper control, **spark ignit. with 150mm flue** in Figure 3.

Given this sensitivity, it can be concluded that detailed information concerning the diameter of the flue and damper control are required for this type of analysis.

Location of heat injection

Heat is injected convectively to the room air with a forced-air heating system. That is, the HVAC system acts immediately upon the room air temperature. Other HVAC systems, such as hydronic, electric baseboards, and in-floor heating, inject heat both radiatively and convectively into the room. These effects are captured in the ESP-r/HOT3000 simulation.

A number of simulations were performed to assess the significance of the location of the heat injection, specifically the ratio of radiant and convective heat injection. Simulations were performed whereby the percent of the heating load met by radiant injection sources were: 0%, 50%, and 100%. The same set-point dry bulb temperature was used in all runs. The metric of interest in this analysis is the heat load as calculated over the heating season.

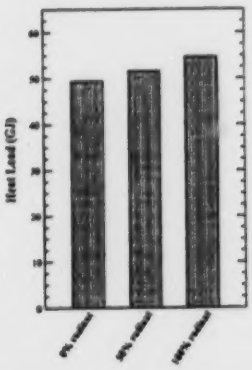

Figure 4: Radiant heat injection into main zone.

The 0% radiant case was taken as the base for this analysis, with a heating load of 49.44 MJ. It can be seen from Figure 4, that increasing the radiant portion of the heat injection to 50% increased the heat load by 4.3%, and simulating 100% radiant heat injection, resulted in a 9.6% increase in the heat load.

With radiant systems, wall and window surfaces are warmed, thus increasing the heat loss through the envelope. This accounts for the increase in heat load predicted in these cases. These results are significant and therefore, the conclusion can be drawn that an explicit representation of heat injection is warranted in this type of analysis.

Convective regime generated by HVAC equipment.

In his paper on ESP-r's adaptive convective algorithm, Beausoleil-Morrison (2001) examined the impact HVAC systems have on the convective regimes in rooms.

Six simulations were performed with the ACA—adaptive convective algorithm. In each case the internal surfaces of the living space were attributed with convection calculation control data to simulate different heating systems and device placements. The scenarios examined were:

- radiators placed under windows
- radiators placed by internal walls
- radiators placed by external walls but not underneath windows
- in-floor heating
- hydronic walls panels placed on internal walls
- forced-air heating system delivering air through registers located under windows[1].

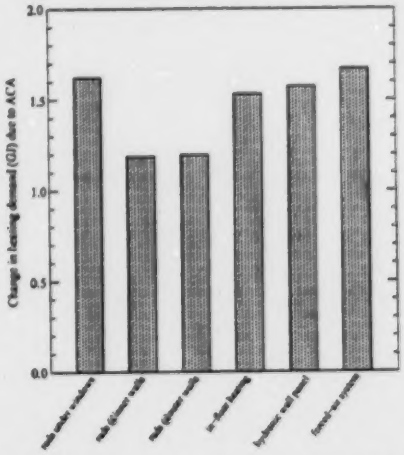

Figure 5: Impact of ACA on annual heating loads

The ACA resulted in greater annual heating load predictions in all scenarios, see Figure 5. Differences ranged from 2.4% to 3.3% of the house's total heating load caused by heat losses through the walls, windows, ceiling, basement, and due to infiltration.

As can be seen in Figure 5, the ACA can discriminate the impact that different HVAC systems have upon

[1] The ACA lacks h_c correlations for this configuration. As such, it was modelled with the closest match, a circulating fan heater.

heating loads. It is important to note that minor alterations to the convection calculation control data can affect these results. Factors such as which walls are adjacent to the radiator, and which surfaces receive the direct stream of the supply air can influence the selection of h_c correlations for each surface.

The interested reader is referred to Beausoleil-Morrison (2001) for further information on this subject.

INTERNAL CONDITIONS

The impact of the modelling of the following conditions internal to the building were examined:

- Set-point temperature.
- Set-back temperature.
- Internal gains.

Again, these specific factors were chosen as they represent a reasonable amount of information that the software user would have access to. Other factors contribute to a building's internal conditions, but they were not considered for this project.

Set-point temperature

The internal set-point temperature—the house's thermostat set-point temperature—for the base case was simulated as 21°C.

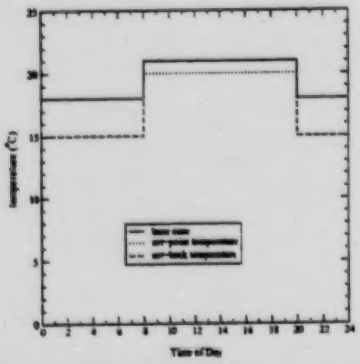

Figure 6: Set-back & set-point control strategies

As is common to energy efficient houses in Canada, nighttime thermostat set-backs were incorporated into the control system of the base case, The set-back control strategy can be seen in **base case** in Figure 6. During the night, between the hours of 8pm and 8am, the thermostat was set to 18°C and during the day—8am to 8pm— the thermostat was set to 21°C.

Reducing the set-point temperature during the day from 21°C to 20°C **set-point temperature** in Figure 6, had a significant impact on the heating load. It can be seen from **lower set-point** in Figure 7, that this 1°C difference, during the day, reduced the annual heating load by 6.3%. Given this sensitivity, accurately representing the set-point temperature of the house is warranted.

Set-back temperature

In this case, instead of reducing the set-point temperature during the day, the set-back temperature, i.e., the set-point temperature during the night, was reduced. As illustrated in **set-back temperature** in Figure 6. Between the hours of 8pm and 8am, the thermostat was set to 15°C and during the day, the internal temperature was maintained at the base case value of 21°C.

This reduction of 3°C during the night had a much smaller but significant impact on the annual heat load than did the 1°C reduction during the day. Reducing the set-back temperature to 15°C lead to a 4.9% decrease in heating load, **lower set-back** in Figure 7.

Information concerning the temperature controls on the furnace has been shown to be of considerable significance to the heating season energy consumption.

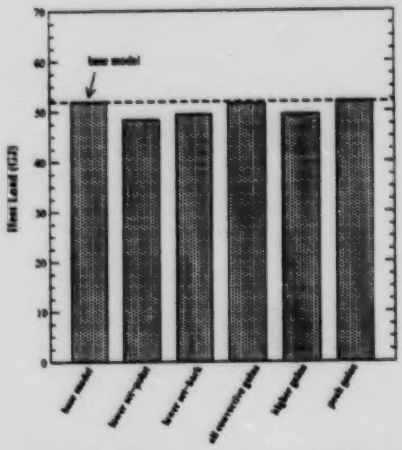

Figure 7: Sensitivity to internal conditions

Internal gains

Internal gains are simply indoor heat generating sources. ESP-r/HOT3000 accounts for the gains from a combination of occupants, lighting, and equipment sources. The user has control over the convection/radiant ratio of these gains as well as the option to define internal gains profiles over a the say. For the base case, a constant 610 W of internal gains were simulated each hour, 50% from convective sources and 50% from radiant sources.

To examine the impact of this convective/radiant ratio, a simulation was performed whereby all of the internal casual gains resulted from convective sources. It can be seen from **all convective gains** in Figure 7 that this lead to a very modest 0.8% decrease in the annual heat load.

Doubling the internal gains lead to a 9% decrease in the annual heat load by, as seen in **higher gains** in Figure 7. Although this represents a significant decrease in the heating load, it results from a very significant increase in internal gains—50%. It can be concluded that accuracy in obtaining the internal gains information is warranted.

In the previous simulations, the internal gains were maintained at a constant value of 610 *W* over the day. To examine the significance of the distribution of the gains over the day, a second simulation was performed, having the same energy addition integrated over the day, but with a lower base load and morning and evening peaks, see Figure 8.

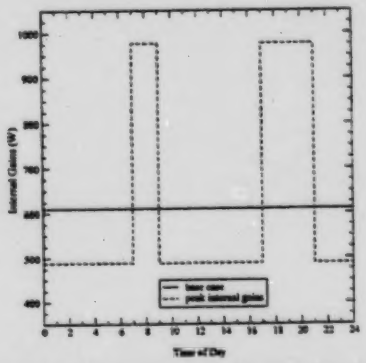

Figure 8: Constant and peak internal gain profiles

The heating load increased by a modest 0.1% (see **peak gains** in Figure 7). For the specific case of an annual heat load calculation, with basic control strategies, creating hourly profiles for the internal gains was not show to have a significant impact on the annual energy prediction.

This investigation did not, however, consider the impact of internal gains profiles on time of use or peak demands. To examine these factors would require a different modelling approach.

CONCLUSIONS

The appropriate degree of modelling resolution depends, of course, upon the objectives of the simulation, the building, and the climate. Predicting a house's annual energy consumption or examining the energy impact of design alternatives demands a very different modelling approach than, for example, estimating the illumination distribution within a daylight office, or predicting the peak electrical demand in a cooling dominated building.

The goal of this research was to determine which factors have the greatest impact on simulated heat loads. Those factors investigated in this second reporting are: the sensitivity of the HVAC system energy consumption, and the sensitivity of the heating load to the internal conditions.

It is important to note that these conclusions are valid for predicting annual residential heating loads in cold climates. Extrapolating these results to other building types and climates and other types of analyses would be inappropriate.

The predicted furnace energy consumption was found to be sensitive to the simulated efficiency and the part load curve. The convective/radiant ratio of heat injection, and the set-point and set-back temperatures had the greatest impact on the predicted heating load.

The next phase of research will involve an empirical comparison of the simulated data to monitored data from the CCHT.

REFERENCES

Barringer C. (1991), Furnace Improvements to the HOT2000 Subroutine - Part B: Furnace and Heat Pump Models, NRCan Report No. ET-91-045.

Beausoleil-Morrison I. (2001), 'Demonstration of ESP-r's Adaptive Convection Algorithm', *Proc. eSim 2001*, Ottawa Canada.

Beausoleil-Morrison I. and Mitalas G. (1997), 'BASESIMP: A Residential-Foundation Heat-Loss Algorithm for Incorporating into Whole-Building Energy-Analysis Programs', *Proc. Building Simulation '97*, (2) 1-8, Int Building Performance Simulation Association, Prague Czech Republic.

Beausoleil-Morrison I. and Strachan P. (1999), 'On the Significance of Modelling Internal Surface Convection in Dynamic Whole-Building Simulation Programs', *ASHRAE Transactions* 105 (2).

Clarke J.A. (1985), *Energy Simulation in Building Design*, Adam Hilger Ltd, Bristol and Boston.

ESRU (2000), *The ESP-r System for Building Energy Simulations: User Guide Version 9 Series*, ESRU Manual U00/1, University of Strathclyde, Glasgow UK.

Haltrecht D., Zmeureanu R., and Beausoleil-Morrison I. (1999), 'Defining the Methodology for the Next-Generation HOT2000 Simulator', *Proc. Building Simulation '99*, (1) 61-68, Int Building Performance Simulation Association, Kyoto Japan.

Henderson H. (1998), Part-Load Curves for Use in DOE-2, Prepared for the Lawrence Berkley Laboratory, CDH Energy Corporation, Cazenovia USA.

Lomas K.J. and Eppel H. (1992), 'Sensitivity Analysis Techniques for Building Thermal Simulation Programs', *Energy and Buildings*, 19 21-44.

Macdonald I. and Strachan P. (2000), 'Practical Application of Uncertainty Analysis', *Energy and Buildings*, (1278) 1-10.

NRCan (2000), *HOT2000: A Comprehensive Tool for the Design of Energy Efficient Homes and Buildings*, Version 8.5, Natural Resources Canada, Ottawa.

NRCan (1994), *R-2000 Technical Requirements*, Natural Resources Canada, Ottawa.

Purdy J. and Beausoleil-Morrison I. (2001) 'The Significant Factors In Modelling Residential Buildings' To be published in *Proc. Building Simulation*, 7th International Building Performance Simulation Association Conference, Rio de Janeiro, Brazil.

Swinton M.C., Moussa H., and Marchand R.J. (2001), 'Commissioning Twin Houses for Assessing the Performance of Energy Conserving Technologies', To be published in *Proc. Integration of Building Envelopes*, Performance of Exterior Envelopes of Whole Buildings VIII, Clearwater USA.

Walker I.S. and Wilson D.J. (1990), *The Alberta Air Infiltration Model: AIM-2*, University of Alberta Dept of Mech Eng, Report 71, Edmonton Canada.

DOE2.1E GEOMETRIC MODELLING:
The Basic Geometric Approach vs. The Complex XYZ Approach

Christopher R. Jones and Curt Hepting
EnerSys Analytics Inc.
Coquitlam, BC
cj@cr-jay.ca chepting@telus.net

ABSTRACT

The DOE2.1e energy modelling program provides different approaches for defining the geometry of a building. The simplest approach involves defining the length, width and direction of building surfaces (basic geometry approach). A more complex model involves defining the co-ordinates of all surfaces (XYZ or detailed geometry approach).

The perceived reason to use the XYZ approach is to better capture the effects of solar shading and daylighting. The XYZ approach can directly model building shades and shading from other parts of the building. However, DOE2 also provides a simple facility for defining horizontal and vertical window shading devices.

The amount of time required to model a building depends on the approach and tools available. The basic geometric approach takes less time than the XYZ approach. This paper examines the building energy use differences for two projects modelled using both approaches. It also compares building energy use and peak loading for both methods following a series of "XYZ simplification" steps.

For the two projects examined, this paper shows there is little difference in total building energy use. These specific results, as well as results from many previous DOE2 modelling projects, reveal that full XYZ geometry is seldom cost-effective.

INTRODUCTION

Building energy simulation programs come with a wide range of complexities and capabilities for accurately defining the geometry of a building design within a thermodynamic model. Some, such as Hot2000 [1], allow for a relatively basic geometric definition and a bin calculation method to model energy use. Creating a model is relatively simple; the area and facing direction of each surface are all that the model needs to capture the building geometry, as it pertains to energy use. Only surfaces of interest need to be modelled. (For example, an adiabatic wall separating units in a duplex need not be modelled if only one unit is of interest.) Others, such as ESP-r [2], are sophisticated and very complex to use. The model must be geometrically contiguous, with all surfaces defined using specific spatial coordinates, dimensions, outward orientation and surface tilt. Further, each zone must have a fully bounded volume, with surfaces joining correctly at all junctures where surface meet each other—in other words, a visually correct representation.

The DOE2.1e [3] energy simulation program (DOE2) allows for complex and/or basic geometric modelling for energy use simulation. Like ESP-r, the user can completely define each surface with its geometric location by using x, y ,z coordinates, defined using a right-hand coordinate system (XYZ approach). Or, the user can define surfaces simply by specifying the area and facing direction (the basic geometric approach). In both cases, the orientation and tilt of walls, roofs and floors are defined as well, even if by default.

The perceived reason to use the XYZ approach is to better capture the effects of solar shading. Windows, in particular, are most affected by shading devices. Hence, the XYZ approach can directly model building shades and shading from other parts of the building. However, solar shading can also be captured using DOE2's simple facility for defining window shading devices. Horizontal shading devices (overhangs) and vertical shading devices (fins) may be defined using DOE2 keywords associated with the window definition. The user usually can use the fins and overhangs to represent most external shading situations.

The time to develop the model depends on which approach is taken. The XYZ approach requires a detailed take-off of all surface coordinates, height, width and facing direction. Each surface in the model is defined by specifying its x, y, z coordinates relative to the containing space origin. Each space's origin is defined relative to the building origin, with its direction defined relative to that of the building. Finally, the

surface azimuth (facing direction) then is defined relative to the azimuth of the space that contains the surface. In contrast, the basic geometric approach only requires input of the area (height and width) and azimuth of each surface. As a result, the drawing take-off time and model definition are reduced significantly.

The accuracy of the DOE2 simulation does not necessarily correlate to the geometric detail of the model. In the majority of cases, the basic geometric approach is sufficient for the desired accuracy of the results.

This paper compares DOE2 simulation results between models constructed using the complex XYZ approach and the basic geometric approach. It examines two building models using "unbundling steps." In other words, the models start with full XYZ geometry and are then modified through a number of steps. Each step logically reduces the geometric detail of the building, ending with a basic geometrically defined model. The analysis includes whole building energy results by end use. This paper also compares energy savings results for daylighting control represented using two different approaches: (1) modelled directly using DOE2's daylighting facility, and (2) approximated by using ASHRAE's daylighting power adjustment approach.

METHODOLOGY

Two exiting DOE2 models, constructed using the XYZ approach, were readily available for evaluating the effects of defining the geometry at different levels of detail. The models were significantly dissimilar, thereby revealing the effects of the two modelling approaches on different building types in different weather regions.

Victoria, British Columbia Office Building

The first model was a 43,296 ft^2 (4,023 m^2) office building in Victoria. It had a unique façade consisting of a curtain wall with a briese soleil (sun shades) constructed of two, sloped horizontal shades near the top of the glazing sections (see the partial building elevation, Figure 1). The building had a narrow footprint situated in a north-south direction. Daylighting potential was high due to eight foot glazing sections. However, the southerly exposure required careful analysis in order to minimize the solar loading and glare, which are known to cause occupants to close internal window coverings.

The client requested application of the XYZ approach to examine the effects of different briese soleil configurations. This included using one, two, or three shades

Figure 1. Briese Soleil, Victoria Office Building

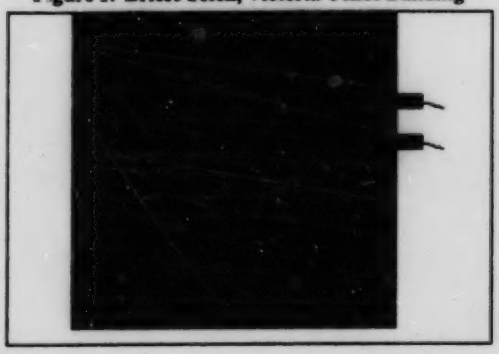

at different angles and spacing. The model described the interior surfaces in their correct locations with the presumption that this would more accurately capture daylighting savings. Additionally, the model applied internal shading (e.g., blinds or drapes) to reduce the sunlight penetration and to slightly increase the window thermal resistance. Application of the internal shading occurred only when the solar intensity or glare index reached a specified level.

Analyzing the impacts of reducing the detailed geometrical representation to a more basic model involved generating six models:

RUN 1. The original model involved creating a detailed geometrical model as described above. Figure 2 shows a visual representation of this model.

Figure 2. Office Building DOE2 Model with Full Geometry

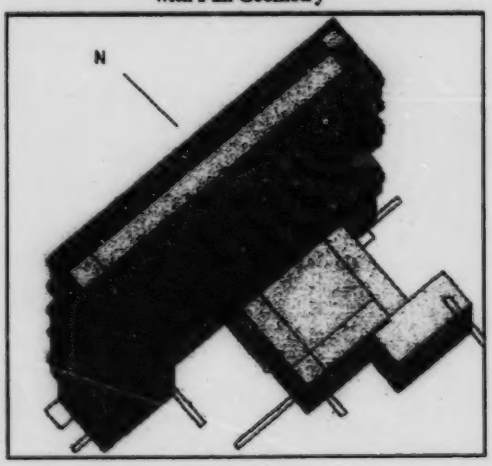

RUN 2. Beginning with the detailed model (run 1), we removed the interior surface positioning by modelling only the area and facing direction of interior surfaces. DOE2 uses a "split flux" method to model daylighting. It uses the reflectance and tilt of interior floors, ceilings and walls, but not the position of these surfaces (Winkleman, 1998).

RUN 3. Continuing from run 2, we modelled the window shading devices using the DOE2 window overhang facility. This was in contrast to the original model where the briese soleil was represented by two angled horizontal shades using the DOE2 "BUILDING-SHADE" settings. In this simplifying step, we removed the two building shades and used a single window overhang. We manually estimated the single overhang projection to represent the same window shading coverage as two building shades. The position of the overhang was set to the same position as the top building shade relative to the window. We kept the DOE2 daylighting control points in the same position as in the original model (i.e., centred in the space).

RUN 4. Using the model defined in run 3, we removed the window positioning. The window position was defined relative to the lower left corner of the containing wall. We let the window X,Y coordinates default to 0,0, thereby placing the window in the lower left corner of the wall.

RUN 5. Building off of run 4, we next removed all space and surface positioning. From a visual standpoint, the model no longer looked like the design, as shown by Figure 3. However, the model was still representative from a thermal standpoint, with the exception of some very minor self-shading on the first level.

Figure 3. Office Building DOE2 Model with Coordinates Removed

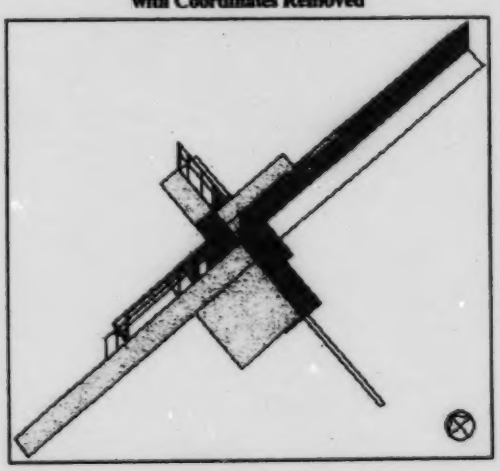

In this step we also simplified the method used to approximate the benefits of daylighting. Instead of using DOE2's daylighting facility, we used the appropriate ASHRAE power adjustment factors (PAFs) for multiple stepped dimming control. ASHRAE Standard 90.1 defines a number of lighting power adjustment factors which are used to effectively reduce the lighting load equivalently for each hour of the year. The PAF for stepped daylighting control is 0.2. In this case, 45% of the lighting load was controlled by daylighting. Hence, the weighted area power adjustment calculation resulted in a connected lighting load reduction of 9.0%.

RUN 6. We were interested in gaining an appreciation of the comparative effects of different building surface characteristics on energy use. Hence, we decided to reduce the exterior wall absorptance since specifying this value oftentimes is neglected. Using the original model in run 1, we reduced the absorptance to 0.65, which is about equivalent to unpainted concrete. The original model used a brick façade with the absorptance set to 0.88.

Toronto, Ontario University Building

The second project was a new 95,000 ft^2 (8,840 m^2) university computer lab building in Toronto. The design consisted of numerous teaching labs and classrooms, central corridors, and lecture theatres. Figure 6 shows how the design appeared when modelled using full geometrical input using DOE2.1e. As the figure shows, the design included several inset areas and articulated wall and window surfaces.

Our approach to analyzing the relative geometry effects on energy performance for the Toronto university building varied from the approach for the Victoria office building. First, the project did not include controlled daylighting and hence, the internal geometry for accommodating daylighting calculations was not described. Second, we thought it would be interesting to provide a relative comparison to an equivalent reference case that complied with Canada's Model National Energy Code for Buildings [4]. In summary, the analysis process followed these steps:

RUN 1. This represents the original model with the full spatial geometry represented, as shown in Figure 4.

Figure 4. University Building DOE2 Model with Full Geometry

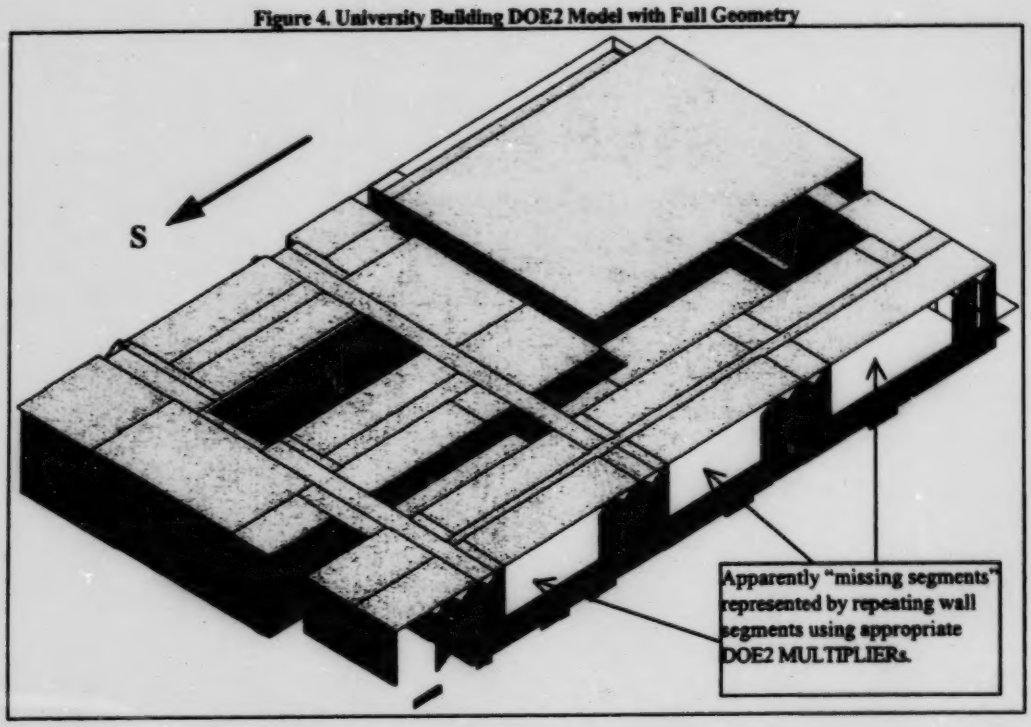

RUN 2. We removed the window positioning, allowing the window(s) to fall to the default lower left corner position within each containing wall surface.

RUN 3. In addition to removing the window positioning (run 2), we disconnected all surface position coordinates. Hence, any self-shading of one part of the building on the other was removed.

RUN 4. We made the changes described in runs 1–3 on an equivalent reference case. This was done to compare the relative differences between the proposed design and reference case.

RESULTS

This section presents the results from the geometry simplification and sensitivity simulations for (1) the Victoria office building and (2) the Toronto university building.

Victoria Office Building

We simulated each of the six models in the Victoria office building project and extracted the energy and plant capacity results from DOE2's results reports, as listed in Table 1. Differences for each run are compared to the base case (Run 1).

Run 2, in which the positioning of the interior walls was removed, showed no difference in energy from the base case. Hence, the XYZ positioning of interior walls was not necessary, confirming that this is unnecessary for accurately modelling daylighting control.

Replacing the more exact sunshades with a representative single overhang (run 3) showed a 7% increase in cooling energy and a slight increase in heating energy. In contrast, lighting energy decreased by 4% (not shown on Table 1). The overall net effect was less than a 1% decrease in total building energy. One might expect that a building shade and an overhang of the same size and shape would have the same effect on building energy. However, the reflection of sun off the sunshades is not captured using window overhangs. Further, the overhangs are an approximation of the two building shades in this case. Note that the length, position, and depth of the overhang could be adjusted to be more representative, but that would defeat the purpose of trying to simplify the modelling process.

Table 1. Modelling Results: Victoria Office Building[1]

Model Run	Energy in mmBtu				Peak Capacities	
	Total	Heating	Cooling	Pumps, Fans	Heating (mmBtuh)	Cooling (Tons)
Run 1	2,213	458	80	646	0.76	22.8
Run 2	2,213	458	80	646	0.76	22.8
Difference:	**0 0.0%**	**0 0.0%**	**0 0.0%**	**0 0.0%**	**0 0.0%**	**0 0.0%**
Run 3	2,207	465	86	648	0.76	23.2
Difference:	**-6 -0.3%**	**7 1.4%**	**6 7.0%**	**2 0.3%**	**0 -0.4%**	**0 1.5%**
Run 4	2,218	461	87	648	0.76	23.3
Difference:	**5 0.2%**	**3 0.6%**	**6 7.3%**	**2 0.3%**	**0 -0.5%**	**0 1.8%**
Run 5	2,231	465	91	647	0.75	23.5
Difference:	**19 0.8%**	**7 1.4%**	**10 11.5%**	**1 0.2%**	**0 -1.5%**	**1 2.8%**
Run 6	2,213	461	79	646	0.76	22.7
Difference:	**1 0.0%**	**3 0.6%**	**-2 -2.4%**	**0 0.0%**	**0 0.2%**	**0 -0.7%**

Removing the window positioning in run 4 had the largest influence on cooling energy (7.8%), compared to the baseline. In addition, lighting energy increased in comparison to run 3, where the windows were appropriately positioned. This illustrates that the window position relative to the daylighting control point affects lighting energy when using DOE2's daylighting facility.

Run 5, with all wall and zone positioning removed and daylighting approximated using the appropriate power adjustment factor (PAF), increased cooling energy by 13%, yet lighting barely changed. This shows that ASHRAE's lighting PAF approach is quite reasonable for estimating lighting energy reduction due to multi-step dimming daylighting control. However, the difference in cooling energy is more than expected as the design has little self-shading modelled. In other words, one would expect that a rectangular building would have little difference in energy between XYZ positioning of the walls and no geometric positioning of the walls. Therefore, it appeared that the timing of when the lighting reduction occured affected the cooling. This made sense as the PAF applied to the lighting over the entire schedule, instead of only when daylighting opportunities existed. In contrast, DOE2 daylighting control reduced lighting primarily during periods of highest cooling demand.

Changing the wall absorptance (run 6) showed a decrease in cooling energy and an increase in heating energy. The change in the energy performance demonstrated the relative importance of this characteristic. However, in comparison to the overall total energy use, it is *also* relatively insignificant. Although it is difficult to estimate the value precisely, it is very quick to change in DOE2.

In summary, the Victoria office building project results show some difference in end use energy at each model simplification step. As expected, the cooling end uses are most affected. Because cooling is a relatively small component of the overall energy use, however, the difference in total building energy is negligible at each step. It is important to note that the difference in total building energy between the full XYZ model and the basic geometric approach is less than 1 percent.

Figures 5 and 6 show the energy and capacity differences between the full XYZ model and the basic

Figure 5. Energy Use Results: Victoria Office Building

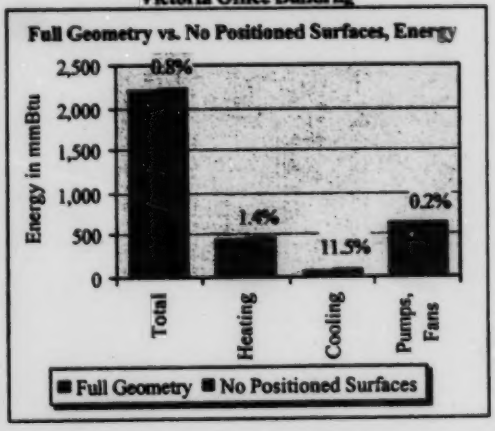

[1] The imperial units of mmBtu stands for millions of British thermal units, as directly reported by DOE2.

Figure 6. Peak Capacity Results: Victoria Office Building

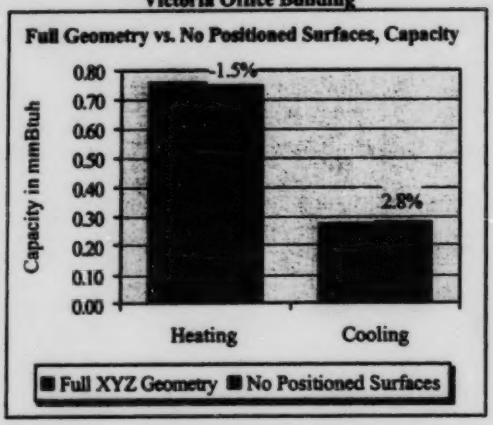

geometric model. As shown in Figure 5, the total building energy increased by 0.8% when reducing the model to the basic geometric approach. The cooling energy difference is the largest, but cooling makes up the smallest part of the total building energy.

Toronto University Building

We extracted the energy and peak capacity results for each of the Toronto building modelling iterations described earlier. The energy use results were taken from the DOE2 building energy performance (BEPS) report while the peak heating and cooling capacities were derived from the equipment sizes determined by DOE2 as listed in the PV-A report.

Table 2 lists the results for the modelling runs on the proposed design in which different geometry aspects were removed (i.e., runs 1–3). As shown in this table, positioning of windows made very little difference on energy use or peak capacity. Removing all self-shading, however, made a significant percent difference on cooling energy and peak capacity, as shown in Figures 7 and 8. This change, however, is on a relatively small number. Further, these relative differences would decrease significantly if appropriate window fins were introduced as an approximation for the self-shading on the windows.

Figure 7. Energy Use Results: Toronto University Building

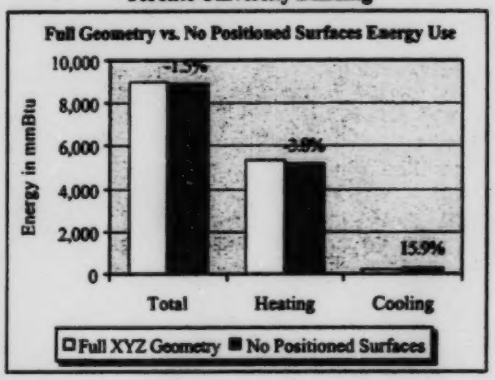

Table 2. Modelling Results: Toronto University Building

Model Run	Energy in mmBtu			Peak Capacities	
	Total	Heating	Cooling	Heating (mmBtuh)	Cooling (Tons)
1) Full Geometry	8,979	5,357	269	4.16	204
2) w/o Positioned Windows	8,990	5,372	267	4.17	202
Difference:	**10 0.1%**	**14 0.3%**	**-3 -1.0%**	**0.002 0.0%**	**-1 -0.7%**
1) Full Geometry	8,979	5,357	269	4.16	204
3) No Positioned Surfaces	8,847	5,162	321	4.14	233
Difference:	**-132 -1.5%**	**-195 -3.6%**	**51 19.0%**	**-0.021 -0.5%**	**29 14.2%**
2) w/o Positioned Windows	8,990	5,372	267	4.17	202
3) No Positioned Surfaces	8,847	5,162	321	4.14	233
Difference:	**-142 -1.6%**	**-209 -3.9%**	**54 20.2%**	**-0.023 -0.6%**	**30 15.0%**

Figure 8. Peak Capacity Results: Toronto University Building

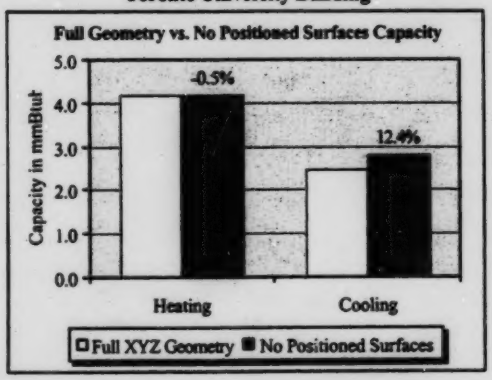

The impact of not fully representing the geometry is much less significant on heating and relatively small overall. Once again, inputting window fins would decrease these differences further.

The final set of runs, where we repeated the three series of simulations for a comparative reference case, produced even smaller differences. The annual energy differences between the proposed case and the reference were relatively small. Heating and cooling energy differences varied by as much as 0.5% and 3.4%, respectively, for the comparison of runs 1 and 3. Total energy use differences were less than 0.005% for the same case. Changes in the heating capacity differences were negligible as well. Cooling tonnage differences, however, changed by 27 tons (5.8%).

As expected, using full spatial geometry makes the biggest difference on cooling due to solar shading. Hence, it is important to pay attention to solar shading. The effort required to input full XYZ geometry to account for these differences, however, may not be worthwhile. In the university building case, cooling only accounts for about 3.0% of the total energy use; without any spatial geometry, this rises to 3.6%. Further, unless the mechanical designer accounts for self-shading in equipment sizing (which is very rare), the exercise of fully representing the spatial geometry becomes academic.

CONCLUSION

The results show that, for the two projects presented, there is little difference in total building energy between models using a full XYZ geometry and those with a basic geometric approach, although it took approximately 30–40% longer to develop the XYZ models. Our findings with these projects, and with over 18 years of combined DOE2 modelling experience, have shown that full XYZ geometry is seldom cost effective. However, no situation is the same and, for some specialized cases, it is worth the extra effort to generate a partial (i.e., for only the surfaces affected) or full geometric model. But, in general, time is better spent focusing on other aspects. As illustrated with the wall absorptance example, the time taken to gather information about the building that is not readily available in the plans and specifications is at least as valuable and in some cases may be more important than the time taken for XYZ modelling.

The results also illustrate that the non-XYZ models tend to make the analysis conservative since cooling is most affected. HVAC designers usually favour more conservative estimates when sizing their equipment and rarely take into consideration the effect of self-shading upon the cooling load. Hence, performing full geometric modelling is usually regarded as academic from an HVAC designer's point of view.

ACKNOWLEDGEMENTS

Figures 1-6 produced using DrawBDL, Joe Huang and Associates, 6720 Potrero Avenue, El Cerrito, CA 94530 Ph/Fax: 510-236-9238.

REFERENCES

Winkleman, Fred (1998), *Building Energy Simulation User News, Vol. 19, No. 1*, Lawrence Berkeley Laboratories.

END NOTES

1 Hot2000 is developed by Canmet Energy Technology Centre, http://www.nrcan.gc.ca/es/etb/cetc/cetchome.htm.

2 ESP-r is developed by the Energy Systems Research Unit, University of Strathclyde, Glasgow, Scotland, http://esru.strath.ac.uk/.

3 DOE2.1e is developed by Lawrence Berkeley National Laboratory, Hirsch & Associates, Consultants Computation Bureau, Los Alamos National Laboratory, Argonne National Laboratory and University of Paris, http://gundog.lbl.gov.

4 *Model National Energy Code of Canada for Buildings*, 1997, Ottawa: National Research Council of Canada.

SIMULATION ON THE EDGE

Dr. Jon W. Hand
ESRU, University of Strathclyde, Glasgow Scotland
jon@esru.strath.ac.uk

ABSTRACT

Consider the following scenarios:

The WWW page describes the tool as "a general first-principles solver for multiple domain assessments" and the practitioner says "the project is an aluminium smelting plant so what's the problem with 3kW/m^2 of casual gains?" Tool developer raises eyebrows - simulation at a newly defined edge.

Gripe from simulationist to tool developer - "we just finished a project with 100,000m^2 floor area and found it difficult to QA the project files". Tool developer imagines scenes from Dante's Inferno - simulation as an endurance contest.

Conversation between tool developer and simulationist - "how do I model stair treads? - where are they? - in the fire escape - why do you think this is important? - they are included in the building section". Simulation drowning in needless complexity.

Planning discussion "the client wants to know how many minutes they have before environmental conditions deteriorate if there is a catastrophic failure of the HVAC on a sunny summer day - if it goes above 26C a collection of rare artifacts will suffer irreversible damage. How shall we approach this?". Gasp - truly simulation at the edge.

This paper reviews some of the singularly amazing, useful, and sometimes misdirected work that practitioners attempt with simulation and the technical and software support which ESRU (the Energy Systems Research Unit) and SESG (the Scottish Energy Systems Group) in Glasgow have recently provided.

The paper will deal with issues such as:

- What was done to support substantial simulation questions and who is well placed to attempt such work?
- How does one gain confidence in projects which are exploring untested uses of a tool?
- What duty is it of the vendor to deprive the practitioner of their chaos and complexity? Sometimes it is necessary to build models which are at the compositional limits of a tool. But does the practitioner realize the incremental cost of such complexity?
- How do those entering the profession develop the skills to deal with issues of model abstraction in realistic design projects?
- What about when the practitioner has a different idea of what the tool is capable of from that of the tool developer?

INTRODUCTION

Simulation tool developers have made great strides in extending tool functionality, they have invested much in tool ease-of-use and are proud of their "better mousetraps". Some even entertain thoughts that these efforts will help pay the rent. So what do practitioners go and do? They apply these tools to real-world projects, unencumbered by the developers inside knowledge of best-practice, successful strategies and "things-to-avoid". Now and again practitioners push the limits of simulation in ways that surprise tool developers.

Whether this results from the ingenuity or naivete of the practitioner, the simulation community can learn much from the radically different views that developers and practitioners hold of simulation tool capabilities. Few developers combine the skills of application coding and application use within the constraints of the design process. Practitioners who successfully explore new facets of design performance and who leverage existing tool facilities will define a new market for their skills and, eventually, influence others in the simulation community. Simulation owes much of its maturity to the random mix of design questions in projects which continually stress tools in hitherto unthought of ways.

Of course, tool developers are not immune to excesses of ingenuity in the design of their tools and naivete regarding those who use their tools. Developers get caught up in facilities which owe more to the dictates of a particular library of interface widgets then on a careful reflection of user requirements. Jargon still masquerades as conventional dialogue, inappropriate interface conventions and arbitrary assumptions abound. Clarity for the developer is often anything but

clear to a practitioner who has a 14h00 deadline.

This paper is particularly interested in occasions where practitioners define new frontiers in simulation. The practitioners working in such areas tend not to be prolific writers, perhaps because of client confidintiality or the intensity of their work, and thus there is little in the literature which addresses this issue.

In the following sections the author will explore some aspects of simulation at the edge which have influenced the evolution of simulation tool design and support which ESRU and SESG have recently provided. Although the case studies were drawn from real projects, for the purposes of this paper some project and participant details have been obscured.

The initial stages of each case study follow a similar pattern. Vendor X advertises their better mousetrap as "a general first-principles solver for multiple domain assessments in the built environment". The web page shows a range of example projects, enumerates the facilities their tool offers and options for skills-acquisition. After careful consideration, Firm Y acquires the tool, allocates resources for initial training and begin to use the tool on the periphery of projects. Gradually they evolve an impression of what they can do with the tool as well as a list of things that they wish they could change about the tool. They develop in-house procedures, they usually, but not always, invest in further training and support. And then...

SIMULATION AT A NEWLY DEFINED EDGE

In a simulation based consultancy, a project arrives that is only moderately challenging in terms of model composition (it is a industrial shed) but operationally complex. The tool interface (in this ESP-r) balked at accepting an internal gain in one zone of 1.5GW. Staff phone the author and the conversation went something like: "Wow, that is a big number...try expressing the load as W/m^2...still to big, try subdividing the main processing hall...ok...and what do the performance reports say...they say '*********', ok try to integrate over a shorter period". At the edge irritants cluster. But hang on, there might be a very good reason the interface rejected the initial number. "What sort of temperatures are being predicted?"...Wow..."What's the wall composed of and is there a radiant component to the load?"... "Ok, we need to confirm additional details of the performance metrics and energy balances, but this output indicates that a) surfaces temperatures are going to be high and b) thermal expansion could be a problem if that load is intermittent."

So why would a model of a smelting plant be cause for concern? Well, the intuition and experiential references which simulationists use to calibrate models might be difficult to acquire. The radiant loads and surface temperatures might lie outside the experimental and theoretical studies underlying the correlations used within the tool. There is uncertainty in the predicted values.

How does one acquire confidence in such a situation. Paranoia (as in "we need to confirm additional details") is a useful guide. What does the CIBSE Guide/ASHRAE Handbook say about this? Each performance metric evolves from the interactions of specific flux and flow paths: Do these make sense? Has zone and surface energy balance been maintained? What is the pattern of longwave radiant exchange within the zone? Where is there thermal mass in the zone and how does it react? What is the sensitivity of the predictions to the magnitude and radiant fraction of the internal gain? Does altering the thickness, conductivity or surface properties of the constructions change the nature of the predictions?

Such questions are predicated on access to a range of performance data (esp-r offers many facilities in this regard) as well as user opinions as to the processes involved and pattern matching skills to find where these overlap. In this case, initial investigations confirmed that the predicted trends were indicative rather than absolute.

Reviewing scores of UK and European consultancy projects, it is as often the case that design questions demand simulations that focus on aspects of performance which are particular to that project. What happens if the exposed ceiling structure is 100mm deeper or the thermostat is moved to a different location or a different crack width is assumed for the doors or the tree near the entrance is removed? Sometimes it is the form of the assessment metric. What is the frequency of predicted mean comfort votes or the rate of change of humidity or the incidence of condensation or the correlation between infiltration rates and wind direction?

Where the focus is narrow and deep there is a chance that it involves simulation facilities which have not been explored by the practitioner. It might involve a simulation facility which has been infrequently used or which has not been used to do exactly what the practitioner demands.

For example, a researcher wished to model an experimental solar drying facility. Measured data from a number of points within the experiment as well as equations representing theoretical moisture losses were available. The intent of the work is to calibrate the simulation model and then conjecture and test different operational regimes to improve the consistency

of the drying process and reduce drying time. The simulations would also provide a platform for evaluating and evolving the moisture transfer equations and the design of the drying facility.

The abstraction of the test facility into a simulation model was straightforward because the zones required were well defined and its design included few areas of complexity. Similarly, the flow network appeared straightforward. The researcher used an explicit geometric representation of the test facility and its contents with imposed heat transfer coefficients. This allowed each convective, conductive and solar and longwave radiant flux exchange within the assembly to be assessed. Code interventions were confined to the core moisture transfer issue.

In reality, the design was is a small scale low-to-medium velocity wind tunnel which had periodic injections of heat from a solar source and was filled with materials which slowly released moisture into the air stream.

During calibration of the model it became apparent that pulses of heat being injected into the collector space were not being "noticed" by downstream zones. This artifact disappeared if the flow rate was reduced below ~1000 ac/h and the simulation timestep increased to one second or longer. This poses some interesting simulation issues:

- How does one represent a solar collector made up of dark course rock layer over a concrete roof in which the total surface area is high and the concrete roof mass is also significant?
- Similarly, how does one represent wood stacked into drying racks within the chamber where the total surface area is high and a complex moisture transfer is active depending on the air stream moisture content?
- What boundary conditions apply when the time constant of the problem is two magnitudes less than the usual lower timestep limits of the simulation tool?
- If the timestep equals the time constant, a three month drying cycle equates to 1.9×10^{7} timesteps (give or take a million). This presumes serious computational and data storage resources even before contemplating how one might might approach the analysis of sub-second performance metrics and long term trends.
- How does one calibrate a model against a limited set of measurement points and uncertainties in the composition of the test facility?

There is a generic simulation issue in the need to understand high frequency performance metrics (say system control feedback loops) in conjunction with long term performance issues. The practitioner must judge where it is acceptable to assess the control response at courser time intervals and the uncertainty this introduces.

SIMULATION DROWNING IN COMPLEXITY

So... "how do I model stair treads? - where are they? - in the fire escape - why do you think this is important? - they are included in the building section".

For any number of reasons practitioners compose models which are not concise representations of the project and they carry out assessments which actually do little to clarify the performance of a design. Practitioners may be lead by the tool to attempt untenable levels of complexity. A typical case is a simulation tool which can import CAD files and the availability of a CAD model which includes items such as door frames, conduits, chairs and standing roof seams. Usually such items have a third order thermal impact but their inclusion in the thermal model requires the practitioner to invest scarce resources in removing them or in their attribution (Hand 1998).

Another classic case is a repetitious design (say 25 near-identical offices) where the user chooses to explicitly model each one (perhaps at low resolution) rather than consider the option to model one or two offices (perhaps at high resolution) and scale the predictions accordingly.

How does one judge how complex a model should be? One approach is to clearly define the performance metrics required by the project and then the related physical processes. Say the design team was concerned about occupant comfort near a west facing facade during the winter. The distribution of solar radiation within the space might contribute to localized discomfort so the model would benefit from addition geometric resolution and from a temporal analysis of shading and insolation distribution within the space. Longwave exchange might cause discomfort so explicit radiation viewfactors within the office would improve the resolution of the metric. One might also consider placing radiant sensors at several points within the office to check for position sensitivity.

Thus, after careful reflection is might turn out that stair treads as an important aspect of a particular design assessment. Required complexity is something which must, somehow, be managed.

SIMULATION AS AN ENDURANCE CONTEST

Having observed scores of projects, there are indeed some which, after sober reflection, demand models of extreme descriptive and/or operational complexity. Given that the use of simulation is hardly a trivial exercise for a constrained project how might one approach the management of large projects?

- Be brutally honest. The relationship between model complexity and project resources does not grow as a linear function. Beyond some nominal level of complexity (which depends on the simulation tool and the practitioners expertise) the resources and attention given to a project is better described as exponential growth. If the vendor offers an improved application or you acquire a faster machine the only thing that actually changes is that point where nominal complexity becomes exponential complexity.
- Have procedures. People loose scraps of paper with critical information, systems which depend on error-free performance invite failure. If it takes more than a few moments to identify the differences between two versions of a model, either the tool or the quality assurance procedure needs to evolve. If the random loss of a file delays the project for more than an hour then use a different archiving strategy.
- Know your skills. When you come to a bottleneck or a puzzle or a crash, is someone in-house or at the other end of an internet or phone connection that can sort it? Can you regularly and consistently build constrained models that work well? How accurate is you estimate of the resources they take? If you intentionally introduce a subtle error in a working model, how long does it take your QA process to find this? Well?
- Know your tools. How well do they accommodate additional complexity? Do simulation staff have strategies for tool use which successfully leverage existing facilities to accomplish their tasks? Do they have strategies for discovering critical performance patterns in large datasets?
- Know the project. Those who rush to the keyboard will be invited to return to it over and over and over. What metrics can you enquire about via simulation that help to answer the project design question(s)? What needs to be represented to deliver those metrics? What can be excluded? Can you design a model which supports these metrics and anticipates follow-on questions from the design team?

If the above questions yield uncomfortable answers what are your options? Can you alter your procedures, skills base or your support contracts to be in a better position to take on the project? Can you influence the tool vendor to adapt the tool?

SIMULATION AT THE EDGE

The catastrophic failure scenario is an excellent example of simulation at the edge. Edges are scary. Engineering almost becomes science. Answers, if they exist at all, have to be prised out of deep and hidden places and held up to the light of extreme sceptism.

The built environment is replete with difficult problems and needs practitioners who are equipped to evolve new methodologies and working practices and leverage the functionality of their tools to support their work. Here is the story of one such project and it began with one question:

The system died, how long have we got?

In the context of archives and museums, a catastrophic HVAC system failure presents a considerable challenge. If an artifact or exhibition is at risk under specific temperature regimes or overly rapid fluctuations in humidity, how can practitioners assess risk within an existing or proposed gallery space? For the majority of buildings without a fully redundant environmental system, contingency plans are a critical design constraint. A 24 hour response may be viable when a 3 hour response is logistically absurd.

This question arose within the planning process for a new exhibition in an English museum. The galleries under consideration had a southwest exposure and the exhibition would be open during the warmest period of the summer. Risk assessment was complicated by the massive construction of the galleries (walls over 1.5m thick were quite common), historic fenestration details and openings between gallery floors as well as an environmental systems design which was planned around a displacement ventilation system.

The exhibition included a mix of free-standing, board-mounted and chambered artifacts with clusters of multimedia terminals. Several displays created voids adjacent to fenestration which were subject to high solar radiation and bespoke lighting schemes were planned.

To find out the nature of environmental degradation it was necessary to understand local response characteristics (e.g. air and surface temperatures, air flow patterns), at a number of points in the galleries, the degree of structural cooling resulting from the raised floor of the displacement ventilation system and the exposed ceiling below it and the mixing of warm air from local casual gains and the display voids near

fenestration.

It was also necessary to understand how the galleries would transition from an air-conditioned state to one driven by buoyancy and boundary conditions. What was the efficacy of the structural mass in delaying overheating? Would artifacts adjacent to the fenestration voids be at greater risk? To what extent would air temperatures stratify and how long would it take for elevated temperatures at the ceiling to extend down into the artifacts?

Clearly, a number of dynamic interactions were at play in the galleries and it would be difficult to perform a risk assessment based on a static analysis or by looking at facets of the design in isolation. The number of points at which performance metrics needed to be tested and the number of paths by which adverse environmental conditions might propagate argued for an integrated assessment of both thermal and air flow domains. This also argued for a degree of redundancy in assessments (i.e. multiple approaches to risk assessment).

In order to determine the onset of critical environmental conditions the following approaches were used:

a) The consultant knew that the project was complex and instituted a cooperative effort with the tool developer.

b) The simulation team prepared models for an integrated simulation tool which supported detailed thermal and network flow analysis and for a CFD package which had been optimized for building analysis.

c) Each model was designed to deliver the specific metrics of the project at critical points within the galleries and artifacts and was structured to support tests of the sensitivity of the model to possible design parameter uncertainty.

d) Assessments were carried out for a number of operational and climatic scenarios with the intent of delivering a "rule-book" for the exhibition managers.

e) Patterns observed in each assessment were cross-correlated with the other simulation tool and with analytical computations.

f) The results of the study would be critiqued by a 3rd party advisor.

Figure 1 shows the model used for the integrated thermal and network flow approach. Each gallery was subdivided into an occupied zone and a ceiling zone with the voids between the displays and the building facade treated as separate zones. A plenum zone for the displacement ventilation system extends under all of the galleries.

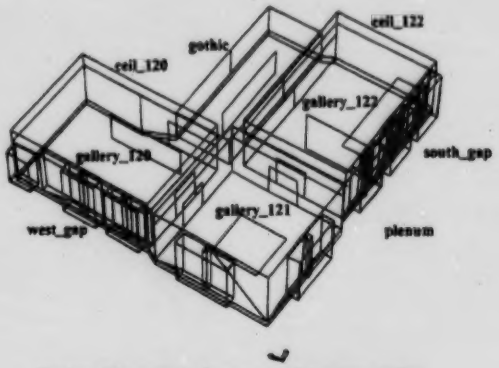

Figure 1: thermal model of museum galleries

This approach allowed the design team to trace the deterioration of environmental conditions and their causal effects before, during, and after system failure.

Figures 2 and 3 show a portion of one of the CFD models used in the study. Each of the display cabinets, internal obstructions and heat sources were included in the model. The stream lines shown are related to one of the extract vents just prior to failure.

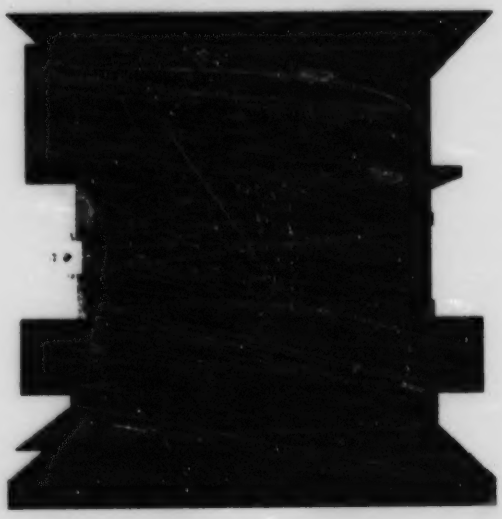

Figure 2: CFD model of gallery (view from above)

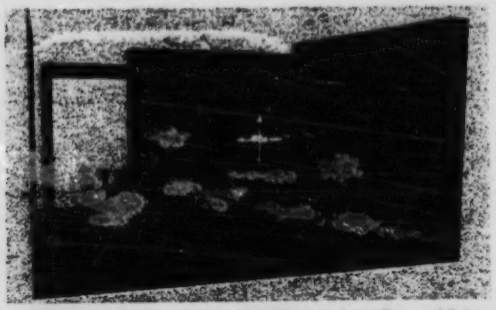

Figure 3: CFD model of gallery (view from side)

To have successfully addressed the catastrophic failure scenario is one measure of the maturity of available tools, practitioner skills and vendor-practitioner cooperation. It indicates that there are ways to approach even the most difficult of problems.

DUE CARE AND ATTENTION

The museum study demonstrated one approach to ensuring that the results of a project stand up to the most critical of analysis by the client and the courts.

The team had evolved working procedures which included robust project planning, model checking and calibration and quality assurance. They had invested the resources needed to become proficient with their tools. They knew that the project required an extension to their skills base and took steps to acquire these skills. This project was an exception only in terms of its intensity, the use of independent (as opposed to cooperative) assessments and the extended testing of uncertainties. Here is what they did:

- the project methodology built on established procedures,
- the metrics of the study were clearly stated and the models designed to deliver those metrics,
- they tested each simulation tool for robustness, sought the advise of the tool vendors and ensured the tool vendor was on call for clarification and advise,
- quality assurance was ubiquitous,
- all assumptions were stated and agreed with the client,
- the simulation team allocated time to evolve a clear understanding of the museum performance and from this communicate clearly with the design team.

Sound familiar? Be brutally honest. Have procedures. Know your skills. Know your tools. Know the project. If this does not sound familiar consult the *CIBSE Building energy and environmental modelling Applications Manual* (CIBSE 1998). It provides recommended QA procedures, guidance on the planning of projects, selection of simulation tools, sources of information. Practitioners who follow these procedures tend not to confront the legal professions and they tend to deliver useful information to their clients.

And sometimes clients want to hear the impossible (like warm air does not rise or that heat absorbing glass does not get warm). In a contest between physics and beliefs, sometimes it is wise to decline the battle. "We never turn down work" keeps the lawyers well fed. Know when to say no.

So what about the stair-tread practitioner? Excessive detail **does not preclude** delivering userful information to a client. Unconsidered detail is a successful strategy for limiting practitioner profits which can, occassionally, have adverse effects for the client. Such approaches can be indicative of a lack of understanding of the underlying interactions within a design.

And what about the smelting plant? Well, here the practitioner might be skating on thin ice without prior experience and/or a finely resolved intuition as to what conditions one might expect within an extreme environment. Paranoia and cynicism are useful vantage points for the use of a tool for an extreme design. Bottom line—don't enter uncharted territory without the skills and resources needed to calibrate the model and confirm performance predictions.

In the case of the material drying facility, it was not possible to identify the numerical problem within the timeframe of the study and pragmatic adjustments to the model were required. In terms of due care and attention this is a boarderline case. The trend was clear, however the absolute values included a degree of uncertainty. Indeed, the simulation community is currently better placed to report on relative performance issues than absolute performance issues. A useful rule for those who wish to use simulation to design experiments— design the simulation model in advance of building the experiment and positioning the instrumentation. This will expose potential unknowns within the model and the experiment. It is easier to change a model than an experiment.

EVOLVING TOOLS

A contributing factor to these case studies has been the continuing evolution of tools to the operational needs to practitioners. Each of these case studies, indeed almost every observation of and participation in such projects has left its mark on the simulation tool (sometimes as an immediate patch). Few of the interventions which were critical to these projects would feature in a vendors glossy brochure. "Even better QA reporting!"

"Now reports frequency of the rate of change of RH!" "Now provides more space for documenting operational strategies!" "Now keeps track of latent gains from wet surfaces!" "Now allows you to adjust small power loads on a minutely basis!"

CONCLUSIONS

The critical requirement in a number of the case studies was to identify the essential characteristics of the design and ensure that the descriptive entities used in the simulation model captured these characteristics. How does one do this? Find a clean notepad and answer the following questions:

- What do I wish to know, at what level of detail?
- Why do I (or the client/design team) want to know this?
- What is the quality and extent of design information that I can access?
- What is the essence of the design in terms of form, composition, operation and control and how might this evolve during the design process?
- What metric(s) signify acceptable performance and how can this be communicated to the design team and/or client?
- What are the essential interactions which need to be preserved within the model in order to deliver the project metrics?
- How can these interactions be represented? Can I sketch out the overall model and explain my approach to the design team (and if not why not)?
- What boundary conditions, over what period(s) would form a reasonable test of the design?
- How do I calibrate the model and arrive at an initial understanding of the design?
- How can I ensure the quality of the model as it evolves and my colleagues understanding of it?

A similar checklist can be found in (CIBSE 1998). Adding observations from simulation at the edge resolves to: **plan the project, find its essence, make a model that can tell the story of the design, be paranoid, live with it long enough to become less paranoid, pass it to someone else to try and break it and only then tell the design team how it works (in four part harmony if necessary).**

A few "secrets" from simulation at-the-edge:

- Practitioners who are uncertain about how to approach an assessment task build quick and nasty disposable models and when they have learned enough they toss them out and use their new knowledge for the "real" model.
- Practitioners who need to see if their tool can deliver a particular metric in a particular way find this out sooner (i.e. they grab and existing model, run a quick simulation and explore data recovery and post-processing options) rather than later (i.e. when the real model is ready).
- (And here is the real secret) No matter how efficient you are at putting together a model and how fast your computer is in doing the calculations—it takes time to understand the performance of a design well enough to "tell its story" to the design team. The bigger the project the longer this tends to take. The closer to the edge you are, the more different views of the performance you need to check. Take the time you gain through good working procedures and staff skills and spend it getting the story.

Simulation is, in many ways, a disruptive technology. In Europe, practitioners working "at the edge" are doing so more frequently and are managing up to a score of simultaneous simulation based projects. The more conservative practices are beginning to notice this.

How will they adapt to this disruptive technology? Some will fail. Currently there is a critical shortage of staff with simulation skills. Few senior partners are in a position to manage simulation based projects. It will take time for new practitioners to work their way to positions of influence. In the interium, simulation based consultancies are thriving on a mix of subcontracted projects from established practices, and increasingly, by drawing clients away from established practices.

REFERENCES

Hand J.W. Irving S.J., Lomas K.J., McElroy L.B., Parand F., Robinson D., Strachan D. *Building energy and environmental modelling, Applications Manual AM11*, The Chartered Institution of building Services Engineers, London, 1998.

Hand J.W. *Removing barriers to the use of simulation in the building design professions*, Thesis, University of Strathclyde, Glasgow 1998.

Session 2 / Séance 2

Energy Calculation Methods, Software Development and New Simulation Programs

Les méthodes de calcul de la consommation énergétique, l'élaboration de logiciels et les nouveaux programmes en matière de simulation

REVUE DE LITTÉRATURE SUR LES AVANTAGES ET LIMITES DES MÉTHODES DE MODÉLISATION DES BÂTIMENTS À DES FINS D'INTERVENTION COMMERCIALE : LE CAS D'HYDRO-QUÉBEC

Michel Parent, Patrice Raymond
Technosim Hydro-Québec
mparent@technosim.com, raymond.patrice@hydro.qc.ca

RÉSUMÉ

La modélisation énergétique de bâtiments commerciaux existants, dans le but d'identifier la répartition de la consommation entre les différents usages, est une tâche fréquemment accomplie par différents intervenants du secteur de l'efficacité énergétique, dont les entreprises de service public, les entreprises de services éconergétiques, les ingénieurs conseils, etc. Étant donné les contraintes de temps et d'apprentissage reliées à une modélisation détaillée des bâtiments commerciaux, plusieurs approches simplifiées sont employées afin d'obtenir la répartition de la consommation d'énergie. La majorité de ces approches se base sur les données de facturation afin de calibrer une simulation ou même de construire l'ensemble du modèle. Afin de déterminer les contraintes et les limites de cette approche ainsi que les autres options de modélisation pouvant être employées, sur une base régulière, pour des bâtiments existants, une revue de la littérature technique sur les méthodes de modélisation des bâtiments commerciaux devant reproduire des données de facturation, ou encore du mesurage plus détaillé, fut effectuée.

La principale observation qui ressort de la revue de littérature est qu'une méthode unique d'analyse et de modélisation des bâtiments commerciaux ne peut être appliquée à grande échelle, par exemple dans le cadre d'audits énergétiques, sans introduire de sérieux problèmes de justesse des analyses ou, à l'opposé, un niveau d'effort injustifié.

INTRODUCTION

Un grand nombre d'intervenants, souvent reliés à des entreprises de services publics, utilisent des modèles empiriques fondés sur des relevés d'équipement (puissance installée), des règles du pouce (coïncidence de charge et heures d'utilisation) et la facture réelle de leurs clients pour répartir la consommation énergétique entre les usages et les équipements de bâtiments commerciaux. Ceci de manière à identifier l'impact de mesures correctives sur la facture du client. Dans la majorité des cas, les valeurs réelles fournies par la facture constituent un point de repère important pour expliquer et justifier auprès du client l'orientation qu'ils lui proposent.

Cette valeur perçue de présenter une analyse énergétique épousant le profil de consommation facturée a amené l'utilisation d'un modèle d'analyse par régression linéaire par certains intervenants du milieu pour l'analyse de la consommation des bâtiment commerciaux. Beaucoup d'utilisateurs sont séduits par les avantages de cette méthode d'analyse par régression dû à sa simplicité d'utilisation et son cycle court d'analyse.

L'évolution de l'approche commerciale d'Hydro-Québec commande l'utilisation d'outils d'analyse les mieux adaptés pour réaliser des diagnostics énergétiques et pour proposer au client des solutions techniques adaptées à ses besoins.

Sachant qu'une approche de modélisation détaillée peut répondre en partie à ces nouvelles exigences, il existe néanmoins des réserves quant à l'utilisation d'une telle approche : elle s'adapte plus difficilement à la reproduction de la facture; elle exige de l'utilisateur une expertise accrue au niveau des systèmes de chauffage, ventilation et climatisation (CVC) et de l'enveloppe du bâtiment; le risque d'erreur d'interprétation des données recueillies est plus élevé; les cycles d'analyse sont plus long.

Les modèles doivent généralement servir à établir la répartition de la consommation selon différents usages et estimer l'impact de mesures d'optimisation de la consommation et de la puissance sur la facture d'un client.Toutefois, les limites d'applicabilité des différentes méthodes d'analyse des bâtiments commerciaux poussent Hydro-Québec à vouloir connaître les différentes options qui sont possibles pour effectuer ce type d'intervention ainsi que les limites de chaque méthode.

MÉTHODE

Pour atteindre l'objectif principal du projet, une revue de la littérature technique sur les méthodes de modélisation des bâtiments commerciaux qui doivent

reproduire des factures énergétiques réelles, ou des mesures, fut effectuée. Une première revue a été effectuée à partir des articles techniques disponibles sur le site Web de l'ASHRAE (American Society of Heating and Air-Condtioning Engineers) ainsi que de ceux référés au chapitre 30 du ASHRAE Handbook – Fundamentals 1997. Cette revue fut jumelée à une recherche sur les principales banques de données techniques, tel Engineering Index et Energy Science and Technology, afin de compléter la revue pour la période entre 1995 et 2000. Les articles pertinents ont été commandés pour procéder à une évaluation détaillée afin de faire ressortir les forces, les faiblesses et les limites de différentes méthodes répertoriées.

Enfin, à la lumière des résultats de la recherche et de l'expérience notre expérience dans l'utilisation et le développement de logiciels de modélisation de bâtiments commerciaux, des orientations possibles de développement et d'utilisation des différentes méthodes sont proposées.

REVUE DES MÉTHODES D'ANALYSE

La revue de littérature a permis d'identifier 4 familles d'approches différentes servant à l'analyse énergétique des bâtiments commerciaux. Ces différentes méthodes d'analyse diffèrent en complexité ainsi qu'au niveau des objectifs visés lors de leur utilisation. Il est à noter que les méthodes complexes de reconnaissance de forme, tel les réseaux de neurones, ont été exclues de l'analyse.

La revue de littérature démontre qu'il n'existe pas de solution unique applicable de manière raisonnable à l'ensemble des bâtiments commerciaux. La diversité des bâtiments, des systèmes, des vocations et les variations d'usage au sein même d'un bâtiment rend l'analyse énergétique de ceux-ci particulièrement difficile. Pour les mêmes raisons, la comparaison directe entre bâtiments en apparence similaires est parfois sujette à une large incertitude.

De manière générale, l'approche à adopter pour l'analyse énergétique d'un bâtiment va dépendre des objectifs visés par l'analyse, de l'information disponible sur le bâtiment et de la complexité du bâtiment. Il est donc peu probable qu'une approche unique sera utilisable pour l'ensemble d'un parc de bâtiments commerciaux.

Indices énergétiques globaux

La méthode la plus simple d'analyse de consommation se base sur les indices unitaires globaux, dont la plus fréquente est la consommation annuelle totale par unité de surface. Des études ont parfois utilisé cet indicateur pour évaluer l'économie d'énergie attribuable à des mesures d'efficacité énergétique par l'analyse des factures avant et après l'implantation de celles-ci (1) ou pour comparer l'efficacité énergétique de bâtiments en apparence semblables.

Une approche souvent employée pour interpréter les indices globaux consiste à utiliser une valeur typique normale, provenant soit de moyennes ou d'un bâtiment considéré comme représentatif, afin d'évaluer la performance d'un bâtiment spécifique. Les bâtiments démontrant une intensité énergétique anormale peuvent alors faire l'objet d'une analyse plus approfondie. La densité de puissance est également un indicateur global fondamental dans l'analyse de premier niveau d'un bâtiment.

Toutefois, une telle analyse ne révèle pas nécessairement un potentiel d'efficacité énergétique ou des anomalies de fonctionnement puisque plusieurs facteurs peuvent expliquer les différences d'intensité énergétique ou de densité de puissance pour des bâtiments apparemment similaires (1). Une normalisation de l'intensité énergétique est parfois employée pour tenter de réduire l'influence de paramètres indépendants comme la température. La correction par l'utilisation des degés-jours de chauffage est une technique relativement courante (ref. Poly-Energie, communication personnelle). Cependant, cette méthode présuppose que la consommation du bâtiment est entièrement proportionnelle à la température et que les variations annuelles ne sont attribuables qu'à ce facteur. Cette hypothèse est rarement applicable dans le secteur commercial. De plus, l'incertitude générale associée aux indices globaux en limite l'utilisation et tout raffinement dans la méthode d'analyse sera obligatoirement restreint par cette incertitude de base.

La répartition entre chauffage, climatisation et les autres usages de l'intensité énergétique est peu appropriée étant donnée le haut niveau d'incertitude reliée à cette méthode très macroscopique d'analyse et aux méthodes également empiriques habituellement utilisées pour répartir l'intensité énergétique en différentes composantes.

Avantages de la méthode :

- Le principal avantage d'une méthode d'analyse par indices globaux repose sur sa simplicité et la rapidité d'évaluation.

- La méthode permet une comparaison rapide de la consommation d'un même bâtiment d'une année à l'autre et ainsi servir d'outil de diagnostic de premier niveau de l'ensemble de la consommation.
- La méthode permet une comparaison d'un bâtiment donné par rapport à une valeur moyenne pour les bâtiments du même type et ainsi servir à détecter des problèmes potentiels ou prioriser des interventions.

Limites de la méthode :

- La méthode ne permet pas de connaître les raisons d'un écart de consommation unitaire d'une année à l'autre pour un même bâtiment.
- La méthode ne peut servir à identifier un potentiel d'efficacité énergétique ou des anomalies de consommation sur la base d'une comparaison entre un bâtiment donné et une valeur de référence.
- La méthode ne peut servir à répartir de manière juste la consommation entre les usages.
- La normalisation des indices globaux est souvent futile puisque les causes réelles de variations peuvent être multiples et non reliées au paramètre de normalisation (ex. température)

Méthode par régression simple

Les méthodes d'analyse par régression simple ont été utilisées avec un certain succès dans le secteur résidentiel pour modéliser le comportement en chauffage. Le modèle le plus connu est PRISM (Princeton Scorekeeping Method).

De façon générale, cette méthode analyse les données de facturation mensuelle d'une résidence et subdivise la consommation en deux composantes, soit une composante de charges fixes, constantes sur toute l'année, et une composante provenant du chauffage des locaux, qui varie linéairement avec la température extérieure. Le modèle ne traite donc qu'une seule variable indépendante, la température extérieure. Toute variation de consommation dont le comportement n'est pas proportionnel à la température extérieure entraînera une violation des hypothèses du modèle et une erreur dans la modélisation du bâtiment.

Pour les bâtiments commerciaux, les gains solaires, les horaires d'exploitation, les gains internes, l'humidité, l'utilisation de climatisation gratuite et les horaires de ventilation variables ont souvent une grande influence qui ne peut alors être saisie par un modèle régressif simple (18, 19). De plus, pour tous les bâtiments ayant des zones centrales qui exigent de la climatisation lorsque d'autres zones sont en chauffage, les modèles régressifs simples ne pourront traiter adéquatement la consommation.

Les résultats de modélisation de bâtiments commerciaux par régression simple sont, au mieux, mitigés dans la littérature (1,18,19). L'utilisation et l'interprétation des données sont sujettes à beaucoup de circonspection (18). Les applications dans les climats froids sont habituellement plus appropriées puisque la température influe plus fortement la consommation. (1,18). De plus, certains types de bâtiments sont plus adaptés à cette méthode. Entre autres, les écoles primaires n'ayant pas ou peu de climatisation ou d'humidification s'adaptent relativement bien à la méthode puisqu'elles respectent en bonne partie les hypothèses sous-jacentes au modèle. Toutefois, même des modèles complexes n'ont pu démontrer des résultats consistants pour des bâtiments en apparence bien adaptés au modèle (i.e. n'ayant pas de climatisation) (19).

À l'opposé, dans le cadre de la vérification d'économies d'énergie attribuables à un important programme de DSM (Demand Side Management) au Texas, les méthodes de régression linéaire se sont avérées les plus utilisées et ont rempli leur rôle adéquatement (12). L'objectif recherché dans ce cas étant beaucoup plus global que l'évaluation du profil précis d'un bâtiment unique.

Plusieurs variantes de la méthode de régression simple existent (12, 15). La plupart de celles-ci permettent de désagréger la consommation selon ses composantes principales, soit la climatisation, le chauffage et les charges indépendantes de la température, de façon automatique. Des méthodes plus complexes de régression existent mais se basent sur des relevés de consommation horaire.

Toutefois, peu importe la méthode sélectionnée, la régression simple utilise toujours l'hypothèse que le chauffage et la climatisation varient uniquement en fonction de la température. Les méthodes plus sophistiquées permettent de tenir compte de certains facteurs temporels, souvent au niveau mensuel, pouvant affecter la consommation d'énergie. Lorsque des données de mesurage journalières ou horaires sont disponibles, la méthode de régression simple peut tenir compte des horaires d'occupation de manière plus appropriée.

Il est également possible d'adjoindre aux méthodes de régression simple des modules de traitement effectuant la répartition de la consommation entre les équipements ou encore entre des zones d'un même bâtiment. Ces ajouts sont faits à l'extérieur de la

méthode de modélisation et ne modifient en rien les limites de la méthode. Dans la plupart des cas, des modèles de répartition empiriques, basés sur des observations pour des bâtiments similaires, sont utilisés.

Notons enfin que la méthode de régression simple reproduira aussi fidèlement que possible le comportement contenu dans les données d'entrée (ex. facturation). Toute anomalie, défaillance ou événement ponctuel sera donc intégré automatiquement au modèle comme étant un comportement normal. Les prévisions ultérieures du modèle et la répartition de la consommation entre les trois usages en seront conséquemment affectées. Lorsque les données comportent des anomalies apparentes, ces données devraient être rejetées (ex. facture sur une période avec défaillance connue, facture estimée,etc) (14). Toutefois, le rejet de certaines données ajoute un élément arbitraire à la méthode et l'utilisateur ne doit pas rejeter toutes les factures ne se conformant pas au modèle (14). En effet, les différences avec les résultats du modèle peuvent provenir autant de ses limites propres que d'anomalies dans la facturation. La régression simple est un outil de diagnostic de premier niveau mais il ne permet pas d'identifier de façon définitive la présence d'une anomalie (14).

Avantages de la méthode :

- Le principal avantage de la méthode de régression simple repose sur sa simplicité d'utilisation.
- La méthode permet une modélisation sur la base des données de facturation.
- La méthode permet souvent une reproduction assez fidèle des données de facturation (de par sa nature de minimisation d'erreurs). L'écart entre la facturation ayant servi à construire le modèle et les prévisions du modèle est un des éléments pouvant servir à établir la validité du modèle pour le bâtiment considéré.
- La méthode permet de reproduire le comportement du bâtiment pour de nouvelles données de température (normalisation).
- La méthode offre de désagréger la consommation entre ses trois principales composantes.
- La méthode permet une utilisation répétitive et relativement uniforme par plusieurs utilisateurs (si la méthode est implantée de manière à effectuer les calculs des points de balance et des charges fixes de façon automatique).

Limites de la méthode :

- La validité de la méthode pour les bâtiments commerciaux est variable. Lorsque les variations de consommation sont fonction de facteurs autres que la température extérieure, la méthode ne pourra modéliser adéquatement le bâtiment et répartir avec justesse la consommation par usage.
- L'interprétation des paramètres des modèles s'avère difficile (ex. température d'équilibre, charge linéaire).
- La répartition de la consommation entre différentes zones thermiques d'un bâtiment n'est pas possible à moins de disposer de mesurages pour chaque zone.
- La répartition entre différents équipements ou systèmes pour un même usage n'est pas possible.
- Le modèle reproduit toute anomalie se retrouvant dans les données de base.
- La méthode ne peut servir à évaluer la majorité des mesures d'efficacité énergétique.
- La méthode exige l'utilisation des données de température correspondant à la période de mesure.

Utilisation type :

Les méthodes de régression simple identifiées sert principalement à mesurer l'impact de mesures d'efficacité énergétique suite à leur implantation (4, 6, 19, 20, 15, 17, 14). La raison principale derrière cette vocation spécialisée des méthodes de régression simple repose sur leur simplicité. La méthode représente un compromis entre la simplicité et la justesse d'évaluation recherchées par les différentes parties (14) lors de contrats de performance.

Dans tous les cas, des mesures de consommation pré-datant et post-datant l'application des mesures sont disponibles. Cette méthode s'adapte à l'une des procédures de vérification d'économie d'énergie suggérée dans l'International Performance Measurment and Verification Protocol (IPMVP 1997) qui sert parfois de guide aux entreprises de service éconoergétique pour valider les économies attribuables à leur intervention. La validité statistique du modèle peut s'évaluer de façon très rigoureuse (réf. 16, 17, 20). Cette validation statistique permet d'établir si le modèle peut au minimum représenter le comportement du bâtiment selon l'hypothèse de base du modèle. Ce test statistique ne permet toutefois pas d'établir si d'autres variables indépendantes (ex. humidité, horaires, ensoleillement) affecteront les prévisions subséquentes du modèle. Dans ces cas, des vérifications doivent être effectuées pour s'assurer qu'il n'y a aucune modification de ces autres variables indépendantes entre la période de référence et la période suivant l'intervention. Ce type de vérification est très difficile à implanter en pratique puisque les valeurs réelles des autres variables indépendantes sont habituellement inconnues ou méconnues.

Méthode par régressions multiples

Pour contourner certaines des limites de la méthode régressive simple dans le cas des bâtiments commerciaux, d'autres méthodes dérivées ont été développées. Ces méthodes utilisent plusieurs variables indépendantes dans l'analyse des factures. Les variables indépendantes fréquemment considérées sont : l'ensoleillement, l'horaire d'utilisation, l'humidité, le vent, l'occupation...

Il n'y pas de limite sur le type de variables indépendantes qui peut être traité. Toutefois, de sérieux problèmes d'auto-corrélation peuvent se produire si les variables sélectionnées ne sont pas totalement indépendantes les unes des autres. La validation statistique de la méthode s'avère également plus complexe.

L'utilisation commerciale des méthodes de régression multiple semble relativement limitée. Une des raisons possibles pour cette apparente faible utilisation provient de la complexité accrue d'implantation de cette méthode et de la difficulté dans la sélection des variables indépendantes. La méthode ne permet d'ailleurs pas d'éliminer toutes les limites des méthodes régressives, dont le traitement du chauffage et de la climatisation simultanée, des zones multiples et de la répartition par équipement. Ce type de modèle requiert beaucoup plus de jugement de la part de l'utilisateur que la méthode simple et les gains de la méthode ne sont donc pas toujours garanties (1).

Avantages de la méthode :

- Le principal avantage de la méthode de régression multiple repose sur sa capacité de saisir plusieurs variables indépendantes affectant la consommation des bâtiments commerciaux.
- La méthode permet d'effectuer une modélisation de phénomènes non linéaires, tel l'arrêt de systèmes.
- La méthode permet souvent une reproduction assez fidèle des données de facturation (de par sa nature de minimisation d'erreurs). L'écart entre la facturation ayant servi à construire le modèle et les prévisions du modèle est un des éléments pouvant servir à établir la validité du modèle pour le bâtiment considéré.
- La méthode permet de reproduire le comportement du bâtiment pour de nouvelles données de température (normalisation).
- La méthode offre de désagréger la consommation entre ses trois principales composantes.

Limites de la méthode :

- L'implantation de la méthode est plus difficile que la régression simple. La méthode peut s'avérer instable lorsqu'un choix inapproprié de variables indépendantes est effectué.
- L'utilisation de la méthode et la sélection des variables indépendantes requiert plus d'expérience que la méthode simple.
- L'interprétation des paramètres des modèles s'avère difficile (ex. température d'équilibre, charge linéaire).
- La répartition de la consommation entre différentes zones thermiques d'un bâtiment n'est pas possible à moins de disposer de sous-mesurages pour chaque zone.
- La répartition entre différents équipements ou systèmes pour un même usage n'est pas possible.
- La méthode ne peut servir à évaluer la majorité des mesures d'efficacité énergétique.
- La méthode exige l'utilisation des données de température correspondant à la période de mesure.

Utilisation type :

Les méthodes de régression multiple identifiées dans la littérature semblent également servir à mesurer l'impact de mesures d'efficacité énergétique suite à leur implantation (12, 14). L'utilisation de cette méthode apparaît beaucoup plus limitée que pour les diverses méthodes de régression simple et sert en dernier recours lorsque les méthodes simples les plus sophistiquées ne permettent pas une modélisation adéquate (12)

Modélisation détaillée des bâtiments

Contrairement aux trois méthodes d'analyse précédentes, la méthode détaillée ne requiert pas de données de mesurage mais uniquement les caractéristiques physiques et opérationnelles du bâtiment. Les modèles détaillés peuvent également varier grandement en complexité. Des modèles simples peuvent être établis pour obtenir des estimés (ex. en suivant le standard ASHRAE TC4.7) ou des outils très détaillés comme DOE2, ESP-r , etc., peuvent permettre des évaluations fines de tous les systèmes et éléments d'un bâtiment. Le niveau de détails requis est toujours fonction des objectifs recherchés.

Pour un modèle détaillé de modélisation, la reproduction d'une facture exige de reproduire fidèlement non seulement les composantes de l'enveloppe, les systèmes et les contrôles du bâtiment mais également son exploitation et tout autre événement (ex. défaillance, interférence humaine) ayant un impact sur la facture. Un tel processus exige un niveau d'effort assez important. Ce type d'effort

est habituellement requis si l'on veut reproduire des anomalies de consommation se retrouvant dans la facture ou si de la vérification d'économie d'énergie doit être effectuée tout en intégrant l'ensemble du comportement actuel d'un bâtiment (Baselining).

Lorsque les objectifs visent tout d'abord l'optimisation de la conception, l'évaluation d'impacts de mesures ou la répartition normale de la consommation entre zones et équipements, une reproduction fidèle de la facture n'amène généralement pas de gains appréciables au niveau de ces évaluations. Dans une optique d'évaluation générique des mesures, il est souvent possible d'effectuer des simulations types qui servent à établir des règles générales de gains énergétiques attribuables à des mesures d'efficacité énergétique. L'évaluation du potentiel pour un bâtiment donné, tant du point de vue de la consommation que du point de vue économique, requiert une évaluation globale précise mais non une reproduction de facture car dans ce cas l'objectif est d'évaluer les mesures et non pas de diagnostiquer des anomalies (ex. de contrôle, d'exploitation, d'équipements).

Plusieurs études visant à calibrer les modèles détaillés à des données de mesurage ont été identifiées (3, 15, 4, 7, 5, 8, 9). Souvent, la calibration d'un modèle détaillé repose sur l'expérience de l'utilisateur du programme de simulation, sur son expertise tant au niveau des bâtiments que des méthodes de modélisation, sur le jugement et sur beaucoup d'essais et erreurs (9). Plusieurs guides, souvent sous forme de graphiques de diagnostic, ont été développés pour réduire l'incertitude reliée à ce processus. Cependant, aucune procédure prédéfinie n'a été identifiée. Même lorsqu'un modèle est dit calibré à l'intérieur de 5 % de la facture rien ne peut garantir que les profils journaliers et horaires sont corrects. Plusieurs solutions peuvent conduire à reproduire une consommation mensuelle et annuelle (9). Il ressort donc des articles techniques qu'une calibration sérieuse d'un modèle détaillé devrait se baser sur des données de mesurage horaires sur de courtes périodes. Cette procédure permet de réduire le nombre de solutions possibles permettant la reproduction des résultats et réduit le volume de données à traiter. De plus, la reproduction d'anomalies et de défaillances souvent contenues dans la facturation mensuelle n'affectera pas artificiellement le processus de calibration.

Un modèle détaillé de modélisation s'adapte donc mal à reproduire les anomalies de fonctionnement, ce qui en fait souvent du même coup un bon outil de diagnostic d'anomalies de consommation. Toutefois, cela limite les possibilités de calibration sur la base de données globales, telle la facturation qui contient trop souvent des événements ponctuels non répétitifs (anomalies). Le résultat d'une telle calibration peut potentiellement être un modèle artificiellement erroné afin de reproduire ce comportement. La calibration d'un modèle détaillé devrait donc être effectuée uniquement lorsque les données disponibles sont totalement fiables et de préférence de type horaire. De plus, une telle calibration devrait se limiter aux cas où elle est absolument requise, comme la vérification des économies d'énergie attribuable à des mesures déjà implantées (Baselining).

Il existe des règles de vérification des modèles détaillés qui diffèrent de la calibration (3). La vérification du modèle ne sert pas à reproduire fidèlement la facture mais à s'assurer de la valeur et de la représentativité globale du modèle pour un bâtiment spécifique. Cette approche est mal adaptée à la vérification d'économie d'énergie (Baselining) mais est beaucoup plus réaliste pour toutes les autres applications cherchant à modéliser un bâtiment existant. Les règles de vérification décrites dans la littérature (3, 1) reposent beaucoup sur les données de facturation mais surtout au niveau de l'appel de puissance puisque celle-ci est mois sujette à être influencée par les nombreux facteurs qui sont invariablement intégrés dans les données de consommation (3, 17). Bien qu'un tel modèle ne reproduise pas nécessairement la facture, il offre un estimé convenable de la consommation normale du bâtiment, il permet de diagnostiquer les anomalies potentielles et il permet une évaluation plus objective du potentiel d'amélioration énergétique du bâtiment.

Avantages de la méthode :

- Le principal avantage de la méthode détaillée repose sur sa capacité à saisir tous les paramètres d'influence de la consommation d'un bâtiment.
- La méthode permet d'identifier la répartition de la consommation et de l'appel de puissance entre les zones d'un bâtiment.
- La méthode permet la répartition de la consommation entre les équipements d'un bâtiment.
- La méthode permet de reproduire le comportement du bâtiment pour de nouvelles données de température (normalisation).
- La méthode offre de désagréger la consommation entre tous les usages dans un bâtiment.
- La méthode permet d'évaluer l'influence de mesures d'efficacité énergétique touchant tant le contrôle, les équipements, les systèmes que l'enveloppe du bâtiment.

- La méthode est rigoureusement valide pour tous les types de bâtiment.
- La méthode représente un bon outil de diagnostic de consommation.
- La méthode permet d'établir la consommation type normale d'un bâtiment spécifique.

Limites de la méthode :

- La méthode exige une expertise plus grande.
- Le nombre d'entrées de données est plus élevé.
- La reproduction de données de mesurage, comme la facture, s'avère difficile.
- La vérification des données doit être très rigoureuse.
- La vérification des résultats est une étape importante et qui requiert une bonne expérience.
- L'utilisation répétitive de la méthode est plus difficile et la reproduction des mêmes résultats pour un même cas par différents analystes est plus difficile que pour les méthodes régressives.
- La méthode est plus dispendieuse d'utilisation.

Utilisation type :

Les méthodes de modélisation détaillée sont normalement utilisées dans le cadre d'évaluation d'impact de mesures avant leur implantation (design), pour l'optimisation de la conception d'un bâtiment et plus rarement pour la vérification des économies attribuables à des mesures suite à leur implantation. Dans ce dernier cas, le niveau de détail des résultats excède de beaucoup ce qui est requis dans ce type d'analyse, ce qui explique que les méthodes par régression sont normalement privilégiées.

CONCLUSIONS

La principale observation qui ressort de la revue de littérature, ainsi que de l'expérience que nous possédons en modélisation énergétique des bâtiments, est qu'une méthode unique d'analyse et de modélisation des bâtiments commerciaux ne peut être appliquée à grande échelle, dans le cadre d'audits énergétiques, sans introduire de sérieux problèmes de justesse des analyses ou encore d'efforts injustifiés.

Il s'avère essentiel d'adopter une procédure d'analyse progressive qui s'ajuste aux objectifs commerciaux, aux besoins techniques, à l'importance et à la complexité du bâtiment à traiter. Une méthode d'analyse énergétique unique pour tous les bâtiments ne constituera jamais la solution optimale. Ainsi, la méthode requise pour un petit bâtiment à vocation unique (ex. petit magasin de détail) ne devrait pas être la même que pour un grand centre commercial où coexistent un grand nombre de vocations. Dans de tels cas, des compromis souvent inacceptables doivent être faits. Si une méthode simple est utilisée, l'analyse du centre commercial risque fortement d'être erronée. Cependant, une approche détaillée dans le cas du petit magasin de détail serait trop longue et dispendieuse en fonction des enjeux commerciaux. Toutefois, si les enjeux commerciaux dominent largement les enjeux techniques, une méthode unique simplifiée peut être employée. Il s'agit dans ce cas d'une décision principalement commerciale et non technique. La valeur ajoutée d'une offre technique basée sur une simulation détaillée est difficile à percevoir pour un grand nombre de propriétaires de bâtiments. La démonstration de la justesse de la méthode détaillée comparativement à une approche simplifiée est potentiellement complexe. De plus, cette méthode n'offre pas, règle générale, une reproduction fidèle de la facture. Cette reproduction est souvent employée comme barème pour juger de la qualité d'une offre technique. Dans ce cadre opérationnel, la méthode détaillée sera perçue comme inadéquate, bien qu'elle soit probablement la seule à pouvoir saisir correctement le comportement normal du bâtiment et permettre un diagnostic de sa consommation.

D'autre part, le niveau d'expertise technique requis pour utiliser les différentes méthodes d'analyse diffère fortement. Une analyse par indices globaux et par régression linéaire peut être effectuée avec un minimum de formation, quoique l'interprétation des résultats exige une connaissance approfondie des hypothèses associées à ces modèles. Les méthodes d'analyse détaillée exigent une bonne connaissance des différents éléments traités par les modèles, tel le CVC, l'enveloppe du bâtiment, l'éclairage, les contrôles et tous les autres systèmes auxiliaires. De plus, afin d'obtenir des résultats fiables, il est essentiel d'avoir une bonne connaissance des hypothèses utilisées par ces modèles détaillés dans leur simulation des bâtiments et des systèmes.

Cette différentiation marquée de l'expertise technique requise pour utiliser les différentes méthodes d'analyse énergétique a comme conséquence fréquente l'utilisation de ressources spécifiques dans un processus d'analyse progressif (12). Ainsi, les traitements de premier niveau sont effectués par un groupe d'individus spécifiquement formés à l'utilisation de méthodes simplifiées. Ceux-ci peuvent alors effectuer une analyse complète pour tous les bâtiments répondant aux hypothèses et limites des méthodes de premier niveau (ex. critères statistiques). Si l'analyse de premier niveau démontre un potentiel mais que le bâtiment est trop complexe, ou l'enjeu trop grand, pour employer des

outils simplifiés, des analyses détaillées peuvent alors être effectuées par un groupe plus restreint d'individus spécifiquement formés dans l'utilisation de méthodes détaillées d'analyse.

Toutefois, peu importe l'outil de modélisation énergétique, la connaissance que l'utilisateur a des limites du logiciel sera toujours l'élément le plus déterminant dans la justesse et l'interprétation des résultats. Par exemple, dans le cas d'un modèle régressif, il est crucial que l'usager soit en mesure de déterminer si l'outil est applicable à un bâtiment donné et que les données de facturation employées ne contiennent pas d'entrées à rejeter (14). Dans le cas de logiciels de modélisation détaillée, l'utilisateur doit comprendre la manière dont fonctionnent réellement les systèmes du bâtiment ainsi que la manière dont ils sont traités dans la simulation. Dans les deux cas, l'expérience et la connaissance de l'usager détermineront la valeur des résultats.

RÉFÉRENCES

1- MacDonald, J. M., Wasserman, D. M., "Investigation of Metered Data Analysis Methods for Commercial and Related Buildings", ORNL/CON-279, Oak Ridge National Laboratory, May 1989

2- "An Expert System for Building Energy Consumption Analysis: Prototype Results", ASHRAE Transactions 1987, pp. 979 – 998 Haberl, J. S., Claridge, D. E.

3- Waltz, J. P., « Practical Experience in Achieving High Levels of Accuracy in Energy Simulations of Existing Buildings », ASHRAE Transactions: Symposia, AN-92-1-2

4- S. Katipamula and D. Claridge, USE OF SIMPLIFIED SYSTEM MODELS TO MEASURE RETROFIT SAVINGS, ASME Solar Engineering 1992, ESL-PA-92/04-06

5- "A Procedure for Calibrating the DOE-2 Simulation Program to Non-Weather Dependent Measured Loads, ASHRAE Transactions: Symposia, 1992, pp. 636 – 652, Bronson, D. J., Hinchey, S. B., Haberl, J. S., O'Neal, D. L.

6- "The Great Building Energy Predictor Shootout II: Measuring Retrofit Energy Savings, Thamilseran, S., Haberl, J. S.

7- Schuldt, M. A., Romberger, J.S., "Alternative Approaches to Baseline Estimation Using Calibrated Simulations", ASHRAE Transactions 1998,V104Pt 2

8- "Graphical Tools to Help Calibrate the DOE-2 Simulation Program, ASHRAE Journal, January, 1993, pp. 27 - 32 Haberl, J. S., Bronson, J. D., Hinchey, S. B., O'Neal, D. L.

9- "An Improved Procedure for Developing Calibrated Hourly Simulation Models, International Building Performance Simulation Association, 4th International Conference, August 14-16, 1995, Bou-Saada, T. E., Haberl, J. S.

10- D. Ruch and D. Claridge, A FOUR-PARAMETER CHANGE-POINT MODEL FOR PREDICTING ENERGY CONSUMPTION IN BUILDINGS, ASME Solar Engineering 1991, ESL-PA-91/03-03, 7 pages

11- D. Ruch, L. Chen, J. Haberl, and D. Claridge (Revised for ASME/JSE June 1993, new copies not yet available), A CHANGE-POINT PRINCIPAL COMPONENT ANALYSIS (CP/PCA) METHOD FOR PREDICTING ENERGY USAGE IN COMMERCIAL BUILDINGS : THE PCA MODEL, ASME Solar Engineering 1991, ESL-PA-91/03-02, 8 pages

12- " Baseline Calculations for Measurements and Verification of Energy and Demand Savings in a Revolving Loan Program in Texas, ASHRAE Transactions 1998, v.104, Pt.2, Haberl, J. S.; Thamilseran, S.; Reddy, A.; Claridge, D. E.; O'Neal, D. L.; Turner, W.D.

13- " Baselining Methodology for Facility-Level Monthly Energy Use - Part 1: Theoretical Aspects, ASHRAE Transactions 1997, v. 103, Pt. 2
Reddy, T. A., Haberl, J. S., Saman, N. F., Turner, W. D., Claridge, D. E., Chalifoux, A. T.

14- Sonderegger, R. C. , "A Baseline Model for Utility Bill Analysis Using Both Weather and Non-Weather-Related Variables", ASHRAE Transactions 1998, V. 104 Pt. 2, TO-98-12-2

15- "A Bin Method for Calculating Energy Conservation Retrofit Savings in Commercial Buildings, 9th Symposium on Improving Building Systems in Hot and Humid Climates 1994, May 19-20, 1994, Arlington, Texas
Thamilseran, S., Haberl, J. S.

16- Reddy, T.A., Haberl, J. S. Elleson, J.S., "Engineering Uncertainty Analysis in the Evaluation of Energy and Cost Savings of Cooling System Alternatives Based on Field-Monitored Data", ASHRAE Transactions: Symposia, SE-99-16-1

17- Reddy, T. A., Claridge, D.E., "Uncertainty of Measured Energy Savings from Statistical Baseline Models", HVAC&R Research, Vol.6, No. 1, January 2000

18- Rable, A., Norford, L, Spadaro, J., "Steady State Models for Analusis of Commercial Building Energy Data"

19- Rabl, A., Rialhe, A., « Energy Signature Models for Commercial Buildings: test with measured data and interpretation », Energy and Buildings, 19 (1992), pp.143-154

20- D. K. Ruch, J. K. Kissock, and T. A. Reddy, MODEL IDENTIFICATION AND PREDICTION UNCERTAINTY OF LINEAR BUILDING ENERGY USE MODELS WITH AUTOCORRELATED RESIDUALS, 1993 Proceedings of the ASME-ASES-SED International Solar Energy Conference, ESL-PA-93/04-03

SIMULATION OF RESIDENTIAL HVAC SYSTEM PERFORMANCE

Iain S. Walker, Jeffrey Siegel and Gwladys Degenetais
Lawrence Berkeley National Laboratory
Berkeley, California
ISWalker@lbl.gov JASiegel@lbl.gov

ABSTRACT

In many parts of North America residential HVAC systems are installed outside conditioned space. This leads to significant energy losses and poor occupant comfort due to conduction and air leakage losses from the air distribution ducts. In addition, cooling equipment performance is sensitive to air flow and refrigerant charge that have been found to be far from manufacturers specifications in most systems. The simulation techniques discussed in this paper were developed in an effort to provide guidance on the savings potentials and comfort gains that can be achieved by improving ducts (sealing air leaks) and equipment (correct air-flow and refrigerant charge). The simulations include the complex air flow and thermal interactions between duct systems, their surroundings and the conditioned space. They also include cooling equipment response to air flow and refrigerant charge effects. Another key aspect of the simulations is that they are dynamic - which accounts for cyclic losses from the HVAC system and the effect of cycle length on energy and comfort performance.

INTRODUCTION

To field test the effect of changes to residential HVAC systems requires extensive measurements to be made for several months for each condition tested. This level of testing is simply impractical due to cost and time limitations. Therefore the Energy Performance of Buildings Group at LBNL has developed a computer simulation tool that models residential HVAC system performance. This simulation tool has been used to answer questions about equipment downsizing, duct improvements and climate variation so that we can make recommendations for changes in residential construction and HVAC installation techniques that would save energy, reduce peak demand and result in more comfortable homes. Although our study focuses on California climates, the simulation tool could easily be applied to other climates.

This paper summarizes the simulation tool and discusses the significant developments that allow the use of this tool to perform detailed residential HVAC system simulations. The simulations have been verified by comparison to measured results in several houses over a wide range of weather conditions and HVAC system performance. After the verification was completed, more than 350 cooling and 450 heating simulations were performed. These simulations covered a range of HVAC system performance parameters and California climate conditions (that range from hot dry deserts to cold mountain regions). The results of the simulations were used to show the large increases in HVAC system efficiency that can be attained by improving the HVAC duct distribution systems and by better sizing of residential HVAC equipment. The simulations demonstrated that improved systems can deliver improved heating or cooling to the conditioned space, maintain equal or better comfort while reducing peak demand and the installed equipment capacity (and therefore capital costs).

This study concentrated on the extreme location for HVAC systems: in the attic (where it is hot during the cooling operation and cold during heating operation). This is the most difficult location to model because the attic has extreme diurnal temperature changes due to solar radiation and is sensitive to other weather conditions because of high ventilation rates. Other more thermally stable duct locations (such as crawlspaces and garages) will be studied in future work.

SIMULATION TOOL OUTLINE

The REGCAP (short for REGister CAPacity) model was developed because existing models of residential HVAC system performance either have too many simplifying assumptions (e.g., proposed ASHRAE Standard 152P, ASHRAE (2000)), or do not adequately model the ventilation, thermal and moisture performance of the ducts and the spaces containing ducts. The attic thermal and air flow elements were developed from existing models outlined previously by Wilson and Walker (1991 and 1992). The attic ventilation and thermal model has been discussed in Forest and Walker (1993a) and (1993b). These models of ventilation and heat transfer, excluding the ducts,

were verified with extensive field measurements. A key attribute for the REGCAP simulation tool that makes it unique is that the ventilation air flow rates are calculated from building envelope leakage parameters, weather data and calculations of wind shelter effects, rather than requiring these air flow rates to be known by the user of the simulation. Previous studies discussed in the above references showed how the capability of calculating attic air flow rates is essential in determining the attic air temperatures, which in turn is very important when determining the HVAC system losses.

The model does not explicitly include any moisture transport phenomena. This is mainly due to the lack of verified models of moisture performance for buildings in general and specifically, those that can be used based on the simple information available for a house. For example, we could not find a simple verified model for air conditioner moisture performance (particularly one that would include the transient effects required in our modeling). Although the attic model has the capability to determine the moisture content of the attic air based on outdoor, indoor and attic wood conditions (Forest and Walker (1993a) and (1993b)), there is no equivalent model for indoor air moisture, mostly due to large unknowns in the hydroscopic performance of the house furnishings and the large impact occupants have on indoor moisture. In addition, the houses tested for verification purposes were in dry climates.

The air flow modeling in REGCAP combines ventilation models for the house and attic with duct, register, and leakage flows using a mass balance of air flowing in and out of the house, attic and duct system. The thermal modeling uses a lumped heat capacity approach so that transient effects are included. The ventilation and thermal models interact because the house and attic ventilation rates are dependent on house and attic air temperatures. Also, the energy transferred by the duct system depends on the attic and house temperatures.

The equipment model for REGCAP (Proctor (1999)) is based on manufacturers' performance data. The capacity and power consumption change with the outside weather conditions, flow rate across the evaporator coil, and the return air conditions. Additional information regarding air conditioner performance changes due to incorrect system charge and system air flow have been adapted from laboratory data (Rodriguez et al. (1995)). The output from the airflow and thermal models are used together with weather data to determine the air conditioner performance. For example, the capacity of the air conditioner is decreased as the outdoor temperature increases, and refrigerant change and air flow across the evaporator decrease. The temperature change across the cooling coil is determined from the volumetric flow rate through the coil (the system fan flow) and the calculated capacity of the equipment. Due to the limited data available and the possible changes in equipment performance for specific A/C units the equipment performance algorithms are as simple as possible and assume that the various effects combine independently. Field measurements on houses with a range of systems in different climates have been used to verify the predictive ability of the model (Siegel et al. (2000)).

The thermal model uses a lumped heat capacity approach in which the attic, house and HVAC system are split into 16 nodes (plus the outside conditions and the equipment capacity). . These nodes are illustrated in Figure 1. Heat is transferred between the nodes by air motion (for the air nodes), convection (between air and surfaces), radiation (between surfaces in the attic, solar effects and night time exterior surface cooling) and conduction (between nodes in contact with each other). Two attic surfaces form the two pitched roof decks and they are important to allow for differential solar heating depending on roof orientation. The attic gable ends are lumped together in the end walls.

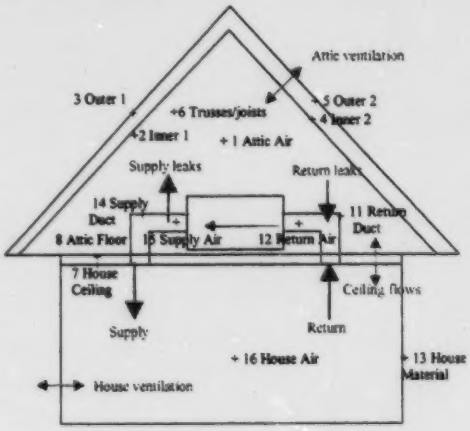

Figure 1. Nodes for thermal model

The model is able to use single nodes for the supply and return duct branches because the all the supply and all the return ducts are in the same space: the attic. If some ducts were in other locations (e.g., a crawlspace) then additional nodes would be required to account for heat transfer to these other spaces. The use of a single node per duct location does is not a large source of

uncertainty because the temperature changes within the supply or return ducts are smaller than the other temperature differences active in the heat transfer calculations. As the verification results show, a single modeled supply temperature air temperature is very close to the average of the measured supply temperatures. This single node approach has also been successfully used by many other researchers (e.g., ECOTOPE (1997)) and in a draft ASHRAE Standard for thermal distribution system efficiency (ASHRAE (2000)).

In order to investigate the effects of system cycling, equipment capacity and alternative thermostat settings, the timestep for the simulations shown here was set to one minute. Shorter timesteps produce too much computational burden for no significant improvement in time response and longer timesteps are too coarse to differentiate the detailed system performance changes (e.g., the changes in cyclic behaviour for reduced capacity systems).

To reduce the input data burden, REGCAP uses simple correlations based on field measurements in attics to correlate the attic floor area and roof pitch to determine the geometry used in the attic heat transfer calculations and the thermal mass of the attic wood.

The attic surfaces experience both natural and forced convection. The forced convection is based on empirical relations developed from standard Nusselt relationships and linearized (Ford (1982)) over the range of temperatures seen in residential buildings. The velocities for exterior surfaces are based on the exterior wind speed at eaves height, and the interior velocities are based on the ventilation air flows and the size of holes through which the ventilation air passes. This assumption is physically more realistic and gives higher velocities for attic interior surfaces than the traditional plug flow assumption used by Ford (1982) and Burch and Luna (1980). Similarly, the natural convection coefficient uses the same length scale and a standard Nusselt relationship (Holman (1981)). Fortunately, changes in the heat transfer coefficient due to surface orientation do not significantly affect the attic heat transfer and a coefficient based on a single orientation can be used. The total heat transfer coefficient is determined from the cube root of the sum of the forced and natural heat transfer coefficients cubed. This makes the larger of the two coefficients most dominant, whilst maintaining a smooth transition from one to the other. For the house the convection heat transfer coefficient is fixed at 7 W/m^2K. This value is based on the correlation given in ASHRAE Fundamentals, Chapter 3 (ASHRAE (1997)) that is not very sensitive to internal air flow velocities.

REGCAP uses a simple single node/zone model for estimating house loads because the model is focussed on HVAC system performance rather than building envelope performance. In addition, without detailed house and site information. a more complex house thermal model was not justifiable.

For air flows, the house and attic are both treated as single zones. Most attic spaces are of open construction and a single zone is a good assumption. Houses tend to be compartmentalized by interior partitions and if doors are closed between rooms the house will have several linked interior zones. If we were interested in predicting heat and air movement for individual rooms, then this would be a concern, but when determining overall values for the whole house the single zone approach is probably adequate. In addition, the extra information on the flow resistance of all the flow pathways between all the rooms of the house is almost impossible to determine - so the required input information for a more complex model is generally unknown. One significant aspect of the single zone assumption is that it ignores heat transfer through the ducts when the air handler is off that is transported by air flow through the ducts from room to room. This is generally not a problem for this study because it is a very small part of the load for the whole house. Some simple calculations show that the room-to-room flows through attic ducts contribute less than 100 W to the house load. Note that REGCAP does include air flows (and the associated heat transfer) between the house and the attic through the duct leaks when the air handler system is off.

FIELD VERIFICATION

To validate the REGCAP simulations, this study used measured data from three different sites: Palm Springs, Sacramento and Las Vegas. These homes have an average floor area of 1500 ft^2 (140 m^2) and have ducts located in the attic. Other houses used to validate REGCAP have ducts brought in to conditioned space and are discussed in Siegel et al. (2000).

The comparisons between measured and predicted results were examined for the house, attic, supply, and return air temperatures. In general, REGCAP gives temperatures close to the measured values (typically within ± 2°C (± 3.6°F)). The equipment model predicts power consumption and capacity very closely for all sites (within 4% of measured values). The differences between measured and predicted values are mainly due to model simplifications and do not significantly change the building load or the predicted HVAC system performance.

House temperature: The average absolute difference between the simulated and the measured data was in the range of 1 to 2 °C (2 to 4°F). Observations of the simulation results and some additional parametric analyses have shown that these differences are mainly due to the simplifications regarding coupling of house thermal mass to the house air, and under-prediction of solar radiation effects.

Attic temperature: The simulation results show average differences of about 3°C (5°F) between measured and predicted temperature. This is a reasonable difference given the highly variable attic temperatures. The simulations are good at reproducing the large diurnal fluctuations in attic temperatures, as shown in Figure 2. The main reasons for the differences are poor estimates of exterior radiation effects (solar gains during the day and radiative cooling at night). This hypothesis is confirmed by the study of other sites for which measured data are lower than predicted data in the morning before sunrise and higher after sun-rise. Factors such as cloud cover and the spectral emissivity and absorptivity of the roof material are not well known and this uncertainty in model input contributes to these differences.

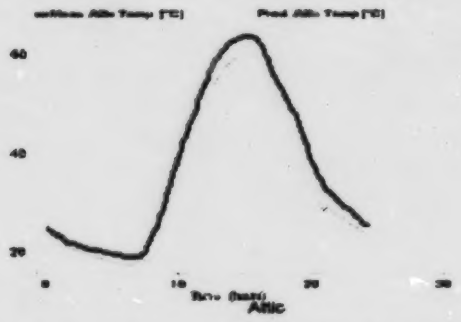

Figure 2. Comparison of measured and predicted attic air temperature

The simulations and measured data show similar variations in attic temperature due to duct system operation. As the system cycles, it cools the attic air when the cooling system is on. The attic air then warms up when the system is off (this can be seen in Figure 4). This cycling shows how the duct losses are conditioning the attic rather than the house. A system with no duct losses would not show this cycling of attic temperature.

Return Duct air: The return duct air temperature agreement is very good when the air handler is on. The return duct air temperature is close to indoor conditions and is dominated by the indoor air flow into the return due to air handler operation. When the air handler is off, the predicted temperatures are higher than the measured results.

Supply duct air: Figure 3 shows that the Supply duct air has the same behavior as return duct air, with good agreement when the air handler is on but not when it is off. The high temperatures for the supply and return duct simulations with the air handler off are due to strong coupling to the hot attic air temperature and radiation exchange with the interior attic surfaces. In addition, any air flows from room-to-room through ducts when the air handler is off will cool the duct air and these multi-zone effects are not taken into account in the simulation. REGCAP only calculates the flow of air passing from the attic to the house or from the house to the attic through duct and ceiling leaks. It should be noted that these errors when the air handler is off do not affect the results when the air handler turns on, and do not have a significant effect on the overall building load or system losses. With the air handler on, the heat transfer is dominated by the air handler flows and equipment operation.

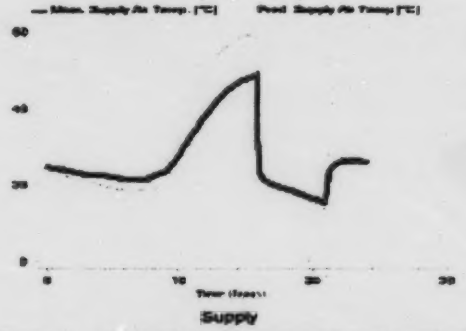

Figure 3. Comparison of measured and predicted supply air temperatures.

SIMULATING IMPROVED HVAC SYSTEMS

REGCAP was designed to answer questions about the effect of heating and cooling system inefficiencies on system performance. Specifically, the goals of this research were to answer the following questions:

1. What are the energy and comfort penalties associated with inefficient heating and cooling systems in California climates?
2. How much does correcting those efficiencies improve system performance?

3. Are there performance penalties associated with downsizing (or, more accurately, rightsizing, equipment)?

In order to answer these questions, some performance parameters need to be defined.

The two **comfort** related issues studied are: **pulldown time** and **Tons At the Register**. A common operating strategy used to reduce energy consumption is to turn off the air conditioning system during the day when the house is unoccupied. The **pulldown time** is the time required to cool the house after it has heated up during the day. A short pulldown time means that the house is comfortable sooner, which is desirable for the occupants. The power delivered to the conditioned space via the register is called **Tons At the Register (TAR)** (although this is a misnomer for heating systems, it is retained for convenience). Higher TAR implies more energy delivered to the conditioned space. TAR is used as a comfort parameter because it changes the occupants perception of cooling system performance and also effects consumer expectations of how much heating or cooling the system should provide (as discussed further in Walker et al. 1998).

This study evaluates the energy related issues of **system performance** by evaluating **duct efficiency, equipment efficiency, total HVAC efficiency, peak power** and **total energy**. The **total energy** represents the energy consumed during the 24-hour period simulation. The three efficiencies are defined as follows:

Equipment efficiency = Equipment Output Capacity / Power Consumption

Duct efficiency = TAR / Equipment Output Capacity

Total HVAC efficiency = TAR / Power Consumption

Cooling simulations were run minute-by-minute for 24 hour periods corresponding to a design day. Weather data for a whole year were searched for a day that represented a design day (99%/1% design conditions from ASHRAE Fundamentals (1997)). The heating simulations were run for 36 hours. The additional 12 hours allow a full night of simulations (when heating loads are highest). The input weather data were the hourly weather data developed by the California Energy Commission for use in residential energy calculations (CEC (1998)). These weather data include all 16 climate Zones for the state of California. The cooling system simulations were performed for climate zones from 8 to 15 because other zones do not require residential cooling. The heating system simulations were performed for all of the 16 climate zones. The hourly weather data include the solar radiation, outdoor temperature, outdoor humidity ratio, wind speed, wind direction and the atmospheric pressure. The one-hour data were linearly interpolated down to one minute for the simulations.

The input data for the house and attic were based on a typical California house defined by the California state energy code for new residential buildings (CEC 1999) and field observations of residential attics by the authors. The house is a 164 m^2 two-storey house with the system in the attic. The characteristics of the house, attic and system are given in more detail in Degenetais et al. (2001). Four systems were simulated:

- **Base case** - This case describes an average new house in California, with duct leakage of 22% of air handler flow (split evenly between supply and return ducts), 85% of correct refrigerant charge and air handler flow, duct surface area of 27% of floor area, nominal R4 duct insulation, and a 4 ton air conditioner.
- **Poor case** - this case describes a below-average house in California. Duct leakage is increased to 28% and charge reduced to 70%,
- **Best case** - this case describes an average new house in California that has been improved by duct sealing (to 12%), refrigerant charge addition (to 100%), and correction of air handler flow.
- **Best resized** – this is the best case with a properly sized air conditioner according to *Manual J* and *Manual S* (ACCA (1986, 1992)). For cooling, this system has one ton less capacity and for heating the capacity reduction is also 25%. The air flow and duct surface area are also reduced by 25%.

RESULTS

An example of the temperatures generated by the simulations are shown in Figure 4. This figure clearly shows the effect of solar gains on daytime heating of the attic. The cycling behavior of the cooling system can be seen in the large temperature variations for supply air and smaller variations for house air. In addition, the cooling losses from the duct system are illustrated by the cyclic fluctuations in attic temperature. These detailed simulation results have been analyzed in order to determine answers to focus on comfort and energy related issues.

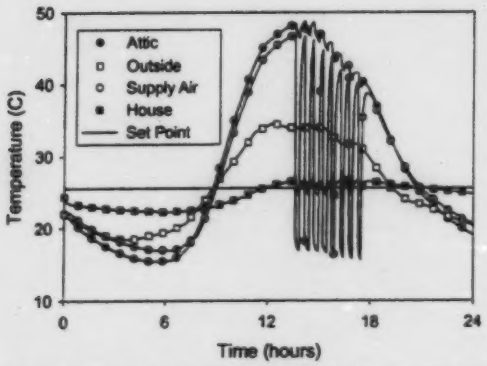

Figure 4. Example of predicted REGCAP temperatures for a base case system in Climate Zone 8.

In the discussion of the cooling simulations, the results are shown for climate zone (CZ) 8 and climate zone 15, which are respectively the mildest (32°C design temperature) and hottest (43°C design temperature) cooling climates. Other climate zones give results between these two extremes. Because the focus of this study was on potential reductions in electricity consumption for residential cooling and for brevity, the heating system results are only discussed briefly.

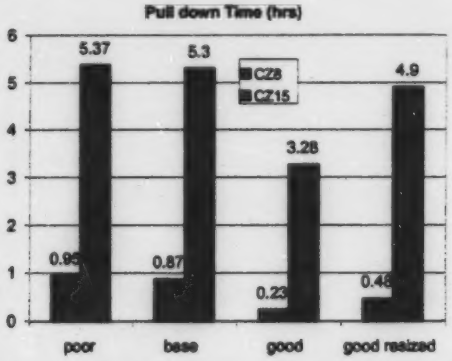

Figure 5. Climate and system dependence of the time required to cool a house (pulldown time)

Climate strongly affects pulldown time, as shown in Figure 5, with less than an hour required to control the indoor temperature in mild climates, but more than five hours required in the hottest climate. Because of the short pulldown times in CZ 8, the 15 to 30 minute differences between the systems are not important to most homeowners. However, in CZ 15 the **good** system takes two hours less to achieve a comfortable indoor temperature than the **base** and **poor** systems. The **good resized** system requires a longer pulldown time then the **good** system, but is still better than the **base** system.

For systems with a long pulldown time, a homeowner is likely to operate the system such that the air conditioning is turned on at an appropriate time to have a comfortable house temperature at 5 p.m. or at 6 p.m. Additional REGCAP simulations were performed to determine the turn on times required for CZ 12 and for the **base** and **good resized** systems only. This procedure is iterative because we cannot know in advance when to turn a system on to achieve the desired temperature at a fixed time. The good resized system can be turned on half an hour later (at 3:15 rather than 2:45) to achieve the same indoor conditions at 5:00 p.m. This causes reduced electricity use during the afternoon peak period.

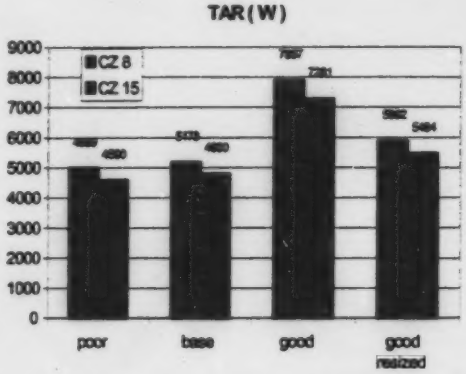

Figure 6. Changes in TAR with climate and system performance

Figure 6 illustrates the range of TAR calculated in the simulations. The **poor** system delivers only 60% of the TAR of the **good** system - the rest being lost because of poor ducts and equipment. The **good resized** system is able to deliver more TAR than the larger **base** system. The difference between the climates is due to the increased ambient temperatures in CZ 15 that increase duct losses and reduce air conditioner capacity. In all cases the TAR is substantially less than the nameplate capacity of the equipment that is four tons or about 14 kW (or 3 tons (10.5 kW) for the **good resized** system). Even the **good** system only delivers about half the nameplate capacity. This is due to the combination of duct losses, poor equipment performance at elevated ambient temperatures and overstating of equipment capacity by manufacturers. For the base and poor systems, the capacity is further reduced by low air

handler flows and low refrigerant charge. The discrepancy between TAR and nameplate capacity is also discussed in Siegel et al. (2000)

The duct efficiency increases as the systems are improved, from about 50% for a poor system to 70% for good systems. The remaining 30% of duct losses can be reduced if the HVAC equipment and ducts are brought inside conditioned space (see Siegel et al. (2000)). The higher duct efficiency implies reduced losses and more of the equipment output going into the conditioned space.

For utilities, the reduced power consumption for resized systems reduces peak demand (currently a key issue in California's power crisis). In addition, the improved efficiency of the **good** systems leads to increased diversity and reduced utility system peak load. The cost to the homeowner for these systems depends on the overall energy consumption. The energy consumed for the design day is shown in Figure 7. The **poor** and **base** systems use about 35% more energy compared to a **good** system. There is no significant difference in energy consumption between the **good** and the **good resized** system.

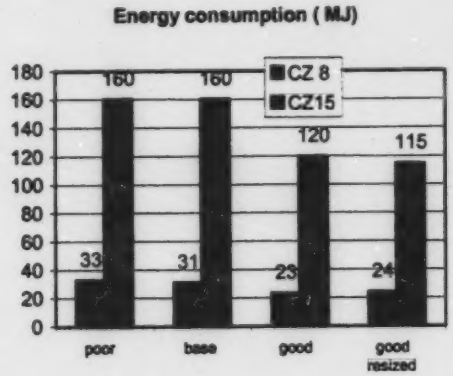

Figure 7. Energy consumption changes with climate and system performance

The results for heating systems are similar to those for cooling, although performance gains are more moderate. Correct air handler flow and less leakage (a **good** system) results in a 10 % improvement in register capacity and a 10 % increase in duct efficiency. It also decreases the energy consumption by 6% in comparison with the **base** system. A **poor** system loses 5% of the register capacity and duct efficiency in comparison with the **base** system. Its energy consumption is about the same as the **base** system energy consumption. In addition to the 25% power (peak) consumption reduction due to resizing, a **good resized** system consumes between 10 % and 12 % less energy than a **base** system for almost all climates and duct locations.

CONCLUSIONS

The REGCAP simulation was developed to examine the performance of residential HVAC systems. REGCAP was developed to be able to use readily available data for a house rather than requiring the user to supply generally unknown input parameters (e.g. attic ventilation rates and temperatures). Comparison to field measurements shows that REGCAP is a good predictor of house and duct system performance, during heating or cooling system operation. When the systems are not operating, the simulations do not match the measured data as well for HVAC system air temperatures, but the errors do not contribute significantly to the energy consumption or system performance results.

Simulations were performed for a typical California house in 16 California climate zones. The typical (**base**) California system used about 35% more energy than a **good** or **good resized** system on a design day for cooling, and about 10% more for heating.

The **good** and **good resized** systems also have significant improvements in thermal comfort. They are able to reach a comfortable indoor temperature hours before typical systems in hot climates. The **good** system is able to deliver more than twice as much cooling to the conditioned space as a base system and still delivers more cooling with a 25% smaller air conditioner.

A properly sized system (about 25% capacity reduction) reduces the power consumption and therefore peak demand. Even though these correctly sized systems have a smaller capacity, they can still provide better or equal comfort than an oversized system. Better comfort is achieved by supplying a higher register capacity and having a shorter pulldown time. For houses operating in pulldown mode (where the house heats up during the day), these correctly sized air-conditioning systems can be turned on later in the day and still achieve the setpoint temperature by the time occupants return to the house in the evening.

ACKNOWLEDGEMENTS

This study was sponsored by the California Institute for Energy Efficiency and the Pacific Gas and Electric Company. In addition the authors would like to thank the following LBNL staff members for their

contributions: Jennifer McWilliams, Darryl Dickerhoff and Craig Wray.

REFERENCES

ACCA. (1986), *Manual J - Load Calculations for Residential Winter and Summer Air Conditioning.* Washington D.C.; Air Conditioning Contractors of America.

ACCA. (1992), *Manual S - Residential Equipment Selection.* Washington D.C.: Air Conditioning Contractors of America.

ASHRAE. (1997), Handbook of Fundamentals, ASHRAE, Atlanta, GA.

ASHRAE. (2000), Standard 152P– Method of test for determining the Design and Seasonal Efficiencies of Residential Thermal Distribution (Second Public Review Draft), ASHRAE, Atlanta, GA.

Burch, D.M. and Luna, D.E. (1980). A Mathematical Model for Predicting Attic Ventilation Rates Required for Prevention of Condensation on Roof Sheathing. *ASHRAE Trans.* 86 201., ASHRAE, Atlanta, GA.

CEC. (1998), *RESACM Weather Data.* California Energy Commission, Sacramento, California.

CEC. (1999), *Residential Manual For Compliance with California's 1998 Energy Efficiency Standards.* California Energy Commission, Sacramento, California.

Degenetais, G., Walker, I.S. and Siegel, J.A. (2001), *Sizing and Comfort Improvements for Residential Forced-Air Heating and Cooling Systems.* LBNL 47309.

ECOTOPE (1997), Development of a Practical Method for Estimating the Thermal Efficiency of Residential Forced Air Distribution Systems, Electric Power Research Institute Report TR-107744.

Ford, J.K. (1982), *Heat Flow and Moisture Dynamics in a Residential Attic.* PU/CEES Report # 148, Princeton University.

Forest, T.W. and Walker, I.S. (1993a), *Attic Ventilation and Moisture.* Canada Mortgage and Housing Report. March 1993

Forest, T.W. and Walker, I.S. (1993b), "Moisture Dynamics in Residential Attics". *Proc. CANCAM '93,* Queens University, Kingston, Ontario, Canada, June 1993.

Holman, J.P. (1981), *Heat transfer- 5th Edition.* Mc Graw-Hill.

Proctor, J. (1999), Air Conditioning Equipment Model. Personal Communication, March 1999.

Rodriguez, A.G., O'Neal, D.L., Bain, J.A., and Davis, M.A. (1995), *The Effect of Refrigerant Charge, Duct Leakage, and Evaporator Air Flow on the High Temperature Performance of Air Conditioners and Heat Pumps.* Energy Systems Laboratory report for EPRI, Texas A&M University.

Siegel, J.A., Walker, I.S., and Sherman, M.H. (2000), Delivering Tons to the Register: Energy Efficient Design and Operation of Residential Cooling Systems. *Proceedings of the 2000 ACEEE Summer Study on Energy Efficiency in Buildings,* 1 295-306. American Council for an Energy Efficient Economy. (LBNL 45315)

Walker, I.S., J. Siegel, K. Brown, M.H. Sherman. (1998), Saving Tons at the Register. *Proceedings of the 1998 ACEEE Summer Study on Energy Efficiency in Buildings,* 1 367-385. Washington D.C.: American Council for an Energy-Efficient Economy. (LBNL 41957).

Wilson, D.J. and Walker, I.S. (1991), *Passive Ventilation to Maintain Indoor Air Quality.* University of Alberta Department of Mechanical Engineering Report #81. University of Alberta, Edmonton, Alberta, Canada.

Wilson, D.J., and Walker, I.S. (1992), "Feasibility of Passive Ventilation by Constant Area Vents to Maintain Indoor Air Quality". *Proc. Indoor Air Quality '92, ASHRAE/ACGIH/AIHA Conference.* San Francisco. October 1992.

AIRTIGHTNESS TESTING AND AIR FLOW MODELLING OF A THREE-UNIT MULTIFAMILY BUILDING

Sebastiano DePani, P.Eng., M.A.Sc.
GES Technologies
Montreal
sdepani@ges-int.com

Paul Fazio, Ph.D
Concordia University
Montreal
fazio@vax2.concordia.ca

ABSTRACT

Older multifamily buildings offer a great opportunity for energy savings because they are typically poorly insulated and not airtight. Weatherization programs, such as Hydro-Quebec's *ISOLACTION* program, have recently targeted this building stock. These programs and the emergence of the renovation market have created a need for practical tools that can be used by the building industry to evaluate the impact of retrofits on energy and ventilation.

This paper presents a ventilation case study for a three-unit multifamily building. Both the external and the inter-unit air leakage characteristics of the building were obtained using a single-fan blower door method. This method produces significantly more valuable data than is currently obtained with the whole building depressurization technique. A steady state ventilation model was used with the in-situ test results to investigate the outdoor air distribution and the impact of exhaust ventilation on a unit-per-unit basis.

INTRODUCTION

Background

Energy use in housing has been the focus of numerous research studies in Canada. So far, the majority of Canada's energy efficiency initiatives have focused on new construction. However, the emergence of the renovation market has shifted interest to the energy efficiency potential of existing housing. This potential was the focus of the recent Hydro-Quebec weatherization program called *ISOLACTION*, which was completed in 1998.

Approximately 1000 low-rise multifamily buildings in the Montreal region were retrofitted as part of the *ISOLACTION* program. The Montreal region was targeted because of its urban environment, which is significantly different from that of other large Canadian cities. A large proportion of the urban building stock in Montreal consists of two and three unit buildings constructed prior to 1970. A distinguishing feature of these dwellings is that individual units usually have separate entrances and civic addresses, as detached houses do.

ISOLACTION brought to light the need for practical methods and tools, which can be used to evaluate the impact of energy measures on ventilation. A sponsoring agency, such as Hydro-Quebec, is responsible for the impact of work on the overall building performance. Ventilation is of particular concern due to the obvious link with occupant heath. A program sponsor must ensure that the retrofit work does not lead to inadequate ventilation.

To gauge the impact of energy retrofits on ventilation for multifamily buildings, both the airtightness of the building shell and of partitions between units must be considered. The performance of ventilation systems, particularly exhaust fans, also depends on the airtightness of both the exterior shell and the interior partitions.

Originally developed as research tools, fan pressurization doors (blower doors) have proven their worth as practical and effective tools for the housing industry. The blower door consists of a heavy-duty fan, pressure and airflow meters, and a supporting frame (figure 1). They have been used extensively to test the airtightness of detached homes in programs and research studies sponsored by agencies such as Natural Resources Canada (NRCan), the Canadian Mortgage and Housing Corporation (CMHC) and Hydro-Quebec. However, blower door testing of multifamily buildings is not widespread.

Standard CAN/CSGB-149.10, *A Method for Testing the Airtightness of Buildings by the Fan Depressurization Method*, provides a methodology for determining the airtightness of the exterior envelope. Other standards include ASTM Standard E779-87, *Test Method for Determining Air Leakage by Fan Pressurization* and

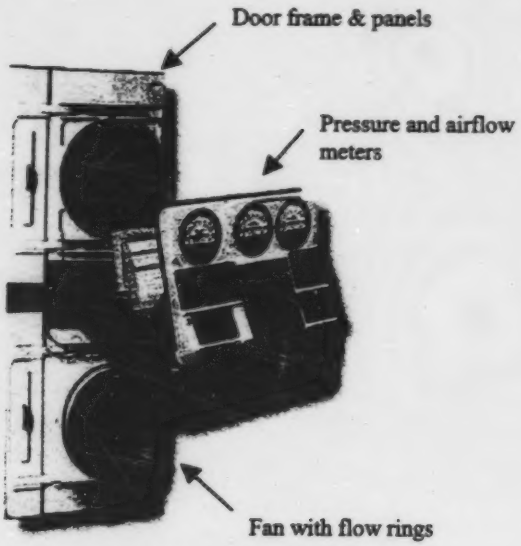

Figure 1. Retrotec Blower Door

ASHRAE Standard 119, *Air Leakage Performance for Detached Single-Family Residential Buildings*. These standards to not address the interior partitions of multifamily buildings. On a practical note, whole building depressurization of multifamily buildings is not cost effective within the scope of a weatherization program.

Several studies have focused on the measurement of interzonal and envelope air leakage in multi-unit buildings. Sheltair Scientific (1987) tested six different approaches for the R2000 Program and the British Columbia Home Builders Association. At the time of the report, a number of multifamily R2000 developments were under construction in British Columbia. Modera and Herrlin (1990) analyzed a two-fan pressurization technique for measuring the interzonal leakage in a multi-unit building. Love (1990) used a similar two-fan technique to test the airtightness of row houses in Calgary, Alberta. Blasnik and Fitzgerald (1992) present methods for diagnosing complex air leakage paths using blower door induced pressures. Tuluca and Sherman (1995) evaluated two single-fan methods and a two-fan method. This research focused on the applicability of these methods for New York State apartment buildings. DePani (1999) defined and evaluated three single-fan methods suitable for Montreal's multifamily building stock. The single-fan methods were benchmarked against a two-fan approach on four case study buildings. One of these compared favorably with the two-fan method.

Objectives

The objective of this paper is to present a ventilation case study for a low-rise multifamily building with three units, typical to Montreal's building stock. The paper aims to demonstrate how blower door test results can be used with a simple modelling tool to investigate ventilation as a function of outdoor temperature and wind speed, on a unit-per-unit basis.

METHODOLOGY

Single-fan Blower Door Method

The single-fan method used in testing the case study building was developed and tested by DePani (1999). The method can be used to test the three building configurations typical to Montreal low-rise multifamily buildings (figure 2).

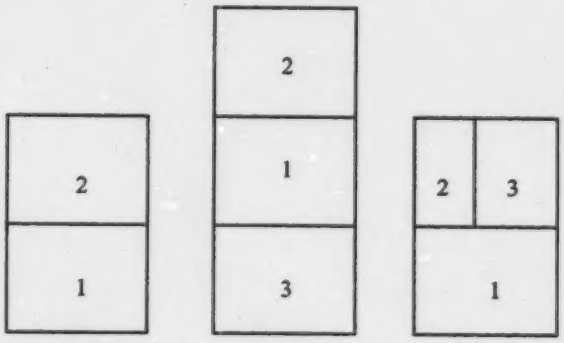

Figure 2 Typical Configurations for Montreal Low-rise Multifamily Buildings

The single-fan method uses a single blower door combined with pressure measurements in adjacent units to calculate the airtightness of the building envelope and of the interior partitions between units. Tests are performed with each unit depressurized in turn to 50 Pa pressure difference. Equations are obtained by balancing airflows through the exterior envelope and the interior partitions, using the power law airflow equation:

$$Q = CP^n$$

Where:

Q = airflow through the leakage path, l/s,
C = flow coefficient of the leakage path, l/(s*Pa^n),
P = pressure difference across the leakage path, Pa,
n = flow exponent of the leakage path, dimensionless.

The flow exponent is assumed to be 0.65, which is the value commonly used in industry for single point blower door tests. When fitting depressurization test data to buildings, the value of n generally lies between 0.6 and 0.7 (ASHRAE Fundamentals, 1993). It is assumed that the flow coefficient C does not vary with the leakage direction through a flow path (no directional valve effect). Current standards and blower door manuals do not specify the measurement of the directional valve effect when establishing the airtightness of buildings (Energy Conservatory, 1996).

The testing protocol for the single-fan method starts with the blower door installed in unit 1. The unit is depressurized to a pressure difference of 50 Pa and the change in pressure to the other units is measured (with respect to initial baseline pressures). The test is repeated with the blower door installed in unit 2 and then in unit 3. The protocol and the flow paths are illustrated in figure 3.

$$C_{x1}50^n + C_{12}P_{12}^n + C_{13}P_{13}^n = Q50_{Fan} \quad (1)$$
$$C_{x2}P_{x2}^n + C_{12}P_{12}^n = 0 \quad (2)$$
$$C_{x3}P_{x3}^n + C_{13}P_{13}^n = 0 \quad (3)$$

The 4th and 5th equations are obtained by balancing the flows in the unit with the blower door in tests B and C:

$$C_{x2}50^n + C_{12}P_{12}^n = Q50_{Fan} \quad (4)$$
$$C_{x3}50^n + C_{13}P_{13}^n = Q50_{Fan} \quad (5)$$

Equations 1 through 5 can be solved with linear algebra techniques to obtain the five unknown flow coefficients C.

The equivalent leakage area (ELA), normalized leakage area (NLA), liters per second at 50 Pa pressure difference (l/s50) and air change at 50 Pa pressure difference (ACH50) can be derived from the flow coefficients.

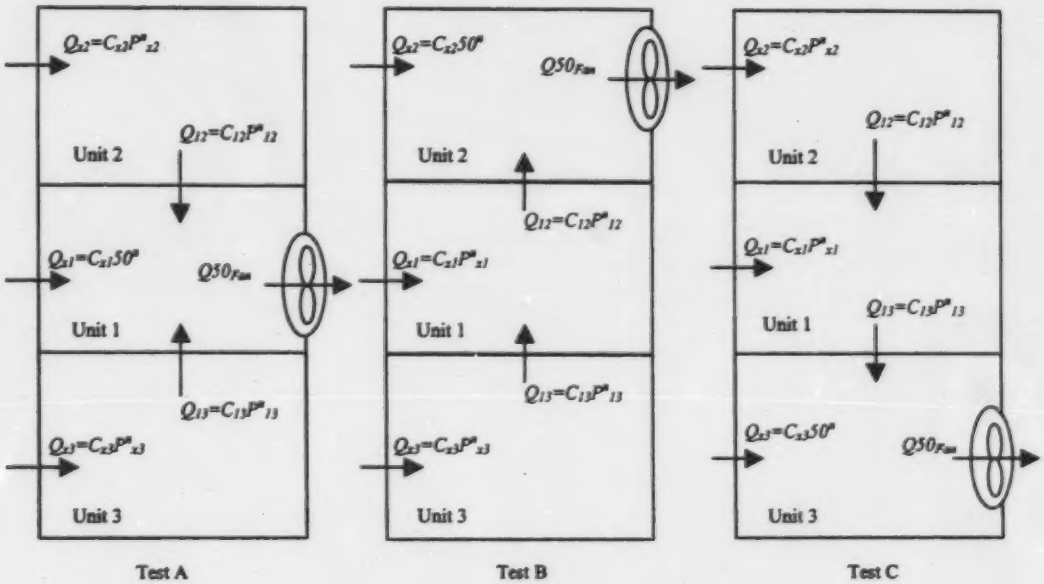

Figure 3 Single-fan protocol

Balancing the flows for units 1,2 and 3, for test A, gives us the following equations:

Computer model

A computer model was used in conjunction with the single-fan blower door test. Multi-unit airflow models are needed to analyze natural and mechanical ventilation rates on a unit-per-unit basis. Most existing airflow modelling tools were designed for research work and are not well suited for use by weatherization teams. The model presented in this paper has a simple graphical interface (figure 4), which requires limited data entry. With further development, this model could be used in-situ to evaluate ventilation in multifamily buildings.

The configuration shown in figure 4 has 3 units, one of which is a basement apartment. Air movement is modeled with 13 nodes. Inter-unit leakage occurs through one direct leakage path between the units. The basement unit is connected to the outside via leakage paths at ground level. The other units have four leakage paths on the exterior walls, two located at one third of the floor height and two located at two thirds of the floor height. The top unit has an additional leakage path through the ceiling. Half of the leakage paths face the wind and the other half are opposite the wind. Each unit also has an exhaust fan. The program solves a set of three non-linear equations with 3 unknowns (unit pressures), using the Newton Raphson iterative approach (Kreyszig, 1983).

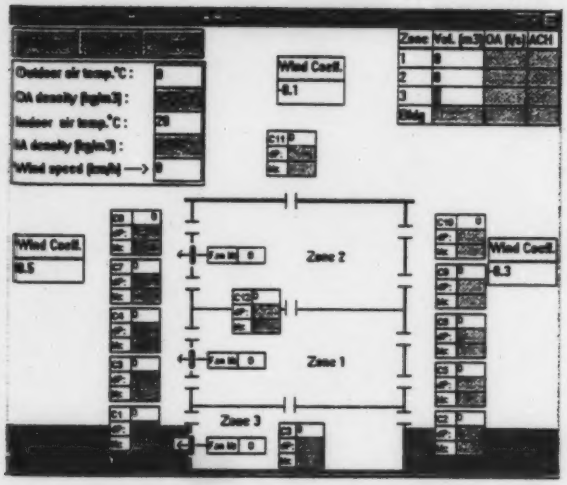

Figure 4 Multizone Airflow Model

CASE STUDY

Building description

The case study building is located at 8399 Dunant in Montreal. It is a semi-detached 3-unit building constructed in 1969 (figure 5). It contains one main unit, which occupies the ground floor and part of the basement. Another unit occupies the 2nd floor and a smaller 3rd unit is located in the basement. The floor areas, volumes and envelope areas are summarized in table 1.

Figure 5 Case Study Building

Table 1 Building Takeoffs

	Unit 1	Unit 2	Unit 3	Total
Floor Area (m^2):	170	135	50	355
Envelope Area (m^2):	165	248	35	448
Volume (m^3):	440	329	122	891

Single-fan blower door test results

The single-fan blower door method was used to obtain the flow coefficients *C*. These coefficients are presented in table 2, along with other derived data.

Table 2 Flow Coefficients and Derived Data

Leakage Path	C l/(s*Pa^n)	l/s50	ELA (cm^2)	ACH50
Exterior - Unit 1	101.2	1286	1808	10.5
Exterior - Unit 2	113.7	1446	2031	15.8
Exterior - Unit 3	30.6	389	547	11.5
Unit 1 - Unit 2	38.7	492	691	-
Unit 1 - Unit 3	26.2	333	467	-
Total Envelope	245.5	3121	4385	12.6

The results indicate that the building is quite leaky, with 12.6 air changes per hour at 50 Pa pressure difference. The top unit was the leakiest, which was expected since it is directly below the attic space. The results also show that the units are relatively well connected, meaning that air movement between units will have an important influence on ventilation.

SIMULATIONS

Simulations were performed to demonstrate how the blower door test results could be used with a computer model to provide information on the following relationships:

1. Outdoor air change as a function of outdoor temperature and wind conditions.
2. Outdoor air change following weatherization work, which reduces the air leakage through the roof.
3. Outdoor air drawn through the envelope of each unit by an exhaust fan installed in the top unit.

Simulations were carried out at outdoor temperatures of -20, -10, 0 and 10°C. Two wind conditions were simulated: calm (no wind) and light wind (10 km/h) conditions.

Leakage distribution

The blower door test data provides the flow coefficients of the exterior walls and interior partitions. However, the tests don't indicate how the leakage area is distributed within the units. Leakage distribution is important when modelling natural and mechanical ventilation because the pressure gradient due to stack and wind pressures is not constant. For the purposes of the simulations, the leakage area was distributed as follows:

- In unit 3 (basement), the exterior leakage area was split evenly between the two leakage paths to the outside.
- In unit 1 (first floor), the exterior leakage area was split evenly between the four exterior leakage paths to the outside.
- In unit 2 (2nd floor), half the exterior leakage area was located at the ceiling node, the remaining leakage area was split evenly between the four leakage paths on the exterior walls.

Simulation Results

The first set of simulations demonstrated natural ventilation trends on a unit-per-unit basis for the existing building (figures 6 and 7).

The second set of simulations demonstrated the impact of sealing the attic space (figures 8 and 9). A common retrofit used in the *ISOLACTION* program consisted of insulating and sealing the attic space with high-density cellulose fiber. In most cases, this technique reduced air leakage through the attic space by 85-95%. For the purposes of this study, it was assumed that the leakage area through the attic space was reduced by 90%.

A third set of simulations demonstrated the impact of a 50 l/s exhaust fan placed in unit 2 of the retrofitted building (figure 10). Exhaust fans are often used in these older buildings for ventilation purposes.

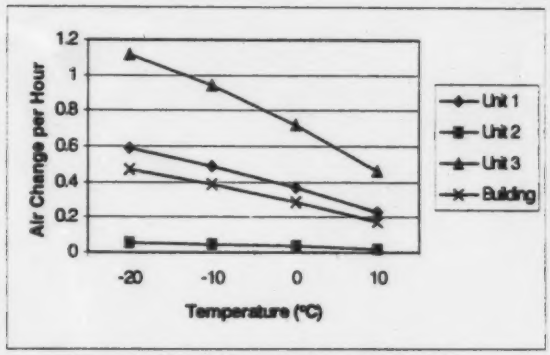

Figure 6 Natural Ventilation - No Wind

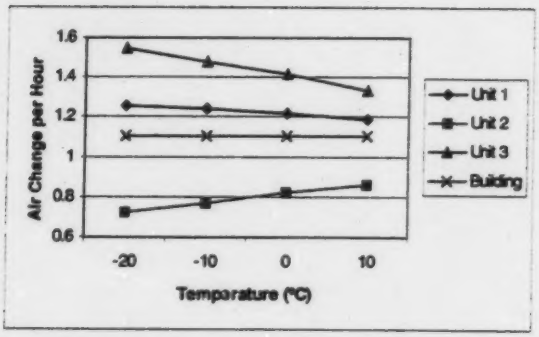

Figure 7 Natural Ventilation - 10 km/h Wind

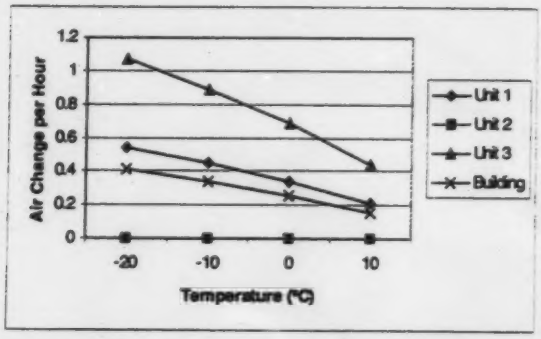

Figure 8 Natural Ventilation - Post-retrofit No Wind

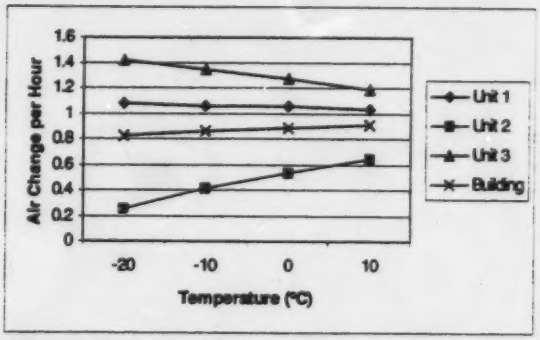

Figure 9 Natural Ventilation - Post-retrofit 10 km/h Wind

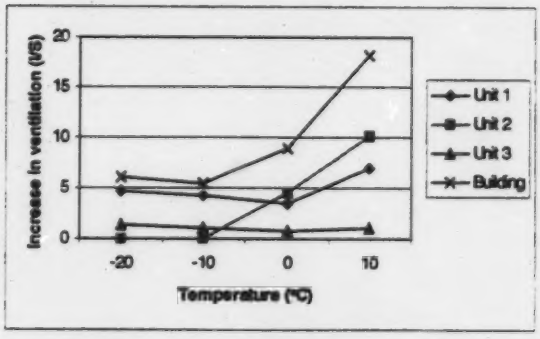

Figure 10 Increase in Ventilation with 50 l/s Exhaust Fan in Unit 2 - Post-retrofit No Wind

Discussion of Results

The key findings are summarized below:

- **A unit's location within the building will influence its ventilation rate.**
  Where units are relatively well connected, the stack effect will affect how outdoor air is distributed. In the absence of wind, ventilation rates for unit 2 were below the 0.35 ACH required by the National Building Code (figure 6).

- **The relationship between ventilation and outdoor temperature is influenced by the unit's location within the building.** With a 10 km/h wind, ventilation for units 1 and 3 decreases as outdoor temperature rises but the opposite occurs in unit 2. Ventilation rates converge as the outdoor temperature approaches the indoor temperature (figure 7).

- **Sealing the attic has an important impact on the outdoor air supplied to the top unit.**
  Weatherization work in the attic lowers the neutral pressure plane. In the absence of wind, unit 3 (top unit) experiences only exfiltration when the neutral pressure plane is lowered below the level of the leakage paths in the top unit (figure 8). Even with a 10 km/h wind, unit 3 may receive much less fresh air than the other units (figure 9).

- **For buildings with well connected units, exhaust fans are ineffective in bringing outdoor air to the top unit.** When the units of a building are well connected, as was the case with the case study building, exhaust fans draw little or no outdoor air directly through the envelope of the top unit. As the outdoor temperature approaches the indoor temperature, the exhaust fan draws more outdoor air into the building. With an outdoor temperature of 10°C, the exhaust fan draws only 10 l/s of additional outdoor air through the envelope of unit 2 and 18 l/s through the envelope of the entire building (figure 10).

CONCLUSIONS

This paper presented a case study where the leakage characteristics of both the exterior envelope and the interior partitions of a three-unit building were obtained with a single-fan blower door method. This method relies on airflow measurements using one blower door, combined with pressure measurements in adjacent units.

This paper also presented a graphical airflow model developed for multifamily building configurations typically found in the Montreal area. The model can be used with the results of the single-fan blower door test to investigate ventilation trends on a unit-per-unit basis. The model can also be used to study the impact of retrofit measures on natural ventilation, the need for mechanical ventilation and the potential for energy savings.

The simulation results showed that ventilation depends on both the exterior envelope and the interior partitions. In cases where the partitions are relatively leaky, the tendency is for the top floor unit to receive much less outdoor air then the other units. Even though the building-has-a-whole meets code requirements for air-change rate, the top unit may only receive air from adjacent units, leading to local indoor air quality problems.

ACKNOWLEDGEMENTS

The concepts presented in this paper were first developed by the authors as part of SIRICON activities in the *ISOLACTION* weatherization program.

REFERENCES

ANSI/ASHRAE Standard 119 (1988), *Air Leakage Performance for Detached Single-Family Residential Buildings*, American Society of Heating, Refrigeration and Air Conditioning Engineers.

ASHRAE Handbook of Fundamentals (1993), Chapter 23, American Society of Heating, Refrigeration and Air Conditioning Engineers.

ASTM Standard E779-87 (1991), *Test Method for Determining Air Leakage by Fan Pressurization*, ASTM Book of Standards, American Society of Testing and Materials, Volume 04.07.

Blasnik M., Fitzgerald J. (1992), *Pressure Diagnostics: Diagnosing Complex Air Leakage Paths*, Tech. Guide.

CSGB Standard 149.10-M86 (1986), *Determination of the Airtightness of Building Envelopes by the Fan Depressurization Method*, Canadian General Standards Board, Ottawa.

DePani (1999), *A Study on Single Blower Door Methods for Multifamily Buildings in Montreal*, M.A.Sc. Thesis, Concordia University

Energy Conservatory (1996), *Minneapolis Blower Door Operation Manuel*.

Feustal H. E. (1988), *Air Permeability Measurements in Multizone Buildings*, Energy and Buildings, Lawrence Berkeley Laboratory, LBL Report 26909.

Furbringer J.M., Roecker C., Roulet C-A (1988), *The Use of a Guarded Zone Pressurization Technique to measure the Air Flow Permeabilities of a Multi-zone Building*, Proceedings of 9th AIVC Conference, 1988.

Kreyszig E. (1983), *Advanced Engineering Mathematics", John Wiley & Sons, 5th Edition.*

Love J.A. (1986), "Airtightness Testing Methods for Multi-unit Housing", prepared for Canada Mortgage and Housing Corporation.

Love J.A. (1990), *Airtightness Survey of Row Houses in Calgary*, Air Change Rate and Airtightness in Buildings, ASTM 1067, American Society for Testing and Materials, Philadelphia.

Modera M.P., Herrlin M.K, "Investigation of a Fan-Pressurization Technique for Measuring Interzonal Airleakage", Air Change Rate and Airtightness in Buildings, ASTM 1067, American Society for Testing and Materials, Philadelphia, pp. 183-192, 1990.

Nylund P. (1981), *Tightness and its Testing in Single and Terraced Housing*, Air Infiltration Instrumentation and Measuring techniques, Proceedings of the First Air Infiltration Centre Conference, England, pp. 159-172.

Sheltair Scientific Ltd (1987), *Methods for Airtightness Testing of Multi-unit R2000 Housing*, prepared for the R2000 Program Administration and the Canadian Home Builders Association.

Tuluca A., Sherman M. (1995), *Simplified Multizone Blower Door Techniques for Multifamily Buildings*, New York State Energy Research and Development Authority and the U.S. Department of Energy, NYSERDA Report No. 95-16

DEVELOPING PROJECT MANAGEMENT AND QUALITY CONTROL APPROACHES FOR IMPROVING THE EE4 BUILDING SIMULATION SOFTWARE

Robert Calla, Phylroy Lopez, and Paul Wyndham-Wheeler
CANMET Energy Technology Centre
Ottawa, Ontario
rcalla@nrcan.gc.ca, plopez@nrcan.gc.ca, pwheeler@nrcan.gc.ca

ABSTRACT

In 1997, Natural Resources Canada (NRCan) developed a highly specialized building energy compliance-checking software called EE4. The need to release a better quality product and to make enhancements and maintenance of the EE4 software more efficient led to several initiatives on behalf of the CANMET Energy Technology Centre (CETC): the development of a detailed project management database to track the various types of work and their level of progress, the implementation of a coding standard, the incorporation of some software configuration management practices and the development of an automated set of testing procedures. These are the initiatives which are discussed in this paper.

INTRODUCTION

Complex building simulation software which are actively used to support energy efficiency programs can become a nightmare to maintain if you do not establish well thought out procedures and strategies for managing the product and improving its quality. This paper describes 4 major initiatives, which CETC incorporated in order to better manage the EE4 building energy compliance-checking software:

- Documenting and implementing formal procedures for tracking the project's progress and other related day-to-day maintenance activities.
- Adopting some software configuration management (SCM) practices.
- Adopting a coding standard.
- Moving towards better-structured testing procedures.

PROJECT MANAGEMENT INITIATIVES

There are different levels of maturity within any organization with respect to project management procedures. When CETC began work on the EE4 software, its level of application of project management procedures to the project was relatively immature.

During this initial phase, we had a highly informal process of requesting and tracking changes to the software. Our bug reporting procedure was (and still is) based on clients' e-mail and telephone-based reporting of problems to the project manager. Changes were then verbally requested by the project manager, based on these comments. They were however uncontrolled and the priority level attached to them was often vague. Two variations of the EE4 software were being supported; one which was used to demonstrate compliance with Canada's Model National Energy Code for Buildings (EE4 CODE) and the other for NRCan's Commercial Buildings Incentive Program (EE4 CBIP). English and French versions were supported for each. Separate project managers were managing EE4 CODE and EE4 CBIP at the time. If changes were required to any of these 2 software, the manager of the project in question would make the request to the programmer - sometimes unbeknown to the other manager. This informal method of requesting changes began breaking down when the number of change requests highly increased as the programs which EE4 supported increased in exposure. The programmer had no indication as to which tasks took priority and in some cases did not know all the required details concerning the requested changes. It was becoming apparent that a better process for handling these requests was needed.

The next phase consisted of developing a template file for documenting change requests. The file contained various types of information fields that were required to describe the problem and the required solution. The template allowed the user to specify which program and linguistic version of EE4 required the change. The communication level between the 2 project managers was also better than in the initial phase in that they now were deciding amongst themselves which tasks took priority. This was necessary as there was only one programmer conducting changes to both versions of

EE4 at the time. Each change request required that a new file be created with the template and submitted to the programmer. All files were stored in a folder on the programmer's local computer. However, no one else knew where they were located and neither did either project manager know what the level of progress was with respect to each task without directly approaching the programmer to enquire about it. Figure 1 shows a partial view of the template.

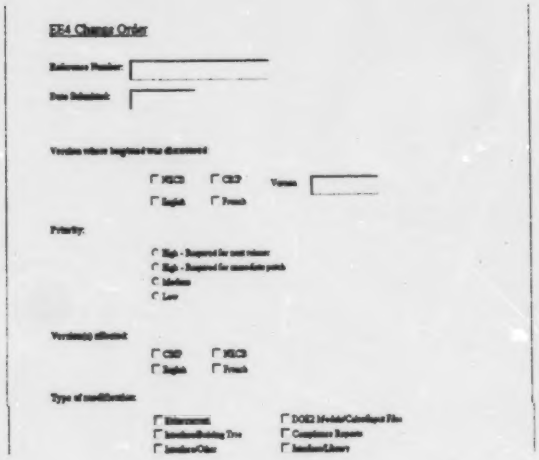

Figure 1: EE4 Change Request Template

The third phase consisted of developing a database to centrally store the data contained in the various files created using the template. Originally, the purchase of an off-the-shelf application was considered, but to allow us the flexibility to make changes as we progressed through various levels of our project management initiatives, it was decided to develop an in-house solution. A Canadian university's IT department provided us with a model database they had devised to track problems related to one of their software. They developed a format that was easy to use and modify and which was an acceptable solution for the multiple platforms they were running off of.

Before actually jumping into the development of the database, additional care was taken in exploring what other items should be included in the change request forms. Once this was finalized, a highly formal database was compiled and the information was transferred to it from the various "loose files". Figures 2 and 3 show the database we are currently using to create and track change requests.

The project manager determines which requests actually make it into the database and sets the priority level. All bug reports are not automatically entered into the database upon report from a client. One of the engineers will usually investigate the request to determine if it actually is a problem before submitting it to the project manager for approval and entry into the database. The project manager together with the team members then determines who is responsible for which part of the task. This is done during periodic (weekly to bi-weekly) meetings. The database is fully searchable and

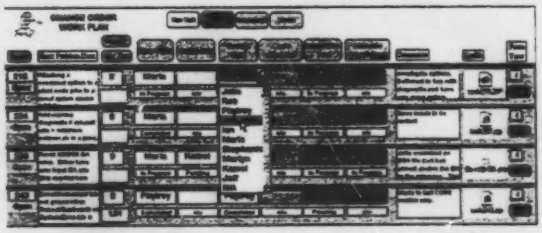

Figure 2: Change Request Database - List View

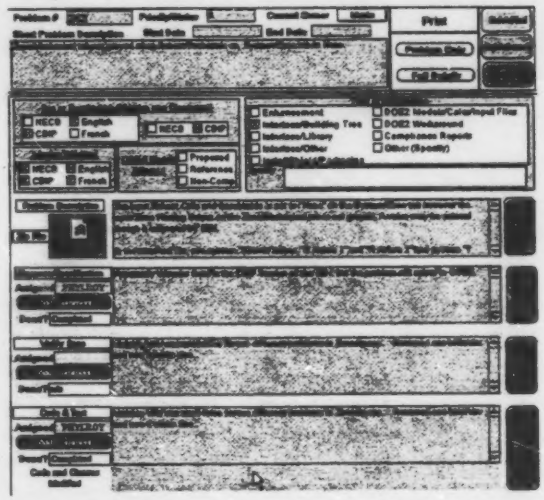

Figure 3: Change Request Database – Form View

there are two project views allowing us to see different levels of detail. One view is primarily used for the project manager's resource allocation strategy for each of the tasks, and the other for describing the task's unique details.

Developing the change request database was a big part of our project management initiative but not the only one that was set in place. Our organization had a long-term goal of developing a formal project management culture, which if expanded and documented, could eventually help us along our path towards ISO-certification in the future.

Recognizing that this was a strong possibility, various procedural documents were compiled over a period of time for the EE4 software and stored in a central location, which could be accessed by anyone in the group. The goal of these documents was to outline proper practice in working with various aspects of the EE4 software – from source code documentation and coding to maintaining the compliance reports that come bundled with the software. Here is a list of some of our documented procedures:

- EE4_01 Repository and Document Control Procedures
- EE4_02 New Document Template
- EE4_04 Change Request Database
- EE4_06 Coding Standard
- EE4_09 Design Documents
- EE4_10 On-line Help

SOFTWARE CONFIGURATION MANAGEMENT

It became apparent to us that we were going to need to centralize all documents once we realized how rapidly the resources we had working on the project and the amount of work that was on the go was growing. Each team member had their assigned tasks and as a natural course of practice, had their working files stored on their individual PC's or on the organization's central server in a location they usually did not publicly share with the rest of the group.

Once the number of people and tasks start growing in this fashion you begin running scenarios like this through your head:

Joe: "I'm leaving – I just got a job offer that pays me $15 000 a year more than what I get here. So long!"

Manager: "What? How about giving some notice ahead of time? Wait! Where is that algorithm we worked on 2 days ago for calculating HVAC system sizing?"

Joe: " I think it's on the back of the Tim Horton's box we scribbled on. Check the second or third drawer of my desk. Careful not to smudge it. I think there's a couple of jelly doughnuts still in there. Gotta go. Have a golf game scheduled with the new boss this afternoon."

Manager: "Good grief – now we're really up the river without a paddle with our star team member gone."

What do you do in this situation? Where is all of Joe's work stored and what state is it in?" When you come to the realization that you don't like the answers to these questions, then you begin exploring ways of sharing information and keeping others in your group aware of the state of your work.

This is where the concept of software configuration management becomes very useful. SCM is a formal process that involves:

- Identifying the configuration of software products and their descriptions at given points in time.
- Systematically controlling changes to the configuration.
- Maintaining integrity and traceability of the configuration throughout the life of the software.[1]

In formal SCM, there are 4 functions: identification, control, configuration auditing and status accounting. The process of SCM can become very heavy and cumbersome and rightfully so if you have a fairly large project which you would like to put under the strictest of control. It is beyond the scope of this paper to explain the process of software configuration management but the reader is encouraged to visit the following Department of Defence mirrored website to get an introduction as to what software configuration management entails:

http://www.pogner.demon.co.uk/mil_498/

In Karl Wiegers' Paper entitled "Twenty-One Project Management Success Tips"[2] one of the tips he presents is "Identify project drivers, constraints, and degrees of freedom." Although it is ideal to follow all the functions of SCM in their entirety, many times, reality does not permit it. So it is left to the judgement of the person developing the SCM plan to evaluate constraints within the organization and implement those parts of SCM which would have the most positive impact. Typical constraints may be limited budget or lack of employer awareness with respect to the advantages of good project management and software configuration management processes.

Some organizations do not have the resources to allocate a full time person(s) to the overseeing of proper SCM processes. They instead rely on the individual team members to do their own part in following agreed upon SCM procedures. This means that extra work is usually loaded onto already very burdened team members. Don't be surprised if you come across

resistance from your team members in attempting to implement an SCM process because of this very reason. When implementing change within an organization, no matter how small, you will usually come up against some resistance. Positive motivation usually works a lot better than negative reinforcement in getting aspects of SCM implemented (in other words bribe your team with goodies like donuts or cookies or other gifts). In our particular case, getting the team to go through stage 1 – identifying configuration items (CI's) was somewhat relatable to pulling teeth and required this type of positive reinforcement. Once all the items were identified and were confirmed to be items that we wanted to control, they were placed in the central repository on a dedicated server for EE4.What are some examples of configuration items? Here are a few of many with respect to EE4: source code, weather files which we distribute with EE4, files which will be compiled to make up the on-line help, compliance report template files and user guides.

Next, we had to tackle the control function which consists of reviewing and assessing the impact of proposed changes to CI's, the tracking of approved changes and the recording of rejected changes. Explaining how we implemented this function for all our CI's would be too lengthy for this paper. Instead we will demonstrate how this function was handled from a "tracking" perspective using EE4 source code as the configuration item being controlled.

After having centralized the source code on our dedicated EE4 server, we needed to develop a systematic and orderly procedure for 3 programmers to access the source code in order to effect the required changes. The following are properties that we felt were required for the third party tool which would help us control and track our source code changes and additions. It had to have the ability to:

1. label all components of the source code at any point in time (baseline) and rollback to this state if need be
2. limit modifications of any specific file to one person at a time and lock out any users from making simultaneous changes to that file
3. track who made changes to which file and for what purpose (have a change history list)
4. easily compare differences between various versions of a file (differential analysis tool)
5. be quick and easy for a new user to learn
6. be relatively inexpensive

In searching for such a tool we easily came across half a dozen different options. In looking closely at their capabilities, most had the basics which we listed above. Others also had more specialized features which we may or may not have required in the future.

Once we purchased the tool, we had to agree on how to effectively use it. Here were some of the basic rules we agreed upon:

1. All users would get the latest version of source code on a periodic basis to load onto their local computer. Once per day (usually at the beginning of the day) was considered good practice.
2. Changes or enhancements with respect to source code would be performed from the user's local computer and tested. Once the programmer felt that changes were implemented properly, only then would he check out the file(s) from the central repository database, make the changes and check it (them) back in.
3. When a file went through the checkin/checkout procedure, we agreed that a comment would be appended to the file concerning the type of change effected to it. The tool automatically documents when the new/modified file was added to the database and by whom.
4. At every new release, the entire source code set is baselined so that if need be, we could rollback and recompile that exact release version.

A few issues had to be clarified as we began investigating setting up a dedicated central server for EE4. Did we want to set up the server as a file server or as an application server? Our budget was a determining factor. Because there was not big support for purchasing an expensive server, we decided to convert one of our current computers into a file server and performed some minor upgrades. We used an existing Pentium Pro computer which had 256 MB RAM and upgraded the hard drive to a 20 Gb capacity. The processor speed was a determining factor in having it used as a file server and having all users do actual compiling, processing, etc. of files from their local computers. We also needed to designate one of the team members as the server administrator. The administrator would maintain the levels of access and perform other day-to-day maintenance activities.

A CODING STANDARD - WHAT IS IT AND WHAT IS IT USED FOR?

We all have a clear understanding of the role software programs like EE4 play in the building industry. The mystery is, how is a well written and robust software application developed?

The coding standard is a small part of the software project, but it has a large impact on the final result and in the software's maintenance and extendibility. It provides the rules by which code is written. If these rules are followed, then the result is a consistent, maintainable and extendable piece of software. In brief, the rules you will find outlined in a coding standard should be similar to the following:

1. Each item in the standard should be labelled as [M] mandatory, [R] recommended or [S] suggested
2. **General recommendations** - (i.e. optimize code only if performance is a problem).
3. **Naming convention** - (i.e. C++ file extension must be cpp; variables must be prefixed with a type descriptor – uiDeviceCount). Source code should be self-documenting through the use of clear variable, subroutine and constant names.
4. **Coding syntax and format** - (i.e. white space and brace placement). A consistent style contributes to clarity, readability and understanding.
5. **The use of function prototypes** - (i.e. void GetDeviceName(char *pName)). This step will help avoid function calling syntax errors.
6. **Compilation rules** - try to avoid conditional compilation. Conditional compilation includes or excludes code at compile time and makes the understanding of code difficult and perhaps misleading.
7. **Fault handling** – check the return codes from all functions, even if these functions seem foolproof. Bad data can be caused by a variety of things and must always be trapped.

Implementing these rules will help software developers produce readable code and develop good consistent coding practices.

To understand the impact of a coding standard, you first have to understand the rules by which software developers work. We are now going to let you into the secret world of software development, by revealing some software developers' working paradigms. In this way we hope to illustrate the value of a good coding standard.

Some software developers try to achieve legacy code guru status through the following tried and true methods of coding:

1. *Save file white space wherever possible. Never line up brackets or write code in a neat and tidy fashion.*

i.e.

```
void TDOE2Data::Calculate(TBuilding& Building,
stringFName,stringWName,boolDelete,TDiagnostic
*Diagnostic){stringpath=TApp::Path+"DOE\\";FN
ame=path+FName+"-
"+Name;stringIName=FName+".doe";string
BName=FName+".bdl";stringOName=Fname
+".sim";WName.prepend(TApp::Path+"Weather\\"
);RunDoe2(path,IName,WName,true);GetResults(F
Name,Building,Diagnostic);if(Delete){DeleteFile(INa
me.c_str());DeleteFile(BName.c_str());DeleteFile(O
Name.c_str());}}
```

Code should be readable and clear. Following a few simple format rules helps other people understand the structure and data flow of the program.

2. *Sacrifice clarity and simplicity - simple and straightforward code is to be avoided at all costs. If your design can be understood in a code walkthrough then you have failed.*

   It is a good possibility that other people will eventually have to work with the source code you have written. Try to make their lives as easy as possible.

3. *Vary coding format - never do things in the same way twice.*

i.e:

```
if( y>9 ) { y=100; } else { y-=200; }

y=x>9?100:200;
```

A consistent coding style is a great aid to clarity and readability.

4. *Continually add to the source lines in a file so that it is impossible to comprehend the intent of the functions that are contained in the file.*

It is very difficult to grasp and understand code that continues for hundreds of lines.

5. *Use the minimalist naming convention. Only use one or two characters for variable names, particularly global variables.*

Following a coding standard naming convention contributes to code readability and design understanding.

6. *Do not document your code (it takes too much valuable time and someone might find your comments useful). If you really feel compelled to place a comment in your code, make it glib and cute:*

i.e. /* don't call the police here */

i.e. TestYear=1967; /* my birthday */

7. *Do not implement any error checking (the bugs in your code will be found after the product is delivered and you will probably be gone by then).*

All functions should trap errors. A function may have to deal with bad data originating from an outside source.

A coding standard is of course not the only part of a software project but it is an important part and a project team that embraces a coding standard in conjunction with code walkthroughs, will produce a quality product that is maintainable, expandable and reliable.

Most large corporations, such as Nortel and IBM insist on enforcing the use of a code standard. They know that to meet market demands in a timely fashion, code must be easily modifiable. That means that it must be in a form that is readable understandable and robust.

We have included several URL's for you to investigate coding conventions and standards which are followed by other organizations:

http://www.possibility.com/Cpp/CppCodingStandard.html

http://oss.software.ibm.com/icu/userguide/conventions.html

http://g.cs.oswego.edu/dl/html/javaCodingStd.html

http://www.cs.mcgill.ca/resourcepages/indian-hill.html

SOFTWARE TESTING

Initially, our testing consisted of compiling and creating builds for all 4 versions of EE4 and having six engineers install them on their computers and perform runs with their own set of unique test files. They would then visually compare the results to those obtained using the previous version. The team members would perform this concurrently. When an error was reported, all testing was halted, the engineer/ programmer would patch the problem, and then the procedure would begin again. This testing strategy was flawed in several respects:

1. **The engineers were testing their own work.** A third party not familiar with the intricacies of the code and who can just interpret the output should ideally perform testing. Programmers, while they are often very diligent, can miss things when their 'nose is close to the grindstone' Programmers are largely interested in coding, not testing for bugs. Someone with a fresh perspective may be able to more easily spot potential problems.

2. **A great deal of time was wasted.** 6 engineers testing concurrently in an unstructured fashion can be frustrating especially when their test cases pass but someone else's doesn't. In this event, the entire process has to be repeated by all engineers regardless of their previous testing results once a fix has been implemented. This can be frustrating and lead to carelessness. This in turn allows for bugs to go undetected.

3. **Testing was inconsistent.** Having people manually do most of the testing introduced human error.

To remedy this situation, new measures were taken to make testing more efficient. A testing plan was created which took into account our current constraints and resource availability.

A test plan is an integral part of any software development strategy. "Testing verifies that a software deliverable conforms precisely to the functional and design specifications that have been agreed to with the users."[3]

While this is the accepted definition, software testing is also used to detect bugs in the software. Even the best programmers will inadvertently produce bugs in their code. The strategy should not be to detect and eliminate all of them. This would require more resources than most organizations can devote. Generally, "bugs are found and eliminated exponentially".[3] That is, as time invested in finding bugs increases, less bugs will be

found. So a cut-off point for testing must be established based on available resources. Emphasis should be placed on eliminating most bugs before shipping the deliverable. Shipping a stable, capable program is possible, but assuming that it is completely bug free is not.

Before testing begins you need to know the requirements of the program. Requirements are the ranges that the program operates under, and the behaviour that the program must exhibit as specified by the designer. Testing should be performed against these requirements. Many types of testing can be undertaken for quality assurance of a software. Here are a few definitions:

- Unit testing: Testing every file or class of code on it's own. This is expensive and time consuming. Every modification to a class requires a modification to the unit testing strategy.
- Integration testing: Testing modules or groups of classes and how they interact with each other and ensuring that no conflicts arise. It is concerned with confirming that no problems arise out of combining unit components into more complex processes. For example, two separate functions might appear to test successfully on their own, but if function B is fed the output of function A as one of its parameters, it might not perform as expected.
- System testing: Concerned with the full build of an application to ensure that system behaviour is correct. Installation, GUI interfaces, registry access, performance, error recovery and error handling are all checked in this process. .
- Regression testing: "The repetition of previously run tests after changes have been made to the source code". [4] This is to ensure that the product still functions in the same manner as it did before. This does not mean that the results have to be exactly the same as before. The changes made to the code might lead to different results. However the results have to be explainable.
- Inspections/Code Reviews: A team of programmers looks at and evaluates the code. It ensures that code is efficient, meets the requirements and follows the organization's accepted coding standards.
- User Acceptance Testing /Beta Testing: This type of testing allows us to see how the software will function in the wild. There are many different versions of operating systems, hardware and third party software that may interact with your products and you will not know the full effect of these interactions until regular users put it through its paces. Finding good testers is the real work here. Users who are familiar with their hardware and the software are ideal candidates.

Unit and integration testing can ensure a very high quality product if they are done correctly. However, the process is very expensive and time consuming and could conceivably double development time. Implementing unit testing on the existing EE4 code would take months if not years due to the sheer volume of code.

A dedicated staff member now conducts system and regression testing procedures for EE4. The tester manually installs all versions of EE4 and ensures that the installation wizard functions correctly. An automated testing protocol (autotester) was developed to run a series of EE4 building test files which contain HVAC system types and scenarios which users would normally incorporate into the modelling of their buildings. We have called these our 'base cases'. They are kept in read-only format on the EE4 server and are a configuration item and therefore subject to the control function of our SCM process. The autotester runs these files with the current release of EE4 and then compares the results to a saved set of output from the previously released version. It then provides a report which details the differences in the output between the new and the old version of EE4. If new functionality is added to the software that will change the output significantly, for example a humidity control which will change the results of the energy use in buildings, select cases are examined manually to predict the percent difference in other base cases output. With this we can normalise the new result set to the old results set. The tester also verifies all dialogs by iterating though them to automatically create a building and to ensure that all dialogs are correctly presented and in the correct language.

Figures 4 and 5 show the interface of the autotester.

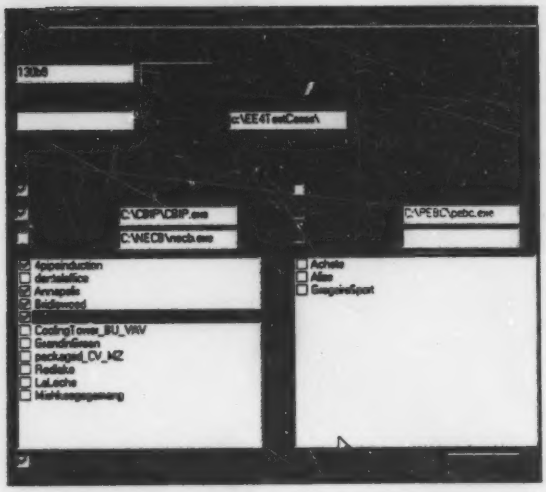

Figure 4: Autotester – User Options Screen

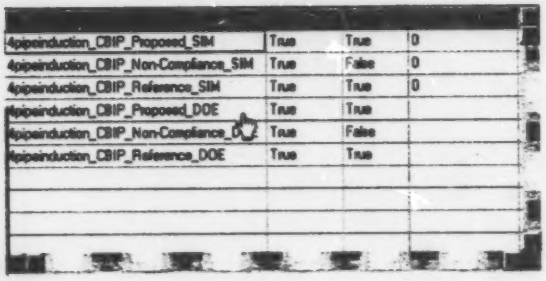

Figure 5: Autotester – Results Screen

Our final test is to go through our checklist to verify that all the help files and documentation have been updated and to determine if the program functions correctly. Figure 6 shows the checklist we are currently using.

CONCLUSIONS

Modifying and improving a large and complicated piece of software is not an easy task and should incorporate several initiatives. Making sure that good project management practices have been put in place is an important first step. Communication amongst the team members is enhanced through the use of configuration management practices. The implementation of proper SCM practices allows for a quick way to determine the status of your project at any point in time. An organization that implements a coding standard recognizes the inherent value in writing consistent and clear code – mainly less timely maintenance-related activities. Developing good software testing procedures is also an indication of an organization's commitment to releasing a quality product. These initiatives enable a team to function with synergy for software production. Time is used effectively, confusion is avoided and quality is assured. These were the major initiatives undertaken by the EE4 team in releasing a better quality product to the Canadian building industry.

1. EE4 Environment
   - The correct executable is in the Install (check time stamp with most recent compiled version)Notice screen text is up-to-date
   - Upon EE4 start-up you do not receive any messages that certain files cannot be loaded
   - All default libraries are present and in the appropriate language
   - "About EE4" dialogue box indicates the correct version number
   - Text in the "User Information" dialogue appears in the correct language
   - EE4 Help File can be launched from within EE4
   - Windows Help can be launched from within EE4
   - The list of recent files under the "File" menu is blank
   - The Help File is up to date
2. InstallShield
   - Title and version appear correctly in the first "Welcome Screen"
   - Software licence text is up-to-date
   - Readme text is up-to-date (Known bugs, planned enhancements, FAQ)
   - Destination Location directory appears correctly
   - EE4 can be opened from Program Groupbox immediately after installation
   - EE4 Help File can be opened from Program Groupbox immediately after installation
   - Readme file can be opened from Program Groupbox immediately after installation
   - Comply can be opened from the Windows Start menu
   - Comply Help File can be opened from the Start menu
   - Readme file can be opened from the Start menu
   - Uninstall works correctly
   - User Guide is up to date
3. EE4 Execution
   - You are able to load building files from previous versions (test – 3)
   - The sample building(s) included return simulation results for all 3 building models
   - File…Print shows the compliance reports checkbox items in their appropriate language
   - The Compliance Reports print in the appropriate language
   - The formatting and text for all compliance reports appear properly (test both E/F)
   - All context sensitive help and on-line help are up to date (refer to detailed list compiled by Mick)
4. User Guide
   - Make sure user guide is up to date

Figure 6: Final EE4 Release Checklist

REFERENCES

1 - Learning Tree International – Software Configuration Management Course Manual p342-1-10

2 - Karl Wiegers, Process Impact "Twenty One Project Management Success Tips" – Proceedings of the Borland 11th Annual Conference

3 - Microsoft – MSDN On-Line Library "The Purpose of Testing"

http://msdn.microsoft.com/library/books/advnvb5/Ch10_2.htm

4 - Microsoft – MSDN On-Line Library "Regression Testing"

http://msdn.microsoft.com/library/books/advnvb5/Ch10_8.htm

SIMULATION SOFTWARE TO DESCRIBE THE THERMAL ENVIRONMENT OF RESIDENTIAL BUILDINGS BASED ON DETAILED PHYSICAL MODELS

Akihito Ozaki*, Toshiyuki Watanabe**, Shigeki Iwaoka*** and Shuho Takase**
* The University of Kitakyushu, Fukuoka, Japan
** Kyushu University, Fukuoka, Japan
***ATOM Indoor Climate Institute, Morioka, Japan
ozaki@env.kitakyu-u.ac.jp

ABSTRACT

A simulation software called THERB has been developed for the purpose of estimating the thermal environment of residential buildings. THERB can simulate dynamic fluctuation of temperature, humidity, sensible temperature such as PMV or SET* (Predicted Mean Vote or Standard Effective Temperature) and heating/cooling load by taking into account both the air temperature and the sensible temperature for multiple zone buildings. The heat transfer models used in THERB such as conduction, convection, radiation and ventilation (or air leakage) are based upon the detailed phenomena describing actual building physics. All the phenomena are calculated without simplification of the heat transfer principles of any building component or element. The paper describes the detailed models used in THERB, and prominent features of the models are explained in detail.

INTRODUCTION

THERB (the simulation software of the thermal environment of residential buildings) is a dynamic simulation software which can estimate temperature, humidity, sensible temperature, and heating/cooling load for multiple zone buildings. The model can be applied to all forms of building design, structure or occupant schedules, etc. The following outlines the algorithms for heat transfer used in THERB, which are derived from fundamental building physics principles.

Conductive Heat Transfer: The successive transition method [1], which is based on a state equation in the modern control theory, is applied to the model of one-dimensional transient thermal conduction of multi-layer walls in the time-discrete domain. One of the principle advantages of the successive transition method compared to the numerical convolution method represented by the response factor [2] are that the successive transition method requires only an input excitation at one time step before from the present time step. An additional advantage of the successive transition method is that the calculation time and storage capacity depends only on the number of exponential terms of the characteristic function. One can take advantage of the superior feature of the successive transition method by making use of a revised four terminals determinant which can dramatically decrease the number of exponential terms [3],[4], the calculation time and storage capacity. Regarding thermal conduction to the ground, the finite difference method is applied to the previous calculation of the ground temperature and then the results are used as the input excitation for conductive calculation of the earthen floor and basement walls by the successive transition method using input data of the building described in THERB. Furthermore, the successive transition method used in THERB utilizes a trapezoid wave instead of an isosceles triangle wave which is easily adaptable to a hold function. This can significantly improve the calculation accuracy of conductive heat because one can adjust the hold function to the time-discrete domain.

Convective Heat Transfer: By default, the convective heat transfer coefficients in THERB are recalculated at every time step on all surfaces of the exterior, interior and cavities of buildings using dimensionless equations which are derived from either the profile method for boundary layer [5] (based on the energy equation, the momentum equation and the fluid friction) or defined from the experimental findings according to natural or forced convection [6],[7]. Furthermore the natural convective heat transfer coefficients are classified into either vertical or horizontal surfaces. It is possible to use the functional equations of the wind direction and velocity for the exterior convective heat transfer coefficients and the functional equations of the temperature difference between surface and room for the interior convective heat transfer coefficients. It is also possible to set constant all day long or during air-conditioning time by every part of the buildings.

Radiant Heat Transfer: On the exterior surfaces of the buildings, the standard method of using the radiant heat transfer coefficients and atmospheric radiation is applied. On the interior of buildings, instead of the general method (that is, the calculation of heat transfer between surface and indoor air and radiation between surfaces), the use of the long-wave absorption coefficient makes possible to simulate a net absorption of radiant heat as a consequence of multiplex reflection among interior surfaces. Mutual radiation between the surfaces of cavities in walls and windows can be also simulated.

Incident Solar Radiation: Incident solar radiation on the exterior and into the interior of buildings is divided into direct and diffuse solar radiation and calculated for all parts of the building in all directions using accurate geometric calculations of shaded and unshaded portions of the building by considering the influence of overhangs and wings. Isotropic model or anisotropic [8] models can be chosen for diffused solar radiation. Transmitted solar radiation is calculated by the multi-layer window model [9] and considers multiplex reflection (depending on an incidence angle of solar radiation) between not only the glazing layers but also between the window and interior shade at every time step. The multiplex reflection of both direct and diffuse solar radiation among interior surfaces including re-transmission of solar radiation from the inside to the outside through the windows is simulated by using the short-wave absorption coefficient. Moreover the absorption coefficients of long and short wave are applied to radiant heat emitted from lights and appliances, etc.

Ventilation: The network airflow model integrating a thermal model with a plant model estimates natural and forced ventilation quantities of each zone (rooms and cavities) caused by air leakage, infiltration and mechanical ventilation. As for independent ventilated cavities in the walls, it is possible to estimate airflow quantities by hydrodynamic analysis as the solution to the equations of motion, energy and continuity [10]. Constant ventilation quantities can be also set every hour for all zones.

Control of space conditioning: Control methods for space conditioning are classified into three types of heating, cooling, and simultaneous heating and cooling. By default, humidity control and temperature control are linked. Temperature and humidity setpoint and ranges can be optionally set every hour. Moreover the control of humidity is automatically performed in case the sensible temperature is set as the setpoint of air-conditioning.

THEORETICAL FEATURE OF THERB

CONDUCTION

The numerical convolution method represented by the response factor method or the transfer function method [11] is well known as a calculation method for transient thermal conduction in the time-discrete domain. The biggest disadvantage of this method is all the past input excitation, which influences the present conductive heat, is required. Thus in the case of walls with large thermal capacity, large calculation time and storage capacity are required. To overcome this problem of the numerical convolution method, the successive transition method is used in THERB. The equations for the successive transition method can be developed from the pulse transfer function with the fundamental wave of input excitation by using the z transformation if it is assumed the characteristic function of multi-layer walls is already known.

Characteristic Function

Unit response $\phi(t)$ of the heat flux on a surface of multi-layer wall with temperature excitation of the surface (or air) is generally expressed by Eq.(1).

$$\phi(t) = A_0 + \sum_{k=1}^{\infty} A_k e^{-\alpha_k t} \tag{1}$$

A_0 is the thermal conductance (or overall coefficient of heat transfer). The maximum value of k cannot be equal to infinity, thus k is broken off K_0 and Eq.(1) is arranged into Eq.(2).

$$\phi(t) = A_0 + \sum_{k=1}^{K_0} A_k e^{-\alpha_k t} + \dot{Q}\delta(t) \tag{2}$$

$\delta(t)$ is Dirac's function. $\dot{Q}$ is the moment heat flux at $t=0^+$ and expressed as follows:

$$\dot{Q} = \sum_{k=K_0+1}^{\infty} \frac{A_k}{\alpha_k} \tag{3}$$

The transfer function $G(s)$ is obtained as the product of the Laplace transformation of $\phi(t)$ and s.

$$G(s) = A_0 + \sum_{k=1}^{K_0} \frac{A_k s}{s+\alpha_k} + \dot{Q}s \tag{4}$$

Hold Function

The following equations are the Laplace transformation of the hold function $G_h(s)$ using a trapezoid wave to approximate time-discrete input excitation. As shown in Fig.1, the trapezoid hold functions are composed of right angle triangles.

$$G_h(s) = \left(\frac{1-e^{-s}}{s}\right) + h\left(-\frac{e^{-s}}{s} + \frac{1-e^{-s}}{Ts^2}\right) \tag{5}$$

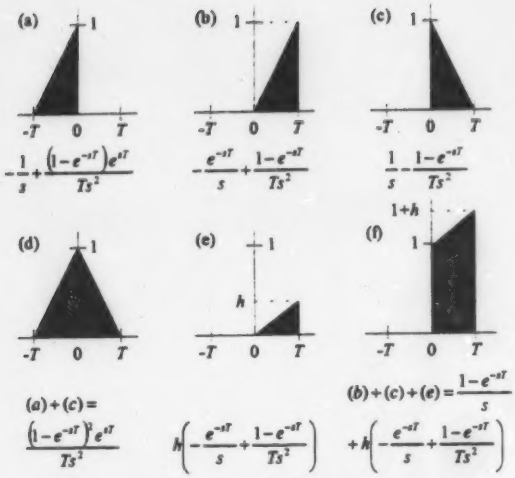

Fig.1 Composition of the trapezoid hold function

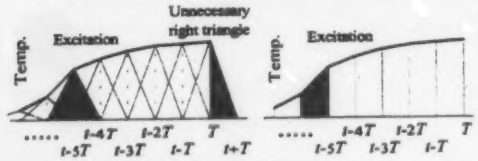

Fig.2 Adjustment of hold function to time discrete domain

The trapezoid hold function has the advantage over the isosceles triangle hold function in that it can adjust itself to the time-discrete domains as in Fig.2.

Pulse Transfer Function

The pulse transfer function $G(z)$ is defined as the z transformation of the product of the transfer function $G(s)$ and the hold function $G_h(s)$ [12].

$$G(z)=Z\{G(s)\cdot G_h(s)\} \tag{6}$$

The pulse transfer function $G_t(z)$ with the trapezoid hold functions $G_{hk}(s)$ are obtained by Eq.(7).

$$G_t(z)=A_0+\sum_{k=1}^{K_0}\frac{A_k(1-z^{-1})}{1-e^{-\alpha_k T}z^{-1}} +h\sum_{k=1}^{K_0}\frac{A_k(1-e^{-\alpha_k T}-\alpha_k T)}{\alpha_k T}\cdot\frac{z^{-1}}{1-e^{-\alpha_k T}z^{-1}}+\frac{\dot{Q}}{T}(1-z^{-1}) \tag{7}$$

where the z transformation of the differentiation of $G_{hk}(s)$ becomes $(1-z^{-1})/T$ [13].

Relation between Input and Output Paramters

The relation between input and output parameters is expressed by Eq.(8) using the pulse transfer function $G(z)$.

$$Q(z)=G(z)\cdot\Theta(z) \tag{8}$$

$\Theta(z)$ and $Q(z)$ are the z transformation of impulse data of the input $\theta(t)$ and the output $q(t)$, and are described by Eqs.(9), (10) for the case when the time-discrete values of the input and output are θ_n and q_n at $t=nT$ (T is an interval of time), respectively.

$$\Theta(z)=\theta_0+\theta_1z^{-1}+\theta_2z^{-2}+\cdots \tag{9}$$

$$Q(z)=q_0+q_1z^{-1}+q_2z^{-2}+\cdots \tag{10}$$

Successive Transition Method

The state transition function $X_k(z)$ with the trapezoid pulse transfer function is defined by Eq.(11) as the product of the right side second and third terms of Eq.(7) and the time-discrete input $\Theta(z)$.

$$X_k(z)=\left\{\frac{A_k(1-z^{-1})}{1-e^{-\alpha_k T}z^{-1}}+h\frac{A_k(1-e^{-\alpha_k T}-\alpha_k T)}{\alpha_k T}\cdot\frac{z^{-1}}{1-e^{-\alpha_k T}z^{-1}}\right\}\Theta(z) \tag{11}$$

Eq.(11) can be re-arranged into Eq.(12).

$$(1-e^{-\alpha_k T}z^{-1})X_k(z)=\left\{A_k(1-z^{-1})+h\frac{A_k(1-e^{-\alpha_k T}-\alpha_k T)}{\alpha_k T}z^{-1}\right\}\Theta(z) \tag{12}$$

By substituting $X_k(z)=x_{k,0}+x_{k,1}z^{-1}+x_{k,2}z^{-2}+\cdots$ and $\Theta(z)=\theta_0+\theta_1z^{-1}+\theta_2z^{-2}+\cdots$ in Eq.(12) and comparing the coefficients of z^{-n} on the left and right sides of the function in Eq.(12), the following state transition equation is obtained.

$$x_{k,n}=e^{-\alpha_k T}x_{k,n-1}+A_k(\theta_n-\theta_{n-1})+h\frac{A_k(1-e^{-\alpha_k T}-\alpha_k T)}{\alpha_k T}\theta_{n-1} \tag{13}$$

The inclination parameter h is obtained by Eq.(14).

$$h\theta_{n-1}=\theta_n-\theta_{n-1} \tag{14}$$

Eq.(13) is rearranged to Eq.(15) by substituting Eq.(14).

$$x_{k,n}=e^{-\alpha_k T}x_{k,n-1}+\frac{A_k(1-e^{-\alpha_k T})}{\alpha_k T}(\theta_n-\theta_{n-1}) \tag{15}$$

where $x_{k,0}=A_k\theta_0$.

The right side of Eq.(8) can be expanded to an infinite series with respect to $x_{k,n}$ (the state transition function) by substituting Eqs.(7), (9) and (15). By comparing the coefficients of z^{-n} on the left and right sides of Eq.(8), the time-discrete output can be defined by Eq.(16).

$$q_n=A_0\theta_n+\sum_{k=1}^{K_0}x_{k,n}+\frac{\dot{Q}}{T}(\theta_n-\theta_{n-1}) \tag{16}$$

Practical Formulas of Successive Transition Method

The followings are the formulas developed from Eq.(16), which express the net heat flux CD on surface $\bar{j}$ taking into consideration the heat flux from the opposite surface j of wall at the present time n.

$$CD_{\bar{j},n} = a_{\bar{j}}\theta_{\bar{j},n} - a_i\theta_{j,n} + D_{\bar{j},n-1} \tag{17}$$

$$\varphi_k = e^{-\alpha_k T}$$
$$p_k = \varphi_k - (1-\varphi_k)/\alpha_k T \tag{18}$$
$$q_k = -p_k - (1-\varphi_k)$$

$$a_m = A_0 + \sum_{k=1}^{K_0} A_{m,k}(1+q_k) + \dot{Q}_m/T$$
$$b_m = \sum_{k=1}^{K_0} A_{m,k} p_k - \dot{Q}_m/T \tag{19}$$

$$D_{\bar{j},n-1} = \sum_{k=1}^{K_k} \varphi_k x_{\bar{j},k,n-1} + b_{\bar{j}}\theta_{\bar{j},n-1} - b_i\theta_{j,n-1} \tag{20}$$

$x_{\bar{j},k,n-1}$ of Eq.(20) is renewed by every time step by Eq.(21).

$$x_{\bar{j},k,n} = \varphi_k x_{\bar{j},k,n-1} + p_k\left(A_{\bar{j},k}\theta_{\bar{j},n-1} - A_{i,k}\theta_{j,n-1}\right) + q_k\left(A_{\bar{j},k}\theta_{\bar{j},n} - A_{i,k}\theta_{j,n}\right) \tag{21}$$

where subscript $m = \bar{j}$ refers to the heat flux of the surface $\bar{j}$, and $m = t$ refers to the heat transmission through the surface j toward the surface $\bar{j}$.

CONVECTION

Table 1 shows the default of the convective heat transfer coefficients, which are developed on the basis of the profile method for boundary layer or experimental findings. THERB recalculates the coefficients by every time step on all surfaces of the exterior, interior and cavities of buildings.

Table 1 Convective Heat Transfer Coefficient

Part of Buildings	Dimensionless Number
Exterior	$Nu = 0.037\,\mathrm{Re}^{0.8}\,\mathrm{Pr}^{1/3}$
Interior (Vertical Plane)	$Nu = 0.24\left(Gr_l \cdot \mathrm{Pr}\right)^{0.4}$ $Gr_l = g\beta\Delta T_a l^3/\upsilon^2$
Interior (Horizontal Plane)	$Nu = C \cdot Ra_f^m$ $Ra_f = Gr_l \cdot \mathrm{Pr}$ $f = (T_s + T_\infty)/2$
Upward	C=0.58, m=1/5
Downward	C=0.54, m=1/4 (Ra_f: 2E4 to 8E6) C=0.15, m=1/3 (Ra_f: 8E6 to 1E11)
Cavity (ventilated)	$Nu = 0.023\,\mathrm{Re}^{0.8}\,\mathrm{Pr}^{0.4}$
Cavity (closed)	$Nu = 0.035\left(Gr_c \cdot \mathrm{Pr}\right)^{0.38}$ $Gr_c = g\Delta T_s l^3/T_m\upsilon^2$

Gr: Grashof number, Nu: Nusselt number, Pr: Prandtle number, Ra: Rayleigh number, T_m: mean temperature of surfaces, ΔT_a: temperature difference between surface and air, ΔT_s: temperature difference between surfaces, g: gravitational constant, l: length, β :expansion coefficient, υ : kinematic viscosity

RADIATION

Multiplex Reflection of Long-Wave Radiation

The multiplex reflection of long-wave radiation between interior surfaces is simulated on the basis of Gebhart's absorption coefficient [14]. The long-wave absorption coefficient $\beta_{l,j}$ is defined as the net ratio of absorbed radiant heat on surface j from the surface l.

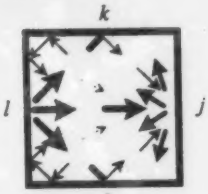

Fig.3 multiple reflection of long-wave radiation

$$\beta_{l,j} = F_{l,j}\varepsilon_j + \sum_{k=1}^{J} F_{l,k}(1-\varepsilon_k)\beta_{k,j} \tag{22}$$

where $F_{l,j}$ is the view factor from the surface l to the surface j and ε_j is emissivity of the surface j.

Thus the net radiant heat emitted from the surface j (see Fig.3) is expressed by Eq.(23).

$$ELR_j = \varepsilon_j\sigma T_j^4 - \sum_{k=1}^{J}\beta_{k,j}\varepsilon_k\sigma T_k^4 S_k/S_j \tag{23}$$

Eq.(23) can be re-arranged into Eq.(25) by using the principle of the conservation of energy and the reciprocal theorem expressed by Eq.(24).

$$\sum_{k=1}^{J}\beta_{j,k} = 1$$
$$\varepsilon_k S_k \beta_{k,j} = \varepsilon_j S_j \beta_{j,k} \tag{24}$$

$$ELR_j = \varepsilon_j\sigma\sum_{k=1}^{J}\beta_{j,k}\left(T_j^4 - T_k^4\right) = \sum_{k=1}^{J}\beta_{j,k}\alpha_{r,jk}\left(T_j - T_k\right) \tag{25}$$

where S_j is the area of surface j. $\alpha_{r,jk}$ is the radiant heat transfer coefficient from surface j to surface k and can be approximated by Eq.(26).

$$\alpha_{r,jk} = 4\varepsilon_j\sigma\left\{(T_j + T_k)/2\right\}^3 \tag{26}$$

The long-wave absorption coefficient can be applied to long-wave radiant heat emitted from lights and appliances and human bodies, etc. If it is assumed that such radiant heat is equally emitted from the ceiling or

floor, the absorption amount ALR_j on the surface j can be described by Eq.(27).

$$ALR_j = \sum_{c=1}^{C} \beta_{c,j} LI_c S_c / S_j + \sum_{f=1}^{F} \beta_{f,j} LH_f S_f / S_j$$
$$= \varepsilon_j \left(\sum_{c=1}^{C} \beta_{j,c} LI_c / \varepsilon_c + \sum_{f=1}^{F} \beta_{j,f} LH_f / \varepsilon_f \right) \quad (27)$$

where LI_c and LH_f are the radiant heat from lights and appliances and human bodies, respectively. Thus the net radiant heat emitted from the surface j can be calculated by Eq.(28).

$$NLR_j = ELR_j - ALR_j \quad (28)$$

Multiplex Reflection of Short-Wave Radiation

Regarding direct solar radiation, when TDN_m is the transmitted direct solar radiation through the window striking a normal surface m, a_l and ρ_l are the solar absorptance and reflectance on the surface l, θ_l is incidence angle upon the interior surface l, and S_l is the insolation area of the surface l. The solar absorption and reflection on the surface l are expressed by $a_l \cdot TDN_m \cos\theta_l$ and $\rho_l \cdot TDN_m \cos\theta_l$, respectively. Solar absorption $ADT_{m,j}$ on the surface j based on TDN_m is expressed as Eq.(30) by using the short-wave absorption coefficient $\gamma_{l,j}$, which is defined as the net ratio on the surface j of absorbed solar radiation reflected from the surface l (see Fig.4).

$$\gamma_{l,j} = F_{l,j} a_j + \sum_{k=1}^{J} F_{l,k} \rho_k \gamma_{k,j} \quad (29)$$

$$ADT_{m,j} = TDN_m \sum_{l=1}^{L} \left(\delta_{j,l} a_l \cos\theta_l + \rho_l \gamma_{l,j} \cos\theta_l S_l / S_j \right) \quad (30)$$

$(\delta_{j,l} = 1 \text{ when } j = l,\ \delta_{j,l} = 0 \text{ when } j \neq l)$

Eq.(30) can be rearranged into Eq.(32) by the reciprocal theorem expressed by Eq.(31).

$$a_l S_l \gamma_{l,j} = a_j S_j \gamma_{j,l} \quad (31)$$

$$ADT_{m,j} = a_j \cdot TDN_m \sum_{l=1}^{L} \left(\delta_{j,l} + \rho_l \gamma_{j,l} / a_l \right) \cos\theta_l \quad (32)$$

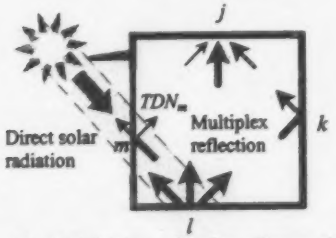

Fig.4 Multiplex reflection of transmitted direct solar radiation

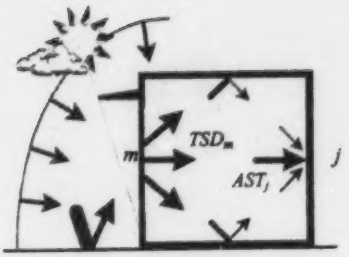

Fig.5 Multiplex reflection of transmitted sky diffuse solar radiation

When ADW_m is the direct absorption of direct solar radiation on window m, the solar absorption ADT_j on the interior surface j is obtained by Eq.(33).

$$ADT_j = \sum_{m=1}^{M} \left\{ \delta_{j,m} ADW_m + a_j \cdot TDN_m \cdot \sum_{l=1}^{L} \left(\delta_{j,l} + \rho_l \gamma_{j,l} / a_l \right) \cos\theta_l \right\} \quad (33)$$

Regarding sky diffuse solar radiation, when TSD_m is the transmitted sky diffuse solar radiation through the window m and ASW_m is the direct absorption of the sky diffuse solar radiation on window m, the solar absorption AST_j on the interior surface j is obtained by Eq.(34) if TSD_m is assumed to spread equally into the room (see Fig.5).

$$AST_j = \sum_{m=1}^{M} \left(\delta_{j,m} ASW_m + a_j \gamma_{j,m} TSD_m / a_m \right) \quad (34)$$

The short-wave absorption coefficient can be applied to short-wave radiant heat emitted from lights and appliances, etc. If it is assumed that the radiant heat is equally emitted from some parts of ceiling, the absorption amount ASR_j on the surface j can be described by Eq.(35).

$$ASR_j = \sum_{c=1}^{C} \gamma_{c,j} SI_c S_c / S_j$$
$$= a_j \sum_{c=1}^{C} \gamma_{j,c} SI_c / a_c \quad (35)$$

where SI_c is the short-wave radiant heat from lights and appliances. Thus the absorption amount NSR_j of the short-wave radiant heat on the surface j is expressed by Eq.(36)

$$NSR_j = ADT_j + AST_j + ASR_j \quad (36)$$

Multi-Layer Window Model

When solar radiation transmits through double-glazing (through 1 to 2 as in Fig.6), the overall transmittance, absorptance and reflectance of the window caused by

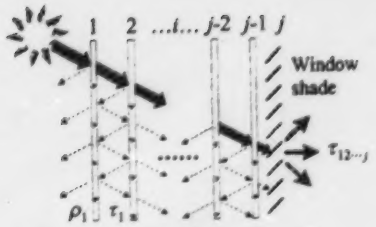

Fig.6 Multi-layer window model

multiple reflections between the glazings can be described by the following infinite series.

$$\tau_{12} = \tau_1\tau_2 + \tau_1\tau_2\rho_1\rho_2 + \tau_1\tau_2\rho_1^2\rho_2^2 + \cdots = \frac{\tau_1\tau_2}{1-\rho_1\rho_2} \quad (37)$$

$$\alpha_{\bar{1}2} = \alpha_1\left(1 + \tau_1\rho_2 + \tau_1\rho_1\rho_2^2 + \cdots\right) = \alpha_1\left(1 + \frac{\tau_1\rho_2}{1-\rho_1\rho_2}\right) \quad (38)$$

$$\alpha_{1\bar{2}} = \alpha_2\tau_1\left(1 + \rho_1\rho_2 + \rho_1^2\rho_1^2 + \cdots\right) = \frac{\alpha_2\tau_1}{1-\rho_1\rho_2} \quad (39)$$

$$\rho_{12} = \rho_1 + \tau_1^2\rho_2 + \tau_1^2\rho_1\rho_2^2 + \cdots = \rho_1 + \frac{\tau_1^2\rho_2}{1-\rho_1\rho_2} \quad (40)$$

where α_1, ρ_1, τ_1 and α_2, ρ_2, τ_2 are the absorptance, reflectance and transmittance of the glazing layers 1 and 2. $\alpha_{\bar{1}2}$ and $\alpha_{1\bar{2}}$ are the overall absorptance of glazing 1 and 2, respectively. ρ_{12} is the overall reflectance on the side of glazing layer 1 of a double-glazed window.

If the overall transmittance, absorptance and reflectance of a double-glazed window are regarded as the properties of an imaginary single glazing, the equations for triple-glazing can be described as follows.

$$\tau_{123} = \frac{\tau_{12}\tau_3}{1-\rho_{21}\rho_3} \quad (41)$$

$$\alpha_{12\bar{3}} = \frac{\alpha_3\tau_{12}}{1-\rho_{21}\rho_3} \quad (42)$$

$$\left(\rho_{21} = \rho_2 + \frac{\tau_2^2\rho_1}{1-\rho_1\rho_2}\right)$$

where ρ_{21} $(\neq \rho_{12})$ is the overall reflectance on the side of glazing layer 2 of the double-glazed window.

By regarding the glazing 2-3 of triple-glazing as an imaginary single glazing, the following equations are obtained.

$$\alpha_{\bar{1}23} = \alpha_1\left(1 + \frac{\tau_1\rho_{23}}{1-\rho_1\rho_{23}}\right) \quad (43)$$

$$\alpha_{1\bar{2}3} = 1 - \tau_{123} - \rho_{123} - \alpha_{\bar{1}23} - \alpha_{12\bar{3}} \quad (44)$$

$$\text{or} \quad \alpha_{1\bar{2}3} = \alpha_{1\overline{23}} - \alpha_{12\bar{3}} \quad (45)$$

Thus the general equations of overall transmittance, absorptance and reflectance of multi-layer glazing including a window shade can be expressed as follows.

$$\tau_{12\cdots j} = \frac{\tau_{12\cdots j-1}\tau_j}{1-\rho_{j-1\cdots 21}\rho_j} \quad (46)$$

$$\alpha_{12\cdots\bar{j}} = \frac{\tau_{12\cdots j-1}\alpha_j}{1-\rho_{j-1\cdots 21}\rho_j} \quad (47)$$

$$\left(\rho_{j\cdots 21} = \rho_j + \frac{\tau_j^2\rho_{j-1\cdots 21}}{1-\rho_j\rho_{j-1\cdots 21}}\right)$$

$$\alpha_{12\cdots\bar{i}\cdots j} = \alpha_{12\cdots\overline{i\cdots j}} - \alpha_{12\cdots\overline{i+1\cdots j}} \quad (48)$$

$$\alpha_{\bar{1}2\cdots j} = \alpha_1\left(1 + \frac{\tau_1\rho_{23\cdots j}}{1-\rho_1\rho_{23\cdots j}}\right) \quad (49)$$

$$\left(\alpha_{12\cdots\overline{i\cdots j}} = \frac{\tau_{12\cdots i-1}\alpha_{i\cdots j}}{1-\rho_{i-1\cdots 21}\rho_{i\cdots j}}\right)$$

$$\left(\alpha_{i\cdots j} = 1 - \tau_{i\cdots j} - \rho_{i\cdots j}\right)$$

$$\left(\rho_{i\cdots j} = \rho_i + \frac{\tau_i^2\rho_{i+1\cdots j}}{1-\rho_i\rho_{i+1\cdots j}}\right)$$

VENTILATION

A standard model, called the network airflow model, is used to calculate ventilation quantities of each zone where zones are represented by nodes. Alternatively set constant ventilation quantities in each zones for each hour can also be defined in THERB. Furthermore the dimensionless buoyant airflow model can be also applied to independent ventilated cavities in the walls.

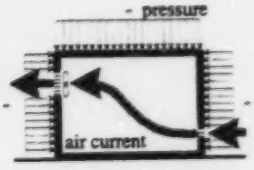

(a) Mechanical Ventilation

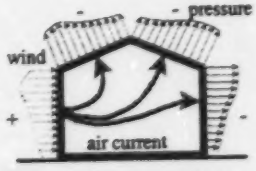

(b) Wind forced ventilation

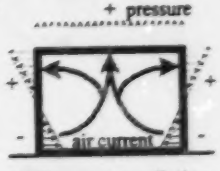

(c) Buoyant ventilation

Fig.7 Mechanical or natural ventilation

Network Airflow Model

The network airflow model, which is based on the equations of continuity and airflow quantities for openings and cracks as shown in Eqs.(50) to (52), is solved

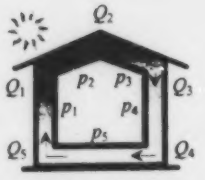

(a) Buoyant airflow

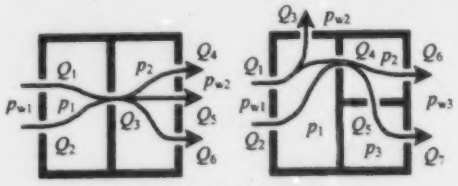

(b) Natural or forced ventilation

Fig.8 Network airflow model based on the equations of continuity and airflow quantities

$$\sum_{i=1}^{I} Q_i = 0 \tag{50}$$

$$Q_i = \alpha_i A_i \sqrt{\frac{2g}{\gamma}|\Delta p_i|} = 4\alpha_i A_i \sqrt{|\Delta p_i|} \tag{51}$$

$$Q_i = a_i l_i \Delta p_i^{1/n} \tag{52}$$

where A is the opening area, Q is the airflow quantity, a is crack constant, g is gravitational constant, l is the length of crack, $n = 1.5$ (constant 1 to 2), Δp is the pressure difference, α is the flow factor and γ is the specific weight of air.

Dimensionless Buoyant Airflow Model in Cavity

Buoyant airflow quantity through a cavity sandwiched between a heating and adiabatic surface as in Fig.9 can be estimated by the equations of continuity, energy and motion described by Eqs.(53) to (55).

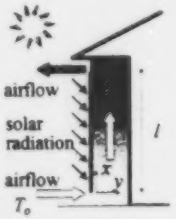

Fig. 9 Wall cavity

$$\frac{\partial u}{\partial x} + \frac{\partial v}{\partial y} = 0 \tag{53}$$

$$\rho c_p u \frac{\partial T}{\partial x} + \rho c_p v \frac{\partial T}{\partial y} = \lambda \frac{\partial^2 T}{\partial y^2} \tag{54}$$

$$u \frac{\partial u}{\partial x} + v \frac{\partial u}{\partial y} = \upsilon \frac{\partial^2 u}{\partial y^2} - \frac{1}{\rho} \frac{\partial P_d}{\partial x} + \beta g (T - T_o) \tag{55}$$

$$\left(P_d = p - p_o,\ \beta = \frac{\rho_o - \rho}{\rho (T - T_o)} \right)$$

Eq.(56) expresses boundary conditions.

$$\left.\begin{aligned} &x = 0,\ 0 < y < b:\ u = \bar{u},\ v = 0,\ T = T_o \\ &y = 0,\ x \geq 0:\ u = 0,\ v = 0,\ T = T_w \\ &y = b,\ x \geq 0:\ u = 0,\ v = 0,\ \partial T / \partial y = 0 \\ &x = 0:\ P_d = 0 \\ &x = l:\ P_d = 0 \end{aligned}\right\} \tag{56}$$

Eqs.(53) to (56) can be rearranged into the dimensionless equations expressed by Eqs.(58) to (61) by applying the following dimensionless number.

$$\left.\begin{aligned} &U = \frac{bu}{\upsilon Gr},\ V = \frac{bv}{\upsilon} \\ &X = \frac{x}{bGr},\ Y = \frac{y}{b} \\ &P = \frac{P_d b^2}{\rho \upsilon^2 Gr^2},\ \Theta = \frac{T - T_o}{T_w - T_o} \\ &Gr = \frac{g\beta (T_w - T_o) b^3}{\upsilon^2},\ \mathrm{Pr} = \frac{\mu c_p}{\lambda} \end{aligned}\right\} \tag{57}$$

Equations of continuity, energy and motion are rewritten as follows:

$$\frac{\partial U}{\partial X} + \frac{\partial V}{\partial Y} = 0 \tag{58}$$

$$U \frac{\partial \Theta}{\partial X} + V \frac{\partial \Theta}{\partial Y} = \frac{1}{\mathrm{Pr}} \frac{\partial^2 \Theta}{\partial Y^2} \tag{59}$$

$$U \frac{\partial U}{\partial X} + V \frac{\partial U}{\partial Y} = \frac{\partial^2 U}{\partial Y^2} - \frac{\partial P}{\partial X} + \Theta \tag{60}$$

Boundary conditions are represented as follows:

$$\left.\begin{aligned} &X = 0,\ 0 < Y < 1:\ U = Q,\ V = 0,\ \Theta = 0 \\ &Y = 0,\ X \geq 0:\ U = 0,\ V = 0,\ \Theta = 1 \\ &Y = 1,\ X \geq 0:\ U = 0,\ V = 0,\ \partial \Theta / \partial Y = 0 \\ &X = 0:\ P = 0 \\ &X = L:\ P = 0 \end{aligned}\right\} \tag{61}$$

where Q (dimensionless buoyant airflow quantity) and L (dimensionless height of a cavity) are defined by Eqs.(62), (63).

$$Q = \frac{b\bar{u}}{\upsilon Gr} = \int_0^1 U dY \tag{62}$$

$$L = \frac{l}{bGr} \tag{63}$$

In the case difference coordinates are used as in Fig.10, the value of Q can be calculated by Eq.(64) on the basis of Simpson's law.

$$Q = \frac{\Delta Y}{3} \left(4 \sum_{j=1}^{(K-1)/2} U_{m+1,2j} + 2 \sum_{j=1}^{(K-3)/2} U_{m+1,2j+1} \right) \tag{64}$$

If Q and Pr are given as initial conditions, the distributions of pressure, velocity and temperature can

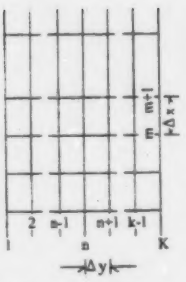

Fig.10 Difference coordinates

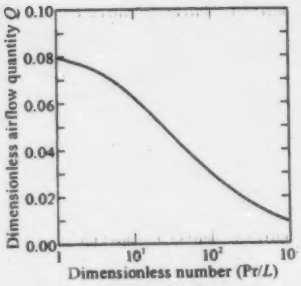

Fig.11 Correlation between Q and Pr/L

be solved from Eqs.(58) to (60) for every height level by convergence calculation as a function of Q, which is obtained from Eq.(64), on the basis of the boundary conditions. When P becomes 0, the dimensionless height L is obtained and then the relationship of Pr/L (revised Rayleigh number) to Q is identified as in Fig.11.

CONCLUSIONS

The theoretical models of heat transfer used in THERB (the simulation software of the thermal environment of residential buildings) are outlined and the following prominent features of the models are highlighted.

1) Calculation time and storage capacity for transient thermal conduction of multi-layer walls in the time-discrete domain are decreased by making use of the successive transition method and the accuracy of conductive heat is increased by applying the trapezoid hold function which can adjust itself to the time-discrete domain.
2) Dimensionless equations, which are derived from the profile method for boundary layer or defined from experimental findings according to natural or forced convection, are used to calculate convective heat transfer coefficients for every part of buildings.
3) The long-wave and short-wave absorption coefficients make it possible to simulate the net absorption of radiant heat and transmitted solar radiation as a consequence of multiplex reflection among interior surfaces of buildings. Furthermore the absorption coefficients are applicable to radiant heat emitted from lights, appliances and human bodies, etc.
4) A multi-layer window model, which defines the overall transmittance, absorptance and reflectance of solar radiation as an infinite series, is proposed.
5) A network airflow model is used to calculate ventilation quantities in each zone where each zone is represented by nodes. Furthermore, the dimensionless buoyant airflow model derived from this network model is applicable to independent ventilated wall cavities.

REFERENCES

[1] Watanabe T., Ozaki A., et al. (1985), 'Practical Methods for Calculating Unsteady-State Heat Conduction of Multi- Layer Walls Based on Pulse Transfer Function', *Journal of Architecture, Planning and Environmental Engineering*, Architectural Institute of Japan, No.391, 8-19

[2] Stephenson D.G. and Mitalas G.P. (1967), 'Cooling Load Calculation by Thermal Response Factor Method', *ASHRAE Transactions*, Vol.73-I

[3] Urano Y. and Watanabe T. (1981), 'Analysis of Conductive Heat Transfer of Multi-Layer Wall by State Transition Determinant – Part 1', *Journal of Architecture, Planning and Environmental Engineering*, Architectural Institute of Japan, No.305, 97-111

[4] Pipes L.A. (1957), 'Matrix Analysis of Heat Transfer Problems', *Journal of Franklin Institute*, Vol.263, No.3

[5] Nishikawa K. and Fujita Y. (1988), *Heat Transfer*, Rikougakusha

[6] Ozaki A., Watanabe T., et al. (1990), 'Heat and Mass Transfer at Outside Surface of Buildings – Wind Tunnel Tests of Heat and Mass Transfer on Horizontal Surfaces', *Journal of Architecture, Planning and Environmental Engineering*, Architectural Institute of Japan, No.407, 11-25

[7] Fujii W. and Imura H. (1972), 'Natural Convection Heat Transfer from a Plate with Arbitrary Inclination', *Int. J. Heat Mass Transfer*, Vol.15, 755-767

[8] Perez R., et al. (1990), 'Modeling Daylight Availability and Irradiance Components from Direct and Global Irradiance', *Solar Energy*, Vol.44, No.5, 271-289

[9] Ono K., Ozaki A., et al. (1996), 'Calculation of Direct Solar Heat Gain through Glazing – Successive Incident Angle Method and Solar Shading Coefficient Method', *Fukuoka University Review of Technological Sciences*, No.58, 67-75

[10] Ozaki A., Watanabe T., et al. (1997), 'Analysis of Draft Quantity through Ventilated Air Space', *Proc. of the 14th International Conference on Passive and Low Energy Architecture*, Vol.2, 33-38

[11] ASHRAE (1972), *ASHRAE Handbook of Fundamentals*, 425-440

[12] July E.I. (1958), 'Sampled-Data Control System', *John Wiley & Sons*

[13] Urano Y. and Watanabe T. (1982), 'Analysis of Conductive Heat Transfer of Multi-Layer Wall by State Transition Determinant – Part 2', *Journal of Architecture, Planning and Environmental Engineering*, Architectural Institute of Japan, No.311, 57-66

[14] Gebhart, B. (1959), 'A New Method for Calculating Radiant Exchanges', *ASHRAE Transactions*, Vol.65

Session 3 / Séance 3

Modelling of Non-Thermal Processes: Lighting, Moisture, Material Emissions

La modélisation des procédés non thermiques : l'éclairage, l'humidité et les émissions produites par les matériaux

A METHODOLOGY FOR DETAILED CALCULATION OF ROOM ILLUMINANCE LEVELS AND LIGHT DIMMING IN A ROOM WITH MOTORIZED BLINDS INTEGRATED IN AN ADVANCED WINDOW

Andreas K. Athienitis, Professor, Centre for Building Studies, athiena@alcor.concordia.ca
Athanassios Tzempelikos, Research Assistant, Concordia University, Montreal, agtzemb@alcor.concordia.ca

ABSTRACT

This paper presents a methodology for detailed lighting/daylighting numerical simulation of an office space with an advanced window system and calculation of dimming levels for electric lights. The particular system considered is a double-glazed low-emissivity window with motorized highly reflective blinds between the two glazings installed in an outdoor test-room and operated by a custom-built computerised building automation system. The daylight transmittance equations for the window system were determined from experimental measurements. A major requirement for on-line control is the automatic determination of the blind tilt angle required in order to avoid glare and simultaneously allow the maximum possible amount of daylight in the room. Numerical simulations indicate energy savings of over 70% in electricity consumption for lighting.

INTRODUCTION

Utilization of daylight in buildings may result in significant savings in electricity consumption for lighting while creating a higher quality indoor environment. The benefits in terms of higher productivity and reduced absenteeism of office workers probably exceed the significant energy savings. Additional energy savings are also realized during the cooling season, when reduction of internal heat gains due to electric lighting results in a corresponding reduction of cooling energy consumption.

The concept of dynamic building envelope technologies introduces a potential for higher quality work environment as well as energy-efficient solutions. Innovative daylighting systems aim to increase daylight levels and improve the daylight uniformity within a space, while controlling sunlight and reducing glare and discomfort for the occupants (*Lorenz, 2000, Beck, 1999*). Simultaneous control of electric lighting systems and building envelope conventional components can minimize energy use (*Vartiainen, 1999*). Predictive control algorithms, can determine the optimal operation of all HVAC components and building envelope systems in order to achieve annual minimization of energy consumption (due to lighting/heating/cooling) while maintaining good human comfort (*Lee, 1995, 1998, Scheatzle, 1990*).

For an office space, it is necessary to avoid glare and high contrast, which cause discomfort to the occupants. Thus, shading provision should be considered as an integral part of fenestration system design, especially for south-facing facades of buildings. Shading devices can be multi-purpose: blocking direct sun and solar gains during the cooling season, allowing the maximum amount of daylight and solar gains during the heating season, controlling the sunlight by diffusing it into the space without causing glare on clear days, while, at the same time, transmitting all the available daylight on overcast days. Human control of moving shading devices is not reliable and causes a constant disruption for the occupants if optimum results are to be achieved. In modern offices, the need for efficient automation systems is greater than ever and motorized shading devices are an attractive option.

The diurnal and seasonal changes in the sun's position and the sky conditions cause a large and complex variation in the daylight transmitted through a window system with an integrated shading device (*Molina, 2000*). Thus a detailed study of all the parameters involved in the transmission process and a balance between the accuracy of calculations and numerical complexity is required (*Tsangrassoulis, 1996*).

This paper presents a methodology for detailed lighting/daylighting numerical simulation of an office space with an advanced window system and calculation of dimming levels for electric lights so as to optimize utilization of daylight and minimize electricity consumption. The particular system considered is a double-glazed low-emissivity window with motorized highly reflective blinds between the two panes installed in an outdoor test-room and operated by a custom-built computerised building automation system. The daylight transmittance equations for the window system were determined from experimental measurements. A technique for detailed simulation of the illuminance level on the

work plane area is then presented together with a dimming control algorithm for a typical office space.

EXPERIMENTAL MEASUREMENTS AND RESULTS

The experiments were performed in an outdoor test-room in Montreal. The interior dimensions of the test-room are 2.3 m wide × 2.7 m wide × 2.4 m high and the window system is integrated on the façade facing 10 degrees east of south (Fig. 1).

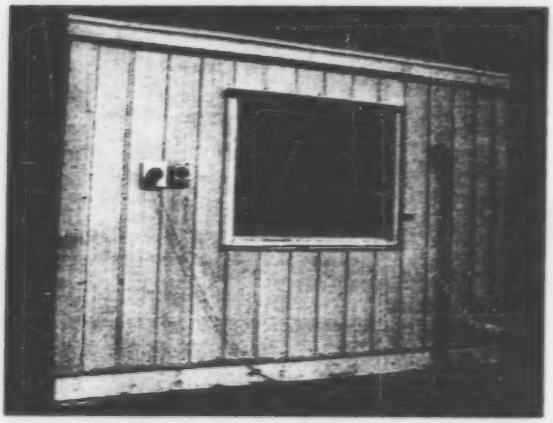

Fig. 1. Outside view of the test-room with the window (daylight and solar radiation sensors are mounted just beside the window).

The window ("Vision Control window"), provided by Unicel Inc., is double-glazed with a low-emissivity coating and highly reflective louvers integrated between the two panes; its dimensions are 1.08 m ×1.08 m. The motorized louvers are made of extruded aluminium, hollow-chambered profile with overlap. They are 35mm wide and 6mm thick at the centre. They can rotate in both directions (180°).

Several solar radiation and daylight sensors were employed to measure solar radiation and its visible portion respectively. Two were mounted on the wall just beside the window (Fig. 1) to measure the solar radiation and daylight incident on the window. There is no single widely used procedure for measuring the transmittance of such non-homogeneous shading devices. A method presented by *Aleo (1994)* is a typical approach. In this study the sensors were mounted at the centre of the inside surface of the window. A detailed investigation of the illuminance uniformity over the whole window area showed that, the daylight uniformity ratio (maximum/minimum value) was less than 110%, taking its maximum value at the centre of the window area. Another movable daylight sensor was installed in the room at a height 0.85m from the floor, to measure the illuminance level at different locations on the work plane. Data were collected for five months, from July 2000 to November 2000.

A customised data acquisition and control (building automation) program was developed in C++ and employed in this project. It was designed to offer the user several options in the control of the blinds and the heating/cooling system. Data were usually sampled every 6 seconds and averaged every 6 minutes. The measurements were detailed and included the collection of data for all blind tilt angles (0°-180°), for all times of the day and for different sky conditions, in order to obtain an accurate characterization of the transmittance properties of the window system.

Transmittance Of The Window And Shading Device

The transmittance equation for the window was determined as a function of sky conditions, blind tilt angle (β) and angle of incidence (θ) (see Fig. 2). Two sky conditions are considered: (i) overcast sky and (ii) the clear sky. Because the two types of days (clear and overcast) cannot be perfectly reproduced, measurements were taken for a large number of days falling into these categories and then statistical analysis of the collected data gave average values for the transmittance on a typical cloudy and on a sunny day.

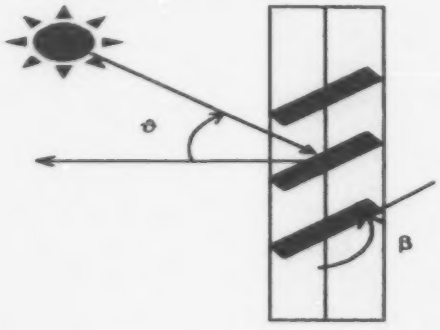

Fig. 2. Schematic of window indicating blind tilt angle, β, and angle of incidence, _.

The angle of incidence is chosen as a parameter of the transmittance equation so that it can then be employed for any window orientation and any location. The transmittance value for a certain blind tilt angle and angle of incidence is found by dividing the illuminance measured on the inside surface of the window by the value measured by the exterior sensors. Figures 3-6 show the visible transmittance

(τ_v) as a function of blind tilt angle (β) and angle of incidence (θ) for both overcast and clear days.

For overcast days, the tilt angle has a strong effect on daylight transmittance (Fig. 3). The curve reaches a maximum at about β=60° for all angles of incidence. For this blind tilt angle, the maximum value is τ_v=38.2%, for θ=27°. The incidence angle has a negligible effect on τ_v, since there is only diffuse daylight; this can also be observed from Fig. 4. These curves can be expressed by an equation independent of θ (only a function of β). Using advanced analytical regression techniques, the following equation was obtained (regression coefficient = 0.99):

$$\tau_v^{diffuse} = \frac{4.5 \cdot 10^{12} \cdot a^{-6}}{e^{\frac{335}{a}} - 1} \qquad (1)$$

For clear sky, the incidence angle has a significant effect on transmittance (Figures 5, 6). The visible transmittance is higher for smaller incidence angles and there is a minimum around θ = 45°. The maximum value (τ_v=55%) is measured for β = 78° and θ=15°. Using multivariate regression techniques the following general equation was obtained (regression coefficient = 0.99):

$$\tau_v^{clear}(\beta,\theta) = 0.55 \cdot e^{-\frac{(\beta-80)^2}{1900}} \cdot (-4.917 \cdot 10^{-7} \cdot \theta^4 + 0.00009 \cdot \theta^3 - 0.00567 \cdot \theta^2 + 0.13 \cdot \theta - 0.00437) \qquad (2)$$

The above equation consists of two terms: the first term describes the effect of blind tilt angle (it is a normal distribution approximation with the maximum of the curve at β=80 degrees as shown in Fig. 5). The second term describes the effect of θ on the transmittance: it is approximated by a 4th-degree polynomial curve (Fig. 6).

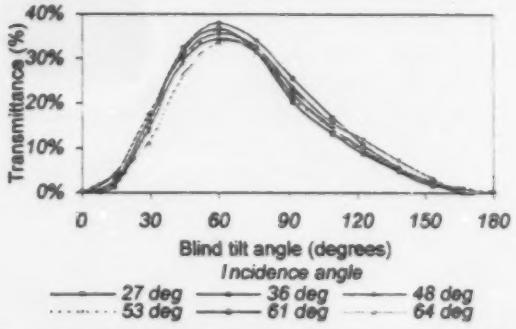

Fig. 3. Daylight transmittance as a function of β for several solar incidence angles, overcast day.

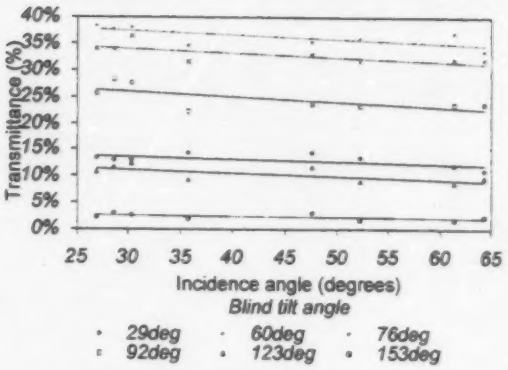

Fig. 4. Daylight transmittance as a function of θ for various blind tilt angles, overcast day.

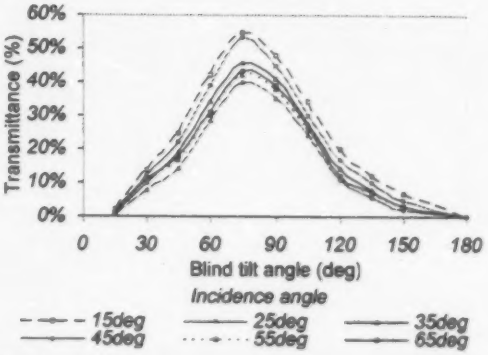

Fig. 5. Daylight transmittance as a function of β for various solar incidence angles, clear day.

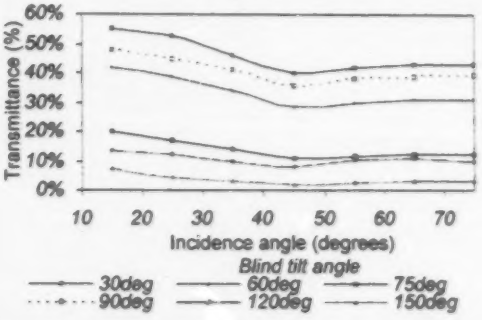

Fig. 6. Daylight transmittance as a function of θ for various blind tilt angles, clear day.

SIMULATION METHODOLOGY

Given the transmittance of a window with a controlled shading device as a function of angle of incidence, shading device position and sky conditions, a simulation of an office space with such a window may be performed. The technique developed determines first the optimum tilt angle of the blinds in order to transmit the maximum possible

amount of daylight without causing glare (by eliminating beam radiation) while allowing the maximum possible view outside. Then, it determines the illuminance due to daylight at several (3-4) points on the work plane (which is assumed to be 0.8 m above the floor) for representative days in each month, once every hour, from 9 am to 5 pm (typical working hours for an office). The dimming levels for the artificial lighting are then determined in order to provide the balance of light required to achieve the required total illuminance levels. Finally, it calculates the energy savings due to electrical lighting from simultaneous control of the blinds and dimming of the lights.

The main input variables in the program are the day number in the year (n) and the solar time (t). Here we considered a 5×5×3m office space located in Montreal, with a 2×4m Vision Control window on the façade facing 10° east of south, with no obstructions and ground reflectance equal to 20%. The reflectance of the floor is assumed to be 30%, the ceiling reflectance 80% and the reflectance of all sidewalls 70%. The angle of incidence is first calculated for every hour of each representative monthly day. The next step is to calculate the illuminance incident on the window. At this point sky conditions must be selected.

CIE Overcast Sky

In this case, there is only diffuse daylight incident on the window coming from the sky and the ground and glare is not much of a concern. In order to allow better view outside and also transmit the maximum possible amount of daylight in the room, the optimum tilt angle is selected, in this case $\beta_{opt}^{diffuse} = 75°$ ($\tau_v \approx 30\%$).

The daylight from the sky is equal to the horizontal illuminance multiplied by the view factor between the sky and the window $F_{w\text{-}sky}$ (0.5 for vertical window). The daylight from the ground is equal to the horizontal illuminance multiplied by the ground reflectance (ρ_g) times the view factor between the ground and the window $F_{w\text{-}gr}$ (0.5). The daylight incident on the window is the sum of these two terms:

$$E_w = E_h \cdot F_{w\text{-}sky} + E_h \cdot F_{w\text{-}gr} \cdot \rho_g \quad (3)$$

The horizontal illuminance under a CIE overcast sky (Murdoch 1985) on a certain day n and time t may be expressed as (lx):

$$E_h^{ov}(n,t) = 1000 \cdot (0.3 + 21 \cdot \sin(\alpha(n,t)) \quad (4)$$

Where _ is solar altitude. Thus the daylight incident on the window on an overcast day at time t will be:

$$E_w^{ov}(n,t) = 500 \cdot (0.3 + 21 \cdot \sin(\alpha(n,t)) \cdot (1 + \rho_g) \quad (4a)$$

The daylight transmitted in the room is equal to:

$$E_{overcast}(n,t) = E_w^{ov}(n,t) \cdot \tau_v^{diffuse}(\beta_{opt}^{diffuse}) \quad (5)$$

CIE Clear Sky

The daylight incident on the window on a clear day consists of three terms: direct sunlight, diffuse light from the sky and reflected light from the ground. The horizontal illuminance due to the sky is given by:

$$E_{hsky}(n,t) = 800 + 15500 \cdot [\sin(a(n,t))]^{1/2} \quad (6)$$

The solar horizontal illuminance is:

$$E_{hsun}(n,t) = E_o \cdot f(n) \cdot e^{-c \cdot m(n,t)} \cdot \sin(a(n,t)), \quad (7)$$

where:

$E_o = 127500\ lx$ is the average illuminance on a surface perpendicular to the sun's rays just outside the earth's atmosphere,

$$f(n) = 1 + 0.033 \cdot \cos(360 \cdot n / 365)$$

is a correction factor to account for the elliptical shape of earth's orbit around the sun, c is the optical atmospheric extinction coefficient (equal to 0.21 for a clear day), and

$m(n,t) = 1/\sin(a(n,t))$ is the relative optical air mass.
The total horizontal illuminance is given by:

$$E_h^{clear}(n,t) = E_{sky}(n,t) + E_{hsun}(n,t) \quad (8)$$

The daylight incident on the window from the ground $E_{wgr}(n,t)$ and from the sky $E_{wsky}(n,t)$ are given by:

$$E_{wgr}(n,t) = F_{w\text{-}gr} \cdot \rho_g \cdot E_h(n,t) \quad (8a)$$
$$E_{wsky}(n,t) = F_{w\text{-}sky} \cdot E_{hsky}(n,t) \quad (8b)$$

The daylight incident on the window directly from the sun is given by:

$$E_{wsun}(n,t) = E_o \cdot f(n) \cdot e^{-c \cdot m(n,t)} \cdot \cos(\theta(n,t)) \quad (8c)$$

Thus the total daylight incident on the window on a clear day may be expressed as follows:

$$E_w^{clear}(n,t) = E_{wgr}(n,t) + E_{wsky}(n,t) + E_{wsun}(n,t) \quad (8d)$$

In the case of clear sky, it is desired to prevent direct sunlight from coming into the room to avoid glare and high contrast. Thus, the blind tilt angle must be adjusted depending on the position of the sun. Since the blinds are horizontal, the solar azimuth has no effect on the daylight transmitted through the blinds and we are only interested in the solar altitude. Fig. 7

shows two adjacent blinds in a horizontal position (β=90°) and at another position at an angle β. The distance between the blinds and the width of each blind are both equal to r. For a random position of the blinds, a direct ray can enter the room (without reflection on the blinds) only for solar altitudes between 0° and α°. In other words, for a certain solar altitude (time), the minimum blind tilt angle that must be set to prevent direct sunlight from coming into the room is the angle β shown in Fig. 7. The reasons for choosing the minimum blind tilt angle are two: first, to allow more daylight into the room (the transmittance values are greater for blind angles closer to horizontal) and second, to allow better view to the outside. Calculating β as a function of solar altitude _ from the geometry of Fig. 7 will give the optimum tilt angle for any time and day on clear days. It is obvious that, because the width of the blinds is equal to the distance between them, for solar altitude angles greater than 45° no direct sunlight is transmitted through the blinds when they are in a horizontal position. Thus, for the hours that α>45°, the blinds will be set at β=90° to maximize view field. For all the other cases the calculations must be performed. Considering triangle ABC we obtain:

$$tan(\hat{a}) = \frac{r - r \cdot sin(\hat{a} - 90°)}{r \cdot cos(\hat{a} - 90°)} = \frac{1 - sin(\hat{a} - 90°)}{cos(\hat{a} - 90°)}$$

Solving this equation for β, we find:

$$\beta_{opt}^{clear}(n,t) = 180° - 2 \cdot \alpha(n,t) \qquad (9a)$$

The optimum blind tilt angle to block beam radiation is selected as follows:

$$if\ a(n,t) > 45°,\ then\ \beta_{opt}^{clear}(n,t) = 90°\ (constant)$$

$$else\ \beta_{opt}^{clear}(n,t) = 180° - 2 \cdot \alpha(n,t) \qquad (9b)$$

The daylight transmitted in the room on a clear day at any time and day is:

$$E_{clear}(n,t) = E_w^{clear}(n,t) \cdot \tau_v^{clear}(n,t) \qquad (9c)$$

Luminous Exitances And Illuminance On The Work Plane

The window interior surface is considered as a diffuse luminous source emitting daylight towards all directions in the room. Although this is true for blind tilt angles near 90° (horizontal), it causes some error for blind tilt angles greater than 130° because for such angles the blinds act like small light shelves, illuminating mainly the ceiling and improving the illuminance distribution at the deepest parts of the room. However, the blinds are highly reflective on both sides and thus a significant amount of thetransmitted daylight is reflected towards the work plane, the floor and the sidewalls.

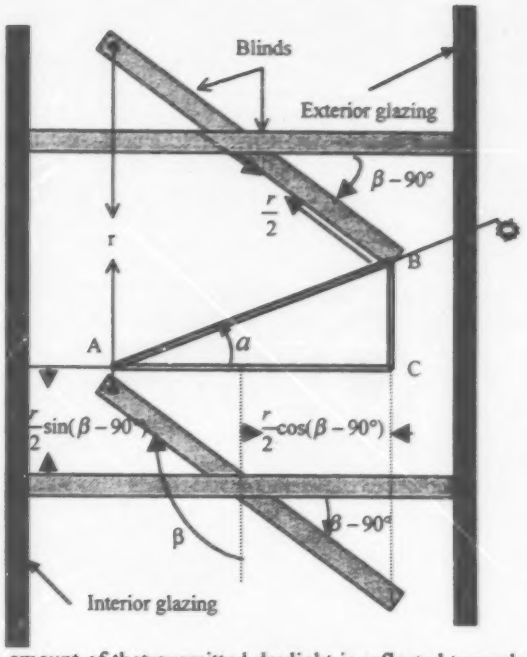

Fig. 7. Cross-section of the window for the calculation of angle β to prevent glare on clear days.

The room is first modelled by 7 surfaces (i=1..7): the window, the wall containing the window, the floor, the ceiling, the back wall and the two sidewalls. Only the window surface has an initial luminous exitance (the transmitted daylight).

The final luminous exitances of all interior surfaces after multiple reflections in the room are next calculated based on radiosity analysis. First, the form factors between all interior surfaces are found. The form factor F_{12} between two surfaces A_1 and A_2 is the ratio of average illuminance on A_2 produced by the flux received directly from A_1 due to the luminous exitance of A_1. Using form factors, the final luminous exitance of each interior surface (M_i) is determined by:

$$M_i = M_{oi} + \rho_i \cdot \Sigma M_j \cdot F_{ij} \qquad (10)$$

where ρ is the surface reflectance. This system of equations may be written in matrix form as follows:

$$M_o = (I - T) \cdot M_i \qquad (10a)$$

where M_o is the initial luminous exitance matrix, I is the 7x7 identity matrix and T is a matrix whose elements are given by $T_{ij} = \rho_i \cdot F_{ij}$.

The matrix of the final luminous exitances of the interior surfaces is calculated from:

$$M(n,t) = (I-T)^{-1} \cdot M_o(n,t) \quad (11)$$

The next step is to select representative points on the work plane and calculate the illuminance. Four points are selected (A, B, C and D) on the work plane 2.5 m from both the left and right wall and at distances from the window given by:
A: 0.94m, B: 1.88m, C: 2.82m, D: 3.76m.
In order to compute the illuminance on the selected points, the configuration factors need to be determined between each of the points and all interior surfaces of the room. The configuration factor c_{Si-A} is defined as the ratio of the illuminance at a differential area (point A) produced by the flux received directly from a surface (S_i) due to the luminous exitance of S_i. The illuminance at each point for all days and times is given by (in matrix form):

$$E_{A,B,C,D}(n,t) = \sum M_i(n,t) \cdot C_{Ai,Bi,Ci,Di} \quad (12)$$

Fig. 8 shows the illuminance profile of the room (at points A, B, C, D) on a clear and on an overcast day in January.

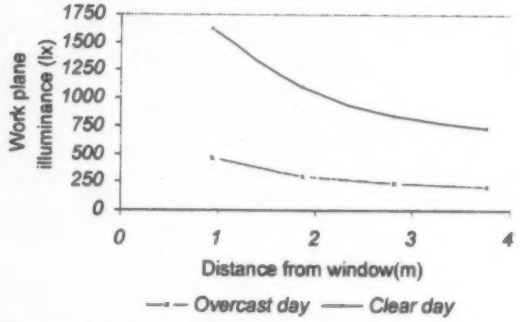

Fig. 8. Illuminance distribution on the work plane, on a typical overcast and clear day in January (10am).

On clear days allows plenty of diffuse daylight is transmitted into the room, without causing glare, and even at 4 m from the window there are more than 750 lx on the work plane. On overcast days artificial lighting is necessary.

SIMULATION RESULTS

The blinds are automatically operated, and based on the above results, electrical lights are automatically dimmed in order to improve the illuminance distribution in the office and provide the necessary additional illumination to reach a pre-selected setpoint (500lx). The luminaires selected for this simulation were chosen based on standard sizing methods (coefficient of utilization, Murdoch 1985). Each luminaire consists of four 60 W rapid start fluorescent lamps with 3850 initial lumens per lamp. The required number of luminaires is two, in order to ensure 500 lx on the working plane. The position of the two luminaires is the following: the first (L_1) is above point B (1.88m from the window) and the second (L_2) is above point D (3.76m from the window). It is assumed that the dimming is not continuous, but it can be applied at four possible levels: 25%, 50%, 75% and 100% of maximum output. Knowing the illuminance at the four points due to daylight, the additional illuminance required to reach 500lx on all points is calculated.

First, L_2 is dimmed (which is deeper in the room) and then, depending on the new illuminance level on points A and B, L_1 is dimmed at the optimum level. The dimming level for both L_1 and L_2 is calculated for all the working hours of the year in matrix form. These calculations are performed for both clear and overcast days. Representative results are shown in figures. On overcast days, this dimming strategy improves significantly the illuminance distribution in the office and ensures that there are always more than 500 lx at each of the four points (Fig. 9, Fig. 10). On clear days, when there is not enough daylight after 3pm, the problem is eliminated and the illuminance distribution is also improved (Fig. 11, Fig. 12).

The results from the calculations of the dimming levels throughout the year are the following: on clear days, L_1 and L_2 are off except for the time between 4 pm and 5 pm in the evening, when L_1 is dimmed at 75% and L_2 (which is deeper in the room) is 100% on. This happens for all months of the year except December, when the lights are dimmed during all the working hours of the day. On overcast days, L_1 is dimmed at all times in winter and only from 4pm to 5pm in the other months, but L_2 needs to be dimmed during all months, as shown in Fig. 13.
On overcast days, L_1 is kept off during 65% of the working hours and L_2 is kept off during 19.4% of the working hours of the year.
On clear days, L_1 is kept off during 73.1% of the working hours and L_2 is kept off during 70.3% of the working hours of the year.
On overcast days, L_1 is never set at 100% output and L_2 is 100% on only for 9.2% of its operating hours in a year. On clear days, L_1 is never set at 100% output and L_2 is 100% on only during the 68.7% of its operating hours in a year.

Comparing with an office space where neither dimming of the lights nor on/off operation is

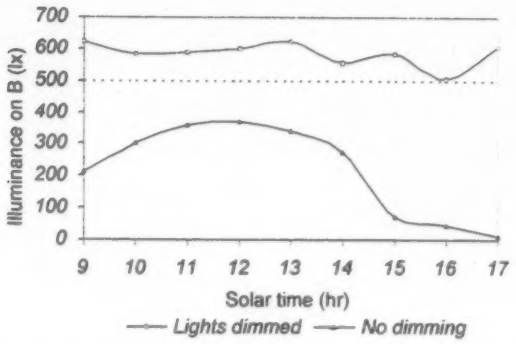

Fig. 9. Horizontal illuminance at point B on a typical overcast day in December (no dimming indicates lights off – only daylight present).

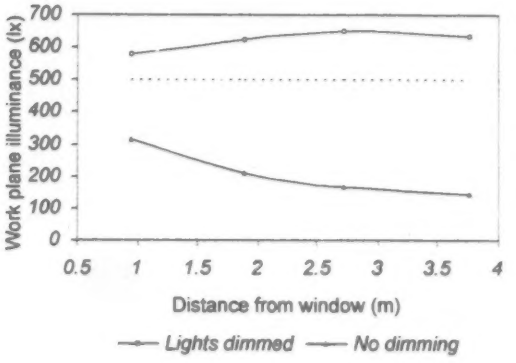

Fig. 10. Illuminance on the work plane at 9am on an overcast day in December (lights are dimmed at 75% (L_2) and 25% (L_1); no dimming indicates lights off).

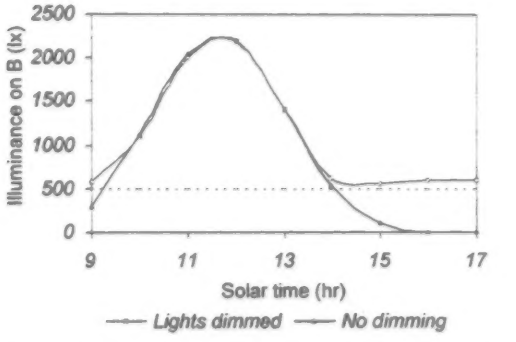

Fig. 11. Horizontal illuminance on point B on a typical clear day in December. Lights remain off from 9:30am to 2:00pm (no dimming indicates lights off).

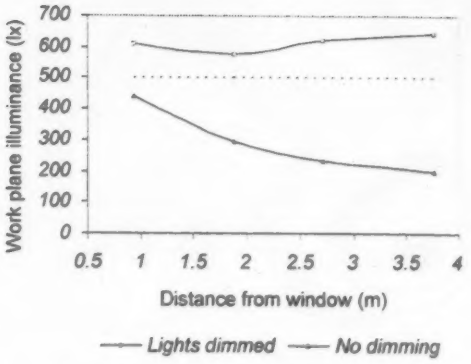

Fig. 12. Illuminance on the work plane at 9am on a typical clear day in December (L_1 is dimmed at 75% after 4pm and L_2 at full output after 2pm; no dimming indicates lights off).

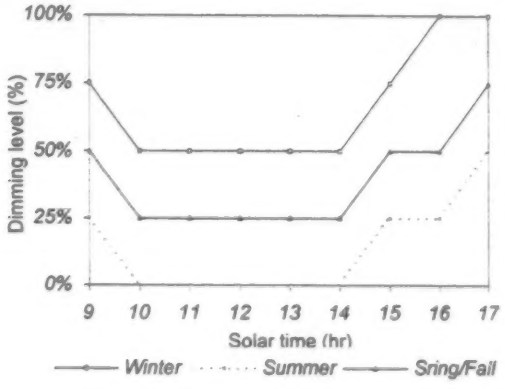

Fig. 13. Dimming levels of L_2 (3.76m from the window) during all seasons of the year.

available (lights are on at 100% output during all the working hours of the year), the energy savings due to electric lighting using the window system and the dimming methodology presented above reach 76.2% for overcast days and 87.6% for clear days.

CONCLUSION

This paper presented a methodology for detailed lighting numerical simulation of an office space with an advanced window system incorporating motorized reflective blinds between the two panes. Based on experimental measurements in an outdoor test-room, the daylight transmittance equations for the window system were determined as a function of sky conditions, blind tilt and angle of incidence. Given the transmittance equations for the window and the blind tilt angle for avoiding glare, the program then calculates the horizontal illuminance on selected

points on the work plane. Then, knowing all the illuminance values due to daylight at the required times, and choosing a required illuminance level on the work plane, the dimming factors needed are computed for the pre-selected luminaires. Finally the computer program determines energy savings from dimming of the lights.

The energy savings due to using the window system and the dimming methodology presented may exceed 70% for overcast days and 85% for clear days. Also, proper control of the blinds provides protection against direct solar radiation and glare.

In the case of partly cloudy days (when there are intervals of direct sunlight), the building automation system will determine the type of the sky conditions at regular times, based on the readings of an exterior sensor. In this case, frequent movement of the blinds must be prevented for psychological reasons (*Vine, 1998*), which should always be taken into account when dealing with advanced shading devices and innovative daylighting components.

Another factor to be investigated in the future is the impact of ground reflectance on the transmittance of the window, expected to be important when there is snow cover. However, in office buildings located in cities without frequent snow cover, this effect is not expected to be significant. Finally, although transmittance was expressed as a function of incidence angle in order to generalize the results, there is a surface azimuth angle effect, that although partly considered needs to be further studied.

ACKNOWLEDGEMENTS

Support of this work from Unicel Inc. and NSERC is gratefully acknowledged.

REFERENCES

Aleo F., Sciuto S., Viadana R. (1994), 'Solar transmission measurements in outdoor conditions of non-homogeneous shading devices', *Proc. European conference on energy performance and indoor climate in buildings*, Lyon, France.

Beck A., Körner W., Gross O., Fricke J. (1999), 'Making better use of natural light with a light-redirecting double-glazing system', *Solar Energy* 66, 215.

Lee E., Selkowitz S. (1995), 'The design and evaluation of integrated envelope and lighting control strategies for commercial buildings', *ASHRAE Trans.* 101, 326.

Lee E., DiBartolomeo D., Selkowitz S. (1998), 'Thermal and daylighting performance of an automated venetian blind and lighting system in a full-scale private office', *Energy and Buildings* 29, 47.

Lorenz W. (2000), 'A glazing unit for solar control, daylighting and energy conservation', *Solar Energy* 70, 109.

Molina L. J., Maestre R. I., Lindawer E. (2000), 'A model for predicting the angular dependence of the optical properties of complex windows including shading devices', *Proceedings of PLEA 2000*, Cambridge, UK.

Murdoch J. B. (1985), *Illumination Engineering-From Edison's Lamp to the Laser*, Macmillan publishing Inc., New York.

Scheatzle D. (1990), 'Computer controlled window blinds', *Proceedings of the 15th AS/ISES National Passive Solar Conference*, Texas, USA.

Tsangrassoulis A., Santamouris M., Asimakopoulos D. (1996), 'Theoretical and experimental analysis of daylight performance for various shading systems', Energy *and Buildings* 24, 223.

Vartiainen E., Peippo K., Lund P. (1999), 'Daylight optimization of multifunctional solar facades', *Solar Energy* 68, 223.

Vine E., Lee E., DiBartolomeo D., Selkowitz S. (1998), 'Office worker response to an automated venetian blind and electric lighting system: a pilot study', *Energy and Buildings* 28, 205.

DEVELOPMENT OF ANALYSIS SOFTWARE FOR THE OPTICAL CHARACTERISTICS AND DAYLIGHTING PERFORMANCE OF CONVENTIONAL AND TUBULAR SKYLIGHTS

Abdelaziz Laouadi and Morad Atif

Indoor Environment Research Program, Institute for Research in Construction

National Research Council Canada, Ottawa, Ontario.

Aziz.laouadi@nrc.ca, Morad.atif@nrc.ca

ABSTRACT

This paper presents an overview of the development of analysis software for the optical characteristics and daylighting performance of conventional and tubular skylights. The software is useful to skylight manufacturers, building designers and fenestration rating councils. The software development process spans over a four-year period, and includes development of prediction models for optical and daylighting performance of different skylight shapes, experimental and analytical validation of the prediction models, and software design. This paper focuses on the software structure, inputs, outputs and analysis modules. Preliminary results from the prediction models are also shown for the beam transmittance of barrel vault skylights, diffuse transmittance of domed skylights under different sky conditions, and average Daylight Factor on internal room surfaces.

BACKGROUND

The skylight market has been booming in recent years. Skylights are found in many modern or retrofitted buildings. In commercial and institutional buildings, skylights are used to simulate the outdoors and to bring natural light and solar heat into the indoor space. In residential buildings and houses, skylights are used mainly for illumination. Recently, tubular skylights have emerged as a new technology in commercial buildings and houses, potentially eliminating some of the drawbacks of the excessive solar heat gains of conventional skylights and extending the application of skylights in areas not reached by conventional skylights and windows (Bajda and Carter 2000; Salih et al. 2000; Shao et al. 1998). Skylights have the inherent potential to save electrical lighting, cooling and heating energy, beside their psychologically positive effects on building occupant satisfaction (HMG 2001, 1999; Heschong and McHugh 2000; Allen 1997; AAMA 1987, 1981; Cassidy 1986; Treado et al. 1983). However, despite these amenities, skylights integrated in building design may result in high-energy consumption if not properly designed. Skylight manufacturers lack design tools to assess the optical characteristics and daylighting performance of skylight products owing to complex skylight shapes that change with design requirements, and large sizes that impede fitting skylight products into measurement facilities. Furthermore, while measurements on some skylight products are possible, they can not be generalised for other products. In addition, fenestration simulation software such as VISION4 (CANMET 1995) and WINDOW (LBL 1992) deal with only planar geometry, such as windows and flat skylights.

OBJECTIVES

The Institute for Research in Construction, PERD (Panel for Energy Research and Development), and NRCan have started a four-year project to develop software to analyse the optical characteristics (transmittance, absorptance and reflectance) and daylighting performance of conventional and tubular skylights. The project is accomplished through three main tasks. The first task is devoted to developing prediction models for skylight optical characteristics and indoor daylight availability. The second task is the experimental and analytical validation of the prediction models. The third task focuses on the design of the software. The software will enable skylight manufacturers to prototype and characterise skylight designs before building them, and will aid building designers in skylight selection to meet design criteria for energy savings. The software will also help fenestration rating councils to rate the optical and daylighting performance of skylight products. The specific objective of this paper is to provide an overview of the software structure, analysis modules, and input and output parameters with some preliminary results from the first task of the project.

SOFTWARE STRUCTURE

Figure 1 shows a flow chart of the software structure. The main components of the software are the inputs, databases, analysis modules and outputs.

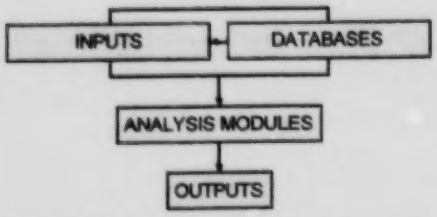

Figure 1 Flow chart of the software structure

INPUTS

The input parameters include general data, sky conditions, skylight system data, and data for the space under the skylight, which include the curb (space above roof), well (space between roof and ceiling) and room (space below ceiling). Databases for glazing optics and climate data are used to simplify the input data process (Figure 2).

General Inputs

The user supplies the site latitude and longitude angles, the ground/surrounding visible and solar reflectances, the simulation day, the floor target illuminance, and the file names for the glazing and climate databases, inputs and outputs. The user may also supply other dummy inputs, which are not used in the computation, such as project identifier, company name, etc.

Sky Conditions

Sky conditions affect the skylight optical characteristics and indoor daylight availability. The user may input a variety of sky conditions, varying from luminance-based to illuminance-based sky conditions. In the luminance-based sky conditions, the sky luminance pattern is known. The user may specify standard skies that are site-independent, or dynamic real skies that change with daytime. Standard sky conditions may be uniform overcast, CIE overcast, CIE intermediate, IES partly cloudy (IESNA 1993), CIE clear with polluted air, CIE clear with clean air (CIE 1990), or dynamic real (Perez et al. 1993). In the illuminance-based sky conditions, the hourly horizontal diffuse illuminance is known. The sky conditions may be uniform overcast, CIE overcast, or dynamic real. In the dynamic real skies, the sky luminance pattern has to be modelled. The model of Perez et al. (1990) is used for this purpose.

Conventional Skylights

Inputs for conventional skylights include the skylight shape and the glazing type. Conventional skylights are classified into four basic classes - dome-Like, vault-like, cone-like, and flat (Figure 3). Skylights with any other shape are converted to the class representative shape through the use of the concept of the Shape Parameter developed by Laouadi and Atif (2001a) and Laouadi et al. (2001). The representative shape for dome-like skylights is a hemispherical dome characterised by its truncation angle and radius. Skylights falling under this class include hemispherical domes with different profiles, segmented domes, square-based bubbles or any other similar shape. The representative shape for vault-like skylights is a barrel vault characterised by its truncation angle, orientation with respect to the south direction, radius and length. The gables (end walls) may be opaque, or glazed with different glazing types from that of the cylindrical part of the skylight. Skylights falling under this class include barrel vaults with different profiles, segmented barrel vaults, ridges, hip ridges, double pitch, rectangular-based bubbles or any other similar shape. The representative shape for cone-like skylights is a circular cone characterised by its cone angle and height. Skylights falling under this class include circular cones, polygons, pyramids, or any other similar shape.

Skylight glazing may be transparent or translucent. When the glazing is transparent, the optical properties (transmittance and front and back reflectances) for the visible and solar spectrums are read from the attached glazing database. When the glazing is translucent, however, the user has to input the diffuse optical properties of the flat sheet the skylight is made of for the visible and solar spectrums.

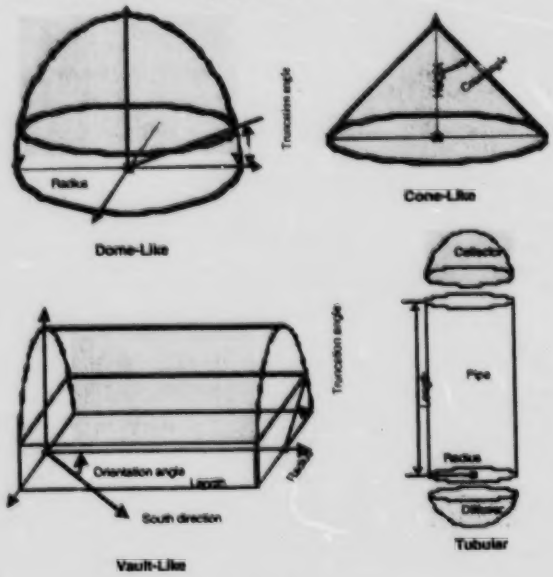

Figure 3 Skylight shape classes

Tubular Skylights

Tubular skylights are made of three components: collector, tube/pipe and diffuser (Figure 3). The collector is a hemispherical clear dome that collects solar rays. Inputs for the collector include the Shape Parameter and the glazing type. The glazing type is supplied from the attached glazing database. The tube or pipe channels solar rays (both beam and diffuse rays) downwards to the indoor space using a highly reflective lining. Inputs include the tube radius, length and surface reflectance. The diffuser is translucent and may take different shapes (flat, dome, rectangular, or other shape). Inputs include the Shape Parameter and the diffuse optical properties of the flat sheet the diffuser is made of.

ANALYSIS MODULES

These are the modules necessary to compute the output parameters (Figure 2). These modules are grouped into three categories: Optics modules, daylighting modules, and sky models.

Optics Modules

The skylight industry employs sophisticated glazing technologies. Most skylights have laminated glazing required for safety raisons. Tinted or solar reflective-coatings are usually employed in conventional skylights to reduce excessive solar heat gains. Low-e coatings are also used to reduce thermal heat loss. Therefore, optics modules have to accommodate all these technologies. These modules compute the optical characteristics of the glazing assembly, conventional skylights and tubular skylights. Glazing optics modules compute the optical characteristics of a composite pane (substrate and coating) and glazing assembly (set of composite panes separated by an air/gas space) at a given incidence angle. Optics modules for conventional/tubular skylights compute the overall optical characteristics of the skylight system under beam and diffuse lights for both solar and visible spectrums.

Daylighting Modules

Daylighting modules compute the outdoor and indoor daylight availability. These include modules to compute the outdoor horizontal illuminance for both beam light and diffuse light under different sky conditions, skylight well efficiency, Daylight Factor (for diffuse light), and indoor illuminance distribution at floor level and normal to walls (for combined beam and diffuse lights).

Sky Models

These modules compute or model the sky luminance patterns for the luminance-based or illuminance-based sky conditions. Sky conditions affect the optical characteristics of skylight and daylight availability. The considered sky models correspond to the sky condition inputs mentioned in Figure 2.

OUTPUTS

The software is used to analyse the optical characteristics and daylighting performance of skylights. The software is also used to produce rating data for a given skylight product under standardised conditions. The optical outputs include the skylight optical characteristics (transmittance, absorptance and reflectance) for beam light as a function of the incidence angle on a horizontal surface, and the optical characteristics for diffuse light as a function of daytime under a given sky condition (Figure 2). The software may also be used to output the optical characteristics of windows and flat skylights. Daylighting outputs include the skylight well efficiency, average Daylight Factor (for diffuse light) at room floor level and at different levels normal to walls, indoor illuminance distribution on the room floor, ceiling and walls (for combined beam and diffuse lights), and outdoor horizontal illuminance for beam and diffuse lights. Rating outputs include beam skylight transmittance at normal incidence angle; diffuse skylight transmittance under CIE overcast, IES partly cloudy and CIE clear sky conditions at noontime in a given location; Solar Heat Gain Coefficient (SHGC); and the ratio of the illuminated floor area to that of the skylight opening under CIE overcast, IES partly cloudy and CIE clear sky conditions at noontime in a given location.

PRELIMINARY RESULTS

Typical outputs of the software from the developed prediction models (project task 1) will be shown. These include transmittance of barrel vault skylights under beam light, transmittance of domed skylights under diffuse light from different sky conditions, and the average Daylight Factor on floor level and normal to walls. Other outputs and details are found in the references: Laouadi and Atif (1998), (1999), (2001a), (2001b), and (2001c).

Figure 4 shows the profile of the equivalent transmittance of barrel vault skylights as a function of the incidence angle on a horizontal surface for relative azimuth angles (difference between the sun and skylight azimuth angles) varying from 0° (sun parallel to the skylight axis) to 90° (sun perpendicular to the

skylight axis). The equivalent transmittance is defined as the ratio of the incident light flux to the transmitted flux that reaches the skylight base surface. The skylight length-to-radius ratio is fixed at L/R=2, and truncation angle = 0°. The top surface of the skylight is grey-tinted with double glass (outer pane is grey and inner pane is clear). The gable surfaces are glazed with double clear glass. The transmittance profile of a flat skylight with double-grey glass is also plotted in the figure. Skylights with tinted top and clear gables gather substantially more beam light at high incidence angles (i.e., low sun altitudes) than do flat skylights. At incidence angle θ_z = 70°, vault skylights may transmit between 122% to 293% more beam light than do flat skylights with similar top glazing, particularly when the sun is parallel to the skylight axis. The equivalent transmittance for incidence angles θ_z < 85° may reach up to 83% higher when the sun is parallel to the skylight axis (relative azimuth = 0°) than that when the sun is perpendicular to the skylight axis (relative azimuth = 90°).

Figure 5 shows the daily profile of the ratio of the diffuse equivalent transmittance (absorptance) to that of a flat glazing for double-clear, fully hemispheric domes during a typical summer day (June 24) in Ottawa, Canada. Transparent domes transmit (absorb) about 18% (80%) more than do similar flat skylights under uniform overcast skies, and 11% (58%) more under CIE overcast skies. The luminance-based models predict that transparent domes transmit (absorb) about 28% (47%) more than under standard CIE overcast skies under standard CIE clear skies, and 15% (25%) more under IES partly cloudy skies, particularly at low sun altitudes. The dynamic sky model predicts the equivalent transmittance and absorptance close to that under the IES partly cloudy skies, which was the case on June 24.

Figure 6 shows a comparison of the average Daylight Factor (DF) at floor level predicted using a newly-developed model and existing models under isotropic overcast skies for a square atrium with a 100% glazed roof. The skylight transmittance is fixed at 0.66. The floor and wall reflectances are fixed at 0.2 and 0.45, respectively. The developed model predicts the average DF values very close to the local DF values at the center of the floor predicted by the model of Liu et al. (1991). The developed model also yields average DF values close to those predicted by the model of Tregenza (1997), particularly for shallow atriums (Well Index, WI<1). Models based on physical scale measurements in artificial skies (Neal and Sharples 1992; Kim and Boyer 1986) overestimate the DF by up to 45% for atriums with WI<3 compared to the developed model. For atriums with WI>3, physical scale models yield approximately similar results as the developed model.

Figure 7 shows a comparison between the local DF normal to walls computed using the developed model, and the finite element method and scale-model measurements of Boubekri and Anninos (1996) under isotropic overcast skies. The well index of the sample atrium is fixed at WI=1.4 (length=31.25 ft, width=52.5 ft, and height =105 ft). The skylight transmittance is fixed at τ_{eq} = 0.7. The floor and wall reflectances are fixed at 0.3 and 0.5, respectively. The predictions from the developed model compare very well with those from the finite element method and physical scale-model measurements, with a maximum difference of 13% occurring at the bottom level of the wall.

CONCLUSIONS

The paper presents an overview of new analysis software for the optical characteristics and daylighting performance of conventional and tubular skylights. The paper focuses on the software structure, input and output parameters, and analysis modules. The software will enable users to vary skylight shape, dimensions and glazing types, sky conditions, and characteristics of the indoor space below the skylight. The software will provide skylight designers with optical characteristics (transmittance, absorptance and reflectance) of the skylight system for direct sunlight and diffuse light, and the indoor daylight availability (Daylight Factor, or illuminance on the floor and normal to walls). The software development process spans over a four-year period, and addresses the development of prediction models for the optical and daylighting performance of different classes of skylight shapes, experimental and analytical validation of the prediction models and design of the software. Preliminary results from the developed models demonstrate their accuracy and utility.

ACKNOWLDGEMENTS

This work is funded by PERD, NRCan and the Institute for Research in Construction of the National Research Council Canada. The authors are very thankful for their contribution.

REFERENCES

AAMA . 1987. Skylight Handbook, Design Guidelines. Des Plaines: American Architectural Manufacturers Association.

AAMA . 1981. Design for Energy Conservation with Skylights. Chicago: Architectural Aluminum Manufacturers Association.

Allen T., Conventional and tubular skylights: An Evaluation of the daylighting systems at two ACT commercial buildings, Proceedings of the 22nd National Passive Solar Conference, Washington DC, pp. 97-129, 1997.

Bajda C. A. and Carter D. J., Passive light pipes as luminaires, Proceedings of the CIBSE national conference, 2000.

Boubekri M. and Anninos W., Daylighting Efficiency of an Atrium: Part 1- The four-sided Type, Architectural Science Review. 39, 75-81, 1996.

CANMET. 1995. VISION 4 Reference Manual. Ottawa: Canadian Centre for Mineral and Energy Technology.

Cassidy V.M., Booming sales have skylight, greenhouse makers smilling, Modern Metals, pp. 20-24, December 1986.

CIE, Spatial Distribution of Daylight -Luminance Distributions of Various Reference Skies, Technical Report, 1995.

Heschong L. and McHugh J., Skylights: Calculating illumination levels and energy impacts, Illuminating Engineering Society, pp. 90-100, Winter 2000.

HMG, Skylighting design guidelines (www.h-m-g.com), 2001.

HMG, Skylighting and Retail Sales, An Investigation into the Relationship between Daylighting and Human Performance, report, Pacific Gas and Electric Company, 1999.

IESNA. Lighting Handbook, Reference And Application Volume. New York: Illuminating Engineering Society of North America, 1993.

Kim K, and Boyer LL, Development of Daylight Prediction Methods of Atrium Design, Proc. Int. Daylighting Conf., Long Beach, CA, 345-359 (1986).

Laouadi A., and Atif M.R. Daylight availability in top-lit atria: prediction of skylight transmittance and Daylight Factor. Lighting Research and Technology, 32(4), in press, 2001a.

Laouadi A., and Atif M.R. Prediction models of optical characteristics for domed skylights under standard and real sky conditions. Submitted to the 7th IBPSA conference, Rio de Janeiro, Brazil, 2001b.

Laouadi A., and Atif M.R. Prediction model of optical characteristics for barrel vault skylights. Submitted to IESNA Annual conference, Ottawa, Canada, 2001c.

Laouadi A., Atif M.R., and Galasiu A., Towards developing design tools for atrium skylights in cold Canadian climates, Part 2: Thermal and energy performance, NRCC report B3204.3, Canada, 2001.

Laouadi A., and Atif M.R. Predicting optical and thermal characteristics of transparent single-glazed domed Skylights. ASHRAE Transactions, 105(2), 325-333, 1999.

Laouadi A., and Atif M.R. Transparent domed Skylights: Optical Model For Predicting Transmittance, Absorptance And Reflectance. Lighting Research and Technology, 30(3), 111-118, 1998.

LBL. 1992. WINDOWS 4.0 User Manual. Berkeley: Lawrence Berkeley Laboratory.

Liu A, Navvab M, and Jones J, Geometric Shape Index for Daylight Distribution Variations in Atrium Spaces, Proc. Bienial Congress of Int. Solar Energy, Denver (1991).

Neal T, and Sharples S, The Influence of Well Geometry on Daylight Levels in Atria, Proc. CIBSE Nat. Lighting Conf. 342-345, 1992.

Perez R., Seals R., and Michalsky J., All-Weather Model for Sky Luminance Distribution – Preliminary Configuration and Validation, Solar Energy 50(3), pp. 235-245, 1993.

Perez R., Ineichen P., Seals R., Michalsky J., and Stewart R., Modeling Daylight Availability and Irradiance Components from Direct and Global Irradiance, Solar Energy 44(5), pp. 271-289, 1990.

Salih A., Shao L. and Riffat S., Study of daylight and solar infrared transmitted through light pipes under UK climate, Proceedings of the CIBSE national conference, pp. 198-207, 2000.

Shao L., Elmualim A.A. and Yohannes I., Mirror lightpipes: Daylighting performance in real buildings, Lighting Research and Technology 30(1), pp. 37-44, 1998.

Treado S., Gillette G., and Kusuda T. Evaluation of the Daylighting and Energy Performance of Windows, Skylights, and Clerestories. Report NBSIR 83-2726. U.S. Department of Commerce, 1983.

Tregenza PR, Daylight Attenuation in Top-Lit Atria, Lighting Res. Technol. 29(3) 151-157 (1997).

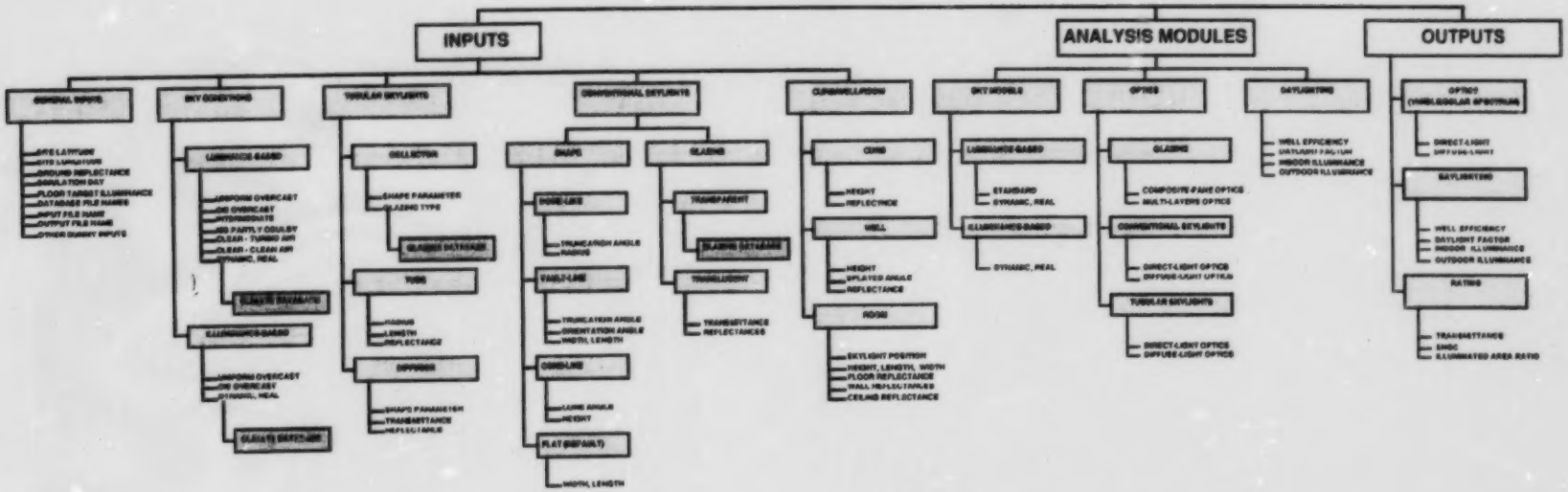

Figure 2 Flow chart of the inputs, analysis modules and outputs of the software

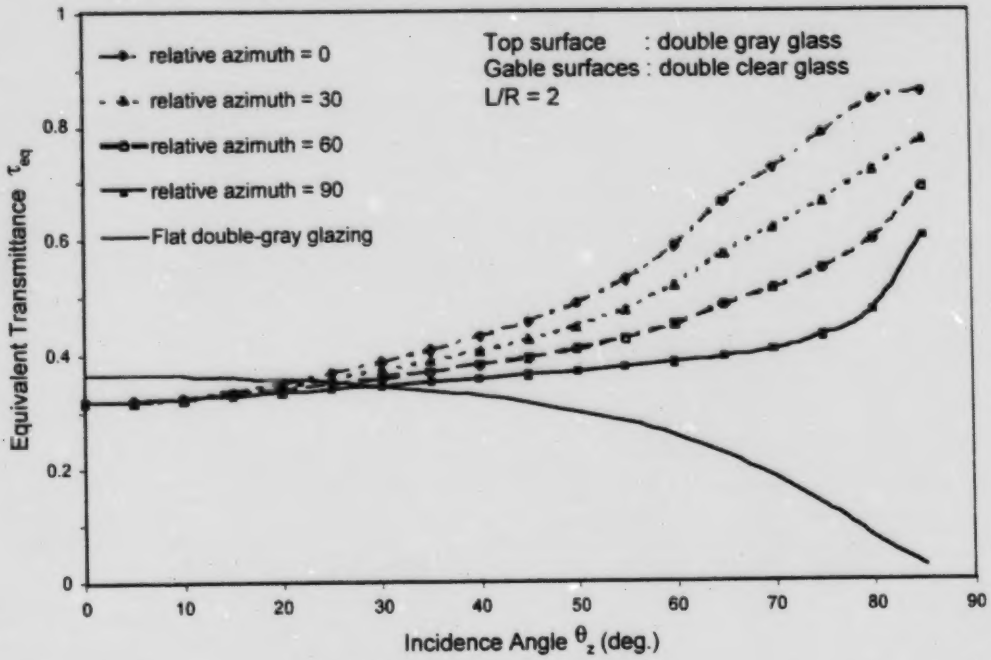
relative azimuth = 0
relative azimuth = 30
relative azimuth = 60
relative azimuth = 90
Flat double-gray glazing
Top surface : double gray glass
Gable surfaces : double clear glass
L/R = 2
Equivalent Transmittance τ_{eq}
Incidence Angle θ_z (deg.)

Figure 4 Profile of the equivalent visible transmittance as a function of the incidence angle on a horizontal surface for barrel vault skylights with tinted top and clear gables.

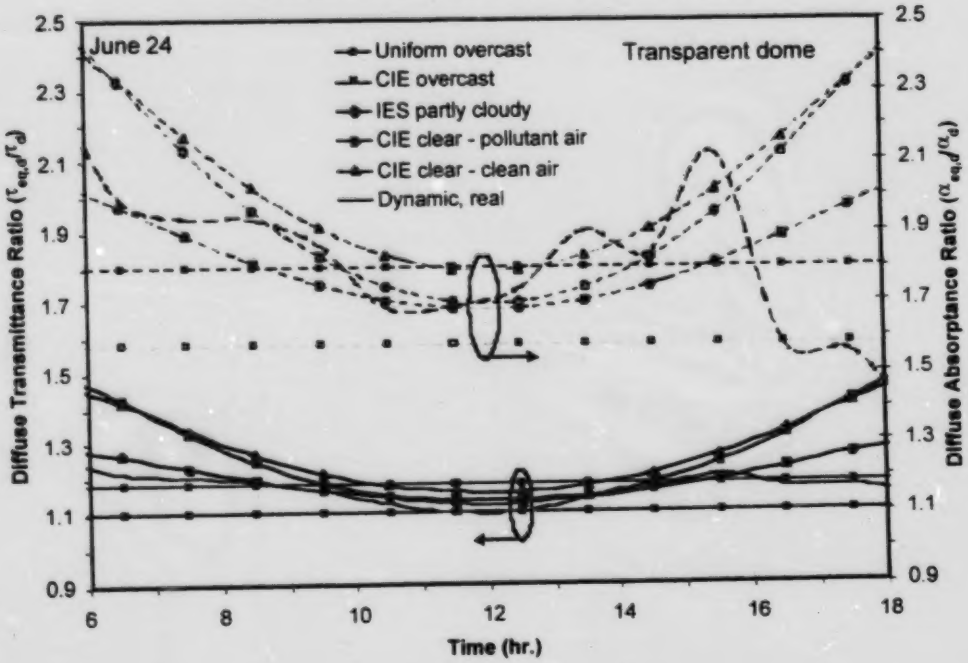

Figure 5 Daily profiles of the diffuse transmittance and absorptance ratios for transparent domes under standard and dynamic sky conditions during a summer day.

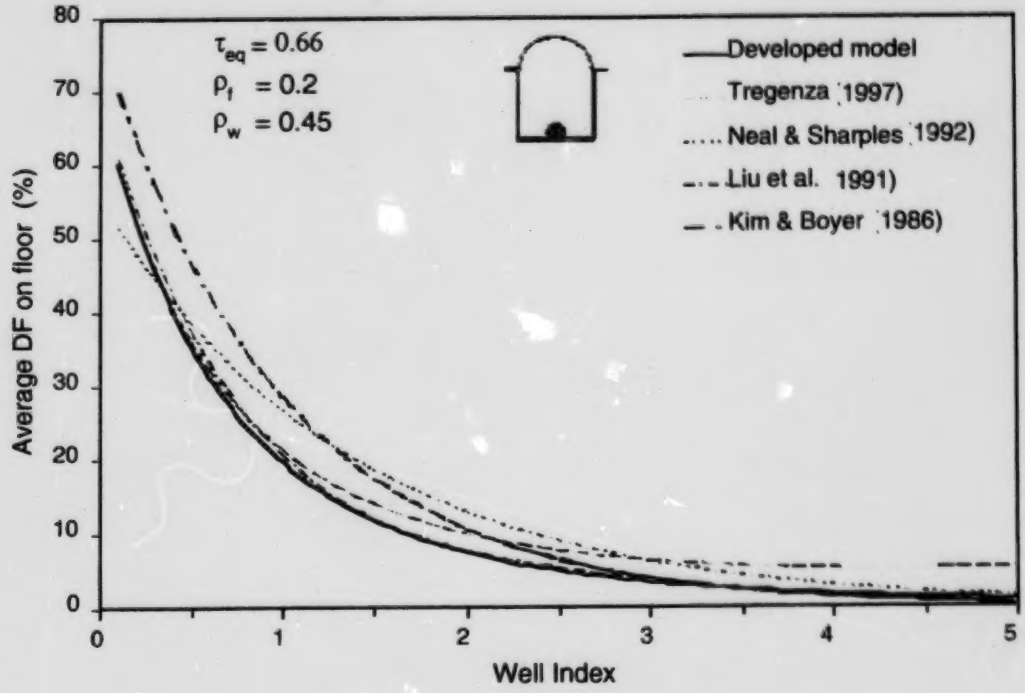

Figure 6 Average Daylight Factor on floor level of an atrium space

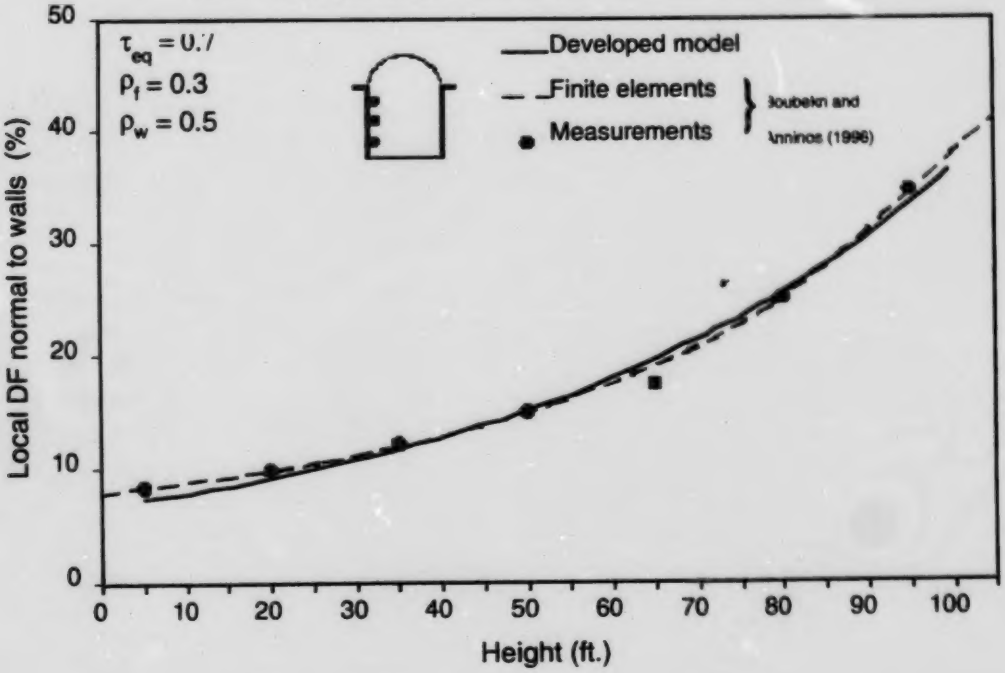

Figure 7 Local Daylight Factor normal to walls of an atrium

A MODEL FOR MOISTURE-CONTENT EVOLUTION IN POROUS BUILDING ELEMENTS: TREATMENT OF IRREGULAR REGIONS

Regina Katsman , Rachel Becker
NRC/IRC, Bld. M-24, Montreal Rd., Ottawa ON K1A 0R6, Canada
Department of Civil Engineering, Technion Israel Institute of Technology, Haifa, 32000, Israel
Regina.Katsman@nrc.ca Becker@tx.technion.ac.il

ABSTRACT

The effects of moisture movement and residual moisture content are becoming a recognized part of a performance based design of buildings. Despite the long-time existence of a basic 3-D formulation of heat and mass transfer within porous materials, the generalized hygrothermal behavior of construction elements that contain hygrothermal bridges and/or air voids has not been studied. Neither have the processes, which occur at the interfaces between different materials, been investigated. Relying on basic energy and mass conservation principles, a general integral form of presentation was applied to establish the coupled heat and mass transfer field equations, which were further transformed to a discrete set of algebraic equations. This form of presentation is more suitable for treatment of irregular regions, such as material interfaces and internal air voids. To treat these regions, specific mathematical procedures were implemented. Two Software packages were written to simulate the evolution of moisture content in non-homogeneous flat planar walls, without and with air voids. Finally, the results of modeling are presented for both types of constructions, thus enabling one to analyse a hygrothermal behavior of irregular wall's regions.

INTRODUCTION

For most planar building elements (usually designated by the general term walls), the main moisture movement is in the direction perpendicular to the element's air-exposed surfaces. However, the non-homogeneous structure of the element within its main plane causes multidirectional moisture movement. The general formulation of simultaneous heat and mass transfer in a porous material has been performed by Luikov [1] in order to analyze moisture transport phenomena in soils. It has then been implemented for building materials by Philip and De-Vries [2] and since then by others [3,4]. The field equations, which emerge from this formulation, have been used since then for analyzing various cases. These works include investigations of 1-D heat and mass transfer phenomena in building elements composed of a homogenous building material [4 to 9]. Despite the long-time existence of a basic 3-D formulation of heat and mass transfer within porous materials, the generalized hygrothermal behavior of construction elements that contain hygrothermal bridges and air voids has not been studied yet. Neither have the processes, which occur at the interfaces between different materials, been investigated. Moreover, the effects of commonly existing air-voids (in the form of large hollow-cores or small deffects) within the materials composing the wall, or at the interfaces between the materials (as usually stems from the construction methods for the jointing), have not been studied either.

This paper is devoted to the mathematical modeling and numerical solution of the moisture-content evolution in walls with hygrothermal bridges, including the case of a construction with air voids, concentrating mainly on methods of mathematical treatment of irregular wall's regions.

MATHEMATICAL MODEL

The basic physical considerations and previous research indicate that the mutual influence of the heat and mass transfer is an inherent property of the explored system. Moreover, the mutual influence of these phenomena on the moisture-content evolution may be particularly significant at the boundaries, where solid meets humid air with variable humidity, and at interfacial zones between different materials.

Generally, the above-mentioned Philip and De-Vries differential equations are actually an outcome of the energy and mass conservation principles. However, for the present aims, the integral form of presenting these basic priciples is the most suitable, as it enables easy inclusion of interfaces between different materials, internal air-voids and their internal boundaries.

General Scheme

The heat and mass field equations at every material point are derived from the basic energy and mass conservation principles:

$$Q_S = Q_I + Q_T + Q_v \qquad (1)$$

$$E_S = E_I + E_T + E_W \tag{2}$$

Where:

Q_S is the heat stored in an arbitrary control-volume V (with a total surface area S) during the time interval dt

Q_T is the total resultant in-flowing heat across S caused by the temperature gradient $\partial T/\partial n$ (at the surface, with the normal n to S pointing outwards at every point on S)

Q_I is the total resultant heat produced within the volume V by internal heat sources and sinks (e.g. due to heat of hydration of cementitious compounds)

Q_v is the total resultant in-flowing latent heat (associated with vaporization and condensation processes) across S, caused by the partial water-vapor pressure gradient $\partial p/\partial n$ (at the surface, with the normal n as above)

E_S is the total moisture stored in the same volume V during the time interval dt

E_I is the total resultant moisture produced within the volume V by internal moisture sources and sinks (e.g. due to the hydration process of cementitious materials)

E_T is the total resultant in-flowing moisture across S caused by the temperature gradient

E_W is the total resultant in-flowing moisture across S caused by the moisture-gradient $\partial W/\partial n$ (at the surface, with the normal n as above).

For the case without internal sources or sinks, delineation of each factor then yields the following integral presentations:

$$Q_S = \int_{t_1}^{t_2} dt \cdot \iiint_V c \cdot \rho \cdot \frac{\partial T}{\partial t} \cdot dV \tag{3}$$

$$Q_T = \int_{t_1}^{t_2} dt \cdot \iint_S \lambda \cdot \frac{\partial T}{\partial n} \cdot dS \tag{4}$$

$$Q_v = \int_{t_1}^{t_2} dt \cdot \iint_S L \cdot D_v \cdot \frac{\partial p}{\partial n} \cdot dS \tag{5}$$

$$E_S = \int_{t_1}^{t_2} dt \cdot \iiint_V \frac{\partial W}{\partial t} \cdot dV \tag{6}$$

$$E_T = \int_{t_1}^{t_2} dt \cdot \iint_S D_T \cdot \frac{\partial T}{\partial n} \cdot dS \tag{7}$$

$$E_W = \int_{t_1}^{t_2} dt \cdot \iint_S D_W \cdot \frac{\partial W}{\partial n} \cdot dS \tag{8}$$

Conducting several transformations, the field equations are thus given by:

$$\int_{t_1}^{t_2} dt \cdot \iiint_V c \cdot \rho \cdot \frac{\partial T}{\partial t} \cdot dV = \int_{t_1}^{t_2} dt \cdot \iint_S \lambda \cdot \frac{\partial T}{\partial n} \cdot dS + \int_{t_1}^{t_2} dt \cdot \iint_S L \cdot D_{vT} \cdot \frac{\partial T}{\partial n} \cdot dS + \int_{t_1}^{t_2} dt \cdot \iint_S L \cdot D_{vW} \cdot \frac{\partial W}{\partial n} \cdot dS \tag{9}$$

$$\int_{t_1}^{t_2} dt \cdot \iiint_V \frac{\partial W}{\partial t} \cdot dV = \int_{t_1}^{t_2} dt \cdot \iint_S D_W \cdot \frac{\partial W}{\partial n} \cdot dS + \int_{t_1}^{t_2} dt \cdot \iint_S D_T \cdot \frac{\partial T}{\partial n} \cdot dS \tag{10}$$

The system of partial differential equations for the simultaneous heat and mass transfer at a regular point within the porous material, which is obtained from the integral equations 9 and 10 when $V \rightarrow 0$, corresponds to the classical Philip and De-Vries formulations and to those given by the IEA Annex 24. However, as presented in the following sections, the integral presentation is more suitable for the general development of the equations in irregular regions, such as material interfaces and internal voids. Moreover, it is more amenable for establishing the numerical integration procedures at irregularities and at all the internal and external boundary points.

Analytical Treatment of Irregular Regions

The following continuity equations emerge at materials' interfaces when the zero-limit is reached for two infinitesimal control volumes that have a mutual interface S:

$$T|_{-S} = T|_{+S} \tag{11}$$

$$p|_{-S} = p|_{+S} \tag{12}$$

$$[\int_{t_1}^{t_2} dt \iint_S (\lambda + L \cdot D_{vT}) \frac{\partial T}{\partial n} dS$$

$$+ \int_{t_1}^{t_2} dt \iint_S L \cdot D_{vW} \cdot \frac{\partial W}{\partial n} dS]\Big|_{-S}$$

$$+ [\int_{t_1}^{t_2} dt \iint_S (\lambda + L \cdot D_{vT}) \frac{\partial T}{\partial n} dS$$

$$+ \int_{t_1}^{t_2} dt \iint_S L \cdot D_{vW} \cdot \frac{\partial W}{\partial n} dS]\Big|_{+S} = 0 \qquad (13)$$

$$[\int_{t_1}^{t_2} dt \iint_S D_W \cdot \frac{\partial W}{\partial n} dS +$$

$$\int_{t_1}^{t_2} dt \iint_S D_T \cdot \frac{\partial T}{\partial n} dS]\Big|_{-S} +$$

$$[\int_{t_1}^{t_2} dt \iint_S D_W \cdot \frac{\partial W}{\partial n} dS +$$

$$\int_{t_1}^{t_2} dt \iint_S D_T \cdot \frac{\partial T}{\partial n} dS]\Big|_{+S} = 0 \qquad (14)$$

The following boundary-condition equations emerge at material-air boundaries when the zero-limit is reached for an infinitesimal control volume with an air-exposed surface S:

$$\int_{t_1}^{t_2} dt \iint_S h_s dT_{aS} dS +$$

$$\int_{t_1}^{t_2} dt \iint_S (\lambda + L \cdot D_{vT}) \cdot \frac{\partial T}{\partial n} dS + \qquad (15)$$

$$\int_{t_1}^{t_2} dt \iint_S L \cdot D_{vW} \cdot \frac{\partial W}{\partial n} dS = 0$$

$$\int_{t_1}^{t_2} dt \iint_S \beta_s \cdot dp_{aS} \cdot dS +$$

$$\int_{t_1}^{t_2} dt \iint_S D_W \cdot \frac{\partial W}{\partial n} \cdot dS + \qquad (16)$$

$$\int_{t_1}^{t_2} dt \iint_S D_T \cdot \frac{\partial T}{\partial n} \cdot dS = 0$$

Derivation of the equations for an element with air-voids is now straightforward. Figure 1 depicts the schemes for the relevant control volumes within the regular porous material (Volume 1) and within the air-void (Volume 2).

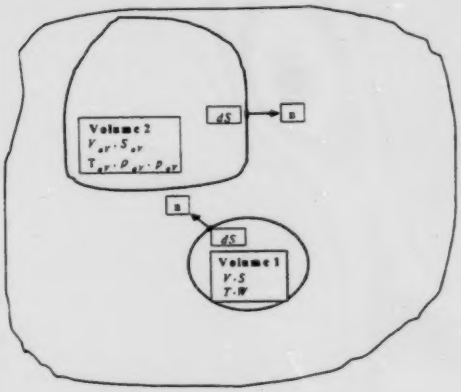

Figure 1: Scheme of general control-volumes within the element's regular material region (Volume 1) and an air-void (Volume 2).

As a first order approximation, it is assumed that within the void the air temperature and partial water-vapor pressure distributions are uniform, except for an extremely thin boundary layer at the interface with the surrounding solid. Thus, across the void the temperature and partial water-vapor pressure are represented by unique values, T_{aV} and p_{aV}. Wherever part of the solid material continuum is replaced by an air-void, equations 9 and 10 re-written for the total entrained air volume V_{aV} that is bounded by the surface S_{aV} (with a normal n into the porous medium). After substitution of 15 and 16 this yields:

$$V_{aV} \cdot \int_{t_1}^{t_2} c_{aV} \cdot \rho_{aV} \cdot \frac{\partial T_{aV}}{\partial t} \cdot dt =$$

$$\int_{t_1}^{t_2} dt \cdot \iint_{S_{aV}} \lambda \cdot \frac{\partial T}{\partial n} \cdot dS + \int_{t_1}^{t_2} dt \cdot \iint_{S_{aV}} L \cdot D_{vT} \cdot \frac{\partial T}{\partial n} \cdot dS +$$

$$\int_{t_1}^{t_2} dt \cdot \iint_{S_{aV}} L \cdot D_{vW} \cdot \frac{\partial W}{\partial n} \cdot dS = -\int_{t_1}^{t_2} dt \iint_{S_{aV}} h_{s_{aV}} dT_{aS} dS \qquad (17)$$

$$V_{aV} \cdot \int_{t_1}^{t_2} \frac{\partial \rho_{aV}}{\partial t} dt = \int_{t_1}^{t_2} dt \cdot \iint_{S_{aV}} D_W \cdot \frac{\partial W}{\partial n} \cdot dS +$$

$$\int_{t_1}^{t_2} dt \cdot \iint_{S_{aV}} D_T \cdot \frac{\partial T}{\partial n} \cdot dS =$$

$$- \int_{t_1}^{t_2} dt \iint_{S_{aV}} \beta_{s_{aV}} \cdot dp_{aS} \cdot dS$$

(18)

This model does not take into account gravitational moisture movement that occurs in pores or cracks outside the capillary range, or within vertical air-voids. Neither does it address the convection inside the porous material, effects of direct rainfall, solar radiation or air transport.

NUMERICAL SOLUTION

General Scheme

The solution procedure adopted here is based on the presentation of the integral equations in a discrete form, including the boundaries and air-voids. An implicit scheme was chosen for the numerical integration process. The ensuing discrete set of algebraic equations with non-constant coefficients is solved by means of an iterative convergence process. In addition, at this stage the solution was limited to the case of an orthogonal x-y coordinate system, as most building walls have only orthogonal internal and external surfaces.

Using an implicit scheme for the linearized set of equations provides the stability of the numerical solution without dependence on time and space steps. In particular, for the iterative process used to solve the equations with variable coefficients this scheme is preferred because of its monotonous behavior. The examples presented in this paper were solved using the "optimal" time steps that stem from the spatial mesh, which was chosen in accordance with the geometric features of the analyzed construction, where the term "optimal" refers in this case to the time step that would be recommended as maximal in order to render an explicit scheme stable (i.e. $\Delta t_{max} = \min[(dn)^2 / (2 \cdot \alpha)]$, where dn designates a mesh step in any direction and α any of the relevant diffusivity coefficients in the equations).

The scheme for the numerical model is shown in Figure 2.

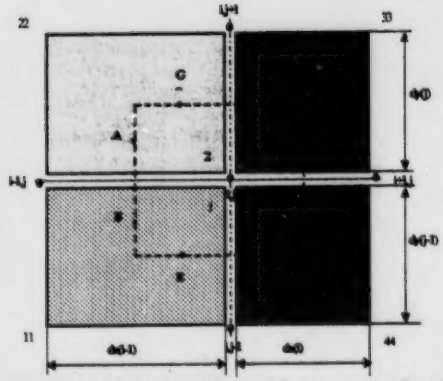

Figure 2: Scheme of the mesh at a general point i,j.

The integration points (nodes i,j) are on an orthogonal grid, with main grid line along all material boundaries. The grid is composed between its main lines by a variable-size mesh. The control volume around every node extends until the mid-distance to the next mesh-node in every direction (rectangle ABEFDCHG in Figure 2). Each of the four parts of the control volume, 1 to 4, may be composed of a different material.

Numerical Treatment of Irregular Regions

In establishing the field and boundary condition equations, the temperature and moisture content within each part are presented by their values at the node i,j. If at a certain node nm different materials meet (nm≤4), moisture-content in these materials at the node, $W_{i,j}^k$ (k=1,...,nm), is different, while the temperature, $T_{i,j}$, and the partial water-vapor pressure, $p_{i,j}$, are identical (i.e. Relative-Humidity values, $\varphi_{i,j}$, are also identical).

The different moisture-contents at the node, generally presented by the four points 1 to 4, are inter-dependent. Their dependence is obtained via the sorption isotherms of the different materials. The following procedure was used for instantaneous linearization of the discrete set of equations: At every iteration-step, m, undertaken within a given time step, dt^n, from n to n+1 (with n=0 at t=0):

$$\left(\frac{\partial W_{i,j}^k}{\partial t}\right)^{n+1} = \left(\frac{\partial W_{i,j}^k}{\partial W_{i,j}^1}\right)^m \cdot \left(\frac{\partial W_{i,j}^1}{\partial t}\right)^{n+1} =$$

$$\left(\frac{\partial W_{i,j}^k}{\partial \varphi} \cdot \frac{\partial \varphi}{\partial W_{i,j}^1}\right)^m \cdot \left(\frac{\partial W_{i,j}^1}{\partial t}\right)^{n+1} =$$

$$(\frac{\xi^k_{i,j}}{\xi^1_{i,j}})^m \cdot (\frac{\partial W^1_{i,j}}{\partial t})^{n+1} \qquad (19)$$

for k that runs from 2 to 4.
Or, re-written in the discrete form:

$$(W^k_{i,j})^{n+1} = (W^k_{i,j})^n + (\frac{\xi^k_{i,j}}{\xi^1_{i,j}})^m \cdot ((W^1_{i,j})^{n+1} - (W^1_{i,j})^n) \qquad (20)$$

For the sake of brevity, $(W^1_{i,j})^n$ and $(W^1_{i,j})^{n+1}$ are denoted in the sequel by $W^n_{i,j}$ and $W^{n+1}_{i,j}$.

For equations at internal and external boundaries, the values of $p^{n+1}_{i,j}$ are unknowns. They depend, however, non-linearly on the unknowns $T^{n+1}_{i,j}$ and $W^{n+1}_{i,j}$. Disceretization and linearization are thus performed by the following:

$$p^{n+1}_{i,j}(T^{n+1}_{i,j}, W^{n+1}_{i,j}) = p^n_{i,j}(T^n_{i,j}, W^n_{i,j}) + fs^m_{i,j} \cdot (T^{n+1}_{i,j} - T^n_{i,j}) + gs^m_{i,j} \cdot (W^{n+1}_{i,j} - W^n_{i,j}) \qquad (21)$$

Where:

$$p^n_{i,j}(T^n_{i,j}, W^n_{i,j}) = p^n_{sat,i,j}(T^n_{i,j}) \cdot \varphi^n_{i,j}(T^n_{i,j}, W^n_{i,j}), \qquad (22)$$

$$fs^m_{i,j} = (\frac{\partial p_{i,j}}{\partial T_{i,j}})^m \qquad (23)$$

$$gs^m_{i,j} = (\frac{\partial p_{i,j}}{\partial W_{i,j}})^m = \frac{p^m_{sat,i,j}}{\xi^m_{i,j}} \qquad (24)$$

The local instantaneous values of all the terms on the RHS of equations 23 and 24, at the intermediate time step m, are thus derived from the local instantaneous values $T^m_{i,j}$ and $W^m_{i,j}$. These parameters are further calculated by means of additional inherent series of sub-iterations applied for each iterative convergence stage, from time step n to n+1.
Two Software packages, MA2DW and MA2DWV, were written to solve numerically the evolution of moisture content in flat planar walls and verified by specific examples. The first one is designed for the solution of walls without air voids and the second for those with.

EXAMPLES

Two examples are given to demonstrate the effects occurring in the irregular regions that are highlighted by the suggested 2-D analysis for a drying process of a block-wall with joints and surface-renderings. These examples are restricted to the case of a symmetrical AAC wall with cementitous-mortar joints and renderings, without and with air-voids, drying symmetrically from a nearly saturated initial state.

Construction data

The element without air-voids is shown in Figure 3,

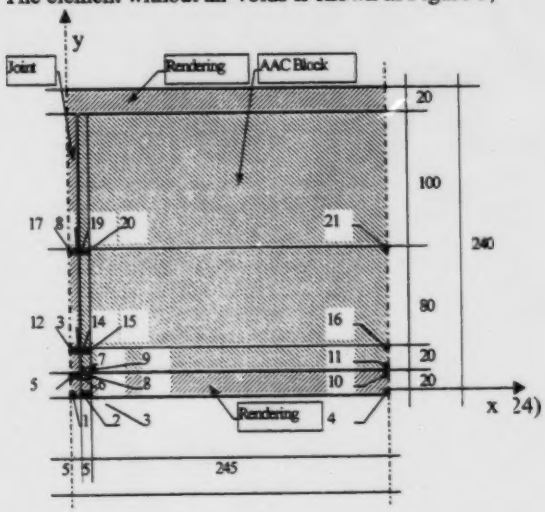

Figure 3: The element without air-voids.

while the one with air-voids is depicted in Figure 4.

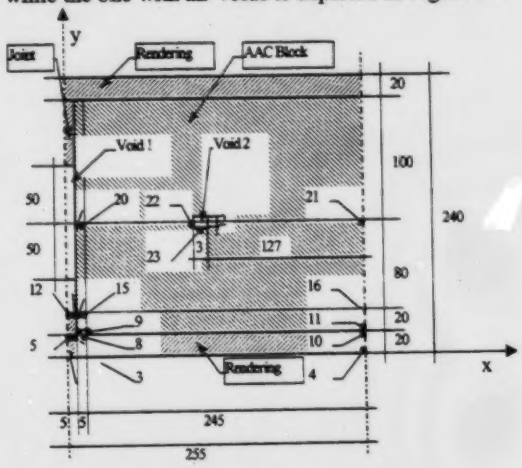

Figure 4: The element with air-voids.

Air-void No. 1 represents a cavity in the joint-mortar in accordance with the manner of construction frequently adopted for block-walls. Air-void No. 2 represents a

small defect in the block. The numbered points depict the locations of results presented in various following figures.

According to accumulated test data [10,12] the moisture-dependence of the water-vapor permeability, moisture diffusivity and thermal conductivity of cementitious materials are given by:

$$D_v = D_{vd} + A_1 \cdot \varphi^{A_2} \qquad (25)$$

$$D_W = D_{Wd} \cdot \exp(C_1 \cdot W) \qquad (26)$$

$$\lambda = \lambda_d (1 + D_1 \cdot W) \qquad (27)$$

Where:

$D_{vd}, D_{Wd}, \lambda_d$ are the relevant properties of the dry material (assuming they do not depend on temperature), and

A_1, A_2, C_1, D_1 are constant coefficients (assuming they do not depend on temperature).

The material data used in these runs represent an AAC block and a cementitious-mortar, with dry densities of 510 and 1822 kg/m^3 respectively, and a common specific heat capacity of 840 $J/(kg \cdot C)$. The mortar's water-vapor permeability is a little smaller than the block's (their ratio changes from ≈3/4 when dry to ≈1/3 when wet), whereas its moisture diffusivity is approximately 15 times larger.

Surface coefficients utilized on the airside surfaces (for both sides of the construction) were [14]:

$$h_S = 8.33 \frac{W}{m^2 \cdot C}, \ \beta_S = 2.6 \cdot 10^{-8} \frac{s}{m}$$

Surface coefficients within the air-void were [14]:

$$h_{S_{av}} = 4.543 \frac{W}{m^2 \cdot C}, \ \beta_{S_{av}} = 2.53 \cdot 10^{-8} \frac{s}{m}$$

Initial and boundary conditions

The initial conditions in all materials correspond to the following values:

$T(0) = 20°C$, $\varphi(x,0) = 95\%$.

With moisture content established according to the sorption isotherm.

The drying process is initiated by a drop in the relative humidity of the air adjacent to both surfaces to 42%, while the temperature remains constant.

Analysis and discussion of results

Figures 5 to 6 present results of the analysis for the element without air-voids, while Figures 7 to 9 present results for the element with the two air-voids.

The element without air-voids

Figure 5 presents moisture-content distributions for the whole cross-section after a period of 1350 hours.

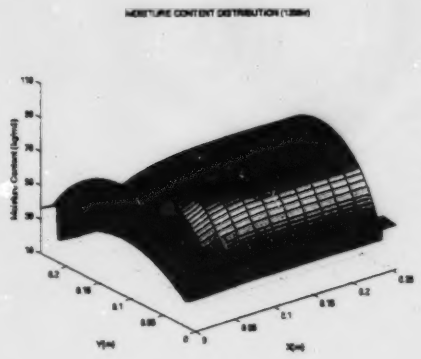

Figure 5: Results for the element without air-voids. Moisture-content distributions after 1350 hours.

Figure 6 presents the evolution of the drying process at points 5 to 11, located at the Block-Mortar intersection (Figure 3).

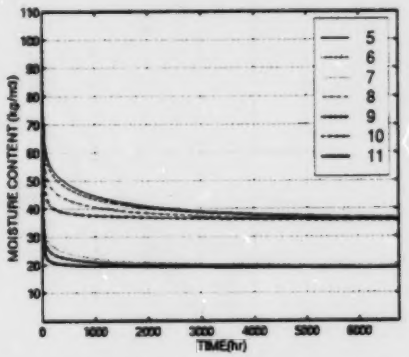

Figure 6: Results for the element without air voids. Moisture-content evolutions at various points within the cross-section.

One can see that, as expected, at the finite state of the drying process moisture contents in the various materials correspond eventually to their sorption isotherms, without dependence on the process that they undergo. The drying pattern of the block is highly influenced by the mortar surrounding it. While the inner part of the block dries extremely slowly (Figure 5), the drying process at points closer to the mortar (joint and renderings) is much faster, with point 11 drying the fastest, and points 9 and 7 only a little slower (Figure 6). These results indicate that the large moisture diffusivity of the mortar is in this case the main cause for the faster drying processes within itself and within

the block material in its vicinity. On the other hand, the smaller moisture diffusivity of the block material does not affect the rate of drying of the rendering (points 5, 6, 8, and 10). Due to the passage of moisture from the blocks into the joint, all along their interfaces, points 5 and 6 in the mortar dry a little slower than point 8.

The element with air-voids

Figure 7 presents moisture-contents distributions throughout the whole cross-section after a period of 1350 hours.

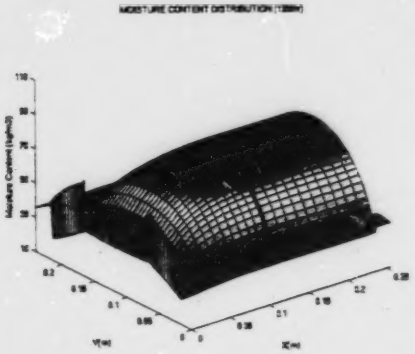

Figure 7: Results for the element with air-voids. Moisture-content distributions after 1350 hours.

Only differences stemming from the presence of the air-voids are discussed.

The substitution of joint mortar by an air-void cuts off the moisture transport by liquid water and enables only vapor transport via the void. The small air-void within the block has obviously only a local effect. The decrease in partial water-vapor pressure and relative-humidity within this void is very slow, thus slowing down even further the drying rate of points 22, 23 in comparison to point 21 all along the drying process (Figure 8).

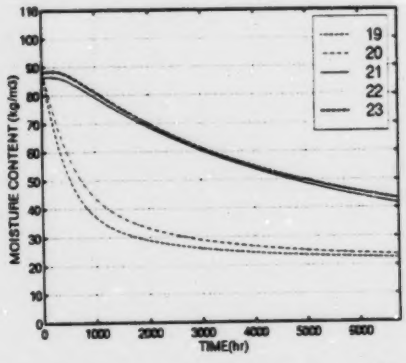

Figure 8: Results for the element without air-voids. Moisture-content evolutions at various points within the cross-section.

The results show that the partial water-vapor pressure in the large void decreases much faster than that in the small one (Figure 9).

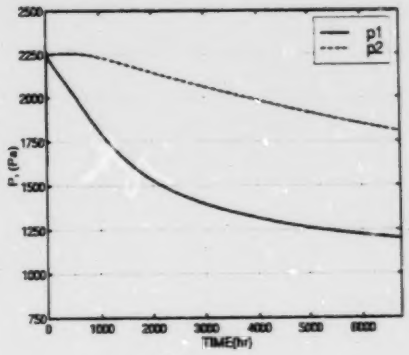

Figure 9: Results for the element with air voids. Partial water-vapor pressure within the two air-voids.

Point 19 exhibits, thus, generically similar behavior to that of points 22 and 23, but quantitatively much less pronounced (Figure 8).

CONCLUSIONS

The paper presents a tool developed for the simulation of moisture evolution in masonry walls, based on the coupled hygrothermal behavior of porous materials.

The 3-D integral form of presentation was used to allow easy inclusion of interfaces between different materials, internal air-voids and their internal boundaries.

The presented numerical procedure has ensured an accurate treatment of the irregular regions.

The developed computer Software packages were designed to allow the analysis of 2-D moisture-content evolution in non-homogeneous building constructions.

To provide analysis of the hygrothermal behavior of the irregular regions, included within real building wall, two examples were exhibited. The wall under analysis was constructed from AAC blocks and cementitious mortar.

Results indicate the severe impact of the mortar's relatively high moisture diffusivity on the processes occurred in other materials in mortar's vicinity. An impact of air voids is estimated to be a local one.

NOMENCLATURE

B_n - Sorption isotherm coefficients

c - Specific heat capacity, $(J/(kg \cdot C))$

h_s - Heat transfer surface coefficient, $(W/(m^2 \cdot C))$

D_T -Thermal moisture diffusion coefficient of the material, $(kg/(m \cdot s \cdot C))$

D_v -Water-vapor permeability coupled to the partial water-vapor pressure gradient, (s)

D_{vT} -Thermal water-vapor diffusion coefficient of the material, $(kg/(m \cdot s \cdot C))$

D_{vW} -Diffusivity of water-vapor coupled to the moisture pressure gradient, (m^2/s)

D_W -Moisture diffusivity, (m^2/s)

L - Latent heat of water-vaporization, (J/kg)

n -Perpendicular to a surface, pointing outwards of control-volume (m)

p -Partial water-vapor pressure, (Pa)

P_a -Absolute air-pressure, (Pa)

p_s -Partial water-vapor pressure at the surface, (Pa)

p_{sat} -Partial water-vapor pressure at saturation, (Pa)

S -Surface, (m^2)

t -Time, (s)

T -Temperature, (C)

T_a -Air temperature, (C)

T_g -Temperature of the reference sorption isotherm for a given material, (C)

T_s -Surface temperature, (C)

V -Control-volume, (m^3)

V_{aV} -Air-void volume, (m^3)

W -Moisture-content, (kg/m^3)

Greek symbols

β_s -Water-vapor transfer surface coefficient, (s/m)

λ -Thermal conductivity, $(W/(m \cdot C))$

ρ -Density, (kg/m^3)

ρ_a -Air density, (kg/m^3)

φ -Relative humidity,

REFERENCES

1. Luikov, A.V. (1966), Heat and mass transfer in capillary-porous bodies. Pergamon Press, (in Russian).
2. de Vries, D.A. (1958), Simultaneous transfer of heat and moisture in porous media. Transactions, American Geophysical Union, Vol. 39, No.5.
3. Andersson, A.C. (1985), Verification of calculation methods for moisture transport in porous building materials. Swedish Council for Building Research, D6.
4. Hens, H. (1996), Heat, air and moisture transfer in insulated envelope parts, Task 1: modeling. International Energy Agency (IEA), Annex 24, Final Report, Volume 1.
5. Burch, D. (1997), MOIST, APC program for predicting heat and moisture transfer in building envelopes. Building and Fire Research Laboratory, NIST, Special Publication 917.
6. Van Der Kooi, J. (1971), Moisture transport in cellular concrete roofs. Ph.D. thesis. Delft. Waltman.
7. Brocken, H.J.P. and Smolders, H.R. (1997), Moisture transport over the brick-mortar interface: water absorption and drying. Heat and Moisture Transfer in Buildings, CIB Proceedings, Publications 213, 1:249-258.
8. de Freitas, V.P. (1993), The moisture migration in building walls, experimental and analytical study. CIB W40 report, pp.1-15.
9. Bomberg, M. (1974), Moisture flow through porous building materials. Report No. 52, Lund Institute of Technology. Lund.
10. Kumar Kumaran, M. (1996), Heat, air and moisture transfer in insulated envelope parts, Task 3: material properties. International Energy Agency (IEA), Annex 24, Final Report Volume 3.
11. Hansen, K.K. (1986), Sorption isotherms, a catalogue. The Technical University of Denmark, Department of Civil Engineering, Building Materials Laboratory.
12. IEA-ANNEX XIV (1991), Condensation and energy, material properties. International Energy Agency (IEA), Annex XIV Report, Vol. 3.
13. Descamps, F. and Hens, H. (1992) Test of the diffusion approach to capillary water transfer in porous building materials, Katholieke Universiteit Leuven, pp.1-50.
14. Billington, S.N. (1967), Building physics: heat. Pergamon Press LTD.

Advanced Hygrothermal Models and Design Models

Achilles N. Karagiozis
Oak Ridge National Laboratory
Building Technology Center
Oak Ridge, TN, 37831-6070
Karagiozisan@ornl.gov

ABSTRACT

Moisture engineering is becoming an important task in the overall design of building enclosures in North America. Assessing the hygrothermal behavior of building components is important to avoid short term and long-term moisture induced damages or additional heat losses. Since experimental investigations are rather expensive and of limited transferability there is a need of heat and moisture calculations tools that give realistic results but that are also easy to use.

Several methods may be used to design wall systems, and modeling is definitively the most flexible approach. Engineers and Architects are commonly asked to perform thermal and moisture analysis of building envelopes. This is increasing the demand for calculation methods to assess the moisture behavior of building components. Modeling analyses are becoming increasingly important to investigate the interrelationships between envelope systems and subsystems and environmental loads.

Recently, the Oak Ridge National Laboratory (Building Technology Center) and the Fraunhofer Institute for Building Physics in an international collaboration developed WUFI-ORNL/IBP, a moisture engineering assessment model that predicts the transient transport of heat and moisture. The WUFI-ORNL/IBP model is an design tool for users in SI and IP units customized for both the USA and Canada.

On the other side, more advanced models such as MOISTURE-EXPERT, developed by the author at ORNL give researchers the capability to predict the behavior of complex multi-dimensional building envelope systems and sub-systems with a higher level of confidence. This hygrothermal model has been used successfully to develop design guidelines for both energy efficient and durable building envelope systems by manufacturers and state regulatory bodies.

In this paper the author will provide an overview of how important both hygrothermal models (design and advanced hygrothermal) are to building science envelope assessment. The limits, assumptions and differences between hygrothermal design tools and advanced modeling is discussed. Several example cases are given to demonstrate the suitability of each model.

INTRODUCTION

Consumers are expecting today a higher level of performance in every purchase they make. They expect products to be engineered. If performance failures occur in the products and systems, it is not generally presumed a normal aspect of consumer goods. Consumers also expect upfront service life data and ratings. This educated form of consumerism is slowly but steadily being requested by today's homebuyers. Home buyers expect a high level of aesthetic and comfort quality in a home that also has superior performance in terms of low yearly maintenance costs, and a high thermal and durability performance. Indoor air quality concerns in buildings are also becoming more important to consumers of new or recently retrofitted buildings.

In countries with cold climates, hot and humid climates, or even mild and mixed climates moisture is one of the most important agents leading to premature building envelope deterioration. Upscale and savvy buildings systems or building components are being introduced in the market place at a much faster rate than ever before. For example, within 1 year of the scientific discovery of the "SMART RETARDER" a vapor retarder that selectively changes it's vapor permeance at higher relative humidities, developed by [Kuenzel, 1998] at the Fraunhofer Institute in Bauphysics, has been installed in building envelopes for more than 3 million square meters. However, at the same time a plethora of building failures have sprouted all across North America and Europe. In Finland, mold and moisture problems have been studied and reviewed by examining the existing building stock. The Finnish National Institute of Public Health, based on the results of an extensive field survey, noted that roughly 50% of all the Finnish detached houses suffered from mold and moisture problems of varying degrees [Salonvaara, 2001]. In Vancouver Canada, a leaky condo crisis exists where many buildings are being repaired for the

third time, each time with a different design (Barret Commission, 2000). This problem/crisis is becoming an emotional and scientifically embarrassing issue for both local and national code/research and training/consulting entities in Canada.

On the positive side, consumer awareness and media attention on these issues is providing a useful educational forum for prospective homebuyers. The issue of moisture control and in particular how well a home manages moisture is inevitably raised more often now than ever before.

Moisture may be transported by diffusion, capillary and convection processes, as well as unintended water penetration. Moisture can be present in any wall system in three thermodynamic physical states, the solid state being ice, the liquid state, and the vapor state. Indeed, all three may be present concurrently in a wall system. This makes the fundamental transport interactions within a construction material complex. Understanding the overall performance of building envelope systems with respect to heat, air and moisture (HAM) excluding durability, is a formidable task. During the transport of moisture, some materials may store and accumulate water in the porous structure. Depending on the amount of water stored, environmental conditions, history and intrinsic material properties of a material, mechanical, biological and chemical damage may occur. In any envelope, some construction materials may be more prone to ageing and damage due to moisture transport than others. Understanding and predicting moisture movement within and through the envelope is therefore of fundamental importance to predicting and improving performance, particularly durability.

Recently several models have appeared that predict the hygrothermal performance of building systems. These models vary significantly and can be ranked according to a new ASTM Manual of Moisture Analysis in Chapter 6 [Karagiozis, 2001], in terms of both mathematical sophistication and inclusions of building system and sub-system performances. This classification approach allows models to differentiate in terms of simplified, design and research tools. In the past few years, simplified models are being used less, especially with the introduction of user friendly hygrothermal design tools, such as the recent one released in North America, the WUFI-ORNL/IBP hygrothermal model [Karagiozis et al, 2001]. However, more sophisticated research models such as WUFI-2D [Holm and Kuenzel, 1999], MOISTURE-EXPERT [Karagiozis, 2001], TRAMO2 [Salonvaara, 2001], TCCC2D [Ojanen, 2001] and LATENITE [Salonvaara and Karagiozis, 1994] can be used to develop design guidelines for the long-term performance of building systems.

In this paper the author will present results from two different hygrothermal models; the WUFI-ORNL/IBP [Karagiozis, et al, 2001] hygrothermal design model and the advanced hygrothermal model, MOISTURE-EXPERT [Karagiozis, 2001]. Results will be presented from both of these models with selective applications to determine the importance of the use of these models to hygrothermally evaluate and design building systems.

BACKGROUND: WUFI-ORNL/IBP

The WUFI-ORNL/IBP hygrothermal model, is a Windows-based PC program for the hygrothermal (heat and moisture) analysis of building envelope constructions. WUFI ORNL/IBP software is an easy-to-use; menu-driven program for use on a personal computer that can provide customized solutions to moisture engineering and damage assessment problems for various building envelope systems. The model was jointly developed by the Oak Ridge National Laboratory (ORNL) in Oak Ridge, Tennessee, USA, and the Fraunhofer Institute for Building Physics (IBP) in Holzkirchen, Germany, both internationally established in the area of building energy performance and durability assessments. The joint effort of these two laboratories has created an easy-to-use and intuitively accessible building moisture engineering software. This model is an excellent educational tool for both the experienced and the novice user, building envelope design engineer and architect. This advanced model has been described in detail in a new ASTM handbook, Moisture Analysis for Buildings, MNL 40 (Treschel 2001).

WUFI-ORNL/IBP Model is a transient, one-dimensional heat and moisture transfer model that can be used to assess the hygrothermal behavior for a wide range of building material classes under climatic conditions found in North America. This version of the model was specifically developed to provide an educational overview of the complicated moisture transport phenomena occurring in construction assemblies, and to allow both building envelope designers and architects insight into design decisions. The WUFI-ORNL/IBP Model can be used to estimate the drying times of masonry and lightweight structures with trapped or concealed construction moisture, investigate the danger of interstitial condensation, or study the influence of driving rain on exterior building components. The program can also help to select repair and retrofit strategies with respect to the hygrothermal response of particular wall assembly subjected to various climates. This allows the comparison and ranking of different designs with respect to total

hygrothermal performance. This design tool can aid in the development and optimization of innovative building materials and components.

Once you have supplied WUFI ORNL/IBP with the data it needs, it will calculate the time evolution of the temperature and moisture fields in the building component. During or at the end of the simulation you will be given three types of distributions results that describe the temporal evolution of certain quantities, taken at specified locations or as mean values over specified layers.

The following parameters are given as courses:

the heat flux densities through the interior and exterior surface, respectively;

- The temperature and relative humidity at monitoring positions of your choice (e.g., at the interior and exterior surfaces, or in the middle of an insulation layer);
- the mean moisture content of each material and the total moisture content of the entire building component.

Additionally profiles (graphs), which show the spatial distribution of a quantity across the building component at a specified point in time of the following quantities, are available:

- The temperature across the assembly,
- The relative humidity across the assembly,
- The moisture content across the assembly.

A film file, which contains the transient profiles over all time steps and thus allows to display the thermal and hygric processes in the building component as an animation .

Courses, profiles, and the film are written to a single file in a compact binary format. This file is currently imbedded in the input file to allow better control of each simulation case. WUFI ORNL/IBP offers graphics functions that allow you to view the computed courses and profiles and print them. The film viewer allows you to view the film at your leisure after completion of the calculation.

The predecessor of this program WUFI was released in Europe in 1994 (Künzel 1995) and has since been widely used by building envelope designers, architects, building physicists, consulting specialists, and universities in Europe. The model has been validated by Künzel (1995) using several field test. The WUFI ORNL/IBP model is an educational tool for understanding the basic principles and interactions present during moisture transport.

In addition to the educational version WUFI ORNL/IBP, IBP (www.wufi.de) offers the professional version WUFI-pro V3.0 with advanced features and options. WUFI-pro V3.0 mainly addresses users with some previous experience in the fields of hygrothermal analysis and moisture transport simulations.

MOISTURE-EXPERT:

Advanced Hygrothermal Model

This model was developed at the Oak Ridge National Laboratory by Dr. Karagiozis to predict the complex heat, air and moisture transport in building envelope systems. This research model incorporates the latest understandings of the physics of hygrothermal processes and to allow extension of this model to durability predictions. Each transport processes has been developed in an object-like representation, where specific indexes store the linkages of the process to other actions or performances. The type of representation allows direct interaction of the magnitude/strength, occurrence, and frequency of various hygrothermal potentials to durability processes. In this regard, this model is unique.

The model is capable in predicting the 1-D and 2-D heat, air and moisture transport in building envelope geometries. The model treats vapor and liquid transport separately. The moisture transport potentials are vapor pressure and relative humidity, and temperature for energy transport. The model includes the capability of handling temperature dependent sorption isotherms, and liquid transport properties as a function of drying or wetting processes.

MOISTURE-EXPERT model includes porous airflow through insulation by solving a subset of the Navier Stokes equations; the Darcy's equations. MOISTURE-EXPERT model accounts for the coupling between heat and moisture transport via diffusion and natural and forced convective air transport. Phase change mechanisms due to evaporation/condensation, freezing/thawing are incorporated in the model. The model includes the capability of handling internal heat and moisture sources, gravity driven liquid moisture, and surface drainage capabilities. The model also captures experimentally determined system and sub-system performances and anomalies of the building envelope. One of the model's unique features is its capability to include temperature dependent sorption isotherms, and directional and process dependent liquid

diffusivity. Currently the model incorporates sub-system drainage performance from a field drainage study performed by Straube et al [2000].

The moisture transfer equation including contributions from liquid, vapor air flow and gravity assisted transfer is:

$$g_u = -D_\phi(u,T,x,y)\nabla\phi - \delta_p(u,T)\nabla P_v + v_a\rho_v + K(u)\rho_w\vec{g}$$

Where:

g_u = Mass flux, kg/m^2·s
D_ϕ = liquid moisture transport coefficient, m^2/s
u = moisture content, kg$_w$/kg$_d$
T= temperature, °C
δ_p = vapor permeability, kg/s·m·Pa
P_v = vapor pressure, Pa
v_a= velocity of air, m/s
ρ_v= density of vapor in the air, kg/m^3
K= moisture permeability, s
ρ_w= density of liquid water, kg/m^3
g= acceleration due to gravity, m/s^2.

MOISTURE-EXPERT is a state-of-the-art moisture engineering building envelope model that integrates experimental material and system and sub-system analysis coupled with advanced mathematical modeling that allows more accurate prediction of the hygrothermal performance of complex building envelope systems. This important development enables building engineers to couple the hygrothermal performance of an envelope to some engineering assessment on how good or bad the building envelope performs relative to new innovative assemblies or existing ones. The model may be inputted with system information about the wall systems as constructed, the aging characteristics and details (how the thermal-hygric-mechanical-chemical properties of a weather resistive barrier change with exposure and time for example).

This advanced moisture engineering analysis capability integrates experimental and analytical approaches to develop performance indexes of a building envelope system and sub-systems for specific interior and exterior loads. This analysis is needed to establish the design life span and durability requirements of a particular building envelope component.

Understanding and predicting moisture movement within and through the envelope is therefore of fundamental importance to predicting and improving performance, particularly durability. Figure 1 shows the transport of vapor and liquid transport of moisture.

Since driving rain deposition on walls and roofs is often quantitatively the largest single source of moisture, controlling rain penetration is essential to a successful moisture control strategy. In fact, failure to control rain is likely the oldest and most common serious building enclosure problem.

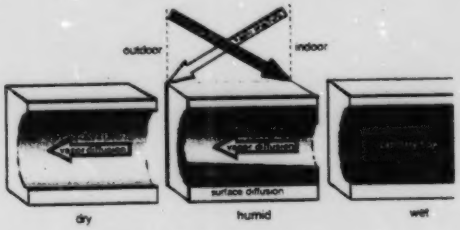

Figure 1: Vapor and Liquid Transport Mecahnism

Differences between design tools and advanced hygrothermal models

The development of an advanced moisture engineering model requires particular attention to:

- Heat and mass transfer physics (these changes as a function of various loads and time)
- Definition of the environmental loads, (now inputs such as fog, water penetration, sky temperature, etc)
- Definition of the construction entity (workmanship, defects, aging-degradation). Design tools do not have the capability to include these types of effects.
- Hygrothermal (structural-biological-mechanical) material properties. The design tools are not equipped with these features.

So far, we have discussed the individual elements that are required for developing an advanced hygrothermal model. An advanced hygrothermal model must also incorporate some key features that will allow the models higher level of confidence in simulations. Depending on the construction type, certain elements may be more important than others. For example airflow through masonry walls is not as important as through light weight wood frame constructions. Understanding the application limits of each model is an important part of applying advanced models to develop design guidelines.

As these two models present the state of the art in both design and advanced research tools, the differences between them are primarily due to:

a) Transient heat, air, and moisture transport formulation (as a minimum)
b) 2-dimensional spatial formulation (as a minimum)
c) Variable material properties; e.g., as functions of moisture content and temperature
d) Incorporating physics of:

- vapor transport
- liquid transport
- air flow
- hydraulic transport
- moisture capacity of the materials
- condensation and evaporation processes
- freezing and thawing processes

e) Incorporating boundary conditions

- incident solar radiation and sky radiation
- wind-driven rain at exterior surfaces
- wind pressure
- interior and exterior temperature and relative humidity
- interior moisture sources

f) Incorporate Building Systems and sub-system effects

- water penetration rates through sub-systems (joints, cracks, etc)
- air leakage (cracks, joints e.g. around a window)
- additional sources of moisture
- drainage and gravity effects

Assumptions

Several assumptions are necessary for the development of moisture engineering models and these must be acknowledged as the limitations of existing advanced models:

1. The material is macroscopically homogeneous
2. The solid phase is a rigid matrix, and thermophysical properties are constants with space
3. Enthalpy of each phase is a function of temperature and moisture
4. Compressional work and viscous dissipation are negligible for each phase
5. Diffusional body force work and kinetic energy are small
6. The gas phase is a binary mixture of ideal gases
7. The three phase system is in local thermodynamic equilibrium (solid-vapor-liquid)
8. Gravity terms are important for the liquid phase mass transfer but not the gas phase mass transfer
9. Fluids are Newtonian and inertial effects are small
10. The transport processes are modeled in a phenomenological way

Example Simulations

In this example, the WUFI-ORNL/IBP hygrothermal design tool was used. The performance of a stucco clad building envelope wall system was investigated as a function of the selection of the weather resistive barrier design. This example illustrates the use of design tools to assist in defining the level of water vapor performance of the weather resistive barrier in a climate as found in Seattle, WA. Figure 2 displays the wall assembly.

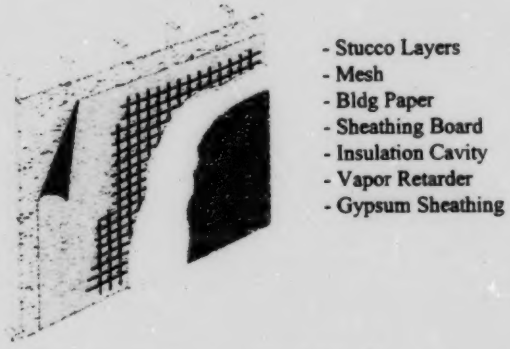

Figure 2: Conventional Stucco Wall

Simulations were performed using interior conditions that changed as a function of season. A three-year simulation with hourly environmental conditions was performed. The interior environmnetal values were obtained by measurements performed by Oak Ridge National Laboratory for the city of Seattle. The interior relative humidity fluctuated between 30 % to 60 % RH, and hourly values were used. For the exterior conditions hourly, exterior temperature, relative humidity, solar radiation, sky radiation, rain, cloud index, wind speed and orientation were used. Thirty years of data were analyzed to determine the 10 % cold year and 10 % hot year, respectively. These years were used in series.

In Figure 3, four simulations were performed for the stucco clad wall system, each characterizing the relative performance of the use of exterior weather resistive barriers. The four simulation cases were:

- No building paper
- 1 layer of Kraft paper
- 2 layers of Kraft paper
- 3 layers of Kraft paper

Wind-driven rain was also included in this analysis, and at present this is a unique feature of the WUFI-ORNL/IBP design model. The results show clearly the benefit of having at least two layers of building paper.

Use of additional layers did not improve the performance of the wall system. Currently design guidance on this issue is important in Vancouver, BC as up to three layers of building paper have been used to enhance the hygrothermal performance. This figure clearly shows the redundancy of using three building papers in a stucco wall system

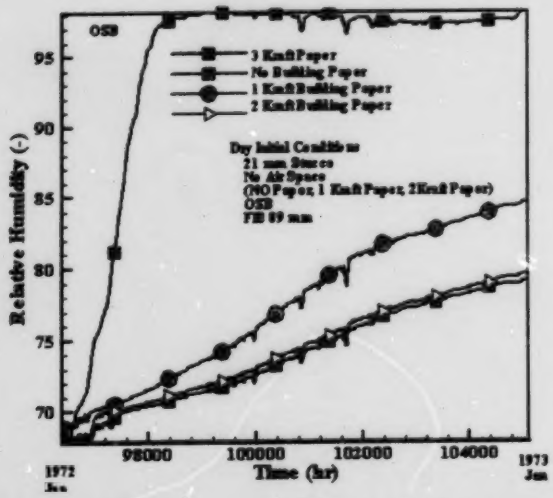

Figure 3: Effectiveness of Weather Resistive Membranes

In another example case, results in Figure 4 show the hygrothermal performance of a stucco clad wall as a function of foam insulation. A plywood sheathing board was used for this simulation. Here the hygrothermally positive influence of thermal insulation on the exterior side of the sheathing board is shown. The interior loads were increased to range between 50 and 70 % RH, and the design without the additional insulation failed. Here is clear the advantageous use of thermal insulation to enhance the durability performance of the wall.

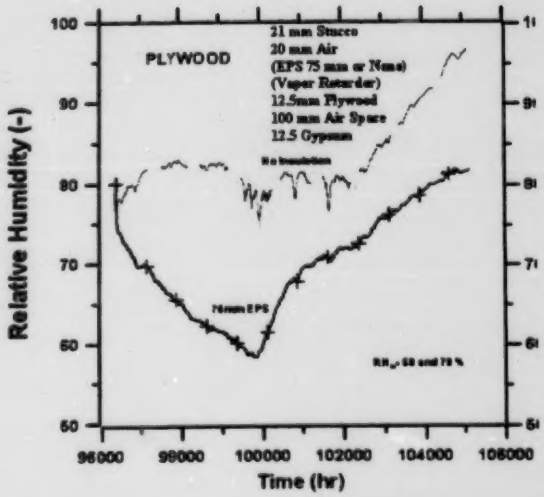

Figure 4:Effectivess of exterior insulation

EXAMPLE OF ADVANCED SIMULATION

A similar stucco clad wall system is investigated using the ORNL advanced hygrothermal MOISTURE-EXPERT. Figure 5 displays the wall assembly. The hygrothermal performance of the wall is investigated in terms of drainage and water management capability of the wall. In a recent publication by Straube, Lstiburek, Karagiozis and Shumacher [2001], the drainage of full wall systems were investigated experimentally for vinyl and stucco clad systems. These experiments allowed the development of sub-system performance data for the water penetration and drainage.

Figure 6 shows the hygrothermal performance of a leaky stucco clad wall system, and another wall positioned under a window. The total moisture content in the OSB sheathing board is shown as a function of time. Both walls were south facing and while the plain wall system did dry out, the one positioned underneath a window did not.

Figure 7 displays the spatial relative humidity distribution at one snap shot in time (Feb 1). The effect of air flow through the wall assembly is also depicted. Air flow can either increase or decrease the moisture accumulation potential in a wall system. From Figure 7 it is evident that moisture transport in building envelope systems is multidimensional for many cases.

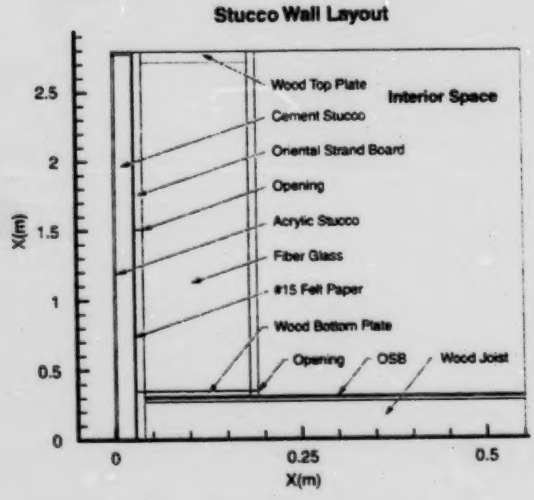

Figure 5: Stucco Clad Wall System

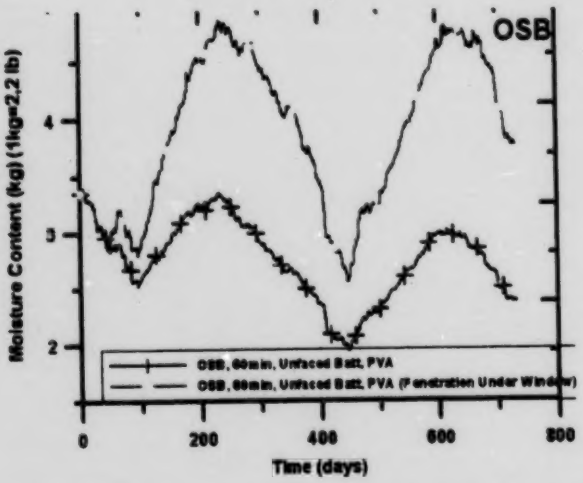

Figure 6: Effect of water penetration (Window/No Window)

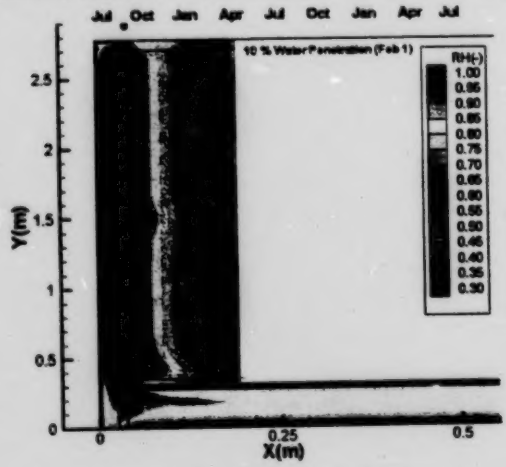

Figure 7: Relative Humidity Spatial Distribution

different water penetration and drainage configurations. This example clearly shows the effect of proper drainage and design, as well as the sensitivity of this particular wall system to moisture penetration. This new approach to classifying the wall's sensitivity to moisture loads and drying potential can be used to develop design guidelines for building envelope practioners.

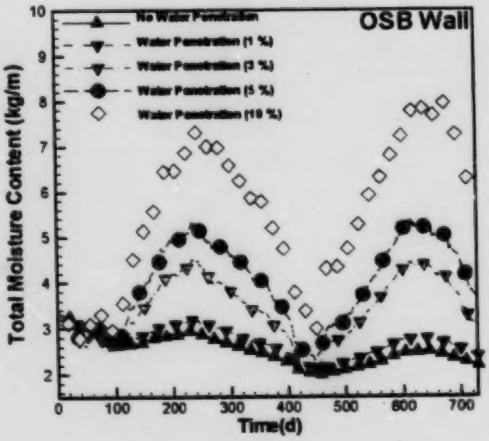

Figure 8: Moisture Acummulation as function of drainage and wetting potential

CONCLUSIONS

Two classes of hygrothermal models have been presented, one the moisture engineering design tools and the more advanced hygrothermal models.

Moisture design tools such as WUFI-ORNL/IBP can be used to evaluate in a comparative manner the hygrothermal performance of various design to a set of hygrothermal loads. Design models must provide the necessary inputs to the users, these being the interior amd exterior environmental conditions, and material properties and other loads. The model is easy to use and provides valuable information that assesses different design options.

The recently released public domain hygrothermal WUFI-ORNL/IBP model has become available to the building design community and can be downloaded at www.ornl.gov/btc/moisture. The WUFI-ORNL/IBP model can be used to assist building envelope designers to assess the relative performance of building systems to real environmental conditions.

Research tools such as MOISTURE-EXPERT not only can assist in evaluating the performance of various building envelope systems, but may optimize "real

systems". In this model, building envelope systems may be optimized for better hygrothermal performance, and additional features such as water penetration, air flow and temperature dependent sorption may be included.

ACKNOWLEDGEMENTS

The author is grateful to DOE Manager Arun Vohra for his continued support of ORNL's Building Technology Center Moisture Management Program. The author would like to thank Drs. Straube and Lstiburek and Mr. Shumacher for the development of a drainage testing methodology. Finally thanks are due to Michael Aoki-Kramer from City of Seattle DCLU for his support in Seattle's first moisture engineering project.

REFERENCES

Holm, A., Künzel, H.M.: Combined effect of temperature and humidity on the deterioration process of insulation materials in ETICS. Proceedings Vol. 2 of the 5th Symposium Building Physics in the Nordic Countries, Göteborg, August 24-26, 1999, S. 677-684.

Karagiozis, A.N., 2001, Advanced Hygrothermal Model MOISTURE-EXPERT, Oak Ridge National Laboratory, Report I

Straube, J., Lstiburek, J., Karagiozis A.N., and Shumacher C., 2001 Report on Investigation of water Drainage in walls systems.

Künzel H.M.: Simultaneous Heat and Moisture Transport in Building Components. - One- and two-dimensional calculation using simple parameters. IRB Verlag (1995).

Künzel, H.M.: 1998., More Moisture Load Tolerance of Construction Assemblies Through the Application of a Smart Vapor Retarder, Thermal Performance of the Exterior Envelopes of Buildings VII, Clearwater, FL, pp.129-132.

Künzel, H.M., Karagiozis, A.N. and Holm A. 2001., WUFI-ORNL/IBP A- Hygrothermal Design Tool for Architects ans Engineers, Chapter ASTM Manual 40 in Moisture Analysis of Buildings

Trechsel, H.R. 1994., Moisture Control in Buildings, Manual, American Society for Testing and Materials.

Trechsel, H.R. 2001., Moisture Analysis for Buildings, Manual, American Society for Testing and Materials.

Salonvaara M. and Karagiozis A., "Moisture Transport in Building Envelopes using an approximate Factorization Solution Method", CFD Society of Canada, Toronto, June 1-3 1994.

Salonvaara M., 2001, TRAMTO2: Advanced Hygrothermal Models, ASTM Manual Moisture Analysis in Buildings, APPENDIX.

Ojanen T., 2001, TCCC2D: Advanced Hygrothermal Models, ASTM Manual Moisture Analysis in Buildings, APPENDIX.

Karagiozis, A., 2001, Advanced Hygrothermal Modeling of Building Materials using Moisture-Expert 1.0, 35th International Particleboard/Composite Materials Symposium, Pullman Washington.

Künzel, H.M., Karagiozis, A.N. and Holm A. 2001., WUFI-ORNL/IBP A- Hygrothermal Design Tool for Architects ans Engineers, Chapter ASTM Manual 40 in Moisture Analysis of Buildings

Karagiozis, A.N., Künzel, H.M., and Holm A. 2001., WUFI-ORNL/IBP Hygrothermal Model , Proceedings of Eight Conference on Building Science and Technology, Solutions to Moisture Problems in Building Enclosures, Feb. 22-23, Toronto pp. 158-183

MODELLING OF VOLATILE ORGANIC COMPOUNDS EMISSION FROM DRY BUILDING MATERIALS

Hongyu Huang Fariborz Haghighat
Department of Building, Civil and Environmental Engineering
Concordia University, Montreal, Canada
hongyu_h@ cbs-engr.concordia.ca haghi@ cbs-engr.concordia.ca

ABSTRACT

A numerical model was developed to predict volatile organic compound (VOC) emission rate from dry building materials. The model considers mass diffusion process within the material and mass convection & diffusion processes in the boundary layer. All the parameters, mass diffusion coefficient of the material, material/air partition coefficient, and mass transfer coefficient of the air can be either found in the literature or calculated using known principles.

The predictions of the model was validated at two levels: with experimental results from the specially designed test and with the prediction made by a CFD model. The results indicate that there is generally a good agreement between the model predictions, the experimental results, and the CFD results.

Keywords: dry building material, VOC emission, diffusion, and numerical model

INTRODUCTION

Volatile Organic Compounds emitted by building materials are recognized as major problems affecting human comfort, health and productivity. Therefore, accurate modeling of the material emission rate in buildings is important for predicting the contaminant concentration, occupant exposure and for the design of mechanical ventilation systems. Recently, there has been a growing interest in the development of mathematical models to predict the quality of indoor air.

Emission models include empirical models and physical models. The parameters of empirical models are determined by fitting experimental data to a predefined model. The main drawback of these models are that nonlinear regression curve fitting might lead to multiple solutions and the resulting empirical parameters may not be scaled up for use in actual buildings. Therefore, physical models based on the mass transfer processes are more attractive to most researchers for building material emission rate modeling.

Physical models are based on the fundamentals of mass transfer processes[1]; diffusion within the material as results of concentration, pressure, or temperature gradient, and surface emission between the material and the overlying air as a consequence of evaporation, convection and diffusion. Fick's second law describes the diffusion within the materials. For wet materials such as paints or wood stain, the diffusion coefficient within the material is very difficult to determine, and studies show that the surface emission usually dominates the emission processes. Therefore, most of the emission models for wet building materials are concentrated on the VOC transport in the air [2-4]. For dry building materials, the diffusion within the material cannot be ignored and the internal diffusion is more likely to be the dominating resistance. Recent review of existing emission models for dry material reveals some of their shortcomings. For example, the diffusion controlled emission models only consider the internal diffusion and ignore the surface convection process[5,6]. This simplification causes the model to underestimate VOC emission at the early stage when the surface concentration is relatively high. The conjugate mass transfer model assumes the VOC concentration at the material bottom is constant and ignores the sorption factor[7]. Those assumptions are not appropriate for real building material, since the concentration distribution inside the material is time dependent and the sorption factor cannot be ignored. Further, the model developed for the semi-infinite materials[8] are not suitable for thin building materials.

Therefore, some researchers turn to CFD to study emission from dry building materials and their concern is mainly on contaminant distributions in the air. Recently developed CFD models consider both the surface emission and the internal diffusion [9,10]. The critical problem of these models is the solution convergence, and the main inherent drawback of this technique is that the CFD simulation would be too expensive and time consuming to be used as a routine

procedure for long term VOC emission prediction.

Although there are a lot of achievements in the development of mathematical models for dry building materials, a model which could overcome the existing shortcomings is not yet available. This paper describes the development of a numerical model.

THE EMISSION MODEL

The physical system considered here is a dry building material (carpet, vinyl flooring, particleboard, etc.) and has its one surface exposed to the air. The VOC emission from this material is composed of three main processes as shown in Figure 1.

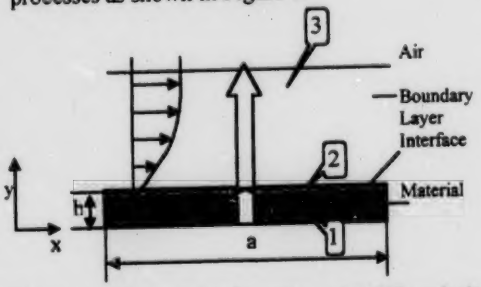

Figure 1: Physical configuration of VOC emission from the dry building material. 1: Internal diffusion; 2: Material /air interface; 3. External advection.

Mass transfer in the boundary layer

When air passes over the material surface, a mass boundary layer exists between the surface material and the main flow. The VOC mass transfer in this mass boundary layer is determined by diffusion and convection. The rate of VOC mass transfer in the boundary layer can be expressed as:

$$R = h(C_{as} - C_a) \qquad (1)$$

Where h is the mean mass transfer coefficient (m/s), C_{as} is the VOC concentration in the air near material surface (ug/m^3) and C_a is the VOC concentration outside the mass boundary layer (ug/m^3).

Material /air interface

At the material/air interface, the material is the adsorbent and the VOC gas is the adsorbate. The material exerts an attractive force normal to the surface plane. Consequently, the concentration of VOC at the material phase exceeds that in the gas phase. Langmuir and BET are the most common isotherm models which may be used to describe this process [11]. At atmospheric pressure, for low VOC concentration and isothermal conditions, equilibrium relation between the VOC concentration in the air phase and the VOC concentration in the material phase can be described by Henry's law [12]:

$$C_m(b,t) = kC_{as} \qquad (2)$$

Where C_m (b,t) is VOC concentration at the material surface (ug/m^3) and C_{as} is the VOC concentration in the air near material surface (ug/m^3), k is the material/air partition coefficient, b is the thickness of the material (m), and t is the time (s).

Mass transfer in the material

For a dry material with homogeneous diffusivity, the transient VOC diffusion in the material can be described by the one-dimensional diffusion equation:

$$\frac{\partial C_m(y,t)}{\partial t} = D_m \frac{\partial^2 C_m(y,t)}{\partial y^2} \qquad (3)$$

Where C_m is the VOC concentration in the material (ug/m^3), D_m is the VOC diffusion coefficient of the material (m^2/s) and y is the coordinate in which the VOC diffusion in the material takes place (m).

Mass balance in the room or chamber

Assuming that the VOC is totally mixed in the room air. The transient mass balance in the room or chamber can be expressed by:

$$\frac{\partial C_a(t)}{\partial t} = NC_{in} - NC_a - LD_m \left.\frac{\partial C_m(y,t)}{\partial y}\right|_{y=b} \qquad (4)$$

Where C_a is the VOC concentration in the room air (ug/m^3), C_{in} is the VOC concentration in the supply air (ug/m^3), N is the air exchange rate (h^{-1}) and L is the material loading factor (m^2/m^3).

Boundary conditions and solutions

Some initial conditions and boundary conditions are needed to close the above equations.

a) Initial conditions:

A homogeneous new material with initial VOC concentration of

$$C_m(y,0) = C_0 \qquad (5)$$

The initial VOC concentration in the room air (C_{a0}) is:

$$C_a(0) = C_{a0} \quad (6)$$

b) Boundary conditions:
At the material bottom, there is no VOC passing through this surface.

$$-D_m \left.\frac{\partial C_m(y,t)}{\partial y}\right|_{y=0} = 0 \quad (7)$$

At the material surface and room air interface, the mass balance can be written as:

$$-D_m \left.\frac{\partial C_m(y,t)}{\partial y}\right|_{y=b} = h(C_{as} - C_a) = h\left(\frac{C_m(b,t)}{k} - C_a\right) \quad (8)$$

There are four key parameters which need to be determined: the mass transfer coefficient in the air, h, the partition coefficient, k, the mass diffusion coefficient in the material, D_m, and the VOC initial concentration, C_0.

Mass transfer coefficient in the air, h
In the mass boundary layer, the following relationships exist [13]:

a) For laminar flow, (Re_l<500,000):

$$Sh = 0.664 Sc^{1/3} \mathrm{Re}_l^{1/2} \quad (9)$$

b) For turbulent flow, (Re_l>500,000):

$$Sh = 0.037 Sc^{1/3} \mathrm{Re}_l^{4/5} \quad (10)$$

c) Combined laminar /turbulent flow, (Re_l<10^7, Re_{tr}=500,000):

$$Sh = (0.037 \mathrm{Re}_l^{4/5} - 8700) Sc^{1/3} \quad (11)$$

Where, $Sh = \frac{hl}{D_a}, Sc = \frac{\nu}{D_a}, \mathrm{Re}_l = \frac{ul}{\nu}$, ν is the kinematic viscosity of the air (m^2/s), u is the mean air velocity over the material (m/s), l is the characteristic length of material (m) and D_a is the VOC diffusion coefficient in the air (m^2/s).

The VOC diffusion coefficient (D_a) can be directly obtained from literature[14] or can be estimated through other methods. Two main methods have been used to estimate the VOC diffusion coefficient in the air[15]: Fuller, Schettler and Giddings (FSG) method and Wilke and Lee (WL) method. FSG method is the most accurate for non-polar gasses at low to moderate temperatures. In this study, the FGS method was used to estimate VOC diffusion coefficient in the air. This method is based on the following correlation:

$$D_a = \frac{10^{-7} T^{1.75} \sqrt{M_r}}{P\left(V_a^{1/3} + V_{VOC}^{1/3}\right)^2} \quad (12)$$

Where $M_r = \frac{(M_a + M_{VOC})}{M_a M_{VOC}}$, T is the absolute temperature (K), P is the pressure (atm), V_a is the air molar volume (cm^3/mol), V_{VOC} is the VOC molar volume (cm^3/mol), M_a is the air molecular weight (g/mol) and M_{VOC} is the VOC molecular weight (g/mol).

Therefore, the mass transfer coefficient can be estimated using Equations 9-12. Those correlations are only valid when the concentration at the bottom of mass boundary layer is constant. Since the VOC concentration at the material surface is very low and the VOC diffusion through the material is very slow: the VOC concentration near the material surface will be relatively stable. Thus, we may assume that the concentration near the material surface is constant in a given time step.

Material/air partition coefficient, k
The material/air partition coefficient describes the relationship between the concentration in the gas phase and the concentration in the material phase. It is a material property and is obtained experimentally [5,16].

Mass diffusion coefficient in the material, D_m
The diffusion coefficient in the material is usually a function of many factors, such as the pore structure, the material type, compound properties and temperature, as well as VOC concentration. The dependence of the diffusion coefficient on the VOC concentration can be ignored considering that the VOC concentration in the material is usually very low. The diffusion coefficient is usually determined experimentally [5,16].

Initial concentration, C_0
Initial concentration in the material can be obtained through solvent extraction, high temperature thermal desorption or direct analysis[17]. Recently a cryogenic grinding/ fluidized bed desorption method was

developed to measure the initial concentration[6]. The VOC concentration in the material, VOC emission rate and the VOC concentration in the room are a function of the initial concentration, thus a small error in initial concentration estimation may cause a significant error in prediction results.

SOLUTION TECHNIQUES

A numerical finite difference method was used to simultaneously solve equations 1-4 using the initial conditions, Equations 5 and 6, and boundary conditions, Equations 7 and 8. The outcomes are:

a) The VOC concentration at the material surface $C_m(b,t)$:

$$\left(\frac{D_m}{\Delta y}+\frac{\Delta y}{\Delta t}+\frac{h}{k}-\frac{Lh^2\Delta t}{k(N\Delta t+Lh\Delta t+1)}\right)C_m(b,t)$$
$$=\frac{D_m}{\Delta y}C_m(b-\Delta y,t)+\frac{\Delta y}{\Delta t}C_m(b,t-\Delta t)$$
$$+\frac{h}{(N\Delta t+Lh\Delta t+1)}C_a(t-\Delta t) \qquad (13)$$

b) The VOC concentration in the room air, $C_a(t)$:

$$C_a(t)=\frac{Lh\Delta t}{k(N\Delta t+Lh\Delta t+1)}C_m(b,t)$$
$$+\frac{1}{(N\Delta t+Lh\Delta t+1)}C_a(t-\Delta t) \qquad (14)$$

c) The VOC emission rate, R(t):

$$R(t)=h\left(\frac{C_m(bt)}{k}-C_a(t)\right) \qquad (15)$$

d) The normalized emitted mass, M/M_0:

$$\frac{M}{M_0}=\frac{\sum_{j=1}^{m}R(t)\Delta t}{bC_0} \qquad (16)$$

Where Δy is the space grid distance (m), Δt is the calculation time step (s).

THE MODEL VALIDATION

The model's prediction was compared with the experimental results of two particleboard tests as well as the predictions made by a CFD model [9].

The model predictions were compared with experimental data obtained at Massachusetts Institute of Technology [9]. The experiments were carried out in a small-scale chamber of 0.5×0.4×0.25 m^3 at a temperature of 23±0.5 ^{0}C, relative humidity 50±0.5%, and air exchange rate 1.0±0.05h^{-1}. Two different specimens of particleboard were tested. Major compounds identified for the tested particleboards were the same: hexanal, α-pinene, camphene, and limonene. The particleboard properties (D_m, k, and C_0) were estimated by using the chamber emission data (concentration vs. time) to fit the CFD model [9]. The physical properties of the particleboard were supplied by the experimenter and they are given in Table 1. The airflow inside the chamber is treated as laminar flow over a flat plate.

Table 1 Physical properties of particleboard emissions

Compound	TVOC	Hexanal	α-Pinene
	Particleboard 1		
$D_m(m^2/s)$	7.65×10^{-11}	7.65×10^{-11}	1.2×10^{-10}
$C_0(ug/m^3)$	5.28×10^{7}	1.15×10^{7}	3.45×10^{6}
k	3289	3289	5602
	Particleboard 2		
$D_m(m^3/s)$	7.65×10^{-11}	7.65×10^{-11}	1.2×10^{-10}
$C_0(ug/m^3)$	9.86×10^{7}	2.96×10^{7}	7.89×10^{6}
k	3289	3289	5602

Figures 2 to 7 show the comparison of the predicted TVOC, hexanal and α-pinene concentrations with the experimental results for particleboard 1. The experiment was carried out for 96 hours. There is good agreement between predicted concentrations and experimental measurements. There are some discrepancies between predicted results (both with the proposed numerical model and the CFD model) and experimental results during the initial hours. This might be due to instability and partial mixing in the chamber at the beginning of the tests.

Figures 5 to 7 compare the model predicted TVOC, hexanal and α-pinene concentrations with the experimental ones for particleboard 2. The experiment was carried out for 840h in the chamber. As shown in the figures the predictions of the TVOC, hexanal and α-pinene made by the proposed model fit the experimental data very well. The predicted results and

experimental results closely follow the same trend, especially for the long term; see Figures 5b, 6b and 7b.

The model predictions were also compared with the prediction of a CFD model [9]. Figures 2 to 7 also compare the model predicted TVOC, hexanal and α-pinene concentrations with the results predicted by a CFD model. In general, there is excellent agreement between predicted numerical results, measurement data and CFD predictions. As shown in Figures 2 and 3, for short term, the predictions made by CFD for sample 1 (PB1) fit the experimental data better than the proposed numerical model. While, for long term, Figures 5, 6 and 7 show that the prediction made by the proposed model fit the experimental data better than the prediction made by CFD. However, over all, the predicted curves of the two models follow the experimental results closely.

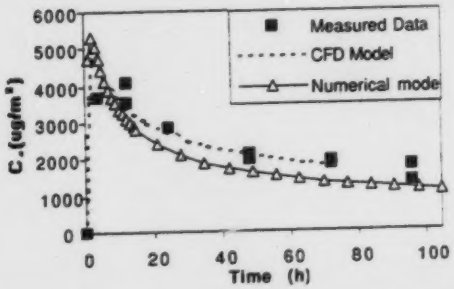

Figure 2 Comparison of TVOC concentrations (PB1)

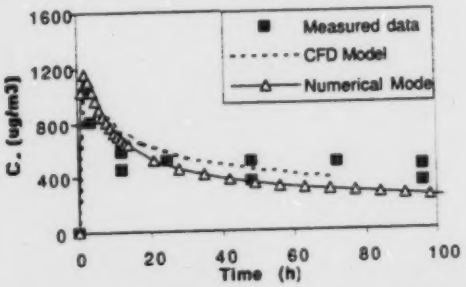

Figure 3 Comparison of hexanal concentrations (PB1)

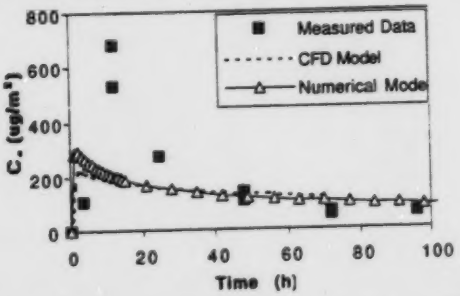

Figure 4 Comparison of α-pinene concentrations (PB1)

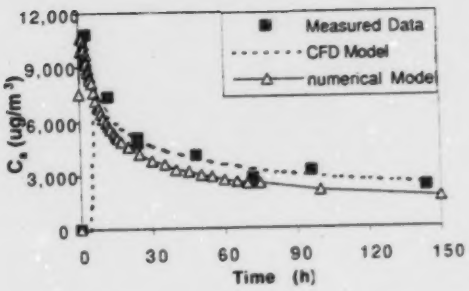

Figure 5 (a) Comparison of TVOC concentrations (PB2)

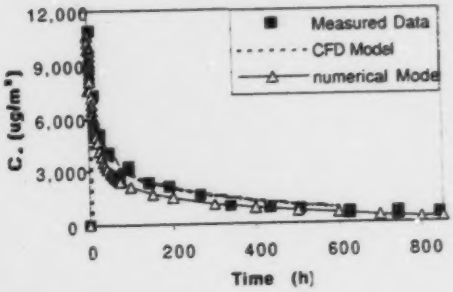

Figure 5 (b) Comparison of TVOC concentrations (PB2)

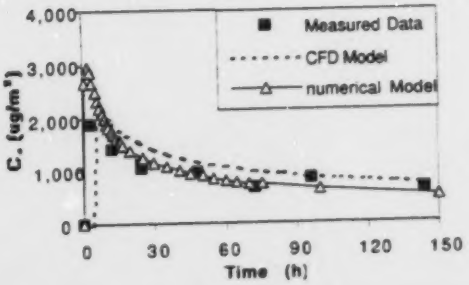

Figure 6 (a) Comparison of hexanal concentrations (PB2)

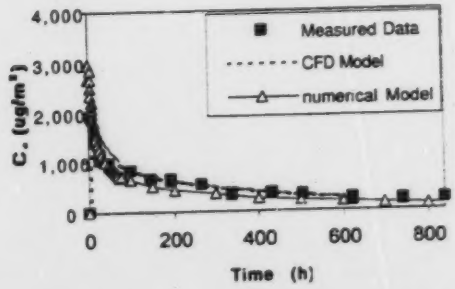

Figure 6 (b) Comparison of hexanal concentrations (PB2)

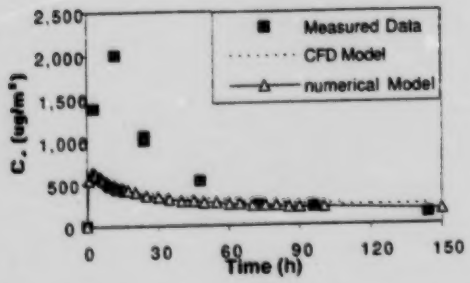

Figure 7(a) Comparison of α-pinene concentrations (PB2)

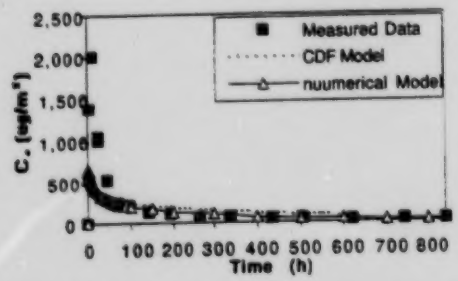

Figure 7(b) Comparison of α-pinene concentrations (PB2)

CONCLUSIONS

A numerical model was developed to predict the VOC concentration within the material, the VOC emission rate and the VOC concentration in the room air. This model uses four parameters, the diffusion coefficient in the material (D_m), material / air partition coefficient (k), the initial concentration in the material (C_0) and the mass transfer coefficient in the air (h). The first three parameters are properties of the material and can be determined by experiment, and the last one, h, can be estimated using fundamentals of fluid dynamics.

The predictions of the model were validated at two levels: with experimental results from the specially designed test and with the predictions made by a CFD model. The results indicate that there is generally good agreement between the model predictions, the experimental results and the CFD results.

ACKNOWLEDGEMENTS

This study was supported by a grant from the National Science and Engineering Research Council Canada and the EJLB Foundation. We thank Dr. Q. Chen of the Department of Architecture, Massachusetts Institute of Technology and Dr. Xudong Yang of the University of Miami for providing the experimental data.

REFERENCES

1. Haghighat, F., and Bellis, L.D., (1998) 'Material emission rates: literature review, and the impact of indoor air temperature and relative humidity', *Building and Environment*, Vol 33, No 5, pp 261-277.
2. Tichenor, B.A., Guo, Z. and Sparks, L.E., (1993) ' Fundamental mass transfer model for indoor air emissions from surface coatings', *Indoor Air*, 3, 263-268.
3. Spark, L.E., Tichenor, B.A., John C.S. Chang and Zhishi Guo, (1996) ' Gas-phase mass transfer model for predicting volatile organic compound emission rates from indoor pollutant sources', *Indoor Air*, 6, 31-40.
4. Haghighat, F. and Zhang, Y. (1999) 'Modeling of emission of volatile organic compounds from building materials-estimation of gas-phase mass transfer coefficient', *Building and Environment*, Vol. 34, pp. 377-389.
5. Little, J.C. and Hodgson, A.T., (1996) ' A Strategy for Characterizing Homogeneous, Diffusion-Controlled, Indoor Source and Sinks', *ASTM STP 1287*, P294-304.
6. Cox, S.S. Little, J.C., and Hodgson, A.T., (2000), ' A new method to predict emission rates of volatile compounds from vinyl flooring', *Proceeding of Healthy Building 2000*, Vol 4, pp169-174.
7. Lee, C. S., Ghaly, W. and Haghighat, F., (2000), ' VOC emission from diffusion controlled building material: analogy with conjugate heat transfer', *Proceeding of Healthy Building 2000*, Vol 4, pp163-168.
8. Dunn, J.E. (1987), ' Models and statistical methods for gaseous emission testing of finite sources in well-mixed chambers' *Atmospheric Environment* 21(2), p425-430.
9. Yang, X., Chen, Q., Zhang, J. S., Magee, R., Zeng, J. and Shaw, C.Y. (2000) 'Numerical simulation of VOC emission form dry materials', *Building and environment*. In press.
10. Murakami, S., Kato, S., Kondo, Y., Ito, K., and Yamamoto, A. (2000), 'VOC distribution in a room based on CFD simulation coupled with emission/ sorption analysis', *Proceeding of the 7th international conference on air distribution in rooms*, v. 1, pp 473-478.
11. Masel, R. I., (1996) *Principles of adsorption and reaction on solid surfaces*, John Wiley & Sons, Inc.

12. Axley, J. W., (1991) 'Adsorption modeling for building contaminant dispersal analysis', *Indoor Air*, 2, p147-171.
13. White, F. M. (1988), *Heat and Mass transfer*, Addison Wesley Series Publishing Company, Inc.
14. Rafson, H., J. (1998) *Odor and VOC control handbook*, McGraw-Hill.
15. Layman, W.J. (1982), *Handbook of chemical property estimation methods*, New York.
16. Bodalal, A. Zhang, J. S. and Plett, E.G. (2000) ' A method for measuring internal diffusion and equilibrium partition coefficients of volatile organic compounds for building materials', *Building and Environment*, p.01-110.
17. Tichenor, B.A. (1996) ' Overview of source/sink characterization methods', *ASTM STP, 1287*, p9-19.

Air Conditioning Simulation

Hisashi YAMAZAKI Toshiyuki WATANABE Hitoshi YAMAZAKI
Kyushu-University Kyushu-University Kanto-Gakuin-University
Fukuoka city Japan Fukuoka city Japan Kanagawa city Japan
yamazaki@beel.arch.kyushu-u.ac.jp tnabe@beel.arch.kyushy-u.ac.jp yamazaki@kanto-gakuin.ac.jp

1.Introduction

In Japan in recent years, utilization of VAV air conditioners is increasing for accomplishment of an air conditioning project owing to their simplicity in structure, low cost, availability for energy conservation, etc. On the other hand, the number of buildings designed to have atrium is also in a trend of increase. However almost none of VAV devices for air conditioning in office in individual buildings are available with the ventilation pipes except with the discharging pipes. "The air conditioning system accordance with the variable air volume method" allows not only the air volume in each room to be changed but also the pressure to be concurrently altered. Despite the above, no consideration is made in performing the pressure control individual office. In almost all of the business buildings in Japan, much importance is hardly attached to the said pressure problems. However it seems likely that the pressure problems are considered with respect to the Century Tower Building designed by Foster Associates at the time of its design. We, the authors of this paper, constructed a computation model based on a variety of information concerning the building, and attempted to make calculation taking up a building having a large-scale atrium as an example with the use of "Heat and Air Environment calculation program" developed by us. With the room pressure problem during the time when the VAV air conditioning attempt is in progress and the problematic points of the air current directed toward the atrium, a method to solve such problems and deal with such problematic points was examined.

2.Outline of the calculation program

In constructing buildings in recent years, research for performance of the buildings is made in advance of starting the construction. Meanwhile even just for the purpose of the preparatory research, simulation technology is exhibiting rapid progress. In case of executing construction design, surrounding air current situation is often available in light environment, or with large-size buildings. However simulation is seldom made with the air environment or air currents in buildings in advance of the setup, notwithstanding that the air environment in the building in which people reside is a matter of importance. On the other hand, realization of good air environment exercises much influence also on the heat environment. The heat environment simulation programs in recent years include in themselves problem of air currents. However heat computation is regarded as a pivotal point of the problems, and almost all of the projects are quite simple ones with which none of air volume calculation, crack air volume computation, and heat balance calculation, and fans, filters, cooling coils, etc. as air conditioner elements can be installed. Thus calculation of the heat/air environment of the system can be made in accordance with a calculation formula almost the same as the one utilized at the time of designing air conditioners. The said program makes its possible to do simulation ranging from small-scale buildings to large-scale construction.

3. Outline of the computation formula

The program in question can arbitrarily make plans for ducts, cracks, FANs, and cooling coils, and makes it possible to control and calculate the temperature, humidity, pressure, CO_2 gas concentration in an arbitrary room. Removal heat quantity calculation of the air handling unit (hereafter abbreviated as AHU) is made in connection with sensible heat and latent heat based on convection current heat conduction computation.

The volume of air flowing through the ducts, cracks, and open mouth is calculated in accordance with Darcy-Wysbach's formula. In other words, the said calculation is made by the local pressure loss and friction loss. Crack air volume calculation is made by parallel plate approximation of laminar airflows, and Colebrook's calculation formula is used for friction resistance in the duct air volume computation. Change of the turbulent flow friction coefficient caused by the change of Reynolds number (hereafter abbreviated as *Re* number) is hyperbola-approximated, and the duct inside roughness and the friction coefficient by the *Re* number are calculated by applying them to Darcy-Wysbach's formula. For that purpose, the friction coefficient in the duct air volume calculation is divided into 6 types of the Re number regions including laminar flow (Table 1). Meanwhile with the static

pressure air volume curve of the FAN which is hyperbola-approximated in consideration of the static pressure and air volume, a curve to allow the axis of the hyperbola whose axis comes to the minus side of the air volume to correspond to minus values of the static air volume one by one is selected.

3.1 Approximated ducts

In this paper , a duct which branches and blows out into the same room was approximated by a single turbulent flow duct. First all, approximation was made on the assumption that the temperature is 20.0 °C. After the duct was constructed, re-calculation made with the coefficient dependent on the temperature in the program corresponding to the change of the temperature and humidity together with change of the air volume. The air volume change by the *Re* number change according to the temperature change in connection with the duct constructed at this stage to be approximated is the same as that of the original turbulent flow duct. This is due to the fact the turbulent flow friction coefficient λ is based equation shown below.

$$\lambda=r_0+(r_1/Re)+(r_2/Re^2) \quad (1)$$

This is furthermore due to the fact that the approximated duct has a term r_0 equivalent to the local pressure loss except r_1, and has a term of r_2 equivalent to a team which is to be a unit of the pressure in the formula of the pressure loss. In addition to the above, the coefficients of r_0, r_1, and r_3 make calculation of the data of the 6 groups (Table 1) corresponding to the *Re* number with respect to the individual ducts at the time of reading the duct data as described before and is in possession of the said data.

3.2 Calculation formula of the room pressure and room temperature

Calculation of the room pressure P_i [pa] in the room i in question is made as shown below from its pressure difference $\Delta P_{i,j}$ on the assumption that the pressure in the room j where open mouths, cracks ducts, etc. are connected is known.

$$P_i=\sum_{j=1}^{N}\{(\Delta P_{ij}+P_j)s_j/(b_{ij}+\sqrt{b_{ij}^2+4\cdot a_{ij}|\Delta P_{ij}|})\}/\sum(s_j/(b_{ij}+\sqrt{b_{ij}^2+4\cdot a_{ij}|\Delta P_{ij}|})) \quad (2)$$

$$\Delta P_{i,j}=(P_j-\rho_j g\cdot h_j)-(P_i-\rho_i\cdot g\cdot h_i)+\delta P_h-\delta P=a_{i,j}\cdot v^2+b_{i,j}\cdot v$$

$$\delta P_h=\rho_d g\cdot(h^*_j-h^*_i) \quad (4)$$

δP: Term concerning r_2 in Eq. (1)

ρ_k: Density of air passing though the open mouths, cracks, ducts, etc. [kg/m^3]

s_k: Representative area the open mouths, cracks and ducts

v: Passing air average speed of the open mouths, cracks, ducts, etc. [m/s]

ρ_d: Duct passing air density [kg/m^3]

h_k: Height from the floor to the pivotal point of a duct open mouth [m]

h^*_k: Absolute height [m]

k: Express i or j. Volumetric flow ranging from j to i is plus.

The calculation formula of the room temperature was obtained from the stationary heat balance equation. This is a heat equilibrium formula of the heat balance of the sensible heat and latent heat of the room inflow/outflow air and the heat balance on the wall surface together with in-room generated heat quantity and in-room generated vapor quantity. On the other hand, the vapor are given by the in-room generated heat quantity on the simulation contains the sensible heat and latent heat together with the heat generation from the equipment and apparatus and solar-radiated inflow heat quantity. The calculation formula of the room temperature t is as shown below.

$$t=[\{(\sum hP_{in,j}\cdot q_{in,j}-G\cdot w\cdot R_w)+h_q+\sum a_k\cdot A_k\cdot t_{s,k}\}/[G\cdot\{c_p(t)+w\cdot c_v(t)\}+\sum a_k\cdot A_k]$$

Where G is given as shown below.

$$G=\sum q_{in,j} \quad (6)$$

$q_{in,j}$: Volume of air flowing from the j chamber to the camber in question [kg/s]

a_k: Convection heat conductivity in the inside of the chamber on the k-th wall in the chamber in question [kW/(m^2·K)]

A_k: Area of the k-th wall in the chamber in question [m^2]

$t_{s,k}$: Surface temperature in the inside of the k-th chamber of the chamber in question [°C]

$hp_{in,j}$: Enthalpy heat quantity [kJ/kg] of air flowing into the chamber though the ducts/cracks

h_q: In-room generated heat quantity [kW]

$c_p(t)$: Isopiestic specific heat [kJ/(kg·K)] to be changed according to temperature, approximately 1.01kJ/ (kg·K)

$c_v(t)$: Vapor specific heat [kJ/(kg·K)] to be changed according to temperature, approximately 1.8282 kJ / (kg·K)

R_w: Vapor latent heat quantity [kJ/kg], 2500.132 kJ/kg

w: Absolute humidity [kg/kg]

4. Calculation model

The data of the Century Tower were available for the calculation model of this time, and were constructed based on the obtained information (Figs. 1 and 2). The information is for construction of the 5th and 6th floors of the building. The structure of the building, which is fundamentally the same as that of the Tower except the 1st and 2nd floors, was designed with respect to the 3rd floor through the 10th floor in accordance with the said information. On the other hand, the offices are placed symmetrically with the atrium as their boundary point. The ducts, which are constructed based on the

information, are used by approximating then as described before. FAN data is constructed based on the information by being hyperbola-approximated as referred to before(fig. 3). No design of the elevator halls was formed.

4.1 Performance of the AHU for simulation

The AHU is constructed by a combination of an air cooling coil and an FAN. Coil specification are read by the data. It is possible to incorporate plural AHUs whose specification are different from each other into a single typo of simulation. Calculation results allow the individual data of the AHU to be outputted. Performance of the cooling coil of the AHU is shown in Fig. 4.

4.2 Pressure control in a room

Settlement of the pressure control was made with respect to the individual systems having respectively an air conditioner. Which this simulation for example, the damper after the ventilating flows were combined was designed to be regulated for the 3rd and 4th floors. In addition, when no heat was generated and no inflow of the outer air was seen, pressure control was made by means of the return VAV of the individual rooms with respect to the individual rooms.

4.3 Pressure settlement method to obstruct the atrium flow in case that the atrium is devoid of heat road

In case that the temperature and humidity in a room are controlled and the atrium is devoid of the heat load from the glass and wall of the atrium, the atrium flow can be obstructed by designation the pressure settlement values of the individual floors as the values in accordance with the calculation formula shown below. When indoor and outdoor temperature difference is brought about in the inside and outside of the room. However when the outer atmosphere on the earth is taken up as a criterion, the pressure difference $\delta P'_h$ is given as shown below.

$$\delta P'_h = gh/v(t_i, w_i) - gh/v(t_o, w_o) \quad (7)$$

$$v(t,w) = 287.055 \cdot (273.15+t) \cdot (0.9995+1.60777 \cdot w)/101325.0 \quad (8)$$

g= 9.80665m/s^2, h: Height [m],

$v(t,w)$: Specific volume assessed from dry-bulb temperature and absolute temperature [m^3/kg]

t: Dry-bulb temperature

w: Absolute humidity i: inside o: outside

By taking up a value of a height in accordance with the calculation formula shown above as a criterion, a control target value is determined. Utilization of the said value for the pressure control in the individual rooms makes it possible to liberate the flow from being directed from the individual floors to the atrium. However in case that difference is noted with the air density of the individual floors, the density difference and the open mouth position are related with each other. From this reason, it is necessary to make calculation with respect to the individual cases.

4.4 Calculation result

The individual Case patterns are listed in Tables 2. No difference is noticed with the north and south buildings for Case 1 though 5, and a symmetrical result is obtained. Therefore the result is described exclusively with the north building. In this connection, the result of the AHU and inputted heat quantity is tabulated exclusively with the 3rd and 4th floors owing to the restriction of the pages in this paper. On the other hand, the values of the atrium ventilation, stairs ventilation, and open mouth inflow quantity are given as the sum of the inflow and outflow owing to the restriction of the page in this paper. Therefore even in case that the numerical values are low, exchange air quantity is sometimes abundant.

4.4.1 Operation with the unrectified air conditioning design data

Although no operation of the air conditioning design is made as a system because the design is made with respect to the individual elements, investigation can be made to check to see if the performance strictly in accordance with the settled settled design is obtained by the operation by means of simulation. First of all, operation is made as Case 1 by being devoid of entire heat generation quantity. The outer atmosphere temperature at that time is 20°C, whereas the outer atmosphere relative humidity is 50%. As a result of the calculation, the volumetric flow from the FAN is obtained as design prediction values. None of natural ventilation is caused because no heat is generated, and no flow is produced on the upper and lower floors.

4.4.2 Heat input operation(room pressure control)

Case 2 reveals that control is made with the area of the glass window facing the outer atmosphere 92.642m^2, room temperature as 26°C, relative humidity as 50% and CO_2 gas concentration as 999ppm under the condition that the heat quantity applied to the individual offices is 24.5kW in Case 1. The crack of the sash was determined to be 22.5m long with the stability floor, whereas the 2 horizontal cracks with a length of 22.5m and 16 vertical cracks with a length of 2.96m were determined. Meanwhile with the mezzanine floor, 3 horizontal cracks with a length of

22.5m and 16 vertical cracks with a length of 2.97m were determined. For the room pressure settlement value in Eq. (7) is used so that the flow on the upper and lower floors will be reduced.

4.4.3 Applied heat quality reduction (room pressure control available and room pressure control unavailable)

Case 3 reveals that the applied heat quantity to be given to the individual offices was determined to be 17.15kW as 30% reduction in Case 2. Also for the pressure settlement in Case 3, the pressure settlement value in Eq. (7) is used likewise in Case 2. Even under the condition that the applied quantity is reduced 30%, the state of equilibrium in the room can be maintained by performing room pressure control.

Case 4 reveals that the applied heat quantity given to the individual offices is determined to be 17.15kW as 30% reduction, but this is the case that no pressure control is performed and affairs are physically the same as the duct state in Case 2. Under the condition that the applied heat quantity is reduced 30% and the affairs are the same in Case 2, the room pressure becomes too low.

4.4.4 Inputting the heat and window cracks to the atrium

To the prevision Case, the atrium unit was devoid of heat load and was placed in a closed state. In Case 5, the heat load brought about by solar radiation and window crack(air-tight sash)data are inputted into the atrium. The atrium has heat load. Therefore when the temperature is higher than in the lower part, it is necessary for the upper room pressure settlement value to be reduced by the amount of the temperature elevation corresponding to the pressure reduction quantity.

4.4.5 In case that the heat quantity is increased exclusively with the 3rd floor of the north building

Case 6 reveals that increased heat quantity more than in other room was supplied exclusively to the 3rd floor of the north building. The generated heat quantity in the room is 24.5kW with the 3rd floor of the north building, whereas the quantity is 17.15kWwith the other floors. Difference is noted with the heat generation quantity, and difference is likewise noted with the volume of air to be supplied to the room for the purpose of the temperature control of the 3rd and 4th floors of the north building. However since room pressure is controlled, the factors including the flow to the atrium are kept low enough without being different from the state in Case 5.

5.Conclusions

(1) It is possible, it is said, foe the VAV unit to correspond to the change, provided that the variation in the heat quantity is as small as 30%.However it is necessary for the variation of the room pressure to be checked. When no correspondence to the room pressure control is made, dangerous pressure lowering liable to allow the room pressure to be lowered to the extent of the outer barometric pressure more than 200Pa is seen.

(2) Also in case that cracks, e.g. windows are in existence, no mitigation of the room pressure lowering can be reached with the air-tight windows in this simulation. As long as the said result is taken into account, a considerable amount of the cracks to mitigate the room pressure lowering becomes necessary.

(3) When the atrium where space is connected with the offices is devoid of heat load, it is possible for the flow directed toward the atrium to be reduced as seen in Case 2.

(4) When the atrium where space is connected with the offices is in possession of heat load and no control is made with the atrium room temperature at the same office room temperature, a flow is produced in the atrium. In Case 5, production of ascending air current together with elevation of the temperature in the upper part was seen. When vigilant to the atrium temperature, room pressure control on the individual floors is possible. Despite the above, temperature difference is noted with the offices and the atrium. Thus exchange of air is brought about as seen in Case 5.

(5) When increase of heat land is seen exclusively with the south office on 3rd floor, pressure balance compels a large amount of air to be directed toward the atrium exclusively with return damper. In that, occasion, control of the individual floors makes it possible to reduce the flow. Meanwhile from the Comparative results in Case 5 and 6, it is explained that the outcomes with which almost none of difference is noted wore obtained with the floors except the floors providing the heat land with change. From this reason, it is imagined that just a small amount of influence in to be exercised on the other floors provided that room pressure control is continuously performed.

Reference

1.ASHRAE Handbook, Fundamentals Volume, American Society of Heating,Refrigerating and Air-Conditioning Engineers,Inc,Atlanta,GA,1989

2. Ian Ranbot and Colin Davis,"Century Tower" , Water Mark publications(UK), September, 1992, Japanese Edition

3.Uichi INOUE, "Air-Conditioning Handbook", Maruzen Inc.,January, 1996,Japanese

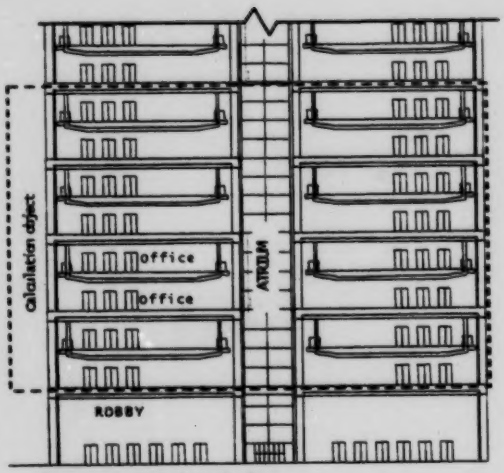

Figure 1 Sectional view

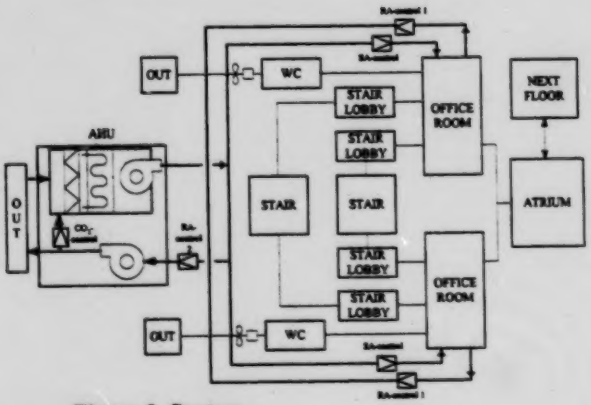

Figure 3 System

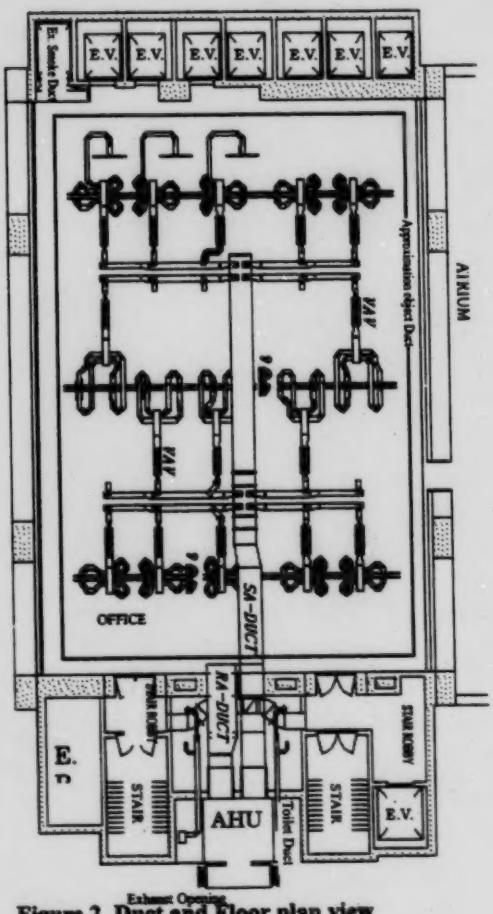

Figure 2 Duct and Floor plan view

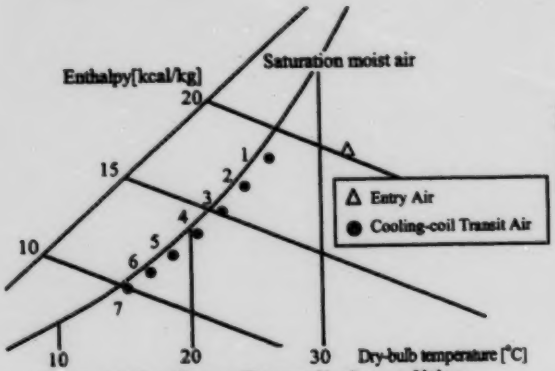

Figure 4 Cooling-coil transit air condition

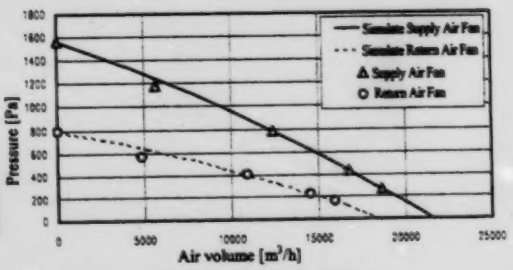

Figure5 The air volume of Fan

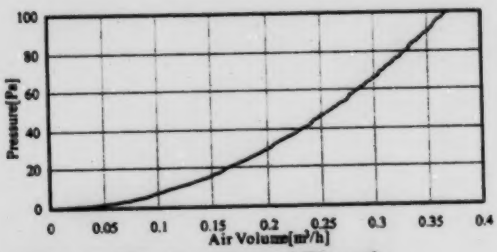

Figure 6 The air volume of Fix sash

	1	2	3
1	Laminar flow.		
2	1000	4000	8000
3	8000	16000	40000
4	40000	80000	200000
5	200000	400000	1000000
6	1000000	2500000	7500000

Table 1 Reynolds areas

Table2 Simulation Calculation result

		Case1	Case2	Case3	Case4	Case5	Case6_H	Case6_S
Supply air VAV	Condition	-	ON*1	ON	ON	ON	ON	ON
Return air VAV	Condition	-	ON	ON	ON	ON	ON	ON
RA-SA VAV	Condition	-	ON	ON	-	ON	ON	ON
ATRIUM 28m	Condition	-	-	-	-	ON	ON	ON
Temperature	℃	26	26.0	26.0	26.0	26.0	26.0	26.0
Relative humidity	%	50	61.4	61.4	61.4	61.4	61.4	61.4
CO_2 concentration	ppm	350	350	350	350	350	350	350
Specific ABS								
The amount of evaporated water	kg/s	-	250	250	250	250	250	250
The amount of evaporated water	kw	-	0	0	0	0	0	0
Outdoor solar-gain temperature	℃	-	5.481	9.300	8.140	9.300	8.900	9.300
Outdoor solar-gain temperature	℃	-	14.059	14.118	13.979	14.118	14.100	14.120
Cooling coil load	kW	-	97.391	82.340	82.340	82.340	80.972	82.403
The amount of latent heat	kW	-	25.000	25.000	25.000	25.000	25.347	25.282
Amount condensation of water	kg	-	36.000	36.000	36.000	36.000	36.000	36.000
Heat data								
Heating the amount of heating	kw	-	26.0	17.13	17.13	17.13	26.0	17.13
Heating Outer wall conduction heat equipment	kW	-	1.314	1.314	1.314	1.314	1.314	1.314
Heating Staying in the room number	person	-	50	50	50	50	50	50
Heating Human body convection heat quantity	kW	-	3.85	3.85	3.85	3.85	3.85	3.85
Heating Human body convection room quantity	kgh	-	5.396	5.396	5.396	5.396	5.396	5.396
Heating CO_2 occupancy quantity	m³/h	-	1.13	1.13	1.13	1.13	1.13	1.13
Maximum The amount of heating	kW	-	26.0	17.13	17.13	17.13	17.13	17.13
Maximum Outer wall conduction heat equipment	kW	-	1.314	1.314	1.314	1.314	1.314	1.314
Maximum stay Staying in the room number	person	-	50	50	50	50	50	50
Maximum Human body convection heat quantity	kw	-	3.85	3.85	3.85	3.85	3.85	3.85
Maximum Human body convection room quantity	kgh	-	5.396	5.396	5.396	5.396	5.396	5.396
Maximum CO_2 occupancy quantity	m³/h	-	1.13	1.13	1.13	1.13	1.13	1.13
Supply air PMV maximum limiting value	kW	-	7.2	7.2	7.2	7.2	7.2	7.2
Minimum PMV minimum limiting value	kW	-	3.6	3.6	3.6	3.6	3.6	3.6
26-4th Floor								
Outdoor Temperature	℃	26.0	26.0	26.0	26.0	26.0	26.0	26.0
Outdoor Relative humidity	%	50.0	50.0	49.4	50.0	50.0	49.4	50.0
Outdoor CO_2 concentration	ppm	350	999	979	999	999	979	999
Kitchen Temperature	℃	26.0	26.0	26.0	26.0	26.0	26.0	26.0
Kitchen Relative humidity	%	50.0	50.0	50.0	50.0	50.0	50.0	50.0
Kitchen CO_2 concentration	ppm	350	999	1000	999	999	1000	999
Infinity	Pa	53.399	5.69	9.89	-280.39	7.39	7.39	7.39
WC (Infinity)	Pa	51.799	7.99	7.99	-280.09	5.99	6.01	6.01
Entrance entry	Pa	53.399	7.99	7.99	-284.09	6.14	6.39	6.31
WC (Entrance)	Pa	51.799	6.79	6.77	-284.17	4.97	4.99	4.99
Supply air (Infinity)	kgh	9,603	9,602	7,899	6,999	7,899	9,519	7,899
Return air (Infinity)	kgh	9,189	9,040	6,603	7,105	6,599	8,979	6,604
Toilet exhaust (Infinity)	kgh	400	400	400	-100	400	400	400
Leakage discharge *2	kgh	0.0	1.4	2.6	-20.5	-499.79	-511.23	-499.96
Aperture inflow (Infinity)	kgh	2.5	-0.6	-0.6	2.5	-0.66	-0.67	-0.67
Recovery discharge *2	kgh	0.0	0.7	0.7	20.4	154	134.85	135.79
Supply air(Entrance)	kgh	9,603	9,602	7,899	6,999	7,899	9,391	7,899
Return air (Entrance)	kgh	9,189	9,040	6,603	7,105	6,599	8,979	6,604
Toilet exhaust (Entrance)	kgh	400	400	400	-100	400	400	400
Leakage discharge *2	kgh	-0.5	-1.6	-2.2	-20.5	-500.1	-493.4	-499.74
Aperture inflow (Entrance)	kgh	2.5	-0.6	-0.9	2.5	-0.72	-0.72	-0.72
Recovery discharge *2	kgh	0.0	0.7	0.7	20.4	154.05	137.72	138.67
Supply air temperature	℃	26	15.64	13.79	13.58	15.79	13.71	13.79
Supply air humidity	%	50	90.39	97.04	86.91	97.02	98.48	97.04

26-4th Floor		Case1	Case2	Case3	Case4	Case5	Case6_H	Case6_S
Outdoor Temperature	℃	26.0	26.0	26.0	26.0	25.99	26.0	26.0
Outdoor Relative humidity	%	50.0	50.0	50.0	50.0	49.97	50.0	50.0
Outdoor CO_2 concentration	ppm	350.0	999.0	999.0	999.0	999	999	999
Kitchen Temperature	℃	26.0	26.0	26.0	26.0	25.99	26.0	26.0
Kitchen Relative humidity	%	50.0	50.0	50.0	50.0	49.96	50.0	50.0
Kitchen CO_2 concentration	ppm	350.0	999.0	999.0	999.0	999	999	999
Infinity	Pa	53.399	6.62	6.62	-280.19	5.33	5.33	5.33
WC (Infinity)	Pa	51.799	5.39	5.39	-280.21	4.12	4.12	4.12
Entrance entry	Pa	53.399	5.68	5.68	-284.39	4.34	4.34	4.34
WC (Entrance)	Pa	51.799	4.48	4.48	-284.52	3.15	3.15	3.15
Supply air (Infinity)	kgh	9,602	9,486	7,899	6,999	7,899	7,899	7,899
Return air (Infinity)	kgh	9,189	9,031	6,603	7,149	6,599	6,791	6,791
Toilet exhaust (Infinity)	kgh	400	400	400	-100	400	400	400
Leakage discharge *2	kgh	0.8	1.38	6.37	-27.48	-250.52	-150.08	-150.34
Aperture inflow (Infinity)	kgh	2.52	-0.65	-0.65	5.31	-0.69	-0.69	-0.69
Recovery discharge *2	kgh	0	0.89	6.33	17.64	98.61	100.6	100.59
Supply air(Entrance)	kgh	9,600	9,486	7,899	6,999	7,899	7,899	7,899
Return air (Entrance)	kgh	9,189	9,040	6,603	7,101	6,674	6,799	6,799
Toilet exhaust (Entrance)	kgh	400	400	400	-100	400	400	400
Leakage discharge *2	kgh	-0.55	-1.38	-7.36	-8.3	-97.11	-49.44	-49.5
Aperture inflow (Entrance)	kgh	3.14	-0.65	-0.65	6.51	-0.54	-0.54	-0.54
Recovery discharge *2	kgh	0	0.81	6.15	7.93	50.09	50.76	57.09
Supply air temperature	℃	26	15.64	13.79	13.58	13.79	13.79	13.79
Supply air humidity	%	50	90.39	97.04	86.9	97.06	97.06	97.04
26-5th Floor								
Outdoor Temperature	℃	26.0	26.0	26.0	26.0	26	26.0	26.0
Outdoor Relative humidity	%	50.0	50.0	50.0	50.0	49.99	50.0	50.0
Outdoor CO_2 concentration	ppm	350.0	999.0	999.0	999.0	999	999	999
Kitchen Temperature	℃	26.0	26.0	26.0	26.0	26	26.0	26.0
Kitchen Relative humidity	%	50.0	50.0	50.0	50.0	49.99	50.0	50.0
Kitchen CO_2 concentration	ppm	350.0	999.0	999.0	999.0	999	999	999
Infinity	Pa	53.399	4.54	4.54	-287.36	3.33	3.33	3.33
WC (Infinity)	Pa	51.799	3.33	3.33	-287.48	2.33	2.34	2.34
Entrance entry	Pa	53.399	3.41	3.41	-288.48	2.67	2.69	2.69
WC (Entrance)	Pa	51.799	2.28	2.28	-288.51	1.45	1.45	1.45
Supply air (Infinity)	kgh	9,602	9,484	7,899	6,999	7,249	7,161	7,152
Return air (Infinity)	kgh	9,189	9,044	6,603	7,133	6,844	6,854	6,855
Toilet exhaust (Infinity)	kgh	400	400	400	-100	400	400	400
Leakage discharge *2	kgh	-0.5	1.38	15.91	-13.58	68.04	22.71	22.4
Aperture inflow (Infinity)	kgh	2.51	-0.65	0.65	5.34	-0.37	-0.37	-0.33
Recovery discharge *2	kgh	0	0.89	0.65	3.04	15.44	18.13	18.39
Supply air(Entrance)	kgh	9,600	9,484	7,899	6,999	7,117	7,129	7,119
Return air (Entrance)	kgh	9,189	9,042	6,603	7,134	6,839	6,850	6,850
Toilet exhaust (Entrance)	kgh	400	400	400	-100	400	400	400
Leakage discharge *2	kgh	-0.55	-1.38	-15.91	15.15	220.45	209.15	206.16
Aperture inflow (Entrance)	kgh	3.14	-0.65	-0.65	6.54	-0.34	-0.34	-0.34
Recovery discharge *2	kgh	0	0.81	0.66	13.55	87.47	91.23	91.76
Supply air temperature	℃	26	15.64	13.79	13.58	13.79	13.79	13.79
Supply air humidity	%	50	90.39	97.04	86.9	97.13	97.14	97.14
26-16th Floor								
Outdoor Temperature	℃	26.0	26.0	26.0	26.0	25.99	26.0	26.0
Outdoor Relative humidity	%	50.0	50.0	50.0	50.0	50.01	49.99	49.99
Outdoor CO_2 concentration	ppm	350.0	999.0	998.9	999.0	999	999	999
Kitchen Temperature	℃	26.0	26.0	26.0	26.0	25.99	26.0	26.0
Kitchen Relative humidity	%	50.0	50.0	50.0	50.0	50.01	50.01	50.01
Kitchen CO_2 concentration	ppm	350.0	999.0	998.9	999.0	999	999	999
Infinity	Pa	53.399	3.57	3.57	-280.86	2.26	2.26	2.26
WC (Infinity)	Pa	51.799	1.97	1.97	-280.98	0.66	0.66	0.66
Entrance entry	Pa	53.399	1.14	1.14	-285.04	1.31	1.31	1.31
WC (Entrance)	Pa	51.799	-0.04	-0.05	-285.06	0.02	0.02	0.02
Supply air (Infinity)	kgh	9,602	9,486	7,899	6,999	7,249	7,161	7,161
Return air (Infinity)	kgh	9,189	9,044	6,603	7,133	6,795	6,872	6,872
Toilet exhaust (Infinity)	kgh	400	400	400	-100	400	400	400
Leakage discharge *2	kgh	-0.5	1.4	14.1	29.2	252.74	261.64	257.34
Aperture inflow (Infinity)	kgh	2.5	-0.5	-0.5	5.3	-0.52	-0.52	-0.52
Recovery discharge *2	kgh	0.0	-0.1	0.3	-14.0	-194.72	-147.69	-147.81
Supply air(Entrance)	kgh	9,600	9,486	7,899	6,999	7,249	7,161	7,161
Return air (Entrance)	kgh	9,189	9,042	6,603	7,115	6,797	6,869	6,869
Toilet exhaust (Entrance)	kgh	400	400	400	-100	400	400	400
Leakage discharge *2	kgh	-0.5	-1.3	-15.7	74.7	466.1	529.14	525.14
Aperture inflow (Entrance)	kgh	3.1	-0.1	-0.1	6.0	-0.14	-0.14	-0.14
Recovery discharge *2	kgh	0.0	-0.2	-0.6	-48.5	-316.64	-310.84	-310.47
Supply air temperature	℃	26	15.64	13.79	13.57	13.77	13.78	13.78
Supply air humidity	%	50	90.39	97.04	86.98	97.36	97.36	97.36

*1 ON mode so that it may become the given condition.
*2 It is flow a node out.

Session 4/ Séance 4

The Role of Simulation in Supporting Energy Efficiency Programmes and Stock Modelling

Le rôle de la simulation à l'appui des programmes d'efficacité énergétique et la modélisation des ensembles de bâtiments

HOT2.XP: ENERGUIDE FOR HOUSES AND THE NEW HOUSING MARKET

Ted Kesik
Architecture, Landscape and Design
University of Toronto
ted.kesik@utoronto.ca

Michael Lio
Lio Associates
Toronto, Ontario
mlio@netcom.ca

ABSTRACT

This paper presents the use of HOT2-XP[1] within a 1999 pilot project sponsored by Natural Resources Canada (NRCan), which involved the evaluation and energy rating of 64 new homes in Ontario according to the EnerGuide[2] for Houses Procedures and Guidelines [1].

Prior to the introduction of the EnerGuide for Houses Program, the only formal method for assessing the energy efficiency of new housing was the R-2000[3] Design Approval Procedures and Guidelines [2]. These were tied to the R-2000 Program criteria and relied on a detailed assessment of house characteristics using HOT2000[4]. HOT2.XP was developed as a derivative of HOT2000 for use within the EnerGuide for Houses Program, aimed initially at improving the energy efficiency of older homes. The Ontario pilot project studied the utility of HOT2.XP in capturing the energy rating of new homes at the pre-construction stage.

The core of this paper explores the variation of EnerGuide ratings among typical new homes, and the differences in ratings between pre-construction and post-construction assessments. The sensitivity of airtightness and solar orientation to the house rating are also discussed. Assessments of the utility of HOT2-XP solicited from the pilot project design evaluators are also discussed. The paper concludes with key recommendations for maintaining energy simulation software integrity within the context of consumer information needs and builder marketing realities.

[1] HOT2.XP is a new member of the HOT2000 family of energy analysis software developed by CANMET Energy Technology Centre, NRCan.

[2] EnerGuide is an energy labeling program administered by the Office of Energy Efficiency, NRCan.

[3] R-2000 is a super energy efficient home program sponsored by NRCan since 1982.

[4] HOT2000 is an energy analysis and design software for low-rise residential buildings developed by CANMET Energy Technology Centre, NRCan.

INTRODUCTION

The EnerGuide for Houses Program seeks to improve the energy efficiency of housing in the marketplace by providing an accurate and effective means of rating the energy efficiency of houses. The EnerGuide ratings for household appliances and energy conversion equipment are familiar to consumers, and a rating system for houses represents a logical extension of information that enables informed decision making by homebuyers.

Initially, the EnerGuide for Houses Program was targeted at existing homes, most of which were significantly less energy efficient than homes currently constructed across Canada. This pilot project was intended to apply program guidelines and procedures to the new housing market to assess its suitability.

The pilot project was limited in scope and confined to new housing in Ontario. While a specific number of homes was not targeted, the intent of the project funding was to maximize the number of houses receiving EnerGuide labels. Based on the available funding and the willing cooperation of Ontario builders, a total of 64 houses were evaluated and assigned energy ratings according to EnerGuide procedures. The houses ranged in location, size, style and market segment, and fairly represent the current mix of new housing in Ontario.

TERMINOLOGY

In this paper, the terms "label" and "standard" are used according to the following definitions:

Labels are markings, with supporting promotion and directories, which show products' energy use or efficiency according to a common measure. The EnerGuide for Houses rating is a label

Standards are mandatory programs (regulations) stipulating the minimum efficiency levels or maximum energy-use levels acceptable for products sold in a particular country or region. Minimum requirements for energy efficiency prescribed in the Ontario Building Code represent standards.

METHODOLOGY

This project was managed by EnerQuality Corporation, an authorized agent of Natural Resources Canada, and involved its network of builders and quality assurance evaluators (QAEs). The recruitment of builders came from within EnerQuality Program members, and involved extensive efforts due to the unusually high levels of residential construction activity across most of Ontario. Request for proposals were forwarded to QAEs across Ontario to obtain quotations for conducting EnerGuide evaluations on a per-house basis. The most competitive quotations were used to match QAEs with willing builders to the extent made possible by available funding.

The pilot pool of builders and QAEs were provided with applicable EnerGuide procedures and guidelines during an orientation workshop in July 1999. Subsequently, the construction, evaluation, site visits and airtightness testing were carried out for the sample of 64 new homes.

Documentation of the evaluations was forwarded to EnerQuality Corporation for review, summarization, and submittal to NRCan for the issuing of EnerGuide labels.

EnerGuide ratings for each of the 64 houses were obtained using the HOT2.XP software and associated evaluation procedures established by Natural Resources Canada.

HOT2.XP evaluation criteria were established by Natural Resources Canada corresponding to assessment scenarios which were investigated to determine:

i. the voluntary energy efficiency improvements found in typical new housing which exceeded 1997 Ontario Building Code (OBC) minimum requirements for energy efficiency (both for the building envelope, and energy conversion equipment, such as furnaces and water heaters);

ii. the sensitivity of the EnerGuide energy ratings to envelope airtightness levels; and

iii. the sensitivity of the EnerGuide energy ratings to the solar orientation of the building.

In order to efficiently assess the variables, QAEs were instructed to perform HOT2.XP simulations involving 7 separate cases, as described in Table 1.

CASE	HOT2.XP EVALUATION CRITERA
1	OBC minimum energy efficiency requirements + HOT2.XP default blower door value (3.57 ach @ 50 Pa)
2	Actual levels of energy efficiency + HOT2.XP default blower door value (3.57 ach @ 50 Pa)
3	Actual + "as operated" blower door test (as per *EnerGuide* procedures)
4	Actual + CGSB procedure blower door test
5	Actual + "as operated" + vary orientation (cardinal direction)
6	Actual + "as operated" + vary orientation
7	Actual + "as operated" + vary orientation
CGSB - Canadian General Standards Board. [3] **Note:** Case 2, blower door values depend upon values specified in the structures library.	

Table 1 HOT2.XP Evaluation Criteria for 7 Cases Assessed in Pilot Study

In all 7 cases, the EnerGuide rating (ER) was derived according to the following equation:

$$ER = 100 - \frac{\text{Estimated Energy Consumption}}{\text{(R-2000 Energy Target)}} \times 20$$

When the energy consumption of a constructed home is estimated above the R-2000 energy target, its rating falls below 80. If the estimated energy consumption is equal to that of the R-2000 target, the rating is exactly 80. As the estimated energy consumption decreases below the R-2000 target level, the energy rating increases beyond 80 to the point where a home with zero purchased energy consumption attains a rating of 100. Typical energy ratings for Canadian housing stock are listed in Table 2.

TYPICAL RATING	HOUSE CHARACTERISTICS
0 to 50	Old house not upgraded
51 to 65	Upgraded old house
66 to 75	More energy efficient upgraded old house or typical new house
68 to 82	Energy efficient new house
80 to 90	Highly energy efficient new house
91 to 100	Approaching zero purchased energy house
Source: Office of Energy Efficiency, NRCan.	

Table 2 Typical EnerGuide Ratings for Canadian Houses

RESULTS

The data in Table 3 reflect the 7 simulation cases described in Table 1, and represent the summarized EnerGuide ratings data for the 64 houses assessed in the pilot project. Due to space limitations, these data have not been included in this paper, but are available in the final report to this project [4].

	ENERGUIDE ASSESSMENT CASE						
	1	2	3	4	5	6	7
Avg.	68	74	74	74	73	73	74
Min	58	69	69	69	69	69	69
Max	77	82	82	83	82	82	82
St. Dev.	3.08	2.38	2.49	2.69	2.53	2.61	2.60

Table 3 Summary of EnerGuide Ratings Corresponding to 7 Assessment Cases for 64 Pilot Project Houses

The data from the computer simulations were also used to derive the level of energy efficiency improvements beyond minimum levels prescribed in the 1997 Ontario Building Code for the sample of 64 pilot study homes. In addition, an assessment of the current level of the sample homes' airtightness was performed.

The results have been summarized in Table 4 according to the following parameters:

OBC '97 - the estimated annual energy consumption of each home assuming it was constructed to the minimum levels of energy efficiency prescribed in the 1997 Ontario Building Code;

ASOP - the estimated annual energy consumption of each home given its actual as-built condition;

CHANGE – (GJ) the improvement in GJ/year between the minimum and actual levels of energy efficiency, and (%), the percentage improvement beyond the minimum levels of energy efficiency prescribed in the 1997 Ontario Building Code; and

ASOP: ACH @ 50 Pa - the measured airtightness of each home based on the "as operated" blower door test required under EnerGuide procedures.

This information was processed in order to gain an estimate of the energy savings captured by energy labeling of voluntary energy efficiency improvements, and to compare HOT2.XP default airtightness levels with those measured in the field.

	OBC '97	ASOP	CHANGE		ASOP
	(GJ)	(GJ)	(GJ)	%	ACH @ 50 Pa
Avg.	202.7	165.3	37.4	18.4%	3.81**
Min	110.6	89.4	-29.5*	-26.7*	1.17
Max	317.2	226.6	152.6	53.5	13.20
St. Dev.	40.76	30.39	27.43	11.1	1.66

* One anomalous house was tested to an airtightness of 13.2 ach @ 50 Pa, resulting in a difference in rating of 8 points on the EnerGuide scale.

** Removing this anomaly from the sample translated into an average airtightness of 3.66.

Table 4 Comparison of Simulated Energy Performance of 64 Pilot Study Houses

Based on the evaluations of the 64 homes in the pilot study, several significant findings emerged:

1. The lowest actual rating among the 64 homes was 69, and the highest rating was 82.

2. The voluntary levels of energy efficiency improvements evidenced in this pilot study translate into an average improvement of 6 points on the EnerGuide rating scale beyond the average energy efficiency rating of 68 for the minimum requirements prescribed in the 1997 Ontario Building Code.

3. The estimated average annual energy consumption of the pilot study homes, assuming they were constructed to OBC minimum levels of energy efficiency, was 202.7 GJ/year. The estimated average annual energy consumption of the actual, as-built condition was 165.3 GJ/year. This average difference of 37.2 GJ represents a 18.4% improvement over minimum levels of energy efficiency. The maximum individual difference observed between the OBC base cases, and the as-operated cases, was 152.6 GJ, a 53.5% improvement.

4. The average airtightness levels in the 64 homes was 3.81 ach @ 50 Pa, compared with the HOT2.XP default value of 3.57 ach @ 50 Pa. The averaged measured airtightness, when corrected for explainable anomalies, was 3.66.

5. The EnerGuide for Houses rating for airtested houses in the "as operated" condition, and those that were evaluated using the HOT2.XP default airtightness of 3.57 ach was virtually identical when comparing ratings across the 64 homes in the pilot study. Of the 64 sets of ratings, 41 (64%) were identical, with 60 (94%) having a difference in rating of 2 or less. The maximum deviation, discounting anomalous data, was 3. This suggests that the difference between default and measured levels of airtightness in new housing does not significantly affect the EnerGuide for Houses rating.

6. The average difference in energy consumption when considering HOT2.XP default airtightness levels versus actual, "as operated" airtightness levels is 0.52 GJ/year, representing less than 1% of annual energy consumption. For any individual building, the maximum difference was 19.5 GJ representing 10% of annual energy consumption, well within the 15% tolerance permitted by the EnerGuide for Houses Technical Guidelines.

7. The differences between ratings due to the effect of orientation for the pilot study homes was insignificant owing to a tendency of these house designs to disregard passive solar potential.

These findings were derived directly from the data appearing in Tables 3 and 4, except for the results discussed in Item 6 above, which were derived from the complete data set appearing in the study report.

ANALYSIS

A number of issues emerged from the findings of this pilot study. These can be categorized as issues relating to the utility of HOT2.XP software, and issues relating to the EnerGuide for Houses Program. The two are interrelated insofar as the results obtained from the HOT2.XP analysis are used to derive an EnerGuide for Houses rating. The utility of the HOT2.XP software should not be confused with consumer and builder perceptions of the EnerGuide ratings. This becomes obvious when the numerous physical measures provided by the software are compared to a single non-dimensional measure.

The issues related to software integrity, accuracy of simulation tools for house energy rating systems (HERS), and the suitability of HOT2.XP are explored later in this paper. The next section of the analysis deals with HOT2.XP as a home energy rating system evaluation tool

Technical Evaluation Using HOT2.XP

HOT2.XP is an express version of HOT2000 which embodies similar modeling capabilities, including:

- Above and below grade envelope heat transfer (opaque and transparent elements);
- Air leakage and ventilation energy loads;
- Solar and internal gains;
- Space and domestic water heating equipment performance; and
- Energy use for appliances and lighting

It is important to note that the HOT2.XP below-grade heat loss modelling capability is not as sophisticated as that provided within HOT2000, however, it is sufficient to accurately model typical basements in older houses.

From a practical perspective, quality assurance evaluators reported difficulties deploying the HOT2.XP software, particularly in the case of less conventional house designs. In comparisons with HOT2000, QAEs indicated that the HOT2.XP software lacked the robustness needed to deal with unusual conditions, especially basement configurations. In general, HOT2000 was preferred by this group - an understandable finding given the many years of experience each evaluator has had with the HOT2000 software. (It is interesting to note that R-2000 Program experience indicates an initial level of resistance to the adoption of new versions of HOT2000 since the 1980s.)

A key observation echoed by most of the QAEs was that the use of HOT2.XP did not appreciably reduce the time, and hence the cost, of performing the technical evaluation. The data requirements for modeling new houses are virtually identical within the EnerGuide and R-2000 Programs, hence the express features geared towards existing homes, which are measured in the field and not from plans, provided no appreciable benefit for new home applications.

A key suggestion for improving HOT2.XP utility within the new home sector of the EnerGuide for Houses Program was to enable HOT2.XP to generate room-by-room heating/cooling load calculations, or to accept inputs from other heating/cooling load calculation software. Heating/cooling load calculations are now required by most Ontario municipalities' building departments prior to issuing permits. Development of a multi-functional tool would better serve the interests of regulatory authorities, mechanical contractors, quality assurance evaluators and the EnerGuide for Houses Program. Issues related to the EnerGuide rating system are now presented within the context of HOT2.XP evaluation.

Airtightness Testing

As previously discussed under the results of the pilot study, changes in airtightness levels within the normal range achieved by Ontario builders in new houses, did not significantly affect the EnerGuide rating. It is important to appreciate that within the existing home market, air sealing and weatherization represent cost effective improvements to the energy efficiency of the home with a correspondingly significant improvement in the EnerGuide rating.

The increased potential for interstital condensation problems leading to degradation of wood-frame house structures is well understood for homes employing high levels of cavity insulation [5]. This aspect of envelope integrity is guarded by stringent airtightness requirements in R-2000 homes. Earlier studies of airtightness levels in Canadian housing, and this pilot study, indicate that new homes are being constructed with higher levels of airtightness [6]. However, the energy implications of airtightness between R-2000 levels, and those evidenced in typical new housing, are not significant. During evaluations of new houses at the design stage, the validity of the HOT2.XP software may be mistakenly questioned by builders who cannot see an appreciable difference in EnerGuide ratings associated with improved airtightness measures. Failure by the rating system to recognize practices, employed for reasons of envelope durability and integrity, conflicts with builder perceptions of the super energy efficient status of R-2000 homes. As a result, confidence in the evaluation software may become eroded among new homebuilders. The relationship of airtightness to envelope integrity, and hence embodied energy, deserves further examination. The energy implications of poorly performing building envelopes are significant when considering repair of defects and possibly retrofit of moisture damaged envelopes. Economic implications to homeowners can easily dwarf the cost of purchased energy. To paraphrase the R-2000 program, perhaps the EnerGuide for Houses rating should be more than operating energy efficiency.

Unrelated to the software, but impacting the EnerGuide program within the new housing market, is the cost effectiveness of mandatory airtightness testing. The testing accounted for between $250 and $300 of the total $450 cost for each house rating assessment, and did not seem to significantly affect the rating when compared with use of the default blower door airtightness of 3.57 ach @ 50 Pa. Again, within the existing home market, airtightness testing is useful in identifying sources of air leakage, as well as confirming the quality of air sealing, but its usefulness within the new home market was questioned.

The requirement to perform an airtightness test caused logistical problems in terms of coordination with builders to ensure that the house was suitably complete to perform a meaningful test. Unlike site visits, which are intended to confirm as-built with submitted plans and specifications, and offer a much wider window of time, airtightness testing requires that the house is substantially complete - shortly thereafter it becomes occupied, hence the window of opportunity is significantly narrower.

QAEs reported that the simplified EnerGuide blower door test procedure was not significantly more economical than the CGSB method, and in general, airtightness testing was seen as a major barrier to widespread uptake of the EnerGuide labeling program within the pilot study participant markets.

Clearly, a qualitative correlation between airtightness and envelope integrity should be provided within the HOT2.XP software to offset views that improved airtightness does not provide homebuyers with added value beyond energy savings alone.

Passive Solar Opportunities

Historically, one of the major advantages of computerized energy evaluation tools has been the ability to predict the utilization of passive solar gains. HOT2.XP provides an accurate and reliable solar utilization model inherited from HOT2000.

An interesting relationship identified in the study involved the absence of passive solar opportunities captured by the sample of houses. Varying the solar orientation of the sample houses did not significantly change their EnerGuide ratings.

Acknowledging that this issue does not directly involve HOT2.XP, it appears from the study that energy efficiency improvements related to passive solar opportunities have not been influenced by this or any other any energy evaluation tool. This suggests that unlike the existing home market sector where solar orientation and fenestration are practically fixed, the EnerGuide Program should seriously consider the active promotion of HOT2.XP as a passive solar optimization tool within the new housing market. This is especially important in view of Canada's commitment to reductions in greenhouse gas emissions.

Issues related to airtightness and passive solar heating afford interesting perspectives on the inherent limitations of energy simulation software and the under-utilization of full software capabilities. As such, HOT2.XP accurately and reliably generates data which is often more sophisticated than the information demands of the new housing market.

DISCUSSION

A recent International Energy Agency publication entitled *Energy Labeling and Standards* [7], has identified the key elements of successful labeling and standards programs as being:

- coherent packages of multiple policy instruments;
- open, transparent and systematic program development procedures -- with extensive stakeholder consultation and thorough engineering and market analysis;
- program elements that reflect product and market realities; and
- solid program credibility -- including conformity assessment and enforcement and program evaluation activities.

The importance of these elements was validated during facilitation of a consumer focus group forming part of the pilot study. EnerGuide for Houses represents an evolving energy labeling program for Canada's low-rise residential buildings, and continues to address each of the key elements listed above. Program credibility is largely founded on the integrity of the HOT2.XP software and accompanying technical guidelines which are intended to reasonably minimize the risk of an inaccurate home energy rating system (HERS).

"Another form of risk is the risk that HERS will suffer serious and long-term credibility problems if consumers, builders, lending institutions, funding agencies or other stakeholders conclude that HERS are significantly less accurate than they were led to believe." [8]

The accuracy and reliability of energy modelling capabilities within HOT2.XP, which is derived from HOT2000, is well validated [9], and generally exceeds the margin of error evidenced in construction practices. However, the technical complexity and sophistication of the measures generated by the software, and the non-energy efficiency implications of the data, require effective communication coupled to extensive consumer and builder education. This current situation is perhaps best illustrated by considering builder interpretations of the EnerGuide rating generated by HOT2.XP.

Some confusion was evidenced as to what the EnerGuide for Houses rating actually measures. Presently, the estimated annual energy consumption associated with the building envelope, energy conversion equipment, appliances and lighting is related to the R-2000 energy target. However, new homebuilders wish to have the energy efficiency of their houses distinguished by the quality of the building envelopes they construct. All of the equipment and appliances they, and/or the homebuyers, supply already bear EnerGuide labels, hence the clarity of the house energy rating has been questioned. It may be more meaningful to relate annual energy demand, accounting for solar and internal gains, to the R-2000 energy demand when deriving the energy rating. Again, HOT2.XP is sufficiently flexible to separate these parameters to readily calculate an energy rating which best reflects market realities and stakeholder interests.

CONCLUSIONS

The following conclusions emerged from the pilot study:

1. Consumers and builders value and respect the credibility associated with NRCan's EnerGuide label. It is viewed as providing a high level of assurance in the marketplace.
2. The present EnerGuide for Houses procedures and guidelines are viewed by builders and quality assurance evaluators as requiring modification, and some streamlining for integration within day-to-day business practices.
3. Consumers are very positive about the EnerGuide label, but somewhat confused about its meaning and interpretation. Builders see potential value in an energy label, but remain concerned that the EnerGuide label may be misunderstood within the marketplace. Both stakeholders believe these issues can be constructively addressed.
4. The sensitivity of the EnerGuide rating scale does not appear to reflect many significant energy efficiency improvements, especially airtightness, and builders have reported that it could serve more as a disincentive if the rating leads to less differentiation in the marketplace.
5. Suggested improvements to HOT2.XP represent less formidable challenges than those associated with the development of ratings that not only reflect market and product realities, but also consistently communicate their meaning to consumers. HOT2.XP software remains well positioned to accommodate the evolution of the EnerGuide for Houses Program development.

ACKNOWLEDGEMENTS

The authors wish to acknowledge the support and cooperation of Natural Resources Canada, and in particular, Messrs. Sylvain Blais and Sylvain Quilliam from the Office of Energy Efficiency. Special thanks to EnerQuality Corporation, its quality assurance professionals and to all of the Ontario homebuilders participating in the pilot study.

REFERENCES

[1] Office of Energy Efficiency (1998), *EnerGuide for Houses Procedures and Guidelines*, Natural Resources Canada, Ottawa, ON.

[2] *R-2000 Design Approval Procedures and Guidelines* (1994), Canadian Home Builders' Association, R-2000 Home Program, Ottawa, ON.

[3] CAN/CGSB-149.10-M86 - Determination of the Airtightness of Building Envelopes by the Fan Depressurization Method, Canadian General Standards Board, Ottawa, ON.

[4] Lio, M. and Kesik, T. (December 1999), *EnerGuide for New Houses Pilot Project: The Assessment and Applicability of EnerGuide for Houses Procedures and Guidelines for the New Housing Market*, EnerQuality Corporation, Toronto, ON.

[5] Waugh, J., Lind, R. and Landry, T. (1994), *Moisture in Atlantic Housing*, Canada Mortgage and Housing Corporation, Ottawa, ON.

[6] Hamlin, T. and Gusdorf, J. (1997), *Airtightness and Energy Efficiency of New Conventional and R-2000 Housing in Canada*, CANMET, Natural Resources Canada, Ottawa, ON.

[7] *Energy Labels and Standards* (August 2000), International Energy Agency (ISBN: 92-64-17691-8).

[8] Stein, J.F. (June 1997), *Accuracy of Home Energy Rating Systems*, Lawrence Berkeley National Laboratory, Berkeley, CA (LBNL Report No. 40394)

[9] UNIES Ltd. (1993), *HOT2000 Program Comparison/Validation with US Blast 3.0 Computer Program*, CANMET, Natural Resources Canada, Ottawa, ON.

WHOLE BUILDING ENERGY SIM. FOR ACCESS TO INCENTIVE FUNDING: LESSONS LEARNED FROM CANADA'S COMMERCIAL BUILDINGS INCENTIVE PROGRAM.

Stephen Pope, François Dubrous
Buildings Group / CETC
Natural Resources Canada
580 Booth Street, 13th Floor
Ottawa ON K1A 0E4 Canada
spope@nrcan.gc.ca fdubrous@nrcan.gc.ca

ABSTRACT

The Commercial Buildings Incentive Program was launched in 1996 by the Canadian federal department of Natural Resources Canada (NRCan). The intent is to curtail greenhouse gas emissions resulting from the use of energy in commercial buildings, and the objective of the program is to lead industry into designing more energy efficient buildings (new or retrofit). Monetary incentives are awarded, based on the amount of energy saved above the Model National Energy Code for Buildings (MNECB) level [NRC, 1997].

To demonstrate compliance with the Commercial Buildings Incentive Program (CBIP) requirements, in particular regarding minimum energy savings and compliance with the MNECB mandatory requirements, applicants most often simulate the energy consumption of the proposed building design. The EE4 software was developed to support this performance approach, and is essentially a custom shell for the DOE-2 engine. In addition to allowing for an accurate evaluation of the energy performance of the proposed design, EE4 automatically generates the MNECB compliant reference building, against which the proposed building is compared and the incremental energy savings calculated.

The Buildings Group of Natural Resources Canada provides the technical support to CBIP. This paper discusses our experience with the use by industry of whole building modelling for the purpose of assessing design energy efficiency. Although the discussion is based on the use of the EE4 software within the CBIP context, emphasis is placed on the generic issues and barriers related to the adoption by the building design and construction community of whole building simulation. Software development, users' issues including training, common design practices and commitment to energy efficient design, and program issues including modelling guidelines and rules, and distinction between modelling for program compliance and energy efficient design, are addressed.

INTRODUCTION

The Commercial Buildings Incentive Program (CBIP) was launched in 1996 by Natural Resources Canada, and continues until 31 March 2004. Its aim is to promote the adoption of the Model National Energy Code for Buildings, encourage increased energy efficiency in commercial buildings, and assist the reduction of greenhouse gas production from the commercial buildings sector.

CBIP provides a monetary incentive to the building owner where the design can be shown to have operating energy performance 25% better than that of the same building constructed to the MNECB minimum requirements. The incentive amount currently is two times the value of energy savings predicted for the first year of operations. The incentive provided was intended to take the risk out of learning new design methods by covering the cost of additional time required for advanced energy efficient design, or to cover the costs of an additional design team member, the building energy simulator. In parallel with the monetary incentive, the program attempts to initiate lasting changes in industry design practices and adoption of energy efficiency.

Potential CBIP participants submit an expression of interest to Natural Resources Canada, which identifies their willingness to follow the terms of the program and makes them eligible for technical assistance with the preparation of CBIP submissions, in particular compliance simulations. Typical CBIP submissions include a simulation of the whole building annual energy performance, which is then reviewed against the building permit documents to confirm the simulation was based on the built version of the project. Once a satisfactory assessment of the performance claim is completed, the incentive amount is calculated based on the energy savings. An agreement is then prepared to provide 80% of the value of the calculated incentive with the final 20% delivered on submission of a copy of the occupancy permit for the completed project.

WHOLE BUILDING SIMULATION FOR INCENTIVE PROGRAMS

The financial incentive programme is based upon a reference building approach, wherein the performance of the proposed design is contrasted against a reference building constructed with representative envelope, lighting, and HVAC systems. A whole-building performance philosophy is used to give designers maximum flexibility. As such, the designer can opt for any solution, within set limits, in terms of HVAC, lighting, and envelope design as long as the overall energy consumption of the building is no more than 75% of the level it would consume had it been built according to the Canadian Model National Energy Code for Buildings (NRC 1997), Figure 1. Conceptually, this reference building approach is very similar to that employed in other energy efficiency standards, codes, and incentive programmes [CEC 1999, ASHRAE 90.1 - 1999].

As an example of the whole-building performance approach, a designer may choose to focus on finding efficiencies in the areas of lighting and HVAC while using conventional envelope construction. Similarly, a conventional HVAC system may be sufficient if high-performance windows and high levels of roof and wall insulation are used in conjunction with reduced lighting power.

The simulation of the proposed building is conducted with standard weather data to estimate the building's annual consumption of electricity, natural gas, oil, and other fuels. A reference building is automatically constructed by the building simulation software, without any input from the user. It has the same size, shape, occupancy, temperature set points, equipment, operating schedules, and orientation as the proposed design. The energy consumption of that reference building is then computed and contrasted against that for the proposed building. It should be noted that the user is specifically prevented from being able to modify or affect the reference building definition process.

Customized simulation software was developed specifically to allow applicants to follow this process within the context of tight design schedules, budgets and limited knowledge of whole building simulation [IBPSA 2001].

COMPLIANCE CHECKING versus DESIGN APPROACH

Figure 1: MNECB / CBIP Compliance Path

Energy simulation for CBIP was intended to standardize the process of compliance without sacrificing design flexibility. HVAC designers are used to building energy simulation software in the context of design tools. Many designers found it difficult to adapt to a compliance checking approach which requires a specific characterization of equipment.

It is commonly understood that the core of the CBIP software is in compliance verification rather than design, and that simulators are therefore required to know the base requirements of the MNECB. For instance, this implies that simulators should have a general idea of the plant size required for the building, or at least as an operative first guess. It has been observed that mechanical designers prefer software that self-size, given the presence of information that would first allow an understanding of exterior loads.

This conflict between the design approach and a compliance checker approach has been debated since the initiation of the MNECB software development work. It was hoped that training for software users would mitigate these issues by providing appropriate methodologies for file creation and review.

Even though these two approaches might seem divergent, both require a fundamental understanding of the building performance along with a high level of input details for successful simulation. It should be noted that the level of effort requires significant time investment from designers.

There are different levels of detail in energy simulation: simulations that are as close to reality as can be made with current tools; and simulations that are intended to show the relative merits of a proposal with respect to a standardized base line building. The first type of simulation is used for accurate predictions of energy bills, which requires an accurate description of yearly weather and operating conditions. The second type is concerned with a more generalized performance characterization. This latter approach was selected for the MNECB to identify changes in applications of code requirements. Accordingly, the software design for the MNECB allows for fair and consistent evaluations of the effects of deviations from MNECB prescriptive requirements.

EE4.CBIP is the software used for verifying compliance to CBIP. It is directly derived from a software developed to demonstrate compliance with the MNECB, which took advantage of the EnergyPro experience. EnergyPro is a DOE-2.1E interface prepared to assist building designers show compliance to the California "Title 24" energy legislation.

SOFTWARE AND INDUSTRY SIMULATION CAPACITY

At the time CBIP started, whole building energy simulation was a small niche in the larger discipline of mechanical design, with consequently few experts available having in-depth knowledge of, and on-going exposure to, whole building simulation. A smooth compliance path for CBIP depended on knowledge of the priorities of the MNECB, a quick integration of whole building energy simulation into design practice, and a rapid expansion of the industry capacity for energy simulation in Canada.

As a result of CBIP, many junior engineers in larger firms have had experience with EE4, but that experience has generally not progressed beyond an introduction to the software and a test of its "user friendliness." In many cases the junior staff were assigned because of the labour intensive character of doing drawing take-offs and data entry, not because of their interest or ability with energy simulation. To date, although a wider group of building designers has been exposed to whole building energy simulation, a small core of practitioners seems to be involved in the majority of the CBIP simulations.

Interestingly, these most experienced simulators tend not use the compliance path outlined above. They are closer to the design approach because they use simulation to optimize the HVAC design. They produce a file that can actually be used in the compliance process however it does not follow the compliance methodology. The most senior simulators are highly proficient in DOE-2, which they use for design optimization. Under CBIP, DOE-2 files are accepted for compliance verification (EE4 uses DOE-2 as its calculation engine).

During the initial phases of CBIP, the need for a simplified compliance-checking tool became quickly apparent. Many developers and designers interested in CBIP desired a preliminary indication of whether the energy performance of their conceptual design was close to meeting the programme target. Using EE4 was an investment difficult to justify at that early design stage, and a quick and easily accessible tool was required. The CBIP Screening Tool was developed as a web-based application to rapidly assess whether a design is likely to comply, and for estimating the energy impact of major design decisions, e.g., type of HVAC system or heating fuel, with limited building information. This software is particularly useful for a quick estimate of the impact of design alternatives at the conceptual design stage when insufficient data are available for performing detailed simulations. The latter feature is popular with designers pitching alternative, i.e., more energy efficient, design concepts to their clients.

The screening tool enables quick exploratory analyses by defaulting a significant number of parameters that affect energy usage. In total, 28 data inputs are required to describe a building. A combination of pick lists, default values, and numerical inputs are used to speed data entry enabling analyses within a two-hour time frame. The screening tool provides results on operational energy consumption and cost and greenhouse gas emissions. Figure 2 illustrates a typical output screen. The screening tool enables a rapid assessment of a building's energy performance with minimal data input. However, this does come at a cost. Only the seven most common building types can be examined and a limited number of HVAC configurations can be considered for each.

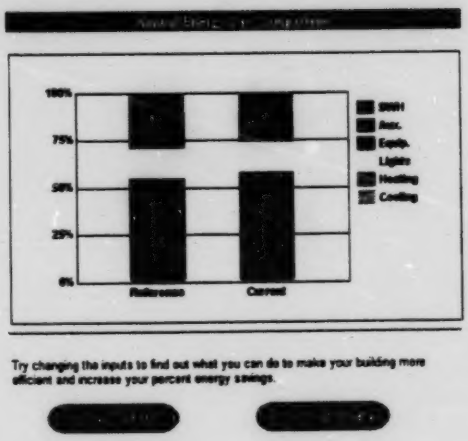
Try changing the inputs to find out what you can do to make your building more efficient and increase your percent energy savings.

Figure 2. A typical Screening Tool output screen

TRAINING IS CRITICAL

The development of compliance-checking software tools was not sufficient in itself to support the incentive programme. A key programme objective was to have the design teams perform their own simulation work. Consequently, as many designers currently use software to size HVAC systems, but not to analyze whole building energy consumption, a substantial effort was placed upon training.

Two courses were developed to train voluntary participants from industry, an introductory course and a specialized modelling course. The introductory course describes the intent and scope of the incentive programme and provides an overview of the technical requirements for compliance. It also includes an overview of the principles of simulating buildings and a demonstration of the EE4 software. This one-day course serves the dual purpose of providing sufficient information to building developers and owners for decision-making purposes while giving designers the introductory information required to start modelling using EE4. This course has proven to be critical in raising awareness of the programme.

The second course is the next logical step in providing CBIP training. It is specifically targeted at the technical staff tasked with performing the EE4 simulations. The objectives of the course are to enhance general building simulation knowledge, to develop modelling skills using EE4, and to encourage standardized procedures that can streamline compliance checking and verification. A combination of lectures, case studies, and hands-on exercises are used throughout the one-day course. Figure 3 illustrates the zoning of an office floor.

Figure 3. A zoning exercise

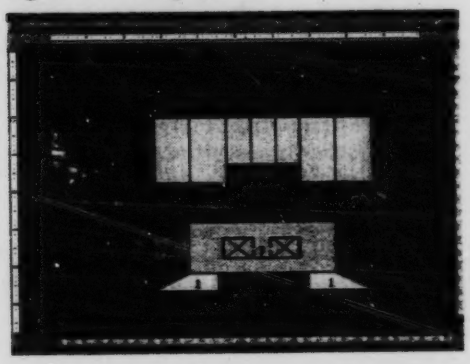

A complementary building modelling guide has also been created. This document acts as a repository for modelling rules and guidelines that are continuously added and developed as new cases are processed. For ease of access of the latest information, the guide is available directly off the web.

A computer based training course (CBT) was developed to complement the training workshops and manuals discussed in the previous section. This CBT serves two purposes: it replaces the workshop for users who are unable to attend a training course due to geographical constraints; and, as it provides in-depth information on specific topics, it acts as a source of reference material for all users. The CBT's total run time is about four hours.

CHANGING DESIGN PRACTICES

The CBIP program is aggressively marketed to generate changes in the marketplace. In addition to a strong presence of CBIP in the building design press, a number of high profile CBIP buildings were opened, and national events covering the subject of building energy efficiency featured design charrettes and awards.

In addition to CBIP being a new programme requiring the use of a new custom software, a number of barriers related to whole building simulation were faced:

- Availability, maintenance and upgrade of the simulation tools and modelling guidelines;
- Availability of energy consultants or mechanical designers familiar with whole building simulation, i.e., industry capacity to perform whole building simulation;

- Recognition of the character of the new tasks and an appreciation that they required an adjustment to working methods;
- Willingness to adopt new working methods, or modify existing methods to accommodate new tasks;
- Lack of perception within the design community at large that whole building energy simulation could be a value added component of design, as opposed to solely a means to recover costs or allow discounted design fees.

Solutions to the technical barriers encompass targeted training, the development of a pool of experts within industry, the use of simplified tools that feed into the sophisticated EE4 software, and a submission framework that allows industry to readily purchase targeted expert simulation assistance when required while minimizing the additional costs to the parties involved.

At the time of publication of this paper, a new strategy was being developed for establishing a technical assistance framework for the purpose of CBIP submission. The strategy reflects the acknowledgement that it is unrealistic to expect most building designers to become sufficiently proficient with EE4 modelling, and become able to readily prepare an EE4 plan take-off acceptable under CBIP. It is proposed that a qualification program be put in place to establish a pool of expert simulators, from which companies preparing submissions could draw expert resources, whether for specific consultations or the entire building take-off. This would assist companies not willing or able to develop internal EE4 expert knowledge to optimize resource usage for the purpose of preparing a CBIP submission. Although fees would be charged for such design assistance, it is precisely the aim of CBIP incentive to cover these additional design costs. From NRCan's perspective, that would ensure a satisfactory and consistent level of quality of the simulation, and would clearly develop industry's simulation capacity. It is hoped that such capacity would then be used beyond the bounds of CBIP.

The CBIP programme benefited indirectly from another federal program, the C-2000 Program for Advanced Commercial Buildings, a demonstration program for high performance building also run through NRCan. A feature of C-2000 is the promotion of an integrated design process where all design disciplines work together in a workshop, or charrette setting, Figure 4. C-2000 design teams take the familiar architectural, structural, mechanical, and electrical disciplines and add an energy simulator, cost consultant, and client and builder representatives to the team. Whole building energy simulations of options discussed around the table are performed on real time, providing checks for the assumptions made throughout the integrated design process. As a result, designs run through the C-2000 process would almost automatically be examined by the design team for submission under CBIP.

Figure 4. An integrated design process session.

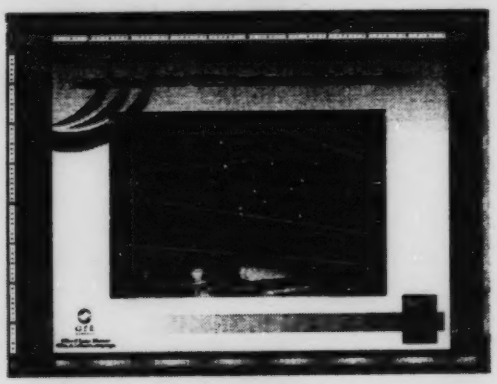

As the CBIP programme matures, there is an increasing interest in emphasizing this type of design process both for its ability to deliver high performance with little added capital cost, and as a quality control strategy that ensures the simulator has an influence on the design. It is clear that such synergy created at these early design stages has enormous potential for influencing the paying clients, and was proven to be one of the most successful way of influencing current design practices.

CONCLUSIONS

Initiating and launching a programme of the technical scope of CBIP was a formidable challenge. The development of the software, technical guidelines and training modules in support of the incentive programme required significant resources in the initial phase of CBIP.

CBIP has completed its early growth phase, and now has the training and tools in place to support an increased use of whole building energy simulation. Both a push from trained consultants and a pull from increasingly interested building owners and developers have contributed towards an accelerated rate of submissions.

One of the main challenges in developing compliance software is to achieve a balance between the needs of novice users and those of experience simulators, while ensuring that the overall technical requirements were respected. In addition to assessing the proposed building performance, EE4 automatically creates the reference building, and generates a compliance report. These steps are critical for code compliance, or for providing financial incentives for energy efficient designs.

Considerable effort has been invested in training and supporting users. The availability of comprehensive on-line help and access to training (either classroom or computer-based) is critical, both in maximizing programme adoption and in minimizing one-on-one support costs.

Training and user support are key elements that should not be overlooked in programme design. In addition to raising awareness of the program and use of its custom software, it is critical to acknowledge that, while a large number of designers may acquire the basis for use of the compliance software, training and qualification of a pool of expert simulators should be performed. These experts will provide support to industry at all stages of the preparation of the CBIP submissions. Simulations performed by professionals would result in faster processing of quality building simulations.

A new element in the CBIP programme, the use of the integrated design process, has shown extraordinary potential. The benefits were made evident by whole building simulation for a number of real projects. The challenge will be to promote the process beyond the small number of firms interested in high performance buildings.

The usual time lines for changes in the building design community are very long. Through CBIP and other programs, whole building energy simulation has demonstrated its value, and requires continued efforts in promotion before it can be said to be part of mainstream design activities.

REFERENCES

NRC (1997), Model National Energy Code for Buildings, National Research Council of Canada, Ottawa.

CEC (1999), Energy Efficiency Standards for Residential and Nonresidential Buildings, P400-98-001, California Energy Commission. Sacramento CA.

ASHRAE (1999), Energy Standards for Buildings Except Low-Rise Residential Buildings, Standard 90.1-1999, American Society of Heating, Refrigeration, and Air-Conditioning Engineers, Atlanta GA.

IBPSA (2001), Using Building Simulation to Support an Energy-Efficient Incentive Programme, paper to be published in Summer 2001 Rio conference, International Building Performance Simulation Association.

THE PRESCRIPTIVE PATH - ITS CONSTRUCTION AND PLACE IN THE COMMERCIAL BUILDING INCENTIVE PROGRAM

Doug Cane Andrew Morrison
Caneta Research Inc.
Mississauga, Ontario
caneta@compuserve.com

ABSTRACT

Hour-by-hour energy simulations using DOE 2.1E were employed to develop the prescriptive path guidelines for Natural Resources Canada's Commercial Building Incentive Program (CBIP). This paper will describe the approach taken to identify and compare current design practice and Model National Energy Code for Buildings (MNECB) requirements, to evaluate potentially cost-effective energy-efficiency measures, to screen measures for life-cycle cost, to bundle and evaluate measure sets (groups of measures), and extend the results to other locations across Canada. Results from each of the development steps are presented. The pros and cons of this approach to small building compliance as opposed to the performance path will be discussed.

INTRODUCTION

On December 15, 1997, Natural Resources Canada (NRCan) announced the implementation of a new program to encourage energy efficient construction in the commercial institutional sector. It was NRCan's stated objective to get more engineers/designers doing energy simulations and offering energy efficient alternatives to developers. Energy simulation was to become a routine part of building design. However, it was recognized that the energy saving and incentive available for smaller buildings may not be large enough in actual dollar terms to offset the additional costs of demonstrating compliance through energy simulation. Thus for buildings under 4,650 m^2 a novel prescriptive path was to be offered. Three months prior to the public announcement, NRCan, following a competitive tender process, awarded contracts to develop Technical Guidelines[1] for the new program. The initial Guideline developments were targetted to the office and hotel sectors. Later, Guidelines for the retail sector were initiated. In Fiscal year 1998 - 1999, Guidelines for the school and MURB (multi-unit residential building) sectors were also undertaken.

Our proposal outlined an approach, where through hundreds of simulations we would identify cost-effective energy measure sets (i.e. groups of measures) from which design teams could select. These measure sets would vary depending on local energy costs and building type and were to yield annual energy savings from the CBIP hurdle rate (25%) to as high as 50% relative to the MNECB[2]. Generally four or five measure sets were developed for each climate zone. Specific areas not impacted on by the individual measures in each set where to be in compliance with the mandatory and prescriptive requirements of the MNECB. This paper will describe the development of the Prescriptive path for multi-unit residential buildings and schools. A similar approach was used for other building sectors.

METHODOLOGY

While the development of the prescriptive path evolved over the two years, it essentially involved the following steps, most involving energy simulation using DOE 2.1E[3] and strict adherence to the MNECB Compliance Supplement[4] and CBIP rules:

- **establish current construction practice** - NRCan wanted to know how stringent current design practice was across Canada and to ensure there were no free riders or at least be aware of free riders. Current practice would also help set specific baseline energy criteria not prescribed by the MNECB.

- **compare current practice to MNECB** - for the building sectors of interest, the performance was compared between current practice and MNECB energy criteria using DOE 2.1E. Model buildings were selected that were representative of large and small buildings in each sector. Comparisons with published whole building energy use data were also made. This was to establish confidence in the DOE 2.1E model predictions used to develop the CBIP Prescriptive path and example results for the Performance Path.

- **pre-screen potentially cost-effective measures** - proposed energy measures were pre-screened against the following criteria - appropriate for building size; type of systems; climate; sensitivity to electricy to gas price ratio (i.e. heat pump systems only where

warranted compared to fossil-fuel/electric cooling systems); whether CBIP credits could apply (e.g. outdoor lighting, elevators, energy management systems (EMS), suite lighting would not receive credit); whether DOE 2.1E could model the energy measure; whether compliance could be easily verified in practice; predicted annual savings and reliability or risk of not achieving the savings.

- **screen individual measures for Life Cycle Cost (LCC)** - DOE 2.1E simulations were undertaken for individual weather-sensitive measures, one at a time in isolation, taking into account fuel/electricity costs. These results were then extrapolated to other climate regions with other fuel/electricity costs. Capital and maintenance costs were developed using Means[5] and other sources for each measure and LCC analysis undertaken. Individual measures were then rank-ordered by discounted payback period for each building type and city, from lowest to highest LCC. The more economical measures were bundled together with others to exceed the CBIP hurdle rate of 25%.

- **perform bundle simulations and evaluate LCC** - this step involved doing DOE 2.1E simulations for both the large and small buildings, in each of the principal cities, in each climate region. Five energy efficiency measure sets or bundles for the small buildings and 3 energy efficiency measure sets, for the large buildings were undertaken. An additional set of DOE 2.1E simulations was undertaken for Yellowknife with different energy efficiency measures considered appropriate for that climate.

- **develop the prescriptive path and extend results to other locations in each climate zone** - this step involved organizing and laying out the simulation results into content for the prescriptive path for the Technical Guide and developing correlations of the DOE 2.1E results for each of the six climate regions to account for fuel/electricity prices and weather differences (i.e. different locations) within each region.

RESULTS

Current Practice Survey - A survey was undertaken of 20 design teams across the five principal regions to get their input on current or typical energy criteria for new buildings based on their knowledge and experience. **Vancouver** - Lighting load was generally higher than the MNECB. Fenestration, opaque walls and roofs had lower U-values in practice than in the MNECB. Outdoor air was higher in current practice than in the model code. In **Regina**, lighting and equipment loads were generally higher than MNECB prescriptions. Assumed occupant density was said to be higher as well. Fenestration, opaque walls and roofs had lower U-value in Regina than the Code prescriptions. Outdoor air was lower in Regina than required by MNECB. **Toronto** current practice energy criteria were often less stringent than the MNECB. Lighting and equipment loads were at Code, whereas fenestration, wall and roof U-values were sometimes higher. Again, as in Regina, outdoor air, in current practice was lower. In **Montreal**, lighting and equipment loads were similar to MNECB provisions, fenestration U-values were higher, wall U-values the same and roof U-values lower. Outdoor air was significantly higher than MNECB. Finally, in **Halifax**, lighting and equipment loads were higher than code, envelopes were more stringent in current practice than Code, but outdoor air was generally higher.

Current Practice and MNECB Energy Use - Current practice energy use in both schools and MURB sectors was found to be lower than MNECB by typically 10%, when energy criteria were applied to the model buildings and modelled in DOE 2.1E. Table 1 presents the whole building energy use resulting from the DOE 2.1E current practice and MNECB model runs.

Adjustments made to the MNECB or baseline models as a result of these comparisons were: lighting and equipment schedules were changed to reflect current practice findings; ventilation was added in garages with make-up air heated to 10 °C and employing CO sensors.

Pre-Screening of Measures - An initial list of measures were drawn-up and screening criteria applied. A large number of energy measures were eliminated for one or more of the reasons stated in Methodology. These were (for MURBs):

- ventilation air pre-heat from solar wall;
- high efficiency ceiling fixtures/lamps in suites;
- reduce hot water distribution piping/circulation losses;
- use compact fluorescents and T-8 fluorescents in fixed fixtures in suites;
- ventilation timer control, to reduce outdoor air at night;
- high efficiency washer/dryers in common area;
- CO_2 sensors controlling suite outdoor air fans to reduce outdoor air during unoccupied periods;
- suite exhaust used for garage ventilation;
- solar water heater for pre-heating SHW;

- low flow showerheads.

Measures eliminated for schools, included:
- high efficiency outdoor lighting;
- waste heat recovery from grey water;
- high efficiency heat recovery chiller;
- low flow showerheads.

Screen Measures for Life-Cycle Cost - This task identified the most economic measures to include in the measure sets for the prescriptive path. None of the more economic measures yielded sufficient savings, by themselves, to exceed the CBIP 25% hurdle. However, when bundled with less economic measures an overall economic bundle resulted that exceeded the CBIP hurdle rate. It was rationalized that a measure was economic if the net present value of savings was positive over the life cycle. This ensured that CBIP yielded societal benefits by creating positive savings over the assumed 20 year measure set life. A discount rate of 10 percent was used in the LCC calculations as required by Treasury Board Guidelines.

Table 2 summarizes the rank-ordering of measures analyzed for small MURBs in Vancouver and Regina. Results for other cities were interpolated, on a degree-day basis, to save on simulation time.

Bundle Simulation and LCC Results - In this task, the measures found to be economic in the previous task were bundled and analyzed using DOE 2.1E. Four measure sets were formulated for each city, with each bundle containing between 3 and 6 individual measures. The resulting whole building energy savings and the discounted payback period for sample bundles are presented in Tables 3 and 4 for small MURBs and primary schools, respectively. Note that the discounted payback period is under 3.5 years for some qualifying measure sets in both sectors.

Extend Results to Other Locations - The DOE 2.1E simulations were restricted to the one representative city in each of 6 regions. There was a need to extend the results from this location to others within the same climate zone. These other locales could have different fuel/electricity costs and heating degree days. Linear best fit equations were developed for each measure between the total building energy savings in each representative city and the heating degree days for each representative city. This resulted in a form of equation as follows:

Adjusted Annual Savings ($\$/m^2$) = $DDF \cdot (A \cdot E_{loc} + B \cdot F_{loc})/100$

Where:
DDF = Degree Day Factor (function of heating degree days (HDD) for design location);
E_{loc} = commercial run-off rate (i.e. last block) for electricity in design location (¢/kWh);
F_{loc} = commercial run-off rate for winter space heating in design location (¢/MJ);
A = correlation factor for electricity (kWh/m^2);
B = correlation factor for fuel (MJ/m^2).

Values for DDF, A and B were provided for each measure set in each climate zone. The prescriptive path participant would only need to have a HDD value for his locale and the run-off electricity and fuel prices.

PRESCRIPTIVE VERSUS PERFORMANCE PATH

Pros - The CBIP prescriptive path is based on energy simulations performed by experienced analysts, featuring generally tried and proven energy measures, and is a relatively easy way to comply with CBIP requirements on small buildings (under 4,650 m^2). The quality control process is simpler as well, both for NRCan and the design teams.

For the uninitiated, the prescriptive path bundles raise awareness of the possibilities for energy efficient design. Today, we use the prescriptive path results to illustrate the paths to CBIP incentive at initial client meetings under the gas utility Design Advisory Program in Ontario.

The prescriptive path bundles provide example starting points (cookbook of ideas) to design teams, even when the performance path is chosen or mandatory (i.e. buildings over 4,650 m^2). In fact, NRCan developed a web-based screening tool from the prescriptive results to help design teams know the potential savings for their proposed measures.

The performance path is subject to errors when simulations are undertaken by the uninitiated. Energy simulation has a steep learning curve. At the outset of CBIP it was speculated that only 1 in 10 buildings used energy simulation. Designers used tools to determine loads and size equipment, but not to model energy use. Many CBIP teams have had to submit and re-submit simulation files seeking approvals. The process is time consuming and may discourage future participation and possibly impact on the long-term goal of encouraging energy efficient design.

Cons - The prescriptive path is felt by some to not encourage innovation. The prescriptive path does not

encourage designers to learn simulation. Others have pointed out that design teams may like certain elements in a measure set, but not others. This is a barrier necessitating the addition of trade-offs that could be selected in lieu of particular measures, a feature that is not there now.

The prescriptive path many not make clear to the developer or design team that a measure set's application to their building will allow, for example, downsizing of the HVAC system components. This downsizing is important as it contributes to keeping incremental costs of the measure down. This was taken into account during the LCC evaluation of the measure sets but needs to be communicated to the user.

The prescriptive path still involves designer time and effort having to comply with the MNECB in areas not impacted on by measures in the selected bundle.

The prescriptive path approach may be counter to NRCan's objective by not engaging the designer enough to permanently change attitudes, methods and the way of thinking about energy efficiency in buildings at the time of design.

CONCLUSIONS

Many have a vested interest in the CBIP Performance Path including NRCan (the investment in the EE4 Software), the CBIP simulators (including the authors) across Canada, and the Gas utilities in Ontario. Simulations were subsidized in the early stages of the Program by NRCan and more recently, the DAP in Ontario provides free simulation support up to $7,800 to teams pursuing CBIP incentives. The prescriptive path also represents a significant investment by NRCan but has not benefited from the same market pull and subsidies that has been the case with the performance path.

The prescriptive path needs software development to shorten the design team time and effort to meet the MNECB requirements beyond the application of the prescriptive measures in the bundles. The same tool could be used in code compliance by design teams in the provinces and territories where the MNECB is eventually mandated.

Is it essential to move the design/development industry into energy simulation on every job? The answer is no. Today, because energy simulations are subsidized this is happening. In small buildings, the emphasis is in rapid design and construction, low initial cost and modest design fees - fees that cannot, in our opinion, support energy simulation. These buildings are ideally suited to the CBIP prescriptive path and there teams should be encouraged to use that path to compliance. If not, when the subsidies end, so could the practice of energy efficient design in small buildings in Canada.

ACKNOWLEDGEMENTS

The authors wish to acknowledge the financial support of the Office of Energy Efficiency for development of the prescriptive path for offices, schools, hotels and MURBs. They also acknowledge the technical support and encouragement provided by the Project Manager, Allen Carpenter, formerly of the Buildings Group, CANMET Energy Technology Centre, Natural Resources Canada.

REFERENCES

[1] Commercial Building Incentive Program for Energy Efficient New Construction. Technical Guide. Natural Resources Canada. 1999.

[2] Model National Energy Code of Canada for Buildings. National Research Council of Canada, 1997.

[3] DOE 2. Version 2.1E. J.J. Hirsch & Associates.

[4] Performance Compliance For Buildings 1996. National Research Council Canada. May, 1997.

[5] Means Mechanical Cost Data, 1998.

Table 1: School and MURB Current Practice and MNECB Energy Use

School	Total Energy Consumption (1,000 ekWh)				
	Vancouver	Regina	Toronto	Montreal	Halifax
Current Elementary School	1,334	1,311	1,313	1,262	1,269
MNECB Elementary School	1,360	1,563	1,440	1,262	1,332
Current Secondary School	4,899	4,903	3,633	4,620	4,455
MNECB Secondary School	4,950	5,366	4,427	4,667	4,579
Current Small MURB	881	1,697	1,291	1,088	1,122
MNECB Small MURB	912	1,769	1,381	1,090	1,164
Current Large MURB	2,578	-	4,261	3,697	-
MNECB Large MURB	2,825	-	4,463	3,673	-

Table 2: Rank-Ordering of Measure LCC - Small MURB

Measure	Whole Building Percentage Savings	Discounted Payback Period (yrs.)
Vancouver		
Install a high efficiency building transformer	0.3 %	3.5
Air-to-air heat recovery (in suites) on fresh air (70% effectiveness)	4.7 %	6.5
Air-to-air heat recovery (whole building) on fresh air (60% effectiveness)	9.6 %	10.5
Two-pipe ground-source heat pump	1.6 %	18.1
Regina		
Common area lighting package	1.0 %	1.4
Daylighting in corridors, stair-wells and garage	0.1 %	1.8
Air-to-air heat recovery (whole building) on fresh air (60% effectiveness)	14.7 %	2.9
Install a high efficiency building transformer	0.3 %	3.0
Parking garage lighting package	0.2 %	10.7
Two-pipe ground-source heat pump system	31 %	18.9

Table 3: Sample Measure Sets - MURBs

City	Measure Set	Whole Building Energy Saving	Discounted Payback Period (yrs.)
Vancouver	- air-to-air heat recovery - low flow showerheads/fixtures - common area lighting package - wall and roof ΔRSI 0.9 above MNECB	25 %	8.7
Regina	- air-to-air heat recovery - low flow showerheads/fixtures - common area lighting package - wall and roof ΔRSI 0.9 above MNECB	29 %	3.5
Toronto	- overall fenestration U-values less than 1.37 W/m^2 - wall and roof insulated to ΔRSI 0.9 above MNECB - air-to-air heat recovery	29 %	11.4
Montreal	- air-to-air heat recovery - low flow showerheads/fixtures - common area lighting package - wall and roof insulated to ΔRSI 0.9 above MNECB - overall fenestration U-values less than 1.37 W/m^2	25 %	2.2
Halifax	- two-pipe ground-source heat pump - air-to-air heat recovery - common area lighting package - low-flow showerheads/fixtures	37 %	16.3

Table 4: Sample Measure Sets - Primary Schools

City	Measure Set	Whole Building Energy Saving	Discounted Payback Period (yrs.)
Vancouver	- air-to-air heat recovery - lighting power density of 11.5 W/m^2 - classroom/offices - low flow showerheads, fixtures and auto-off faucets	25 %	2.7
Regina	- air-to-air heat recovery - overall fenestration U-value less than 1.37 W/m^2	31.5 %	6.0
Toronto	- overall fenestration U-value less than 1.37 W/m^2 - lighting power density of 11.5 W/m^2 - classroom/offices - water-loop heat pump system	33.2 %	immediate
Montreal	- air-to-air heat recovery - overall fenestration U-value less than 1.37 W/m^2	26.5 %	2.6
Halifax	- air-to-air heat recovery - lighting power density of 11.5 W/m^2 - classroom offices - low flow showerheads, fixtures, auto-off faucets	27.7 %	0.1

A RESIDENTIAL END-USE ENERGY CONSUMPTION MODEL FOR CANADA

A.S. Fung, M. Aydinalp, V. I. Ugursal, H. Farahbakhsh
Canadian Residential Energy End-use Data and Analysis Centre
Department of Mechanical Engineering
Dalhousie University
Halifax, Nova Scotia
Alan.Fung@Dal.Ca Ismet.Ugursal@Dal.Ca

ABSTRACT

The residential sector is the third largest end-use energy consumer in Canada. With the increasing pressure on Canada to reduce its energy consumption and the associated carbon dioxide emissions, reducing energy consumption in the residential sector is very important. To quantitatively assess the impact of the large number of measures that can be adopted to reduce the residential energy consumption, a residential energy model for Canada (Canadian Residential Energy End-use Model - CREEM) was developed. This paper presents the model, the characteristics of the residential energy consumption in Canada, and impact of various energy consumption reduction scenarios.

INTRODUCTION

There is an increasing pressure on Canada to reduce its energy consumption and the associated carbon dioxide emissions. One of the effective means of reducing emissions is through reducing energy consumption in the residential sector because this sector is responsible for close to 20% of the end-use energy consumption in Canada. Improving the end-use energy efficiency is one of the most effective ways to reduce energy consumption in the residential sector and the associated pollutant emissions. To identify strategies that would improve the energy efficiency in the residential sector in an economically and environmentally feasible manner, a large number of scenarios need to be considered. Such scenarios include improving envelope characteristics, replacing existing standard efficiency heating equipment, household appliances and lighting with higher efficiency units, and switching to less carbon-intensive fuels for space and domestic hot water heating. Energy efficiency improvements have complex interrelated effects on the end-use energy consumption of houses and the associated pollutant emissions. For example, improving the efficiency of lighting reduces the heat gain from lights, increasing the space heating energy consumption. Owing to such interrelations, detailed computer models are necessary to evaluate the effect of various energy efficiency improvement scenarios on residential end-use energy consumption and associated emissions. Such models would help policy makers and analysts in government agencies, energy suppliers, and utilities to evaluate the impact of a wide range of energy efficiency measures and strategies on the energy consumption and emissions in the residential sector.

An accurate residential energy model is therefore required that can be used to study the characteristics of residential energy end-use, and to evaluate the impact of various energy efficiency measures, such as increasing envelope insulation and integrity, increasing appliance efficiencies, increasing heating/cooling system efficiencies, etc. on residential energy consumption. In this paper a new residential energy model for Canada and the results of several case studies are presented to illustrate the uses of the model. The Canadian Residential Energy End-use Model (CREEM) is the most comprehensive residential energy end-use model in Canada that integrates previous efforts (Ugursal and Fung, 1996) and existing data bases (Statistics Canada, 1993; NRCan, 1994; Scanada 1992). A more detailed description of CREEM and the results of case studies are presented elsewhere (Farahbakhsh et al., 1997, Farahbakhsh, 1997, Fung et al., 2000)

CONTRIBUTING FACTORS TO RESIDENTIAL ENERGY CONSUMPTION

The residential sector in Canada includes five major types of dwellings: single detached, single attached, apartments (less than 5 stories), high-rise apartments (5 stories and more), and mobile homes. Single attached houses include semi-detached houses (double), row or terrace houses, and duplex units. The distribution of these dwelling types in Canada is given in Table 1 (Statistics Canada, 1993).

As it is indicated in Table 1, single detached and single attached houses account for about 68 percent of the

households in Canada, accounting for the largest share of residential energy use. As a result, most of the data collection efforts have been focused on these, with little data available on apartments and mobile homes. Therefore, only single-detached and single-attached dwellings are considered in this study.

Energy consumption in a house is due to four major categories of end-uses: space heating, water heating, appliances and lighting, and space cooling. In cold climates like that of Canada, space heating is the major contributor to the overall household energy consumption, accounting up to 62% of it (NRCan, 1996). Thus, reducing the energy consumed by space heating equipment, through upgrading of the thermal envelope and improving the efficiency of the heating system, is vital in reducing the energy consumption of a house.

Space heating energy consumption is influenced largely by house type since the amount of exposed surface area to the outside environment varies for different house types. Single detached houses have the largest surface area because all six sides are exposed to outside air and the ground. With semi-detached houses, at least one side is common with another dwelling, preventing heat loss through that side. The difference between row and semi detached houses is that the middle units of row houses have two walls common with adjoining units. Thus, space heating energy consumption for a row unit is lower compared to a semi-detached house with the same characteristics (thermal envelope, heating systems, life style, etc.). Duplex houses have either their main floor or ceiling common with another dwelling preventing heat loss from the common surface.

Water heating is another major contributor to the household energy consumption, accounting for up to 22 percent of the total, including the energy required for heating water for clothes washers and dishwashers (Wilson and Morrill, 1993). Energy consumed for water heating is the amount of heat required to bring the city water to about 50°C to 60°C for cleaning and other uses. Reducing the energy required for water heating by increasing insulation around the hot water tank, using more efficient systems, and by reducing the hot water usage reduces the overall residential energy demand.

Energy use by appliances and lighting represents about 20% of the residential end-use energy consumption. As such, improving the energy efficiency of household appliances and lighting present a valuable potential to reduce the overall energy consumption and carbon dioxide emissions of houses in Canada. Space cooling accounts for less than one half of one percent of the total residential energy use in Canada. Thus, it is not of any great significance in the overall residential energy consumption.

CANADIAN RESIDENTIAL ENERGY END-USE MODEL (CREEM)

To study and analyze the characteristics of the residential energy end-use in Canada, and to evaluate the impact of various energy efficiency measures on energy consumption and the associated carbon dioxide emissions, the Canadian Residential Energy End-use Model (CREEM) was developed. CREEM is an Engineering Method (EM) based model[1] of the Canadian residential sector.

To model the energy consumption in the residential sector using the EM, a database of dwellings that is representative of the residential sector is needed. In a representative database, each dwelling represents a certain number of dwellings in the residential sector, i.e.

$$NDRS = \sum_{i=1}^{n} M_i \qquad (1)$$

where,
NDRS = number of dwellings in the residential sector
M_i = multiplier for dwelling i in the database
n = number of dwellings in the database.

Thus, if the annual energy consumption of each dwelling in the database can be estimated, the total annual energy consumption of the residential sector can be calculated from:

$$AERS = \sum_{i=1}^{n} AED_i M_i \qquad (2)$$

where,

[1] Engineering Method refers to the bottom-up modeling of the residential energy consumption. A database of houses with detailed house description files representative of the national housing stock is used along with a building simulation program to estimate the annual energy consumption, and the results are extrapolated to the national housing stock using weighting factors. A detailed discussion of the EM as well as other methods used for residential energy modeling can be found in Aydinalp, et al. (2001)

AERS = annual energy consumption by the residential sector
AED_i = annual energy consumption of dwelling i

The EM involves the estimation of the annual energy consumption of each dwelling in the database using a building energy simulation program, and then extrapolating the energy consumption of the dwellings in the database to the entire residential sector using Eq. (2). Therefore, the available information on each dwelling in the database must be sufficiently detailed to develop an input data file to be used with a building energy simulation program.

CREEM was developed using data from the 1993 Survey of Household Energy Use (SHEU) (Statistics Canada, 1993), the Modified STAR-HOUSING database (STAtistically Representative HOUSING Stock) (Ugursal and Fung, 1996; Scanada, 1992), the 1993/94 "200-House Audit" project database (NRCan, 1994), HOT2000 building energy simulation program default values (NRCan, 1995), and minor contributions from other sources. Brief descriptions of the data sources and the building simulation program are given in Appendix A, and the structure of CREEM is shown in Figure 1.

The data from the Modified STAR-HOUSING database, the 1993/94 "200-House Audit" project database, and HOT2000 default values were used to develop 16 house archetypes to be used in CREEM. The archetypes are based on vintage (pre-1941, 1941-1960, 1961-1977, 1978 and later) and regional location (Western Canada, Prairies, Central Canada, Atlantic Canada). The rationale for this categorization of archetypes is given elsewhere (Farahbakhsh et al., 1997, Farahbakhsh, 1997, Fung et al., 2000). The archetype descriptions were augmented with the information from the SHEU database, and a HOT2000 input file was developed for each one of the 8767 houses in the SHEU database.

Actual energy billing data obtained from fuel suppliers and utility companies for a complete year are available for 2524 of the 8767 houses in the SHEU database. These billing data were used to verify the accuracy of the annual unit energy consumption (UEC) estimates obtained from the simulations of the 2524 house files. To do this, the UEC estimates were compared with the actual billing data, and some systemic errors in the input files were identified from these comparisons. After several cycles of simulation and input file improvement, an acceptable level of agreement was achieved between the actual billing data and the HOT2000 estimates. The refinements identified from the verification process were applied to the rest of the 8767 house files as necessary to improve the accuracy of the simulation results. To ensure the validity of the billing data, houses with auxiliary heating with other fuels (such as wood or propane) were excluded, and the UEC estimates were corrected for the actual weather using degree day ratios between the actual degree days and the typical year degree days for each region. The details of the verification and file improvement process, and its results are given elsewhere (Farahbakhsh et al., 1997, Farahbakhsh, 1997, Fung et al., 2000).

The refined HOT2000 house files were simulated using the HOT2000 simulation program (Batch version 7.14) to estimate the annual UEC of all of the 8767 houses in the SHEU database. HOT2000 simulations were done using weather files for the location of each house. The weather files represent long term (~30 year) averages of weather data obtained by Environment Canada. Thus, the simulation results are estimates of "typical" or "average" energy consumption that can be expected in an "average" year.

The unit energy consumption (UEC) by space heating fuel, by house type, by province, and by vintage were calculated from the simulation results. The refined HOT2000 house files and the results of simulations performed on these files using the HOT2000 simulation program form the Canadian Residential Energy End-use Model (CREEM). Since the SHEU database is representative of the Canadian housing stock, CREEM is also representative of the Canadian housing stock. Hence, the simulation results for UEC were extrapolated to estimate the energy consumption characteristics of the Canadian housing stock. These estimates are in agreement with those from other studies (Ugursal, V.I., Fung, A.S., 1994, Scanada, 1992)

CREEM was then used to assess the reductions in energy consumption and carbon dioxide emissions from the Canadian residential sector as a result of various energy efficiency measures.

As stated above, CREEM is largely based on the data in 1993 SHEU database. A new version of CREEM that will incorporate the data from the 1997 SHEU is currently under development. The 1997 SHEU database was made public by Statistics Canada in the beginning of 2001.

ENERGY CONSUMPTION CHARACTERISTICS OF THE CANADIAN HOUSING STOCK

Results of simulations conducted using CREEM indicate that the average annual heating energy requirement [2] of single detached houses in Canada is 65 GJ/year/house, while the average annual heating energy requirement of single attached houses is 46 GJ/year/house. Thus, the heating energy requirement of single attached houses are about 30 percent less than that of single detached houses. This is in accordance with the explanation given earlier regarding the difference in the exposed envelope surface area.

The average annual UEC (which includes the energy consumption for space heating and cooling, domestic hot water heating, appliances and lights, and heat recovery ventilators and fans) of single detached and single attached houses are found to be 144 and 113 GJ/year/house, respectively. The UEC of single attached houses are about 22 percent less than that of single detached houses due to their lower space heating requirement.

The breakdown of energy consumption by end use in Canadian houses is given in Table 2. Due to the colder climate of Canada, space heating is the major contributor to the overall energy consumption of Canadian houses, accounting for 56 percent of the total energy used.

The overall annual energy consumption of single detached and single attached Canadian housing stock is 1000 PJ/year in 1993. Single detached houses contribute 91% of this total, or 907 PJ/year. The overall annual energy consumption was determined by multiplying the average annual UEC of single attached and single detached houses by the projected number of houses in each house type in the Canadian housing stock.

The average annual space heating energy consumption and the average annual UEC of houses by province and for all of Canada are given in Figure 2. As it can be seen from Figure 2, Saskatchewan, Alberta and Prince Edward Island (PEI) have the highest UEC per house, while British Columbia (BC) has the lowest. The high UEC of houses in Saskatchewan and Alberta are largely due to the cold climate. In the case of PEI, the high UEC is due to the fact that space heating fuel is predominantly oil (77 percent) followed by wood (19 percent). Both of these fuels have lower end-use efficiency than electricity. On the other hand, BC has the warmest climate among all provinces. There are also a large number of electrically heated houses in BC resulting in a lower UEC.

The average annual UEC's of Canadian houses categorized by vintage are given in Table 3. It can be seen that newer houses have lower UEC. This is to be expected since newer houses are better built with higher insulation and lower infiltration rates.

IMPACT OF UPGRADING OF CANADIAN HOUSES ON RESIDENTIAL END-USE ENERGY CONSUMPTION

To demonstrate its capabilities, CREEM was used to study the impact of upgrading of Canadian houses on end-use energy consumption. To accomplish this, each HOT2000 house file in the CREEM database was modified to reflect the upgrade evaluated using a global editor developed for this purpose. Some results for upgrading houses to R-2000 standards (CHBA/NRCan, 1994) are summarized here. Detailed results and discussion of these and other energy saving measures, including upgrading houses to the National Energy Code for Housing (NECH) standards (NRC, 1996), and the impact of these upgrades on carbon dioxide emissions are presented elsewhere (Farahbakhsh, 1997, Ugursal and Fung, 1998, Guler et al., 1999, Guler et al., 2000)

The R-2000 standards provide homeowners and constructors the basis for the design and construction of energy efficient and healthy housing. Various aspects of the house structure are dealt with in the R-2000 standards to address energy efficiency and indoor air quality. Among these are higher envelope insulation, air tightness, orientation, heating, cooling, lighting, and ventilation.

The R-2000 standards specify the requirements for space and water heating in the form of an energy target. This target comprises of two components, i.e. space heating and DHW, each of which depends on certain

[2] "Space heating energy requirement" is the amount of energy required to maintain the temperature of a house at the required level. It does not include the efficiency of the space heating units. "Space heating energy consumption" is the total energy (fuel) consumed by the space heating equipment, taking into account the efficiency of the heating units.

characteristics of the house. The R-2000 energy target for space heating takes into account the climate condition, heated area of the house, and the type of space heating fuel, while the target value for water heating accounts for local water mains temperature, hot water temperature, and efficiency of water heating equipment.

As it was mentioned earlier, houses in CREEM are divided into four vintage categories: pre 1941, 1941-66, 1967-78, 1978 or later. It is unlikely that upgrading older houses to improve energy efficiency would be feasible due to their shorter remaining useful life. Furthermore, the amount of energy savings will not likely justify the cost of upgrading. Thus, only upgrading of houses built in 1967-78 and 1978 or later is considered here. Since it is unrealistic to assume that all houses would be upgraded, scenarios were evaluated which assumed that upgrading would be done by implementing the R-2000 standards to 10, 20, 30, 50, and 90 percent of the houses built in 1961 or later. Differences in energy consumption and pollutant generation levels were determined between the base case and upgrading scenarios in terms of the decrease in UEC and carbon dioxide emissions. These values were then projected to all houses in Canada using the number of houses in each province.

The reductions in the average UEC of single attached and single detached houses in Canada as a result of upgrading 10-90 percent of the housing stock to R-2000 standards are given in Figure 3. The resulting overall reduction in the energy consumption of houses in Canada is shown in Table 4 for each house type. It can be seen that the energy savings associated with the upgrading of single-detached houses are higher than the energy savings for single-attached units. This is because single-detached houses have larger heat losses through the building envelope as compared to single-attached units. Consequently, improving the house envelopes as part of R-2000 upgrade results in bigger savings.

The reductions in the average UEC of houses in each province and for all of Canada as a result of upgrading 10-90 percent of houses to R-2000 standards are given in Figure 4. As it can be seen from this figure, the impact of R-2000 upgrades is the highest in Newfoundland and the lowest in Ontario. This is partly due to the difference between the existing building practices in these two provinces. The other reason is that over 21 percent of houses in Newfoundland use wood for space heating, which results in the highest energy savings when upgraded to the R-2000 standards. The total energy savings resulting from the R-2000 upgrades for each province is shown in Figure 5. These values have been calculated by multiplying the energy savings per house by the total number of houses in each province in 1993.

As Figure 5 shows, Alberta has the highest potential for energy savings, followed by Ontario, Quebec, and British Colombia. On the other hand, the energy saving associated with the R-2000 upgrades is the lowest in PEI. This low energy saving reflect the low population and number of houses in this province, otherwise PEI has the second highest energy saving on a per house basis.

CONCLUSIONS

A residential energy model for Canada was developed using all available data on the Canadian residential sector. The Canadian Residential Energy End-use Model (CREEM) is representative of the Canadian housing stock.

Using CREEM, the characteristics of the Canadian housing stock was studied, and some results are presented in this paper. Also, the impact of two upgrading options on the residential energy consumption in Canada was assessed using the model. The upgrading options were applied to a fraction of newer houses in Canada, and it was found that significant energy savings can be achieved as a result of upgrading.

ACKNOWLEDGEMENTS

The authors gratefully acknowledge the financial support from Natural Resources Canada. H. Farahbakhsh is thankful to ASHRAE for a Graduate Grant-In-Aid.

REFERENCES

Aydinalp,M., V.I. Ugursal & A.S. Fung, "Modeling of Residential Energy Consumption at the National Level", IEMS and ICC&IE 2001 Joint Meeting, Florida, March 5-7, 2001.

CHBA/NRCan, 1994. R-2000 Home Program Technical Requirement, Canadian Home Builders Association (CHBA) and Natural Resources Canada (NRCan), Ottawa.

Farahbakhsh, H., Fung, A, and Ugursal, V.I., 1997. Space Heating Thermal Requirements and Unit Energy

Consumption of Canadian Homes in 1993. CREEDAC Report, May.

Farahbakhsh, H., 1997. Residential Energy and Carbon Dioxide Emissions Model for Canada, MASc Thesis, Dalhousie University, Halifax.

Fung, A., Guler, B., Aydinalp, M., and Ugursal, V.I., 2000. Development of Canadian Residential Energy End-use and Emission Model (CREEEM), CREEDAC Report No. 2000-8-3, September.

Guler, B., Fung. A., Aydinalp, M., and Ugursal, V.I., 1999. The Technoeconomic Analysis of Home Retrofit Activities and Associated Energy Savings in the Residential Sector of Canada, CREEDAC Report No. 1999-12-6, December.

Guler, B., Fung. A., Aydinalp, M., and Ugursal, V.I., 2000. The Technoeconomic Evaluation of the Impact of Potential Retrofit Activities on GHG Emissions, CREEDAC Report No. 2000-4-2, April.

NRC, 1996. The National Energy Code for Housing, Draft 6.1, Canadian Commission on Building and Fire Codes, National Research Council, Ottawa.

NRCan, 1994. 200-House Audit Project, Natural Resources Canada, Ottawa.

NRCan, 1995. HOT2000 V.7.10 User's Manual for DOS and MacIntosh Computers, CANMET/EAETB, Ottawa.

NRCan, 1996. Energy Efficiency Trends in Canada, Natural Resources Canada, Ottawa.

Scanada, 1992. Statistically Representative Housing Stock, Final Report, Submitted to Canada Mortgage and Housing Corporation, Ottawa.

Statistics Canada, 1993. The Survey of Household Energy Use, Microdata User's Guide, Ottawa, February.

Statistics Canada, 1995. *Energy Statistics Handbook*, Catalogue 57-601, Ottawa.

Ugursal, V.I., Fung, A.S., 1994. Energy Efficiency Technology Impacts - Appliances, Final Report, Volumes 1 and 2, Submitted to Canada Mortgage and Housing Corporation, Ottawa.

Ugursal, V.I., Fung, A.S., 1996. "Impact of Appliance Efficiency and Fuel Substitution on Residential End-use Energy Consumption in Canada", Energy and Buildings, V. 24/2, pp. 137-146.

Ugursal, V.I., Fung, A.S., 1998. "Residential Carbon Dioxide Emissions in Canada: Impact of Efficiency Improvements and Fuel Substitution", Global Env. Change, 8/3, 263-273, Oct. 1998.

Wilson, A. and Morrill, J., 1993. Consumer Guide to Home Energy Savings, Third Edition, American Council for an Energy Efficient Economy, Washington, D.C. and Berkeley, Ca.

APPENDIX A

A.1 Survey of Household Energy Use (SHEU)

The 1993 Survey of Household Energy Use (SHEU) was conducted by Statistics Canada on behalf of Natural Resources Canada, in cooperation with the provinces of Nova Scotia, New Brunswick, Ontario, Manitoba, Saskatchewan, and with SaskPower. SHEU was commissioned to enrich the residential sector data in Canada. The target population for this survey was composed of all the housing units in Canada (excluding Yukon and North Western Territories) occupied as primary residences, both owned and rented. It is based on a mail out survey that included 376 questions. The database includes detailed information on 8767 houses from all provinces of Canada.

A.2 Modified STAR-Housing Database

STAtistically Representative HOUSING Stock (STAR-HOUSING database) was first developed by Scanada Consultants Limited on behalf of Canada Mortgage and Housing Corporation (CMHC) in 1992. As its name implies, STAR-HOUSING database is a statistically representative database of housing characteristics and energy consumption data of the existing Canadian housing stock. The original STAR-HOUSING database was later improved and expanded by Thermal Engineering on behalf of CMHC in 1994. This revised version of STAR is called Modified STAR-HOUSING database.

A.3 200-House Audit Project Database

There are total of 197 house files in various versions of Audit2000 file formats. These house files contain detailed house envelope characteristic and energy usage pattern based on house energy audit conducted by NRCan in different province across Canada.

A.4 HOT2000 Building Energy Simulation program

HOT2000 was developed under the direction of the R-2000 Home Program of Natural Resources Canada. It is specifically written to simulate houses rather than large buildings. Its calculations are based on monthly average hourly weather data.

Table 1: Distribution of dwelling types in Canada

House Type	Number	Share (%)
Single Detached	5823176	56
Mobile Home	246970	2
Row or Terrace	489576	5
Apartment, Flat	2073859	20
High-Rise Apartment	936434	9
Semi-Detached	460305	4
Duplex	328896	3
[illegible]	[illegible]	[illegible]

Table 2: Distribution of residential energy consumption by end use

End-uses	Space Heating	DHW Heating	Appliances Light	HRV Fans	Space Cooling
UEC (GJ/Year)	76.7	26.8	34.6	1.5	1.2
(%)	54.5	19.0	24.6	1.1	0.8

Table 3: Average annual UEC by vintage category

Vintage	Before 1941	1941-1960	1961-1977	1978 or Later
UEC (GJ/Year)	157.4	139.7	139.5	133.5

Table 4: Total annual energy savings with upgrading houses built in 1961 or later to R-2000 standards

Total Energy Saving Associated with the R-2000 Upgrade (PJ/Year)		
Penetration Level	Single-Detached	Single-Attached
10%	14.0	0.6
20%	26.9	1.5
30%	41.3	2.1
50%	67.3	3.3
90%	125.2	7.3
Basecase UEC	Single-Detached	Single-Attached
(PJ/Year)	906.7	92.8

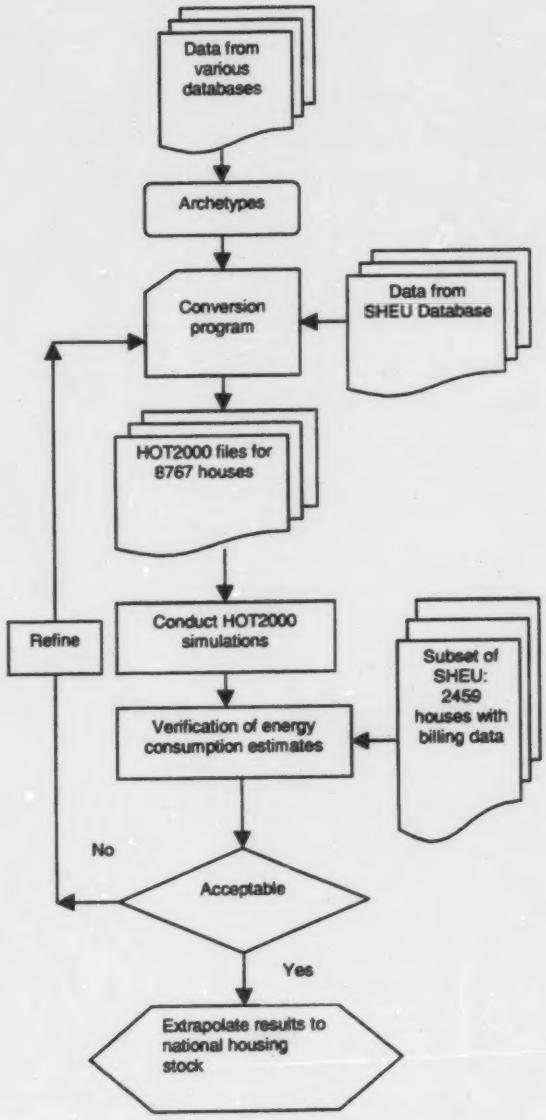

Figure 1: Structure of the CREEM Model

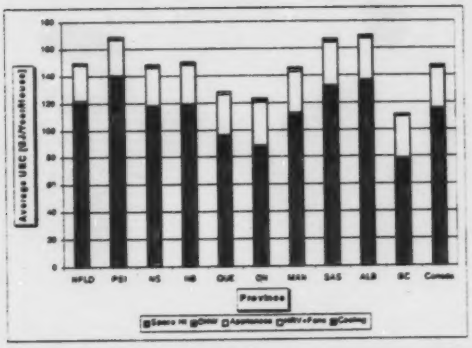

Figure 2: Average annual end-use energy consumption per house by province

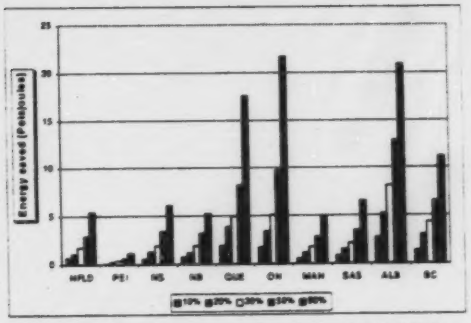

Figure 5: Total energy saving due to the R-2000 upgrades of 1961 or newer houses by province for different market penetration levels

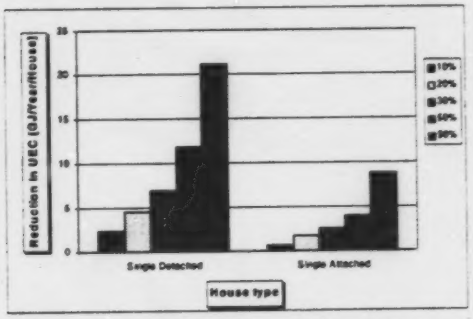

Figure 3: Effect of the R-2000 upgrades on the average UEC of Canadian houses by dwelling type

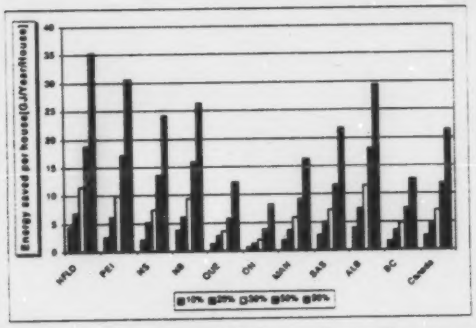

Figure 4: Effect of the R-2000 upgrades on the average UEC of houses by province for different market penetration levels

REAL-WORLD INTEGRATED DESIGN PRACTICE AND TOOLS: EFFECTIVE ENERGY PERFORMANCE ANALYSIS APPROACHES

Graham Henderson, P.Eng.
BC Hydro
Burnaby, British Columbia
graham.henderson@bchydro.bc.ca

Curt Hepting, P.Eng. and Diane Ehret
EnerSys Analytics Inc.
Coquitlam, British Columbia
enersys@telus.net

ABSTRACT

To help design teams investigate energy-efficiency opportunities in the early design stages, BC Hydro conducts "Energy Performance Workshops." The workshops act as a key component of an integrated design process by providing energy simulations, integrated design workshop facilitation, and Commercial Building Incentive Program verification. The resulting building designs are both cost effective and energy efficient.

This paper discusses the EPW concept within the framework of the integrated design process. It discusses both qualitative and quantitative lessons by providing insights on the successful components of the EPW format, as well as an overview of which energy efficiency measures we consistently have found to be most cost effective. Finally, we present program results to date.

INTRODUCTION

What answer might a building owner expect from their design team if the owner asked the question "Did you design me an energy efficient building?" The answer, of course, would be a resounding "Yes!" It would be somewhat akin to the building owner asking the design team if the building would continue to stand after being constructed. No design team would provide a negative response to such a "motherhood and apple pie" sort of question. The difference in the acuity of these two responses is that the building is entirely likely to stand after being constructed, and there would be ample visual evidence to the contrary if it did not. The same, unfortunately, cannot be said for energy efficiency.

A prudent building owner who actually was concerned with ongoing operating costs, and who had just received the obligatory answer to the aforementioned energy efficiency question, would be well advised to ask the design team on what basis they staked their answer. The owner would be further well advised to reject out of hand such answers that suggest the building must be energy efficient, because either 1) we designed this building exactly like we designed the last building, and it was energy efficient, or 2) because we used a vast array of energy-efficient technologies.

The building owner should reject the first response because there is a notorious discontinuity between estimates of a building's energy performance during design, and the actual building's energy performance. As well, follow up regarding a building's energy performance simply does not happen (in our juris diction and experience). Not only does it not happen regularly, it does not happen at all. Thus, there is no basis for determining that an "energy efficient" building had been built.

The building owner should reject the second response because, as will be discussed in this paper, there is a significant amount of misinformation currently existing in the market place regarding which technologies are required to make a truly energy efficient building. The net effect of this unfortunate situation is that any designer is able to say they have designed an energy-efficient building because the chances they will be proven otherwise are negligible. The chances that they will be held accountable are non-existent. What, then, is a conscientious building owner to do?

It was partly in response to this situation that BC Hydro developed its Design Assistance program, whose primary objective is to assist commercial building owners address the issue of cost-effective design from an energy performance perspective. The Design Assistance program has three primary components:

1) building energy modelling and analysis,
2) facilitating an integrated design session, and
3) completing the application and providing verification for the Commercial Building Incentive Program (CBIP).

The program contains technical and process-oriented aspects. The technical aspect has to do with the

provision of quality computer simulation, provided at relatively low cost, early on in the design cycle. The process-oriented aspect has to do with providing the results of the computer simulation in a context that enhances and complements the team's integrated design efforts.

ENERGY PERFORMANCE WORKSHOP

The integrated design session, called the Energy Performance Workshop, is the key deliverable in the program. The workshop typically begins in the morning, and carries on until the early afternoon. In the workshop, we use three terms to discuss the building energy models. The "Reference" building is the CBIP-compliant building that just meets the Model National Energy Code. The "Proposed" building is the design team's current building design. The "Baseline" building is the Proposed building at the beginning of the workshop, without any of the energy efficiency measures proposed by the design team that would typically exceed standard practice (those items are modelled, but are left out of the baseline analysis, and are "tested" later according to a life-cycle costing analysis). It is from the Baseline building that all energy efficiency measures are tested. The design team is presented with the following energy end-use breakout graph of their project at the beginning of the workshop (Figure 1).

Figure 1. Sample Pre-Workshop Results

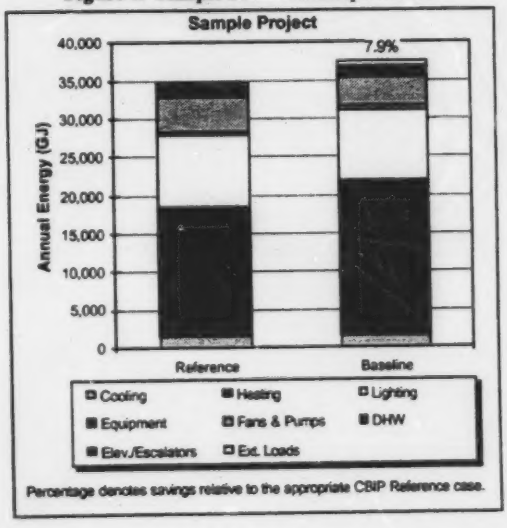

The workshop itself has three ingredients which contribute to its success. The first ingredient is the presence of all interested parties in the design process. At a minimum, this must include the architect, mechanical and electrical consultants, and someone who can address the issue of capital costs (this may be either the consultants, contractors, or quantity surveyors). Additional attendees may include the owner or owner's representatives, and/or personnel from the maintenance department.

The second ingredient is the simulation software. Our process uses an in-house tool called the Building Energy Simulation Tool (BEST), which is an in-house, specialized front-end to the DOE2.1e energy performance simulation program. BEST minimizes set up time for energy simulation, presents results in an easy-to-understand format, and applies a calculational approach which taps into the results from hundreds of detailed hourly simulations. More specifically, the tool makes use of response factors produced from performing dozens of simulations on a specific building project. Each simulation represents a discrete change to a building characteristic (roof insulation, for instance). By also applying the engineering principles of how the discrete change affects energy use, the tool can calculate the end-use impacts from changing a building characteristic by nearly any amount. The approach is similar to that used by Natural Resources Canada's CBIP web screening tool (Hepting et al., 2000), and the results agree very closely with the full DOE2 simulations (Hepting 1996; Hepting and Ehret, 1998).

Using this approach, measures which have a continuum of possible values (e.g. insulation, efficiency, power density, glazing characteristics, overhangs), and are determined to be important to energy use or have been identified by the design team to have special significance are "connected" in the BEST software. We can then manipulate the characteristics as required by the design team at the time of the workshop to quantify the impact of any change on annual energy cost. On the other hand, issues that have discrete values or outcomes (e.g. schedules, mechanical systems, building form, zoning) must be coordinated in advance of the workshop, and cannot be handled ad hoc.

The advantage of using BEST is that it provides for quick feedback, which is important in a workshop setting. Moreover, it presents the results by providing instantaneous comparisons to baseline and reference cases. It also provides for peak load reduction estimates, which may affect HVAC sizing and costing. Coupled with its ability to perform life-cycle costing, the design team is able to make informed decisions that often lead to design changes *during the course of the workshop*.

The third ingredient leading to success is the fact that an energy target is set and referenced constantly throughout the workshop. During the early stages of the program (before CBIP), an appropriate ASHRAE 90.1-1989 "energy cost budget reference" provided an energy target. Now, the CBIP Reference building provides the basis for the target. The CBIP program requires that the Proposed building be shown to use 25% less energy than the Reference building in order to attain an incentive. During the workshop, the team is able to continually view their progress against the required energy target as various measures are introduced.

The typical agenda for a workshop includes an overview of the BC Hydro Design Assistance program, followed by a relatively high level review of the assumptions used in modelling the Proposed building. If changes are required based on feedback from the design team, the changes can often be incorporated on the spot. Other issues requiring discussion are economic factors, such as the discount rate or the escalation rate of utility costs, used in the life-cycle costing analysis.

After this introduction, the rest of the session is spent reviewing how cost and energy results change by altering various design parameters. For example, the architect may be interested in exploring alternative window types. This may include changes to either the U-value or the shading coefficient. Once the alternative window values are entered into the BEST program, the change in operating cost is calculated in a matter of seconds. The design team provides the marginal capital cost of the measure, as well as the impact on maintenance costs, and the payback of the measure is calculated. At the same time, the design team is able to see the sensitivity of operating costs to changes in window properties, the progress toward the energy target, and the impact of altering the building shell on the required capacity of the mechanical systems. The following figures show samples of the energy analysis charts presented during the workshops that summarize these results.

Figure 2. Sample Economic Analysis Workshop Results

Economic Analysis	
Incremental Costs ($)	
Equip. & Labor	$47,000
Annual O&M	$0 /year
Cooling System**	$500 /ton
Heating System**	$4 /kBtuh
Fans & Pumps**	$0 /hp
Net Savings/Year	*$13,035*
Net Capital Cost	*$40,979*
Payback @ 7.0%	***3.5 years***
LCC: $24.37 million, (-$115,546)	

Figure 3. Sample Peak Load Workshop Results

Maximum HVAC Contribution During Peak*			
HVAC END-USE	Demand Base	Demand ECM	Peak Load Reduction
Fossil Heat (kBtuh out)	10,222	9,728	493.3 (4.8%)
Steam Heat (kBtuh out)	0	0	0.0 (0.0%)
Electric Heat (kBtuh out)	0	0	0.0 (0.0%)
Cooling (tons output)	402.2	394.1	8.1 (2.0%)
Fans & Pumps (hp)	368	360	8.4 (2.3%)
*Coincident with building; thus, values do not necessarily reflect absolute maximums.			
Reference Savings - GJ:	7,609 (16.2%)		Incent: $0

It is important to note that life-cycle economic efficiency, not energy efficiency, is typically the focus of the program. However, this can vary from project to project, depending on the owner's interests and objectives. *The primary component that Design Assistance brings to the workshop is the ability to show the impact of various measures on annual operating costs.* Energy efficiency is allowed to seek its appropriate level within the context of the project's life-cycle costs.

At the end of the session, all measures deemed acceptable are "rolled up" into a single package. This is necessary to determine the overall progress towards the energy target, and is also necessary because some measures will affect the savings from other measures (e.g., the savings from improved windows will be diminished when paired with a more efficient boiler).

RESULTS

After applying this integrated design approach to many buildings, we have been able evaluate our results both qualitatively and quantitatively. We base the qualitative assessments on the process: What components lead to an interactive, "successful" project? The quantitative results summarize general trends we have found from performing energy

simulations: Which technologies lead to cost effective, energy-efficient buildings? Which measures don't make sense economically?

Process Lessons Learned

Each workshop and design team has its own ambiance and team dynamics. In our experience, however, the most positive and successful workshops occur when the participants park their egos at the door, and open their minds to unexpected outcomes.

We have had the opportunity to attend several conferences where the theme of integrated building design is presented as a kind of Holy Grail: an item worthy of searching and striving for, but is ultimately complicated, convoluted, and costly. On the contrary, our experience has shown that integrated design does not require excessive use of the design team's time, yet does allow the full quantification of the interactions among the building shell, mechanical, and electrical systems.

The earlier the process begins, the better the outcome. The most successful projects begin once the building's basic form has been decided, but prior to any detailed mechanical design, or even mechanical system selection. Beginning a project at this stage not only allows for energy-efficient measures to be integrated most cost effectively, but it also leads to team interaction throughout the entire design.

In summary, the Design Assistance integrated design process involves the following steps:

- The design team provides information about the building, typically in the form of floor plans, sections, and elevations from the architect, and design development documents from the mechanical and electrical consultants.
- An energy analyst then constructs building energy models of the Proposed and Reference buildings, contacting the design team for clarification as necessary. Coordination with the mechanical consultants at this stage is a priority. The mechanical consultants dictate which mechanical systems are modelled, and they must have buy-in to the simulation results. For instance, it would not make sense to model a mechanical system the mechanical consultant was neither willing nor able to design. The modeller must also discuss CBIP-compliance issues that may run contrary to various mechanical engineering "rules of thumb," such as the delivery rate of supply air.
- Approximately 3 weeks after collecting the information from the design team, the Energy Performance Workshop is held. The workshop report is typically made available within 2 weeks of the completion of the workshop. There is no need for the design team to wait for the workshop report to proceed with their design if the project is time constrained, as the report is only a summary of the workshop findings, and typically contains no new information.
- If further analysis is required after the workshop, additional modelling can be completed. It has been suggested that an iterative workshop approach would be more effective, but that has yet to be determined. To date, providing as-needed modelling feedback has been satisfactory.
- After the completion of tender drawings, the models are finalized and the results are sent to CBIP for processing.

It should be noted that the above process is different than the standard end-of-process CBIP evaluation via the EE4 Comply compliance software. In this regard, Design Assistance has special dispensation from CBIP (based on our historical involvement in the CBIP program and advanced level of modelling expertise). That is, we develop the required models using "raw" DOE2 files and make the incentive application without completing an EE4 Comply file. We use EE4 Comply to assist with inputting the physical description of the building, but not to test compliance. With our approach, the design team receives substantial feedback prior to starting working drawings. Thus, they are able to make design changes as necessary to ensure the building meets CBIP energy targets. This is not the case if the team waits until the creation of tender documents to confirm compliance, which is typically the time the EE4 Comply file would be created.

There seems to be a balance between inviting as many players as possible to the integrated design workshop and maintaining a flow to the session. While we recognize that the process can be more "informed" with more participants, we have also experienced sessions that drag on interminably while non-technical people struggle with basic design concepts, and non-prime players (e.g., structural consultants) are forced to spend hours listening to issues which have no bearing on their design. In essence, we like to invite a good cross section of involved people, while keeping the meeting small and focused.

One of the key issues to a successful workshop is the energy target provided by the CBIP Reference building model. This aspect adds a singularly compelling dynamic to the workshop by boiling all the analysis down to a single indicator of success or failure. A workshop populated with highly motivated professionals all focusing on the same result is capable of producing excellent and sometimes surprising results. Upon careful reflection, it should come as no surprise that this is the case. Standard practice for most of the buildings we have modelled has been in the range of 10%–15% better than the CBIP Reference building. However, given the benefit of a target, and a means of measuring the results of their various design decisions against the target, very few teams have failed to comfortably exceed the required 25% target.

Having said all that, the success of achieving energy performance targets increases with the active participation of the entire design team since the forum allows everyone to beneficially contribute to the process (as further supported by Case and Wingerden, 1998; Montross and Fraser, 1998; Hayter et al., 1998). In particular, the interest and motivation of the mechanical consultant and the building owner are primary indicators for a successful project

Technical Lessons Learned

Although we now have three years and a couple of dozen projects under our collective belt, we never know the outcome of a project until we completely finish the analysis. In other words, every building is different with its own set of unique dynamics on energy performance. Having said that, there are several broadly applicable technical lessons we have learned:

- The two most important issues that affect a building's energy use have to do with ventilation air. First, we have repeatedly found that the amount of air should be controlled carefully by scheduling the volume appropriately for the number of building occupants and/or by using other forms of demand ventilation (e.g., CO_2 sensors). Second, heat should be recovered from exhaust air with the most effective means possible that meets the client's cost-effective criteria. This issue typically has the greatest impact on energy use (with the possible exception of office buildings, depending on the HVAC system type).
- We rarely have found daylighting and lighting occupancy controls to be cost-effective. These measures are only cost-effective when a single point can control a large number of luminaires, or when the sensors can be used in conjunction with a demand ventilation strategy. The most cost-effective lighting control is multiple switching coupled with occupant education.
- Building massing options and orientation are *not* major energy items in most commercial buildings. While important issues may arise in regard to massing and orientation, it is rarely worthwhile investing in the time to quantify the associated energy impact. We have routinely rotated buildings to determine the impact of orientation, and found resulting changes in annual operating cost vary by only 2% at most. This is not to suggest that anything goes for the building shell, but rather that detailed energy simulation is not necessarily the most cost-effective means of assessing the effects. We would suggest not explicitly quantifying the relative impacts, but instead, have good practice for optimizing solar exposure combined with the owner's program and site issues be the driving forces in addressing massing issues.
- Mechanical system selection is a critical decision that will make or break any chance of success for a project. Preferred mechanical systems include heat pumps (water loop and ground source), fan coils, VAV, and unit ventilators (which currently have a reputation for being a cheap system, but show good potential for both demand ventilation and even heat recovery). Ground-source heat pumps save a significant amount of energy, but have not yet been shown to be cost-effective in the B.C. market, except in projects where the loop installation costs can be ameliorated.
- Condensing boilers were rarely cost-effective, even without considering additional maintenance issues. However, with the dramatic gas price increases recently, this has been changing in some cases. Typically, the most cost-effective boiler option is a medium efficient (85%), fully modulating boiler.
- The issue of reheat can be a significant factor, based on the type of mechanical system and zoning. (Reheat occurs when air from a central system is cooled to meet the cooling requirements of the warmest zones on the system, but then requires terminal heating for other zones which otherwise would become too cold.) However, in other cases, the issue is overstated. This all depends on how the HVAC systems and associated zones are defined.

- Glazing results are very building dependent. No strong trend has emerged, although we have not found a project where the most energy efficient of glazing systems (e.g., triple low-e glazing) is cost-effective.
- Roofs are often over insulated from a life cycle costing perspective. R20 seems to be in the ballpark for a cost-effective value, with the recent increases in gas prices included. Likewise, cost-effective wall insulation values are in the range of R12. We have often shown that values in excess of these are not cost-effective. The design team may prefer to see the capital re-allocated to more important mechanical items, depending on the budget constraints.

It is important to note that the trends we have observed are based on studies of building designs primarily in the southwestern B.C. area, where temperatures are relatively mild and electricity prices are among the lowest in North America. However, we have also found similar trends in other jurisdictions. The life-cycle cost-effectiveness of more aggressive energy-efficient measures may increase in colder climates and/or when higher utility costs are applied. Therefore, it is important to examine measures on a building-by-building basis.

One important issue that bears commenting on is the noticeable difference in technologies implemented in buildings that have been heavily marketed as "green," and the results of our own Energy Performance Workshops. We are having a hard time resolving the difference between our results, which have been repeatedly verified with computer simulations, and various projects that are being advertised as green and energy efficient which incorporate technologies that we believe are neither cost-effective nor save significant amounts of energy. The following technologies are those that seem to have the widest positive "green" press coverage, but provide the least cost-effective energy savings:

- Natural ventilation: We have repeatedly shown that if the opportunity cost of providing for natural ventilation means that heat recovery can't be used, this technology is a losing proposition from the energy perspective. Fan energy is a very small piece of the energy pie compared to the amount of energy required to heat outdoor air. Also, there often is a significant cross effect issue with space heating. Any fan energy (which eventually ends up as heat in the airstream) that is avoided would need to be replaced by the conventional heating source during the heating season. The image of a building that saves large amounts of energy by simply drawing in its own air as required without mechanical effort belies all analysis we've done to date. This is not to say that natural ventilation is not a good opportunity, but that it needs to be fairly assessed on its own merits and in relationship to other measures.
- Daylighting: While we are fully supportive of any effort to introduce natural light into the building from a psychological and human productivity standpoint, it has little bearing on overall energy use. Thus, it rarely is cost effective to install the associated controls required to harvest it. This becomes even more exacerbated in cases where cooling is negligible (e.g., most schools in B.C.) due to the reduction of heat gains from lights.
- Super Insulation: This may work in the residential sector, but analysis has repeatedly shown that over insulating a building is not cost-effective.

Program Results to Date

The Design Assistance program originated in mid-1998. Not including the initial pilot projects, we have conducted analysis on 27 buildings, totaling approximately 350,000 m^2. There have been private and public sector projects, including offices, schools, lab buildings, airport facilities, long term care facilities, a maintenance facility, and a fire hall. Of the 27 projects, 20 have been through the complete program, including the Energy Performance Workshop. For the remaining seven projects, we have conducted some analysis, including CBIP facilitation, but no workshop. Of the 27 projects, 25 projects were interested in applying for a CBIP incentive (two projects were owned by the Federal government, which cannot apply for CBIP incentives). Of the 20 projects that have been through the Design Assistance program, all but two have been shown to qualify for a CBIP incentive. The summary statistics for those 20 projects is below.

Savings vs. Reference		Savings vs. Baseline	
Dollars	GJ	Dollars	GJ
$695,603	103,561	$644,549	99,200

Note that the above table contains summaries of historical information, and many projects were completed prior to the recent increase in gas prices, which would increase the dollar savings item considerably.

We have been pleasantly surprised since the middle of this summer by the emergence of a trend that has seen projects surface from workshops with the best possible outcome of reduced energy and capital cost compared to the Baseline, while attaining a maximum CBIP incentive. In other words, energy was saved while construction costs was *reduced*. In all, four projects have achieved this outcome.

The first thought most people have when talking about energy efficiency is: "How much will it cost?" That is one reason why we position Design Assistance as maximizing economic efficiency, not just energy efficiency. Typically, we have been happy to mine all of our projects for any energy efficiency measure which will come in under a (typically) 5-10 year payback, depending on the payback tolerance of the client. However, this new trend shows that a careful review of various measures can actually reduce energy consumption and the capital cost of the building by re-allocating resources to the most cost-effective energy conservation measures. This is certainly not a general trend that applies in all cases, but nevertheless is gratifying to witness on occasion.

The following table is a companion to the previous table, showing the average additional capital and maintenance costs. It also shows the associated energy savings and resulting overall payback of the 20 projects. The payback is assessed by comparing the final bundle of energy efficiency measures from the workshop to the baseline model, using a discount rate (typically 7%) over a 20-year analysis period.

Economic Analysis			
Incremental Capital	Annual Savings		Payback in Years*
	O&M	Energy	
$84,038	$762	$51,145	2.8

*Includes discount rate.

CONCLUSION

Our experience has shown that the process produces more energy efficient buildings with an attractive payback. The Energy Performance Workshop approach to integrated design is able to take any team and project through its design session and focus the team on achieving significant savings. This has come at a relatively small incremental design cost and with the likelihood of achieving those savings with a reasonable payback, if not actually reducing the cost of the building.

We would like to further consider two other aspects of the Design Assistance approach. Firstly, we do not replace anyone on the design team. As we often state in our workshops, "The design team is the artist, we only want to be a better paint brush." We do not tell the design team what to do, nor are we the "energy police." Secondly, while emphasizing that we were not necessarily interested in creating a budget-oriented service, the approach responded to market pressures (alleviated to a certain degree by CBIP incentives) in arriving at a scope of work which would improve the commercial building design process, but at a price that was acceptable in the market. This second point is key, as the industry needs to come up with a sustainable alternative design process for a post-CBIP world. That process cannot be onerous and expensive, or it will not stand the test of time and contribute to market transformation.

It is also important to view our findings in the proper context. All buildings are different, and measures that were or were not cost-effective in our studies may have different outcomes in other regions with different climates and/or utility rates. Therefore, instead of emphasizing the results of the program, we would like to emphasize that the process of using modelling in an integrated design setting allows the design team to bring forth ideas and discuss the potential, often leading to innovative, energy-efficient, and cost effective solutions.

REFERENCES

Case, M.E. and J. Wingerden (1998), Incentive Program for Energy Efficient Design of State Buildings, *ACEEE 1998 Summer Study on Energy Efficiency in Buildings*, American Council for an Energy-Efficient Economy, 4.37–4.48.

Hayter, S.J., P.A. Torcellini, R. Judkoff, and M.M. Jenior (1998), Creating Low-Energy Commercial Buildings through Effective Design and Evaluation, *ACEEE 1998 Summer Study on Energy Efficiency in Buildings*, American Council for an Energy-Efficient Economy, 3.181–3.192.

Hepting, C. (1996), Hourly End-Use Energy Analysis as a Value-Added Customer Service, *ACEEE 1996 Summer Study on Energy Efficiency in Buildings, Commercial Buildings: Program Design, Implementation, and Marketplace Issues*, American Council for an Energy Efficiency Economy.

Hepting, C. and D. Ehret (1998), The "BEST" New Commercial Design Program, *Green Building Challenge '98: An International Conference on the Performance Assessment of Buildings, Volume 2,* Natural Resources Canada.

Hepting, C., D. Ehret, and M. Mottillo (2000), Web-Based Building Performance Assessment: The CBIP Screening Tool, *Building Energy Simulation User News*, 21(6), Lawrence Berkley National Laboratory. A variation of this paper was also presented as a poster paper at the Sustainable Buildings 2000 conference in Maastricht, The Netherlands, Oct. 2000.

Montross, C. and M. Fraser (1998), Building Design for a Sustainable Future. *ACEEE 1998 Summer Study on Energy Efficiency in Buildings*, American Council for an Energy-Efficient Economy, 4.285–4.295.

ACKNOWLEDGEMENTS

This paper would not be complete without recognizing the contribution of Natural Resources Canada's Commercial Building Incentive Program, which has indirectly provided the financial engine for our program.

Session 5/ /Séance 5

Modelling Conventional and Innovative HVAC Systems

La modélisation de systèmes classiques et originaux de CVC

ANNUAL SIMULATIONS OF HEAT PUMP SYSTEMS WITH VERTICAL GROUND HEAT EXCHANGERS

Michel A. Bernier Duo Randriamiarinjatovo
École Polytechnique de Montréal
Département de génie mécanique
mibern@meca.polymtl.ca rduo@meca.polymtl.ca

ABSTRACT

This article presents a methodology that has been developed to perform annual hour-by-hour simulations of a single zone building heated/cooled by water source heat pumps coupled to a vertical ground heat exchanger.

The computer program simulates the three distinct parts of the system: i) building load; ii) heat pump; iii) and ground heat exchanger. The coupled governing equations of these three models are solved simultaneously until a converged solution is obtained at each time step. Simulations are performed using a commercially-available equation solver called EES.

Results of annual simulations are presented. It is shown that the program can be useful to balance ground heat exchanger length against heat pump energy consumption.

INTRODUCTION

Ground-coupled heat pump (GCHP) systems are becoming increasingly popular because of their energy saving potential. The system under study is presented in figure 1. It consists of a single-zone building with one heat pump, a circulating pump and a vertical ground heat exchanger. As shown in figure 1, a vertical GCHP system is usually composed of a series of boreholes (only one is shown on figure 1). After its passage through the heat pump, a certain amount of heat, identified as "q" in figure 1, is released into the loop to the circulating fluid. The fluid enters the ground at a temperature $T_{out,HP}$. Heat is then exchanged, at a rate equal to q, between this fluid and the surrounding ground. The fluid leaves the borefield at a temperature $T_{in,HP}$.

The rate at which heat is exchanged in the ground will depend on the temperature level which, in turn, depends on heat pump performance. Thus, heat pump performance and ground heat transfer are coupled via the temperature in the loop.

The economic decision to select a GCHP system for a particular application is most often dictated by the length of the ground heat exchanger and by energy saving potential offered by GCHP systems. An undersized heat exchanger will lead to unacceptably low (high) inlet temperatures in the winter (summer) months. An oversized heat exchanger, on the other hand, while providing safe heat pump operation, may lead to prohibitive installation costs.

This article presents a method to perform annual simulations of GCHP systems which can be used to optimise the length of the ground heat exchanger and provide annual energy consumption.

CURRENT METHODS

Ground heat exchanger sizing

There are several methods of sizing vertical ground heat exchangers. These methods have been reviewed and compared by Shonder et al. (1999, 2000). In essence, they use precalculated peak heating and cooling loads and average monthly building loads. The building loads are converted to ground loads using given values of COP and EER (which, in some sizing programs, are constant throughout the year). Then, the length required in heating and cooling is estimated using these ground loads in conjunction with the minimum and maximum entering water temperatures. The length estimation is based on ground heat exchanger models which use different methods to handle transient heat transfer in the ground. Models based on the cylindrical heat source method (e.g. Kavanaugh and Rafferty, 1997 and Bernier, 2000, Morrison, 2000) and the g-function (Yavuzturk and Spitler, 1999) are available.

The main characteristics of these approaches is that the building load is decoupled from the ground. In other words, loads and ground heat transfer are treated sequentially with no interaction between the two.

Whole system simulations

To our knowledge there are only two simulation programs that can perform annual simulations of a complete GCHP system including building load

interactions. The first of these programs is DOE. As reported by McLain and Martin (1999), DOE-2.1E has a subroutine to handle ground heat transfer. However, its performance seems to be relatively poor when compared to experimental data.

The second simulation program is TRNSYS coupled with the DST model of the University of Lund (Hellström et al., 1996). There is a general consensus in the GCHP research community that the DST-TRNSYS combination is probably the best available to perform whole system simulation. However, based on our own experience the TRNSYS environment is difficult to learn (Bernier, 1999).

This paper presents a methodology to perform accurate simulations of complete systems in a user-friendly environment. The building load, ground heat transfer, and heat pump performance are calculated simultaneously at each time step.

METHODOLOGY

Building load calculations

The load calculation portion of the proposed approach accounts for heat transfer through opaque surfaces; solar heat gains and conductive gains/losses through windows; and internal heat gains.

Heat transfer through opaque surfaces. There are six opaque surfaces in the monozone building used here. The four walls are assumed to be identical while the roof and the floor have different configurations. As shown in figure 2, it is possible to specify up to three different layers in the walls, as well as in the roof and floor. Assuming one-dimensional heat flow, transient heat transfer in the opaque surfaces is governed by :

$$\rho C_p \frac{\partial T}{\partial t} = \frac{\partial}{\partial x}\left(k \frac{\partial T}{\partial x}\right) \qquad (1)$$

where ρ is the density (kg/m^3), C_p is the specific heat (J/kg-K), k is the thermal conductivity (W/m-K), t is the time (sec), x is the position in the wall (m), and T is the temperature (°C).

The boundary conditions are also shown on figure 2. The interior temperature, T_{int}, as well as the temperature in the adjacent room, T_{adj}, are assumed constant throughout the year. Exterior temperature and solar radiation vary on an hourly basis. These last two parameters are combined using the concept of sol-air temperature (ASHRAE, 1997).

The value of $q_{ext,i}$ (Figure 2) is then given by:

$$q_{ext,i} = h_o \, (T_{sol\text{-}air,i} - T_{s,ext,i}) \qquad (2)$$

where,

$T_{sol\text{-}air,i}$ is the sol-air temperature for surface "i"; h_o is the outside film coefficient (this coefficient is assumed constant and equal to 16.94 W/m^2-K); $T_{s,ext,i}$ is the external surface temperature for surface "i" .

Convective heat exchanges on internal surfaces are given by:

$$q_{conv,in,i} = h_{conv,i} \, (T_{int} - T_{s,int,i}) \qquad (3)$$

where $T_{s,int,i}$ is the internal surface temperature of surface "i" and $h_{conv,i}$ is the convective film coefficient. The terms associated with long-wave radiation, $q_{lw,i}$, represents the sum of two terms:

$$q_{lw,i} = q_{lw,surf,i} + q_{lw,gains} \qquad (4)$$

where $q_{lw,surf,i}$ is the net long-wave radiation incident on surface i coming from the other five surfaces and $q_{lw,gains}$ is the incident long-wave radiation received from the radiative portion of the internal gains. In this work, it is assumed that the radiative portion of the internal gains is equally distributed among all six surfaces. The values of $q_{lw,surf,i}$ are obtained by solving:

$$q_{lw,surf,i} = \frac{Eb_i - J_i}{1 - \varepsilon_i}$$

$$q_{lw,surf,i} = \sum_{k=1}^{6} \frac{J_i - J_k}{\frac{1}{A_i F_{i,k}}} \quad for\ i = 1\ to\ 6 \qquad (5)$$

where Eb_i is the emissive power ($\sigma T_{s,int,i}^4$), J represents radiosity, A_i is the surface area, $F_{i,k}$ is the form factor between surface i and k, and ε_i is the emissivity of surface "i".

The last boundary condition is $q_{solar,f}$. It is the amount of solar energy transmitted through the window and intercepted by the floor. It is assumed here that all of the solar energy transmitted through the windows is absorbed evenly by the floor. Consequently, $q_{solar,f}$ is given by:

$$q_{solar,f} = \sum_{i=2}^{5} G_{t,i} \times \tau_i \times \frac{A_{window,i}}{A_{floor}} \qquad (6)$$

where the summation extends from i=2 (south wall) to i=5 (east wall) and τ_i is the solar transmittance of window "i". Incident solar radiation on each surface, $G_{t,i}$, is calculated using:

$$G_t = G_{ND} \cos\theta + G_{dH} \frac{(1+\cos\beta)}{2} + \rho G_{tH} \frac{(1-\cos\beta)}{2} \qquad (7)$$

where G_{tH} is the total horizontal radiation, G_{DN} is the direct normal radiation, and G_{dH} is the diffuse radiation on the horizontal. These three values of solar radiation are obtained from meteorological data files. The angle between the normal to the surface and the solar rays is θ while β is the slope (from horizontal) of the surface and ρ is the albedo.

To summarise, equation 1 is the governing equation to be solved and the boundary conditions are given by equations 2,3,4,5,and 6 . This problem is solved using the control-volume approach proposed by Patankar (1980). With reference to figure 3, the fully implicit form of the discetization equation for an internal node is given by :

$$a_P T_P = a_E T_E + a_O T_O + b \qquad (8)$$

where

$$a_P = a_E + a_O + a_P^0,\ a_E = \frac{k_e}{\delta x_e},\ a_O = \frac{k_o}{\delta x_o},$$

and $a_P^0 = \frac{\rho C_p \Delta x}{\Delta t}$, $b = a_P^0 T_P^0$

Δx is the width of the control volume, T_P^0 is the temperature at point P prevailing at the preceding time interval, k_e and k_o are so-called interface conductivities which account for different thermal conductivities between adjacent nodes (Patankar,1980). With this approach, sudden changes in the value of k can be handled even with a coarse mesh near the interface.

Boundary nodes require a special treatment. Taking the floor surface temperature as an example ($T_{s,int,f}$ in figure 2 and node B in figure 3), the values of a_B^0 and b are given by:

$$a_B^0 = \frac{\rho C_p (\Delta x/2)}{\Delta t},$$

$$b = a_B^0 T_B^0 + q_{lw,f} + q_{conv,f} + q_{solar,f} \qquad (9)$$

As indicated in figure 3, nine grid points, three in each layer, were selected. This grid spacing is the result of a compromise between accuracy and calculation speed. Figure 4 presents the result of a comparison between the TFM method (ASHRAE,1997) and the method used here with 9 and 15 grid points. These results show that there is good agreement between the three sets of results. The 15 grid points solution is closer to the TFM solution than the 9 grid point solution. However, a 9 grid point spacing was retained to reduce calculation time. Finally, it should be noted that over a 24 hour period, the average value of $q_{conv,in,i}$ obtained with 9 grid points and the TFM method agree within 1%.

Internal heat gains. The treatment of internal heat gains, q_{gains}, is relatively straightforward. The convective portion of the internal gains, which contributes immediately to the heating/cooling load is given by:

$$q_{gains,conv} = F_{conv} \times q_{gains} \qquad (10)$$

where F_{conv} is the convective fraction of internal heat gains. The radiative portion of the heat gains, $q_{gain,rad}$, is simply given by:

$$q_{gains,rad} = q_{gains} - q_{gains,conv} \qquad (11)$$

Solar heat gains through windows. As indicated earlier in conjunction with equation 7, the amount of solar energy that enters the room, $q_{solar,in}$ is given by:

$$q_{solar,in} = \sum_{i=2}^{5} G_{i,j} \times \tau_i \times A_{window,i} \qquad (12)$$

Convective heat gains/losses through windows. These gains/losses are evaluated simply by solving:

$$q_{conv,window} = \sum_{i=2}^{5} U_i \times A_{window,i} \times (T_{ext} - T_{int}) \qquad (13)$$

where U_i is the heat loss coefficient of window "i".

Calculation of the heating/cooling load. Equations 1 to 13 are solved simultaneously until a converged solution is obtained. The heating/cooling load is then obtained by:

$$q_{load} = \sum_{i=1}^{6} q_{conv,in,i} + q_{gains,conv} + q_{conv,window} \qquad (14)$$

Ground loop calculations

Figure 5 presents the main components of a vertical ground heat exchanger. This figure is in fact an input screen extracted from the software. The left portion of the figure shows the borefield arrangement. In this case there are a total of 4 boreholes, arranged in a 2×2 grid. Their center-to-center distance is 6 m and the total length of the loop is 75 m. The initial ground temperature is 10°C. The right portion of the figure shows the internal configuration of the borehole. It consists of two tubes separated by a certain distance and located away from the borehole wall (configuration "B" of Remund, 1997). The borehole is filled with a grout whose thermal properties might be different from the ones of the adjoining soil.

The characteristics that are needed to define transient heat transfer in the ground are presented on the right portion of the figure. From top to bottom, these

characteristics are: soil thermal diffusivity (α_s), soil thermal conductivity (k_s), grout thermal conductivity (k_g), borehole diameter, pipe internal and external diameters and thermal conductivity (k_p).

Transient heat transfer in the ground is similar to transient heat transfer in a wall in that energy storage, or the "thermal history" as to be accounted for. However, in the case of ground heat transfer, the thermal history as to be kept relatively long. Computationally, this complicates calculations. In the approach proposed in this paper, transient heat transfer in the ground is calculated using the cylindrical heat source method with a load aggregation scheme which reduces computational time. This method will now be described briefly. The readers are referred to other publications (e.g. Kavanaugh and Rafferty, 1997 and Bernier, 2001) for a more complete description of the method.

With reference to figure 6, the mean fluid temperature in the borefield at time n, referred here as $T_{f,n}$, is given by:

$$T_{f,n} = \frac{q_n}{L} R_b - \frac{1}{k_s L}\left[q_{mean,m}\left(G_{Fo_{\alpha_s t_m}} - G_{Fo_{\alpha_s t_0}}\right) + q_{m+1}\left(G_{Fo_{\alpha_s t_{m+1}}} - G_{Fo_{\alpha_s t_m}}\right) + q_{m+2}\left(G_{Fo_{\alpha_s t_{m+2}}} - G_{Fo_{\alpha_s t_{m+1}}}\right) + \ldots + q_n\left(G_{Fo_{\alpha_s t_{m+A-1}}} - G_{Fo_{\alpha_s t_{m+A}}}\right)\right] - T_{g,n} \qquad (15)$$

where,

q_n is the heat transfer rate during the last time interval, from t_{m+A-1} to t_n, (Watts). A positive value of "q" implies heating, i.e. heat transfer from the ground to the fluid; R_b is the effective borehole thermal resistance, (m-K/W); L is the total length of the boreholes (not to be confused with the pipe length which is twice the borehole length),(m); $q_{mean,m}$ is the aggregated load, i.e. the average heat transfer rate during the time interval from 0 to t_m, (Watts); A (= t_n-t_m) is the "short term thermal history" time interval, (hours); $T_{g,n}$ is the far field ground temperature at time n.

The "G" function requires some further discussion. As shown in equation 15, this function is evaluated for a given Fourier number, Fo, which is defined by:

$$Fo = 4\alpha_s t / d^2 \qquad (16)$$

where,

t is the time (in days) and d is the borehole diameter (m). The "G" function is in fact the analytical solution to transient heat transfer (Ingersoll et al., 1954) from a cylinder embedded in an infinite medium subjected to a constant heat transfer rate. The ratio G_{Fo}/k_s represents an effective thermal resistance. The "G" function is relatively complex. In this work, the curve fitted expression suggested by Bernier (2001) has been used.

Equation 15 reflects the use of the principle of superposition to accommodate variable heat transfer rates. For example, the term associated with q_{m+1} represents the contribution of q_{m+1} to the final value of $T_{f,n}$. It is calculated by assuming that q_{m+1} prevails over the time interval from t_m to t_n from which is subtracted the superimposed effect of q_{m+1} over the time interval from t_{m+1} to t_n.

Recognising that the immediate short term thermal history is more important than the past thermal history in the determination of $T_{f,n}$, the past thermal history is averaged into a single term while the short term thermal history is kept intact. Yavuzturk and Spitler (1999) have referred to this as "load aggregation". This technique is illustrated schematically in figure 6 with an example of a calculation performed at hour 5168 and where the short term thermal history consists of the last 168 hours prior to hour 5168. By using load aggregation, equation 15 contains 169 terms (instead of 5168 terms if load aggregation was not used) with the impact of the first 5000 hours combined into a single term, $q_{mean,m}$.

The first term on the right hand side of equation 15 represents heat transfer form the fluid to the wall of the borehole. It is assumed that this process occurs in steady state and that it can be described using an equivalent borehole thermal resistance, R_b, based on the concept of shape factors (Remund 1999).

When a borefield is composed of several boreholes, heat gets stored (retrieved) between boreholes, thereby increasing (decreasing) the value of T_g . Kavanaugh and Rafferty (1997) have proposed a correction procedure that was used in the present approach. The readers are referred to the book by Kavanaugh and Rafferty for more details.

To summarise, equation 15 is the main governing equation to evaluate ground heat transfer. It calculates the mean fluid temperature in the borefield at time t_n. It accounts for two groups of heat transfer rates. The first one is associated with the immediate thermal history, i.e. interval A in figure 6. The second heat transfer rate is an aggregated load that covers the time period prior to the immediate thermal history.

Ground loop calculations using equation 15 have been validated successfully against the DST model. Results are presented in a related paper (Bernier, 2001).

Heat pump performance

Heat pump performance depends mainly on four factors: room air temperature, air flow rate, water flow rate, and entering water temperature. Generally, the first three factors are fixed by design and only the entering water temperature varies during the course of a year.

In this work, heat pump performance, characterised by the Coefficient of Performance (COP), is calculated using "lookup tables". One such table is presented in figure 7 for both heating and cooling. These tables are generated by entering catalogue data.

During calculations, the operating COP is evaluated at the entering water temperature based on a linear interpolation between values contained in the lookup tables. Once the COP is known, the amount of heat rejected (HR) (or the amount of heat extracted (HE), if the building is in cooling mode), and the heat pump energy consumption (EC_{HP}) are calculated using:

$$HR = q_{load} \times \left[1 + \frac{1}{COP_{cooling}}\right] \quad (17)$$

$$HE = q_{load} \times \left[1 - \frac{1}{COP_{heating}}\right] \quad (18)$$

$$EC_{hp} = \left| \frac{q_{load}}{COP_{cooling\ or\ heating}} \right| \quad (19)$$

SOFTWARE IMPLEMENTATION

The equations described in this paper were implemented in a commercially-available solver called EES which stands for Engineering Equation Solver (Klein, 2000). One of the nicest feature of this solver is the diagram window capability which makes entering data very user-friendly. One such graphic is presented in figure 5.

EES uses a variant of Newton's method to solve the set of non-linear algebraic equations. The Jacobian matrix is evaluated at each iteration. Blocking algorithm and sparse matrix techniques are used to break the problem into smaller problems and improve calculation efficiency.

Since the governing equations of ground heat transfer and heat pump performance are coupled, an iterative solution procedure is needed. In a nutshell, the iteration procedure assumes different values of $T_{in,HP}$ until the amount of energy rejected into the loop is equal to the amount of energy released into the ground.

RESULTS

Simulations are performed for a 3×3×3 m single-zone building located in Montréal and maintained at 24°C all year round. The four walls are facing the four cardinal points and each has a 4 m^2 window. Using the building material terminology of ASHRAE (page 28.19 of the ASHRAE Handbook of Fundamentals, 1997), the construction of the building envelope is the following:

Window: U=3.3 W/m^2-K, τ = 0.8

Walls: A2-B16-E1

Roof: B7-B16-E1

Floor: E1-C12-E13

with h_o = 16.94 W/m^2-K and $h_{conv,i}$ = 3.4 W/m^2-K. All surfaces are assumed to have an emisivity of 0.9.

Internal heat gains are assumed constant and equal to 2500 W with a convection/radiation split of 50/50.

The borefield arrangement as well as the ground properties are shown in figure 5. The heat pump COP is given in figure 7 for both heating and cooling. The flow rate is set at 0.24 L/sec. Finally, ground heat exchanger simulations were performed with a 24 hour load aggregation period.

Figure 8 shows the resulting building loads. The peak loads are -3.6 kW in heating and 4.8 kW in cooling. At this point, if current sizing methods are used, the length determination of the ground heat exchanger would proceed by estimating ground loads based on an average annual COP. Using the data of figure 8 and based on an average annual COP of 3.5, it can be shown that: i) the average power (on a yearly basis) released into the ground is 270 W (a positive ground load means that heat is being transferred from the ground to the circulating fluid); ii) the average monthly power rejected/absorbed into the ground is -1.9kW/+1.7kW for the most severe months (July/January); iii) the maximum hourly heat rejection into the ground occurs in July and is equal to -6.2 kW. In January, the ground provides +2.6 kW of heat to the heat pumps. Using these values and the ground properties indicated in figure 5 in a sizing program (Bernier, 2000), it can be shown that the required heating length is 95 m while the required cooling length is 79 m. These lengths are based on maximum entering water temperatures of +1.5°C and +32.5°C in heating and cooling, respectively.

Figure 9 presents the results of annual hour-by-hour simulations for two different heat exchanger lengths, 75 and 67.5 m. Both graphs show the variation of the inlet

temperatures to the heat pumps. As shown on the left graph, a heat exchanger length of 75m is adequate to remain within the lower and upper temperatures used in the sizing procedure described above. Thus, in this particular case, the heat exchanger length estimation is lower when using annual simulations. This is due to the fact that hour-by-hour simulations can "follow" the ground loads more precisely while current sizing procedure are based on the maximum hourly, monthly, and yearly thermal pulses.

The other main advantage of hour-by-hour simulations is that heat pump energy consumption can be calculated precisely using hourly values of COP. For instance, with a 75m heat exchanger, annual heat pump energy consumption is 3300 kWh. The graph on the right of figure 9 shows the impact of a 10% reduction (from 75m to 67.5m) in heat exchanger length on T_{inHP} and annual heat pump energy consumption. The lower and upper limits of T_{inHP} are lower/higher than for the case where the length is 75m. In fact, temperatures of -1.6°C and 39°C are dangerously close to the safe operation limit of heat pumps. In addition, results in Figure 9 show that heat pump energy consumption increases by 6% due to lower COP values attributable to lower/higher values of T_{inHP} in heating/cooling.

CONCLUDING REMARKS

A methodology has been presented to solve simultaneously the coupled governing equations of building load, heat pump performance, and ground heat transfer. These equations are solved using a commercially-available equation solver called EES.

Hourly simulations for a complete year are presented for a $27m^3$ cube subjected to Montréal weather conditions. This room is coupled to a 75m vertical ground heat exchanger and heated/cooled by a single heat pump. Results show that the proposed methodology has the advantage of giving a more precise estimate of heat exchanger length when compared to current sizing procedures. Furthermore, heat pump energy consumption can be calculated more accurately since hourly COP values, obtained from predictions of the outlet ground temperature, are used.

REFERENCES

ASHRAE. (1997). *ASHRAE Handbook of Fundamentals*.,ASHRAE.

Bernier, M.A. (1999). L'apprentissage de TRNSYS/IISiBat par des étudiants en génie climatique, *2ième séminaire TRNSYS francophone*, 12 pages, Montréal,.

Bernier M. (2001). Ground-Coupled Heat Pump System Simulation, *ASHRAE Transactions* 107 (1).

Bernier, M. (2000). A Review of the Cylindrical Heat Source Method for the Design and Analysis of Vertical Ground-Coupled Heat Pump Systems. *4th International Conference on Heat Pumps in Cold Climate*, Aylmer, Québec.

Hellström, G., Mazzarella, L., Pahud,D. (1996). Duct ground storage model – TRNSYS version. Department of Mathematical Physics, University Of Lund, Sweden.

Ingersoll, L.R., Zobel, O.J., Ingersoll, A.C. (1954). *Heat Conduction With Engineering, Geological, And Other Applications*, University Of Wisconsin Press.

Kavanaugh S.P., Rafferty, K. (1997). *Ground-Source Heat Pumps : Design Of Geothermal Systems For Commercial And Institutional Buildings*. ASHRAE, Atlanta, GA.

Klein, S.A. (2000). *EES – Engineering Equation Solver*, F-chart software, Madison, Wisconsin.

McLain, H.A., Martin, M.A., (1999). A Preliminary Evaluation of the DOE-2.1E Ground Vertical Well Model Using Maxey School Measured Data. *ASHRAE Transactions*, 105 (2).

Morrison, A. (2000). GS2000™ software, *4th International Conference on Heat Pumps in Cold Climate*, Aylmer, Québec.

Patankar, S.V., (1980). *Numerical Heat Transfer and Fluid Flow*, McGraw-Hill.

Remund, C.P. (1999). Borehole Thermal Resistance : Laboratory and Field Studies, *ASHRAE Transactions* 105 (1) : 439-445.

Shonder, J.A., Baxter, V., Thornton, J., Hughes, P., (1999). A New Comparison Of Vertical Ground Heat Exchanger Design Methods For Residential Applications. *ASHRAE Transactions*, 105 (2).

Shonder, J.A., Baxter, V.D., Hughes, P.J., Thornton, J.W., (2000). A Comparison of Vertical Ground Heat Exchanger Design Software for Commercial Applications, *ASHRAE Transactions* 106 (1).

Yavuzturk, C., Spitler, J.D., Rees, S.J. (1999). A Transient Two-Dimensional Finite Volume Model For the Simulation of Vertical U-Tube Ground Heat Exchangers, *ASHRAE Transactions* 105 (2).

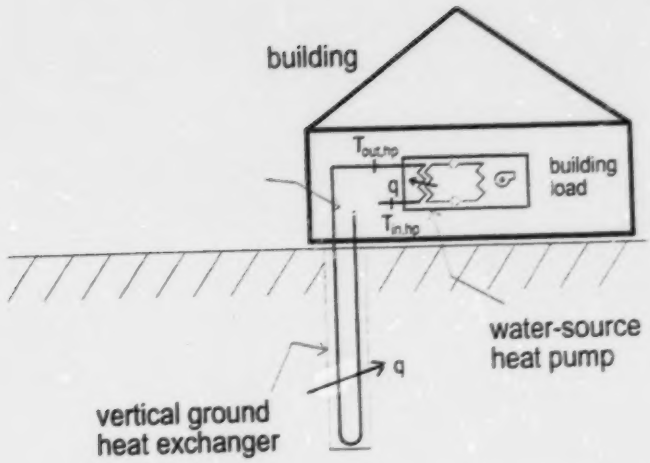

Figure 1. Schematic representation of the problem under study.

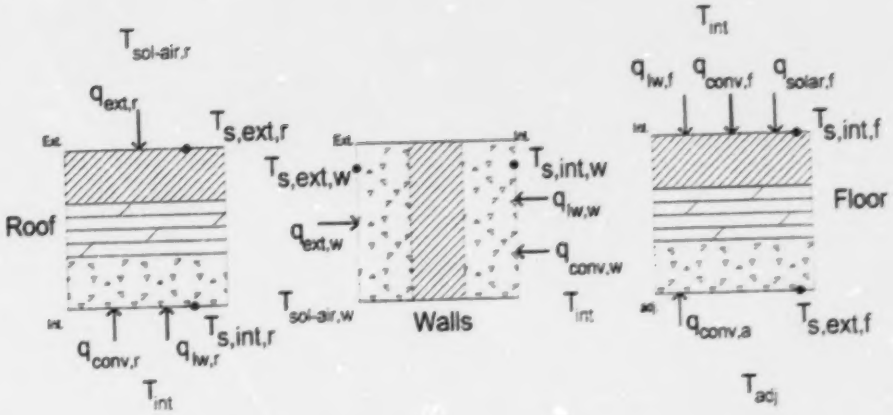

Figure 2. Nomenclature used to describe heat transfer through the walls, the roof, and the floor.

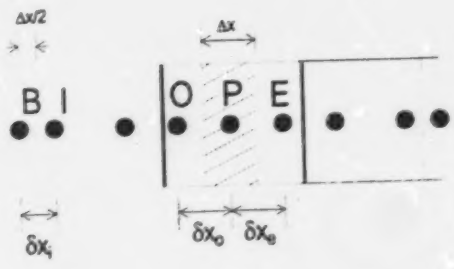

Figure 3. Grid arrangement for a three layer opaque surface.

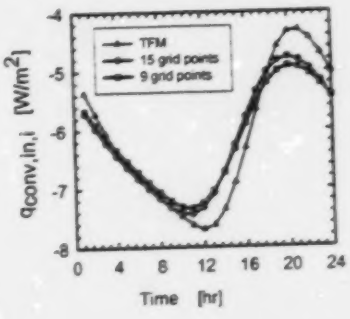

Figure 4. Heat transfer at the internal surface. Comparison between the TFM and the proposed method.

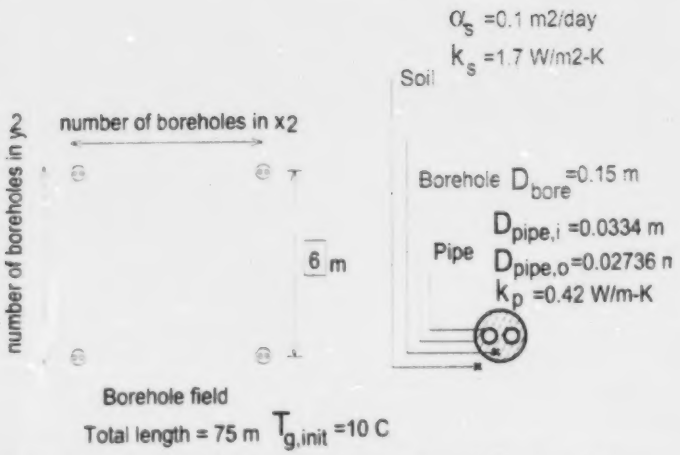

Figure 5. Input screen for borefield and for the ground/bore properties.

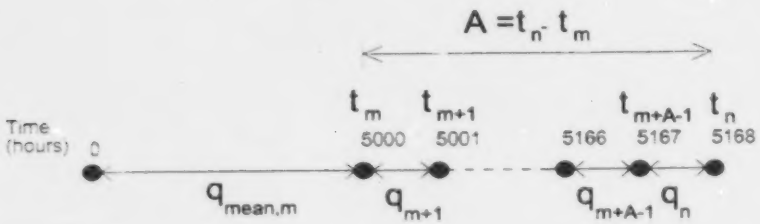

Figure 6. Schematic representation of load aggregation

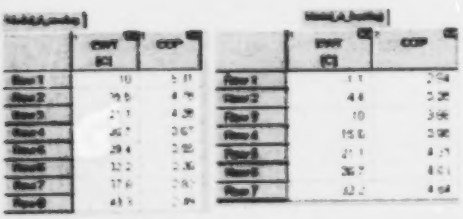

Figure 7. Lookup table to calculate heat pump COP.

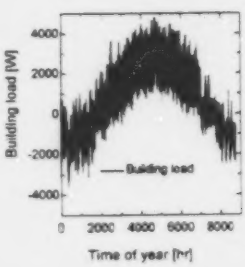

Figure 8. Building load

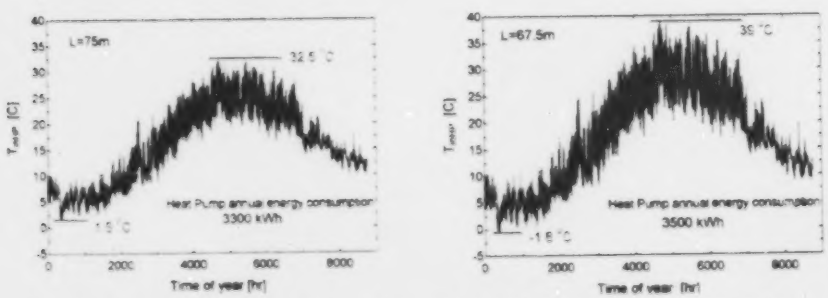

Figure 9. Inlet temperature to the heat pumps for two different heat exchanger lengths.

MODÉLISATION D'UN CHAUFFE-EAU SOLAIRE COUPLÉ À UN SYSTÈME À COMPRESSION DE VAPEUR

Simon SANSREGRET, Stéphane BILODEAU
Groupe Énerstat, inc
Sherbrooke (Québec)
ssansregret@groupeenerstat.com, sbilodeau@groupeenerstat.com

RÉSUMÉ

Cet article présente la modélisation d'un système biénergie (solaire et thermique) servant à préchauffer l'eau sanitaire. Ce système, en phase développement, est composé d'une thermopompe dont l'évaporateur puise principalement son énergie du rayonnement solaire. La modélisation de ce système a été effectuée à l'aide du logiciel EES (Engineering Equation Solver). Le modèle numérique présenté a la particularité de coupler un modèle avancé d'un système à compression de vapeur avec la modélisation d'un capteur solaire. Les résultats du modèle, comparés avec des essais expérimentaux, permettent d'observer une hausse appréciable des performances du système en fonction :

- d'une diminution de la température de l'eau à l'entrée du condenseur
- d'une augmentation de la température extérieure
- d'une augmentation du rayonnement solaire

INTRODUCTION

Les systèmes à compression de vapeur et les systèmes solaires impliquant des capteurs sont deux secteurs d'activité du génie mécanique qui ont été largement étudiés. Plusieurs modèles caractérisent le comportement de ces systèmes. Un modèle de thermopompe souvent cité est celui développé par Fischer et Rice du ORNL (Oak Ridge National Laboratory). La modélisation de systèmes impliquant l'utilisation de capteurs solaires est aussi bien développée. Le logiciel TRNSYS est un outil souvent utilisé pour ce type d'application. La présente étude combine ces deux sujets dans une seule modélisation : un modèle de thermopompe, prenant en considération la charge et les pertes de pression du réfrigérant dans les échangeurs, couplé à un capteur solaire modélisé par différences finies.

DESCRITION DU SYSTÈME

Le système héliothermique développé permet de préchauffer l'eau sanitaire en utilisant l'énergie solaire via un système à compression de vapeur. Ce système est basé principalement sur le fonctionnement d'une thermopompe. La particularité provient de l'évaporateur, qui absorbe la majeure partie de son énergie du rayonnement solaire, ce qui permet une utilisation efficace du système à de faibles températures extérieures. Dans ce système, on retrouve un circuit d'eau et un circuit de réfrigérant. Le réfrigérant à basse pression s'évapore dans le capteur en absorbant l'énergie solaire et l'énergie de l'air extérieur par convection. Un compresseur vient augmenter la pression et la température du réfrigérant. Celui-ci transmet sa chaleur à l'eau à l'intérieur d'un condenseur coaxial. Par la suite, une valve de détente apporte le réfrigérant à basse pression et le cycle recommence. Le circuit d'eau, opérant en boucle fermée, est entraîné par une pompe de recirculation qui envoie l'eau réchauffée par le condenseur dans un réservoir d'eau, servant de source au chauffe-eau en service. Un schéma descriptif du système est présenté à la figure 1.

Le système est présentement installé sur un site d'expérimentation. Un capteur solaire, d'une superficie de 5,5 m^2, est placé sur un mur extérieur du bâtiment. Le capteur pointe dans la direction sud-est, ce qui confère un ensoleillement débutant tôt le matin jusqu'à environ 14 h. À l'intérieur du bâtiment, une unité de thermopompe comprenant un condenseur à eau et un compresseur a été installée. L'eau préchauffée est emmagasinée dans un chauffe-eau hors-fonction, faisant office de réservoir. Un chauffe-eau électrique puise l'eau dans ce réservoir à température tempérée, réduisant ainsi sa consommation électrique. Un contrôleur programmable gère un fonctionnement sécuritaire et efficace du système en fonction de plusieurs paramètres mesurés :

- Température extérieure
- Intensité du courant au compresseur
- Intensité du rayonnement solaire
- Température de l'eau (plusieurs points)
- Température du réfrigérant (plusieurs points)

Les données expérimentales recueillies jusqu'à présent ont permis de valider le comportement global du système modélisé.

DESCRIPTION DU MODÈLE

La modélisation du système héliothermique est basée sur un découpage modulaire du système où les variables de sortie d'une composante deviennent les variables d'entrée pour d'autres. Diverses méthodes (différences finies, modélisation semi-empirique, équations algébriques, etc.) sont utilisées pour modéliser les différentes composantes du système. La résolution du couplage des équations des différentes composantes est assurée par le logiciel EES (Engineering Equation Solver) développé par F.L. Avarado et S.A. Klein du Solar Energy Lab, University of Wisconsin. Ce logiciel utilise une variante de la méthode de Newton pour résoudre des systèmes d'équations non linéaires. Plusieurs fonctionnalités intéressantes élargissent son utilisation : fonction d'optimisation, calcul d'incertitude et utilisation de fonction des propriétés physiques de plusieurs fluides.

La thermopompe est modélisée en régime permanent et l'impact des arrêts et des démarrages a été négligé. Un schéma illustrant les entrées et les sorties (associées au réfrigérant) des différentes composantes modélisées est présenté à la figure 2. L'évaluation du sous-refroidissement à la sortie du condenseur est contrôlée par l'équation de conservation de la masse de réfrigérant à l'intérieur du système. La suite de cette section présente la modélisation spécifique des composantes.

1- Élément de détente

Un orifice est utilisé comme élément de détente dans ce circuit. Une détente isenthalpique est considérée. L'équation suivante associée à la perte de pression d'un écoulement fluide incompressible subissant une brusque contraction est utilisée.

$$\Delta P = \frac{1}{2}\left(\frac{m_{réf}}{C_D \cdot A}\right)^2 \qquad (1.1)$$

Une valve thermostatique a également fait l'objet d'un autre modèle. L'hypothèse d'un fonctionnement parfait, c'est-à-dire une température de surchauffe constante à la sortie de l'évaporateur a été considérée. Une détente isenthalpique est également pris en compte.

2- Compresseur

Le compresseur utilisé est hermétique et de type alternatif. La cylindrée et la révolution sont respectivement de 27 cm^3 et 3450 rpm.

Une méthode semi-empirique, inspirée du projet ASHRAE RP-870, est employée pour modéliser le compresseur. La référence et le détail de ce projet proviennent de [1]. Les équations classiques des différents rendements associés au performance du compresseur sont utilisées :

$$\eta_{vol} = \left[1 + C - C \cdot \left(\frac{P_2}{P_1 \cdot (1-\Delta P_1)}\right)^{1/n}\right] \qquad (1.2)$$

$$\eta_{is} = \frac{m_{réf} \cdot \left(h_{2,is} - h_1\right)}{W_{réf}} \qquad (1.3)$$

$$\eta_{mécanique} = \frac{W_{requise}}{W_{réf}} \qquad (1.4)$$

Ces équations possèdent des paramètres propres caractérisant le compresseur utilisé : le volume mort du cylindre C, la perte de pression relative ΔP_1 à l'entrée du cylindre, le rendements isentropique η_{is} et le rendement électromécanique $\eta_{méc}$. Pour déterminer C et ΔP associés au compresseur modélisé, une fonction d'optimisation du logiciel EES a été utilisée afin de minimiser la différence entre les débits massiques calculés et ceux mesurés expérimentalement. Le débit massique de même que les états thermodynamiques du réfrigérant (pression, température) à l'entrée et à la sortie du compresseur ont été mesurés lors de tests expérimentaux. Les paramètres caractéristiques $\eta_{méc}$ et η_{is} ont été obtenus directement à l'aide des résultats expérimentaux.

3- Condenseur

Le condenseur utilisé est de type coaxial. Il est modélisé par la méthode des différences finies en utilisant la méthode NTU. L'échange de chaleur entre l'eau et le réfrigérant est régit par une série de

résistances thermiques. La conductance d'un élément k de l'échangeur est :

$$UA_k = \frac{1}{R_{k,réf} + R_{k,tube} + R_{k,eau}} \qquad (1.5)$$

La résistance de convection due à l'écoulement de l'eau est évaluée par une relation provenant d'essais expérimentaux réalisés par Kausik [2]. Par ailleurs, le coefficient de chaleur associé au réfrigérant est évalué par une relation développée par Shah [3]. Selon Shah, cette relation a admis un écart de ± 15.4 % avec 474 points de mesure.

Le calcul de la charge du réfrigérant à l'intérieur des échangeurs est basé sur le modèle homogène. Ce modèle suppose que les deux phases à l'intérieur d'un écoulement diphasique sont en équilibre thermique et dynamique (T, P, V ont les même valeurs). Le modèle stipule que la fraction de la surface α occupée par la vapeur à l'intérieur d'une coupe d'un écoulement diphasique se traduit par :

$$\alpha_k = \left(1 + \left[\frac{1-\chi}{\chi}\right]\frac{\rho_g}{\rho_l}\right)^{-1} \qquad (1.6)$$

où $\chi \rightarrow$ titre du mélange de l'élément k

La masse de réfrigérant dans un élément k de l'échangeur est donc donnée par :

$$M_{k,réf} = Vol_k \cdot \left[\alpha_k \rho_g + (1-\alpha_k)\rho_l\right] \qquad (1.7)$$

Les pertes de pression du réfrigérant à l'intérieur de l'échangeur sont également prises en compte. Les pertes dues au frottement et les pertes dues à la variation de densité du fluide ont été calculées pour chaque élément. Dans un but de concordance, le modèle utilisé pour le calcul des pertes de pression en écoulement diphasique est basé également sur le modèle homogène.

4- Capteur/Évaporateur

Le capteur utilisé est constitué d'une plaque de cuivre sur laquelle sont soudés des tubes de cuivre également espacés. Aucun vitrage n'est employé.

La modélisation du capteur solaire est basée sur l'ouvrage de Duffie et Beckman [4]. Le capteur a été discrétisé en plusieurs éléments pour faciliter l'évaluation du coefficient de transfert de chaleur en évaporation du réfrigérant. La méthode NTU a été utilisée comme dans le cas du condenseur. La figure 3 présente une vue du capteur solaire.

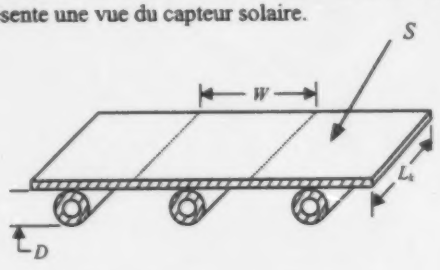

Figure 3 : Vue du capteur solaire

Le schéma résistif illustrant l'échange de chaleur entre l'environnement et le réfrigérant circulant dans le capteur est donné à la figure 4.

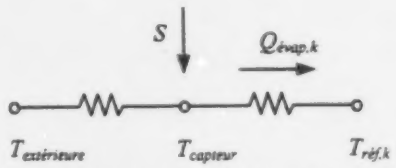

Figure 4 : Schéma résistif de l'échange de chaleur entre l'environnement et le réfrigérant

L'équation 1.8 exprime l'échange de chaleur $Q_{évap,k}$ calculé en fonction de la température du réfrigérant et de la température extérieure. Cette équation est obtenue en éliminant le terme de la température du capteur par l'utilisation d'un rendement F_k (éq. 1.9).

$$Q_{évap,k} = W \cdot L_k \cdot F_k \left[S - h_{air}(T_{extérieure} - T_{réf,k})\right] \qquad (1.8)$$

$$F_k = \frac{1/h_{air}}{W\left[\frac{1}{h_{air}\left[D + (W-D)\eta\right]} + \frac{1}{\pi D_i h_{réf,k}}\right]} \qquad (1.9)$$

Le rendement η est calculé par les équations classiques du rendement d'une ailette longitudinale dont les bouts sont adiabatiques.

L'évaluation de l'échange de chaleur d'un élément permet le calcul des propriétés du réfrigérant à l'entrée de l'élément suivant à la suite du gain de chaleur absorbé. L'échange thermique total vers le réfrigérant est obtenu en additionnant l'échange de chaleur de tous les éléments k. Les pertes de pression et la charge du réfrigérant dans le capteur sont évaluées suivant le même principe que la modélisation du condenseur.

Une relation développée par Chen pour le calcul du coefficient de transfert du chaleur en évaporation a été utilisée, comme le recommande Braun [1]. Cette relation est jugée précise à ± 15 % par la comparaison de 200 points de mesure.

5- Réservoir d'eau

Le réservoir d'eau n'a pas été modélisé directement. Une température d'eau à l'entrée du condenseur est utilisée comme entrée au modèle.

RÉSULTATS

Plusieurs simulations ont été effectuées dans le but d'observer l'influence de certains paramètres sur les performances du système.

Jusqu'à présent, le modèle a été comparé à des résultats expérimentaux portant sur l'influence de la température de l'eau à l'entrée du condenseur. Des simulations montrant l'influence de la température extérieure et du rayonnement solaire sont présentées. De plus, deux modèles distincts possédant un élément de détente différent (orifice et valve thermostatique) ont été utilisés pour observer leur impact.

1- Influence de la température de l'eau

La température de l'eau à l'entrée du condenseur a une influence importante sur le coefficient de performance du système, le C.O.P. Ce coefficient est définit comme étant la puissance transmise à l'eau divisée par la puissance consommée par le compresseur. On observe (figure 5) une diminution du C.O.P. en fonction d'une augmentation de la température de l'eau. Une chute de 3,25 à 2,75 a été calculée. Par ailleurs, la puissance transmise à l'eau tend à demeurer sensiblement constante. Une température de l'eau élevée implique une température de condensation plus haute, ce qui se traduit par une augmentation de la puissance consommée par le compresseur.

Les résultats du modèle suivent la même tendance que les résultats expérimentaux. Par contre, le modèle sous-estime d'environ 20 % la puissance thermique transmise à l'eau. Plusieurs raisons peuvent expliquer cet écart. D'une part, l'imprécision des mesures expérimentales apportent une incertitude évaluée ± 10 %. D'autre part les incertitudes sur les relations utilisées pour les coefficients de convection en changement de phase et dans l'air ambiant influencent la précision du modèle.

2- Influence de la température extérieure et du rayonnement solaire

La température extérieure et le rayonnement solaire absorbé par le capteur ont un effet direct sur la puissance disponible à l'évaporateur. On observe (figures 6 et 7) que la puissance thermique transmise à l'eau et le C.O.P augmentent en fonction d'une augmentation de la température extérieure ou du rayonnement solaire.

Une différence de performance notable est observée entre les deux éléments de détente modélisés. L'utilisation de l'orifice à comme conséquence de transmettre deux fois moins de puissance comparativement à la valve thermostatique. Ce résultat est observé pour une température élevée et/ou un rayonnement solaire important. Cette différence est attribuable à une augmentation considérable de la surchauffe à la sortie de l'évaporateur lorsque l'orifice est utilisée. Ce gain d'énergie sensible n'est pas favorable à l'augmentation de la puissance transmise à l'eau.

Les conditions d'opération d'un tel système sont excessivement variables et la sélection d'un élément de détente approprié est très important.

CONCLUSIONS

La modèle développé permet de bien simuler le comportement d'un chauffe-eau solaire couplé à un système à compression de vapeur. La comparaison d'une simulation avec des résultats expérimentaux permet de valider le comportement du système selon les paramètres établis. En bref, le code numérique permet :

- d'observer l'influence de paramètres importants (températures de l'eau à l'entrée du condenseur, température extérieure et rayonnement solaire) et de définir plus précisément les conditions d'opération du système.

- d'analyser le système en simulant différents éléments de détente et de mieux comprendre le comportement du système en fonction de l'élément de détente utilisé.

Nous envisageons actuellement de raffiner le modèle et de le valider en fonction de la température extérieure et du rayonnement solaire. De plus, la modélisation d'autres types d'éléments de détente est prévue dans le but d'optimiser le fonctionnement du système.

NOMENCLATURE

α : Surface occupée par la vapeur (%)
ρ : Masse volumique (kg/m^3)
η_{is} : Rendement isentropique
$\eta_{méc}$: Rendement électromécanique
ΔP_l : Perte de pression relative (%)
η_{vol} : Rendement volumétrique
A : Surface (m^2)
C : Volume mort relatif (%)
C_D : Coefficient de décharge
D : Diamètre (m)
$h_{2,is}$: Enthalpie du réfrigérant à la sortie du compresseur, considérant une compression isentropique (J/kg)
h_{air} : Coefficient de chaleur de convection entre l'air et le capteur (W/m^{2}K)
L : Longueur (m)
M : Masse (kg)
$m_{réf}$: Débit massique (kg/s)
n : Indice isentropique de compression
P : Pression (Pa)
P_1 : Pression d'aspiration (Pa)
P_2 : Pression de refoulement (Pa)
R : Résistance (K/W)
S : Rayonnement solaire (W/m^2)
T : Température (K)
UA : Conductance (W/K)
V : Vitesse (m/s)
Vol : Volume (m^3)
W : Espacement entre les tubes (m)
$W_{réf}$: Puissance transmise au réfrigérant (W)
$C.O.P.$: Coefficient de performance
$W_{requise}$: Puissance requise au compresseur (W)

Indices

g : Vapeur
i : Intérieur
k : Élément k
l : Liquide
$réf$: Réfrigérant

BIBLIOGRAPHIE

[1] Braun, J. E., Groll, E., et Klein, S.A., *Modeling And Design of Vapor Compression Systems Sort Course*, June 1-4, 1999, Ray W. Herrick Laboratories, School of Engineering, Purdue University

[2] Kausik N., Azer N.Z., « Condensation Heat Transfer Enhancement by Doubly Augmented Tubes », *ASHRAE Transaction 1988* (2), Vol. 94, pp. 1367-1374

[3] Shah, M.M., « A General Correlation for Heat Transfer during Film Condensation Inside Pipes », *International Journal of Heat and Mass Transfer*, Vol. 22, pp. 547-556

[4] Duffie J. A., Beckman W. A., *Solar Engineering of Thermal Processes*, 2nd ed., John Wiley & sons, 1991, 919 p.

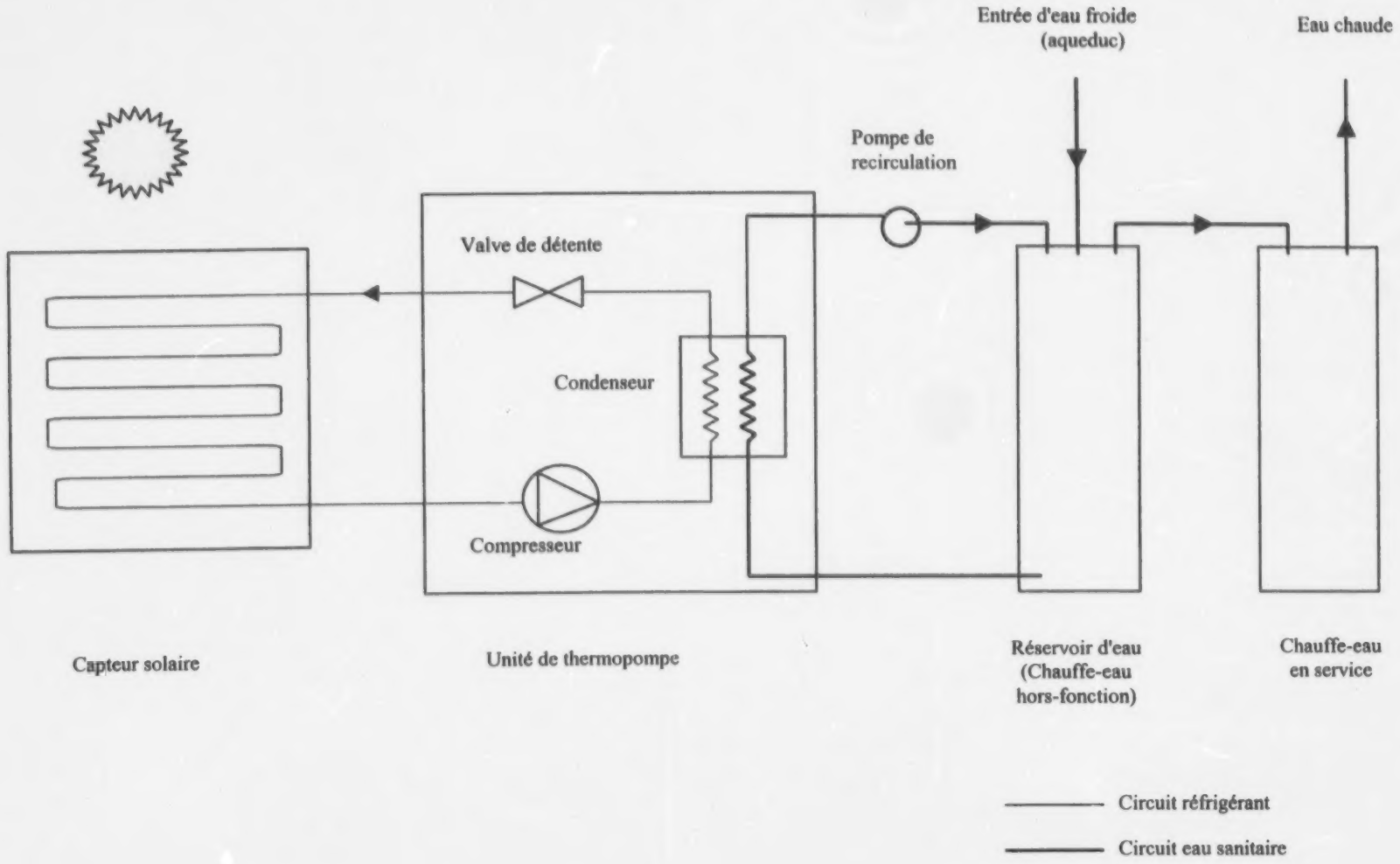

Figure 1 : Schéma de fonctionnement du système héliothermique

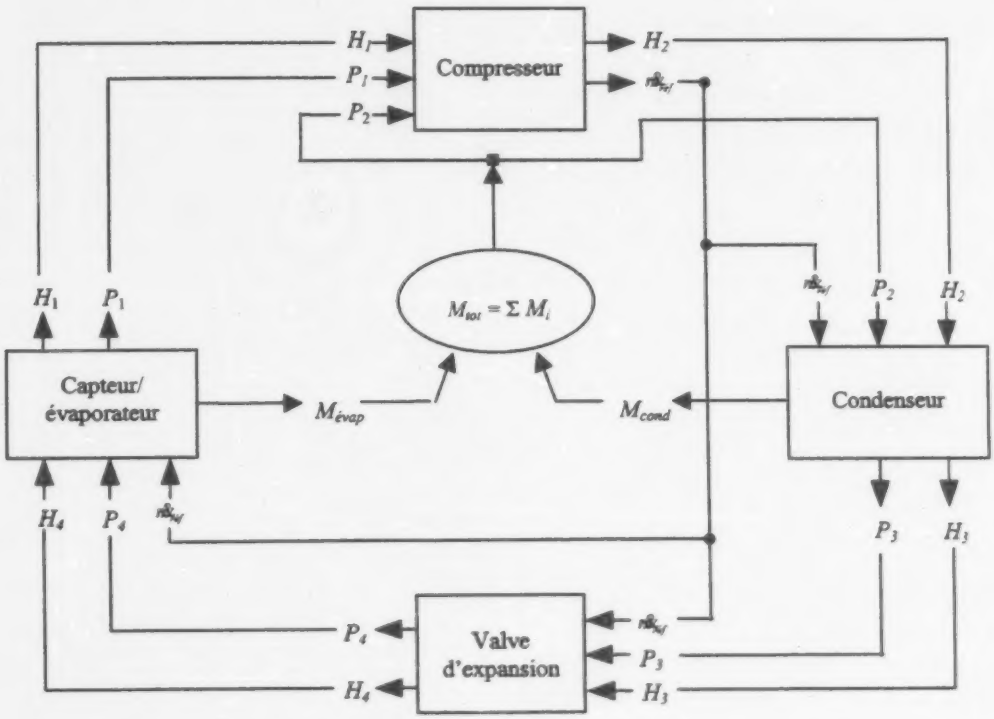

Figure 2 : Illustration des entrées et sorties du modèle (associées au réfrigérant)

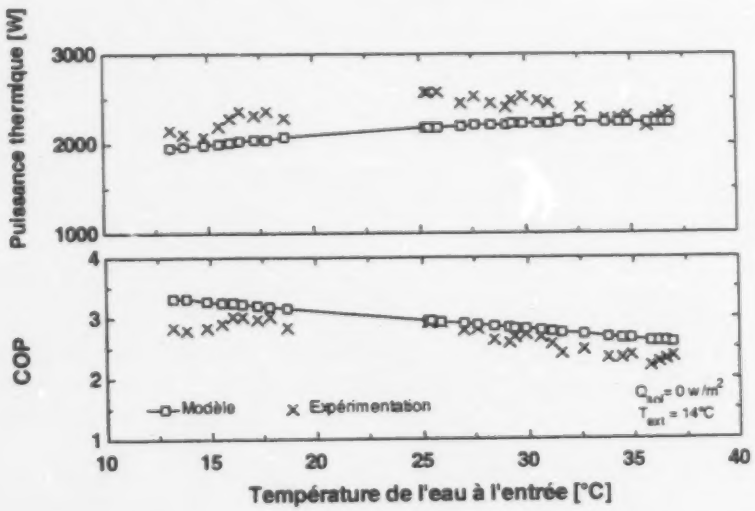

Figure 5 : Influence de la température de l'eau à l'entrée du condenseur

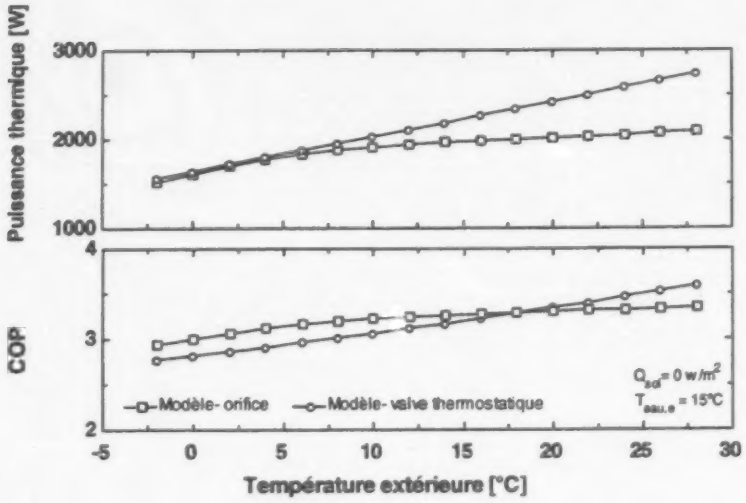

Figure 6 : Influence de la température extérieure

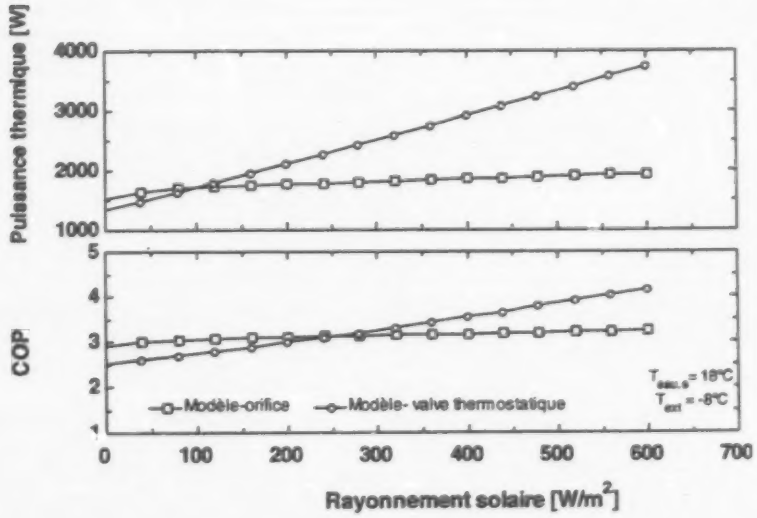

Figure 7 : Influence du rayonnement solaire

SIMULATION OF A COMBINED SPACE AND WATER HEATING SYSTEM FIRING PELLET FUEL FOR COMMERCIAL/RESIDENTIAL APPLICATION

Bruce R. Clements, Bill Pearson, A.C.S. Hayden
CANMET Energy Technology Centre
Nepean, Ontario
clements@nrcan.gc.ca, bpearson@nrcan.gc.ca, shayden@nrcan.gc.ca

ABSTRACT

This paper describes the development of a real-time dynamic simulator that is configurable to simulate a variety of commercial / residential combined space heating and domestic hot water systems. The simulation allows the designer the ability to test different physical configurations under various operating conditions and to optimize a system design for specific operating requirements. The simulator was built using the G2 expert system shell which is a product of the Gensym Corporation.

INTRODUCTION

Efficiency gains, improved system performance, and low consumer cost are all recognizable benefits associated with the development of oil and gas integrated residential energy systems. With natural gas, high efficiency integrated space and hot water heating systems can have seasonal efficiencies over 90%, with overall fuel savings and pollutant reductions of 35-45%, when compared to conventional non integrated systems. Properly integrating oil-fired space and tap water heating systems can raise overall efficiencies by 10-30%, with a commensurate reduction in NO_x and CO_2 emissions, with an even greater reduction of incomplete combustion products.

Biomass fuel technology advancements, particularly in the area of pellet fuel, are now revolutionizing how biomass is likely to be used in our homes for generation to come. Pellet fuel overcomes many of the major impediments that seriously limit the attractiveness of biomass as fuel. The pellet industry turns a biomass residue destined for non-productive landfill into a valuable energy commodity that is very competitive as a fuel. Unlike traditional wood use which varies widely in fuel quality, pellet fuel is high grade, conforming to industrial standards that define ash content (less than 1%), moisture content (less than 5%) and dry calorific value of 19,773 kJ/kg (8,500 Btu/lb). Biomass pellets are much easier to handle, transport, and store compared to conventional core wood. Biomass pellet fueled stoves are very energy efficient, clean burning and offer the customer automation and convenience.

CANMET Energy Technology Centre is focused on developing advanced residential integrated systems using biomass pellets as a fuel. Combining two or more end uses, such as space and tap water heating, with one energy generator into an integrated system has the potential to be an effective means to substantially increase efficiency and to reduce emissions from residential biomass combustion appliances, at reduced overall capital costs. However, the design of an integration energy system poses many equipment and systems challenges along with a host of operational variables that have to be optimized. Considerations include: furnace sizing, burner modulation requirements, furnace startup and shut down scenarios, hydronic systems configurations, tap water segregation, optimal thermal fluid temperature, heat storage, load following and optimization, and systems's reliability. This set of complex design considerations and trade-off can best be effectively optimized using appropriately designed simulation software.

The simulator was originally developed to design and test various combined space and water heating system designs firing pelletized wood fuel. It not only tests the design but can be used to develop and test control strategies and operating practices. Although the simulator was originally used for pellet fire systems, the technology applies equally to the more conventional gas and oil fired systems.

This paper will present the configuration of the pellet fired system, the theory used for the major components in the system and then the architecture and design of the simulator. It will comment briefly on how the simulator was used in the design process.

THE PELLET-FIRED SPACE AND WATER HEATING SYSTEM

High-efficiency pellet-fired integrated home energy systems (Figure 1) comprised components that can be configured in a number of ways to suit site specific installation needs. Major system components include, a fuel storage and supply system, a pellet burner, fuel and ash removal system, a furnace air supply and exhaust module, boiler, hot water storage tank, a forced air fan coil unit and a plate to plate domestic hot water heat exchanger (Figure 2).

The fuel storage management and handling system allows a typical home owner to receive and store 800 kg. of fuel, sufficient fuel to cover a homeowner's space and hot water energy requirements for a month during Canadian winter conditions. Fuel from the storage bin is monitored and augered to the furnace fuel supply hopper.

The specific control strategy is designed to achieve the desired set points to ensure safe operation, maximum energy efficiency, reduced furnace cycling, comfort, optimum fan speeds to optimize comfort and to minimize noise levels. Features of the control strategy include intelligent defaults and occupant controlled set points for space and hot water heating, air coil settings, furnace monitoring for proper combustion startup and shutdown, proof of fluid flows and temperature monitoring, furnace startup and shut down and modulating fuel firing rates .

The furnace incorporates a variable speed induced draft fan to minimize excess air requirements, optimize combustion performance and load following with a step down ratio of 3 to 1. Overall operating efficiencies are in the range of 80 %. The control strategy also focuses on minimizing furnace cycling.

The combustion burner is encased in a waterwall boiler, the burner is air cooled by its own air supply, and the ash dump is appropriately lined and insulated to meet all standards and code requirements. The furnace exhaust will be fitted with a high temperature cut-off switch.

Space Heating

Space heating capacity of the system as proposed would be 14 kW (77,000 Btu/hr). Three furnace firing rates are controlled to follow the heating load in a fashion that maximizes energy efficiency. The water supply temperature to a forced air fan coil unit is controlled between 60 and 71 deg C.(140 to 160 deg F).

The space heating control can be set to ensure that under all conditions the space heating supply air temperature of 47C (117F) is maintained. At design conditions, our air handler will have a supply air temperature of 51C (123F).

Domestic Hot Water

The smart control that prioritize domestic hot water over space heating means the actual water available for domestic use is much greater than current guidelines. The recovery rate is 300 litres/h (80 usgph) (based on 50C/90F temperature rise). The first hour rate is 416 litres (110 usg).

The burner input of 34 kW (maximum120,000 Btu/hr) with an output of 28kW (96,000 Btu/hr) is capable of meeting the 14kW (77,000 Btu/hr) space heating load with a 20% reserve for domestic hot water. The smart controls that prioritize domestic water over space heating means the actual water available for domestic use will be much greater than measured using the current guideline rating method. The delivery temperature is monitored to ensure it will not exceed 60C (140F) using a mixing valve and bypass configuration.

The hot water tank will be fitted with electrical resistance heating to provide backup for domestic hot water and space heating needs.

THEORY

For the simulator to behave as required, certain components must have transient behaviour. Transient behaviour is required for the space and the tank, due to their ability to store heat. All other components in the system have minimal thermal capacitance (the ability to store heat) and therefore were treated as behaving in steady state. This steady state assumption is used for the air coil, domestic hot water heat exchanger, boiler and piping. It could be argued that the boiler should have a transient behaviour, however, it was treated as instantaneously coming to thermal equilibrium. This assumption may be improved in the future.

The theory that will be presented in this section will be for the major components including the treatment of the heated space and the storage tank.

The other components in the system were modeled using simple heat and mass balances. The domestic hot water heat exchanger was modeled using the NTU method.

Modeling of the Heated Space

The heated space can be treated as an enclosure that transfers heat to the outside environment through a single equivalent wall. This is a simplification of the heated space, however, the purpose of this project was to concentrate on the behaviour of the heating system. This gives the appropriate overall behaviour of the heated space because it replicates the overall conductance to the temperature sink and the overall thermal capacitance of the space.

The heat transfer of the wall of an enclosed space can be expressed as:

$$Q = \frac{A \times (T_o - T_i)}{(1/h_o + \Delta x/k + 1/h_i)} \qquad ...(1)$$

Where:

Q	Heat transfer (kW)
A	Equivalent heating surface of the house(m^2)
To	Outside temperature (deg C)
Ti	Inside temperature (deg C)
ho	Equivalent outside film coefficient (kW/m^2.deg C)
hi	Equivalent outside film coefficient (kW/m^2.deg C)
? x	Equivalent thickness of the wall (m)
k	Equivalent conductivity of the wall (kW/m.deg C)

An overall equivalent heat transfer coefficient (U) can be solved for the enclosure

$$U = \frac{1}{1/h_o + \Delta x/k + 1/h_i} \qquad ...(2)$$

Therefore, the expression in equation (1) can be simplified to:

$$Q = U \times A \times (T_o - T_i) \qquad ...(3)$$

For the sake of this analysis the product U x A can be written as a single conductance (G) which can be called the heat loss factor .

This reduces the equation to

$$Q = G \times (T_o - T_i) \qquad ...(4)$$

Determination of Heat Loss Factor (G)

The heat loss factor factor describes how quickly heat is being lost on average from a space. This heat output would be required to be supplied by the heating system.

The average temperature differential is :

$$\gamma = Degree-days / heating\_period \qquad ...(5)$$

Therefore the average outside temperature is :

Average Outside Temperature
= The Reference Temperature - ? ...(6)

Using as an example Ottawa, Ontario, Canada as a design condition we know the following:

Design Temperature	-25 deg C
Degree Days	4763 deg C- Days
Reference room temp	18 deg C
?	23 deg C
Average Outside Temp	-5 deg C
Annual fuel consumption	75 GJ/yr (14880 KJ/hr based on 210 heating days/yr)
Heat loss factor (G)	647000 kJ/deg C . hr

Although infiltration can be a factor, this heat loss is included in the heat loss factor using this analysis method.

Heat Capacitance Factor (C)

Space heating requires transient modeling because dwellings of different sizes, construction and materials will store various amounts of heat. Heat lost from the space will cause an overall drop in temperature of the space depending upon the equivalent thermal capacitance of the space.

$$G \times (T_o - T_i) = \frac{C \times (T'_i - T_i)}{d\theta} + Q_{delivered} \qquad ...(7)$$

d?	Time period (s)
T'i	New temperature after d? (deg C)
Q delivered	Heat supplied by the heating system (kW)

If $Q_{delivered} = 0$ (the heating system is not running)

then this equation can be used to determine heat capacitance factor (C) of the space:

$$C = \frac{G \times d\theta \times (T_o - T_i)}{(T'_i - T_i)} \qquad ...(8)$$

This equation can be solved experimentally using a cool down test. At the required temperature differential (?) and no heat delivered from the heating system, the rate of temperature drop (ß) of the enclosure needs to be recorded.

$$\beta = \frac{(T'_i - T_i)}{d\theta} \qquad ...(9)$$

Therefore

$$C = \frac{G \times \gamma}{\beta} \qquad ...(10)$$

Modeling of the Storage Tank

The change in heat over a time period within the storage tank is equal to the difference between the heat input and the heat output and losses during that period. A generalized heat balance for the tank can be written as follows:

$$\Delta Q_{tank} = Q_{input} - Q_{output} - Q_{losses} \qquad ...(11)$$

Heat Input (Q_{input})

$$Q_{input} = \dot{m}_{boiler\_water} \times Cp \times (T_{boiler} - T_{tank}) \qquad ...(12)$$

Where:

$$Q_{input} = (\eta / 100) \times Q_{fired} \qquad ...(13)$$

Where:

m_{boiler_water}	Mass flow of the boiler water(kg/hr)
Ttank	Temperature of water in tank (deg C)
Tboiler	Temperature of water out of boiler (deg C)
Cp	Specific heat of water (kJ/kg.deg C)
?	Efficiency of boiler (%)
Q_{fired}	Heat input from fuel firing (kJ/hr)

Heat Storage Differential

The difference in heat of the tank will cause the temperature of the tank to vary in accordance with:

$$\Delta Q_{tank} = \frac{m_{tank} \times Cp \times (T'_{tank} - T_{tank})}{d\theta} \qquad ...(14)$$

Heat Output

The heat leaving the tank is the sum of the heats to the heat exchanger and the air coil:

$$Q_{out} = Q_{heat\_exchanger} + Q_{air\_coil} \qquad ...(15)$$

Where:

$Q_{heat\_exchanger}$	Heat duty of the heat exchanger
Q_{air_coil}	Heat duty of the air coil

Solving equation (14) for the next temperature of the tank:

$$T'_{tank} = \frac{d\theta}{m_{tank} \times Cp} \Delta Q_{tank} + T_{tank} \qquad ...(16)$$

SIMULATOR DESIGN

The simulator was built using an expert system shell called G2 developed by the Gensym Corporation. The shell uses an object oriented data structure and therefore, objects can be created having specific functions and attributes.

Data Objects

The objects used in this simulation are :

TANK	a tank
HEX	the domestic hot water heat excanger and mixing valve assembly
SHOWER	a domestic hot water draw that could represent a shower, sink, washer etc by user configuration
SPACE	this is the heated space that can be configured for different geographical locations and various types of use and construction
COIL	the air coil used to heat the forced air system
BOILER	a hot water boiler

Each object is configurable by the user. There are three types of attributes (data) associated with each object.

- Real time user modifiable input
- Configuration input (must be set before the simulation starts and will be constant for the simulation)
- Output (values which) are calculated by the simulation and these values are simply

displayed to the user

Real Time User Input
The user can control the following time-variant boundary conditions in real time throughout the simulation:

For the space:
- room thermostat set-point temperature (deg C)
- outside ambient temperature (deg C)

For the domestic water:
- set-point temperature for hot water (deg C)
- service water supply temperature (deg C)

For the tank:
- boiler cut-out temperature (deg C)
- boiler cut-in temperature (deg C)

The user can also turn on and off any number of configurable domestic hot water demands.

Configuration Input
These include the size of the tank, flowrates of the domestic hot water demands, physical attributes of the components etc. These inputs have been configured to be established at the beginning of the simulation and not configurable in real time.

Rules
There are two types of rules that govern the operation of the simulator, "initially" rules and "whenever" rules.

"Initially" rules are run at the beginning of the simulation. In this simulation these rules are used to initialize data and to start continual procedures. In this case there is one rule to set the conditions of the tank at startup and another to start a continuous procedure called "space_proc". The 'space_proc' starts the calculation of the heat loss of the space which is a continual process during the heating season.
"Whenever" rules are triggered by events such as reaching cut-in temperatures.

Procedures
Procedures are usually triggered by a rule and are used to perform a computational task. There are two types of procedures used in this simulation. There are those that perform a heat balance and mass balances on specific system components, and those used to start, stop and initialize values for components .

The procedures that perform the heat and mass balances are:

TANK_PROC
SPACE_PROC
SHOWER_NUMBER_PROC

A brief descrciption of these procedures is as follows:

TANK_PROC
This procedure is used to perform a heat balance on the tank and calculate all temperatures associated with the tank and water entering and exiting the tank. This heat balance is a transient balance that takes into consideration the heat storage ability of the tank. This balance is run throughout the simulation and as components such as the air coil, boiler and domestic hot water heat exchanger are turned on and off and numerical values such as the tank cut-in and cut-out temperature are modified by the user.

SPACE_PROC
This procedure performs the heat balance on the space based upon the physical and environmental attributes of that space. This, once again, is a transient analysis based on the theory presented.

SHOWER_NUMBER_PROC
This procedure, upon noticing that there is domestic hot water being drawn from the system, will do a complete heat balance on the domestic hot water heat exchanger using the NTU method. It will also resolve the heat balance and mass balance associated with the mixing valve.

There are also a number of less consequential procedures that perform the tasks of turning components on and off and set appropriate flows and temperatures when these components are operating.

Logic Flow
The main logic flow is as follows:

1. Start the simulation
2. Initialize the tank data
3. Calculate the heat balance on all system components that are operating
4. Start at time = 0
5. Wait for a time step

6. Calculate new temperatures within the system including the space and perform a heat balance on all components that are operating
7. Repeat steps 5 and 6 until simulator is shutdown

The space loses heat continually with various realtime changes in the thermostat setpoint and the outside temperature condition. Once the room temperature decreases to below the lower deadband on the thermostat, the air coil will turn on and heat will be drawn from the tank to heat the space.

Heat is also removed from the tank as domestic hot water is drawn from the system by a variety of user controlled demand systems such as showers. Once the temperature of the tank decreases below the cut-in temperature the boiler will automatically turn on and deliver heat to the tank.

Graphical User Interface

The graphical user interface (Figure 3) shows a variety of configurable graphics. To change the attributes of the tank for example the user selects the tank which causes a table to appear. The user then enters a different value in the table. Data sliders that are used to change many of the real time inputs for the components. Values can be graphed at the bottom to monitor the simulation as it proceeds. Water demands can be configured and turned on and off using the action buttons to the side of water draw object (noted as shower1, shower2, etc.).

USE OF THE SIMULATOR

The simulator was used to design the heating system shown in figure 1 and to configure the control system. This use can be summarized as follows:

- size the tank, boiler, air coil and heat exchanger
- establishing firing rates for the boiler and under which conditions to use these firing rates
- determine the best cut-in and cut-out tank temperatures for starting and stopping the boiler
- establishing an acceptable deadband on the thermostat
- determining how the heating system will perform on different houses for various ambient temperature and hot water use scenarios

DISCUSSION AND CONCLUSIONS

The simulator was used to develop a preliminary design for the pellet fired combined space and domestic hot water and to give us an idea of how to control the system. Many different design and control scenarios were tested before developing an optimal arrangement for a specific set of constraints.

The specific design features for this installation that that were derived from the simulations were

- boiler firing rates and flowrates
- optimum storage tank capacity
- domestic hot water heat exchanger size, flowrates
- mixing valve parameters
- fan coil size, flowrates and temperatures
- control set-points such as cut-in and cut-out temperatures and thermostat dead bands

In the next phase of this project the actual performance of the system will be tested and compared against the simulator runs.

The major conclusions from this work were

1. It has been shown that an appropriately designed simulation software can effectively be used to analyze complex design considerations and optimize the design of a system of this nature.
2. Use of a simulator is an extremely valuable tool in developing and testing control strategies.
3. In the future there would be some value in developing a transient behaviour for the boiler component.

REFERENCES

1. Chapman, A.J., 'Heat Transfer', MacMillan Publishing, 1974.
2. Jennings, B., 'Environmental Engineering Analysis and Practice', Harper and Row, 1970.
3. "Heating with Gas, Office of Energy Efficiency, NRCan, Cat. No. M91-23/3, 1999.
4. Hayden, A.C.S., Braaten, R., 'Efficient Residential Oil Heating', NRCan report # SP 88-1, Cat. No. M38-15/88-1, 1988.

Figure 1 Schematic Integrated Space and Water Heating Furnace

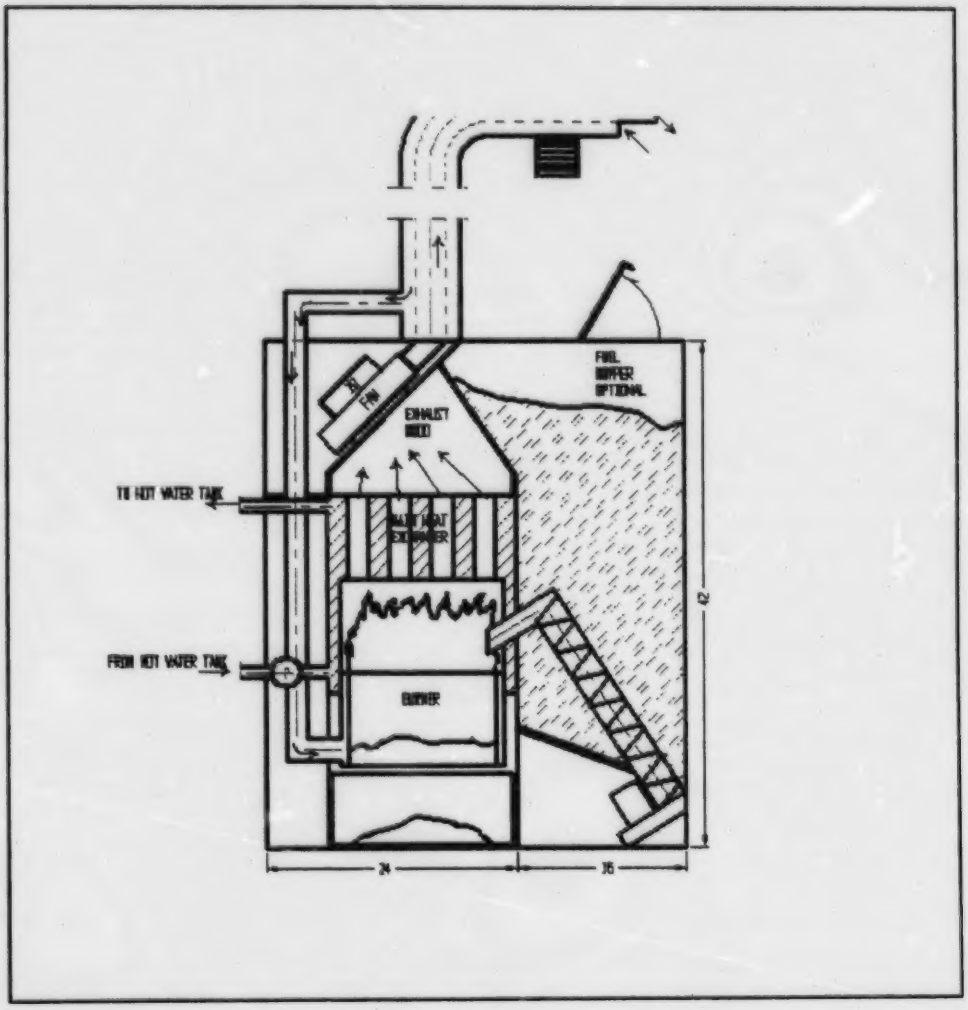

Figure 2 Schematic Space and Water Heating System

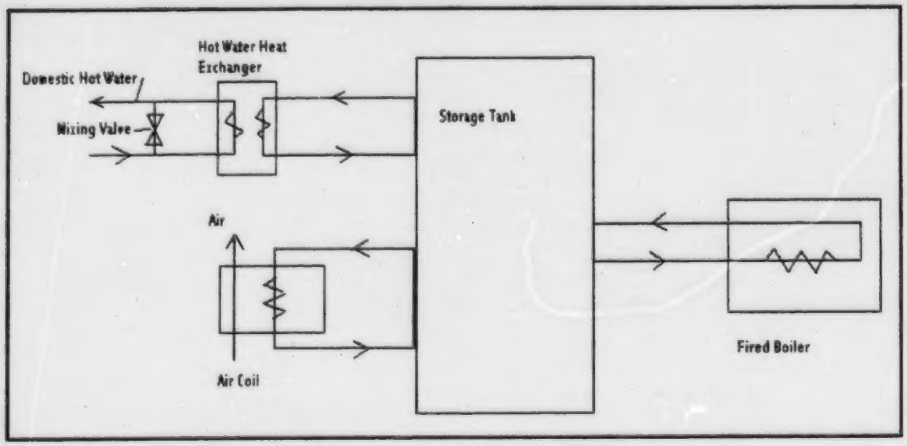

Figure 3 Simulator Graphical User Interface

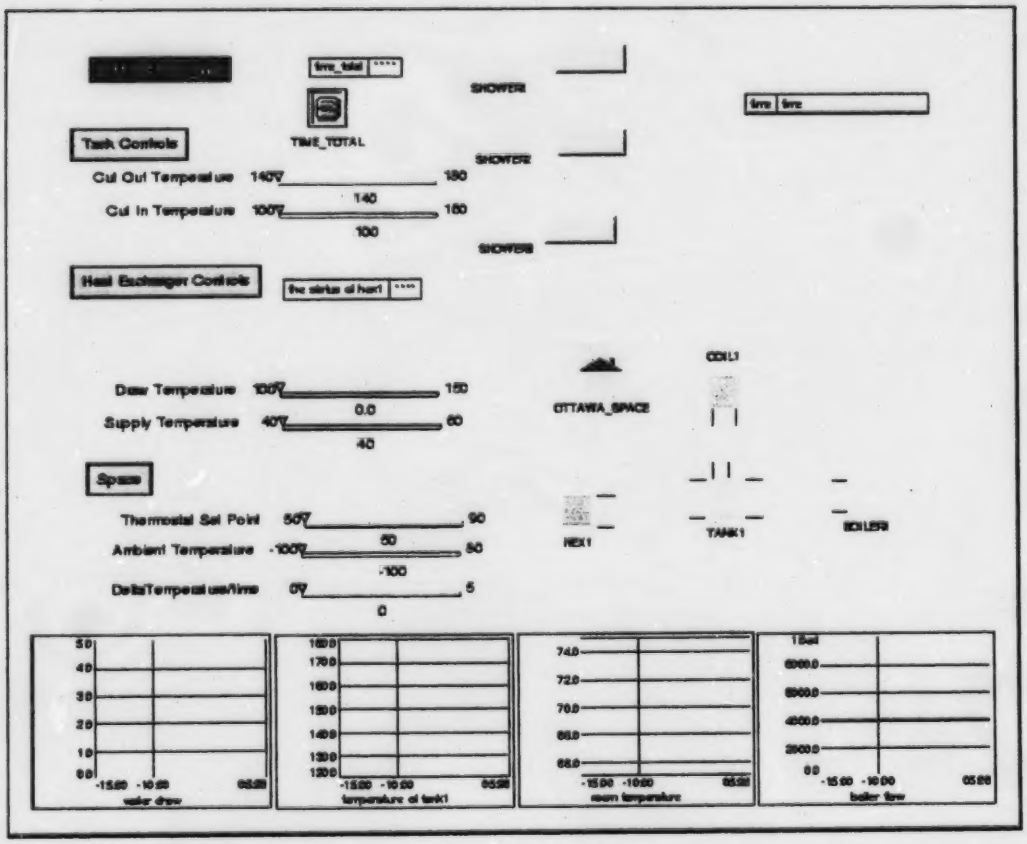

MODELLING AND ANALYSIS OF BUILDING SYSTEMS THAT INTEGRATE COGENERATION AND DISTRICT HEATING AND COOLING

Marc A. Rosen Wey H. Leong Minh N. Le
Department of Mechanical, Aerospace and Industrial Engineering
Ryerson University
Toronto, Ontario, M5B 2K3, Canada
mrosen@ryerson.ca weyleong@ryerson.ca

ABSTRACT

The modelling and analysis of building systems that integrate cogeneration and district heating and cooling are described. The analysis work uses exergy methods, in addition to the more conventional energy analysis, to evaluate overall and component efficiencies and to identify and assess thermodynamic losses. Exergy analysis is a relatively new analysis technique that provides enhanced understanding of the characteristics of energy systems and can assist design and improvement efforts. The modelling efforts focus on simplified models that can be assessed relatively straightforwardly and facilitate the application of simulation tools. The use of thermal energy storage and the impact of heat losses in the ground are considered. The latter can be significant for the system components that can be on- or below-ground, including the buildings, any present thermal storage and the district heating and/or cooling piping. The results should assist in the enhancement of simulation techniques for building energy systems.

INTRODUCTION

This paper considers integrated energy systems in buildings, including such technologies as cogeneration, district heating and cooling, and thermal energy storage. Such building energy systems can be complex, relative to conventional systems, in that integrated systems often carry out the provision of electrical, heating and cooling services simultaneously.

Two particular aspects of the modelling, simulation and design of such building energy systems are emphasized in this paper:

- the benefits of using exergy analysis in such activities, and
- the difficulties in dealing with systems involving many in-ground components (e.g., underground distribution pipes in district heating and cooling networks, and underground thermal energy storages).

Rather than focus exclusively in this paper on the simulation of building energy systems, we concentrate more on modelling activities, bearing in mind the fact that the resulting models can be incorporated into simulation codes. Also, analyses based on exergy methods can be incorporated into simulation codes.

In this paper, consequently, the following topics are covered:

- background on exergy analysis and its use in simulation codes,
- efficiency analysis of a system design for an integrated building energy system, and
- discussion of the aspects of such systems involving in-ground components, and how they can be dealt with.

The objectives of this paper are to improve understanding of (i) models for whole building simulation, (ii) the benefits of using exergy analysis in such work, and (iii) the need to consider carefully heat transfer through the ground in systems where extensive use is made of in-ground components. It is anticipated that the work will assist developers and users of simulation tools for building systems.

BACKGROUND ON EXERGY METHODS

Energy and exergy analyses (Moran and Sciubba, 1994; Moran and Shapiro, 2000; Kotas, 1995) are used to perform thermodynamic performance comparisons in the present study. Energy analysis is based on the first law of thermodynamics, which is concerned with the conservation of energy. Exergy analysis is based on the second law, and generally allows process inefficiencies to be better pinpointed than does an energy analysis, and efficiencies to be more rationally evaluated. Many researchers propose that the thermodynamic performance of a process is best evaluated with exergy analysis.

Exergy is defined as the work which can be produced by a stream or system as it is brought into equilibrium with a reference environment, and can be thought of as a measure of the quality (or usefulness) of energy, work having the highest quality. In simple terms, exergy is that portion of energy that is available for performing useful tasks. Exergy is consumed during real processes, and conserved during ideal processes. The exergy consumption during a process is proportional to the entropy created due to process irreversibilities.

Applications of exergy analysis have increased in recent years, and have included investigations of electricity generation and cogeneration (Moran and Shapiro, 2000; Kotas, 1995; Rosen and Le, 1998; Rosen and Berry, 1989; Rosen and Scott, 1985). For conventional energy technologies, energy and exergy analyses have been performed and have yielded useful results. For advanced energy technologies, the use of energy and exergy analyses can be expected to provide meaningful insights into performance that will assist in achieving optimal designs.

EXERGY AND SIMULATION

The second law of thermodynamics is often not considered in modelling and simulation. The present authors believe the lack of second-law considerations is one of the main weaknesses of simulators. Violations of the second law sometimes occur in modelling and simulation (e.g., thermal energy passing of itself from a lower to a higher temperature, and entropy being consumed in a system) if only the first law is considered.

One of the present authors has enhanced two process-simulation computer codes, Aspen Plus and Salt, for exergy analysis (Rosen and Berry, 1989; Rosen and Scott, 1985). The enhancements and their applications are detailed elsewhere (Rosen and Berry, 1989; Rosen and Scott, 1985). It is expected that similar enhancements for exergy analysis can be made to simulation codes for building energy systems.

MODELLING AND ANALYSIS OF A WHOLE BUILDING SYSTEM

Edmonton Power proposed for downtown Edmonton, Alberta, Canada a major cogeneration-based district heating and cooling project having (Edmonton Power, 1991): (i) an initial supply capacity of 230 MW(thermal) for heating and 100 MW(thermal) for cooling, with the potential to expand to about 400 MW(thermal) for heating over the next ten years; (ii) the capacity to displace about 15 MW of electrical power used for electric chillers through district cooling; and (iii) the potential to increase the efficiency of the Rossdale power plant that would provide the steam for district heating and cooling from about 30% to 70%. The design incorporated central chillers and a district cooling network. Screw chillers were to be used originally, and absorption chillers in the future.

This section is based on previous research by the authors (Rosen and Le, 1998) in which the Edmonton Power design for cogeneration-based district heating (using a district heating network and heat exchangers) and district cooling (using central, electrically-driven centrifugal chillers and a district cooling network) was modelled and evaluated thermodynamically. Then, the design was modified by replacing the electric centrifugal chillers with heat-driven absorption chillers, and the evaluation was repeated.

The intent of the present work, in part, is to reveal insights that will aid the designers of such systems in simulation and optimization activities, and in the selection of the proper type of systems for different applications and situations. It is hoped that the present results will permit energy utilities to improve existing plants where appropriate, and to develop better designs.

A second motivating factor in the present work relates to some of the difficulties associated with the types of analysis tools often used for cogeneration/district energy systems. In general, energy technologies are normally examined thermodynamically using energy analysis, although a better understanding is attained when a more complete thermodynamic view is taken. Exergy analysis provides an additional thermodynamic perspective and, in conjunction with energy analysis, permits the performance of more complete thermodynamic analyses. Consequently, both energy- and exergy-based approaches to thermodynamic analysis are considered in this study, both to improve the quality of the results and to demonstrate the usefulness of exergy analysis.

Approach and Methodology

There are two main stages in this study. First, the Edmonton Power design for cogeneration-based district heating and cooling is modelled and evaluated. The system is shown in Figure 1. Then, the design is modified by replacing the electric centrifugal chillers with heat-driven absorption chillers (single- and double-effect types), and re-examined. The modified portion of the system is shown in Figure 2.

The plant is divided into six major components for modelling and analysis purposes. Efficiencies of the individual components and the overall cogeneration-based district energy system are examined. Also,

several subsystems, comprised of selected combinations of the components, are evaluated to pinpoint better the locations and causes of inefficiencies. Both energy and exergy analyses are used throughout the thermodynamic assessments.

For simplicity, economics and part-load operation are not considered in the present understanding. The results and findings are thus correspondingly limited. Also, several simplifying energy-related assumptions are used to keep the paper concise and direct, while still permitting the differences between the energy and exergy results to be highlighted.

Annual energy transfer rates for the cogeneration-based district energy system are shown in Table 1, with details distinguished for the three chiller options considered. The data in Table 1 are used to calculate energy and exergy efficiencies of the systems for the year and for winter (October to April) and summer (May to September) periods.

Analyses of System Components

Cogeneration of Electricity and Heat

The electricity production rate $\dot{W}$ can be expressed for a cogeneration-based system using electric chillers as a function of the product-heat generation rate $\dot{Q}_H$ as

$$\dot{W} = \left(\frac{\eta_{elec}^{CHP}}{\eta_{heat}^{CHP}} \right) \dot{Q}_H \qquad (1)$$

and for a cogeneration-based system using absorption chillers as a function of the product-heat generation rates, $\dot{Q}_H$ and $\dot{Q}_{gen}$, as

$$\dot{W} = \left(\frac{\eta_{elec}^{CHP}}{\eta_{heat}^{CHP}} \right) \left(\dot{Q}_H + \dot{Q}_{gen} \right) \qquad (2)$$

where η_{elec}^{CHP} and η_{heat}^{CHP} denote respectively the electrical and heat efficiencies of the cogeneration, or combined heat and power (CHP), plant. The total energy efficiency can be written for cogeneration using electric chillers as

$$\eta_{tot}^{CHP} = \frac{\dot{W} + \dot{Q}_H}{\dot{E}_f} \qquad (3)$$

and for cogeneration using absorption chillers as

$$\eta_{tot}^{CHP} = \frac{\dot{W} + \dot{Q}_H + \dot{Q}_{gen}}{\dot{E}_f} \qquad (4)$$

where $\dot{E}_f$ denotes the fuel energy input rate. The corresponding total exergy efficiency can be expressed for cogeneration using electric chillers as

$$\psi_{tot}^{CHP} = \frac{\dot{W} + \tau_{Q_H} \dot{Q}_H}{(R\dot{E})_f} \qquad (5)$$

and for cogeneration using absorption chillers as

$$\psi_{tot}^{CHP} = \frac{\dot{W} + \tau_{Q_H} \dot{Q}_H + \tau_{Q_{gen}} \dot{Q}_{gen}}{(R\dot{E})_f} \qquad (6)$$

where τ_{Q_H} and $\tau_{Q_{gen}}$, respectively, are the exergetic temperature factors for $\dot{Q}_H$ and $\dot{Q}_{gen}$. For heat transfer at a temperature T, $\tau \equiv 1 - T_o/T$ (Moran and Shapiro, 2000; Kotas, 1995), where T_o denotes the environmental temperature. Here, R denotes the energy grade function, values of which for most fossil fuels are between 0.9 and 1.0 (Moran and Shapiro, 2000; Kotas, 1995).

Chilling

Edmonton Power has annual free cooling of 33 GWh/yr; the cooling requirement of the chilling plant is 169 GWh/yr. The *COP* of the centrifugal chiller in the design is 4.5 (Edmonton Power, 1991). Thus, the annual electricity supply rate to the chiller is $\dot{W}_{ch}$ = 169/4.5 = 38 GWh/yr. For the chilling operation, including free cooling and electrical cooling, *COP* = (169 + 33)/38 = 5.32. The net electricity output ($\dot{W}_{net}$) of the combined cogeneration/chiller portion of the system is 433 – 38 = 395 GWh/yr, where the electrical generation rate of the cogeneration plant is 433 GWh/yr. Similarly, the coefficient of performance for the chilling operation, including free cooling, using single-effect absorption cooling is *COP* = 202/252 = 0.80, and using double-effect absorption cooling is *COP* = 202/141 = 1.43. It is noted for the absorption chiller cases that, since the work required to drive the solution and refrigeration pumps is very small relative to the heat input (often less than 0.1%), this work is neglected here.

The exergy efficiency can be written for the chilling operation using electric chillers as

$$\psi_{ch} = \frac{-\tau_{Q_C} \dot{Q}_C}{\dot{W}_{ch}} \qquad (7)$$

and using absorption chillers as

$$\psi_{ch} = \frac{-\tau_{Q_C} \dot{Q}_C}{\tau_{Q_{gen}} \dot{Q}_{gen}} \qquad (8)$$

Transport of Heat and Cool

District heating utilizes hot water supply and warm water return pipes, while district cooling utilizes cold water supply and cool water return pipes. The pipes are assumed here to be perfectly insulated so that heat loss or infiltration during fluid transport can be neglected. Hence, the energy efficiencies of the district heating and cooling portions of the system are both 100%. The exergy efficiency can be evaluated for district heating as

$$\psi_{DH} = \frac{\tau_{Q_H^u} \dot{Q}_H^u}{\tau_{Q_H} \dot{Q}_H} \qquad (9)$$

and for district cooling as

$$\psi_{DC} = \frac{-\tau_{Q_C^u} \dot{Q}_C^u}{-\tau_{Q_C} \dot{Q}_C} \qquad (10)$$

Utilization of Heat and Cool

Heat loss and infiltration for the end-use heating and cooling components are assumed negligible here so that their energy efficiencies are 100%. The exergy efficiency can be expressed for end-use heating as

$$\psi_{UH} = \frac{\tau_{Q_H^{u,s}} \dot{Q}_H^{u,s} + \tau_{Q_H^{u,w}} \dot{Q}_H^{u,w}}{\tau_{Q_H^u} \dot{Q}_H^u} \qquad (11)$$

and for end-use cooling as

$$\psi_{UC} = \frac{-\tau_{Q_C^{u,r}} \dot{Q}_C^{u,r}}{-\tau_{Q_C^u} \dot{Q}_C^u} \qquad (12)$$

The left and right terms in the numerator of Eq. 11 represent the thermal exergy supply rates for space and hot-water heating, respectively.

Analysis of Overall System

Since there are three different products generated (electricity, heat and cool), application of the term energy efficiency here is prone to be misleading (Rosen and Le, 1995), in part for the same reason that "energy efficiency" is misleading for a chiller. Here, an overall-system "figure of merit" f_{sys} is used, and calculated as follows (Rosen and Le, 1995):

$$f_{sys} = \frac{\dot{W}_{net} + \dot{Q}_H^{u,s} + \dot{Q}_H^{u,w} + \dot{Q}_C^{u,r}}{\dot{E}_f} \qquad (13)$$

The corresponding exergy-based measure of efficiency is simply an exergy efficiency, and is evaluated as

$$\psi_{sys} = \frac{\dot{W}_{net} + \tau_{Q_H^{u,s}} \dot{Q}_H^{u,s} + \tau_{Q_H^{u,w}} \dot{Q}_H^{u,w} - \tau_{Q_C^{u,r}} \dot{Q}_C^{u,r}}{(\dot{E})_f} \qquad (14)$$

Results and Discussion

Efficiencies of the overall cogeneration-based district energy system, for the three chiller cases considered, are presented in Table 2. The efficiencies for the heating and cooling sides of the overall system are also presented in Table 2. The overall energy efficiencies are seen to vary, for the three system alternatives considered, from 83 to 94%, and exergy efficiencies from 28 to 30%.

The results demonstrate that energy efficiencies do not provide meaningful and comparable results relative to exergy efficiencies when the energy products are in different forms. For example, the energy efficiency of the overall process using electric chillers is 94%, which could lead one to believe that the system is very efficient. The exergy efficiency of the overall process, however, is 28%, indicating that the process is far from ideal thermodynamically. The exergy efficiency is much lower than the energy efficiency in part because heat is being produced at a temperature (120°C) higher than the temperatures actually needed (22°C for space heating and 40°C for hot-water heating). The low exergy efficiency of the chillers is largely responsible for the low exergy efficiency for the overall process.

The exergy efficiencies of the cooling side of the system are relatively low, ranging from 9% to 14% (Table 2). These low efficiency value can be explained by noting that the cool-water supply temperature (11°C) needed for space cooling (to 22°C) is relatively near to the environmental temperatures (in summer). The exergy of the cool is small compared with the work input to drive the electric centrifugal chiller. The excess exergy input via work is destroyed due to irreversibilities.

The exergy-based efficiencies in Table 2 are generally different than the energy-based ones because the energy efficiencies utilize energy quantities which are in different forms, while the exergy efficiencies provide more meaningful and useful results by evaluating the performance and behaviour of the systems using work equivalents for all energy forms. The exergy and energy for electricity are the same while the exergy for the thermal energy forms encountered here is less than the corresponding energy.

The results for cogeneration-based district energy systems using absorption chillers (single-effect and

double-effect types) and using electric chillers are, in general, similar. Generally, the results appear to indicate that the three integrated cogeneration and district energy systems considered have similar efficiencies. It is likely, therefore, that the choice of one option over another will be strongly dependent on economics and other factors (e.g., environmental impact, space availability, noise limitations, etc.).

MODELLING OF IN-GROUND BUILDING SYSTEM COMPONENTS

The impact is considered of heat losses in the ground, which can be significant for system components that are on- or in-ground.

Heat and Moisture Transport in Ground

Heat and moisture transport in ground is a complex phenomenon. The governing equations are coupled and usually must be solved simultaneously using numerical methods. A computer model based on finite element methods, called G-HEADS (Tarnawski and Leong, 1990), has been developed for analyzing ground thermal energy storage with a ground heat exchanger. The performance of a ground-coupled heat pump system depends strongly on the moisture content and the soil type (Leong, Tarnawski and Aittomäki, 1998). Besides the natural variation of soil moisture content throughout a year, moisture variation in ground can be further augmented by the temperature gradients due to heat extraction and deposition, leading to significant change in soil thermal properties. With modifications, G-HEADS can be used for predicting thermal energy and exergy losses or gains for district pipes in the ground within a heating or cooling season.

District Heating and Cooling

District heating utilizes hot water supply and warm water return pipes, while district cooling utilizes cold water supply and cool water return pipes. The pipes can be on or below ground. For a realistic analysis, the heat loss or gain during fluid transport should be considered, even if the pipes are insulated. Hence, the energy efficiencies of the district heating and cooling portions of the system are both actually less than 100%. The thermal interaction between heating/cooling pipe and ground can be very complex. A dynamic simulation of the process should include weather data for the ground-air boundary interaction and soil thermal and hydraulic properties for heat and moisture transport in soils. The exergy efficiency can be evaluated by extending Eqs. 9 and 10 to account for thermal losses/gains for district heating as

$$\psi_{DH} = \frac{\tau_{Q_H^a}\,\dot{Q}_H^a - \tau_{Q_H^l}\,\dot{Q}_H^l}{\tau_{Q_H}\,\dot{Q}_H} \qquad (15)$$

and for district cooling as

$$\psi_{DC} = \frac{-\tau_{Q_C^a}\,\dot{Q}_C^a + \tau_{Q_C^g}\,\dot{Q}_C^g}{-\tau_{Q_C}\,\dot{Q}_C} \qquad (16)$$

The right terms in the numerator of Eqs. 15 and 16 represent the piping thermal exergy loss and gain in the ground, respectively.

The corresponding exergy-based measure of efficiency is simply an overall system exergy efficiency, and is evaluated by similarly extending Eq. 14 as

$$\psi_{sys} = \frac{\begin{pmatrix} \dot{W}_{net} + \tau_{Q_H^{a,s}}\,\dot{Q}_H^{a,s} + \tau_{Q_H^{a,w}}\,\dot{Q}_H^{a,w} \\ -\tau_{Q_C^{a,r}}\,\dot{Q}_C^{a,r} - \tau_{Q_H^l}\,\dot{Q}_H^l + \tau_{Q_C^g}\,\dot{Q}_C^g \end{pmatrix}}{(RE)_f} \qquad (17)$$

Thermal Energy Storage

Building energy systems may involve thermal energy storage. For example, a ground-coupled heat pump system can extract low-grade heat, which may be deposited in the ground during summer using the waste heat from a central chiller and/or by natural means, for space heating in winter. This low-grade heat can also be extracted using a heat pump for domestic hot water during both winter and summer. Utilizing thermal energy storage may increase energy and exergy efficiencies of building energy systems.

LONG-TERM RESEARCH NEEDS

Two key areas of research related to building energy systems and their simulation that appear to be needed emanate from the present work:

- the inclusion of exergy methods in building energy system simulation, and
- better accounting for the heat losses associated with in- or on-ground components of whole building systems.

CONCLUSIONS

This work has helped improve our understanding of the efficiencies of the components that comprise an integrated system for cogeneration and district energy. In particular, exergy analysis provides important insights into the performance and efficiency. The present results indicate that the complex array of energy forms involved in cogeneration-based district energy systems make them difficult to assess and compare thermodynamically without exergy analysis. This difficulty is primarily attributable to the different nature and quality of the three product energy forms:

electricity, heat, and cool. The difficulties in dealing with systems involving many in-ground components (e.g., underground distribution pipes in district heating and cooling networks, and underground thermal energy storages) have also examined. The results are expected to aid designers of such systems in development and optimization activities, and to assist developers and users of simulation tools for building systems.

ACKNOWLEDGMENTS

Financial support was provided by the Natural Sciences and Engineering Research Council of Canada.

NOMENCLATURE

COP	coefficient of performance
E	energy
f	figure of merit
Q	heat
T	temperature
W	work
R	energy grade function
η	energy efficiency
τ	exergetic temperature factor
ψ	exergy efficiency

Subscripts

C	cooling
ch	chiller
DH	district heating
DC	district cooling
elec	electrical
f	fuel
gen	generator of absorption chiller
H	heating
heat	heat
net	net
o	environmental state
sys	system
tot	total
UH	end-use heating
UC	end-use cooling

Superscripts

.	rate with respect to time
CHP	combined heat and power (cogeneration)
g	gain
l	loss
r	room
s	space
u	end-use
w	water

REFERENCES

Edmonton Power (1991) (approx.), City of Edmonton District Energy Development Phase, Section 2: Engineering Report.

Kotas, T.J. (1995), *The Exergy Method of Thermal Plant Analysis*, reprint edition, Krieger, Malabar, Florida.

Leong, W.H., Tarnawski, V.R. and Aittomäki, A. (1998), 'Effect of Soil Type and Moisture Content on Ground Heat Pump Performance', *Int. J. Refrig.*, 21, 595-606.

Moran, M.J. and Sciubba, E. (1994), 'Exergy Analysis: Principles and Practice,' *J. Engineering for Gas Turbines and Power*, 116, 285-290.

Moran, M.J. and Shapiro, H.N. (2000), *Fundamentals of Engineering Thermodynamics*, 4th ed., Wiley, New York.

Rosen, M.A. and Berry, G.F. (1989), 'The Enhancement of the SALT Simulation and Analysis Code for First- and Second-Law Analysis.' In *Thermodynamic Analysis and Improvement of Energy Systems*, ed. Cai Ruixian and M.J. Moran, Pergamon, Toronto, 472-480.

Rosen, M.A. and Le, M.N. (1995), 'Efficiency Measures for Processes Integrating Combined Heat and Power and District Cooling.' In *Thermodynamics and the Design, Analysis and Improvement of Energy Systems*, AES-Vol. 35, ASME, New York, 423-434.

Rosen, M.A. and Le, M.N. (1998), 'Thermodynamic Assessment of the Components Comprising an Integrated System for Cogeneration and District Heating and Cooling.' In *Proc. ASME Advanced Energy Systems Division*, AES-Vol. 38, ASME, New York, 3-11.

Rosen, M.A. and Scott, D.S. (1985), 'The Enhancement of a Process Simulator for Complete Energy-Exergy Analysis.' In *Analysis of Energy Systems - Design and Operation*, AES-Vol. 1, ASME, New York, 71-80.

Tarnawski, V.R. and Leong, W.H. (1990), *Computer Simulation of Ground Coupled Heat Pump Systems*, Report submitted to National Research Council, Ottawa.

Table 1. Annual Energy Transfer Rates (in GWh) for the Cogeneration-Based District Energy System[1]

Type of energy	Winter period, T_o = 0°C	Summer period, T_o = 30°C
District heating, $\dot{Q}_H$	0.8946 × 1040 = 930	0.1054 × 1040 = 110
Water heating, $\dot{Q}_H^{u,w}$	(22 GWh/yr/mo.) × 7 mo. = 154	0.1054 × 1040 = 110
Space heating, $\dot{Q}_H^{u,s}$	930 – 154 = 776	0
Space cooling, $\dot{Q}_C$	0	1.00 × 202 = 202
Electric chiller case		
Total electricity, $\dot{W}$	0.8946 × 433 = 388	0.1054 × 433 = 45.6
Input energy, $\dot{E}_f$	0.8946 × 1733 = 1551	0.1054 × 1733 = 183
1-stage absorption chiller case		
Heat to drive absorption chiller, $\dot{Q}_{gen}$	0	1.00 × 252 = 252
Total electricity, $\dot{W}$	0.8946 × 433 = 388	25/60(110 + 252) = 151
Input energy, $\dot{E}_f$	0.8946 × 1733 = 1551	(110 + 252)/0.6 = 603
2-stage absorption chiller case		
Heat to drive absorption chiller, $\dot{Q}_{gen}$	0	1.00 × 141 = 141
Total electricity, $\dot{W}$	0.8946 × 433 = 388	21/64 × (110 + 141) = 82
Input energy, $\dot{E}_f$	0.8946 × 1733 = 1551	(110 + 141)/0.64 = 391

[1] The winter period (October-April) accounts for 89.46% of the annual heating load and 0% of the annual cooling load, and the summer period (May-September) for the remaining annual heating and cooling loads.

Table 2. Overall and Subsystem Efficiencies for the Cogeneration-Based District Energy System

Subsystem	Energy efficiency, η (%)			Exergy efficiency, ψ (%)		
	Centrifugal chiller	1-stage absorption chiller	2-stage absorption chiller	Centrifugal chiller	1-stage absorption chiller	2-stage absorption chiller
Heating side[1]	85	85	85	30	31	31
Cooling side[2]	532[3]	80[3]	143[3]	14	9	12
Overall system	94	83	88	28	29	29

[1] The heating side includes cogeneration, district heating and end-use heating.
[2] The cooling side includes chilling, district cooling and end-use cooling.
[3] These are coefficient of performance (*COP*) values when divided by 100.

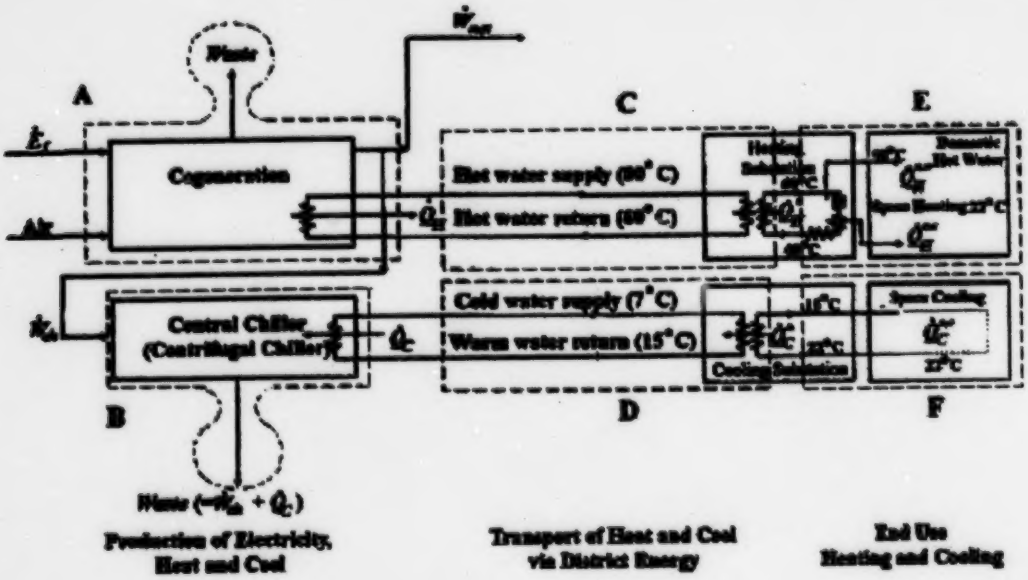

Figure 1. Simplified diagram of the cogeneration-based district energy system proposed by Edmonton Power. The system, which uses electric chillers, is divided into six subsections within three categories. On the left are production processes, including cogeneration of electricity and heat (A) and chilling (B). In the middle are district-energy transport processes, including district heating (C) and district cooling (D). On the right are end-user processes, including user heating (E) and user cooling (F).

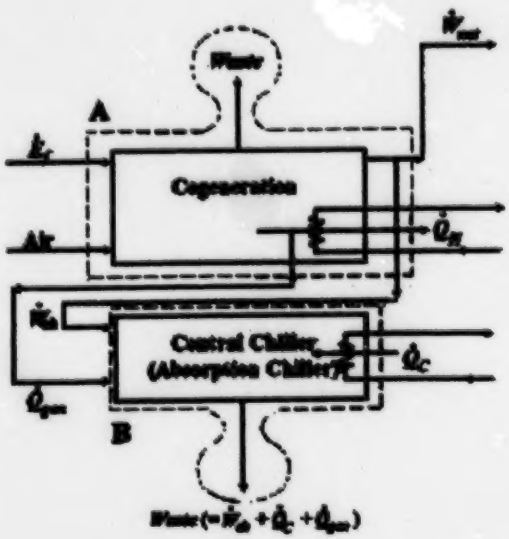

Figure 2. Modified version of production processes (units A and B) for the simplified diagram in Figure 1. In the modified system, the electric chillers are replaced with absorption chillers (single- or double-effect), driven mainly by heat from the cogeneration plant. The rest of the system in Figure 1 (units C to F) remains unchanged in the modified system. The temperature of the heating medium supplied to the absorption chillers is higher for the double-effect chiller relative to the single-effect machine.

DYNAMIC SIMULATION OF BUILDING HEATING SYSTEMS CONNECTED TO A DISTRICT HEATING SYSTEM

L. Yang C. W. Snoek
CANMET Energy Technology Centre
Natural Resources Canada
1 Haanel Dr., Nepean, ON K1A 1M1
Phone: (613) 995-0191 (613) 992-1832
Fax: (613) 947-9691
E-mail: lyang@nrcan.gc.ca csnoek@nrcan.gc.ca

ABSTRACT

A novel methodology for simulating and evaluating energy and cost performance of buildings connected to a district heating (DH) system is presented in this paper. The simulation includes the entire DH system, which consists of the heat production plant, the heat distribution system, the buildings to be supplied and their heating systems. This methodology used a simple model to represent a complex district heating system, which makes the long-term time-series simulations easy and fast.

The developed methodology was demonstrated using a heating system for commercial buildings, connected to a DH network supplied by a combined heat and power (CHP) plant. This system was simulated for an entire heating season with measured hourly weather data, using fully dynamic simulation models that were developed based on general heat transfer theory and thermodynamic principles.

The simulation results were used to compare the performance of building heating systems with different configurations, control strategies and operating parameters. From the results, a cost-performance optimization of building heating systems can be determined.

Furthermore, the simulation methodology can be used as a design tool for consulting engineers to evaluate the performance of conceptual building heating systems not only under peak load, but also under partial loads. Also, it can be a valuable diagnostic tool for examining the performance of existing building heating systems.

INTRODUCTION

In many countries where district heating is used extensively, there is a discernable trend towards low temperature operation of these systems. Also, increasing the temperature difference between supply and return results in monetary savings to the DH companies due to lower pumping energy requirements. Decreasing the temperature levels in DH systems reduces heat losses, gives better performance potential of combined heat and power plants and provides the possibility for utilization of low grade energy sources.

A DH system consists of three main components: the heat production plant, the heat distribution system and the buildings to be supplied and their heating systems. Low temperature operation of DH systems, however, increases the building heating systems capital cost because more heat transfer surface is required. The minimum supply temperature in the DH system is ultimately limited by the performance of the building heating systems. To thoroughly simulate and evaluate the thermodynamic and economic performance of different building heating systems connected to a DH system, all three components should be taken into consideration as an integrated whole.

Different building heating system configurations which have similar performance at peak load (design load) can have significantly different characteristics at partial load (Van der Meulen 1991). The more statistical data available on system performance under different operating conditions, the more accurately energy recoverable from waste heat sources and backup boiler operation can be predicted. Therefore, long-term time-series simulations are necessary in order to carry out accurate energy and cost performance studies of different building heating systems (Snoek 1997 and Onno 1998).

The simulation and analysis of entire DH systems are complicated by the great number of parameters involved. Furthermore, the structure of the network is complicated as it may involve hundreds of different diameters, heat loss coefficients, flow rates, etc. It obviously will require an enormous amount of effort to

build a computer model and a long time to perform these time-series simulations.

Most of the previous work on simulating and evaluating the performance of building heating systems connected to a DH system concentrated on the building systems themselves (Hjorthol 1992, Yang 1994 and Volla 1996).

Snoek (1997) demonstrated a methodology for cost-performance optimization of building heating systems by modeling an entire DH system for a full year. However, a very simple distribution network system with only three consumers was modeled.

Under Annex V of the International Energy Agency (IEA) Implementing Agreement on District Heat and Cooling, studies on optimization of operating temperature of district heating were performed (Woods 1999). The optimization included all three components of the DH system. Complex distribution networks were selected. However, the network models were steady state (i.e., the thermal storage capacity of the network and transportation time delay were not considered in the model.) The heat production plant and the distribution network were simulated in spreadsheet software only, for 16 typical days of the year using output data from a full-year dynamic simulation of the building heating systems.

There is a need to develop a methodology to make long-term time-series dynamic simulations of the entire DH system simple, fast and accurate. This paper describes a methodology for simulating and evaluating energy and cost-performance of building heating systems, connected to a DH system, by using a simplified district heating system model.

METHODOLOGY FOR SIMULATING DH SYSTEMS

Studies (Zhao, 1995) have shown that a complicated DH network can be simplified to an equivalent network with one consumer connected to the power plant by a pair of pipes (the supply and return). The simplified network model is generated by gradually reducing the topological complexity of the original network (without loops) using an aggregation method. During this reduction, the relevant model parameters of the network are transformed in such a way that the dynamic behavior of the network resembles the original one. Zhao (1995) verified the accuracy of the method for creating equivalent systems, and concluded that the simplified network with a single pair of pipes still represented the dynamic behavior of the original complex network with reasonable accuracy.

In this paper, a simple model of the DH system presented by Bøhm (1981, 1988) is adopted. The simple model illustrated in Figure 1 is used to represent a DH system with a complex network. The DH system is approximated as a single pipe, a single consumer, and a single bypass. However, as stated above, the dynamic behavior of the simple model resembles the original one.

Computer models of components with thermodynamic effects on the system were created using Simulink® software by the Math Works Inc. These fully dynamic models were developed based on general heat transfer theory and thermodynamic principles. All models were pre-built in Simulink® as subsystems in icon form. The simulation model for the DH system was created by connecting these component models based on the actual system configuration.

The district heating system was simulated for an entire heating season since it was assumed that there were no load requirements in the summer. Measured hourly weather data were used in the simulations. The weather data will be described in detail in the "Description of the DH System Model" section.

The simulation raw output data can be examined in time-series format, leading to a better intuitive understanding of the more subtle aspects of the

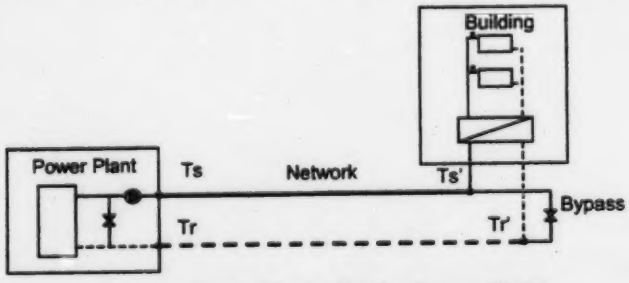

Fig. 1 A Simple District Heating System Model.

building heating system performance. System economic studies can be accomplished accurately even if the cost of fuel and/or electricity is a time dependent variable.

SYSTEM DESIGN

The methodology for simulating and evaluating the energy and cost performance of building heating systems connected to DH systems can be best demonstrated by a simple example. In this example, we assumed that a DH end user was connected to a DH network which was supplied by a CHP plant with internal combustion (IC) engine. Two building heating systems were simulated and compared. One was designed as the reference system (System A). The other was a system with larger radiator heat transfer area (System B), which resulted in lower DH return temperatures, compared to the reference system.

It should be mentioned that the objective of this paper is to demonstrate the methodology of simulating and evaluating the energy and cost performance of the entire DH system. Therefore, emphasis is placed on the methodology rather than the complexity of the physical situation and validity of the assumptions.

The detailed descriptions of the CHP plant, the distribution network and the building systems are as follows.

Power Plant

The power plant is a CHP plant with an internal combustion engine using natural gas as the fuel. The available waste heat is about 50% of the total fuel energy input to the IC engine. The breakdown of the energy balance of the IC engine is listed in the following.

- 31% electrical energy
- 18% jacket cooling water (at 95°C), recoverable heat
- 26% exhaust gas (at 410°C), recoverable heat
- 6% lubrication oil (at 80°C), recoverable if the return DH temperature is low enough
- 19% exhausted and radiated heat which are non-recoverable.

A constant electricity output of 2.5 MW_e, was assumed in this example. Therefore, the available waste heat was constant as well (4.1MW_{th}). The methodology is also applicable to variable electricity output, but this option is not pursued in this paper. The assumed CHP plant was able to cover 40% of the building heating peak load. A natural gas fired peaking boiler with an efficiency of 90% was used to supply the remaining heat load. The supply temperature at the power plant was 90°C and constant. Figure 2 shows the flowchart of the CHP plant heat recovery system.

Distribution Network

As discussed in the previous section, the distribution network was simplified to one pair of pipes. The equivalent length of the network was 1000 meters and the equivalent diameter was 350 mm.

A bypass is located at the end user to avoid the system water cooling off to the point where it is unsuitable for the radiator heating, see Figure 1.

Building Heating Systems

The end user was assumed to represent a group of seven identical commercial buildings. These buildings were located in Toronto, Ontario. Each building had a peak heating load of 1.45 MW, for a total of 10.2 MW_{th}. The room temperature set point was kept at a constant 20°C. The building heating system was indirectly connected to the DH network, as shown in Figure 3.

Domestic hot water usage was not supplied by the DH system and was not included in the simulations.

Two building heating systems were studied. The first system (System A) was designed so that the DH return temperature from the building is 80°C at design

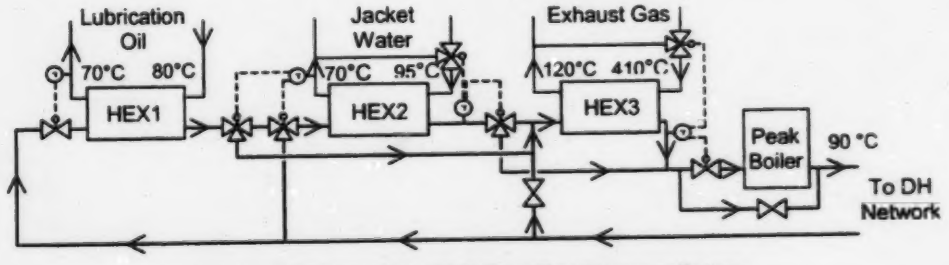

Fig. 2 Flowchart of the CHP Plant Heat Recovery System.

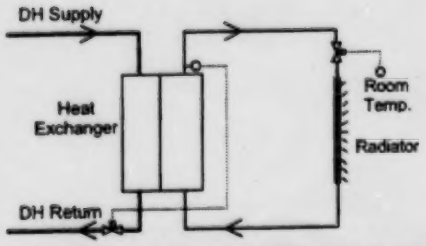

Fig. 3 Diagram of the Building Heating System.

conditions. In the second system (System B), the radiator surface area was enlarged to give a lower DH return temperature, 65°C, at design condition.

DESCRIPTION OF THE DH SYSTEM MODEL

Hardware components that have thermodynamic impact on the DH system were available in the form of numerical models. For the example systems, these components were the building, and the heat exchangers and radiators of the building heating system. Models of the plate heat exchangers and fin-coiled heat exchanger for the extraction of energy in the lubrication oil, cooling water and exhaust gas in the CHP plant heat recovery system were also available, as were models of the distribution pipes in the DH network and control valves. Some of the simulation models were based on a previous IEA Annex V project done by the CES group of CANMET (Woods 1999).

Computer models were created using Simulink® software by the Math Works Inc. Simulink® is a visually programmed mathematical modelling tool which offers direct simulation of graphically-constructed block diagrams. The block diagram interface makes the models easy to build and easy to understand.

A description of the different models is given in the following sections.

Building Model

In order to accurately simulate a complete district heating system, the building model must realistically respond to steady state and dynamic effects of weather conditions and building occupancy. Since the DH system simulation studies are aimed at discovering the effects of changes to the heating systems while keeping the building envelope constant, high absolute accuracy of any given building model is not necessary. Therefore, a number of simplifications were incorporated to speed up the simulation process. Figure 4 shows the diagram of the simplified building model. The primary emphasis of the building model was to include all transfer functions that have a significant influence on the characteristics of the various buildings that make up a typical community. A detailed model description and verification can be found in Onno (1998).

The heat loss factor and thermal masses were estimated from monitoring data obtained during the winter of 1996-97 in a school in Cornwall, Ontario, Canada.

Although they are included in the building model, solar radiation and internal gain were not considered in this example.

Heat Exchanger Models

The heat exchanger models were based on general heat transfer theory and thermodynamic principles. The heat exchanger was divided into a number of elements in water flow direction. A general energy balance equation was developed for the cold fluid, hot fluid and the plate/tube material for each of these elements respectively. The energy balance resulted in a set of first order differential equations. The outlet temperatures of the cold and hot fluid were obtained by solving these equations. Detailed description of the heat exchanger model can be found in Yang (1994) and Woods (1999).

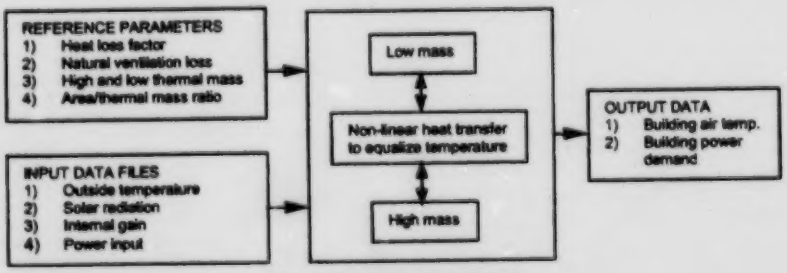

Fig. 4 Simplified Building Model.

Plate Radiator Model

The radiator model was developed using the same methodology used for developing the heat exchanger model. The heat transfer from the radiator to the surrounding space was by free convection and radiation from the outside surface area. The modeled radiator was divided into a number of elements in the water flow direction. The outlet temperature of the water was obtained by solving the general energy balance equations. A description and verification of the plate radiator model can be found in Woods (1999).

DH Network Model

The network model is used to calculate heat losses from the DH pipes and required pumping energy for transporting the DH water. As described earlier, an equivalent network with one pair of supply and return pipes was used to represent the DH network.

The simplified network model can be generated by gradually reducing the topological complexity of the original network (without loops) using an aggregation method. The relevant model parameters of the network were transformed in such a way that the dynamic behavior of the equivalent network resembled the original one. The time delay of the equivalent network was equal to the average time delay of all consumers weighted by the flow to each consumer. The heat loss of the equivalent network was equal to the heat loss of the real network.

The following assumptions were used in the aggregation method:

- All dimensional data of the pipes are known and the network is a tree type network.
- The supply and return pipe are identical and isothermal.
- All consumers have the same temperature difference between the DH supply and return water.

Since the supply pipe and return pipe were assumed to be identical, only one pipe was considered in the aggregation. The water volume of the equivalent network (pipe) is the sum of the water volume in pipes where flow is non zero.

$$V_w = \sum_{i \neq j} V_{w,i}$$

where volume flow f_j=0 and i is the pipe number.

The steel volume V_s and overall heat loss coefficient H_e (W/°C) of the equivalent network can be obtained in the same way.

After a diameter of the equivalent pipe, D_e, is selected (e.g. as the diameter of the largest pipe in the network), the length of the equivalent pipe can be obtained by

$$L_e = \frac{V_w}{(\pi/4)D_e^2}$$

The time delay of the equivalent pipe is calculated by

$$\tau_e = V_e / f_e$$

where f_e is the volume flow rate (m^3/s) of the equivalent pipe and V_e is the volume (m^3) of the equivalent pipe.

$$V_e = V_w + V_s(\rho_s c_s / \rho_w c_w)$$

where is density (kg/m^3) and c is specific heat capacity (J/kg·°C). Subscript w is for water and s is for steel.

Since the original network is simplified to a single pair of supply and return pipes, the outlet temperature of the equivalent pipe, at time t, then can be calculated by

$$T_{o(t)} = T_{in(t-\tau_e)} \cdot e^{-\frac{H_e}{L_e(V_w\rho_w C_w + V_s\rho_s C_s)}\tau_e}$$

$T_{in(t-\ )}$ is the inlet temperature of the pipe at time t- , °C.

The heat loss of the equivalent pipe was calculated by

$$Q_l = H_e[(T_o + T_{in})/2 - T_g]$$

where T_g is the undisturbed ground temperature, °C.

In this example, the network model calculated the heat loss based on a winter season average undisturbed ground temperature of 2°C.

The DH pump was modeled as a variable flow unit, adding sufficient head to the system to provide 100 kPa pressure drop at the end user. The pressure drops in the supply and the return lines were assumed the same. The required electrical pumping energy was calculated as a function of flow, pressure loss and overall pump efficiency.

Control Valve Models

There are two-way and three-way control valves in this DH system. It was assumed that these control valves were proportional quadratic valves. The computer models calculated the flow rates through the heat exchangers/radiators based on the set point of the control parameters, see Woods (1999).

Weather Data

As stated previously, the buildings were assumed to be located in Toronto. Toronto weather data was obtained

from the University of Waterloo WATSUN laboratory. The data consists of "20-year average" outdoor temperature and solar radiation data. The calculation of the "average" has been accomplished by taking months with a degree-day accumulation equal to the 20-year average, and using their exact hourly temperature and solar radiation measurements. The normal temperature and radiation variability was therefore included in the data.

The hourly outdoor temperature was used to calculate the required building energy in the building model. For simplicity, solar radiation was not considered in the example simulations.

Overall System Model

All models were pre-built in Simulink® as subsystems in icon form. The Simulink® model for the DH system was created by connecting these component models as required. The CHP plant model was created by connecting the heat exchanger and control valve models based on the configuration shown in Figure 2. Similarly, the model for the DH network and the building heating system was created by connecting the models of network, building, heat exchanger, radiator and control valves together based on the configuration shown in Figure 3.

The CHP plant was simulated separately using the output data (flow and return temperature at the plant) from the simulation of the DH network and the building heating system. This two-stage approach avoided a more complex iterative process between the two models with no loss of accuracy.

The inputs to the model were Toronto hourly weather data, DH supply temperature profile, flow and inlet temperature of the waste heat sources (lubrication oil, jacket cooling water and exhaust gas), as well as the set point of each control parameters.

The outputs were DH water flow and inlet/outlet temperatures at the building and at each heat exchanger in the CHP Plant heat recovery system. The heat losses and required pumping energy of the DH system were also outputs from the model. These outputs were all in time-series format. A time interval of 10 minutes was selected for recording the simulation output data.

The Simulink® model can also easily be programmed in such a way that the data outputs correspond closely to the data available to maintenance engineers on an actual system. This will provide a valuable diagnostic tool for examining the performance of existing building heating systems.

RESULTS AND ANALYSIS

Based on the simulation output data, the amount of energy recovered by the CHP plant waste heat sources and the peaking boiler, heat losses and electrical pumping energy can be easily computed on an hourly, daily, monthly or yearly basis. A cost performance analysis then can be carried out based on the installation cost of the DH system and the price of the fuel, electricity and thermal energy. This section describes the energy and cost performance analyses that were carried out for the systems.

As described in the "System Design" section, two building heating systems were studied. One was a reference system with a design return temperature of 80°C (System A). The other was a modified system with a design return temperature of 65°C (System B). The DH systems were simulated for an entire heating season, from Oct. 1 to April 30.

Using the output data (DH flow and inlet/outlet temperatures at each heat exchanger in the CHP plant heat recovery system), the energy extracted from each waste heat source was computed. Figure 5 shows the hourly value of energy extracted from the different engine waste heat sources when the heating load was high during February.

The simulation results showed that, at high building heating loads, System A (90/80°C) could extract only a fraction of the heat from the lubrication oil and jacket water. Partial heat recovery happened when the building return temperatures were high. System B (90/65°C), however, could recover all available heat from these two waste heat sources due to its relatively low building return temperatures. At times, when the building loads were low (resulting in low building return temperatures), both systems could extract similar amounts of heat from the lubrication oil and jacket cooling water. Figure 5 also shows that both System A and B could extract approximately the same amount of heat from the exhaust gas. This is because the exhaust gas temperature was high compared to either of the building return temperatures.

Table 1 shows the thermal energy recovered from the different heat sources for the entire heating season for building heating System A and B respectively. Also shown in Table 1 is the fuel consumption, the electricity generation by the CHP Plant, the pumping energy and heat losses. The comparisons, between systems A and B, are shown in Table 1 as well.

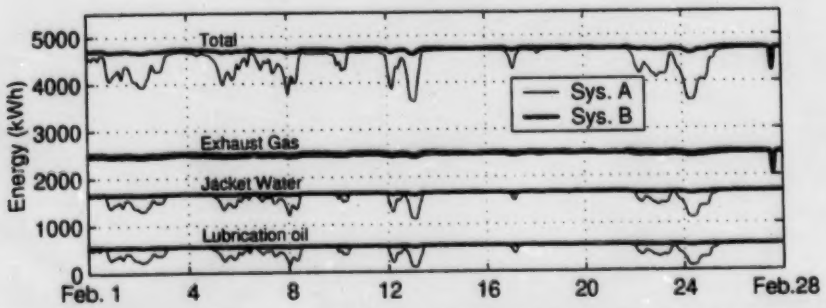

Fig. 5 Energy Extracted from the Different Waste Heat Sources during February.

Table 1 Annual Thermal and Electrical Energy Generation and Fuel Consumption.

	System A (90/80°C)	System B (90/65°C)	Difference % (B-A)
Thermal Energy (MWh_{th})			
Energy recovered from lubrication oil	2,173	2,349	7.2
Energy recovered from jacket cooling water	6,856	7,023	2.3
Energy recovered from exhaust gas	9,270	9,429	1.5
Total Energy Recovered from Waste Heat Sources	**18,299**	**18,801**	**2.5**
Thermal Energy (MWh_{th})			
Total energy recovered from waste heat sources	18,299	18,801	2.5
Energy supplied by the peaking boiler	12,225	11,475	-6.1
Heat losses from the DH system	(2,881)	(2,633)	-8.6
Total Building Thermal Energy Consumption	**27,643**	**27,643**	-
Electrical Energy (MWh_e)			
Electricity generated by the CHP plant	12,600	12,600	-
Pumping energy	(97)	(33)	-66.0
Total Electricity Available to Grid	**12,503**	**12,567**	**0.5**
Fuel (Natural Gas) Consumption (MWh)			
CHP plant consumption	40,645	40,645	-
Peaking boiler consumption	13,583	12,750	-6.1
Total	**54,228**	**53,395**	**-1.5**

Table 2 Annual Net Equivalent Worth Comparison.

	System A (90/80°C)	System B (90/65°C)	Difference (B-A)
Expenses ($)			
CHP capital cost	(305,550)	(305,500)	-
Peaking boiler capital cost	(62,129)	(62,129)	-
Distribution network capital cost	(141,360)	(141,360)	-
Building heating system capital cost	(55,476)	(66,705)	(11,229)
Operation and maintenance cost	(126,000)	(126,000)	-
Labour cost	(25,000)	(25,000)	-
CHP plant fuel cost	(812,900)	(812,900)	-
Peaking boiler fuel cost	(271,667)	(255,000)	16,667
Total	**(1,800,081)**	**(1,794,644)**	
Income ($)			
Sale of electricity to grid	750,180	754,020	3,840
Sale of thermal energy to consumers	1,105,720	1,105,720	-
Total	**1,855,900**	**1,859,640**	
Annual Net Equivalent Worth ($)	**55,819**	**65,096**	**9,278**

Capital cost: CHP $1200/kWe, Peaking boiler $100/kWth, Network $1388/m
Capital recovery factor: 0.10185 (Interest rate: 8%, Amortization period: 20 years)
Operation and maintenance cost: 1¢/kWhe
Natural gas: 2¢/kWh, Electricity: 6¢/kWhe, Thermal energy: 4¢/kWth

The results shown in Table 1 indicate that the building heating system with the lower return temperature (System B) recovered 2.5% more energy from the waste heat sources than System A. The major heat recovery increase resulted from using the heat from the lubrication oil which has a relatively low temperature. System B reduced the overall fuel consumption by 1.5%. This is because the DH water flow in System B was reduced significantly due to the larger difference in supply and return temperatures at the building. The heat losses from System B were also reduced because of the lower temperature in the return pipeline.

Table 2 shows the annual net equivalent worth of the two example systems. Net equivalent worth is the difference between the income and expenses. The economic analysis shows that System B has the higher building heating system capital cost, in order to reduce the return temperature. However, System B utilized more waste heat, and operated with reduced pumping energy and network heat losses. Therefore, System B consumed less fuel and electricity. The net saving of System B was over $9,000, an increase of 16.6% of the annual net equivalent worth.

As mentioned previously, the purpose of this paper was to demonstrate a methodology of simulating a building system connected to a DH system. The analysis shown here is merely an example. More rigorous energy and economic analysis can be carried out by using the simulation output data. Building heating systems with different configurations and control strategies can also be compared using this methodology.

CONCLUSIONS

A methodology for simulating and evaluating energy and cost performance of buildings connected to a DH system is presented. This methodology used a simple model to represent a complex district heating system, which makes the long-term time-series simulations easier and faster.

The simulation results can be used to compare the performance of building heating systems with different configurations, control strategies and operating parameters. From the results, a cost-performance optimization of building heating systems can be determined.

Furthermore, the simulation methodology can be used as a design tool for consulting engineers to evaluate the performance of conceptual building heating systems not only under peak load, but also under partial loads. Also, it can be a valuable diagnostic tool for examining the performance of existing building heating systems.

REFERENCES

Bøhm, B. and Jesen P.T. (1981), *Energy Economic Operation of Existing District Heating Networks*, Energiministeriets Fjernvarmeprogram, rapport nr 2.

Bøhm, B. (1988), *Energy-Economy of Danish District Heating System-A Technical and Economic Analysis*, Technical University of Denmark.

Hjorthol, E.M. and Ulseth, R. (1992), *Consumer Heating System Simulation*, IEA District Heating and Cooling Project Report published by NOVEM, Sittard, The Netherland.

Onno, T. (1998), *Optimization of Building Heating and Domestic Hot Water Systems Supplied by Low Temperature District Heating Water*, Gagest Developments Inc.

Snoek, C. W. et. al. (1997), *Cost-Performance Optimization of Low-Temperature Heating Systems by Statistical Analysis of Full-Year Simulation*, Proceedings of the 6th International Symposium on District Heating and Cooling Simulation, August 28-30, 1997, Reykjavik, Iceland.

Van der Muelen, S.F. et. al. (1991), *Investigation on District Heating*, Final Summary Report, Twente University, Holland.

Volla, R. et. al. (1996), *Efficient Substations and Installations*, SINTEF, the Norwegian Institute of Technology, IEA District Heating and Cooling Annex IV Project Report published by NOVEM, Sittard, The Netherlands.

Woods, P. et al. (1999), *Optimization of Operating Temperatures and an Appraisal of the Benefits of Low Temperature District Heating*, IEA District Heating and Cooling Annex V Project Report published by NOVEM, Sittard, The Netherlands.

Yang, L (1994), *District Heating House Stations with Hot Water Storage-Simulation and Evaluation of Dynamic Performance*, Ph.D. thesis, Technical University of Denmark.

Zhao, H (1995), *Analysis, Modeling and Operation Optimization of District Heating Systems*, Ph.D. thesis, Technical University of Denmark.

Session 6 / Séance 6

Calibration, Validation and Inverse Methods

L'étalonnage, la validation et les méthodes inversées

USE OF SOFT COMPUTING TECHNIQUES FOR THE EVALUATION OF ENERGY PERFORMANCE OF EQUIPMENTS IN BUILDINGS

R. Zmeureanu and L. Farinaccio
Centre for Building Studies
Department of Building, Civil and Environmental Engineering
Concordia University, Montreal, Quebec, CANADA
zmeur@cbs-engr.concordia.ca

ABSTRACT

The paper presents the use of pattern recognition and neural networks techniques for the evaluation of energy performance of equipments. Two methods were developed and validated using measurements of existing equipments.

INTRODUCTION

Soft computing is a collection of methodologies, which aim to exploit tolerance for imprecision, uncertainty and partial truth to achieve tractability, robustness and low solution cost (WFSC 2001). These techniques have been applied to some engineering problems as an alternative to the conventional approaches. The paper presents the application of two of these techniques for the evaluation of energy performance of equipments used in buildings.

APPLICATION NO.1

The breakdown of whole-house electricity consumption among the major end-uses can help to increase of homeowners' awareness about how the energy is used in the house and the potential impact of changing the people's behaviour (e.g., the frequency of usage of clothing washer, or the number and duration of hot showers) on the annual energy cost. Traditional load monitoring techniques can be described as intrusive techniques because the physical placement of sensors on individual appliances to gather end-use load data. Researchers have developed non-intrusive techniques of load monitoring as an alternative to long-term intrusive metering (Hart 1992, Norford 1996, Sharp 1994). Non-intrusive techniques of load monitoring are based on the analysis of appliance energy signatures. An appliance signature gives information about the operating state of an individual appliance, using the monitored whole-house electric demand. The main advantage of defining appliance signatures in terms of the whole-house load is that, afterwards, only a appliance single monitoring point in the house is required to gather end-use load data. The signature is assumed to remain constant for the life of the appliance provided that no modifications are made or malfunctions occur.

Farinaccio and Zmeureanu (1999) and Marceau and Zmeureanu (2000) developed two new rule-based pattern recognition approaches to disaggregate the total electricity consumption of a house into the major end-uses.

Although the two methods use different algorithms, their application has in common the following two phases: (1) a one-time training process required to tune the generic algorithms, to the characteristics of electric demand of each particular house under investigation; during this phase, the electric current is monitored at the main electric entrance of the house as well as at several appliances of interest such as the domestic hot water tank; and (2) the application phase, in which only the electric current at the main electric entrance is monitored.

PATTERN RECOGNITION APPROACH

The new approach is based on the top-down mental process of recognizing an object (Grey 1997), which in this case is the shape of variation of electric current, monitored at the main electric entrance of the house, during the operation of a particular appliance. The step-increase or decrease of the electric current, due to the activation or disactivation of an appliance, is a distinct feature which can be used for the preliminary recognition of objects. The pre-existing knowledge is used to generate a hypothesis about the object (e.g., the increase of electric current is due to the activation of a refrigerator). However, the hypothesis could be false for at least two reasons: (i) the signal is generated by the simultaneous operation of other appliances and not by a single appliance, and (ii) there are two or more appliances which can generate almost the same initial signal. Moreover the noise generated by the operation of several small appliances or by the variation of electric voltage in the utility lines could

mask the real signal. In the following step, the hypothesis is tested, using additional features of each class of objects such as the variation of electric current in time or the frequency of activation. The hybrid combination strategy is preferred to connect the rules used for the recognition of objects: (i) some rules are applied sequentially, one after the another, to reduce the preliminary set of possible objects, and (ii) other rules are applied concurrently and independently, and their results are integrated using weighting factors.

The generic algorithms presented in this paper are developed from the analysis of electric current, monitored in a test house over a training period of one week. The house is heated by a central hot water system using oil as energy source. The monitoring equipment consisted of clamp-on sensors and data loggers to record the measurements, performed every 16 seconds. Since the electric demand (W) is better perceived by the readers, the energy signature is developed in terms of electric demand, using a constant voltage. This substitution does not affect the accuracy of results, mainly the evaluation of energy share, which is defined as the contribution of each appliance to the whole-house electricity consumption.

The algorithms are only based on monitored data and do not need information about the occupants' lifestyle and usage of appliances. Once the generic algorithms have been developed, they can be applied to other houses. However, some parameters used by the generic algorithms will have to be modified, through the training process, to fit the electric characteristics of appliances in each house.

The first pattern recognition approach is used to recognize the operation of DHW heater based on the total demand profile. The algorithm consists of three stages: (1) the detection of the activation (ON or start event) or disactivation (OFF or end event) of the appliance, by using its energy signature, (2) the estimation of the appliance's demand profile, and (3) the calculation of energy use.

The first stage of the algorithm consists of five pattern-recognition rules, which are used to identify start and end events from the monitored total demand profile. The first rule, or the *state change detection* rule, is applied to determine a preliminary set of possible start and end events based solely on the detection of a given step-increase or decrease in the total demand profile. The following three rules: the *profile vector norm* rule, the *number of data points* rule, and the *total demand* rule are then applied to each possible event. An aggregate score of the performance for these three rules is then attributed to each event. This aggregate score is then used to confirm or refute the occurrence of an event as recognized by the first rule. The *minimum score* rule is used to filter out the weak events from the data set of possible events, that is, those events with low aggregate scores. The remaining set of selected start and end events proceed to the second stage of the algorithm, which consists of three constraining rules: the *highest scoring event* rule, the *minimum ON and OFF interval* rule, and the *minimum total demand* rule. Unlike the first stage of the algorithm, where the rules try to match the variation in total demand with the characteristic increase of each appliance, the goal of these rules is to verify that the DHW ON periods estimated in the first stage of the algorithm are consistent with the frequency of appliance usage and the monitored data observed from the training period. Similar to the first rule, these rules are applied on a pass or fail basis. For example, an event is either confirmed as a start event or is recognized as a false start event, in which case, it is eliminated from the data set of possible start events. Consecutive start and end events are then linked together to obtain the sequence of activation periods of the DHW heater. Once the ON and OFF periods of the appliance are estimated, the DHW energy consumption for the duration of the day is then calculated.

The accuracy of the algorithm is assessed in terms of three performance indices: (i) daily DHW energy consumption, (ii) daily DHW demand profile, and (iii) daily energy share, that is the ratio of the DHW energy consumption to the whole-house energy consumption.

The error in estimating the daily DHW energy consumption, with respect to the monitored values, is under 7%. Only for four out of 19 days of testing, the error was between -10.5% and 15.9%.

Two statistics are used to evaluate the accuracy of the estimated DHW demand profile compared to the monitored profile: the coefficient of determination (R-squared) and the average error, which is calculated using the absolute values of errors for each individual cycle. For any given day, the estimated profile tracks the monitored profile fairly well. The average error varies between 11 W and 312 W, that is, 0.2 and 7% of the average electric demand of 4455 W, observed during the training period.

From the homeowner's point of view, the most useful result is the estimation of the energy share, that is,

the contribution of this appliance to the whole-house energy consumption and cost. For any given day, the error in estimating the DHW heater energy share is between –5.1% and 5.5%. On a weekly basis, the average difference is below 2.5%.

APPLICATION NO.2

Energy Monitoring and Control Systems (EMCS) installed in buildings should allow for the comparison of monitored energy performance of HVAC equipments with the predicted performance. This comparison can help the building managers to detect abnormal operating conditions, due to failures or deterioration of the equipment efficiency, or unexpected changes due to people's habits. This function can also evaluate the cost-effectiveness of the equipment retrofit or replacement.

There are two elements preventing the implementation of such capabilities in the EMCS: (1) the increase of initial cost due to the type and number of sensors, which are required for the monitoring of relevant parameters, and (2) the complexity of application software, used to compare the monitored and predicted energy performance.

This paper presents a new approach, based on the artificial neural networks, to be implemented in the EMCS. It was developed and tested using measurements taken on two rooftop units installed about 15 years ago in Montreal. These units will be identified in the rest of paper as unit A, with a supply air flow rate of 3000 L/s, and unit B with 2400 L/s. The manufacturer's catalogue indicates the following operating characteristics at the design conditions: the total cooling capacity of 33.7 kW, the electric demand of 11.6 kW, and the Coefficient of Performance of 2.9.

Data was collected every 32 seconds during two cooling seasons (from July to September, 1997 and 1998), using five sensors for each unit: (1) one clamp-on probe for the electric current at the compressor and the fans of air-cooled condenser, and (2) four sensors for the temperature and relative humidity of air entering and leaving the cooling coil. The cooling load from the supply air flow rate and the enthalpy difference across the coil. Data was processed to obtain the daily values of parameters relevant to the performance of these two units, during the operation between 6:00 am and 6:00 pm. The corresponding daily average dry-bulb and dew-point air temperatures were calculated from the hourly values measured at the Dorval airport.

NEURAL NETWORKS APPROACH

The approach used for predicting the COP of existing rooftop units is based on the General Regression Neural Networks (Specht 1991). It was assumed that the information from the electric current at the compressor and the fans of air-cooled condenser can be used alone or coupled with another parameter to evaluate the COP.

This approach reduces the installation cost since only a minimum number of sensors is needed, and also during the operation it reduces the costs for re-calibration or replacement of sensors. The method has two components: (1) the learning component, in which the pattern of operation over a representative period is "learned," using data from the set of five sensors; and (2) the evaluation component, which predicts the COP by applying the "learned" pattern to the new operating conditions; during the evaluation period, a smaller number of sensors are needed.

The learning period of unit A is composed of 27 days of July, August and September, 1997. The unit A was tuned in June 1998, at the beginning of the new cooling season. The evaluation period is composed of nine days of July and August 1998. The daily average COP was 1.09 during the learning period and 1.68 during the evaluation period. In the case of unit B, the learning period is composed of 18 days of July and August 1997. The old expansion valve of unit B was replaced on August 28, 1997 with an experimental valve. The evaluation period is composed of eight days of September 1997. The daily average COP was 2.20 during the learning period and 1.86 during the evaluation period.

Several models were tested (Table 1). The base model, identified as no.1, uses data only from the monitoring of electric current at the compressor and the fans of the air-cooled condenser: the average (E_{avge}) and maximum (E_{max}) electric demand measured from 6:00 am to 6:00 pm, and the operation factor, which is the proportion of time the compressor runs. The models 2 to 12 were developed by adding to the base model other monitored data: (1) the average dry-bulb outdoor air temperature (T_{db}), (2) the average dew-point outdoor air temperature (T_{dp}); and (3) the average, maximum and minimum temperature of air leaving the cooling coil, respectively (T_{avge}, T_{max}, T_{min}).

Three types of methods were compared for learning the pattern of operation: (1) Multiple Linear Regression (MLR), (2) Backpropagation Neural Networks (BNN), and (3) General Regression Neural Networks (GRNN). Two commercial software

packages were used: STATGRAPHICS (1989) for the MLR models, and NeuroShell 2 (1998) for the BNN and GRNN models. In the case of BNN and GRNN models, 80% of data available for learning was randomly selected for training the networks, and 20% for testing. The number of input parameters used by the BNN and GRNN models is equal to the number of relevant parameters presented in Table 1. For instance, the GRNN model 4 uses five input data. The BNN models use one hidden layer with seven nodes. All BNN models use the sigmoid [0,1] transfer function $f(x) = 1/(1+\exp(x))$. The GRNN models use one hidden layer, on which the number of nodes is equal to the total number of patterns in the training and testing sets (27 sets for unit A, and 18 sets for unit B). The output layer has only one node, corresponding to the COP. The GRNN models use the linear [0,1] transfer function $f(x) = x$. A genetic adaptive algorithm is used to find the appropriate smoothing factor adjustment for each input.

RESULTS FROM THE LEARNING PERIOD

The fitness of each model for predicting the COP during the learning period was evaluated using three statistical indicators: the regression coefficient r^2, the standard error, and the mean absolute error (Table 1).

The three statistical indicators prove that all GRNN models perform well for both rooftop units, and much better than the MLR and BNN models. For instance, the standard error and r^2 of model 1 for unit B are, respectively, 0.063 and 0.993 (GRNN) compared with 0.135 and 0.671 (MLR), and 0.089 and 0.860 (BNN). It is important to note that the base model 1, which uses only measurements of electric current, performs well for both units ($r^2 > 93\%$, and mean absolute error < 5%). Models 2 to 4 present a particular interest for this application, since they need one or two sensors for outdoor air temperature, which are already available in the EMCSs installed in some buildings.

RESULTS FROM THE EVALUATION PERIOD

The difference between the measured and predicted COP is used to evaluate the reduction of energy cost; negative values indicates the degradation of performance, hence the increase of energy cost. The calculations were performed by considering the rooftop units run 12 hours/day and 22 days/month, and using the following electricity rates: \$11.72/kW plus \$0.0372/kWh (HQ 1998).

The unit B experienced a change of the COP from 2.20 to 1.86. The models did not face conditions which are significantly different from those of the learning period, and as a result the difference between the predictions of COP, given by all models, is small (Table 2). The GRNN model 1, using only the measurements of electric current, provides a good evaluation of the expected COP of 1.94 compared with the measured COP of 1.86. The addition of other sensors increases the initial cost, without increasing significantly the accuracy of prediction. For instance, the model 12 which uses all parameters leads to the largest error (predicted COP of 2.1compared with the measured COP 0f 1.86). On the other hand, the three statistical indicators show that the model 12 is the best fit to the learning data. More important is the evaluation of the reduction/increase of energy cost due to the replacement of valve. The model 1 predicts an increase of energy cost of \$3.3/month, while the model 12c predicts \$7.9/month, a difference of \$4.6/month or \$13.8 for the cooling season. The increase of initial cost for the installation of three additional sensors (the dry-bulb outdoor temperature, the dew-point outdoor temperature, and the leaving air temperature) is not justified by the value of information obtained, that is \$13.8/summer.

The COP of unit A significantly increased from 1.09 to 1.68, due to the tuning of June 1998. The models appear to be very sensitive to the new conditions, and their predictions are different (Table 2). For instance, the base model 1 predicts COP = 0.77, while model 2, which uses in addition the dry-bulb outdoor temperature, predicts COP = 1.17, compared with the measured COP of 1.68. The measurements of electric current alone do not provide enough information to the GRNN model to accurately predict the COP and the energy savings. The addition of a sensor for the dry-bulb outdoor air temperature improves significantly the accuracy of predictions from COP = 0.77 to 1.17.

In the case when no significant changes of operation or failures occur, the GRNN model can predict the COP using only the measurements of electric current. Otherwise, two sensors are needed, one for the electric current, and another for the dry-bulb outdoor air temperature. If the EMCS system installed in the building already monitors the weather conditions, this information can be retrieved and therefore only the electric current must be monitored.

ACKNOWLEDGEMENTS

The authors acknowledge the financial support received from the Natural Sciences and Engineering

Research Council of Canada.

REFERENCES

Farinaccio, L. and Zmeureanu, R. (1999) "Using a pattern recognition approach to disaggregate the total electricity consumption in a house into the major end-uses," *Energy and Buildings*, 30 245-259.

Grey, P. (1997) *Psychology*, chapter 9: Perception. Worth Publishers.

Hart, G. W. (1992), "Non-Intrusive Appliance Load Monitoring," *Proceedings of the IEEE*, 80 (12) 1870-1891.

HQ. (1998) *Electricity Rates Bylaw*, Hydro Québec, Montreal.

Marceau, M. and Zmeureanu, R. (2000) "Nonintrusive load disaggregation computer program to estimate the energy consumption of major end-uses in residential buildings," *Energy Conversion and Management Journal*, 41 1389-1403.

NeuroShell 2. (1998) Ward Systems Group, Inc. Frederick, MD, USA.

Norford, L. K. and Leeb, S. B. (1996) "Non-Intrusive Electrical Load Monitoring in Commercial Buildings Based on Steady-State and Transient Load Detection Algorithms," *Energy and Buildings*, 24 51-64.

Sharp, T. R. (1994) "Non-Intrusive Load Monitoring Systems: Considerations for Use and Potential Applications," *ACEEE Summer Study on Energy Efficiency*, 2 241-247.

Specht, D.F. (1991) "A General Regression Neural Network," IEEE Transactions on

Neural Networks 2 568-576.

STATGRAPHICS. (1989) *Statistical Graphics System. Version 6.0.* Manugistics, Inc, Rockville, MD, USA.

WFSC. (2001) The Official Journal of the World Federation on Soft Computing (WFSC) http://www.bioele.nuee.nagoya-u.ac.jp/WFSC/.

Table 1. Evaluation of the fitness of Genaral Regression Neural Network models to predict the COP during the "learning" period. All models contain E_{avge}, E_{max} and $time_{ON}$. First line is for unit A, and second line for unit B.

Model	Other parameters					r^2	standard error	mean absolute error
	T_{db}	T_{dp}	T_{avge}	T_{max}	T_{min}			
1						0.931 0.933	0.077 0.063	0.047 0.040
2	x					0.968 0.886	0.055 0.077	0.023 0.060
3		x				0.980 0.993	0.045 0.025	0.017 0.007
4	x	x				0.973 0.989	0.045 0.032	0.021 0.011
5			x			0.890 0.933	0.095 0.063	0.071 0.041
6			x	x	x	0.984 0.998	0.032 0.020	0.015 0.003
7				x	x	0.975 0.967	0.045 0.045	0.023 0.025
8	x		x			0.988 0.885	0.032 0.077	0.012 0.060
9		x	x			0.973 0.983	0.045 0.032	0.018 0.022
10	x	x	x			0.988 0.993	0.032 0.020	0.012 0.006
11	x		x	x	x	0.990 0.922	0.032 0.071	0.014 0.041
12	x	x	x	x	x	0.990 0.995	0.032 0.020	0.013 0.012

Table 2. Use of the GRNN model to estimate the reduction of energy cost savings during the evaluation. First line is for unit A and second line for unit B.

Model	Measured post-retrofit COP	Predicted post-retrofit COP (based on the pre-retrofit pattern)	Reduction of energy cost [CAN$/month]
1		0.77 1.94	65.0 -3.3
2		1.17 1.92	26.0 -2.7
3		0.84 1.91	55.0 -2.4
4		1.24 2.02	22.0 -5.7
5		0.85 1.94	54.0 -3.3
6	1.68 1.86	0.83 1.89	56.0 -1.8
7		0.81 1.89	59.0 -1.8
8		1.31 1.91	18.0 -2.4
9		0.93 2.05	45.0 -6.5
10		1.31 1.89	18.0 -1.8
11		1.30 1.85	19.0 -0.4
12		1.27 2.10	21.0 -7.9

MEASUREMENT AND SIMULATION OF THE THERMAL ENVIRONMENT OF A LOW ENERGY HOUSE WITH AIR-CIRCULATION IN BRICK WALLS

Shuho Takase*, Toshiyuki Watanabe*, Tetsuo Hayashi* and Akihito Ozaki**,
Mikiko Nakamura***, Mayuko Nagata*, Masako Osato*
* Kyushu University, Japan
** Kitakyushu City University, Japan
*** Japan Science and Technology Corporation
shuho.t@beel.arch.kyushu-u.ac.jp

ABSTRACT

Brick houses are high-grade in terms of life cycle assessment, life span and maintenance costs after construction. However, earthquakes made brick infamous as a fragile material in Japan. Now quakeproof brick houses have been developed and they will be authorized in the near future in Japan. We can control the indoor thermal environment and reduce cooling and heating loads using a passive system and the large thermal capacity of bricks. This paper reports the development of Passive Brick Houses with Air-circulation Systems. We have made predictions about the indoor thermal environment and cooling and heating loads using the simulation software "Triple P" (TrP = Program for Passive System Simulation with Personal Computers). The prediction using TrP is useful because currently there are no brick houses in Japan.

INTRODUCTION

There are no brick houses in Japan for two reasons. One is their fragility in earthquakes. Masonry structures are regulated by the building code in Japan. The other reason is condensation. The Japanese hot and humid climate in summer further reduced the popularity of brick houses because of mold. The structural difficulty in making large openings interfered with ventilation and the large temperature caused dew on walls and was a sanitary disaster.

Now quakeproof brick houses with large openings have been developed (the "Distributed Unbond Pre-stress Method" by Matsufuji 1992). If we can control the indoor thermal environment and reduce cooling and heating loads using a passive system and the large thermal capacity of bricks, brick houses will become popular in Japan. We have measured the indoor thermal environment and cooling and heating loads of a test brick room that was constructed, and made predictions about the environment and the loads of a test brick house that is under construction using the simulation software TrP (Program for Passive System Simulation with Personal Computers).

DESCRIPTION OF THE TEST ROOM

A test room was constructed and its thermal performance was measured to evaluate a newly proposed air-circulation system. Then the test room was simulated using the software TrP and we compared the results of measurement and simulation. Furthermore we changed it to many types of model and made predictions about each of them.

The test room was built in 1998 in Kumamoto prefecture, in the southern part of Japan (Figure 1 to 4). The test room has three main passive systems. One is a Trombe wall on the south side. The other is a solar collector, 16.2 m^2, about 1m above the ground. Another is two 20 m lengths of cool tubes at 3 m depth below the ground. The north, east and west walls have air cavities between brick walls.

In winter, outdoor air is drawn into the solar collector and warmed up. The warmed air is sent to the air cavity of the north wall through the space under the floor. And then the air comes into the room from the north air cavity. The air in the room goes through the lower slits in the east and west walls, goes up to the attic space through the air cavity of the east and west walls and is exhausted to the outside. On the other side, the room air goes through the lower slits in the south wall, goes up in the cavity of the Trombe wall and comes back to the room through the upper slits. (See Figure 4(a))In summer, the outdoor air cooled by two 20 m lengths of cool tubes goes into the room directly. The air in the room goes up to the attic space through the upper slits in the east and west walls. The air in the attic space is exhausted to the outside using the forced ventilation. The Trombe wall and windows are solar-shaded by the shutter all day long. (See Figure 4(b))

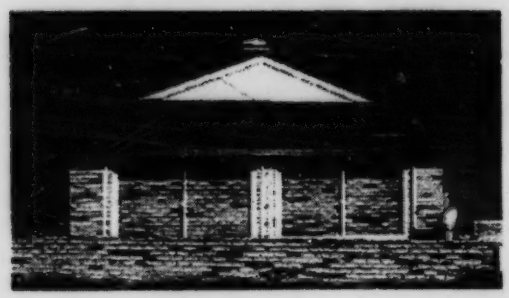

Figure 1 Outside View of the South Facing Face of the Test Room

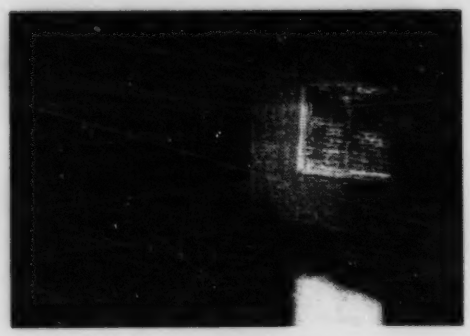

(a) South Aspect (Trombe Wall)

(b) North Aspect (Cavity Brick Wall)

Figure 2 Inside View of the Test Room

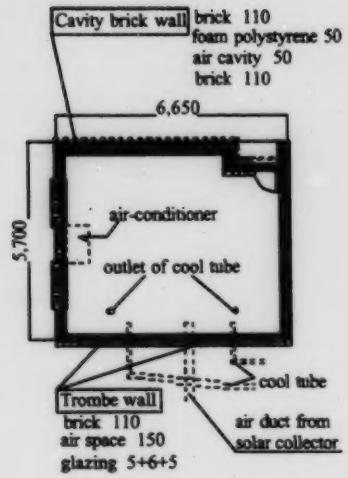

Figure 3 Floor Plan of the Test Room [unit : mm]

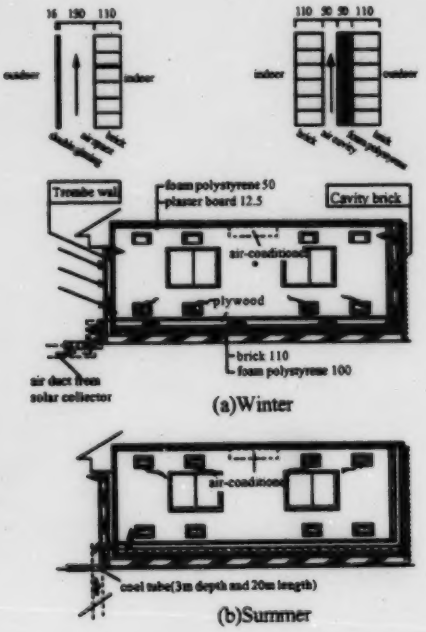

Figure 4 Sections and Details of the Test Room [unit : mm]

COMPARISON OF MEASURED AND SIMULATED RESULTS FOR THE TEST ROOM

We made predictions using the simulation software TrP (Program for Passive System Simulation with Personal Computers). We input outside air temperature, outside absolute humidity mixing ratio, solar irradiance, wind direction, wind velocity and cloud cover from the standard weather data for Kumamoto. We were able to get room air temperature, PMV and heating/cooling loads for each hour as output. Assumptions for the simulation are shown in Table 1. TrP has some suppositions as premises. (See Table 2)

Table 1 Conditions for the Simulation

weather data :
standard weather data (Kumamoto in Japan)
simulation interval time : 1 hour
date : December 7 (winter)
August 14 (summer)

Table 2 Suppositions for TrP

Rooms are rectangular parallelepiped
Rooms have 6 faces
(east, west, south, north, floor, ceiling)
Walls are divided into some parts
Heat conducts one-dimensionally in every part
Parts have no temperature distribution
Room temperature is the same in each rooms
Heat diffuses all over the room immediately

Figure 5(a) shows air temperature in the room and under the floor in winter. The results of measurement and simulation are almost the same.

Figure 5(b) shows the temperature of the surface of the south brick wall in winter. Temperatures in simulation rose a little bit higher than in reality. This is because the air tightness of the double glazing on the south Trombe wall in the simulation was better than in actual measurements. The maximum difference was about 3 K.

Figure 6(a) shows the room air temperature in summer. In the morning, actual temperatures were about 2 K higher than in the simulation. This is because the outdoor air cooled by the cool tubes is re-warmed just before it goes into the room.

Figure 6(b) shows inside air temperature of the cool tube in summer. The results were very similar and the maximum difference was less than 1 K.

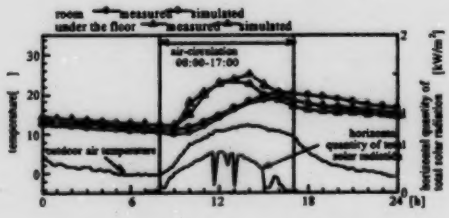

(a) Room and Under Floor Air Temperature

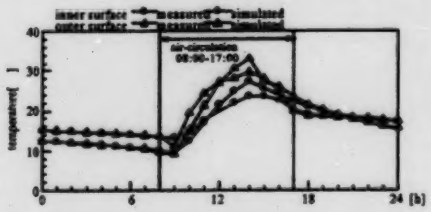

(b) Temperature of the Surface of the South Brick Wall

Figure 5 Room and Surface Temperature in Winter (December 7, 1999)

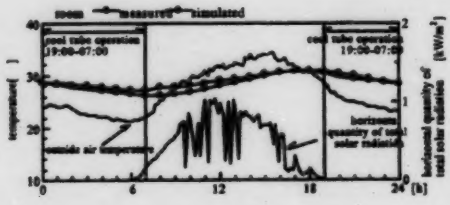

(a) Room Air Temperature

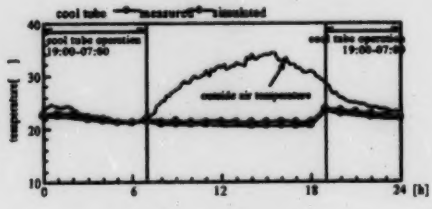

(b) Cool Tube Air Temperature

Figure 6 Air Temperature in Summer (August 14, 1999)

SIMULATION OF THE TEST ROOM

We made predictions about the indoor thermal environment and cooling and heating loads using the simulation software TrP while changing some parameters.

SIMULATION IN WINTER

In winter we changed the surface area of the solar collector. Figure 7 shows the room air temperature. When the surface area of the solar collector was large, the room air temperature was high, but the rate of temperature increase was small. We also changed the mass flow rate of the solar collector. A mass flow rate of 100m³/h resulted in better temperatures than a rate of 200 m³/h. Too much mass flow rate prevents the air drawn into the solar collector from becoming warm enough.

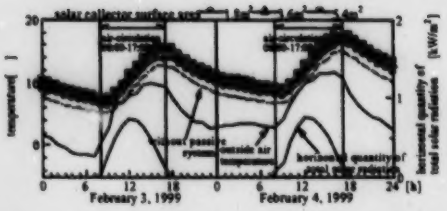

Figure 7 Room Air Temperature

We also changed the thickness of the brick layer of the Trombe wall. Figure 8 shows the room air temperature and Figure 9 shows the inner surface temperature of the brick wall. A thickness of 50 mm resulted in the best room air temperatures in the daytime but all types resulted in almost the same temperatures at night. The inner surface temperature showed a similar tendency in the daytime but a wall thickness of 200 mm resulted in the highest temperatures at night.

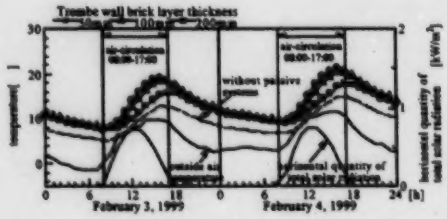

Figure 8 Room Air Temperature

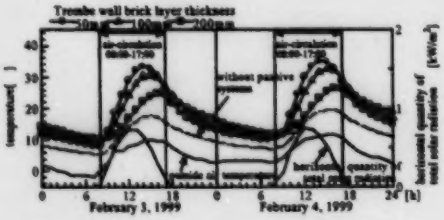

Figure 9 Inner Surface Temperature of the Brick Wall

Figure 10 shows the comparison of seasonal heating loads. The target temperature was 22 and the heating time was from 17:00 to 08:00. When the surface area of the solar collector was 5.4m², the mass flow rate of the solar collector was 100m³/h and the thickness of the south brick layer of the Trombe was 100mm, the seasonal heating load was lowest. It was 6.6 GJ which was 2.8 GJ (30%) lower than the load of the house without passive systems.

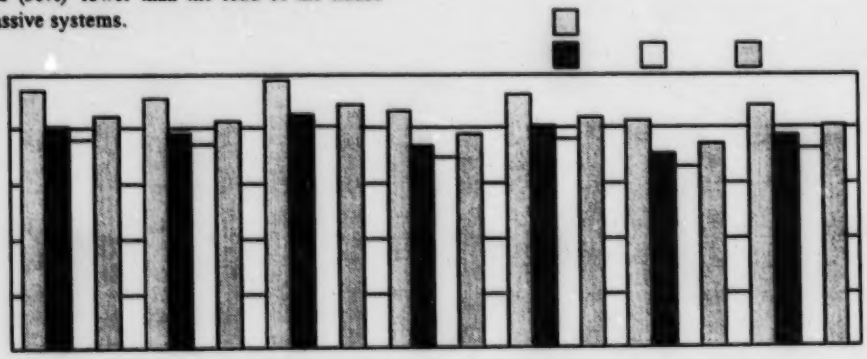

Figure 10 Comparison of Heating Load

SIMULATION IN SUMMER

In summer we changed the length of the cool tubes. Figure 11 shows the room air temperature. In the daytime, the longer the cool tube, the lower the room air temperature. But there was little variation at night.

In summer we also changed the mass flow rate of the cool tube. Figure 12 shows the room air temperature. The larger the mass flow rate, the lower the room temperature. When the mass flow rate became large, the room air temperature became low, but the rate of decrease became small.

Figure 13 shows the comparison of seasonal cooling loads. The target temperature was 26 and cooling time was from 07:00 to 19:00. When the length of the cool tubes was 30m and the mass flow rate of the cool tubes was 300m³/h, the seasonal cooling load was lowest. It was 2.7 GJ which was 0.9 GJ (25%) lower than the load of the house without passive systems.

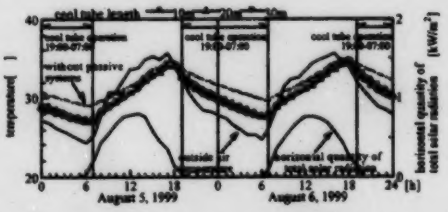

Figure 11 Room Air Temperature

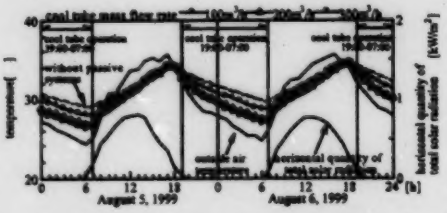

Figure 12 Room Air Temperature

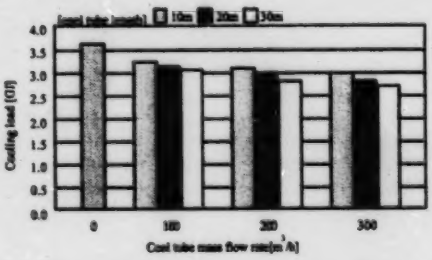

Figure 13 Comparison of Cooling Load

DESCRIPTION OF THE TEST HOUSE

We have explained about the test room that was constructed and measured. For the next stage, we propose a test house as large as an actual residence. The test house is under construction next to the test room and so currently we have only a computer model. We have made predictions about the indoor thermal environment and cooling and heating loads using the simulation software TrP.

Figure 15 is the plan of the proposed house and Figure 16 shows the sectional diagram of the passive system. The brick house with air-circulation is a two-story house and the total floor area is 194m². The exterior walls are cavity brick structure.

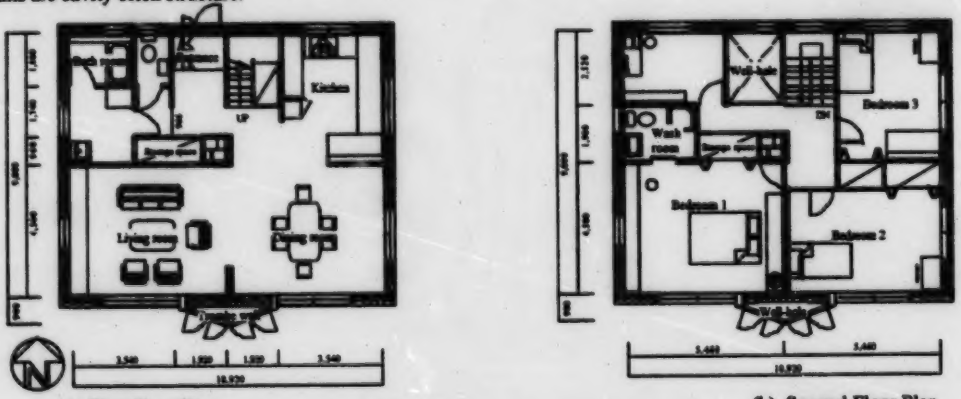

(a) First Floor Plan

(b) Second Floor Plan

Figure 14 Plans of Passive Solar House [unit: mm]

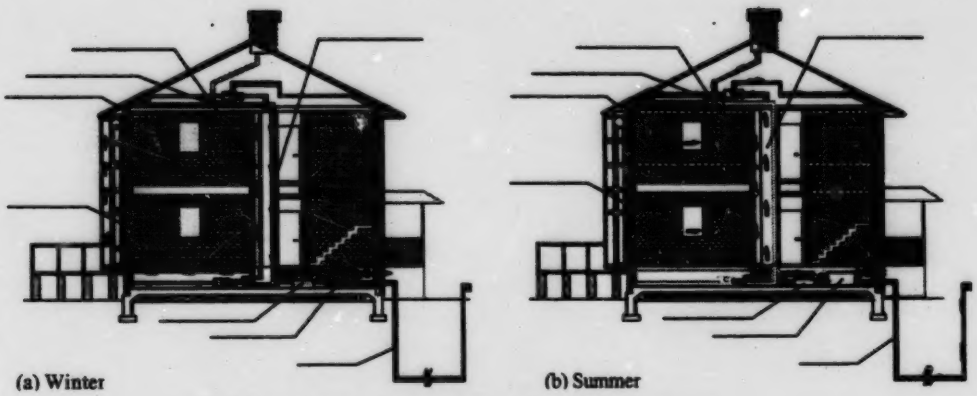

(a) Winter (b) Summer

Figure 15 Sectional Diagram of Passive Devices [unit: mm]

In winter, the room air goes into the heat exchanger under the floor through the central duct. The air from the solar collector is pre-heated in the air space in the Trombe walls facing to the south and drawn into the solar collector by the electric fan in the air-handling box. The air from the solar collector and the return air from the rooms exchange sensible heat at the heat exchanger. The warmed air is sent to the rooms through the air cavities in the cavity brick walls, and returned to the heat-exchanger. In the night, heat radiation into the room from the Trombe walls and the cavity brick walls keeps the room comfortable and the pulled-down shutter on the Trombe walls prevents heat loss. (See Fig. 15 (a))

In summer, the room air goes into the heat exchanger under the floor through the central duct. The air from the cool tube and the return air from the rooms exchange sensible heat at the heat exchanger to prevent mold caused by the moist air in the cool tubes. The cooled air is sent to the rooms through the air cavities in the cavity brick walls, and returned to the heat-exchanger under the floor through the central duct. The Trombe walls and the windows are solar-shaded by the shutter, the outdoor air is drawn in to the air space in the Trombe walls, led to the attic space and exhausted to the outside by an electric fan to prevent the temperature from rising. (See Fig.15 (b))

SIMULATION OF THE TEST HOUSE

We made predictions using the simulation software TrP. The presumptions for the simulation are shown in Tables 3 to 5. Table 3 shows the components of the wall structures of the proposed solar house. However, five types of wall structure were examined to compare their thermal performance. The first type was a passive

Table 3 Components of Wall Structures

Roof	plywood	10mm
	clay tile	40mm
1F ceiling	plaster board	10mm
2F ceiling	plaster board	10mm
	thermal insulating board	50mm
Floor	plywood	10mm
Ground	concrete	200mm
	crushed stone	50mm
	soil	50mm
Foundation	brick	110mm
	thermal insulating board	50mm
	brick	110mm
Exterior wall	brick	110mm
	air cavity	50mm
	thermal insulation board	50mm
	brick	110mm
Exterior wall	plywood	10mm
	mortar	10mm
	air cavity	50mm
	urethane foam	30mm
	plaster board	10mm
Trombe wall	brick	330mm
	air space	100mm
	double glazing	5+10+5mm
Trombe wall	concrete	330mm
	air space	100mm
	double glazing	5+10+5mm
Interior wall	brick	110mm
Interior wall	plaster board	10mm
	air cavity	50mm
	plaster board	10mm

brick house with an air-circulation system, the same as the test house that is under construction. The second type was termed brick house A and had the same wall structure but no air-circulation. The third type was termed brick house B and had an exterior wall with inside insulation. The fourth type was a wooden house with air-circulation with the exterior brick walls replaced by plywood panels. The fifth type was a wooden house, the same as the fourth one but without an air-circulation system or a Trombe wall.

The thermal performances of the five types of house shown in Table 4 were compared to confirm the validity of the proposed system. In winter, the surface area of the solar collector was 28.7 m² and the mass flow rate was 500 m³/h. The electric fan was operated when the air temperature in the air-handling box exceeded 25 . The shutter on the Trombe wall was pulled up from 08:00 to 17:00. In summer, the cool tube was 3 m deep, 50 m long and had a mass flow rate of 500 m³/h. The electric fan was operated from 19:00 to 07:00.

SIMULATION IN WINTER

Figure 16 shows air temperatures in bedroom 1 and outside on February 10 and 11. The room air temperature of all three brick houses was stabler than that of the two wooden houses because of the large thermal capacity of the indoor brick walls. In the daytime, the room air temperature of the brick house with air-circulation was lower than that of the wooden house with air-circulation. However, the former was about 5 K higher than the latter at night.

Figure 17 shows a comparison of the seasonal heating loads in winter among the five types of house. The target temperatures and air-conditioning time shown in Table 5 were applied to these simulations. The thermal capacity of the brick walls reduced the temperature decrease at night. Therefore, the seasonal heating load of the passive brick house with air-circulation was lowest. Compared with the seasonal heating load of the wooden house, that of the brick house with air-circulation was 38% lower.

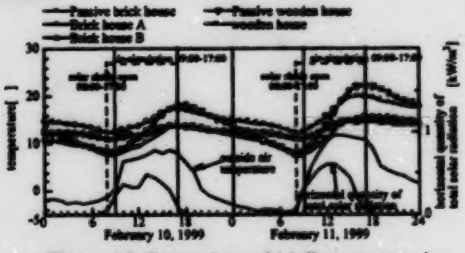

Figure 16 Comparison of Air Temperatures in Winter (Bedroom1)

Table 4 Specification of Simulation Models

<<Passive brick house>>
(air-circulation, over-all heat loss coefficient: 1.69)
Standard type (wall type)
<<Brick house A>>
(no air-circulation, over-all heat loss coefficient: 1.69)
Change Trombe wall to exterior wall
<<Brick house B>>
(no air circulation, over-all heat loss coefficient: 1.69)
Change Trombe wall to exterior wall
Change outside insulation to inside insulation
<<Passive wooden house>>
(air-circulation, over-all heat loss coefficient: 2.19)
Change wall type to
<<Wooden house>>
(no air-circulation, over-all heat loss coefficient: 2.51)
Change wall type to
Change Trombe wall to exterior wall

Table 5 The Conditions for Simulation Data

Weather data: Expanded AMeDAS Weather Data (Kahoku)
Simulation interval: 1 hour
Active heating
Period: December – March
Time: 17:00-08:00
Target temperature: 22
Active cooling
Period: June – September
Time: 07:00-19:00
Target temperature: 26

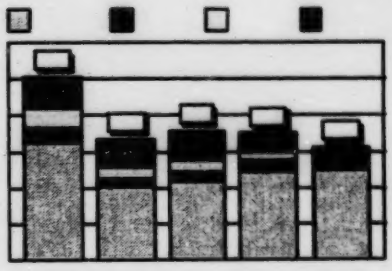

Figure 17 Comparison of Air Heating Load (Winter)

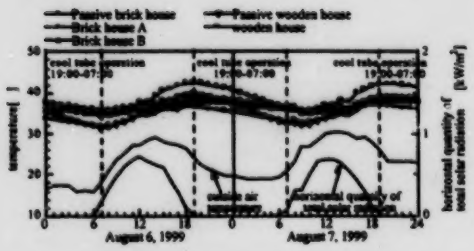

Figure 18 Comparison of Air Temperatures in Summer (Bedroom1)

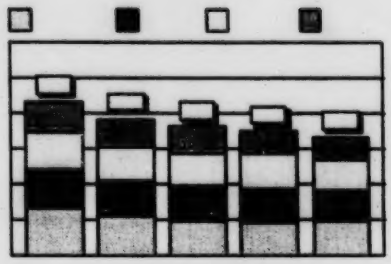

Figure 19 Comparison of Air Cooling Load (Summer)

Figure 18 shows the air temperature in bedroom 1 and outside on August 6 and 7. The room air temperature of the brick house with air-circulation was higher than that of the wooden house with air-circulation at night. However, the former was about 3K lower in the afternoon.

Figure 19 shows a comparison of the seasonal cooling loads in summer among the five types of house. The target temperatures and air-conditioning time shown in Table 5 were applied to these simulations. The seasonal cooling load of the passive brick house with air-circulation was lowest. Compared with the seasonal cooling load of the wooden house, that of the brick house with air-circulation was 24% lower.

CONCLUSIONS

In the first stage of this research, a test room was constructed and its thermal performance was measured. Then the test room was simulated using the simulation software TrP and a comparison was made of the results of measurement and simulation. The results were very similar and so the simulation software TrP was considered to be suitable for making predictions about the environment and the heating and cooling loads of houses.

In the second stage, predictions were made about the environment and the loads of several types of test houses using TrP. Comparisons were made for different solar collector surface areas and mass flow rates, different thicknesses of brick in the Trombe wall and different cool tube lengths and mass flow rates. In winter, the lowest heating load was 6.6 GJ which was 2.8 GJ (30%) lower than the load of the house without passive systems. In summer, the lowest cooling load was 2.7 GJ which was 0.9 GJ (25%) lower than the load of the house without passive systems .

In the third stage, a passive system utilizing the thermal capacity of brick walls and earthen floors was proposed and its thermal performance was simulated. The passive system was combined with a solar air-heater, Trombe walls and air-circulation. As for the seasonal heating load, the passive brick house with air-circulation was 38% less than a normal wooden structure house. In summer, the proposed passive system combined with earth cool tubes decreased by 24% the seasonal cooling load in comparison with a normal wooden structure house.

REFERENCES

Matsufuji, Y. (1992). Reinforced Brick Wall System for Semi-Dry Brick Work, *Doc. Division of Building, Construction and Engineering CSIRO*, (personal communication)

Hayashi, T. (1992). Development of Thermal Performance Simulation Program for Multi-Space Dwellings Using Personal Computers, *Annual Report Housing Research Foundation*, No.19, pp. 337-346, (in Japanese)

VALIDATION DYNAMIQUE DES MODELES DE SIMULATION DES BATIMENTS EXISTANTS

Roberge Marc-Antoine, Kajl Stanislaw, Bellemare René
École de technologie supérieure, 1100, rue Notre-Dame Ouest, Montréal H1C 1K3, Canada.
(514) 396-8517, fax. (514) 396-8530, courriel : skajl@mec.etsmtl.ca

RÉSUMÉ

L'article présente une approche dynamique de validation des modèles de simulation des bâtiments existants. La normalisation des résultats de simulation, ainsi que la répartition mensuelle des factures d'énergie sont effectuées en tenant compte des températures de base pour les degrés-jours de chauffage et de refroidissement qui peuvent varier suite aux ajustements apportés pendant la validation. Ces températures, une fois choisies, sont dans la majorité de cas considérées comme constantes. La validation est réalisée en tenant compte des fractions de consommations mensuelles relatives au chauffage, au refroidissement et à la consommation de base identifiées à partir des factures. Les modifications des modèles pendant la validation ne portent que sur les données cueillies avec le degré de véracité faible. Ce degré de véracité est identifié pendant un relevé détaillé de données techniques qui est indispensable pour ce type de validation. L'application de cette procédure de validation à l'analyse énergétique d'un bâtiment existant est aussi présentée dans cet article.

INTRODUCTION

De nos jours, on a recours à l'analyse énergétique sur les bâtiments existants afin d'évaluer l'impact de l'application de certaines mesures d'économie d'énergie sur la consommation d'énergie comme par exemple : le changement des séquences de contrôle, le remplacement des équipements CVCA ou le nouvel horaire d'utilisation de ceux-ci, etc. L'utilisation d'un logiciel performant ainsi que la qualité du fichier météorologique utilisé sont les deux éléments clés permettant d'effectuer une analyse juste et précise. Différents logiciels sont reconnus pour leur performance tels DOE-2 ou BLAST. Cependant, les modèles de simulation développés pour ces logiciels exigent un relevé détaillé de données dans le bâtiment étudié. Certaines de ces données, comme par exemple les horaires d'utilisation des équipements et d'occupation des locaux, sont difficiles à cueillir avec un degré de certitude raisonnable. Il est donc important d'évaluer le degré de véracité des données recueillies afin d'identifier les plus problématiques. Quant au fichier météorologique, il est recommandé d'utiliser le fichier de l'année pour laquelle la validation du modèle de simulation est réalisée. Malheureusement, le fichier météorologique pour le site de l'établissement à l'étude n'est parfois pas disponible ou bien n'existe pas. Lors de telles situations, un fichier météorologique type est utilisé pour la simulation. Les résultats de simulation obtenus dans ce cas doivent alors être normalisés avant de les comparer avec les consommations d'énergie facturées. La normalisation est faite en utilisant les degrés-jours de l'année de validation et du fichier météorologique type. Il est cependant à noter que cette normalisation exige l'identification des fractions de consommations mensuelles totales d'énergie facturées relatives au chauffage et à la climatisation. Cette identification est parfois difficile à réaliser dans les bâtiments utilisant une source et un compteur d'énergie.

Lors du processus de validation, il est rare que les critères de validation soient atteints dès la première simulation. La validation consiste donc à ajuster le modèle afin d'obtenir les profils de consommations et de puissances maximales mensuelles semblables aux profils provenant des factures mensuelles d'énergie. Par conséquent, la validation des modèles de bâtiments existants, lorsque le fichier météorologique type est utilisé pour la simulation, peut comporter les étapes suivantes :

1. Identifier la température d'équilibre pour le bâtiment donné qui sera considérée comme la température de base pour les degrés-jours utilisés dans la normalisation des résultats;
2. Normaliser les résultats de simulation qui dépendent des conditions météorologiques comme par exemple, la consommation attribuée au chauffage ou à la climatisation;
3. Comparer les résultats normalisés avec les factures d'énergie en identifiant, si possible, les fractions de factures relatives à la consommation due au chauffage, à la climatisation et à la consommation de base (éclairage et équipements);
4. Ajuster le modèle de simulation du bâtiment si les critères de validation ne sont pas atteints.

DESCRIPTION DE LA PROCÉDURE

Dans cet article, on présente une nouvelle approche relative aux trois premières étapes du processus de validation mentionnées ci-dessus. Cette approche a été

appliquée sur un bâtiment existant comportant des laboratoires de recherche, des bureaux et de multiples espaces communs. Il est à noter que les simulations ont été réalisées à l'aide du logiciel DOE-2. Le modèle de simulation du bâtiment a été développé en tenant compte des résultats des relevés détaillés de données effectuées sur celui-ci. Afin de faciliter l'ajustement du modèle lors de la validation, le degré de véracité a également été identifié pour certaines données considérées comme étant incertaines ou difficiles à évaluer. Il est à noter que le degré de véracité résulte d'un jugement subjectif fait par le cueilleur de données selon la qualité des informations disponibles. L'approche utilisée lors de la validation peut être résumée de la façon suivante :

1. Déterminer, pour le fichier météorologique type (doe) et pour l'année de la facturation (ref), les degrés-jours mensuels de chauffage (djch_doe, djch_ref) et de refroidissement (djre_doe, djre_ref) pour différentes températures de base (te_ch pour chauffage et te_re pour refroidissement) afin d'établir les courbes mensuelles des degrés-jours;
2. Comparer, respectivement pour le chauffage et la climatisation, les courbes de consommation mensuelle d'énergie obtenues par simulation avec les courbes mensuelles de degrés-jours établies à l'étape précédente. Trouver la courbe de degrés-jours pour le chauffage, et par la suite, pour la climatisation, dont l'allure correspond le mieux à la courbe de consommation mensuelle en calculant l'erreur cumulative entre les courbes adéquates. Les températures de base des courbes ainsi trouvées peuvent être considérées comme étant les températures d'équilibre pour la période de chauffage et celle de climatisation;

Pour chaque température de base et pour chaque mois :

$$rap\_ch\_doe = \frac{ch\_men\_doe}{ch\_ann\_doe}$$

$$rap\_re\_doe = \frac{re\_men\_doe}{re\_ann\_doe}$$

$$rap\_dj\_ch\_doe = \frac{dj\_ch\_men\_doe}{dj\_ch\_ann\_doe}$$

$$rap\_dj\_re\_doe = \frac{dj\_re\_men\_doe}{dj\_re\_ann\_doe}$$

$$err\_cumul\_ch = \sum_{i=1}^{12} (rap\_dj\_ch\_doe - rap\_ch\_doe)$$

$$err\_cumul\_re = \sum_{i=1}^{12} (rap\_dj\_re\_doe - rap\_re\_doe)$$

Choix des températures de base :

$$\min(err\_cumul\_ch) \qquad \min(err\_cumul\_re)$$

3. Normaliser les résultats de simulation en utilisant les degrés-jours de chauffage et de climatisation pour les températures d'équilibre déterminées à l'étape précédente;

Normalisation typique consiste à appliquer la formule suivante

$$VAL_{norm} = VAL_{doe} * \frac{dj\_ref}{dj\_doe}$$

Afin d'éviter division par zéro (lorsque dj_doe est zéro et dj_ref est supérieur à zéro), nous avons utilisé pour la normalisation de résultats relatifs au chauffage la formule suivante :

$$ch\_men\_doe_{norm} = ch\_ann\_doe * \left(rap\_ch\_men - \frac{dj\_ch\_men\_ref - dj\_ch\_men\_doe}{dj\_ch\_ann\_doe} \right)$$

Pour les résultats relatifs au refroidissement, la formule semblable était utilisée;

4. Identifier les fractions de consommations mensuelles totales d'énergie facturées relatives au chauffage et à la climatisation. Pour le faire, dans les bâtiments ne comportant qu'un compteur d'énergie, on prend en considération les résultats de simulation. D'abord, on soustrait la consommation d'énergie de base (éclairage, équipements, etc.) obtenue par la simulation de l'énergie facturée. On considère le reste comme l'énergie consommée par les systèmes de chauffage et de refroidissement. La répartition pour le chauffage et le refroidissement est fait en tenant compte de relation entre ces deux types de consommations obtenue par la simulation;
5. Comparer les résultats de simulation normalisés (chauffage et climatisation) et non normalisés (consommation de base : éclairage, équipements, etc.) avec les factures d'énergie fractionnées obtenues à l'étape précédente;
6. Analyser les résultats de comparaison faite à l'étape 5 afin de vérifier si les critères de validation sont atteints;
7. Identifier les ajustements à apporter sur le modèle du bâtiment et répéter la procédure de validation à partir de la deuxième étape en utilisant le modèle de simulation ajusté.

La procédure itérative se termine lorsque les critères de validation sont atteints à l'étape 6. Elle a été développée dans le logiciel MATLAB et elle inclus aussi la saisie des résultats de simulations réalisées à l'aide du logiciel DOE-2, requise pour la validation. Il est à souligner que les températures de base pour les degrés-jours de chauffage et de refroidissement

peuvent varier suite aux ajustements apportés pendant la validation. Sonderegger [5] propose aussi la variation de ces températures sauf que dans ce cas elles sont déterminées différemment. Dans la majorité de cas, ces températures, une fois choisies, sont considérées comme constantes.

EXEMPLE DE VALIDATION

Description du bâtiment

Le bâtiment étudié est un centre de recherche hospitalier universitaire situé au Québec. L'édifice comporte un sous-sol et quatre étages (*rez-de-chaussée inclus*) pour une superficie brute d'environ 1560 m_. On retrouve l'animalerie au sous-sol, des bureaux administratifs au rez-de-chaussée et enfin, des bureaux et laboratoires de recherche sur les trois autres étages. La fenestration varie de 18 à 38 % dépendamment de l'orientation de mur. Les résistances thermiques (RSI) des murs et des fenêtres sont respectivement de 4.1 et de 0.39 $m^2°C/W$. Pour climatiser les zones thermiques, l'édifice possède trois systèmes centraux de traitement de l'air desservis par deux chaudières à vapeur au gaz naturel et à un refroidisseur. Les trois systèmes sont à débit constant, à température d'alimentation variable avec les serpentins terminaux de réchauffage et le chauffage périphérique assuré par des plinthes électriques. Les serpentins de refroidissement et chauffage sont alimentés respectivement en eau refroidie et en eau chaude. Les systèmes # 1 et 3 sont à 100% d'air frais et ils desservent respectivement l'animalerie et les laboratoires aux étages. Ils comportent des récupérateurs de chaleur dont l'efficacité est évaluée à environ 50%. Les laboratoires et la salle de culture du bâtiment (desservis par système # 3) sont équipés de hottes d'évacuation contrôlées par l'utilisateur. Lorsque l'une d'elles est en fonction, le ventilateur de retour du système d'alimentation réduit son débit proportionnellement au débit d'évacuation de la hotte en opération. Il y a alors une réduction de la quantité de chaleur récupérée par le serpentin de récupération placé dans l'évacuation d'air en aval du ventilateur de retour du système concerné. Seul le système # 2 comprend un économiseur pour contrôler le débit d'air frais dont le minimum est 20%.

Les chaudières ont une capacité de 370 kW chacune et une efficacité à pleine charge de 80%. Il faut noter qu'une seule chaudière et qu'une seule pompe sont en opération et que les autres équipements ne sont utilisés qu'en cas de bris mécaniques. La puissance frigorifique du refroidisseur est de 345 kW et son COP est de 2.64. Il est refroidi à l'air avec dix ventilateurs d'une puissance motrice totale de 11.19 kW. De plus, selon les renseignements, les chaudières sont mises en marche relativement tard, c'est-à-dire vers la mi-novembre et arrêtées dans la période du 15 mai. Quant au refroidisseur, il suit la cédule inverse des chaudières.

Pour combler les besoins en eau chaude sanitaire (*ECS*), le bâtiment dispose d'un chauffe-eau au gaz naturel, d'une puissance de 88 kW et un réservoir d'une capacité de 260 l. L'efficacité estimée de combustion à pleine charge du chauffe-eau est de 72%. De plus, la puissance de l'ascenseur est de 30 kW et aucun système d'éclairage extérieur n'a été relevé.

Modèle de simulation

Pour modéliser le bâtiment sous le format DOE-2, nous avons identifié 42 zones thermiques (36 externes et 6 internes). Le relevé précis portait sur les données architecturaux des locaux et sur les caractéristiques de charges internes des zones telles que l'éclairage, les équipements, l'occupation, etc. Pour ces données, le relevé était si détaillé que nous les avons considérés avec un degré de véracité très élevé. Un degré de véracité élevé a aussi été attribué pour les débits des ventilateurs étant donné que nous disposions des rapports de balancement effectués peu de temps avant la modélisation. Par contre, certaines données ont été relevées avec un degré de véracité considéré comme faible. Il s'agit notamment du contrôle des points de consigne tels que la température du local (thermostats non protégés) et la température de soufflage (contrôle manuel). Il était de même pour la date de mise en service de la chaudière à gaz qui est évaluée à la mi-novembre. Étant donné que la chaudière ne dessert que les serpentins de chauffage et que les serpentins de réchauffage et les plinthes électriques complètent le chauffage dans les zones, la date de mise en opération peut varier selon les priorités du gestionnaire de bâtiment.

Pour compléter la description des paramètres du modèle, certains points spécifiques du modèle de simulation méritent d'être mentionnés :

- Ajout d'une fonction permettant de simuler l'horaire d'éclairage de l'animalerie semblable au cycle de l'éclairage de jour [1];
- Ajout d'une fonction permettant de simuler l'horaire d'utilisation de la protection solaire en fonction de l'intensité de l'ensoleillement (variation du coefficient d'ombrage SC) [1]. Application de la méthode des longueurs de fissures pour tenir compte de l'infiltration de l'air dû au vitrage. La valeur utilisée dans le modèle est 0.287 l/s m à 12 Pa, qui correspond à une fenestration de bonne qualité, et ce, pour une fenêtre ouvrante fermée;
- Usage de trois (3) systèmes de type RHFS (Constant Volume Reheat Fan System) et d'un

système de type PTAC (Packaged Terminal Air Conditioner System). Ce dernier permet de simuler des zones sans refroidissement et sans ventilation mécanique;

- Ajustement du point de consigne de température d'alimentation de façon linéaire en fonction de la température extérieure selon la plage suivante (*alimentation / extérieure*) : (13°C / 13°C , 18°C / –28.9°C);
- Ajustement des points de consigne des thermostats de toutes les zones thermiques entre 21.1 et 23.3°F selon la saison;
- Concept de modélisation des hottes des laboratoires. Étant donné que ces équipements sont utilisés sur une base irrégulière, ils ont été considérés, lors de la simulation, comme n'étant jamais utilisées. Cette hypothèse n'engendre pas d'erreurs majeures parce que lorsque l'une d'elles est en fonction, le ventilateur de retour du système d'alimentation réduit son débit proportionnellement au débit d'évacuation de la hotte en opération. Elle n'entraîne qu'une sur-évaluation de la récupération d'énergie du serpentin de récupération du système alimentant les laboratoires.

Validation

L'objectif de la validation est d'obtenir une différence de moins de 10% mensuellement et de moins de 5% annuellement, et ce, entre les résultats normalisés du DOE-2 et la facturation. La validation présentée ci-dessous comporte cinq (5) itérations suivant la procédure décrite dans cet article. Les ajustements du modèle de simulation consiste à modifier les éléments dont le degré de véracité pendant les relevés techniques du bâtiment a été identifié comme faible.

La validation sera présentée en respectant les étapes de la procédure proposée dans l'article. Il est à noter que l'étape 1 est commune pour chaque itération. Les étapes 2, 5 ,6 et 7 sont identifiées pour chaque itération. Les étapes 3 et 4 sont omises pour alléger la présentation. De plus, pour l'ensemble des figures présentées ci-dessous, les lignes continues correspondent aux répartitions mensuelles de la facturation et les barres aux résultats normalisés de la consommation du modèle adéquat de DOE-2.

Première simulation

Étape 2

Température de base pour le chauffage (élec.) : 24 °C
Température de base pour le refroidissement : 10 °C
Température de base pour le chauffage (gaz) : 24 °C

À titre d'exemple, les erreurs cumulatives (calculées selon les formules présentées dans l'étape 2 de la description de la procédure) servant au choix de ces températures sont présentées dans le tableau 1.

Tel que mentionné ci-dessus, ces températures ont été utilisées pour normaliser les résultats de DOE-2 pour les comparer aux factures d'électricité et de gaz. La température de base des degrés-jours de chauffage est tellement élevée qu'elle exige des explications.

Tableau 1: Erreurs cumulatives

Temp. [°C]	Chauffage élec.	Refroidissement
0	0.8041	0.3612
5	0.5619	0.1682
10	0.3684	0.0725
15	0.2082	0.2866
18	0.1395	0.3978
20	0.1076	0.5200
24	0.0778	1.2930

Premièrement, tel qu'il est déjà mentionné, les degrés de véracité relatifs au point de consigne dans les locaux et à la température de soufflage sont considérés comme faibles à cause des thermostats non-protégés installés dans les locaux et du contrôle manuel de la température de soufflage. Deuxièmement, les plinthes électriques assurent le chauffage d'appoint dans les locaux desservis par les systèmes de climatisation sans avoir une séquence de contrôle adéquate pour éviter le soufflage d'air relativement froid et le chauffage simultané. Cette lacune nous a été confirmée par observation de l'opération des plinthes électriques qui fonctionnaient souvent en été ce qui peut expliquer le choix des températures de base pour le chauffage (24°C) et la climatisation (10°C).

Étant donné que ces températures ont un impact important sur la normalisation des résultats obtenus par la simulation, il est à souligner que grâce à l'une des originalités de la procédure, le choix des températures de base est tel que présenté ci-dessus. Sans appliquer la procédure, le choix porterait plutôt sur les températures souvent utilisées pour ce type de bâtiment, soit une température entre 10 et 18°C pour le chauffage et une autre entre 12 et 20°C pour le refroidissement.

Étape 5 et 6

Les Figures 1 et 2 présentent une comparaison entre la répartition mensuelle de la facturation et la normalisation de la consommation du 1er modèle DOE-2. L'analyse des résultats révèle une erreur relative sur la consommation annuelle de 28,96% pour l'électricité et de 48% pour le gaz naturel. Même si l'erreur relative sur l'électricité est très importante, nous avons essayé de corriger d'abord les résultats relatifs à la consommation du gaz. On peut constater en analysant

les résultats qu'il y a une différence importante pour la consommation du gaz de base en période estivale. Il est à noter que la demande de l'ECS a été établie dans ce modèle selon le code de plomberie et que la cédule utilisée de la demande horaire correspondait aux recommandations du Code Modèle National de l'Énergie dans les bâtiments *(CMNEB)* pour les laboratoires [2].

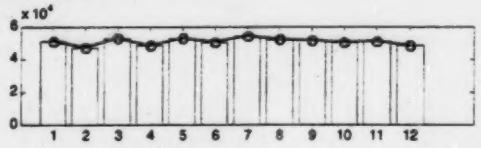

Figure 1: Répartition de la consommation d'électricité du 1er modèle

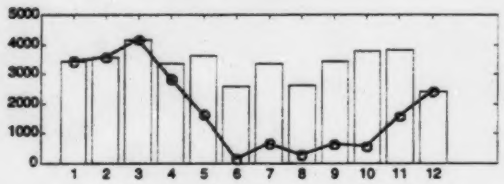

Figure 2: Répartition de la consommation de gaz naturel du 1er modèle

Étape 7

Étant donnée que durant la période d'été, le seul poste de consommation qui nécessite du gaz naturel est l'ECS, la demande maximale a été modifiée de façon à ce que la consommation de gaz en été soit comparable à celle facturée.

Deuxième simulation

Étape 2

Température de base pour le chauffage (élec.) : 24 °C
Température de base pour le refroidissement : 10 °C
Température de base pour le chauffage (gaz) : 15 °C

Étape 5 et 6

Il n'y a pas de changement au niveau des températures de base de chauffage électrique et de refroidissement et au niveau de la consommation d'électricité parce que l'ajustement du premier modèle portait seulement sur le gaz naturel. Les Figures 3 et 4 présentent une comparaison entre la répartition mensuelle de la facturation et la normalisation de la consommation du 2ième modèle DOE-2. L'erreur concernant la consommation d'énergie électrique n'a pas changé. Par contre, l'erreur sur la consommation annuelle du gaz a augmenté jusqu'à 95.57 %. Il est à noter que la consommation simulée de gaz en hiver est inférieure à celle facturée et que, pour la même période, la consommation d'électricité est trop élevée. L'ajustement doit donc viser ces anomalies.

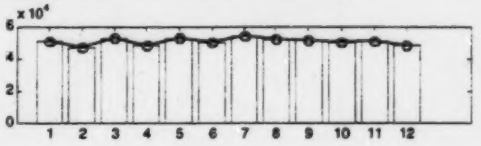

Figure 3: Répartition de la consommation d'électricité du 2ième modèle

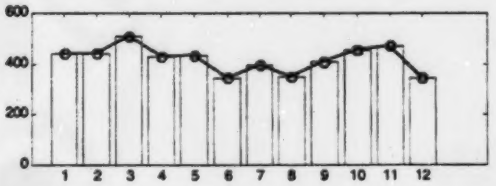

Figure 4: Répartition de la consommation de gaz naturel du 2ième modèle

Étape 7

Tel qu'il est déjà mentionné, le relevé détaillé a démontré un degré de véracité faible sur les consignes

d'opération, notamment, sur les températures de consigne de pièce et les températures de consigne d'alimentation. Tout en respectant les règles de l'art, on a proposé l'ajustement suivant :

- Le point de consigne de la température d'alimentation a été fixé à 15.8°C et 18°C respectivement en période d'hiver et d'été, contrairement au mode de contrôle du devis qui suggérait un ajustement de cette dernière en fonction de la température extérieure. Cette mesure a créé une augmentation de la consommation de gaz naturel (*serpentin de chauffage centrale*) et une diminution de la consommation d'électricité en période de chauffage. En période de refroidissement, elle s'est concrétisée par une diminution de la consommation d'électricité pour le refroidissement et le chauffage.

Troisième simulation
Étape 2
Température de base pour le chauffage (élec.) : 24 °C
Température de base pour le refroidissement : 10 °C
Température de base pour le chauffage (gaz) :10 °C

Étape 5 et 6
On peut constater une nette amélioration tant au niveau de consommation de gaz que d'électricité. Les figures 5 et 6 présentent une comparaison entre la répartition mensuelle de la facturation et la normalisation de la consommation du 3ième modèle DOE-2. L'erreur concernant la consommation annuelle d'énergie électrique est de 9.2 % et celle sur la consommation annuelle du gaz a diminuée jusqu'à 2.27 %.

Étape 7
En se référant aux degrés de véracité résultant du relevé de données, nous avons proposé les ajustements suivants :

- Le point de consigne de température des pièces a été fixé à 25°C en période de refroidissement et entre 22.9°C et 24°C en période de chauffage. Cette modification a eu pour effet d'augmenter la consommation électrique des plinthes en période de chauffage et de diminuer la consommation de chauffage en période de refroidissement.
- La date de mise en opération de la chaudière a été repoussée de 15 jours afin de diminuer la consommation de gaz pour le mois de novembre et d'augmenter la consommation d'électricité pour le chauffage. Cet ajustement résulte des anomalies décelées sur les résultats du mois de novembre.

Figure 5: Répartition de la consommation d'électricité du 3ième modèle

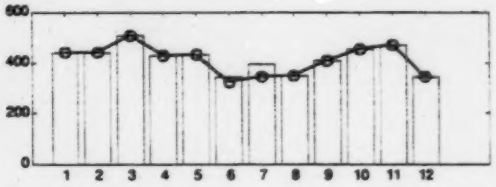

Figure 6: Répartition de la consommation de gaz naturel du 3ième modèle

Quatrième simulation
Étape 2
Température de base pour le chauffage (élec.) : 24 °C
Température de base pour le refroidissement : 10 °C
Température de base pour le chauffage (gaz) : 10 °C

Étape 5 et 6
Les figures 7 et 8 présentent une comparaison entre la répartition mensuelle de la facturation et la normalisation de la consommation du 4ième modèle DOE-2. L'erreur concernant la consommation annuelle d'énergie électrique est de 0.46 %, tandis que l'erreur mensuelle varie de 0.29 % en octobre à 8.69 % en novembre. L'erreur concernant la consommation annuelle du gaz est de 3.47 %. Par contre, l'erreur mensuelle varie beaucoup. Elle est surtout inacceptable en novembre.

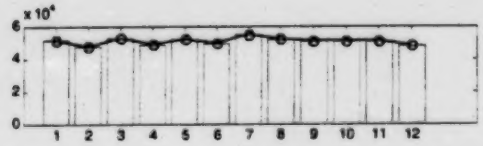

Figure 7: Répartition de la consommation d'électricité du 4ième modèle

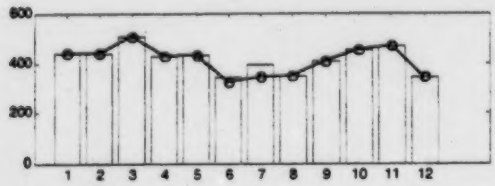

Figure 8: Répartition de la consommation de gaz naturel du 4ième modèle

Étape 7
Les ajustements suivants sont alors proposés :

- Repousser encore de 10 jours la mise en service de la chaudière à gaz. Selon le gestionnaire du bâtiment, cette mise en service était souvent retardée sans les conséquences graves sur le confort thermique, parce que les systèmes CVCA comportent des serpentins de réchauffage dans les gaines d'alimentation;
- Faire varier la température de soufflage de 15.8 à 16.9°C en novembre et décembre.

Cinquième simulation
Étape 2
Température de base pour le chauffage (élec.) : 24°C
Température de base pour le refroidissement : 10°C
Température de base pour le chauffage (gaz) : 5°C

Étape 5 et 6
Les figures 9 et 10 présentent une comparaison entre la répartition mensuelle de la facturation et la normalisation de la consommation du 5ième modèle DOE-2. Étant donné qu'il s'agit des résultats finaux, les erreurs annuelles et mensuelles relatives aux consommations de gaz et d'électricité sont présentées dans le tableau 2.

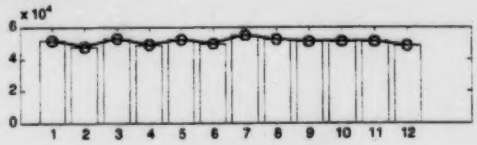

Figure 9: Répartition de la consommation d'électricité du 5ième modèle

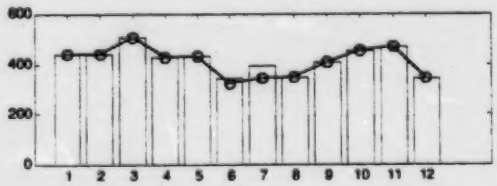

Figure 10: Répartition de la consommation de gaz naturel du 5ième modèle

L'analyse des résultats démontre que nous avons atteint les objectifs de validation pour l'électricité tant pour la consommation annuelle que pour les consommations mensuelles. Pour le gaz, l'objectif n'est atteint que pour la consommation annuelle. Le profil de consommation mensuelle correspond très bien au profil mensuel de facturation mais les erreurs relatives pour les consommations mensuelles exigent quelques explications.

- Les erreurs relatives concernant les mois d'août et de septembre sont élevées mais il s'agit des

différences absolues de l'ordre de 140 m^3 de gaz. Étant donné l'irrégularité d'utilisation de l'ECS surtout avec une animalerie dans le bâtiment, cette erreur est tout à fait acceptable.

- Pour les autres mois avec des erreurs supérieures à 10%, les différences absolues sont de 427 m_ en mai et jusqu'à 2100 en décembre. Même pour le mois de novembre avec l'erreur relative de 52.5%, cette différence n'est que de 483 m_ de gaz. Ces différences sont vraisemblablement dues à l'impact de l'utilisation des hottes de laboratoire sur l'efficacité des récupérateurs de chaleur des systèmes #1 et 3 tel qu'il est expliqué précédemment. Dans nos modèles, nous avons fixé l'efficacité de ces récupérateurs. En réalité, pour diminuer les différences au niveau de consommations mensuelles, il a fallu introduire au logiciel DOE-2 une fonction permettant de simuler une cédule appropriée d'utilisation des hottes et de calculer l'efficacité qui en résulte. Cependant, étant donné l'irrégularité d'utilisation des hottes, il nous semble que le modèle validé, sans comporter une telle fonction, peut pleinement servir à évaluer la majorité des mesures d'économie d'énergie.

Tableau 2: Sommaire des erreurs relatives à la consommation de gaz et d'électricité

Mois	DOE (électricité)	Facture (électricité)	Erreur (abs.) relative	DOE (gaz)	Facture (gaz)	Erreur abs.) relative
	MWh	MWh	%	m^3	m^3	%
1	88.47	93.85	6.1	8298	7309	13.5
2	87.05	90.17	3.6	10667	11339	5.9
3	87.66	83.08	5.2	7193	6898	4.3
4	79.82	72.87	8.7	4780	4148	15.2
5	73.11	69.25	5.3	1525	1098	38.9
6	74.49	70.08	5.9	365	331	10.1
7	90.30	86.69	4.0	477	443	7.7
8	84.09	86.11	2.4	385	522	26.1
9	76.62	79.59	3.9	435	574	24.2
10	76.02	74.50	2.0	452	452	0
11	94.52	98.39	4.1	1402	919	52.5
12	93.33	101.76	9.0	10089	12187	17.2
Total	1005.48	1006.34	0.09	46069	46222	0.33

REMERCIMENTS

L'étude présentée dans cet article réalisé par l'École de technologie supérieure fait partie d'un mandat octroyé par GES Technologies inc. dans le cadre d'un projet de développement du logiciel Best Building Facility Management.

CONCLUSION

Les éléments originaux de la procédure de validation présentée dans l'article sont les suivants :

Premièrement, la procédure de validation est dynamique, parce que la normalisation des résultats de simulation, ainsi que la répartition mensuelle des factures d'énergie sont effectuées en tenant compte des températures de base pour les degrés-jours de chauffage et de refroidissement. Ces températures, comme il est démontré dans cet article, peuvent varier suite aux ajustements apportés pendant la validation, tandis que dans la majorité de cas, ces températures, une fois choisies, sont considérées comme constantes. Le choix de ces températures est réalisé selon le critère présenté dans l'article. Il est à souligner que les températures de base pour les degrés-jours ont un impact indirect mais très important sur l'ajustement des modèles de simulation pendant la validation;

Deuxièmement, la validation est réalisée en tenant compte des fractions de consommations mensuelles relatives au chauffage, au refroidissement et à la consommation de base identifiées à partir des factures. La comparaison ainsi réalisée permet de cibler davantage les secteurs à ajuster. Comme il est présenté dans cet article, la procédure appliquée à un bâtiment complexe du point de vue de diversité énergétique s'avère efficace et rapide, parce que les critères de validation ont été atteints après seulement cinq itérations;

Troisièmement, les modifications apportées aux modèles de simulations portent en premier lieu sur les données techniques cueillies ayant un degré de véracité faible. Il est cependant à noter qu'un relevé détaillé de données techniques est indispensable pour ce type de validation.

BIBLIOGRAPHIE

1. DOE-2 Engineers Manual, Lawrence Berkeley Laboratory and Los Alamos National Laboratory, November 1982.
2. Code modèle national de l'énergie pour les bâtiments – Canada 1997
3. Fundamentals, ASHRAE Handbook, Atlanta, 1997.
4. Air-Conditioning Systems Design Manual, Prepared by the ASHRAE 581-RP Project Team Harold G. Lorsch, Principal Investigator, Atlanta, 1993
5. Sonderegger, R. (1998), A Baseline Model for Utility Bill Analysis Using Both Weather and Non-Weather Related Variables, ASHRAE Transactions, TO-98-12-2

VALIDATION AND CALIBRATION OF A MULTIZONE NETWORK AIRFLOW MODEL WITH EXPERIMENTAL DATA

Amy Musser, University of Nebraska-Lincoln, Omaha, NE
Oliver Schwabe, University of Nebraska-Lincoln, Omaha, NE
Steven Nabinger, National Institute of Standards and Technology, Gaithersburg, MD
amusser@unl.edu, oliver.schwabe@gmx.net, steven.nabinger@nist.gov

ABSTRACT

This paper chronicles the development and refinement of a multizone network airflow model to represent a two-story classroom-office building. The model is initially developed during construction based on architectural plans and published leakage information. After construction is complete, envelope leakage is refined based on fan pressurization tests. Measured fan flow rates are then used to refine the air handling system portion of the model. A final revision makes use of automated tracer gas decay tests to fine-tune the flow rates to individual rooms. Predictions of the multizone model with these varying levels of refinement are then compared with additional tracer gas decay tests. The ability of the model to simulate the conditions of the experimental tests is evaluated at each stage of refinement. The experimental effort required for each step in the refinement process is discussed.

INTRODUCTION

Multizone network airflow models allow engineers to predict infiltration, ventilation rates, contaminant transfer, and pressure differences in buildings. Although the mathematics behind these models is well understood, it can be difficult to determine input parameters, particularly for envelope leakage. This may be dealt with by analyzing a range of possible leakages to obtain a bounded solution. Fan flows are easier to estimate, based on the mechanical system design.

In existing buildings, leakage and flow characteristics can be field measured. Fan pressurization, tracer gas tests, and flow measurement are three common techniques that could assist in fine-tuning model inputs. This paper documents the modeling process for one such ongoing project. A two-story classroom building is initially modeled during the design phase using published leakage data and architect's plans. The building leakage is refined based on results of a fan pressurization test, and flows adjusted based on field measurements. The modeled air handling system flows are then further adjusted based on a set of tracer gas decay tests. The refined models are then used to predict future tracer gas concentrations. This work discusses a process that can be used to refine a building model using experimental data. It also provides validation of the model as it might be applied to non-residential buildings.

MULTIZONE MODELING

The public domain multizone network airflow model CONTAMW (Dols et al 2000) was used for this study. In CONTAM, buildings are represented as networks of connected zones (e.g., rooms), within which uniform contaminant concentration is assumed. Zones are connected to one another and the outdoors via paths that represent the building component leakage. A mass balance calculation determines the flow between the zones and concentrations of contaminants distributed by this flow.

Defining the building leakage is perhaps the most difficult aspect of using these models. Buildings have many leakage paths, which may not be obvious from design drawings. The leakage associated with identical components can also vary significantly with construction. Fan driven flows in non-residential buildings can also vary from the design values shown in construction documents. When a building is being modeled in the design phase, it is common to model a range of leakages and fan flows. Modeling of existing buildings allows fine-tuning based on field measurements.

BUILDING DESCRIPTION

A two-story classroom/office building located on a college campus in the United States was used for this case study. Its design was intended to demonstrate innovative technologies and design techniques for reducing the environmental impacts of buildings. Some of its unique features include operable windows, CO_2 demand control, and an onsite biologically engineered wastewater treatment facility called a living machine.

The building has a classroom/office wing that is separated from an auditorium by a large atrium. The living machine is housed in an unconditioned glass enclosure adjacent to the atrium and auditorium and is maintained at a negative pressure relative to these spaces. A

primary air handling system serves the classroom/office wing, while another serves the auditorium and atrium.

The air handling system design seeks to supply 100 % outdoor air for ventilation, in quantities modulated based on CO_2 demand control. Many of the occupied spaces are equipped with occupancy and CO_2 sensors. When a room is occupied, its supply damper is opened 50 %. When the CO_2 concentration exceeds 800 ppm(v)*, the supply damper opens to 100 %. A pressure sensor in the supply duct is intended to modulate the total outdoor airflow supplied by the air-handling unit.

EXPERIMENTAL MEASUREMENTS

Fan pressurizations tests are commonly used to measure exterior envelope leakage in residences and other small buildings (ASTM 1999). The building is pressurized using a calibrated fan and the resulting pressure difference between indoors and outdoors is measured. Results over a range of pressures can be correlated to a powerlaw relationship that can be used to estimate the leakage at a given pressure difference. This method quantifies the gross exterior envelope leakage, without regard for location of specific leakage sites.

The building studied here was small enough that it could be pressurized up to 40 Pa using two calibrated fans of the type that are normally used in residences. One test was conducted with all interior doors open to obtain the overall exterior leakage. Since the auditorium wing was easily isolated from the rest of the building, it was tested separately as well.

Fan driven flows throughout the building were also verified. Flow rates for localized exhaust fans were measured using a flow hood. Gross air handling system supply and return flow rates were measured by pitot tube duct traverse, a method commonly used in testing and balancing (ASHRAE 1988). A pitot tube and differential pressure gauge are used to measure the velocity pressure at evenly spaced points over a cross section of the duct, to obtain air speed. These readings are then averaged and multiplied by the duct cross sectional area to obtain the duct flow rate.

Smoke tests are another useful method to qualitatively document airflow behavior in buildings. Tubes, candles and other devices can be used to generate a small amount of smoke for flow visualization. This technique was used to verify the direction of flow between rooms under normal operating conditions.

Building air change rates under actual operating conditions were measured using tracer gas decay (ASTM 2000a). Sulfur hexafluoride (SF_6) tracer gas was periodically released upstream of the air handling unit supply fan to maximize mixing and achieve as uniform as possible distribution throughout the building. This technique allows calculation of the building air change rate based on decay of the tracer gas over time.

Automated tracer gas injections were enabled at each of the two air-handling units at two-hour intervals. Pressure switches were used to indicate fan on/off status so that no injection would be made when an air-handling fan was off. Air sampling pumps collected samples from nine building rooms and the outdoors via a network of polyethylene tubing. These samples were analyzed using a gas chromatograph equipped with an electron capture detector, calibrated to determine SF_6 concentration between 5 and 300 ppb(v).

CONSTRUCTION STAGE MODEL

During construction, the architect's plans were used in conjunction with published leakage data to obtain a model representation of the building. Building envelope leakage was specified for the CONTAM model using a hybrid approach that considered some easily identified leakage sites (such as doors and windows) and a distributed envelope leakage to describe wall construction and other details. This approach allowed the impact of easily identified leakage sites to be applied in the correct location, while reducing the input effort for less obvious leakage paths.

Door and window leakages were taken from ASHRAE residential data (ASHRAE 1997). Distributed envelope leakage of 0.75 cm^2/m^2 was also specified. This leakage was chosen to provide an overall leakage of 1.1 cm^2/m^2 (at 10 Pa, C_D=0.6) in a simulated fan pressurization test. This leakage is slightly lower than the average of 79 office and school buildings in the US, Canada and UK that were surveyed in a recent review (Persily 1999). Interior partitions, ceilings, and floors were modeled with twice the leakage of the exterior walls. An air handling system, with diffuser flows taken from the mechanical design drawings was also specified. Figure 1 shows the layout of zones, leakage paths, and HVAC diffusers for a portion of one floor of the building.

---

* ppm(v), is traditionally used to denote concentration in this application. 1 ppm(v) CO_2 = 1.80 mg/m^3 and 1 ppm(v) SF_6 = 5.97 mg/m^3

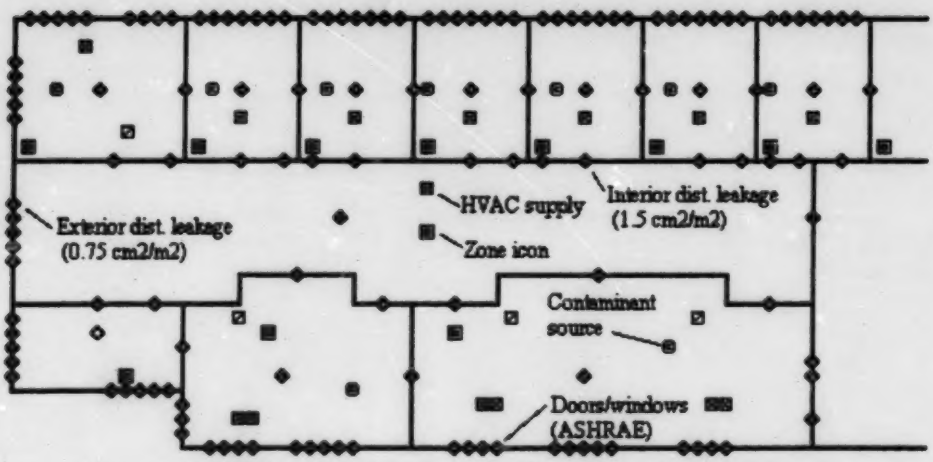

Figure 1. CONTAM model of representative floor and modeling assumptions.

FAN PRESSURIZATION MODEL

After construction of the building was complete, fan pressurization tests indicated that the exterior envelope of the building was roughly four times leakier than was originally assumed. Based on this result, the distributed exterior envelope leakage of the model was changed from 1.1 cm^2/m^2 to 4.3 cm^2/m^2 to match the experimental test. This was a significant increase, so the interior leakage was also adjusted to maintain a ratio of 2:1 between interior and exterior leakage.

The isolated pressurization test of the auditorium was used to specify large leakage paths that were visually apparent between that space and the attached living machine. This was done by assuming that the distributed exterior leakage was the same as for the building as a whole, and the excess measured leakage was used to define a path connecting to the living machine.

Figure 2 shows simulated fan pressurization tests for the construction stage model (leakages estimated from published data) and the fan pressurization model (leakages adjusted to match the actual fan pressurization tests). The large differences in the two curves underscores the importance of modeling a range of leakages in cases where the actual leakage cannot be measured.

MEASURED FLOW RATE MODEL

The next step in collection of experimental data was to field verify as many fan-driven flow rates as possible. Several "service" areas located on the first floor are ventilated by local exhaust fans. These are controlled using a variety of means including thermostat, occupancy sensors, and switch. Flow rates for all of the accessible fans were verified using a flow hood. A few of these fans were not accessible, so the design flow rate listed on the mechanical schedule was used.

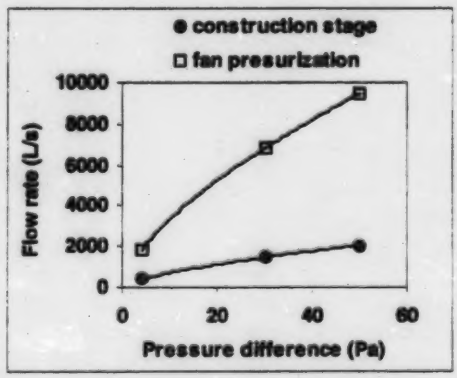

Figure 2. Fan pressurization test of construction stage and fan pressurization models.

The exhaust fan used to depressurize the living machine was too large for use of a flow hood. It was originally specified to operate at constant flow rate, but was oversized and the doors had to be kept locked to keep them from blowing open when the fan was operating. To solve the problem, a variable speed drive was installed and controlled to maintain a 20 Pa pressure difference between the living machine and the adjacent atrium. In CONTAM, this fan was therefore specified to maintain a pressure difference of 20 Pa.

Duct traverse velocity measurements were used to determine the overall supply and return volumes of the two air handling systems. Duct velocity measurements taken with the dampers in the spaces with CO_2 demand control dampers commanded to various positions

showed that the duct pressure feedback mechanism did not reduce the total volume of outside air supplied to the building. Therefore, the design flow rate was supplied by the system at all times, regardless of damper position in the individual spaces. The operation of dampers at each of the rooms served to change the distribution of the ventilation air among the spaces, rather than reduce the overall volume of supply air to the building. This was not easily remedied, and this operating scenario continued throughout the tests.

It was also discovered at this stage that the auditorium had not been scheduled for classes during the first semester of building operation. As a result, the air handling system serving that part of the building was usually off and was deactivated in the CONTAM model.

The primary air handling system design supply and return flow rates at each diffuser were scaled down proportionally to match the measured overall system flow. Little change was made to the supply flow, which was within about 10 % of the design volume. The measured return volume was only about 60 % of that which was expected based on the design drawings, so it was scaled back more significantly in the model.

To evaluate the performance of this and the previous two models, their predictions were compared with the results of ten tracer gas decay tests. In CONTAM, each decay test was modeled separately; with initial concentrations of SF_6 tracer gas specified as the measured concentration in each room at the start of the decay period. For spaces in which the SF_6 concentration was not measured directly, the concentration for a similar space was used. This did not cause much of a problem, because most of these spaces were depressurized with respect to those in which SF_6 concentration was measured. However, the corridors were an exception. The corridors received a large volume of supply air from the air handling system, and communicated significantly with the atrium and auditorium through flow driven by the large exhaust fan in the living machine. At this step, the initial concentrations of tracer gas in the two corridors (C_{cor}) were estimated using a simple mass balance for a tracer gas that is uniformly mixed in the supply air and the design supply flow rate. The quantity VC_{cor}/Q_s in the corridor was approximated by the average of VC_{meas}/Q_s in the rooms in which SF_6 was measured. Here, V denotes the room volume, C_{meas} is the measured initial SF_6 concentration, and Q_s is the volume of air supplied to each room by the air handling system.

CONTAM simulations for the three levels of model refinement were compared with measurements of SF_6 concentration in each room taken at ten minute intervals. These comparisons were quantified using correlation coefficient and normalized mean square error as defined by the ASTM Guide for Statistical Evaluation of Indoor Air Quality Models (ASTM 2000a).

The correlation coefficient (r) is defined as:

$$r = \frac{\sum_{i=1}^{n}\left[\left(C_{m,i}-\overline{C_m}\right)\left(C_{p,i}-\overline{C_p}\right)\right]}{\sqrt{\left[\sum_{i=1}^{n}\left(C_{m,i}-\overline{C_m}\right)^2\right]\left[\sum_{i=1}^{n}\left(C_{p,i}-\overline{C_p}\right)^2\right]}}$$

where, C_m is the measured concentration and C_p is the concentration predicted by the model. Correlation coefficient measures the degree of linear relationship between the two data sets. Its maximum value of 1 indicates a perfectly linear positive relationship, while the minimum value of –1 signifies a perfect negative relationship. It is important to note that either data set could be multiplied by a constant without changing r (Devore 1987). This means that two parallel decay curves would have r=1, even though the concentrations might be very different. However, since in this case all modeled concentration curves begin with the same concentration as was initially measured, different concentrations at later times must be accompanied by a difference in the slope of the decay curve.

The normalized mean square error (NMSE) measures the magnitude of the difference between the predicted (C_p) and measured (C_m) concentrations, and is defined as,

$$NMSE = \frac{\overline{\left(C_p-C_m\right)^2}}{\overline{C_p}\,\overline{C_m}}$$

NMSE will equal zero when the predicted and measured concentrations are equal. For cases in which the two data sets differ consistently by 50 %, NMSE will be about 0.2, and when they differ by 100 %, NMSE will be about 0.5. When considered in conjunction with the correlation coefficient, NMSE helps to identify cases in which the concentration profiles are parallel but not equal.

The correlation coefficients and NMSE values shown in Table 1 are averages for ten decay periods. In most of the spaces, the model predictions did not improve significantly as the model was refined. Because the flow in these rooms is primarily fan-driven, the predictions of the first two models are not very different, even though the building envelope is much leakier in

the second model. This would not be expected to be the case in the absence of fan-driven flow, since the infiltration performance of the two models would depend on building leakage. In the third model, the fan flows were adjusted to reflect the overall measured flow to the building. However, since the overall supply flow was close to design, this did not result in a significant change for these spaces either.

Tracer gas decay rates in the administration, classrooms, conference room, and library all tended to be over-predicted by the three computational models. A typical decay period for one of these spaces is shown in Figure 3a. These spaces tended to be pressurized by the air handling system with respect to the outdoors and corridors. Therefore, the experimental profile is similar to an ideal exponential decay curve.

The spaces discussed above all utilize CO_2 demand control. The building was lightly occupied during the test period and CO_2 levels (also documented by our instrumentation system) rarely exceeded 800 ppm(v), so the dampers serving these spaces would have been in the 50 % open position during most hours of operation. Since the system is still supplying the same volume of supply air to the entire building, some of the supply air intended for these spaces would be diverted to duct leakage and the spaces without demand control. These include the six offices (represented by typical office 1) and the corridors on the first and second floors. Visual inspection of the concentration profiles for the office verified a higher measured tracer gas decay rate than was planned during design. Based on this observation, it is likely that a larger than intended volume of supply air was supplied to the corridors as well.

The much lower correlation coefficients obtained for the auditorium indicate a difference in shape between the predicted and measured concentration profiles. This effect was also present in the atrium, but to a somewhat lesser degree. During the decay period, the tracer gas concentrations in these spaces did not follow an exponential decay profile. This is because the air handling system that supplies ventilation air directly to these spaces was not operating during the tests. The large exhaust fan in the living machine created an airflow pattern that moved air from corridors into the atrium, through the auditorium and out via the living machine. Figure 3b shows typical measured and modeled concentration profiles for the atrium. These show a tendency of the three models to predict some transfer of tracer gas into the atrium after the injection, but it is not as high as was measured. This is consistent with the three models under-predicting the volume of supply air (and thus tracer gas) delivered to the corridors.

Likewise, there was not a notable reduction in the NMSE with these three model refinements. One exception is that the fan pressurization model improves the auditorium prediction. This happens because the leakier building components allow more tracer gas to enter the auditorium. However, the predicted tracer gas concentrations are still lower than were measured.

All three models also consistently under-predicted the tracer gas decay rate in the mechanical room. The flow rate of the exhaust fan in that room could not be measured using a flow hood because access to the fan was blocked by equipment. Therefore, the under-prediction in airflow rates by all three models suggests that the fan is actually removing more air than is specified on the design drawings.

Space	Construction stage model		Fan pressurization model		Measured flow rate model	
	r	NMSE	r	NMSE	r	NMSE
Administration	0.94	0.31	0.94	0.25	0.94	0.29
Atrium	0.91	0.25	0.89	0.27	0.90	0.26
Auditorium	0.47	0.73	0.71	0.38	0.77	0.33
Classroom 1	0.96	0.26	0.96	0.24	0.96	0.30
Classroom 2	0.97	0.26	0.97	0.26	0.97	0.29
Conference	0.96	0.48	0.96	0.42	0.95	0.53
Library	0.96	0.32	0.97	0.24	0.97	0.30
Mechanical	0.96	0.23	0.97	0.21	0.95	0.30
Office 1	0.97	0.10	0.96	0.15	0.96	0.16

Table 1. Average Correlation Coefficient and Normalized Mean Square Error.

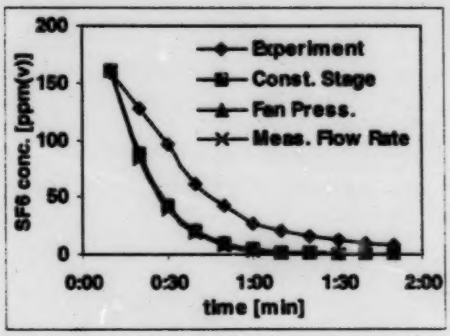

(a) Classroom 1

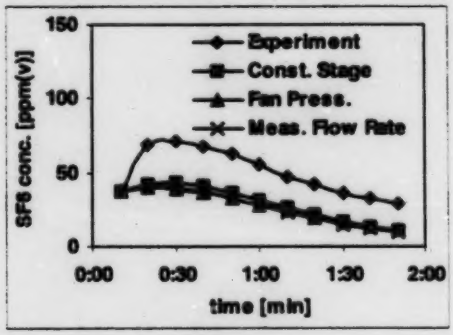

(b) atrium

Figure 3. Measured and Predicted tracer gas decay.

TRACER GAS DECAY MODEL

The final model refinement considered average air change rates in each of the rooms based on one month of tracer gas data. The tracer gas decay technique estimates air change rates in any enclosure that acts as a single zone. Testing of an entire building requires that the tracer gas be at a uniform concentration throughout the building at the start of the test. The method could also be applied to a single room provided that no tracer gas enters it from adjacent spaces during the test. In this case, modeling and smoke testing had shown that the rooms receiving supply air from the air handling unit were pressurized with respect to most of the neighboring spaces, with little tracer gas leaking back into them. This was supported by the observation that the tracer gas decay profiles for these rooms resembled exponential decay curves. For these spaces, average air change rates for the month were estimated based on tracer gas decay for each room, and are shown in Table 2.

Tracer gas was only released when the air handling system was operating, so Table 2 represents this condition. Air change rates were then compared with the prediction of the measured flow rate model for the rooms in which tracer gas concentration was measured directly. Again, air change rates in spaces with CO_2 demand control tended to be overestimated by the model while the air change rate in the office, which is not demand controlled, was under predicted.

Space	Experiment*		Measured flow model
	Air chg. rate (1/hr)	Std. Dev.	Air chg. rate (1/hr)
Administration	1.00	0.43	1.73
Classroom 1	1.00	0.19	2.63
Classroom2	1.60	0.27	4.19
Conference	1.22	0.24	3.87
Library	1.10	0.23	2.07
Office 1	1.30	0.24	0.93

Table 2. Air Change Rates For Spaces Served by Primary AHU.
**averaged for one month*

In the final model refinement, supply air volumes to each room were fine-tuned to match the air change rates shown in Table 2. Because the air handling system was not capable of reducing its overall supply volume, the amount of air supplied to the two corridors was determined by adding together the supply volumes for all of the other spaces, and subtracting that sum from the total system supply.

This adjustment resulted in a larger amount of ventilation air supplied to the corridors by the air handling system. In the CONTAM model, the initial concentration of tracer gas in the corridors was estimated using the same technique as for the measured flow rate model. This resulted in higher initial SF_6 concentrations in the corridors.

The tracer gas decay model was then used to simulate five future tracer gas decay tests. Figure 4 shows the predictions of all four models compared with one of these future decay periods. This final model refinement produces a tracer gas decay profile in classroom 1 that is much closer to the measured profile.

In the atrium (Fig. 4b) and auditorium, the higher initial concentration modeled in the corridors resulted in model predictions that were closer to the experimental measurement, but the agreement was still not as good as for the other rooms. This would be expected, since

these large spaces would not be as well represented by a single concentration measurement.

Figures 5 and 6 show the correlation coefficient and NMSE for the tracer gas decay model compared with those obtained for the other models as shown in Table 1. The increased correlation coefficient in nearly every room indicates that the tracer gas decay model improves the predicted air change rate. Likewise, the NMSE drops significantly for these rooms as well.

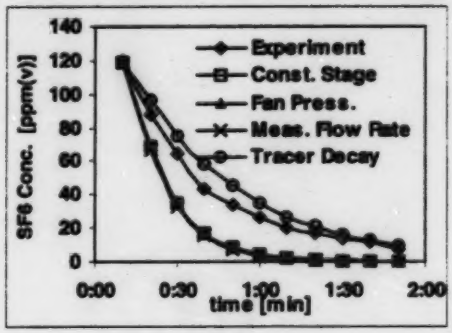

(a) Classroom 1

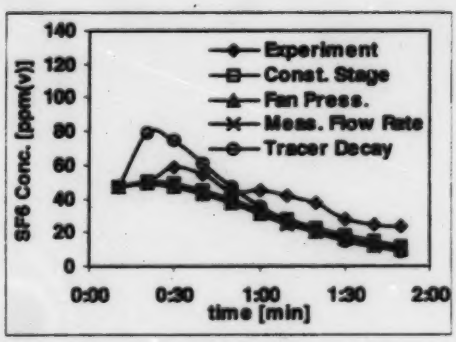

(b) atrium

Figure 4. Measured and predicted tracer gas decay.

Classroom 2 is the single exception to this trend. Upon investigation, it was noted that during three of the five decay intervals used to analyze the tracer gas decay model, the CO_2 readings in this room were above 800 ppm(v). Since this had rarely occurred during the prior month, it would be expected that the damper to this space would now be 100 % open and the model would underpredict the supply flow rate to this room. Thus, to make its predictions more accurate, one would have to devise a mechanism for linking the model to the actual changing room flow condition.

DISCUSSION

Building leakage characteristics have often been stressed as an important contributor to realistic model predictions. However, in this study properly defining the fan driven flows more directly influenced the model results. This occurs because the air change rate under the model conditions is primarily fan driven. Infiltration data collected for this building showed air change rates of approximately 0.25 h^{-1}, compared with approximately 1 h^{-1} when the fan was on. Therefore, the fan flow rate is most important to properly represent the building when the fan is on. If the model were being used to predict infiltration (fan off) conditions, or if the fan flow rate were determined based on pressure control, however, the leakage of the exterior envelope would undoubtedly play a more significant role.

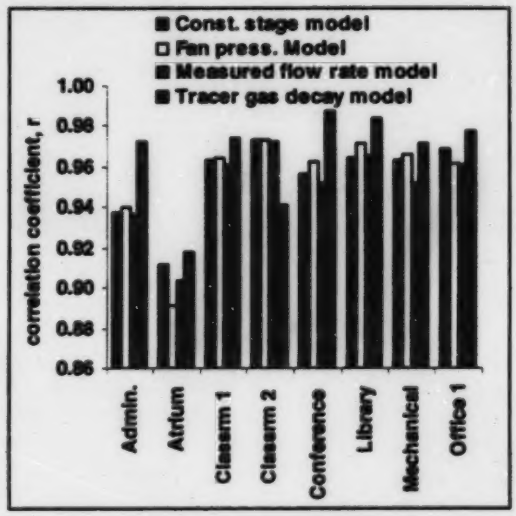

Figure 5. Correlation coefficient

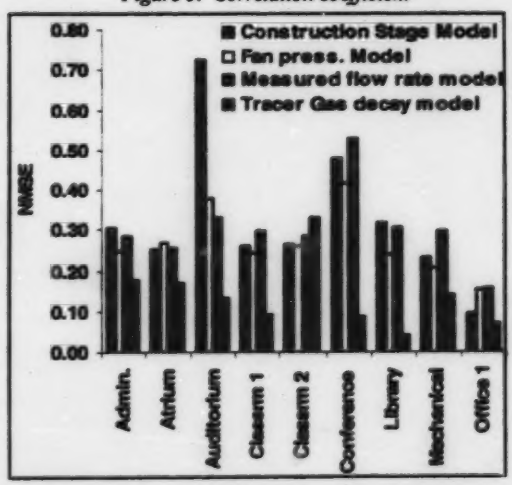

Figure 6. Normalized mean squared error.

Of the experimental techniques used for refinement of the model, the tracer gas decay tests required the most effort. The fan pressurization tests were completed in a half-day and the data analyzed in an hour. Likewise, the flow hood measurements, smoke test, and duct traverses were conducted in about one day. The tracer gas decay tests required a long-term installation of tubing, measurement equipment and an automation protocol. A temporary setup could have been implemented more quickly, but a significant computing effort was also required to sort and analyze the collected data.

The level of effort needed to adequately characterize fan-driven flows depends on the type of ventilation system and its configuration. A duct traverse at the air handling system is a good first step to verify that the overall volume of supply air is close to what is expected. This measurement is often done as a part of the testing and balancing process. If the system has a mechanism to reduce the overall volume of supply air, a repeated duct traverse in the same location at this partial flow condition can uncover irregularities in part load operation.

Additional duct traverses in downstream branches of the system or flow hood measurements might also be used to field verify the distribution of supply air. In the case of a variable volume system, measurement of another control quantity, such as CO_2 or temperature could help to estimate flow under specific operating conditions. Unique aspects of this building simplified the process somewhat. Despite the fact that damper control did change the distribution of supply air among the spaces, low occupancy resulted in less variability in air change rates in these spaces.

CONCLUSIONS

In comparison to the measured data, the CONTAM predictions were quite good for the pressurized spaces once the flow rates to individual rooms were defined based on experimental measurements. Because this air handling system was not operating as designed at part load, significant measurement effort was required to understand and quantify the actual operating condition.

Proper definition of the fan driven flows was the most important experimental measurement contributing to agreement of the model and the experiment. This is because the building air change rate during the experiment was primarily driven by fan flow and because flow rates were defined directly in the model. If the building fans had been controlled to provide defined pressure differences or if the model had been used to predict infiltration for a period in which the air handling system was off, proper definition of the exterior envelope leakage would have been more critical.

REFERENCES

ASHRAE 1988. "Best Practices for Measurement, Testing, Adjusting, and Balancing of Building Heating, Ventilation, Air-Conditioning, and Refrigeration Systems." ASHRAE Standard 111. American Society of Heating, Refrigeration, and Air-Conditioning Engineers, Inc. Atlanta, GA, USA.

ASHRAE 1997. *Handbook of Fundamentals*. American Society of Heating, Refrigeration, and Air-Conditioning Engineers, Inc. Atlanta, GA, USA.

ASTM 1999. "Standard Test Method for Determining Air Leakage Rate by Fan Pressurization." ASTM E 779-99. The American Society for Testing and Materials, Philadelphia, PA, USA.

ASTM 2000 (a). "Standard Guide for Statistical Evaluation of Indoor Air Quality Models." ASTM E 741-00. The American Society for Testing and Materials, Philadelphia, PA, USA.

ASTM 2000 (b). "Standard Test Method for Determining Air Change in a Single zone by Means of a Tracer Gas Dilution." ASTM E 741-00. The American Society for Testing and Materials, Philadelphia, PA, USA.

Devore, J. 1987. *Probability and Statistics for Engineering and the Sciences*. 2nd Ed. Brooks/Cole Publishing Company. Monterey, California.

Dols, S., G. Walton, and K. Denton. 2000. "CONTAMW User Manual." NISTIR 6476. National Institute of Standards and Technology, Gaithersburg, MD.

Persily, A. 1999. "Myths About Building Envelopes." ASHRAE Journal. 41(3):39-47. American Society of Heating, Refrigeration, and Air-Conditioning Engineers, Inc. Atlanta, GA, USA.

Session 7 / Séance 7

Recent Developments in Modelling Thermal and Other Physical Processes

Les plus récents développements dans la modélisation des procédés thermiques et des autres procédés physiques

ADVANCES IN MODELLING THERMAL BRIDGES IN BUILDING ENVELOPES

Stephen Carpenter
Enermodal Engineering Limited
Kitchener, ON, Canada
scarpenter@enermodal.com

ABSTRACT

This paper describes recent techniques developed to simplify the analysis and improve the accuracy of modeling thermal bridges. Two techniques are presented for determining the overall wall thermal resistance. The first is a hand technique using weighting factors between the isothermal planes and parallel path results. The second is a MS-WINDOWS finite-volume computer program. A technique is presented that accounts for the impact of thermal bridges on the transient response of wall systems. The equivalent wall model involves creating a fictitious multi-layer wall with properties selected so that its dynamic response to the transient conditions is the same as the real wall with two- and three-dimensional effects.

INTRODUCTION

Most building envelopes have thermal bridging: locations where the thermal resistance of the assembly is comprised for structural or framing reasons. Common thermal bridges include steel or wood studs in cavity walls, junctions between floors and walls, balconies and other structural protrusions, corners and extra framing around doors and walls. These thermal anomalies increase heat transfer to the outdoors and can be a site for condensation. Despite their common nature, many building simulation programs and program users ignore the impact of thermal bridging or attempt to account for thermal bridging with a simple correction factor to the R-value. This paper describes recent techniques developed to simplify the analysis and improve the accuracy of modeling thermal bridges. These techniques account for the impact of thermal bridges on thermal resistance and transient response of the wall system.

BUILDING ENVELOPE THERMAL RESISTANCE

Traditional Approach

The negative impact of thermal bridges has been known for a long time. Most building designers are aware of the reduction in wall R-value due to wood and steel framing. The traditional analysis technique to determine this reduction has been the "Parallel Path" method as described in the ASHRAE Handbook of Fundamentals. The resistances of each layer are added together to get a total path R-value. If there is more than one path through the wall (e.g., through the wood stud and through the cavity insulation), the total resistance of each path is calculated. The U-value (reciprocal of R-value) of each path are area-weighted to determine the total wall R-value.

This approach implies that the heat flows in parallel paths and does not adjust its direction to find an easier route through the wall. The reality of course is that heat takes the path of least resistance, and as such the parallel path method always over-predicts the actual R-value.

Table 1 lists the R-value over-prediction of the parallel path method for two common wood and steel frame wall systems. The over-prediction was calculated by comparing the results of the parallel path method to the results from 2-D finite volume analysis (see Section 2). The over prediction is most severe with steel frame walls but also has an effect in wood frame walls.

Table 1: Parallel-Path R-value Over-Prediction (%)

Wall Type	Wood Frame	Steel Frame
38 X 89 @ 400 mm centers with 25 mm ins. Sheathing	2.2 %	54 %
38 X 140 @ 400 mm centers with 25 mm ins. sheathing	2.2 %	86 %

Hand Calculation Correction Factors

The ASHRAE Handbook of Fundamentals recommends that both the parallel path method and the isothermal planes method be used to determine wall R-value. The correct wall R-value will be somewhere between these two results. In the isothermal planes method, the effective R-value of each layer is added together. If a layer is made up of more than one material, the material thermal conductivites are area-weighted.

Unfortunately, the two methods give very different results and some information is needed to determine where between these two extremes the correct answer lies. The results from the two methods can be weighted as follows:

$$R_{wall}=R_{isothermal\ planes}*K+R_{parallel\ path}*(1-K)$$

Where K is a weighting factor between 0 and 1

Figure 1 shows the weighting factor (K) for a variety of steel and wood stud assemblies [Enermodal, 1996]. A value of 1.0 means that the isothermal-planes result is correct and a value of 0.0 means that the parallel-path result is correct. The lower the value K is, the higher the R-value will be. As the studs are placed closer together, thermal bridging is more significant and a higher weighting factor is required. Similarly, deeper studs cause more thermal bridging.

The above approach is useful for assessing thermal bridging in simple stud walls, however, it does have three major limitations. First, the weighting factors are limited to the wall systems studied. Second, the method cannot be easily applied to non-parallel geometries such as corners and wall/floor junctions. Third, the method does not account for lateral heat transfer caused by highly conductive layers. Two-dimensional finite-volume heat transfer overcomes all of these limitations.

Figure 1: Weighting Factor between Isothermal Planes and Parallel Path Results

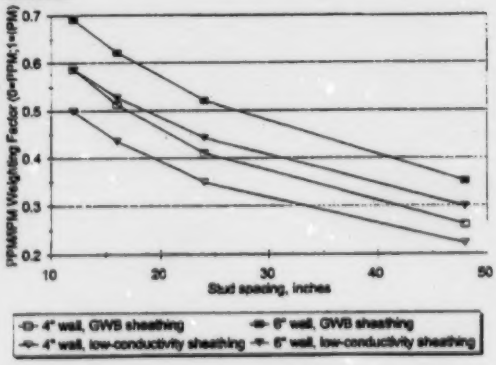

Two-Dimensional Heat Transfer

Several two-dimensional computer programs (such as FRAMEplus, Enermodal, 2001a) are available to analyze more complicated wall assemblies. The speed of analysis and ease of use of these programs means that practitioners can use them on a daily basis as part of their design practice.

The latest version of FRAMEplus (5.0) allows users to draw and analyse wall and window sections in a MS-WINDOWS environment. The program has a comprehensive materials library and automatically assigns environmental boundary conditions, meshes the geometry and performs the calculations (usually within a few seconds). For complex walls and windows, the program area-weights individual results to obtain total wall (including corners etc) and window results.

Figure 2 shows the FRAMEplus screen of an insulated concrete block drawing. Figure 3 shows the main screen where the component area-weighting is performed.

This and similar computer programs provide a simple and accurate means of determining total wall properties to account for the thermal resistance impact of thermal bridging. However, these thermal anomalies can also have an impact on the thermal or transient response of wall assemblies. The time-lag benefits of a thermal massive wall system can be partially negated by thermal bridging. This speeds up the thermal response of the wall. A different approach is needed to account for transient effects.

Figure 2: FRAMEplus Model of an Insulated Concrete Block

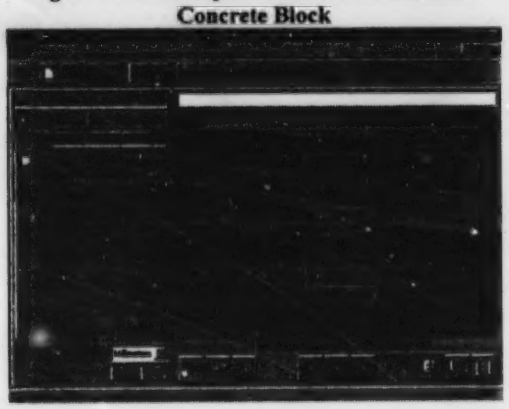

Figure 3: FRAMEplus Screen for Displaying Total Window/Wall Results

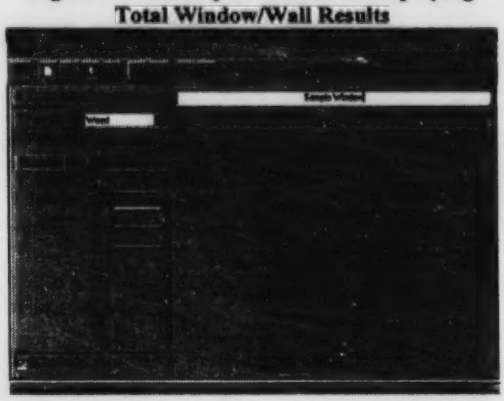

BUILDING ENVELOPE TRANSIENT RESPONSE

Equivalent Wall Model

Most building energy analysis programs model the transient response of walls as a series of one-dimensional layers, ignoring the impact that thermal bridges have on the transient response of the assembly. A recent ASHRAE project developed the concept of equivalent wall layers to account for this impact [Enermodal, 2001b]. The equivalent wall technique is a relatively simple way to model complex building assemblies in whole-building energy programs that use a nodal network or require input of thermo-physical properties of wall layers.

The equivalent wall model involves creating a fictitious multi-layer wall with properties selected so that its dynamic response to the transient conditions is the same as the real wall with two- and three-dimensional effects. Thus, for example, a homogenous wall layers could be defined with specific conductivities, densities, specific heats, etc., to give the same dynamic (and steady-state) response as a steel-framed wall with gypsum wallboard sheathing.

The equivalent wall method, developed by Kossecka and Kosny [1996, 1997], is incorporated into a specialized version of HEATING 7.2 [Childs, 1993], called

EQV_WALL. This computer tool aids in the modeling of dynamic thermal performance of complex wall systems with significant thermal mass, and is utilized for these simulations.

The equivalent wall method uses, as its mathematical basis, conditions imposed on the response factors and z-transfer function coefficients by thermal structure factors. Thermal structure factors are dimensionless quantities representing the fractions of heat stored in the wall volume, in transition between two different states of steady heat flow, which are transferred across each wall surface.

Structure factors φ_{ii} and φ_{ie} for a wall composed of n plane homogeneous layers, numbered from 1 to n with layer 1 at the interior surface, are given as follows:

$$\varphi_{ii} = \frac{1}{R^2 C} \sum_{m=1}^{n} C_m \left[\frac{R_m^2}{3} + R_m R_{m-e} + R_{m-e}^2 \right]$$

$$\varphi_{ie} = \frac{1}{R^2 C} \sum_{m=1}^{n} C_m \left[-\frac{R_m^2}{3} + \frac{R_m R}{2} + R_{i-m} R_{m-e} \right]$$

where R is the total thermal resistance per unit cross section area, R_m and C_m denote the thermal resistance and capacity of the m-th layer, whereas R_{i-m} and R_{m-e} denote the resistance for heat transfer from surfaces of the m-th layer to inner and outer surroundings, respectively.

There are several ways the equivalent wall technique may generate a simple one-dimensional multi-layer structure with the same thermal properties and dynamic behaviour as the actual wall. The first step is to assume some number of 'equivalent' layers for the wall structure. Experience has shown that three-layer equivalent wall models provide the best results. A simple way to solve for equivalent layer properties is to first generate, randomly or with some logic, a set of capacitances C_n (or resistances R_n) for each layer. Then seek the resistances R_n (or capacitances C_n) to satisfy the above equations. The thermal structure factors and overall R-value must match those for the 3-D wall assembly. Thermo-physical properties of the layers may then be established, if necessary, to match R_n and C_n values and total thickness of the wall.

The development of the equivalent wall model is an iterative procedure. By adjusting the number and capacitances of equivalent wall layers, the equivalent wall model can generate results that more closely resemble those of the 3-D model. The equivalent wall model results are not unique; however, different equivalent wall models have, in general, very similar dynamic thermal properties. If desired, one may examine several generated models to choose the best one.

Equivalent Wall Model Example

A comparison was made between the thermal response of the three-dimensional computer model and the equivalent wall model for an insulated concrete block wall (as shown in Figure 2). The equivalent wall layers are shown in Table 2. The comparison was made for a one-day period shown in Figure 4. The quantity Te is the exterior air temperature and Tes is the exterior sol-air temperature. The indoor air temperature was held constant at 68 F (20 C).

The results of the comparison are shown in Figure 5. There is very good agreement between the 3-D and the equivalent wall model. For reference, the response assuming instantaneous heat flow (i.e., no thermal lag) is also shown, labeled "steady-state". The 3-D transient analysis results in a 4-hour shift in peak load and a considerably smoother daily response.

A tabulation of equivalent wall properties for 20 common wall systems is contained in Enermodal, 2001b.

Table 2: Equivalent Wall Layers for an Insulated Concrete Block Wall

WALL DESCRIPTION

Components	*Total R-Value* ft^2-°F-h/ Btu
11.625 in. 2 Core Concrete Block 0.375 in. Mortar 1.875 in. Foam inserts	2.3

EQUIVALENT WALL THERMOPHYSICAL PROPERTIES

N	R_n ft^2-°F h/Btu	C_n Btu/f t^2-°F	l_n in	k_n Btu-in/h-ft^2-°F	ρ_n lb/ft^3	c_{pn} Btu/lb-°F
1	0.51	5.78	3.13	6.1	111	0.2
2	1.26	1.81	5	4.0	21.7	0.2
3	0.52	6.79	3.5	6.7	116	0.2
Total	2.3					

Figure 4: Daily Profile of the Exterior Air (Te) and Sol-Air (Tes) Temperatures

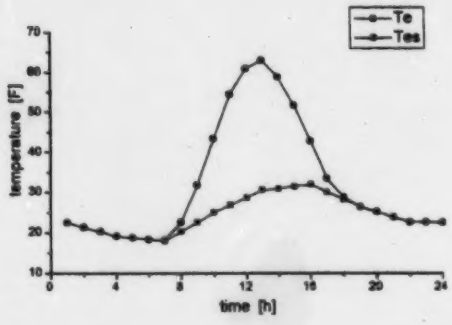

Figure 5: Comparison of Results for 3-D Transient Model and Equivalent Wall Model

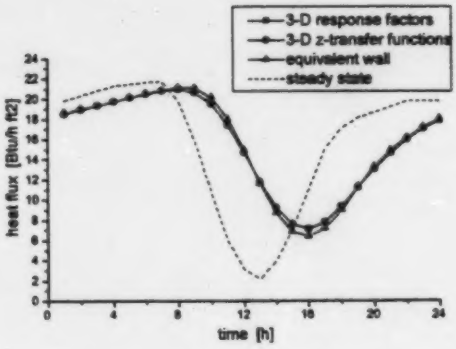

CONCLUSIONS

The conventional parallel-path method can significantly over-predict the R-values of walls with thermal bridging. This over-prediction can be corrected using one of two simple techniques. First, a weighting factor between the isothermal planes and parallel-path methods is the easiest technique for simple wall assemblies. Second, user-friendly 2-D computer simulation tools can be used for more accurate assessment and for more complex assemblies.

Thermal bridging can also impact the transient response of walls. An "equivalent wall" model is a simple way of accounting for the transient response. This technique shows excellent agreement with detailed 3-D heat transfer models.

REFERENCES

Childs K.W. 1993. HEATING 7.2 User's Manual". ORNL/TM-12262. Oak Ridge National Laboratory, Oak Ridge, TN.

Enermodal, 1996. Building Insulation System Thermal Anomalies – 785-RP, report prepared for ASHRAE, Atlanta, GA

Enermodal, 2001a. FRAMEplus Computer Program Version 5.0 (www.frameplus.net) developed for Natural Resources Canada, Kitchener, ON

Enermodal, 2001b. Modeling Two- and Three-Dimensional Heat Transfer Through Composite Wall and Roof Assemblies in Hourly Energy Simulation Programs (1145-RP), report prepared for ASHRAE, Atlanta, GA

Kossecka E. and J. Ko_ny. 1996. Relations between structural and dynamic thermal characteristics of building walls. Proceedings of 1996 International Symposium of CIB W67 *Energy and Mass Flows in the Life Cycle of Buildings"*, Vienna, 4-10 August, pp. 627-632.

Kossecka E. and J. Ko_ny. 1997. Equivalent wall as a dynamic model of the complex thermal structure. *Journ. of Thermal Insulation and Building Envelopes,* Vol. **20**, 249-268.

ACKNOWLEDGEMENTS

The author wishes to acknowledge the work of the co-authors of the ASHRAE research project on equivalent wall models: Jan Kosny of Oak Ridge National Laboratory, Elizabeth Kossecka of the Polish Institute of Sciences and Tracey Forrest of Enermodal Engineering Limited.

DEMONSTRATION OF ESP-r's ADAPTIVE CONVECTION ALGORITHM

Ian Beausoleil-Morrison

CANMET Energy Technology Centre, Natural Resources Canada, Ottawa
(ibeausol@nrcan.gc.ca)

ABSTRACT

A flow responsive algorithm was devised and implemented within the ESP-r simulation program to advance the modelling of internal surface convection. The impact of this method is demonstrated with two case studies. The method is able to resolve the impact that HVAC systems have upon room convective regimes and can substantially affect simulation results. The total annual heating load predictions of an energy efficient house were found to increase by up to 3.3%. The method had an even greater impact on the simulation of a typical office building conditioned with a air-based heating and cooling system. In this case, the method increased the predicted annual heating coil load by 9% and the cooling coil load by 19%.

INTRODUCTION

The convective heat exchange between internal building surfaces (walls, windows, etc.) and indoor air significantly affects a room's energy balance. For example, this mechanism determines the timing and degree to which solar gains absorbed by internal surfaces warm the room air. The common approach for modelling this important heat flow path within dynamic whole-building simulation programs is to employ the so-called *well-stirred* assumption (refer to Figure 1). This treats the room air as uniform and characterizes surface convection heat transfer (q''_{conv}) by a convection coefficient (h_c) and by the temperature difference between the room air and the internal surface.

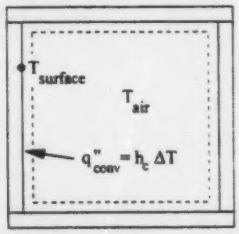

Figure 1: Well-stirred convection model

Convection heat transfer varies from surface to surface in the building, as well as with time, in response to local air flow patterns. Therefore, the calculation of convection coefficients must respond to local flow conditions in a dynamic fashion in order to accurately capture this effect. This contrasts with the simplified treatments commonly employed in building simulation programs: many programs employ time-invariant h_c values or use correlation equations which characterize h_c for a single flow regime (most often buoyancy driven flow).

The significance of the choice of h_c algorithm (made by program developer or user) on simulation results has been well demonstrated (Waters 1980; Irving 1982; Bauman et al 1983; Alamdari et al 1984; Spitler et al 1991; Clarke 1991; Lomas 1996; Fisher and Pedersen 1997; Beausoleil-Morrison and Strachan 1999). Energy prediction sensitivities in the order of 20-40% have been observed. More significantly, in some cases the predicted benefits from design measures were found to be sensitive to the approach used to model internal surface convection.

Clearly more detailed calculation approaches are required for this significant heat transfer path. One solution to address this need has been implemented in the ESP-r simulation program (ESRU 2000). Known as the *adaptive convection algorithm* (ACA), this method responds the calculation of h_c to the configuration and to the time-varying flow conditions.

This paper illustrates the application of the ACA using two case studies: an energy efficient Canadian house and a typical Canadian office building. Simulations are performed using a version of ESP-r modified for the HOT3000 program (see Purdy and Beausoleil-Morrison 2001a for a description). An overview of the ACA is provided in the following section. The case studies, the analysis method, and the simulation results are then described. Conclusions are then drawn and recommendations made for further work.

ADAPTIVE CONVECTION ALGORITHM

A brief description of the ACA is provided in this section. The interested reader is referred to Beausoleil-Morrison (2000; 2001b) for detailed coverage of the ACA's approaches and building blocks.

The ACA is built upon a foundation of 28 h_c correlation equations and employs a series of automated assessments and user prompts during the problem definition stage to appraise conditions in each room.

Each internal surface is attributed with a set of h_c equations appropriate for the flow conditions anticipated over the duration of the simulation. As the simulation progresses, a controller monitors the operational state of HVAC equipment (other control schemes are possible) to assess the flow regime. Based upon this assessment, the controller dynamically assigns (for each surface) an appropriate h_c algorithm from amongst the set attributed at the problem definition stage. One of the ACA's calculation control schemes is illustrated in Figure 2.

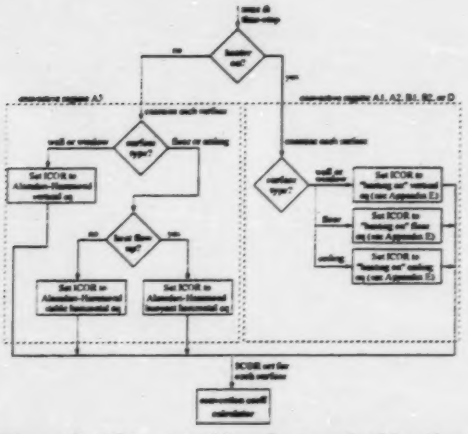

Figure 2: ACA control law for terminal heating

Consider, for example, a room heated by a radiator placed next to an internal wall. When the radiator is on, the temperature difference between the radiator and the surrounding air generates buoyant plumes. These rise and generate a convective regime within the room. The nature of the convective regime is spatially dependent: stronger convective currents are expected nearest the radiator. When the radiator is off, however, no buoyant plumes will form over the radiator. Rather, a weaker convective regime will be established in the room, this generated by buoyancy caused by temperature differences between the room air and internal surfaces. These surface-air temperature differences could be caused by heat transfer through the envelope (e.g. the cold surface of a window) or by sun patches, for example.

The ACA makes use of three h_c correlation equations for the walls to capture these effects. A correlation produced by Khalifa (1989) from experimental data collected in a room-sized test cell heated by a radiator is used for the walls adjacent to the radiator,

$$h_c = 1.98 \cdot \Delta T^{0.32} \qquad (1)$$

where ΔT is the temperature difference between the room air and the internal vall surface[1] $\{^oC\}$ and the units of h_c are $\{W/m^2K\}$.

Another Khalifa correlatior is used for the other walls in the room,

$$h_c = 2.07 \cdot \Delta T^{0.23} \qquad (2)$$

As equations 1 and 2 are only applicable when the radiator is on, a third equation is used when the ACA detects that the radiator is off. This correlation is one recommended by Alamdar and Hammond (1983) for buoyancy driven flow generated by surface-air temperature differences,

$$h_c = \left\{ \left[1.5 \cdot \left(\frac{\Delta T}{H} \right)^{1/4} \right]^6 + \left[1.23 \Delta T^{1/3} \right]^6 \right\}^{1/6} \qquad (3)$$

where H is the height of the wall $\{m\}$.

Using the logic illustrated in Figure 2, the ACA toggles between equations 1 to 3 to calculate h_c values for the walls. For a given time-step, the ACA uses equations 1 or 2 to calculate h_c for the walls if it detects that the radiator is supplying heat to the room. And equation 3 is used if the ACA detects that the radiator is off. The same logic (but different equations) are used to calculate h_c for the windows, floors, and ceilings.

ACA calculation control schemes are available to resolve the convective regimes generated by the following HVAC configurations:

- radiators located under windows;
- radiators located elsewhere in the room;
- in-floor heating;
- heated wall panels;
- circulating fan heaters;
- air-based heating and cooling systems.

The ACA is based upon experimentally derived h_c correlations and the method has undergone both analytical and empirical validation tests (Beausoleil-Morrison 2000). The ACA technique is unique to ESP-r. Most simulation programs use a single h_c correlation for all surfaces and do not vary the equation with time. In fact, many programs simply assign a fixed value for h_c. The next sections illustrate the impact the ACA has upon simulation results.

[1] Khalifa chose to regress the data using the average room air temperature, rather than the temperature of the plume rising from the radiator.

RESIDENTIAL CASE STUDY

One of the houses at the Canadian Centre for Housing Technology (CCHT) was selected as the residential case study to demonstrate the ACA. The CCHT (Swinton et al 2001) represents a typical modern energy efficient Canadian house, being airtight, well insulated, and having high performance windows. and being airtight. A model of the CCHT was constructed in ESP-r making use of infiltration and ground contact algorithms added for HOT3000. Purdy and Beausoleil-Morrison (2001a) provide a detailed description of the modelling approaches employed.

Impact of ACA on h_c calculations

Three simulations were performed with the CCHT model to investigate the ACA's impact on h_c calculations. ESP-r's default internal convection treatment was employed in the first simulation. With this, the Alamdari and Hammond (1983) h_c correlations for buoyancy-driven flow are used for all surfaces and at all time-steps of the simulation (a common approach with simulation programs and the approach usually employed by ESP-r users). The ACA was then invoked for the second simulation. All internal surfaces in the house's living space were attributed with convection calculation control data for the case of rooms heated with radiators located under windows[2]. ESP-r's default h_c treatment was retained for the other three zones. The simulation was then repeated using the same weather data and simulation parameters.

This process was repeated for the third simulation but this time the surfaces were attributed with convection calculation control data for the case of rooms heated with radiators which are not located under windows.

No other changes were made to the model between variants. Typically when comparing different heating systems, alterations would be made to the zone control data to specify which nodes interact with the plant components (e.g. a portion of the heat output from a radiator would be convective and thus would inject to the air node while a portion would be radiative and thus would inject to surface nodes). However, all runs presented here assumed the plant injected heat to the zone air-point, this to isolate the impact of the ACA. A 10-minute time-step was used in all simulations.

The h_c values calculated for an east facing window on a typical winter day (February 10) are plotted in Figure 3. This figure compares the h_c values resulting from the three simulations. As can be seen, the ACA produces substantially higher h_c for the majority of the day: from midnight to 7h00; from 11h00 to 19h30; and from 20h30 to midnight. For the case of radiators not located under windows, the h_c values are 25 to 30% more than the default treatment. When the radiators are placed under the windows the values are 40 to 45% greater.

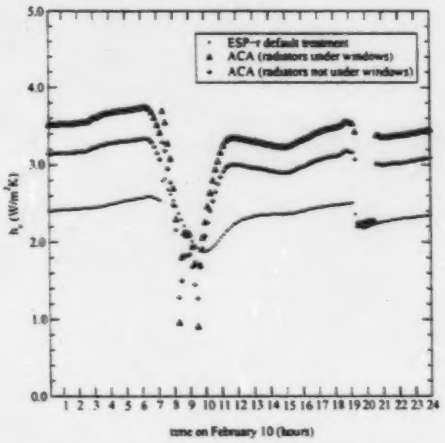
ESP-r default treatment
ACA (radiators under windows)
ACA (radiators not under windows)
5.0
4.0
3.0
2.0
1.0
0.0
1 2 3 4 5 6 7 8 9 10 11 12 13 14 15 16 17 18 19 20 21 22 23 24
time on February 10 (hours)

Figure 3: Impact of ACA on h_c calculations

From about 7h30 until 11h00 the h_c values drop substantially in all three simulations. There are significant solar gains to this east facing window during this morning period. This warms the window's internal surface to near the room air temperature. The resulting small surface-air temperature differences produce low h_c values (see equations 1 to 3).

When the nightly thermostat set-back comes into effect the three simulations produce similar h_c values. No heating is supplied for about one hour following the set-back as the house cools to the lower temperature setting (see the period around 20h00 in Figure 3). As explained in the previous section, the ACA toggles to the Alamdari-Hammond correlation when the radiator is off (see Figure 2). Therefore, during this cooling period the ACA employs the same equation as ESP-r's default approach to calculate the window's h_c. This toggling behaviour of the ACA's performance is clearly seen in Figure 3.

These results demonstrate that the ACA has a substantial impact on the calculation of h_c values. The actual impact of these h_c differences on temperature and energy flows is examined in the next section.

Impact of ACA on zone energy balance

ESP-r is based upon a control-volume heat-balance methodology. The building is discretized by representing air volumes, solid-air interfaces, and envelope

[2] The optional window correlations were not used in any of the simulations reported here due to their tendency to overestimate h_c (Beausoleil-Morrison 2000).

components with nodes. An energy balance is written for each node and the resulting set of equations solved to predict nodal temperatures and inter-nodal energy flows. These energy balances are reformed and resolved each time step of the simulation.

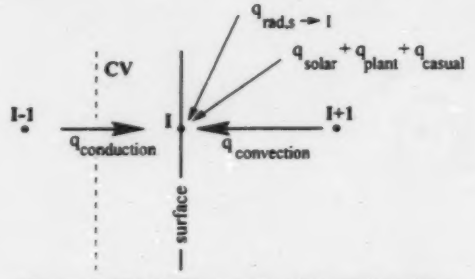

Figure 4: Heat balance at an internal surface

Figure 4 focuses on a node (*I*) located at an internal surface (e.g. the window considered above). This node's energy balance takes the following form (where *CV* is the control volume represented by the node),

$$\left\{\begin{matrix}\textit{storage of}\\ \textit{heat in CV}\end{matrix}\right\} = \left\{\begin{matrix}\textit{net conduction}\\ \textit{into CV}\end{matrix}\right\} + \left\{\begin{matrix}\textit{source of heat}\\ \textit{within CV}\end{matrix}\right\} \quad (4)$$

$$+ \left\{\begin{matrix}\textit{net longwave}\\ \textit{radiation}\\ \textit{into CV}\end{matrix}\right\} + \left\{\begin{matrix}\textit{net convection}\\ \textit{into CV}\end{matrix}\right\}$$

The rate of change of the control volume's temperature characterizes the storage term. The source term includes the radiant portion of heat injected from the HVAC system, solar gains, and longwave radiation from sources of heat within the room (e.g. lighting, occupants). The longwave radiation term represents the net heat exchange with the room's other internal surfaces.

The previous section showed how the ACA affects h_c values, and therefore the last term in equation 4. The resulting impact on temperature and energy flow predictions depends upon the importance of convection relative to the other terms in equation 4. To explore this, some of the temperatures predicted in the three simulations were compared. Figure 5 plots the zone's air-point temperature and the internal surface temperatures of the east facing window and a south facing wall. The time period examined is the same as in Figure 3.

The influence of the thermostat's nightly set-back can be clearly seen. For the sake of clarity, only the air-point temperatures predicted with the default convection treatment are shown in the figure. The ACA simulations predicted very similar air-point results, with

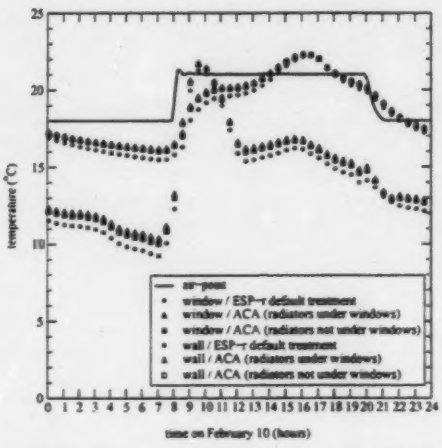
temperature (°C)
time on February 10 (hours)
air-point
window / ESP-r default treatment
window / ACA (radiators under windows)
window / ACA (radiators not under windows)
wall / ESP-r default treatment
wall / ACA (radiators under windows)
wall / ACA (radiators not under windows)

Figure 5: Impact of ACA on T_{air} and T_{surf}

only slight differences observed in the reaction to the nightly set-back.

The ACA had a significant impact on the internal surface temperature predictions, however. As can be seen, the wall and window surfaces are consistently warmer in the ACA simulations. The radiator responds to the zone's energy balance to maintain the set-point temperature. The greater h_c predicted by the ACA therefore results in higher internal surface temperatures, the degree of augmentation depending on the relative strength of the terms in equation 4. In this case, the ACA increases the window's internal surface temperature by up to $1.1°C$ and the wall's by up to $0.6°C$. These higher internal surface temperatures consequently increase the heat transferred through the envelope components, this increasing the energy usage of the radiator (the impact on energy will be discussed shortly).

The energy exchange between the room air and the envelope components is also significantly affected by the ACA. Figures 6 and 7 plot the convective heat transfer to the east facing window and the south facing wall[3] (the figures cover the same time period as before). The convection component is more dominant in the window's energy balance (principally due to the wall's high insulation level). As such, the ACA has a greater impact on the window than on the wall. The convection to the window can be as much as 24% higher with the ACA while the convection to the wall

[3] ESP-r's default approach was used to calculate h_c at the *external* surfaces as a function of wind velocity. Simulation results have been shown to be less sensitive to the treatment of external h_c than to internal h_c (Beausoleil-Morrison and Strachan 1999).

can be 12% higher. This effect is clearly seen in the figures as is the significance of the placement of the radiator.

Therefore, the ACA substantially affects the zone energy balances. The impact upon predicted energy consumption is examined in the following section.

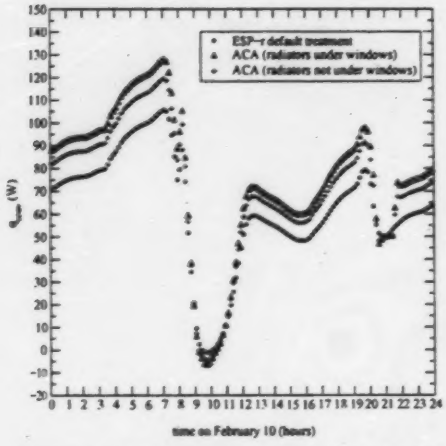

Figure 6: Convection to east facing window

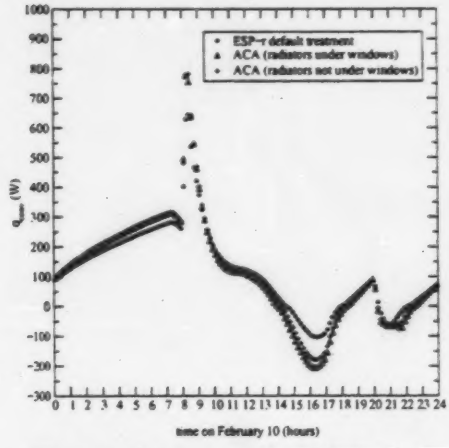

Figure 7: Convection to south facing wall

Impact of ACA on heating loads

An annual simulation was performed with the CCHT model using ESP-r's default convection treatment. This predicted an annual heating load of 50.2 GJ. Six simulations were then performed with the ACA. In each case the internal surfaces of the living space were attributed with convection calculation control data to simulate different heating systems and device placements. The scenarios examined were:

- radiators placed under windows;
- radiators placed by internal walls;
- radiators placed by external walls but not underneath windows;
- in-floor heating;
- hydronic walls panels placed on internal walls;
- forced-air heating system delivering air through registers located under windows[4].

The ACA resulted in greater annual heating load predictions in all scenarios (see Figure 8). Differences ranged from 2.4% to 3.3% of the house's total heating load caused by heat losses through the walls, windows, ceiling, basement, and due to infiltration. This sensitivity is significant. In fact, the CCHT model was found to be less sensitive to a substantial change in the house's internal thermal mass; to neglecting shading by the roof overhang; and to a 10% change in the SHGC of the windows (Purdy and Beausoleil-Morrison 2001b). Additionally, the ACA had a similar impact on annual heating load predictions as the following factors:

- increasing the U-value of the windows by 10%;
- ignoring damper control on the furnace flue;
- changing models for predicting the diffuse solar radiation distribution;
- ignoring shading by neighbouring houses.

As can be seen in Figure 8, the ACA can discriminate the impact that different HVAC systems have upon heating loads. It is important to note that minor alterations to the convection calculation control data can affect these results. Factors such as which walls are adjacent to the radiator, and which surfaces receive the direct stream of the supply air can influence the selection of h_c correlations for each surface.

It is worth noting that the sensitivity of load predictions to h_c modelling is highly dependent upon the building envelope construction. The CCHT is a well insulated building with low U-value windows. The ACA was found to have a much greater impact (up to 16% for the heating scenarios examined here) on the loads predicted for a less insulated building modelled with British weather data (Beausoleil-Morrison 2001b). To further examine this effect two additional simulations of the CCHT were performed. In this case the thermal characteristics of the envelope were derated (2x4 rather than 2x6 construction and standard double-glazed windows). In this case, the ACA simulation with the forced-air heating system produced a

[4] The ACA lacks h_c correlations for this configuration. As such, it was modelled with the closest match, a circulating fan heater.

heating load that was 4.9% greater than the default case. These results demonstrate that simulation results are more sensitive to h_c values is less insulated buildings, when convection plays a more dominate role in the surface energy balances (refer to equation 4).

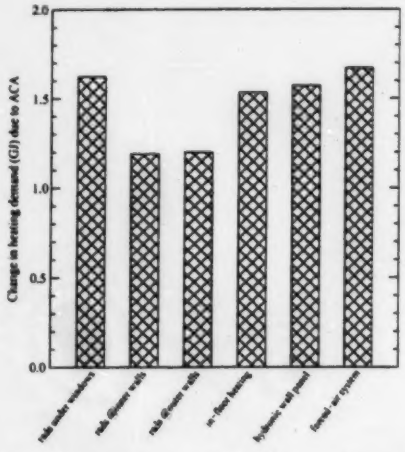

Figure 8: Impact of ACA on annual heating loads

OFFICE BUILDING CASE STUDY

An ESP-r model of a hypothetical shallow-floor-plate office building was created. A single storey was modelled and this was divided into east and west facing zones (150 m^2 floor area per zone). The envelope assemblies, insulation levels, and internal gains are typical of Canadian construction (NRC 1997) and 35% of the external wall area is glazed. Each zone is conditioned with a constant-volume forced-air mechanical system whose supply-air temperature varies from 13°C to 43°C in response to loads. During occupied hours the system delivers 60 L/s of outdoor air to each zone. The building is heated to 22°C, with an 18°C setback during unoccupied hours. The cooling set-point is 24°C but the building is allowed to free float during unoccupied periods in the summer. At 6 ac/h, the HVAC system is adequately sized to meet the peak heating load but cannot satisfy the peak cooling load (Ottawa weather conditions).

Impact of ACA on heating and cooling loads

Two annual simulations—identical except for the treatment of internal convection—were performed to compare ESP-r's default convection treatment with the ACA. In this case, the ACA was configured to employ a set of h_c correlations for mixed flow, in which both forced effects and buoyancy effects are important (Beausoleil-Morrison 2001a). When the HVAC system is supplying air to the zones, the ACA calculates h_c in response to the flow rate and temperature of the air supplied at the diffuser, and in response to the room air and internal surface temperatures. The ACA again toggles to the Alamdari-Hammond correlations when the fan system is shut down.

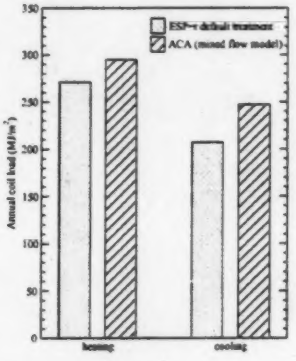

Figure 9: Impact of ACA on annual coil loads

The annual loads (normalized by floor area) placed on the HVAC system's heating and cooling coils are shown in Figure 9. Clearly, the choice of h_c algorithm has a significant impact on the prediction of annual heating and cooling loads (and thus energy consumption). The ACA predicts significantly higher heating and cooling loads (9% and 19% respectively). The cooling loads are more affected by the ACA because ESP-r's default treatment predicts very low h_c during much of the cooling season, this due to low surface-air temperature differences (refer to the functional form of equation 3).

Impact of ACA on assessment of design options

As mentioned, at design conditions the constant volume HVAC system does not meet the peak cooling load. Examination of the zone air-point temperature predictions on days with high cooling loads revealed that comfort conditions could not be maintained. The designer might explore a number of options to address the overheating problem, including:

- increasing the system's cooling capacity by 50% by increasing the air flow rate from 6 to 9 ac/h;
- increasing the cooling capacity by approximately 25% by lowering the minimum supply air temperature from 13°C to 10°C;
- changing to a VAV system with a constant supply temperature of 13°C, a minimum flow of 6 ac/h, and a maximum flow of 9 ac/h, effectively increasing cooling capacity by 50%;

- reducing solar gains by adding window overhangs.
- pre-cooling the building by night purging with 100% outdoor air at 6 ac/h.

Each of these design options was simulated twice: first with ESP-r's default convection treatment and then with the ACA. All measures reduced the peak zone temperatures, with varying degrees of success, and all had an influence on cooling loads. Figure 10 plots the impact of the design changes on the cooling load for the month of July.

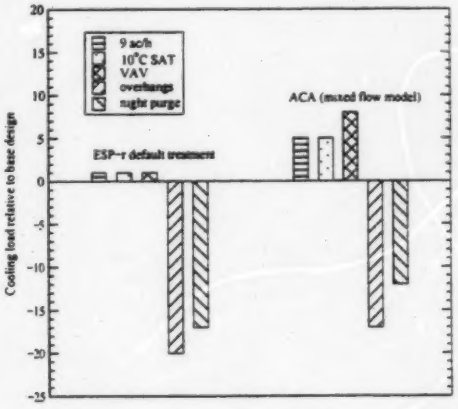

Figure 10: Impact of design options on cooling coil loads for July

The first three design options alter the convective regime: different air flow rates and supply air temperatures result. The ACA is able to respond to these changes. It predicts higher cooling loads (5%, 4%, and 8%, respectively) for the first three design options, a result of the increased cooling capacity *and* increased surface convection. In contrast, ESP-r's default approach is not capable of responding to these changes in the flow regime. Consequently, cooling load predictions are only slightly higher (about 1%) and due entirely to the fact that the cooling system was able to extract more energy because of its higher capacity. In contrast, the default approach predicted greater savings with overhangs and night purging. These measures reduced cooling loads substantially with both convection methods, but the lower h_c produced in the default runs overpredicted the savings.

CONCLUSIONS

There is substantial evidence in the literature to demonstrate the importance of accurately modelling internal surface convection within building simulation programs. Despite this, most programs still employ simplified approaches.

To address this need, a flow responsive method to improve the modelling of internal surface convection has been implemented in ESP-r. This *adaptive convection algorithm* (ACA), employs a series of automated appraisals and user prompts during the problem definition stage to appraise conditions in each room. Each internal surface is attributed with a set of h_c equations appropriate for the flow conditions anticipated over the duration of the simulation. As the simulation progresses, a controller monitors critical simulation variables to assess the flow regime. Based upon this assessment, the controller dynamically assigns (for each surface) an appropriate h_c algorithm from amongst the set attributed at the problem definition stage. The ACA currently supports 28 experimentally derived h_c correlations and has been structured such that new correlations can be easily incorporated when they become available. The method has undergone both analytic and empirical validation tests.

This paper demonstrated the ACA's impact on simulation results using two case studies. In simulations of an energy efficient house, the ACA gave h_c predictions that were up to 45% greater than ESP-r's default approach. These simulations also demonstrated that the ACA's calculations are highly sensitive to subtle changes to the convective regime, such as the placement of radiators in the room. The ACA's h_c calculations were found to have a substantial impact upon internal surface temperature and convective heat flow predictions. Compared to ESP-r's default treatment, the ACA raised the window's internal surface temperature by up to $1.1°C$ and the wall's by up to $0.6°C$. Convection heat transfer from the room air to the window was as much as 24% higher with the ACA while the convection to the wall was up be 12% higher. The ACA also lead to greater annual heating load predictions. Results were sensitive to the type and placement of the heating system, and were up to 3.3% of the house's total heating load caused by heat losses through the walls, windows, ceiling, basement, and due to infiltration. The sensitivity of load predictions was found to be highly dependent upon the building envelope construction. In general terms, the lower the envelope's resistance to heat transfer, the greater the impact of the ACA.

The ACA was found to have an even greater impact on the simulation of a typical office conditioned with an air-based HVAC system. In this case, the ACA lead to annual heating and cooling coil loads that were 9% and 19%, respectively, greater than found with ESP-r's default convection treatment. The examination of a number of design measures aimed at mitigating an

overheating problem illustrated that the ACA is able to respond to changes in the flow regime resulting from mechanical system alterations, but ESP-r's buoyancy-only default approach cannot. As a result, it was found that the ACA could influence design decisions drawn from a simulation-based analysis.

The ACA draws heavily upon the experimental work of others who provide h_c correlations for various convective regimes. Approaches were found to characterize most of the principle convective regimes, however further research in this field is required. Clearly the operation and placement of HVAC equipment has a profound impact on internal surface convection. Many systems have yet to be investigated. For example, for the residential results reported here an h_c correlation for a circulating fan heater was used to approximate the convective regime generated by a forced-air furnace. Given the importance of this heating system in residential applications, the accuracy of this approximation should be tested and, potentially, new h_c correlations developed for forced-air furnaces. Finally, further validation of the ACA is warranted. This will require the collection of high quality empirical data sets.

REFERENCES

Alamdari F. and Hammond G.P. (1983), 'Improved Data Correlations for Buoyancy-Driven Convection in Rooms', *Building Services Engineering Research and Technology*, 4 (3) 106-112.

Alamdari F., Hammond G.P., and Melo C. (1984), 'Appropriate Calculation Methods for Convective Heat Transfer from Building Surfaces', Proc. 1st U.K. National Conf. on Heat Transfer, (2) 1201-1211.

Awbi H.B. and Hatton A. (1999), 'Natural Convection from Heated Room Surfaces', *Energy and Buildings*, 30 233-244.

Bauman F., Gadgil A., Kammerud R., Altmayer E., and Nansteel M. (1983), 'Convective Heat Transfer in Buildings: Recent Research Results', *ASHRAE Transactions*, 89 (1A) 215-232.

Beausoleil-Morrison I. and Strachan P. (1999), 'On the Significance of Modelling Internal Surface Convection in Dynamic Whole-Building Simulation Programs', *ASHRAE Transactions* 105 (2) 929-940.

Beausoleil-Morrison I. (2000), *The Adaptive Coupling of Heat and Air Flow Modelling within Dynamic Whole-Building Simulation*, PhD Thesis, University of Strathclyde, Glasgow UK.

Beausoleil-Morrison I. (2001a), 'An Algorithm for Calculating Convection Coefficients for Internal Building Surfaces for the Case of Mixed Flow in Rooms', *Energy and Buildings* 33 (4) 351-361.

Beausoleil-Morrison I. (2001b), 'Flow Responsive Modelling of Internal Surface Convection', to be published in *Proc. Building Simulation '01*, Int. Building Performance Simulation Association, Rio de Janeiro Brazil.

Clarke J.A. (1991), *Internal Convective Heat Transfer Coefficients: A Sensitivity Study*, Report to ETSU, University of Strathclyde, Glasgow U.K.

ESRU (2000), *The ESP-r System for Building Energy Simulations: User Guide Version 9 Series*, University of Strathclyde, Glasgow UK.

Fisher D.E. and Pedersen C.O. (1997), 'Convective Heat Transfer in Building Energy and Thermal Load Calculations', *ASHRAE Transactions*, 103 (2) 137-148.

Irving S.J. (1982), 'Energy Program Validation: Conclusions of IEA Annex 1', *Computer Aided Design*, 14 (1) 33-38.

Khalifa A.J.N. (1989), *Heat Transfer Processes in Buildings*, PhD Thesis, University of Wales College of Cardiff, Cardiff UK.

Lomas K.J. (1996), 'The U.K. Applicability Study: An Evaluation of Thermal Simulation Programs for Passive Solar House Design', *Building and Environment*, 31 (3) 197-206.

NRC (1997), *Model National Energy Code of Canada for Buildings*, National Research Council of Canda.

Purdy J. and Beausoleil-Morrison I. (2001a), 'Modelling Residential Buildings: Which Factors are Significant', *Proc. eSim 2001: The Canadian Conference on Building Energy Simulation*, Ottawa.

Purdy J. and Beausoleil-Morrison I. (2001b), 'The Significant Factors in Modelling Residential Buildings', to be published in *Proc. Building Simulation '01*, Int. Building Performance Simulation Association, Rio de Janeiro Brazil.

Spitler J.D., Pedersen C.O., and Fisher D.E. (1991), 'Interior Convective Heat Transfer in Buildings with Large Ventilative Flow Rates', *ASHRAE Transactions*, 97 505-515.

Swinton M.C., Moussa H., and Marchand R.J. (2001), 'Commissioning Twin Houses for Assessing the Performance of Energy Conserving Technologies', To be published in *Proc. Integration of Building Envelopes*, Clearwater USA.

Waters J.R. (1980), 'The Experimental Verification of a Computerised Thermal Model for Buildings', *Building Services Engineering Research & Technology*, (1) 76-82.

MULTI-DOMAIN MODELLING USING THE ESP-r SYSTEM

Kelly N J and Strachan P A

Energy Systems Research Unit, University of Strathclyde, Glasgow, Scotland, G1 1XJ
nick@esru.strath.ac.uk; paul@esru.strath.ac.uk

ABSTRACT

Prediction of building performance is inherently a multi-domain problem. This is particularly true of many modern buildings where the aim is to provide energy efficient operation and high levels of comfort (thermal, visual, acoustic) and indoor air quality. Such buildings may employ sophisticated environmental control systems, and/or energy efficient design features such as natural daylighting, natural ventilation and building-integrated renewables.

The ESP-r system allows the analysis of coupled, inter-domain processes, e.g, detailed air flow and dynamic building temperature variation. The program has the capability to model, in an integrated manner, the following domains to variable levels of resolution: thermal, lighting, ventilation (network air flow and CFD), moisture, HVAC, electrical power flow (including renewable energy sources). All of these domains can be subjected to user-defined control action. The modeller can select, based on the particular design, which domains to include in the analysis.

This paper discusses the importance of multi-domain modelling and illustrates this with an example of an application where it is important to model interactions between different domains: the detailed modelling of an HVAC system, coupled with the building it serves. The model highlighted is one developed in support of HOT3000 developments at Natural Resources, Canada (NRCan).

INTRODUCTION

Buildings are an inherently complex energy system, whose constituent energy-related sub-systems (fabric, HVAC, lighting, etc.) interact and evolve dynamically with time due to environmental excitation, human occupation and control action. Capturing this complexity in a simulation program requires a coherent and integrated mathematical model of the problem.

This paper describes an integrated approach to building simulation, applied in the ESP-r simulation program. The building is modelled as a set of domains, each representing a sub-system. Coupling the domains together in a single model and solving simultaneously with real climate data allows a solution to be obtained of the dynamic performance of the whole building. This simultaneous solution can only be undertaken if the domains of the model are fully compatible, requiring a common approach to the representation of all the constituents of the model. However, in order to avoid over-complexity, it is important to ensure that only those domains relevant to the particular design issues of interest are selected for study.

There are many examples of building performance where the different domains interact and where the use of multi-domain models would be advantageous. Examples include:

- thermal/lighting interaction: using light sensors to control light switching;
- thermal/airflow interaction: using air flow through a double facade to provide pre-heating of building ventilation air;
- thermal/CFD interaction: studying dynamic variations in local comfort conditions in a large glazed space;
- thermal/HVAC interaction: using thermal mass to moderate heating/cooling requirements;
- thermal/power flow interaction: using electrical power and thermal heat recovery from hybrid photovoltaic modules on a building facade;
- thermal/moisture flow interaction: studying local condensation and mould growth potential.

MULTI-DOMAIN MODELLING

ESP-r applies the same basic modelling principle to all aspects of the building, which is broken down into many small control volumes. A control volume is a region of space, represented by a node, to which the principles of conservation of mass, energy and momentum can be applied. A building modelled using this technique may require the use of many thousands of control volumes to describe its fundamental components: opaque and transparent structures, plant components, fluid volumes, etc. The technique may be

summarised thus [1]:

"... ESP-r will accept some building/plant description in terms of three-dimensional geometry, construction, usage and control. This continuous system is then made discrete by division into many small, but finite volumes of space. These finite volumes then represent the various regions of the building within and between which energy can flow."

An energy conservation equation can be derived for each control volume describing the fundamental physical processes, e.g. heat conduction and storage, air flow, moisture flow, convection, etc. Sets of these equations can be extracted from the building model and grouped according to the physical process they represent. Solution of the equation sets, with real climate data and user defined control actions as boundary conditions, allows the determination of the transient energy and fluid flow processes occurring within the building.

The Form of the Multi-Domain Model

A typical ESP-r model of a building consists of a number of coupled polyhedral zones that describe the geometry and fabric. Augmenting these zones are a series of networks, each of which describes an individual domain: heating and air conditioning plant, air flow, water flow and moisture flow. This multi-domain modelling approach is efficient in terms of both the complexity of the model and the numerical solution. In a multi-domain ESP-r model, each domain adds functionality and detail. The requirements of a particular simulation will dictate the form and complexity of the model, with extra domains being added by the modeller as needed. Table 1 describes the functionality added by the various domains within ESP-r.

The multi-domain approach to modelling allows flexibility in both the types of system that can be modelled and the level of detail to which they are defined. The modeller can describe a building and its systems abstractly and then add more detailed domain descriptions as required. For example, the most basic energy simulation would involve only one domain in a model, e.g. the geometry and fabric of the building. If more functionality were required, the model could be augmented with air flow, CFD, plant and electrical networks, etc.

This flexible approach to the problem definition is made possible by the consistent application of the control volume in the description of every constituent of the building model. Hence, while the model can be constructed from many different and diverse domains (e.g. moisture flow, electrical networks, air flow networks), each domain is based on the same elemental components: control volumes. When the domains of the building model are connected together, they form a consistent mathematical description of the building.

Numerical Solution of the Multi-Domain Model

ESP-r's solution method complements the program's flexible approach to model description in that it can be tailored to suit the constituents of any particular model. ESP-r employs a range of solvers to process each domain of the building model using the most appropriate and efficient means. These solvers are essentially individual blocks that can be linked together to form a unified solution process for the entire model. The exact form of the solution process is variable: different combinations of solvers may be used at any one time. The number and type of solvers used will depend upon the characteristics of a particular model. The domains of the model (fabric, plant, flow, CFD, etc.) will use the relevant solver as required (Figure 1).

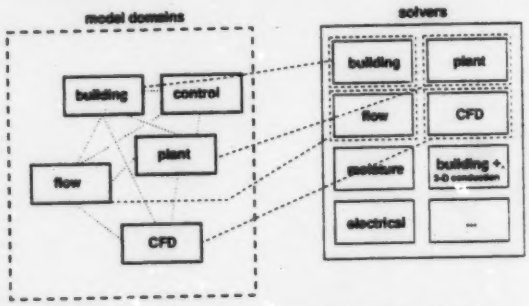

Figure 1: A multi-domain model and associated solvers.

The framework upon which the ESP-r solution process is built is provided by a governing control algorithm: a simulation controller (this is described in [1]). The combination of the solvers and the simulation controller forms ESP-r's "numerical engine", which is able to simultaneously solve all of the subsystems of the building model. This controller determines the structure of the solution process for a particular model, both in terms of the solvers that are employed, their couplings, and their temporal relationships. The use of both a simulation controller and solvers was designed to be flexible enough to enable such functionality as variable frequency processing of the equation sets, iteration and variable time-stepping within an ESP-r simulation. All these functions are useful for the successful execution of an integrated simulation, accounting for the complex couplings between the various domains.

CASE STUDY: CANADIAN BUILDING

The case study discussed here demonstrates the multi-domain modelling approach discussed above when applied to a typical Canadian dwelling. The domains involved in this particular model are described in the following paragraphs.

The Building

The building is described using 14 thermal zones, describing the basement, ground floor rooms, first floor bedrooms and roof space. The basic zone geometry is augmented with details of the constructions and occupancy schedules. A wireframe geometry of the building is shown in Figure 2.

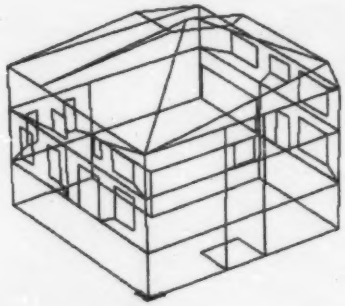

Figure 2: ESP-r Canadian building model.

The development of the original building model is described in [2]; the model shown here has been enhanced with CFD and HVAC domains to allow the investigation of local room conditions resulting from HVAC operation. The model enables accurate representation of the interacting heat transfer processes. Although it is possible to include enhanced resolution such as 3-D conduction and detailed sun-patch analysis, it was not considered necessary in this model.

Plant Network

Plant is represented within ESP-r in two complementary ways. Firstly, conditions can be controlled using abstract control: essentially an idealised representation of coupled HVAC systems. Secondly, a more detailed representation of plant can be integrated into the model: a plant network with a detailed representation of each plant component.

In this case, detailed plant modelling was used. The building was modelled with an advanced integrated mechanical system (AIMS). Such systems are being developed by a consortium of Canadian companies with Government support - they are domestic systems that integrate space and water heating with ventilation, fuelled by natural gas. They can also include air conditioning and heat recovery components. The intention is, by integrated design and intelligent control, to achieve high levels of energy efficiency and performance.

The AIMS system is shown in Figure 3. This system combines the functions of domestic hot water storage and supply with mechanical ventilation and warm air heating. In the corresponding ESP-r plant network 16 components are used to model the AIMS system; these describe ductwork, heat exchangers, mixing boxes, heating coils, fans, etc. These components are adapted from the basic plant component templates available in ESP-r's plant component databases. The network also includes a heated water storage component (described in detail in [3,4]), which serves the heating coil and also supplies the scheduled hot water demand of the building. The plant network is augmented with several control loops, which govern the operation of the system. These are summarised in Table 2.

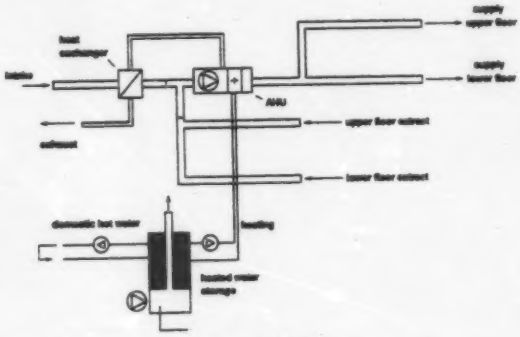

Figure 3: The AIMS system

Flow Network

The flow network, consisting of fluid components and control volumes, describes the air flow through the building and plant domains. In the building domain, the fluid control volumes correspond to the thermal zones, while connections represent doors, windows, etc. In the plant system the connections represent the individual plant components, and the control volumes represent the coupling points between the components. Air flows throughout the network are calculated as a function of pressure difference between control volumes and connecting component characteristics.

CFD

To facilitate detailed analysis of air temperature distributions, the living room zone is augmented with a CFD domain. The integration of CFD within the ESP-r model is achieved by replacing the single control volume describing the air inside a room with the CFD equivalent comprising many hundreds of smaller control volumes [5]. The CFD model facilitates the extrapolation of surface temperatures to the interior of the zone. The ability of CFD to calculate temperature distributions, air velocities, humidity and contaminant concentrations enables more detailed environmental performance analysis than would be possible with a simple homogeneous zone air volume model. It allows, for example, investigation of local thermal comfort, air quality and ventilation system performance.

Inter-Domain Couplings

The individual domains described above are all coupled together. The nature of these couplings is as follows.

building-plant: Plant components can supply and extract air to and from a zone (in convective plant systems). Hydronic systems can supply a mixed radiant/convective heating flux into a zone (e.g. radiators), or a heating flux to a structural element in the case of chilled/heated ceilings and floors. Plant interaction is integrated into the overall zonal energy balance calculations. Similarly the air temperature of the zone determines return air temperatures in convective systems and convective output from radiators and chilled/heated ceilings and floors; zone surface temperatures influence the radiant output from the same components.

flow-building-plant: The flow network calculates the flows in the building and plant network. On the building side, the flow network calculates buoyancy and wind pressure driven air flows between the building and outside and between zones. On the plant side, the flow network calculates inter-component air flows and can be used to represent the action of dampers and valves. The flow network is also used to calculate the flows between the plant and building (in convective systems) and so explicitly couples these two domains. Finally, temperatures calculated in the plant and building domains are used in the calculation of buoyancy driven flows in the flow network.

CFD-building-plant-flow: The CFD domain relies on the building plant and flow domains for the supply of its boundary conditions, and in turn provides temperature and flux data back to these other model domains. The flow domain supplies boundary flow rates to the CFD model, either from connected plant components (supply and extract) or other openings such as doors and windows. The building and plant domains supply the temperatures of these boundary flows. In addition, the temperatures of surrounding surfaces are also boundary conditions for the CFD domain, with convective heat transfer occurring between the surface and air. The convective heat transfers into and out of the CFD domain are calculated using the local surface-to-air temperature difference and a heat transfer coefficient h_c. New empirical correlations for the calculation of h_c, appropriate to the flow regimes found in buildings, have recently been added to provide more accurate estimations of convective heat transfer to and from the CFD domain [6].

Additionally, the new expressions for h_c enable the modelling of mixed natural and forced convection regimes. For the model in question both flow regimes operate: forced flow when the AIMS system is active and natural convection during quiescent periods.

Finally, as mentioned previously, control action pervades all the participating domains and as such is a major coupling mechanism in an ESP-r model. In the case of the Canadian building, model control spans the flow, plant and building domains:

- the flow rate of the pump supplying the heater coil (part of the plant network) is controlled based on the temperature of the lower floor living room in the building domain.
- the flow rate of the combustion air supply fan (calculated by the flow network) is controlled based on the heated water storage burner status (again located in the plant network).

In summary, the linkages between the various domains of the model take the form of "handshaking" of critical coupling variables: temperatures and flow rates. Control also acts as a coupling mechanism between variables in different domains e.g. flow in plant and temperature in the building.

Simulation of the Integrated Model

The model of the Canadian dwelling presented here uses 4 of ESP-r's customised domain solvers: the building solver, plant solver, flow solver and CFD solver. Note that the solution process employs the use of both iterative solvers to process the flow network and CFD equations and direct solvers to process the building and plant domains.

The solution of the CFD domain is a special case as the user has the option of activating the CFD solution for each time step of the simulation period (this is computationally expensive) or for shorter periods of

interest, e.g. during plant ON state and OFF state. Outside the active period, the CFD domain is replaced by a single control volume representing the air in the living room. The advantage of this "swapping" mechanism is that the computational overhead associated with the CFD solution is reduced.

The integrated model was simulated using Ottawa climate data over the course of a winter week (8th - 14th January). The simulation was conducted using 5-minute time steps on the building side and 1-minute time steps on the plant and flow-side. These short time steps allow the dynamics of the HVAC system and associated control to be captured in the simulation output. This allows a detailed picture of plant performance to be gained from the simulation, both in terms of the performance of individual components, but also the overall performance of plant and control on environmental conditions. A more detailed picture of environmental conditions in the living room is gained using the CFD model, which is activated during a plant ON and plant OFF state to examine the prevailing temperature distributions.

Analysis of the Integrated Model

The results presented here demonstrate the detail that can be obtained from an integrated simulation. Figure 4 shows the variation in temperatures of the living room (located on the ground floor) and an upstairs bedroom along with external temperatures. The output clearly shows the effect of the ON-OFF control strategy employed in the plant system. Also evident is the effect of night-time set-back on the temperatures.

Figures 5 to 7 show output from the plant domain, with heating coil and duct temperatures shown in Figures 5 and 6 respectively. The output indicates that air is occasionally delivered to rooms at temperatures up to 40°C, a value that may have implications for occupant comfort. This temperature could be reduced in a number of ways, e.g. down-sizing the heating coil or reducing the set point temperature of the hot water storage. Figure 7 shows the variation in temperature of the hot water storage. Again the effect of the ON-OFF cycling of the heating coil pump is evident. However, the temperature of the hot water is maintained at close to the 60°C set point.

Figure 8 shows infiltration into the living room zone, as calculated using the flow network. More detailed output regarding living room conditions is shown in Figures 9 and 10, which show output from the CFD model with the heating system active. Figure 9 shows the temperature distribution in a cross-section through the room and shows a thermal plume rising above the heating outlet (located at floor level below the living room window). Figure 10 also shows the thermal plume for a length-wise cross-section. The near uniformity of room air temperature (in the regions outside the thermal plume) and the absence of a cold down-draught indicate that, in terms of homogeneity of air temperatures, the system performs well in this room.

CONCLUSIONS

The intention of this paper was to demonstrate the need for multi-domain modelling to permit proper study of whole building performance. Given that the simulation program has the capability for such modelling, users then need appropriate skills to identify the required domains for the design questions in hand, to construct the models and to interpret the large data volumes resulting from simulations of the model.

By way of example, the paper has presented the development of a detailed model focussed on the investigation of local conditions within part of a residential building, as influenced by the heating, ventilation and control system, together with the building fabric. Such models allow designers to optimise the design of such systems without unnecessary simplification of the real building response.

REFERENCES

[1] Clarke J A, 'Energy Simulation in Building Design', Adam Hilger, Bristol, 1985.

[2] Swinton M C, Moussa H, and Marchand R J, 'Commissioning Twin Houses for Assessing the Performance of Energy Conserving Technologies', to be published in Proceedings of Integration of Building Envelopes, Performance of Exterior Envelopes of Whole Buildings VIII, Clearwater USA, December 2-6, 2001.

[3] Kelly N J, 'Development of a Heated Water Storage Plant Component Model ', Technical Report TRE 150/01, ESRU, University of Strathclyde, Glasgow, March 2001.

[4] Parent M, 'Combo/AIMS Model Description', Technosim Report for CANMET, Buildings Group, Natural Resources Canada, May 2000.

[5] Negrao C O R, 'Conflation of Computational Fluid Dynamics and Building Thermal Simulation', PhD Thesis, University of Strathclyde, 1995.

[6] Beausoleil-Morrison I, 'The Adaptive Coupling of Heat and Air Flow Modelling Within Dynamic Whole-Building Simulation', PhD Thesis, University of Strathclyde, 2000.

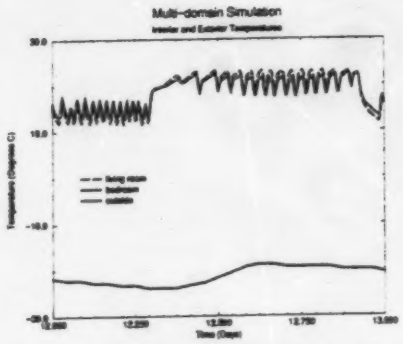

Figure 4: Internal and external temperatures

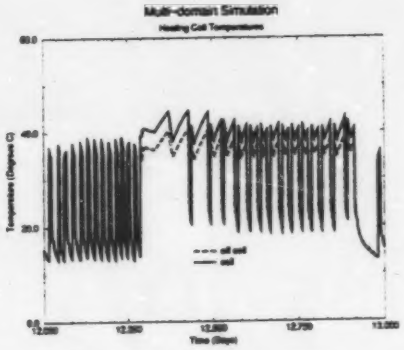

Figure 5: Heating coil temperatures

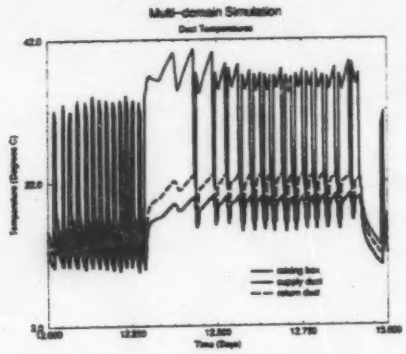

Figure 6: Duct temperatures

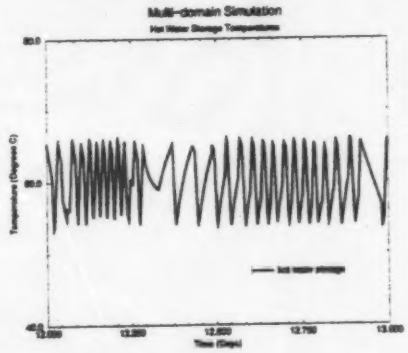

Figure 7: Hot water temperature

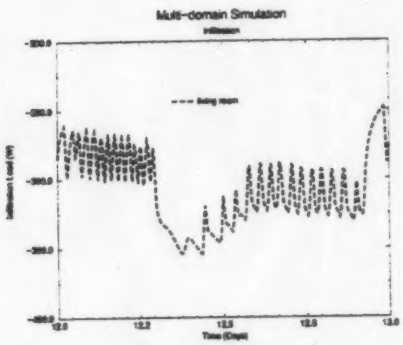

Figure 8: Infiltration

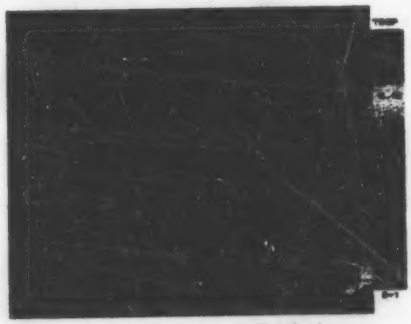

Figure 9: Temperature distribution

Figure 10: Thermal plume

Table 1 The added functionality from different domains of an ESP-r model.

Model Domain	Functionality	Typical Uses
the essential model "core": building fabric, climate, occupancy, idealised ventilation and infiltration	basic fabric thermal energy flows, air, surface and fabric temperatures	free floating environmental conditions driven by climatic and internal excitations, daylight factor calculations, solar distribution, overheating and summer comfort analysis, basic lighting studies
+ zone based control	logically and temporally controlled heating, cooling, lighting, etc.	control strategy testing, heating/cooling loads, plant sizing, lighting control, heated/cooled floor and ceiling models
+ enhanced fabric modelling: 3-D conduction, non-linear material properties, special materials	three dimensional conduction, detailed fabric thermal and non thermal (i.e. electrical energy) flows, advanced materials	thermal bridging, detailed floor heat flows, phase change materials, photovoltaics, advanced glazing studies
+ air flow network	pressure driven air flow and ventilation, inter-zonal air flow and moisture transport, detailed fan models	natural and forced ventilation studies, detailed overheating analysis, passive/ambient cooling strategies, e.g. night flushing
+ HVAC and component level control	detailed component-based plant descriptions, component temperatures and energy flows, local component-based control loops	detailed air conditioning systems modelling, control strategy analysis, etc.
+ CFD	air velocities and momentum, temperature distributions, surface boundary layer information	detailed forced and natural ventilation studies, convective heat transfer coefficient calculations, displacement ventilation modelling, detailed heating or cooling studies, atrium airflow patterns, indoor air quality etc.
+ moisture network	humidity distribution	local condensation, mould growth studies
+ electrical power network	voltage and current levels, power factors	building-integrated renewable energy studies, load control

Table 2: Control loops used with the plant network.

loop 1	ON-OFF and timer control on the pump supplying the heater coil: the pump is ON if the temperature in the ground floor zone is less than 19°C during the day and ON below 14°C at night.
loop 2	Timer control on the ventilation fan.
loop 3	ON-OFF control on the HWS burner, maintaining the water temperature at 50°C ± 5°C.
loop 4	ON-OFF control on the combustion air supply fan (ON when the burner is activated).

Author Index / Index des auteurs

Author Index / Index des auteurs

Athienitis, Andreas K. 77

Atif, Morad 85

Aydinalp, M. 144

Beausoleil-Morrison, Ian 11, 245

Becker, Rachel 93

Bellemare, René 220

Bernier, Michel 163

Bilodeau, Stéphane 171

Calla, Robert 58

Cane, Doug 138

Carpenter, Stephen 239

Clements, Bruce R. 179

Degenetais, Gwladys 43

DePani, Sebastiano 51

Dubrous, Fracois 132

Ehret, Diane 152

Farahbakhsh, H. 144

Farinaccio, Linda 205

Fazio, Paul 51

Fung, A.S. 144

Haghighat, Fariborz 109

Hand, Jon W. 26

Hayashi, Tetsuo 212

Hayden, A.C.S. 179

Henderson, Graham 152

Hepting, Curt 19, 152

Huang, Hongyu 109

Iwaoka, Shigeki 66

Jones, Christopher R. 19

Karagiozis, Achilles N. 101

Katsman, Regina 93

Kelly, N. 253

Kesik, Ted 125

Laouadi, Abdelaziz 85

Le, Minh N. 187

Leong, Wey H. 187

Lio, Michael 125

Lopez, Phylroy 58

Morrison, Andrew 138

Musser, Amy 228

Nabinger, Steven 228
Nagata, Mayuko 212
Nakamura, Mikiko 212
Nichols, Laurier 3
Osato, Masaki 212
Ozaki, Akihito 66, 212
Parent, Michel 35
Pearson, Bill 179
Pope, Stephen 132
Purdy, Julia 11
Randriamiarinjatovo, Duo 163
Raymond, Patrice 35
Roberge, Marc-Antoine 220
Rosen, Marc A. 187
Sansregret, Simon 171
Schwabe, Oliver 228
Siegel, Jeffrey 43
Snoek, C. W. 195
Stanislaw, Kajl 220
Strachan, PA 253
Takase, Shuho 66, 212
Tzempelikos, Athanassios 77
Ugursal, V. I. 144
Walker, Iain S. 43
Watanabe, Toshiyuki 66, 116, 212
Wyndham-Wheeler, Paul 58
Yamazaki, Hisashi 116
Yamazaki, Hitoshi 116
Yang, L. 195
Zmeureanu, Radu 205